

# Optimal construction and transportation method for gravity based foundations for offshore wind farms on commercial scale

Application of a new developed design method

Justin Tuin  
26-9-2018



**OPTIMAL CONSTRUCTION AND TRANSPORTATION METHOD FOR GRAVITY  
BASED FOUNDATIONS FOR OFFSHORE WIND FARMS ON COMMERCIAL SCALE**

*Application of a new developed design method*

BY JUSTIN TUIN

MASTER THESIS  
DELFT UNIVERSITY OF TECHNOLOGY  
SECTION: CIVIL ENGINEERING AND GEOSCIENCES  
26<sup>TH</sup> SEPTEMBER 2018

TO OBTAIN THE DEGREE OF MASTER OF SCIENCE IN CIVIL ENGINEERING  
AT THE DELFT UNIVERSITY OF TECHNOLOGY

Graduation committee:	prof dr. ir. S.N. Jonkman	(TU Delft)
	ir. K. J. Reinders	(TU Delft)
	dr. E.J. Houwing	(TU Delft)
	ir. E. Van Putten	(DIMCO)

## PREFACE

---

This report is the result of the executed master thesis to obtain the master degree in civil engineering at the faculty of Civil Engineering and Geosciences at the University of Technology in Delft. The master thesis is performed in cooperation with Deme Infra Marine Contractors (DIMCO, Dordrecht), part of the Deme-group.

This report contains a new developed design method to develop the most optimal construction and transportation method for gravity based foundations for offshore wind turbines on commercial scale. Because gravity based foundations are large caissons, the design method could also be applied on other types of caissons when the project characteristics are similar. A realistic case study, where the developed design method is applied on, is considered in this master thesis report.

I would like to thank several persons for making this master thesis possible. I would like to thank the graduation committee: Prof. dr. ir. Bas Jonkman, ir. Kristina Reinders, dr. Erik-Jan Houwing and ir. Eelco van Putten for the guiding and the constructive criticism during the graduation period. In special, I appreciated the committee meetings to discuss problems and the progress of the master thesis.

I would like also thank the colleagues of the Deme-group, from which I get information and new ideas. Not only the colleagues from Dimco have supported me but also some colleagues from GeoSea and Dimco nv. In special I would thank Jan-Mark van Mastwijk, Gerry Jonkheijm, Paul Kips and Wart van der Velde for the meetings and information they provided.

At last I would thank my family, friends and girlfriend for supporting me to pass the courses at the TU Delft and to accomplish the master thesis.

Delft, 26<sup>th</sup> September 2018

Justin Tuin

## ABSTRACT

---

A new trend to found offshore wind turbines at larger depths or on harder soils is to apply gravity based foundations (GBFs). These foundations are caissons with a set of properties which are different with respect to other caisson types. The draught is large and the horizontal dimensions are relatively small. The number of constructed caissons is high and the timeframe for construction and transportation from land into water is small when these foundations are applied on offshore windfarms on commercial scale. In general, an offshore wind farm is constructed in two years and all GBFs must be constructed and transported into the water in a tight time schedule.

To accomplish the construction and installation a large number of GBFs in a tight timeframe a new design method is developed. A realistic case study is composed and the target is to construct and install 64 GBFs in front of the Belgium coast in a timeframe of 2 years.

The design of these foundations generally consists of, from bottom to top, a large circular base slab with a cylindrical part, then a conical part and at last the tower which is partly above water. The minimal base slab dimensions to ensure stability are calculated and the result is a minimal diameter of 33 meter. The result is a caisson with a weight of 9157 tons, and a draught of 10.45 meter. The construction time is quite large with 26 weeks for each foundation.

To reduce the large construction time the design is adapted. The base slab is changed into a hexagonal base slab and the tower is elongated till the base slab. Because the circular base slab is the most efficient geometry the change in design increases the amount of material, the weight and therefore the draught of the element. The decrease in construction time is 6 weeks, which is 23% of the construction time. The stability is again calculated for this GBF design and results in a weight of 10,495 ton and the draught is larger with 11.21 meter.

When the design of the GBFs is known, the transportation method from land into water is considered. According to the decision matrix, developed in the literature study, the only feasible method is to apply a semi-submersible vessel, however this solution is quite expensive with a rental and operational cost of 10.5 or 13.8 million euro depending on the storage location, a new alternative method could be feasible. In a brainstorm session several new ideas are created and the most promising solution is chosen with the help of a multi-criteria analysis: The immersion structure.

Because time is the most important factor the construction planning and construction area layout is considered. Three options are considered and the most optimal construction planning is to construct the GBFs with the use of a production line, on four locations the construction activities are optimized and with this solution it is possible to construct the 64 GBFs in time with a minimal use of area and equipment. Because of the small area left, the storage location cannot be designed on the construction area. Therefore the semi-submersible vessel must be rented a longer period and cost 13.8 million.

The construction of 64 GBFs in two years is feasible and the immersion structure is designed. The platform consists of H-beams and the foundation consists of two concrete hollow legs. The immersion structure is innovative because it is placed directly on sand and no foundation works are needed. When the project is executed, water is pumped out from the legs, the immersion structure floats, and can be towed to a storage location until a new project arises where caissons must be constructed and transported into the water. Due to the large capacity the main part of the caisson types can be transported with this structure.

At last the construction and operational costs of the immersion structure, 19.7 million euro, are compared with the cost of renting a semi-submersible vessel, which costs 13.8 million euro. The semi-submersible vessel seems to be the best solution but when the immersion structure is applied at multiple projects it could be a profitable solution. The depreciation and interest costs for the immersion structure are calculated and the immersion structure is profitable when a minimal utilization rate of 22% is achieved during a service lifetime of 20 years. Depending on the market development and the amount of applicable caisson construction projects the immersion structure could be profitable. Comparing with the case study the immersion structure is profitable if three comparable projects are executed in the timeframe of 20 years.

## CONTENTS

---

List of figures .....	IX
List of tables .....	XV
Nomenclature .....	XVII
List of abbreviations .....	XXII
Chapter 1: Introduction .....	1
1.1 Cause of the research .....	1
1.2 Research goal .....	2
1.3 Research question .....	2
1.4 Research method .....	2
1.5 Sub-questions .....	5
1.6 Research method for sub-questions .....	5
1.6.1 Analysis .....	6
1.6.2 Synthesis .....	6
1.6.3 Simulation .....	6
1.6.4 Evaluation .....	7
1.6.5 Decision .....	7
1.6.6 Applicability on the several subjects .....	7
1.7 Reading guide .....	8
Chapter 2: Construction and transportation methods of large caissons .....	11
2.1 Caissons .....	11
2.2 Elementary construction and transportation actions .....	11
2.3 Construction methods .....	12
2.3.1 Casting concrete .....	12
2.3.1.1 Prefab .....	12
2.3.1.2 In-situ .....	12
2.4 Transportation methods .....	13
2.4.1 Transportation methods on land .....	13
2.4.1.1 Rail system .....	14
2.4.1.2 Skid system .....	14
2.4.1.3 Self Propelled Modular Transporter .....	14
2.4.1.4 Land based crane .....	15
2.4.1.5 Portal crane .....	16
2.4.2 Transportation methods from land into water .....	16
2.4.2.1 Heavy lift vessel/barge .....	16
2.4.2.2 Syncrolift .....	17
2.4.2.3 Semi-submersible vessel .....	17

2.4.2.4	Dry dock.....	17
2.4.2.5	Floating dock .....	17
2.4.2.6	Building on pontoons .....	17
2.4.2.7	Factory with double dock .....	18
2.4.2.8	Casting basin.....	18
2.5	Construction location.....	18
2.5.1	Fixed location.....	18
2.5.2	Production line.....	18
2.6	Decision matrix .....	19
2.7	Gravity based foundations.....	19
2.8	Conclusion construction and transportation methods.....	20
Chapter 3:	Short history of wind energy development .....	21
3.1	First electricity producing wind turbine.....	21
3.2	From onshore to offshore .....	22
3.3	Offshore wind turbine foundations .....	23
3.4	Conclusion history of wind industry.....	25
Chapter 4:	Case description .....	26
4.1	Reference case: C-Power project on the Thornton Bank.....	27
4.1.1	Project characteristics.....	27
4.1.1.1	Project location.....	27
4.1.1.2	Construction area .....	28
4.2	Case study: Seastar and Mermaid offshore wind farms .....	29
4.2.1	Construction area .....	29
4.2.1.1	Soil conditions .....	31
4.2.1.2	Environmental conditions .....	31
4.2.1.2.1	Water level in port of Oostende .....	31
4.2.1.2.2	Weather conditions .....	32
4.2.1.2.3	Wave conditions .....	33
4.3	Conclusion case study.....	34
Chapter 5:	Materialefficient GBF design .....	35
5.1	GBF properties .....	36
5.2	Program of requirements GBF design.....	37
5.3	GBF design .....	38
5.3.1	Starting points.....	39
5.3.2	Weight.....	40
5.3.3	Draught .....	41
5.3.4	Static stability.....	42
5.3.5	Dynamic stability.....	43

5.3.6	Shear capacity .....	45
5.3.7	Bearing capacity .....	46
5.3.8	Rotational stability .....	48
5.3.9	Optimal diameter for stability .....	49
5.4	Construction planning.....	50
5.4.1	Learning curve.....	50
5.5	Conclusion materialefficient GBF design .....	52
Chapter 6: Adapted GBF design .....		53
6.1	Problematic construction elements in original design.....	54
6.2	Program of requirements construction method.....	54
6.3	Starting points.....	54
6.4	Optimal diameter.....	56
6.5	Construction planning.....	57
6.6	Conclusion hexagonal design .....	60
Chapter 7: Transportation and construction method.....		61
7.1	Applying the decision matrix.....	62
7.2	Program of requirements .....	65
7.3	Brainstorm session.....	66
7.3.1	Method 1: Slipway .....	67
7.3.2	Method 2: Prefabrication method .....	68
7.3.3	Method 3: Prefabrication on quay wall, completion on water.....	69
7.3.4	Method 4: Construct GBF on quay wall, lift action with portal crane .....	70
7.3.5	Method 5: Immersion platform .....	71
7.4	Applicability of the new methods .....	73
7.4.1	Method 1: Slipway .....	73
7.4.1.1	Slipway construction .....	73
7.4.2	Method 2: Prefabrication method.....	75
7.4.2.1	Construction of GBF element .....	75
7.4.2.2	Portal crane .....	75
7.4.2.3	Land based cranes .....	77
7.4.3	Method 3: Prefabrication on quay wall, completion on water.....	78
7.4.3.1	Construction of GBF element .....	78
7.4.3.2	Portal crane .....	78
7.4.4	Method 4: Construct GBF on quay wall, lift with portal crane in water .....	80
7.4.4.1	Construction of GBF.....	80
7.4.4.2	Portal crane .....	80
7.4.5	Method 5: Immersion structure .....	81
7.4.5.1	Construction of GBF.....	81

7.4.5.2	Immersion structure .....	81
7.5	Multi-criteria analysis.....	82
7.5.1	Criteria .....	82
7.5.2	Conclusion of the MCA .....	82
7.6	Conclusion construction and transportation methods .....	87
Chapter 8:	Construction and transportation planning.....	88
8.1	Minimizing learning curve.....	89
8.2	Program of requirements .....	89
8.3	Construction on fixed location .....	90
8.4	Construction with a production line .....	92
8.4.1	Production line with three locations.....	92
8.4.2	Production line with four locations.....	94
8.5	Decision on construction and transportation planning .....	95
8.6	Optimizing planning .....	97
8.7	Conclusion construction and transportation planning .....	99
Chapter 9:	Design of immersion structure.....	100
9.1	Function of immersion structure .....	101
9.2	Starting points design immersion structure.....	101
9.3	Program of requirements .....	103
9.4	Design procedure.....	103
9.4.1	Platform design.....	104
9.4.2	Lifting mechanism.....	105
9.4.3	Foundation.....	106
9.4.3.1	Load conditions .....	107
9.4.3.2	Structural analysis .....	108
9.4.3.3	Stability.....	112
9.4.4	Construction of immersion structure .....	114
9.5	Conclusion and recommendations .....	114
Chapter 10:	Cost calculation.....	116
10.1	Applicability of immersion structure .....	117
10.1.1	Applicability on other caisson types .....	117
10.1.2	Applicability of immersion structure on port locations .....	118
10.1.3	Conclusion of applicability of immersion structure .....	120
10.2	Construction cost estimation of immersion platform.....	120
10.3	Operational cost of immersion structure.....	125
10.4	Immersion structure applied on more projects .....	125
10.5	Conclusion.....	126
Chapter 11:	Conclusions and recommendations.....	127

11.1 Conclusions .....	127
11.2 Recommendations .....	128
Bibliography .....	129

## **ANNEXES**

Annex A Construction and transportation methods of reference projects .....	135
Annex B Matlab scripts .....	148
Annex C Construction of Thornton bank Phase I .....	164
Annex D Bathymetry offshore wind farm locations .....	168
Annex E Detailed bathymetry Port of Oostende .....	169
Annex F Cone Penetration tests .....	171
Annex G Concrete hardening .....	173
Annex H Wave characteristics .....	174
Annex I Leaflet of applicable semi-submersible .....	177
Annex J Design calculation immersion structure .....	182

## LIST OF FIGURES

---

Figure 1-1 –Developed design method to develop optimal construction and transportation method for a large number of GBFs.....	4
Figure 1-2 - Design method (Hertogh, Bosch-Rekvelde, & Houwing, 2017).....	5
Figure 1-3 – Chapters indicated in design method .....	10
Figure 2-1 - Use of caisson as bridge pier (severnbridges.org) .....	11
Figure 2-2 - Caisson used as flood defence (thinkdefence.co.uk, 2015).....	11
Figure 2-3 - Caisson used as quay wall (research.engineering.ucdavis.edu) .....	11
Figure 2-4 - Prefab concrete structure (theconstructor.org) .....	12
Figure 2-5 - Traditional formwork (theconstructor.org) .....	12
Figure 2-6 - System formwork (directindustry.es) .....	13
Figure 2-7 - Crane-climbing formwork (peri-usa.com).....	13
Figure 2-8 - Self-climbing formwork at bridge of Millau (engineersireland.ie).....	13
Figure 2-9 - Skid system (mammoet.com) .....	14
Figure 2-10 - Self Propelled Modular Transporter (scheuerle.com) .....	15
Figure 2-11 - SPMTs transporting a tripod foundation (scheuerle.com) .....	15
Figure 2-12 - Crane with 1200 ton lifting capacity (liebherr.com) .....	15
Figure 2-13 - Ring crane (Mammoet.com) .....	15
Figure 2-14 - Portal crane (directindustry.com).....	16
Figure 2-15 - Taisun gantry crane (cimc-raffles.com).....	16
Figure 2-16 - Lifting GBF with the heavy lift barge Rambiz (c-power.be) .....	16
Figure 2-17 - Lift capacity of heavy lift vessels (Data: Wikipedia.org).....	16
Figure 2-18 – Syncrolift used to transport the caissons into the water (newcivilengineer.com, 2011) .....	17
Figure 2-19 - Transportation of caisson on semi-submersible vessel (Krabbendam, 2016) .....	17
Figure 2-20 - Gravity based foundations for wind turbine in dry dock (bam.com).....	17
Figure 2-21 - Use of a floating dock to construct a caisson (acciona-construccion.com, 2018) .....	17
Figure 2-22 - Construction phase FLOATGEN foundation (Floatgen.eu).....	17
Figure 2-23 - Tunnel Element Factory for Fehmarnbeltunnel (femern.com) .....	18
Figure 2-24 - Casting basin Barendrecht (beeldbank.rws.nl) .....	18
Figure 3-1 - Wind turbines from Blyth and Brush (energyclassroom.com, 2004).....	21
Figure 3-2 - Two test turbines from Poul la Cour (drømstørre.dk, 2003) .....	21
Figure 3-3 - Wind turbines built by F.L. Schmidt (drømstørre.dk, 2003) .....	21
Figure 3-4 - Modern wind turbine (mwps.world, 2015) .....	21
Figure 3-5 - Upscaling of wind turbine capacity (sciencedirect.com) .....	22
Figure 3-6 - Size of constructed and under construction offshore wind farm .....	23
Figure 3-7 - Foundation onshore wind turbine (cte-wind.com).....	23
Figure 3-8 - Different types of offshore wind turbine foundations (energy.gov, 2017) .....	23
Figure 3-9 - Main types of offshore wind foundations (theengineer.co.uk, 2012).....	23
Figure 3-10 - Applicability per foundation type as function of water depth (carbontrust.com, 2015) .....	24
Figure 3-11 - Characteristics of a GBF (4coffshore.com, 2013).....	25
Figure 3-12 - Fécamp GBF (4coffshore.com, 2013).....	25
Figure 3-13 - Strabag GBF (slideshare.net, 2012).....	25
Figure 3-14 - Blyth GBF (strukton.nl, 2016).....	25
Figure 4-1 – Chapter 4 indicated in design method .....	26
Figure 4-2 - Planning C-Power offshore wind farm (c-power.be) .....	27
Figure 4-3 - Belgium offshore wind farm locations (otary.be).....	27
Figure 4-4 - Wind turbine Thornton bank phase I.....	27
Figure 4-5 - Layout of C-Power wind farm (c-power.be).....	28
Figure 4-6 - Port of Oostende.....	28
Figure 4-7 - Halve Maan and C-Power location with dimensions .....	28
Figure 4-8 - REBO Offshore Site with dimensions .....	29

Figure 4-9 - Lifting operation of GBF from the quay wall into the water (c-power.be) .....	29
Figure 4-10 - Port of Oostende map with guaranteed depth .....	30
Figure 4-11 - Frequencies of High Water levels (afdelingkust.be) .....	31
Figure 4-12 - Frequencies of Low Water tides (afdelingkust.be) .....	31
Figure 4-13 - Cumulative density function of high water levels at Port of Oostende .....	31
Figure 4-14 - Cumulative density function low waters at Port of Oostende.....	32
Figure 4-15 - Weather characteristics at Oostende (meteoblue.com) .....	32
Figure 4-16 - Wind rose at Oostende (meteoblue.com) .....	33
Figure 4-17 - Maximum temperatures at Oostende (meteoblue.com) .....	33
Figure 4-18 - Wave rose for port entrance location (metoceanview.com).....	34
Figure 4-19 - Size of case study indicated in existing and under construction offshore windfarms .....	34
Figure 5-1 – Chapter 5 indicated in design method .....	35
Figure 5-2 - Forces on installed GBF.....	36
Figure 5-3 - Preliminary design of GBF.....	38
Figure 5-4 - Load factors according the Eurocode .....	39
Figure 5-5 – Stability of a floating element .....	42
Figure 5-6 - Wave spectrum at port entrance (Data: metoceanview.com) .....	44
Figure 5-7 – Wave spectrum at Mermaid location (Data: metoceanview.com) .....	44
Figure 5-8 – Principle of effective dimensions of a circular foundation .....	46
Figure 5-9 - Stability criteria as function of base slab diameter.....	49
Figure 5-10 - Construction planning circular GBF .....	51
Figure 6-1 – Chapter 6 indicated in design method .....	53
Figure 6-2 - Elements of GBF.....	54
Figure 6-3 - Adapted design for better constructability.....	55
Figure 6-4 – Principle of ring connection Detail A.....	55
Figure 6-5 – Principle of post-tensioned connection detail B .....	55
Figure 6-6 - Dimensions of hexagon.....	56
Figure 6-7 - Stability determination of hexagonal GBF by using unity checks for varying base slab diameter.....	56
Figure 6-8 - Hexagonal and circular base slab .....	57
Figure 6-9 - Construction planning of GBF .....	59
Figure 7-1 – Chapter 7 indicated in design method .....	61
Figure 7-2 - Top view method 1 .....	67
Figure 7-3 - Cross-section A-A Method 1 .....	67
Figure 7-4 - Construction parts in production line .....	68
Figure 7-5 – Top view method 2 .....	68
Figure 7-6 - Top view method 3 .....	69
Figure 7-7 - Top view method 4 .....	70
Figure 7-8 - View A-A method 4 .....	70
Figure 7-9 - Cross-section BB method 4.....	71
Figure 7-10 - Top view method 5 .....	71
Figure 7-11 - Cross-section A-A method 5 .....	72
Figure 7-12 - Top view method 1 .....	73
Figure 7-13 - Dimensions slipway platform.....	73
Figure 7-14 - Height of slipway platform with L=40m .....	73
Figure 7-15 - Forces on the slipway construction .....	74
Figure 7-16 – Top view prefabrication method .....	75
Figure 7-17 - Geometry of portal crane .....	76
Figure 7-18 - Forces on portal crane .....	76
Figure 7-19 - Forces on foundation portal crane .....	76
Figure 7-20 - Moment line portal crane.....	76
Figure 7-21 - Capacities and working range of Demag AC 650 (peinemann.nl).....	77
Figure 7-22 – Top view method 3 .....	78
Figure 7-23 - Geometry of portal crane .....	79

Figure 7-24 - Forces on portal crane method 3a.....	79
Figure 7-25 - Foundation forces method 3a.....	79
Figure 7-26 - Moment line method 3a.....	79
Figure 7-27 - Geometry portal crane .....	79
Figure 7-28 - Forces on portal crane method 3b .....	79
Figure 7-29 - Foundation forces method 3b .....	79
Figure 7-30 - Moment line method 3b.....	79
Figure 7-31 - Top view method 4 .....	80
Figure 7-32 - Geometry of portal crane .....	80
Figure 7-33 - Forces on portal crane .....	80
Figure 7-34 - Reaction forces on foundation .....	80
Figure 7-35 - Moment line for portal crane .....	80
Figure 7-36 - Cross-section A-A method 5 .....	81
Figure 7-37 - Top view method 5 .....	81
Figure 8-1 – Chapter 8 indicated in design method.....	88
Figure 8-2 - Layout of REBO site with 16 fixed construction locations .....	90
Figure 8-3 - Project planning with 16 fixed locations.....	91
Figure 8-4 - Grouped construction actions .....	92
Figure 8-5 - Construction planning with the use of three locations (option 1).....	92
Figure 8-6 - Production lines on the REBO site with three locations (option 1) .....	93
Figure 8-7 - Construction planning with the use of four locations (option 2).....	94
Figure 8-8 - Production line on REBO site with four locations (option 2) .....	94
Figure 8-9 - Number of constructed GBFs.....	97
Figure 8-10 - GBF production adapted planning.....	98
Figure 8-11 - Number of GBFs in stock.....	98
Figure 9-1 – Chapter 9 indicated in design method.....	100
Figure 9-2 - Transportation of GBF from land into water .....	101
Figure 9-3 - Load factors according the Eurocode .....	102
Figure 9-4 - Material factors for concrete structures (Molenaar & Voorendt, 2018).....	102
Figure 9-5 - Material factor for steel (Molenaar & Voorendt, 2018) .....	102
Figure 9-6 - Final design H-beam.....	104
Figure 9-7 - Stresses in H-beam .....	104
Figure 9-8 - Deflection of H-beam.....	104
Figure 9-9 - Principle of steel beam supporting system.....	105
Figure 9-10 - Plate of immersion platform placed on H-beams.....	105
Figure 9-11 - Winch system at Venice Mose project (newcivilengineer.com, 2011).....	105
Figure 9-12 - Platform of Venice Mose project (newcivilengineer.com, 2011) .....	105
Figure 9-13 – Starting point of design foundation legs.....	106
Figure 9-14 - Forces on concrete foundation (hydrostatic forces depends on water depth) .....	107
Figure 9-15 - Immersion platform as Scia Engineering model .....	108
Figure 9-16 - Immersion platform transparent view.....	109
Figure 9-17 - Load combinations used in Scia .....	109
Figure 9-18 - Bending moment in x-direction for bottom slab .....	111
Figure 9-19 - Decision on foundation leg width .....	113
Figure 9-20 - Dimensions of available dry docks (Data: Wikipedia.org).....	114
Figure 9-21 - Dimensions of floating docks .....	114
Figure 9-22 - Final design H-beam.....	114
Figure 9-23 - Preliminary design immersion structure.....	115
Figure 10-1 – Chapter 10 indicated in design method .....	116
Figure 10-2 - Area of applicability of immersion platform .....	117
Figure 10-3 - Solution for too high quay wall.....	119
Figure 10-4 - Solution for a lower quay wall .....	119
Figure 10-5 - Solution for a longer element .....	120

Figure 10-6 - Construction planning immersion structure .....	123
Figure 10-7 - Depreciation and interest costs as function of utilization .....	126
Figure 11-1 - Decision matrix with immersion structure .....	128
Figure A-1 - Map Fehmarnbeltunnel (femern.com) .....	135
Figure A-2 - Tunnel Element Factory for Fehmarnbeltunnel (femern.com) .....	135
Figure A-3 - Production process tunnel element .....	136
Figure A-4 - Location of the Tuas port expansion (maritime-executive.com).....	137
Figure A-5 - Transportation of caisson on semi-submersible vessel (Krabbendam, 2016).....	138
Figure A-6 - Construction method Singapore harbour extension (Maritime and Port Authority Singapore).....	138
Figure A-7 - Gravity based foundation for wind turbine in dry dock (bam.com) .....	139
Figure A-8 - Location of the Blyth project (vallourec.com, 2016) .....	139
Figure A-9 - Dimensions of available dry docks (Data: Wikipedia.org) .....	139
Figure A-10 - Width and lengths of available floating docks (Data: Wikipedia.org) .....	140
Figure A-11 – Animation of installed FLOATGEN foundation (Floatgen.eu) .....	141
Figure A-12 - Construction phase FLOATGEN foundation (Floatgen.eu) .....	141
Figure A-13 - Heavy lift vessel lifting a gravity based foundation (Peire, Nonneman, & Bosschem, 2009).....	142
Figure A-14 - Lift capacity of heavy lift vessels (Data: Wikipedia.org) .....	143
Figure A-15 - Lifting capacity Deme fleet (Data: deme-group.com) .....	143
Figure A-16 - Ring crane (Mammoet.com).....	143
Figure A-17 - Type of flood defence, plan view of flood defence, location of immersing caissons (dutchwatersector.com, 2013) .....	144
Figure A-18 - Drawing of Syncrolift (tehnoros-ship.ru) .....	144
Figure A-19 - Construction area of flood defence in Venice lagoon (newcivilengineer.com, 2011).....	144
Figure A-20 - Depth of dry docks (Data: Wikipedia.org) .....	146
Figure A-21 - Depth of floating docks (Data: Wikipedia.org) .....	146
Figure A-22 - Bathymetry map Seastar offshore wind farm (navionics.com) .....	168
Figure A-23 - Bathymetry map Mermaid offshore wind farm (navionics.com) .....	168
Figure A-24 - Port of Oostende map with guaranteed depth .....	169
Figure A-25 - Bathymetry map at Otary/Halve Maan [dm LAT].....	170
Figure A-26 - Bathymetry map at REBO Offshore Site [dm LAT].....	170
Figure A-27 - Available CPTs at REBO Offshore Site .....	171
Figure A-28 - Available CPTs at Halve Maan .....	171
Figure A-29 - CPT at Halve Maan.....	172
Figure A-30 - CPT at REBO Offshore Site .....	172
Figure A-31 -Compressive strength of concrete in time .....	173
Figure A-32 - PDF of the wave height at the Mermaid offshore wind farm (Data: metoceanview.com) .....	174
Figure A-33 - CDF of the wave height at the Mermaid offshore wind farm (Data: metoceanview.com) .....	174
Figure A-34 - Spectral density at Mermaid location (Data: metoceanview.com) .....	175
Figure A-35 - Wave rose for port entrance location .....	175
Figure A-36 - Probability density function of wave heights at Oostende port entrance (Data: metoceanview.com).....	176
Figure A-37 - Cumulative density function of wave heights at Oostende port entrance (Data: metoceanview.com).....	176
Figure A-38 - Wave spectrum at port entrance (Data: metoceanview.com) .....	176
Figure A-39 - Transportation of GBF from land into water .....	182
Figure A-40 - Load factors according the Eurocode .....	183
Figure A-41 - Material factors for concrete structures (Molenaar & Voorendt, 2018).....	183
Figure A-42 - Material factor for steel (Molenaar & Voorendt, 2018).....	183
Figure A-43 - Preliminary design immersion platform .....	185
Figure A-44 - Geometry and supports of immersion platform .....	186
Figure A-45 - Distributed load of GBF, skid system and steel platform .....	186
Figure A-46 - Foundation reaction forces .....	186
Figure A-47 - Bending moment (purple) and shear force (blue).....	186

Figure A-48 - Bending moment in 2D platform .....	186
Figure A-49 - Definitions for a H-profile (Bijlaard, Abspoel, & Vries, 2013) .....	187
Figure A-50 - H-beam design .....	189
Figure A-51 – Von Mises criteria plotted as function of x-coordinate .....	190
Figure A-52 - Stress in H-beam due to $q_{tot}$ .....	191
Figure A-53 - Displacement of H-beam .....	191
Figure A-54 - Final design H-beam .....	192
Figure A-55 - Von Mises criteria plotted as function of x-coordinate .....	192
Figure A-56 - Stresses in final design H-beam .....	193
Figure A-57 - Deflection of final H-beam.....	193
Figure A-58 - Forces on reinforcement concrete cross-section (Hordijk & Lagendijk, 2017) .....	193
Figure A-59 - Maximum reinforcement ratio per concrete class (Cement&Betoncentrum, 2016) .....	194
Figure A-60 - Preliminary design prestressed concrete girder.....	195
Figure A-61 - Principle of prestressing (Walraven & Braam, 2018) .....	196
Figure A-62 - Principle of steel beam supporting system .....	198
Figure A-63 - Plate of immersion platform placed on H-beams.....	198
Figure A-64 - Winch system at Venice Mose project (newcivilengineer.com, 2011).....	198
Figure A-65 - Platform of Venice Mose project (newcivilengineer.com, 2011) .....	198
Figure A-66 – Starting point of design foundation legs.....	200
Figure A-67 - Forces on concrete foundation (hydrostatic forces depends on water depth) .....	200
Figure A-68 - Immersion platform as Scia Engineering model .....	202
Figure A-69 - Immersion platform transparent view .....	202
Figure A-70 - BG 2: Hydrostatic pressure on immersion structure .....	203
Figure A-71 – BG 3: GBF load on platform .....	203
Figure A-72 – BG 4: Lifting mechanism on side inner walls .....	204
Figure A-73 - BG 5: Skidding beams and plate .....	204
Figure A-74 - Values of hydrostatic pressure on immersion platform .....	205
Figure A-75 - Load combinations used in Scia .....	205
Figure A-76 - Load distribution side outer wall .....	206
Figure A-77 - Bending moments at the supports for a fixed-fixed beam (Molenaar & Voorendt, 2018) .....	206
Figure A-78 - Result of bending moment in x-direction for side outer wall.....	207
Figure A-79 - Result of bending moment in y-direction for side outer wall.....	207
Figure A-80 - Result of shear force in x-direction for side outer wall .....	207
Figure A-81 - Result of shear force in y-direction for side outer wall .....	208
Figure A-82 - Result of axial force in x-direction for side outer wall.....	208
Figure A-83 - Result of axial force in y-direction for side outer wall.....	208
Figure A-84 - Forces on reinforcement concrete cross-section (Hordijk & Lagendijk, 2017) .....	210
Figure A-85 - Principle of shear reinforcement (Hordijk & Lagendijk, 2017) .....	211
Figure A-86 - Bending moment in x-direction for bottom slab .....	214
Figure A-87 – Stability of a floating element.....	217
Figure A-88 - Draught and metacentric height as function of foundation leg width .....	219
Figure A-89 – Stability criteria as function of foundation leg width .....	222
Figure A-90 - Decision on foundation leg width.....	223
Figure A-91 - Dimensions of available dry docks (Data: Wikipedia.org) .....	224
Figure A-92 - Dimensions of floating docks.....	224
Figure A-93 - Final design H-beam .....	224
Figure A-94 - Preliminary design immersion structure .....	226
Figure A-95 - Result of bending moment in x-direction for upper slab .....	227
Figure A-96 - Result of bending moment in y-direction for upper slab .....	227
Figure A-97 - Result of shear force in x-direction for upper slab .....	228
Figure A-98 - Result of shear force in y-direction for upper slab .....	228
Figure A-99 - Result of axial force in x-direction for upper slab.....	228
Figure A-100 - Result of axial force in y-direction for upper slab.....	229

Figure A-101 - Result of bending moment in x-direction for bottom slab .....	229
Figure A-102 - Result of bending moment in y-direction for bottom slab .....	230
Figure A-103 - Result of shear force in x-direction for bottom slab .....	230
Figure A-104 - Result of shear force in y-direction for bottom slab .....	230
Figure A-105 - Axial forces in x-direction for bottom slab .....	231
Figure A-106 - Axial forces in y-direction for bottom slab .....	231
Figure A-107 - Result of bending moment in x-direction for front wall .....	232
Figure A-108 - Result of bending moment in y-direction for front wall .....	232
Figure A-109 - Result of shear force in x-direction for front wall .....	232
Figure A-110 - Result of shear force in y-direction for front wall .....	233
Figure A-111 - Result of axial force in x-direction for front wall .....	233
Figure A-112 - Result of axial force in y-direction for front wall .....	233
Figure A-113 - Result of bending moment in x-direction for side inner wall .....	234
Figure A-114 - Result of bending moment in y-direction for side inner wall .....	234
Figure A-115 - Result of shear force in x-direction for side inner wall .....	235
Figure A-116 - Result of shear force in y-direction for side inner wall .....	235
Figure A-117 - Result of axial force in x-direction for side inner wall .....	235
Figure A-118 - Result of axial force in y-direction for side inner wall .....	236
Figure A-119 - Result of bending moment in x-direction for side outer wall .....	236
Figure A-120 - Result of bending moment in y-direction for side outer wall .....	237
Figure A-121 - Result of shear force in x-direction for side outer wall .....	237
Figure A-122 - Result of shear force in y-direction for side outer wall .....	237
Figure A-123 - Result of axial force in x-direction for side outer wall .....	238
Figure A-124 - Result of axial force in y-direction for side outer wall .....	238
Figure A-125 - Result of bending moment in x-direction for connecting beam .....	239
Figure A-126 - Result of bending moment in y-direction for connecting beam .....	239
Figure A-127 - Result of shear force in x-direction for connecting beam .....	239
Figure A-128 - Result of shear force in y-direction for connecting beam .....	240
Figure A-129 - Result of axial force in x-direction for connecting beam .....	240
Figure A-130 - Result of axial force in y-direction for connecting beam .....	241
Figure A-131 - Result of bending moment in x-direction for inner walls .....	241
Figure A-132 - Result of bending moment in y-direction for inner walls .....	242
Figure A-133 - Result of shear force in x-direction for inner walls .....	242
Figure A-134 - Result of shear force in y-direction for inner walls .....	242
Figure A-135 - Result of axial force in x-direction for inner walls .....	243
Figure A-136 - Result of axial force in y-direction for inner walls .....	243

## LIST OF TABLES

Table 1-1 - List of symbols.....	XXI
Table 1-2 - List of abbreviations .....	XXII
Table 1-1 - Design methods (Hertogh, Bosch-Rekvelde, & Houwing, 2017).....	6
Table 1-2 - Example of Multi Criteria Analysis .....	7
Table 2-1 - Decision matrix.....	19
Table 4-1 - Properties REBO Offshore site quay walls .....	30
Table 4-2 - Sand layers at REBO Offshore Site and Halve Maan .....	31
Table 4-3 - Important wave parameters at Mermaid location and port entrance .....	33
Table 5-1 - Properties GBF of reference projects (c-power.be) .....	37
Table 5-2 - Weight of GBF of 35m diameter .....	41
Table 5-3 - Factors used to calculate the distance KG for a GBF diameter of 35 meter .....	43
Table 5-4 - Most important wave parameters .....	43
Table 5-5 - Result of shear capacity calculation for GBF with 35m diameter .....	46
Table 5-6 - Values for bearing capacity .....	47
Table 5-7 - Input and results of rotational stability for GBF with 35m diameter.....	48
Table 5-8 - Properties of 33 meter diameter base slab.....	49
Table 5-9 - Concrete volumes of circular GBF .....	50
Table 6-1 - Parameters hexagonal GBF design with a diameter of 37.5 meter and circular GBF with diameter of 33 meter.....	57
Table 7-1 - Decision matrix applied on project with GBF.....	62
Table 7-2 - Cost estimation semi-submersible vessel with storage area at construction site .....	64
Table 7-3 - Cost estimation semi-submersible vessel with storage area in water .....	65
Table 7-4 - Weights of GBF-parts .....	75
Table 7-5 - Lifting weights for method 3 .....	78
Table 7-6 – Multi-criteria analysis.....	82
Table 7-7 - Explanation of multi-criteria analysis.....	86
Table 8-1 - Comparing the equipment of construction planning variants .....	95
Table 8-2 - Multi-criteria analysis construction and transport planning.....	95
Table 8-3 - Comparison of construction and transportation planning.....	96
Table 8-4 - Renting costs of semi-submersible vessel.....	99
Table 9-1 - Result of internal forces of all structural elements.....	110
Table 9-2 – Calculated minimal thickness and estimated mean thickness of structural elements .....	111
Table 9-3 - Values for immersion structure leg width=9m .....	112
Table 9-4 - Thickness of concrete elements.....	114
Table 10-1 - Properties of caisson construction projects.....	118
Table 10-2 - Starting points cost estimation immersion structure .....	121
Table 10-3 - Cost estimation immersion structure .....	124
Table 10-4 - Total operational costs of immersion platform .....	125
Table 10-5 - Input for depreciation and interest cost estimation .....	125
Table A-1 - Projects from literature study where the construction method is described .....	135
Table A-2 - Decision matrix .....	147
Table A-3 Values for circular GBF-design with a diameter of 35 meter.....	152
Table A-4 - Values for circular GBF-design with a diameter of 33 meter.....	153
Table A-5 - Values for hexagonal GBF-design with a 'diameter' of 37 meter .....	158
Table A-6 - Values for immersion structure with a foundation leg width of 3 meter.....	162
Table A-7 - Values for immersion structure with a foundation leg width of 9 meter.....	163
Table A-8 - Short explanation of construction method of GBF for the Thornton bank Phase I (Pictures: C-Power.be).....	167
Table A-9 - Sand layers at REBO Offshore Site and Halve Maan .....	171
Table A-10 - Important wave parameters at Mermaid location and port entrance .....	175

Table A-11 - Properties designed steel beam (S355) .....	189
Table A-12 - Dimensions of heavier designed H-beam .....	191
Table A-13 - Properties prestressed concrete element .....	196
Table A-14 - Result of internal forces of all structural elements .....	209
Table A-15 - Maximum internal forces for side outer wall .....	212
Table A-16 - Minimal thicknesses due to the internal forces at one location .....	214
Table A-17 - Estimated mean thickness of structural elements .....	215
Table A-18 - Factors used to calculate the distance KG .....	218
Table A-19 - Result of shear capacity calculation.....	220
Table A-20 - Values used to calculate bearing capacity of subsoil.....	221
Table A-21 - Input and results of rotational stability .....	222
Table A-22 - Values for immersion structure leg width=9m .....	223
Table A-23 - Thickness of concrete elements .....	224
Table A-24 - Maximum values of internal forces upper slab .....	229
Table A-25 - Maximum values of internal forces upper slab .....	231
Table A-26 - Maximum values of internal forces upper slab .....	234
Table A-27 - Maximum values of internal forces side inner wall .....	236
Table A-28 - Maximum values of internal forces side outer wall.....	238
Table A-29 - Maximum values of internal forces connecting slab .....	241
Table A-30 - Maximum values of internal forces inner walls.....	243

## NOMENCLATURE

Symbol	Description	Unit
$A$	Circular area blades	$[m^2]$
$A$	Contact area structure and soil	$[m^2]$
$A$	Area of concrete in vertical cross-section	$[m^2]$
$A$	Annuity	$[-]$
$A_c$	Cross-sectional area concrete	$[mm^2]$
$A_{eff}$	Effective area of foundation	$[m^2]$
$A_s$	Cross-sectional area steel profile	$[mm^3]$
$A_{s,needed}$	Minimal amount of longitudinal reinforcement needed	$[mm^2]$
$A_{s,req,c}$	Minimal amount of longitudinal reinforcement needed for compression	$[mm^2]$
$A_{s,req,t}$	Minimal amount of longitudinal reinforcement needed for tension	$[mm^2]$
$A_{sw}$	Cross-sectional area shear reinforcement	$[mm^2]$
$b_e$	Effective width of circular foundation	$[m]$
$B_{eff}$	Effective width of foundation area	$[m]$
$b_{leg}$	Width of immersion structure foundation leg	$[m]$
$b_w$	Working width of concrete element	$[mm]$
$\overline{BM}$	Distance centre of buoyancy and metacentre	$[m]$
$c'$	Effective cohesion	$[kN/m^2]$
$C_b$	Betz optimum	$[-]$
$C_{D+I}$	Depreciation and interest costs	$[€]$
$C_{D+I,IS}$	Depreciation and interest costs of immersion structure	$[€]$
$c_h$	Friction coefficient skidding system	$[-]$
$C_{ss}$	Rental cost of semi-submersible vessel	$[€/day]$
$d$	Draught	$[m]$
$d_0$	Initial estimated concrete thickness in Scia model	$[mm]$
$D_{bs}$	Base slab diameter	$[m]$
$D_f$	Discount factor	$[-]$
$D_{in}$	Inner diameter of cylindrical part GBF	$[m]$
$d_m$	Minimal thickness for bending moment capacity	$[mm]$
$d_{mean}$	Mean of concrete element thickness of immersion platform	$[mm]$
$d_{min}$	Minimal thickness of concrete elements of immersion platform	$[mm]$
$d_{nc}$	Minimal thickness of concrete element due to compression force	$[mm]$
$D_{out}$	Outer diameter of cylindrical part GBF	$[m]$
$d_{rent}$	Rental days of semi-submersible vessel	$[days]$
$d_{rent,year 1}$	Rental days of semi-submersible vessel in year 1	$[days]$
$d_{rent,year 2}$	Rental days of semi-submersible vessel in year 2	$[days]$
$D_w$	Diameter wind energy area	$[m]$
$e$	Eccentricity	$[m]$
$E$	E-modulus	$[Nm]$
$e_i$	Distance between centre of gravity of element I and reference level	$[m]$
$f$	Drape of tendon	$[m]$
$F_{buoy}$	Bouyancy force	$[kN]$
$f_{ck}$	Characteristic compressive strenght of concrete	$[N/mm^2]$
$f_{cm}$	Mean compressive strength concrete	$[N/mm^2]$

$F_{Ed}$	Design load	[various]
$f_f$	Coefficient of friction	[-]
$F_p$	Push or pull load	[kN]
$F_{Rd}$	Resistance design capacity	[various]
$f_{yd}$	Maximum design yield stress	[N/mm <sup>2</sup> ]
$f_y$	Characteristic yield strength reinforcing steel	[N/mm <sup>2</sup> ]
$f_{yd}$	Design yield strength reinforcing steel	[N/mm <sup>2</sup> ]
$f_{ywd}$	Design strength of shear force reinforcement	[N/mm <sup>2</sup> ]
$g$	Gravitational acceleration	[m/s <sup>2</sup> ]
$H_1$	Significant wave height	[m]
$\frac{H_1}{3}$		
$h_c$	Height of concrete element	[m]
$h_{COG}$	Height of centre of gravity	[m]
$H_j$	Height of the j'th wave	[m]
$h_m$	Metacentric height	[m]
$H_{platform}$	Height of slipway platform	[m]
$H_t$	Sum of horizontal characteristic load	[kN]
$H_{Wind turbine}$	Horizontal force due to wind turbine	[kN]
$i_\gamma$	Inclination factor on effective weight	[-]
$i_c$	Inclination factor on cohesion	[-]
$i_q$	Inclination factor on surcharge	[-]
$I_{yy}$	Area of moment of inertia	[m <sup>4</sup> ]
$I_{polar}$	Polar moment of inertia	[m <sup>4</sup> ]
$I_{xx}$	Polar moment of inertia around z-axis	[m <sup>4</sup> ]
$I_{yy}$	Polar moment of inertia around x-axis	[m <sup>4</sup> ]
$j$	Polar inertia radius of element	[m]
$k$	Shear force influencing k-factor	[-]
$\overline{KB}$	Distance of centre of buoyancy and bottom element	[m]
$\overline{KG}$	Distance between bottom element and centre of gravity	[m]
$l$	Span length	[m]
$l_{cable}$	Length of cables	[m]
$l_e$	Effective length of circular foundation	[m]
$L_{eff}$	Effective length of foundation	[m]
$l_{leg}$	Length of immersion structure foundation leg	[m]
$L_{platform}$	Length of slipway platform	[m]
$M_{10MW}$	Bending moment of 10MW wind turbine	[kNm]
$M_{8MW}$	Bending moment of 8MW wind turbine	[kNm]
$M_{c,mid}$	Bending moment at midspan in concrete element	[kNm]
$M_{E,G}$	Bending moment at midspan in prestressed element due to selfweight and permanent loads	[kNm]
$M_{E,G+Q}$	Bending moment at midspan in prestressed element due to selfweight, permanent and variable loads	[kNm]
$M_{Ed}$	Design value bending moment	[kNm]
$M_{Ed,x}$	Design value bending moment in X-direction	[kNm]
$M_{Ed,y}$	Design value bending moment in Y-direction	[kNm]
$M_{mid}$	Bending moment at midspan	[kNm]
$M_{Rd}$	Resistance design capacity	[kNm]
$M_{wind turbine}$	Moment due to wind turbine	[kNm]

$m_x$	Bending moment in x-direction	[kNm]
$m_y$	Bending moment in y-direction	[kNm]
$N$	Number of waves	[-]
$N_\gamma$	Bearing capacity factor on effective weight	[-]
$N_c$	Bearing capacity factors on cohesion	[-]
$N_c$	Compressive force in concrete	[N]
$N_q$	Bearing capacity factor on surcharge	[-]
$N_{Rd}$	Resistance design capacity	[kN]
$N_s$	Tension force in reinforcement steel	[N]
$N_x$	Axial force in x-direction	[kN]
$N_y$	Axial force in y-direction	[kN]
$P$	Power production	[W]
$P_{current}$	Water pressure due to current	[kN/m <sup>2</sup> ]
$p_h(d)$	Hydrostatic pressure water as function of depth	[kN/m <sup>2</sup> ]
$P_{Hydrostatic}$	Hydrostatic pressure water	[kN/m <sup>2</sup> ]
$p_{m,\infty}$	Prestressing force in tendon	[kN]
$p'_{max}$	Maximal bearing capacity subsoil	[kN/m <sup>2</sup> ]
$P_{Wave}$	Wave pressure	[kN/m <sup>2</sup> ]
$q_c$	Distributed characteristic load concrete weight	[kN/m]
$q_{cd}$	Distributed design load concrete weight	[kN/m]
$q_{GBF}$	Distributed load due to GBF weight	[kN/m]
$q_{Hydro}$	Distributed hydraulic load	[kN/m]
$q_{H-beam}$	Distributed load due to steel weight of H-beams	[kN/m]
$q_p$	Upward force caused by tendons	[kN/m]
$q_{skid+plate}$	Distributed load due to skidding beams and steel plate	[kN/m]
$q_{tot}$	Total distributed load	[kN/m]
$R$	Radius	[m]
$R_{in}$	Inner radius of cone bottom	[m]
$r_{in}$	Inner radius of cone top	[m]
$R_{out}$	Outer radius of cone bottom	[m]
$r_{out}$	Outer radius of cone top	[m]
$RC_{sv}$	Renting cost of semisubmersible vessel	[€/day]
$\rho_{lm}$	Reinforcement ratio needed for bending moment	[%]
$s$	Distance between shear force reinforcement	[mm]
$s$	Cement degrading factor	[-]
$S_{y,f}^a$	Shear moment flange	[mm <sup>3</sup> ]
$S_{y,w}^a$	Shear moment web	[mm <sup>3</sup> ]
$S_\gamma$	Shape factor on effective weight	[-]
$S_c$	Shape factor on cohesion	[-]
$S_q$	Shape factor on surcharge	[-]
$\sigma'_n$	Effective normal stress under foundation	[kN/m <sup>2</sup> ]
$\sigma'_q$	Effective normal stress due to surcharge	[kN/m <sup>2</sup> ]
$t$	Age of concrete	[days]
$t$	Service time	[years]
$T_0$	Natural oscillation period	[s]
$T_c$	Total construction costs immersion structure	[€]

$T_{c,ss}$	Total renting costs semi-submersible vessel	[€]
$t_f$	Flange thickness	[mm]
$T_p$	Peak period wave spectrum	[s]
$t_w$	Web thickness	[mm]
$t_1$	Reference time (=1 day)	[days]
$TC_{is}$	Total cost of constructin immersion structure	[€]
$U$	Utilization factor	[-]
$UC$	Unity check	[-]
$v_a$	Wind velocity	[m/s]
$V_{Bottom\ slab}$	Volume of concrete of immersion structure foundation in bottom slab	[m <sup>3</sup> ]
$V_c$	Volume of concrete	[m <sup>3</sup> ]
$V_{dw}$	Volume of immersed part of element	[m <sup>3</sup> ]
$V_{front\ back\ wall}$	Volume of concrete of immersion structure foundation in front and back wall	[m <sup>3</sup> ]
$V_i$	Volume of element i	[m <sup>3</sup> ]
$V_{Inner\ walls}$	Volume of concrete of immersion structure foundation in inner walls	[m <sup>3</sup> ]
$V_{leg}$	Volume of concrete of immersion structure foundation leg	[m <sup>3</sup> ]
$v_{min}$	Minimal shear stress capacity concrete	[N/mm <sup>2</sup> ]
$V_R$	Residual value factor	[%]
$V_{Rd}$	Resistance design capacity	[kN]
$V_{Side\ wall}$	Volume of concrete of immersion structure foundation in side wall	[m <sup>3</sup> ]
$V_t$	Sum of vertical characteristic load	[kN]
$V_u$	Volume of immersed part	[m <sup>3</sup> ]
$V_{Upper\ slab}$	Volume of concrete of immersion structure foundation upper slab	[m <sup>3</sup> ]
$V_{Wind\ turbine}$	Vertical force due to wind turbine	[kN]
$v_x$	Shear force in x-direction	[kN]
$v_y$	Shear force in y-direction	[kN]
$V_{z,ED}$	Design shear force in z direction	[kN]
$V_{z,Rd}$	Shear force resistance design capacity	[N]
$W$	Transportation weight	[kN]
$W_{bs}$	Moment of resistance of base slab	[m <sup>3</sup> ]
$W_{cables}$	Weight of cables	[kN]
$W_{cb}$	Area moment of resistance bottom	[mm <sup>3</sup> ]
$W_{ct}$	Area moment of resistance top	[mm <sup>3</sup> ]
$W_{GBF}$	Weight of GBF	[ton]
$W_{leg}$	Weight of immersion structure foundation leg	[kN]
$w_{mid}$	Deflection at midspan	[m]
$W_{min}$	Minimal needed moment of resistance	[mm <sup>3</sup> ]
$W_{plat}$	Weight of immersion structure platform	[kN]
$W_{tot}$	Weight of entire immersion structure	[kN]
$W_{y,min}$	Minimal moment of resistance around y-axis	[m <sup>3</sup> ]
$x$	Angle between the horizontal and slipway beams	[°]
$z$	Internal lever arm	[m]
$B_{cc}(t)$	Coefficient depending on the age t of concrete	[-]
$\delta$	Angle of friction between sand and concrete	[°]
$\gamma'$	Effective volumetric weight of soil under foundation	[kN/m <sup>3</sup> ]
$\gamma_c$	Volumetric density of concrete	[kg/m <sup>3</sup> ]

$\gamma_c$	Partial factor concrete capacity	[-]
$\gamma_G$	Partial factor on permanent load	[-]
$\gamma_i$	Volumetric weight of element i	[kN/m <sup>3</sup> ]
$\gamma_m$	Partial factor steel	[-]
$\gamma_Q$	Partial factor on variable load	[-]
$\gamma_{Rh}$	Partial factor on sliding capacity	[-]
$\gamma_{Rv}$	Partial factor on bearing capacity	[-]
$\gamma_s$	Partial factor on reinforcing steel strength	[-]
$\rho_a$	Mass density air	[kg/m <sup>3</sup> ]
$\rho_c$	Volumetric weight concrete	[kN/m <sup>3</sup> ]
$\rho_{l,max}$	Maximum reinforcement ratio	[%]
$\rho_s$	Volumetric weight steel	[kg/m <sup>3</sup> ]
$\rho_w$	Volumetric weight of water	[kN/m <sup>3</sup> ]
$\sigma_{cd}$	Compressive design strength of concrete	[N/mm <sup>2</sup> ]
$\sigma'_{GBF,max}$	Maximum vertical pressure under GBF foundation	[kN/m <sup>2</sup> ]
$\sigma_x$	Stress in x direction due to bending moment	[N/mm <sup>2</sup> ]
$\sum H$	Sum of horizontal design loads	[kN]
$\tau$	Stress due to shear force	[N/mm <sup>2</sup> ]
$\tau_d$	Design load shear stress	[kN/m <sup>2</sup> ]
$\tau_{Ed,flange}$	Shear stress in flange due to shear force	[N/mm <sup>2</sup> ]
$\tau_{Ed,web}$	Shear stress in web due to shear force	[N/mm <sup>2</sup> ]
$\tau_{max}$	Maximum shear capacity	[kN/m <sup>2</sup> ]
$\varphi'$	Angle of internal friction	[°]

Table 1-1 - List of symbols

## LIST OF ABBREVIATIONS

Abbreviation	Meaning
<b>GBS</b>	Gravity Based Structure
<b>GBF</b>	Gravity Based Foundation
<b>TAW</b>	Tweede Algemene Waterpassing
<b>HW</b>	High Water
<b>LW</b>	Low Water
<b>LAT</b>	Lowest Astronomical Tide
<b>PDF</b>	Probability Density Function
<b>CPT</b>	Cone Penetration Test
<b>REBO</b>	Renewable Energy Base Oostende
<b>CDF</b>	Cumulative Density Function
<b>MCA</b>	Multi-Criteria Analysis

*Table 1-2 - List of abbreviations*

## Chapter 1: INTRODUCTION

---

In this report a new developed method to design the most optimal construction and transportation method for large caissons is performed. This chapter includes an introduction to the report. First the cause of the research is described, thereafter the research goal with the research questions are given. A new developed design method which is used in this report is presented and the sub-questions which have to be answered to give a complete answer to the research question are given. Finally a reading guide is presented with the report structure.

### 1.1 CAUSE OF THE RESEARCH

Immersing caissons is a technique which is applied for more than 100 years. This technique was first applied for immersed tunnels where the subsoil consists of weak soil layers. This immersing technique is now applied on more types of construction projects where caissons are applied. The definition of a caisson is (Voorendt, Molenaar, & Bezuyen, 2016):

*“A retaining watertight case (or box), in order to keep out water during construction, but also for more permanent purposes. Caissons are always part of a larger structure, such as a breakwater, substructure or foundation”*

Commonly, caissons were built in dry docks and when the construction of the caisson was finished water was let in the dry dock and the caissons float. The caissons are towed by tugs to the project location. On the immersion location the caissons are ballasted. The weight of the caisson increases, exceeds the buoyancy forces and the caisson is immersed to the bottom with a high precision. In the past decades, caissons are widely used for different purposes like quay wall construction, gravity based foundations for wind turbines, bridge piers and flood defenses. The construction method of using a dry dock is still applicable but more construction methods arise, constructing caissons on a quay wall and transport them from the dry into the wet is now an important alternative.

Caissons in general have a large weight, in most cases larger than 10,000 tons. The main challenge is the transportation of the caissons from the dry into the wet. There are several methods possible to transport caisson from the dry to the wet like a dry dock, floating dock, lifting operations with heavy lift vessels or using a semi-submersible vessel.

A new trend in caisson construction is the use of caissons as gravity based foundations for offshore wind turbines. At the moment only some small numbers of these wind turbines are installed as test and demonstration projects, but when the projects are on commercially scale, the most important change is the large amount of caissons what is needed. This will change the project execution with respect to other caisson projects where, in general, a small number of caissons are needed. The construction time is very important and the risks are huge when there is a delay. Only in the installation window GBFs can be installed, when a delay is present the GBFs must be stored a halfyear and this will cost a lot of money. Also, the gravity based foundation has other properties than most caisson types, the horizontal dimensions are relatively small and the vertical dimensions are large which causes a large draught. Most common transportation methods are now impractical or even impossible to execute because of the large draught of these caissons. Because gravity based foundations are a promising alternative to other foundation types for offshore wind turbines, this report is focused on this type of caissons with the help of a case study. The question is what influence the large number of GBFs, which must be constructed and transported, has on the project execution with respect to a small number of GBFs.

A secondary question on what is the most optimal transportation method to transport the GBFs from land into water must be considered. The weight of a gravity based foundation is large, nowadays mostly in the range of 5000 till 15,000 tons. Crane operations for this large weight are (nearly) impossible to lift the gravity based foundations from the dry to the deep water. The weight is too large to find appropriate equipment to fulfil the

transportation of the foundations. In future the offshore wind turbines capacity will increase and therefore larger and heavier gravity based foundations are needed. For the Thornton Bank Offshore Wind Farm the gravity based foundations have a dead weight of approximate 3000 tons to ensure stability of a 5MW wind turbine (Peire, Nonneman, & Bosschem, 2009). The Blyth Offshore Demonstrator Project foundations have deadweight of approximately 13,000 tons, to ensure stability for an 8.3MW turbine (bamnuttall.co.uk, 2016). The weight of the foundation is dependent on the installed capacity of the wind turbine, the depth of the sea, environmental conditions and soil properties. The trend is that gravity based foundations increase in weight following the development of capacity increase of the wind turbines.

## **1.2 RESEARCH GOAL**

A major challenge is the construction and transportation of the heavy gravity based foundations. There are some demonstration and test locations where a few offshore wind turbines are installed on gravity based foundations. This type of foundations is still not applied on offshore windfarms on commercial scale. With a commercial scale offshore windfarm a large number of GBFs must be build. To be competitive against other foundation types like jackets or monopiles a large number of GBFs must be constructed on a relatively small construction area and transported into the water in a relatively short time which is the main challenge. The most important parameter to be competitive is the constructability and a small construction time per GBF. Large risks are on the construction planning: a delay on the construction has large consequences on the installation planning, because the installation can only takes place in a certain time window all GBFs must be constructed in time.

To reduce the risks on delay and decrease the construction time per GBF an optimal construction and transportation method must be developed. When the construction time per GBF can be decreased and the cost for transporting the GBFs from land in water can be minimized the competitiveness of GBFs compared to other foundation types can be increased. To reach the research goal, a research question is formulated where after sub-questions and the research method is given.

## **1.3 RESEARCH QUESTION**

The goal of the research is summarized in the research question, after presenting the research question the research method and several sub-questions are formulated to give a complete answer to the research question.

The research question is formulated as follows:

*“What is the most optimal construction and transportation method for a large number of gravity based foundations for offshore wind turbines?”*

## **1.4 RESEARCH METHOD**

To give a complete answer to the research question a design method is developed, especially for the case of construction and transportation of a large number of gravity based foundations in a relatively short period. The most important parameter is construction and transportation time of the GBFs. Because the construction and transportation interacts with each there is not a single answer to which design is the most optimal. Therefore the start is made to the materialefficient GBF. If within the project characteristics this GBF can be constructed in a certain timeframe this design could be used. But when the construction time is relatively large so that a large number of construction locations and thus also area is needed a design can be chosen with a good constructability. When both designs are given a combination of the design, construction method and transportation method must be found. In general, the designer or contractor takes a look to reference projects or expertise with methods. If there are no transportation methods applicable or if they are expensive a new method could be developed. If an existing or new developed transportation method is chosen, the construction of the GBFs must be considered. With a large number of GBFs a production line could be profitable. Then the

(temporary) structures must be designed and at last a cost calculation is performed. If a question is answered with 'no' the design of the GBFs could be adapted to make other methods possible. The design method is graphically presented as a flowchart given in Figure 1-1. All questions between the initiative and the execution of the project are answered with help of the sub-questions given in the next paragraph.

The method assumes that with the use of sub-optimizations an optimal result is obtained. Because designing is all about interactions it could be that another solution could be more optimal. This could be investigated and the design method can be optimized in a next research, this is included in the recommendations at the end of this report.

The new developed design method consists of some questions which could be interpreted differently by people. Therefore an explanation to the different questions is given:

- Is the construction time relatively large?  
The term relatively large means that problems occur with the construction area or construction time. With a large construction time a lot of construction locations are needed and this takes a lot of area.
- Is the applicable method too expensive?  
An applicable method to transport the GBFs from land into water could be expensive. Now the question is: How much may this action cost? In the stage of answering this question only a hand calculation is made to estimate the order of magnitude of the costs. In the report no strict boundary is set for too expensive or not. It is concluded on the large amount of money and therefore it is tried to found a cheaper solution. A recommendation is mentioned to investigate the boundary of too expensive by investigate reference projects with different types of transportation methods.
- Is the number of elements large enough to use a production line?  
To answer this question several construction planning options are considered to determine the effectiveness of a production line. There is no hard boundary for which construction process is profitable. Some different solutions can be designed and the most optimal must be chosen.
- Is the demand of construct and transport X GBFs in X time realistic?  
With the planning and construction area known the question is if the construction of X GBFs on area X in X time is realistic. There must be sufficient place to construct and transport all GBFs in the restricted timeframe.
- Are the (temporary) structures constructible?  
The transportation method could exist of (temporary) structures which must be constructed. The structures must be constructible and a preliminary design must be given to apply a cost calculation.
- Is transportation method profitable?  
The cost calculation must be executed and a comparison between different methods can be made to present the most cost effective solution for the project.

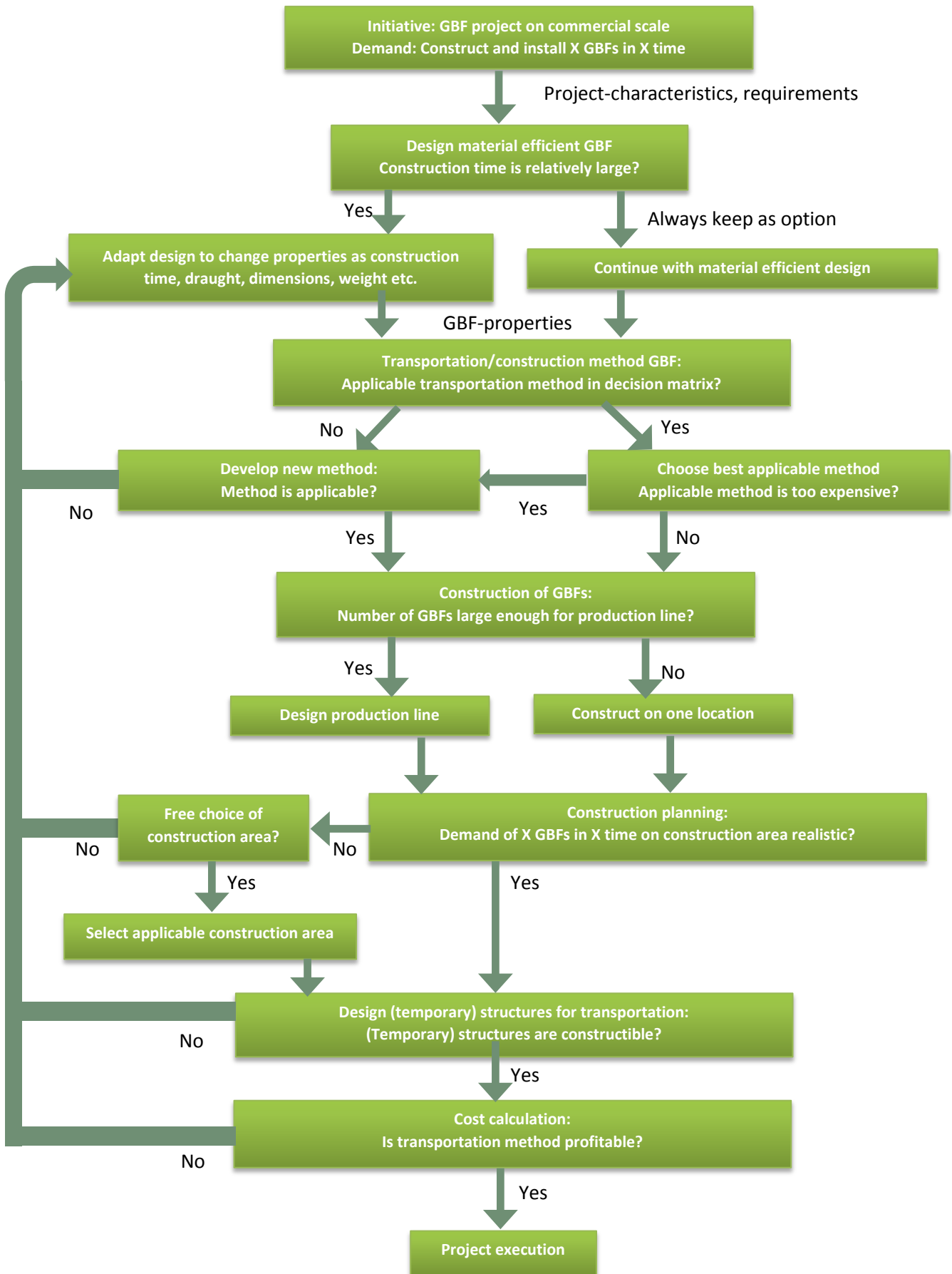


Figure 1-1 –Developed design method to develop optimal construction and transportation method for a large number of GBFs

## 1.5 SUB-QUESTIONS

To give a clear answer to the research question several sub-questions are formulated, these sub-questions, excluding sub-question 1, are the same questions as in the design method in Figure 1-1 are present:

1. *What are the main constructing and transportation methods for large caissons?*
2. *What is a realistic case for an offshore wind farm founded on GBFs on commercial scale?*
3. *What is the most materiaefficient design of a GBF?*
4. *What is the construction time of the materiaefficient GBF?*
5. *What adaptations on the design can be performed to increase the constructability and decrease the construction time?*
6. *What transportation method is the most applicable on the GBFs as described in the case?*
7. *What alternative transportation method could be designed which is cheaper and/or has less risk on time delay?*
8. *What is the most optimal construction method of the GBFs, a production line or construction on a fixed location?*
9. *Is the planning and construction layout realistic to construct a number of X GBFs in X time?*
10. *What is the optimal design for (temporary) structures to realize the transportation operation of the GBFs from land into water?*
11. *Is the new developed transportation method profitable comparing with other commonly applied applicable methods?*

## 1.6 RESEARCH METHOD FOR SUB-QUESTIONS

To give a satisfactory answer to the research question a secondary design method is followed to give answers on the sub-questions, see Figure 1-2. This secondary design method is applied on all questions in the design method of Figure 1-1. Sometimes this design method is quite straightforward when for example one demand is the most important or only one solution is feasible, then the evaluation phase are very short because no alternatives are present.

The applied design method in this report consists of 5 phases.

- Analysis
- Synthesis
- Simulation
- Evaluation
- Decision

In the next paragraph the five design phases and the output of each phase is described.

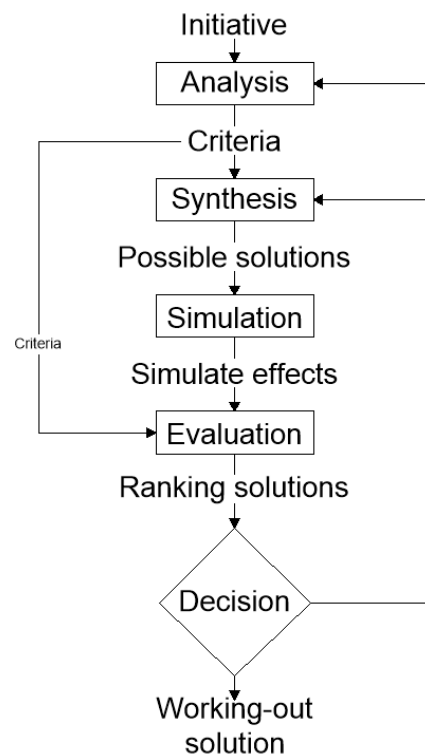


Figure 1-2 - Design method (Hertogh, Bosch-Rekvelde, & Houwing, 2017)

### 1.6.1 Analysis

In the analysis phase the problem is analysed. Questions as: “What are the main functions and sub-functions of a system?” are important in this phase. A program of requirements is described and boundary conditions are determined. Important examples of boundary conditions at the project location could be:

- Soil properties
- Water levels
- Bathymetry maps
- Wave conditions
- Weather conditions
- Legislation at the location
- Available facilities at the location
- Feasible construction materials

Also the program of requirements is given on which the solutions must comply on. This program of requirements is used later in the multi-criteria analysis to decide which solution is the most applicable.

In the analysis phase no detailed drawings or ideas are used. The analysis is only meant to describe the problem and give an overview of the situation and reference projects. Therefore only a schematic drawing of the situation is allowed.

### 1.6.2 Synthesis

In the synthesis part the first ideas and drawings are given. All information from the analysis is merged and this leads to new ideas. Sometimes one specific property or requirement is that important that no other ideas have to be considered. When more requirements are important there are different methods for generating new solutions, see Table 1-1 (Hertogh, Bosch-Rekvelde, & Houwing, 2017). In Table 1-1 the most appropriate method for creating new solutions for four situations are given.

	Solutions unknown	Solutions known
Design target unknown	Research	Technician
Design target known	Brainstorm	Standard solution

Table 1-1 - Design methods (Hertogh, Bosch-Rekvelde, & Houwing, 2017)

For each sub-question a different design approach for the synthesis phase is applied:

- Design materialeefficient GBF: Standard solution
- Adaptation GBF-design: Technician
- Transportation method in decision matrix: Technician
- Develop new transportation method: Brainstorm
- Construction method and construction area layout: Technician
- Construction planning: Technician
- Design temporary structures for transportation operation: Technician

The benefits of a brainstorm session are the large amount of new thoughts and ideas. With all methods a number of solutions could be selected and can be worked-out to a level where the system is clear.

### 1.6.3 Simulation

The selected solutions from the synthesis phase are now simulated. A check is performed on the functions, sub-functions and the program of requirements. Also the feasibility of the solutions is checked. When a solution is practically impossible this solution is rejected. The solutions which comply with the program of requirements, the functions and sub-functions are selected and are evaluated in the evaluation phase.

### 1.6.4 Evaluation

The evaluation phase is used to give the solutions a score and to rank the solutions. The method to give the solutions a certain score is a Multi-Criteria Analysis (MCA). In a MCA several factors are given where the solutions score a mark per criteria. Examples for criteria could be:

- Time
- Safety
- Constructability
- Risks
- Durability
- Applicability

A score is given between 1 and 10. Each criterion has a certain weight. All weights summed up are equal to one, therefore the final score per solution is also between 1 and 10. With the final scores the solutions can be ranked.

With these criteria an example of a MCA is given in Table 1-2. In this table it can be seen that for this case solution 3 is the best solution. The MCA is the end product of the evaluation phase.

		Rating				Score			
Criterion	Weight	Sol. 1	Sol. 2	Sol. 3	Sol. 4	Sol. 1	Sol. 2	Sol. 3	Sol. 4
<b>Time</b>	0.2	8	6	5	8	1.6	1.2	1	1.6
<b>Safety</b>	0.15	5	3	6	7	0.75	0.45	0.9	1.05
<b>Constructability</b>	0.2	4	5	8	4	0.8	1	1.6	0.8
<b>Risks</b>	0.15	2	8	7	1	0.3	1.2	1.05	0.15
<b>Durability</b>	0.15	6	7	4	4	0.9	1.05	0.6	0.6
<b>Applicability</b>	0.15	8	4	4	8	1.2	0.6	0.6	1.2
<b>Total</b>	<b>1</b>					<b>5.55</b>	<b>5.5</b>	<b>5.75</b>	<b>5.4</b>

Table 1-2 - Example of Multi Criteria Analysis

### 1.6.5 Decision

The last phase of the design method is the decision phase. In this phase the conclusion is given and the direction in the design method is determined.

### 1.6.6 Applicability on the several subjects

The secondary design method is executed on the development of a construction and transportation method for GBFs. In the initiative the research question is given and at the end the decision must be made to work out the selected solution. Before making the solution the secondary design loop is executed several times. For each subject the applicability of the design loop is described:

- Material efficient GBF design:  
The design of the GBF is investigated with the most important criteria which is stability, in transportation phase and in operational phase. Because for these criteria a circular base slab is the most optimal choice no other geometries are investigated in this chapter. Therefore this design loop is very short because there is only one variant.
- GBF constructability:  
For a better constructability some design experts of DIMCO are interviewed and in consultation the decision was to change the circular base slab to a hexagon. Because a circular foundation is still the most optimal geometry a hexagon is assumed to be profitable due to a better constructability. A larger diameter might be needed and more material is needed but the construction process can be executed in less time and with lower risks. Therefore no other variants are treated. This design loop is therefore

small due to one variant. After this design loop the GBF design is given with the dimensions and properties.

- Construction and transportation method:  
For the transportation method the decision matrix is applied. The only applicable transportation method is to make use of a semi-submersible vessel, but this solution seems to be very expensive. As input the design for the circular and hexagonal with their construction times are used. With a brainstorm session several new ideas are given, this is the synthesis phase. The ideas are treated and the systems are investigated at headlines. Questions as: what are the dimensions, effects and system properties of the solutions are given in the simulation phase. All systems are reviewed with the program and requirements and applying a multi-criteria analysis in the evaluation phase the most optimal system is determined.
- Construction planning and construction area layout:  
After the most optimal transportation method is determined, the outcome is used as input for the construction planning and design of the construction area layout. In the synthesis phase three possible solutions are given, drawings of the different area layouts are included. The construction planning for each solution is given and the effects on the layout of the REBO Offshore site are investigated in the simulation phase. Then the solutions are checked with the program of requirements and by applying a multi-criteria analysis the most optimal construction planning is chosen.
- Design of structure used for transportation:  
Now the logistical procedures in the execution and the location of the immersion structure are known, the immersion structure is considered. After giving the program of requirements the immersion platform is designed. Three materials are selected of which the platform could be build. In the simulation phase the applicability is determined. From the simulation phase the conclusion was that only one material is applicable and therefore this material is chosen in the evaluation phase. The foundation is designed of reinforced concrete, this is the most logical choice due to the requirement of stability on the subsoil and a large contact area is needed. Therefore no alternatives are designed and no synthesis, simulation and evaluation phase are performed.
- Cost comparison:  
For the cost comparison the design method is not applicable.

## 1.7 READING GUIDE

The report includes several design steps to answer the research question. In chapter 2 an extensive analysis is given to provide information about caissons, the common construction and transportation methods to construct and transport caissons on land and from land into water are described. A decision matrix is given, which is derived in a previous literature study. In this matrix the most common project characteristics present in a caisson project are used to decide which transportation methods from land into water are applicable.

Because this report is in first instance not about all types of caissons, the focus is set on gravity based foundations for offshore wind turbines. In chapter 3 a short history of the wind energy development is given. To give some knowledge about the wind industry in general and to explain the trend of increasing dimensions and capacities of the offshore wind industry. Also the foundation types are described with their applicability in the range of water depths.

Because the report is focusing on gravity based foundations for offshore wind turbines, a case study is described in chapter 4. Two offshore wind farms, called Mermaid and Seastar, in front of the Belgium coast are assumed to be founded with gravity based foundations. Several years ago the C-Power wind farm is realized, at a close distance to the Mermaid and Seastar, with a majority of jacket foundations and five gravity based foundations. These foundations are built in the port of Oostende. This case is applied with the upscaling from

five to 64 gravity based foundations. With this change the whole construction process is changed. Risks on time are very important and the main challenge in the design method is to give a method statement to construct and install 64 gravity based foundations in a period of two years.

The first technical challenge is to design the gravity based foundation. In chapter 5 a design based on reference projects is used and the diameter of the circular foundation is determined which ensure stability during transport and during the operational phase. The circular shape is used to design a materiaefficient design. The foundation is stable but the constructability leads to problems in the challenge to construct 64 of these foundations in a relatively short timeframe.

In chapter 6 the constructability is addressed, the geometry of the gravity based foundation is adapted from a circular to a hexagonal shape. Also the tower design of the GBF is adapted. The cone on the original gravity based foundation is changed into twelve plates which are prefabricated and can be placed by land based cranes. The constructability is better with this design and the construction period and the risks are decreased.

After having changed the geometry for a better constructability the transportation process of the GBFs from land into the water is addressed in chapter 7. A brainstorm session is organized to create new ideas which are applicable. In the decision matrix only a semi-submersible vessel could be used to fulfil the transportation action but this is an expensive solution. A new solution could be profitable and is tried to found. From the multi-criteria analysis the immersion structure is found to be the most optimal solution.

When the GBF design and the transportation process is known the construction planning and construction area layout are addressed. In chapter 8, three options for the construction planning are given and the most optimal is chosen. A planning is given and the layout of the construction area is drawn in the REBO terminal at the port of Oostende.

In chapter 9 a preliminary design of the immersion structure is given. The immersion platform is designed and a choice is made between three materials: Steel, reinforced concrete, prestressed concrete. The most appropriate material is chosen and this design is worked out in more detail. The foundation of the immersion structure is made of reinforced concrete and the main advantage of the immersion structure is the possibility to let the immersion structure float and tow it to another location where it can fulfill its function for a next project.

In chapter 10 the cost calculation of constructing the immersion structure is performed. If the immersion structure is profitable compared to the semi-submersible vessel the immersion structure is chosen to be the best solution. If not, another transportation method must be chosen or a new method must be designed which is profitable.

At last, in chapter 11 the conclusions and recommendations are given.

In Figure 1-3 the chapters are indicated in the design method to give a clear overview of the report structure.

In the report chapters some references are made to annexes, they are included at the end of this report.

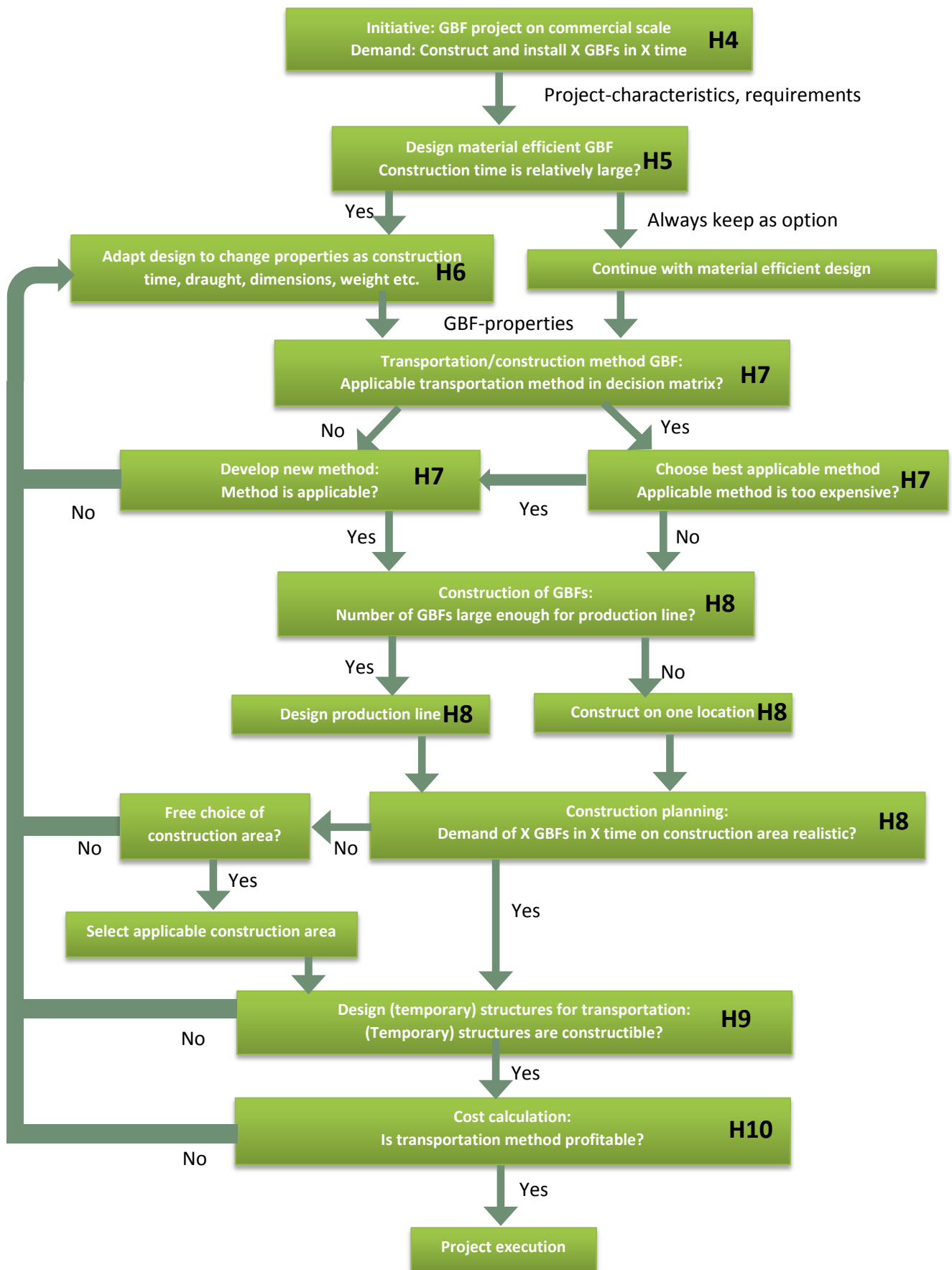


Figure 1-3 – Chapters indicated in design method

## Chapter 2: CONSTRUCTION AND TRANSPORTATION METHODS OF LARGE CAISSONS

This chapter contains the main construction methods of constructing caissons. A large variety of construction possibilities are present to construct caissons. Thereafter the transportation methods are described. For the transportation operation of large caissons the possibilities are lower in number.

### 2.1 CAISSONS

Large caissons are present in multiple types of projects. Caissons are used among other to build flood defenses, bridge piers, quay walls or foundations. Caissons are large concrete boxes which are constructed in the dry and are transported into water, and then the caissons are towed by tug boats to the project locations where the caissons are immersed. In Figure 2-1 till Figure 2-3 three examples of caissons are shown.



Figure 2-1 - Use of caisson as bridge pier ([severnbridges.org](http://severnbridges.org))



Figure 2-2 - Caisson used as flood defence ([thinkdefence.co.uk](http://thinkdefence.co.uk), 2015)



Figure 2-3 - Caisson used as quay wall ([research.engineering.ucdavis.edu](http://research.engineering.ucdavis.edu))

### 2.2 ELEMENTARY CONSTRUCTION AND TRANSPORTATION ACTIONS

To develop a new construction and transportation method the elementary construction works of caissons are listed in this paragraph. The construction of caissons can be roughly distinguished in several important actions. There are important construction and transportation actions. First the different available concrete construction techniques are given:

- Construction of caisson:
  - In-situ
    - Traditional formwork
    - System formwork
    - Climbing formwork
      - Crane climbing
      - Self-climbing
      - Gliding
  - Prefab

The following techniques are available to transport the caissons on land:

- Transport on land
  - Rail system
  - Skidding system
  - SPMT
  - Lifting solutions
    - Land based crane
    - Portal crane

The following techniques are available to transport the caissons from land into water.

- Transport from land into water
  - Syncrolift
  - Lifting solutions
    - Land based crane
    - Heavy lift vessel
    - Portal crane
  - Dock
    - Dry dock
    - Floating dock
  - Semi-submersible vessel
  - Building on pontoons

The transport from the water in the port to the final location is not considered in this report, because the transportation of the GBFs from the construction area to the immersion location for all different methods is executed by tug boats. Only with the floating dock and the dry dock the transportation can mainly be fulfilled with these equipment but the last phase tug boats are needed.

These different concrete construction techniques, transportation methods on land and from land into water are all explained in the next paragraph. These techniques are needed to develop the optimal construction and transportation method for GBFs.

## 2.3 CONSTRUCTION METHODS

Before the transport of the caissons from the land into the water can be executed the element must be constructed. The caissons consist mainly of reinforced concrete. In this paragraph different methods to construct reinforced concrete are described.

### 2.3.1 Casting concrete

The realization of concrete constructions can be done in two ways, connecting prefabricated concrete elements or casting the concrete construction at the construction area (in-situ).

#### 2.3.1.1 Prefab

A concrete structure could be composed of several parts. These parts could be prefabricated, transported to the structure and connected to the structure. In this way the concrete quality could be better and the time needed to realize the structure can be decreased. Especially for complex geometries with a large number of elements needed the prefab construction method could be profitable. A disadvantage of the use of prefab is the connections between the elements. When large internal forces are expected the connections are hard to design because the reinforcement is not connected as in an in-situ casted structure.



Figure 2-4 - Prefab concrete structure  
(theconstructor.org)

#### 2.3.1.2 In-situ

Another method to construct concrete structures is to cast concrete at the construction area. Concrete is delivered at the construction area and a formwork must be applied to realize the geometry of the concrete structure. There are different main types of formwork and in one of the main types, the climbing formwork, three subtypes are possible:

- Traditional formwork:  
Wooden formwork is applied to realize the geometry of a concrete structure, see Figure 2-5. This type of formwork is labour-intensive and the wood is not very durable and in



Figure 2-5 - Traditional formwork  
(theconstructor.org)

general cannot be used more than 30 times (concreteconstruction.net).

- System formwork:

A system formwork is in most cases a steel formwork, which can be used multiple times. This type of formwork is less labour-intensive than the traditional formwork and therefore profitable when this formwork can be used in sequence. This type of formwork is applied when a structure is made with a high repetition factor. The system formwork is shown in Figure 2-6.



Figure 2-6 - System formwork (directindustry.es)

- Climbing formwork:

For high constructions with a quite uniform geometry, climbing formwork is commonly applied. Because the geometry of the formwork does not have to be adapted this type of formwork can be profitable due to the little time of installation. There are three main types of climbing formwork:

- Crane-climbing formwork:

The formwork is lifted upward by a crane when the concrete hardening is sufficient. In Figure 2-7 a crane-climbing formwork is displayed.

- Self-climbing formwork:

The formwork is elevated by mechanic equipment that is part of the formwork itself. The formwork can be elevated when the concrete hardening is sufficient without the use of external equipment. The self-climbing formwork is displayed in Figure 2-8.

- Gliding formwork:

The gliding type of formwork is quite similar to the self-climbing formwork; the main difference is that the gliding formwork is continuously elevating. The casted concrete is seamless and has a high quality. A disadvantage is that the process is continuously, day and night and seven days a week, and that an interruption of the casting process causes problems to the quality of the concrete.



Figure 2-7 - Crane-climbing formwork (peri-usa.com)



Figure 2-8 - Self-climbing formwork at bridge of Millau (engineersireland.ie)

## 2.4 TRANSPORTATION METHODS

When the caisson is constructed, the caissons must be transported from the construction place to the quay wall. After the caisson is transported on land the next operation is to transport the caissons from the land into the water. In this paragraph both transportation methods, on land and from land into water are discussed with the possibilities of each method.

### 2.4.1 Transportation methods on land

Because these elements are heavy, a lot of common transportation methods are not applicable. The possible transportation methods on land are as described in paragraph 2.2:

- Rail system
- Skid system
- Self propelled modular transporter
- Lifting with a land based crane
- Lifting with portal cranes

These methods will be discussed with respect to the range of possibilities and a short discussion about the advantages and disadvantages.

#### 2.4.1.1 Rail system

A rail system as is used for the transportation of the caissons for the Venice MOSE project to protect the city Venice for high water levels could be used. The caissons that are transported by the rail system weight around 23,000 ton (strukton.com, 2014). The main disadvantage of a rail system is that sharp bends are impossible to create.

#### 2.4.1.2 Skid system

Skidding beams are widely used to transport large weights. The load is placed on a platform on several swivels, the push/pull unit is fixed to the rail and with a hydraulic cylinder the skid shoe is moved on the skidding track.

To advantage of skidding beams is the small horizontal force needed to transport large weights horizontally. To horizontal load can be calculated with:

$$F_p = c_h \cdot W \quad (1)$$

Where:

$$F_p = \text{Push or pull force [kN]}$$

$$c_h = \text{Friction coefficient [-]}$$

$$W = \text{Transportation weight [kN]}$$

The friction coefficient is around 4% and therefore a pushing load of 4% of the total weight is needed to push the load (polyfluor.nl). The pushing load per push unit ranges from 20 till 125 tons, so with the use of several skidding beams and push units the transportation on land is feasible (Mammoet.com). With a pushing load of 125 ton a load of 3125 ton can be transported. Per skid shoe a maximum vertical load of 863 tons is feasible, large weights till several ten thousands of tons could be transported by using skid systems. A skid system is displayed in Figure 2-9 for some clarification of the system.

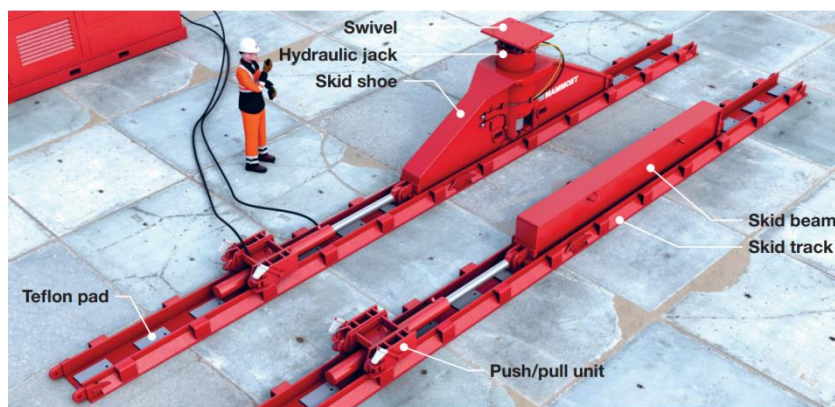


Figure 2-9 - Skid system (mammoet.com)

#### 2.4.1.3 Self Propelled Modular Transporter

A Self Propelled Modular Transporter (SPMT) is a vehicle that consists of an engine, a lot of axles and a platform where the load is placed on. A SPMT is displayed in Figure 2-10. A SPMT is a modular system which means that more SPMTs can be deployed simultaneously to carry a heavy load. The transport of a large load, where the transport operation with SPMTs is executed is shown in Figure 2-11. SPMTs have a capacity that is expressed in tons per axle. The maximum axle load is 60 tons per axle (Mammoet.com). With this axial load heavy construction can be transported. The amount of SPMTs can simply be calculated with the transported load. SPMTs have the advantage that the load can be transported in every direction. Another advantage is that no extra construction on the quay wall has to be made for the transportation operation.



Figure 2-10 - Self Propelled Modular Transporter (scheuerle.com)



Figure 2-11 - SPMTs transporting a tripod foundation (scheuerle.com)

#### 2.4.1.4 Land based crane

Elements also can be transported by lifting the elements and place them on the right location. Mobile land based cranes as displayed in Figure 2-12 have lifting capacities to 1200 tons at 2.5 meter (liebherr.com). When the load is at larger distance from the crane this lifting capacity will decrease rapidly. The largest land based cranes, ring cranes, as displayed in Figure 2-13 have larger lifting capacities till 5000 ton.

The mobile crane has the maneuverability as a large advantage in comparison to the ring crane. On the other hand, the ring crane has a much larger lifting capacity.



Figure 2-12 - Crane with 1200 ton lifting capacity



Figure 2-13 - Ring crane (Mammoet.com)

### 2.4.1.5 Portal crane

A portal crane is a type of crane that is supported on both sides with a steel leg to a rail. Portal cranes can maneuver in one direction on a rail. A portal crane is displayed in Figure 2-14. The advantage is that the crane can maneuver with the load and the lifting capacity not decreases as is the case for mobile and ring crane. The disadvantage is that the load only can be transported in the covering area of the portal crane. Another disadvantage is that the portal crane limits the height of the element that has to be lifted. This element may not be higher than the height of the portal crane. With large elements this results in very high portal cranes. The largest existing portal crane is displayed in Figure 2-15, this crane is able to lift weights up to 20,000 ton, has a span of 120 meter and a height of 80 meters (cimc-raffles.com).



Figure 2-14 - Portal crane (directindustry.com)



Figure 2-15 - Taisun gantry crane (cimc-raffles.com)

## 2.4.2 Transportation methods from land into water

The transportation from land into water is a more complex transportation action. The lifting capacity of common material is mostly insufficient to simply lift the caisson from the quay wall into the water. The most common transportation methods are given in this paragraph. The described transportation methods are:

- Heavy lift vessel/barge
- Syncrolift
- Semi-submersible vessel
- Dry dock
- Floating dock
- Building on pontoons
- Factory with double dock
- Casting basin



Figure 2-16 - Lifting GBF with the heavy lift barge Rambiz (c-power.be)

### 2.4.2.1 Heavy lift vessel/barge

The transportation method with a heavy lift vessel or barge are very similar, the only difference is the presence of the propulsion power. With this method the caisson is lifted from the quay wall into the water with a heavy lift vessel/barge. See Figure 2-16 for the transportation of the GBF from the quay wall into the water. In Figure 2-17 the capacity of existing heavy lift vessels are shown. A quite low number of heavy lift vessels could lift loads more than 5000 tons and higher than 10.000 tons are quite exceptional.

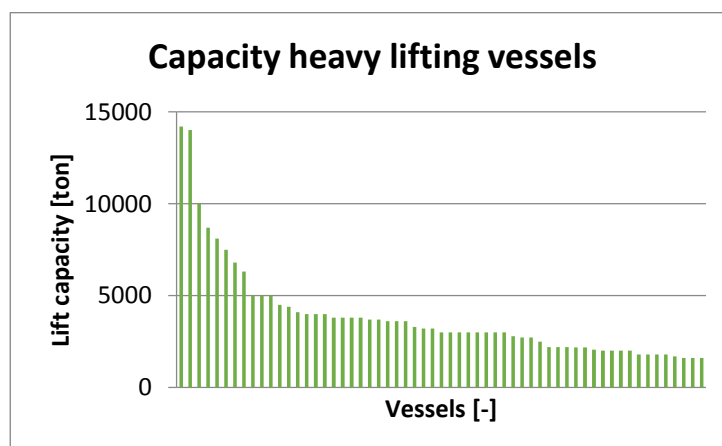


Figure 2-17 - Lift capacity of heavy lift vessels (Data: Wikipedia.org)

#### 2.4.2.2 Syncrolift

A syncrolift originates from the shipbuilding industry. A syncrolift is a platform that could be lowered and raised to transport vessels from the water to land and vice versa. In the MOSE project where a flood defense for the Venice city is constructed a type of syncrolift is constructed to transport the caissons from the land into the water. In Figure 2-18 this platform is displayed. This platform is not able to lift the caissons from the water to the land, but obviously that is not needed.



Figure 2-18 – Syncrolift used to transport the caissons into the water (newcivilengineer.com, 2011)

#### 2.4.2.3 Semi-submersible vessel

The caisson is constructed on a quay wall. With a transport method on land it is transported on a semi-submersible vessel. A semi-submersible vessel is a vessel that can bear large weights and is able to submerge partly. When the semi-submersible vessel submerges deeper than the draught of the caisson, the caisson will float and it can be towed to the final location. In Figure 2-19 a caisson on a quay wall before a semi-submersible vessel is displayed.



Figure 2-19 - Transportation of caisson on semi-submersible vessel (Krabbendam, 2016)

#### 2.4.2.4 Dry dock

A dry-dock originates from the shipbuilding industry. A dry-dock is used for the repair and maintenance of a vessel. A vessel sails in the dry dock, the door closes, water is pumped out and the vessel can be maintained in the dry.

The use of a dry dock is also applicable for the construction of caissons. The caissons are built in the dry dock, when the caisson is constructed water is letting in the dry dock and the caissons float. When it floats one caisson at a time can be towed out from the dry dock and can be immersed at the project location. A dry dock with five constructed gravity based foundations is displayed in Figure 2-20.



Figure 2-20 - Gravity based foundations for wind turbine in dry dock (bam.com)

#### 2.4.2.5 Floating dock

A floating dock is quite similar to the dry dock but the main difference is that it floats on water. On this floating dock the caisson is constructed and the floating dock submerges to give the caisson sufficient depth to float. Then the caisson can be towed from the floating dock to the location of immersion.



Figure 2-21 - Use of a floating dock to construct a caisson (acciona-construccion.com, 2018)

#### 2.4.2.6 Building on pontoons

A less known construction method is to build a caisson on one or more pontoons, see Figure 2-22. When the caisson is fully constructed the pontoons are towed to a sluice, the water is pumped out, the pontoons with the caisson lies on the bottom and the pontoons are ballasted. Then water is let in the sluice and the caisson floats and can be towed to the location of immersion.



Figure 2-22 - Construction phase FLOATGEN foundation (Floatgen.eu)

### 2.4.2.7 Factory with double dock

For some large projects where a large number of caissons are needed a special factory could be built. A specially built factory often is applied with the use of one or two basins. In the factory the caissons are constructed and with one or two basins the caisson is transported into deeper water. In Figure 2-23 a factory is displayed what will be used for the construction of the tunnel elements for the Fehmarnbelttunnel. In this figure the presence of the two basins are shown, the upper basin is controlled by the sliding gate and the lower one with a floating gate.

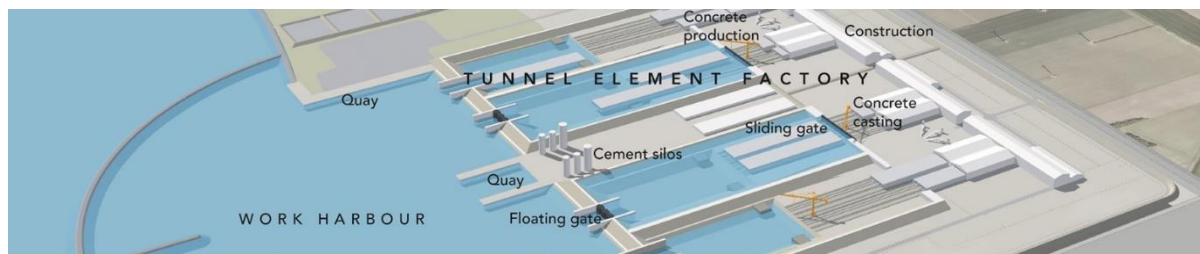


Figure 2-23 - Tunnel Element Factory for Fehmarnbelttunnel (femern.com)

### 2.4.2.8 Casting basin

As last transportation method the casting basin method is described. A casting basin is displayed in Figure 2-24. A casting basin is a basin where construction activities in the dry are possible on a height which is lower than the surrounding water level. When the tunnel segments are constructed, the dike is removed and water flows in the casting basin. The tunnel segments float and can be towed to its final location.



Figure 2-24 - Casting basin Barendrecht (beeldbank.rws.nl)

## 2.5 CONSTRUCTION LOCATION

After describing the construction methods and transportation methods one important choice must be made. The construction of caissons can be performed in two ways, at a fixed location or on a production line. The production of caissons at a fixed location or in production line depends on the construction and transportation method. One important parameter is the available space on the construction area.

### 2.5.1 Fixed location

All construction actions are executed with the caisson on a fixed location. When the caisson is fully constructed it is transported to the quay wall where it is transported into the water. This method is often applied when the construction takes place at a dry dock, casting basin, floating dock or on pontoons.

### 2.5.2 Production line

The construction of the caissons is executed in a serial production. On location 1 the first part of the element is constructed, on location 2 the next part, etcetera. With this type of construction the locations can be optimized for the execution of that specific construction action. The production time decreases but the amount of required space presumably increases. This method could be applied when the construction takes place in a factory or on a quay wall where the transportation from land into water is executed by a syncrolift, semi-submersible vessel or heavy lift vessel.

## 2.6 DECISION MATRIX

The most complex construction action is the transportation of the caisson from the dry into the wet. In a previous study, included in Annex A, the applicability of transportation methods from land into water for caissons is studied. By studying reference projects where caissons are constructed and immersed some project characteristics are determined. The project characteristics are:

- Horizontal dimensions
- Draught
- Weight
- Number of elements
- Level of existing infrastructure

The most common construction methods to build large caisson and transport them into deep water are displayed in the first column of Table 2-1. In Annex A, the positive and negative elements of each construction method are described, also the range of possibilities is given with data of key factors of certain construction methods.

Construction method	Dimensions up to Length x Width [m x m]			Draught of element [m]			Weight [ton]			Number of elements			Level of existing infrastructure		Casting independent on weather conditions
	<50x50	50x50 - 150x75	>150x75	<5	5-10	>10	<5,000	5,000-15,000	>15,000	<10	10-20	>20	Little	High	
Factory	✓	✓	✓	✓	☐	✗	✓	✓	✓	✗	✗	✓	✗	✓	+
Casting basin	✓	✓	✓	✓	☐	✗	✓	✓	✓	✓	✗	✗	✗	✓	-
Syncrolift	✓	✓	☐	✓	☐	✗	✓	✓	✓	✗	✓	✓	✓	✓	-
Semi-submersible vessel	✓	✓	✓	✓	✓	☐	✓	✓	✓	✓	✓	✓	✓	✓	-
Dry dock	✓	✓	✓	✓	☐	✗	✓	✓	✓	✓	✓	✗	✗	✓	-
Floating dock	✓	☐	✗	✓	✓	☐	✓	✓	✓	✓	✓	✗	✓	✓	-
Building on pontoons	✓	☐	✗	☐ <sup>(1)</sup>	☐ <sup>(1)</sup>	☐ <sup>(1)</sup>	✓	✓	✓	✓	✗	✗	✓	✓	-
Land based crane	✓	✗	✗	✓	✓	✓	✓	✗	✗	✓	✓	✓	✓	✓	-
Heavy lift vessel	✓	☐	✗	✓	✓	✓	✓	☐	✗	✓	✓	✗	✓	✓	-

(1): Depends on available dimensions of sluices in the proximity

Table 2-1 - Decision matrix

The result is a decision matrix that gives an overview of the construction methods including the applicability of some important project characteristics. This overview is based on reference projects with different caisson functions and properties. Applying a project where large caissons have to be constructed and transported into deeper water a first overview of applicable construction methods are given by using some project characteristics.

## 2.7 GRAVITY BASED FOUNDATIONS

In the field of caisson construction a new type of caissons arises the last years: The GBF for offshore wind farms. These GBFs now are only produced in low numbers for some test locations and often a dry dock or a semi-submersible vessel to transport them from land into the water is used. The use of a dry dock is caused by the low number of caissons. The semi-submersible vessel is applicable but the renting costs for this vessel are quite high. When the number of GBFs for offshore wind is scaled up to commercial scale a new type of project comes to the market and a new solution could be developed which is profitable comparing the semi-submersible vessel.

In the next chapter a short history of wind energy development and the main characteristics of the foundations types are given.

## 2.8 CONCLUSION CONSTRUCTION AND TRANSPORTATION METHODS

There are a lot of construction and transportation methods to construct caissons and transport caissons from land into water. The construction generally takes place in the dry and the fully constructed caisson is transported from the dry into the wet. The most important project parameters which decide what transportation method is applicable are:

- Dimensions of caisson
- Draught
- Weight
- Number of caissons
- Level of existing infrastructure

With these project parameters a first indication of which construction and transportation methods are feasible is given in the decision matrix. Because each project have an identical set of boundary conditions and project characteristics certain exceptions are possible.

## Chapter 3: SHORT HISTORY OF WIND ENERGY DEVELOPMENT

As introduction to the construction of GBFs a short history of the development of wind energy is given. First a short history about the first wind turbines is given where after the upscaling of the wind turbines is described. Then the transition from onshore to offshore wind energy production is considered. At last the major difference between the onshore and offshore foundations are treated.

### 3.1 FIRST ELECTRICITY PRODUCING WIND TURBINE

The first wind turbine which converts wind energy into electricity was the wind turbine built by Professor James Blyth in 1887 (theguardian.com, 2008). A half year later Professor Charles Brush built a wind turbine with a rotor diameter of 17 meter producing a maximum power of 12 kW. With the produced electricity he charged 408 batteries to store the energy to use in his mansion (cleantechnica.com, 2014). This windmill has produced for 20 years electricity for his mansion. The wind turbines of Blyth and Brush are both displayed in Figure 3-1. Poul la Cour, a Danish scientist found out that a vertical wind turbine with fewer blades is more efficient (drømstørre.dk, 2003). Two of his wind turbines in 1897 are given in Figure 3-2.

The next step in the history of the wind turbine was the step to the modern wind turbine design. During the Second World War the Danish engineering company F.L. Schmidt built two and three rotor blades wind turbines (drømstørre.dk, 2003).

After the Second World War the progress of the wind turbine development was quite low due to low oil and gas prices. After the oil crises in 1973 the political opinion changes and the development of wind turbines increased (windenergyfoundation.org). The modern wind turbine is displayed in Figure 3-4. After this type of wind turbine has been developed no major changes are executed on the design. Only the efficiency is improved and the dimensions are scaled up.

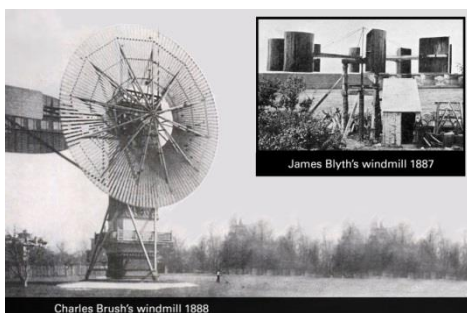


Figure 3-1 - Wind turbines from Blyth and Brush (energyclassroom.com, 2004)



Figure 3-2 - Two test turbines from Poul la Cour (drømstørre.dk, 2003)



Figure 3-3 - Wind turbines built by F.L. Schmidt (drømstørre.dk, 2003)



Figure 3-4 - Modern wind turbine (mwps.world, 2015)

The turbines are scaled up from 12 kilowatt for the first wind turbine until several megawatts nowadays. The largest installed wind turbine has a capacity of 9.5 megawatt and plans are to construct wind turbines of 12 megawatt (genewsroom.com, 2018). The upscaling of wind turbine dimensions in time is displayed in Figure 3-5.

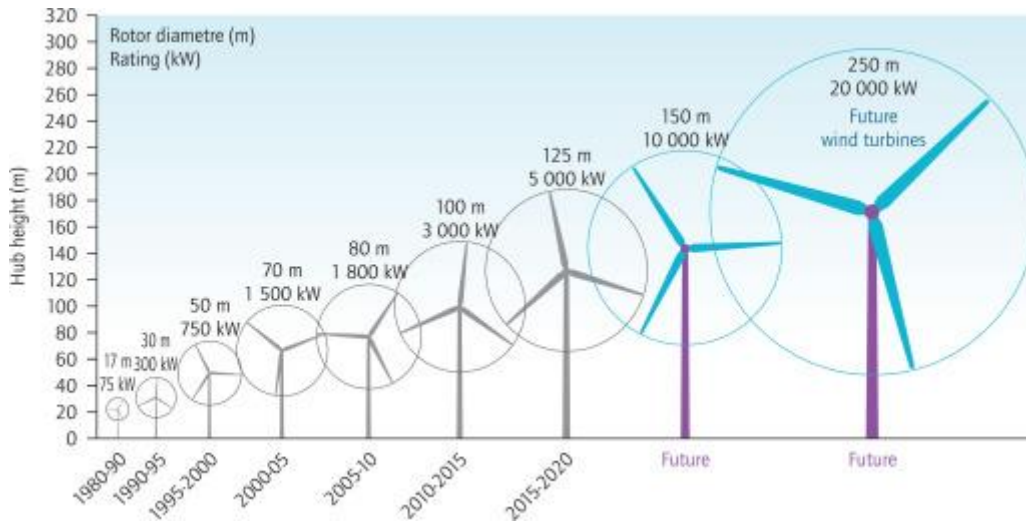


Figure 3-5 - Upscaling of wind turbine capacity (sciencedirect.com)

### 3.2 FROM ONSHORE TO OFFSHORE

Most people want green energy because it is better for the environment than energy produced with coal and gas. But when a wind farm is planned to be built in sight the public opinion, in general, is negative. This is a classic example of the “not in my backyard” principle: the majority is positive about wind energy but few people would deal with the consequences like the turbines at their view or at the horizon. With the upscaling as displayed in Figure 3-5 the public debate will be more active. A solution to this debate is to install wind turbines at the sea. Then the wind turbines have no negative impact to the value of the landscape where people live. An important positive side effect is the higher wind velocities offshore. The energy production of a wind turbine is given by:

$$P = \frac{1}{2} \cdot \rho_a \cdot A \cdot C_b \cdot v_a^3 \quad (2)$$

Where:

$$\begin{aligned} P &= \text{Power production [W]} \\ \rho_a &= \text{Mass density air [kg/m}^3\text{]} \\ A &= \text{Circular area blades [m}^2\text{]} \\ C_b &= \text{Betz optimum [-]} \\ v_a &= \text{Wind velocity [m/s]} \end{aligned}$$

The area is given by the formula:

$$A = \frac{1}{4} \pi D_w^2 \quad (3)$$

Where:

$$D_w = \text{Diameter wind energy area [m]}$$

With the use of formulas 2 and 3 it can be seen that the energy production  $P \propto D_w^2 \cdot v_a^3$ . The offshore conditions with a higher wind velocity and the increase of the diameter generates a lot more energy and could be more attractive than projects onshore if the higher construction costs are compensated with the extra energy production. The number of wind turbines per wind farm and the capacity of the turbines of constructed offshore wind farms are shown in Figure 3-6.

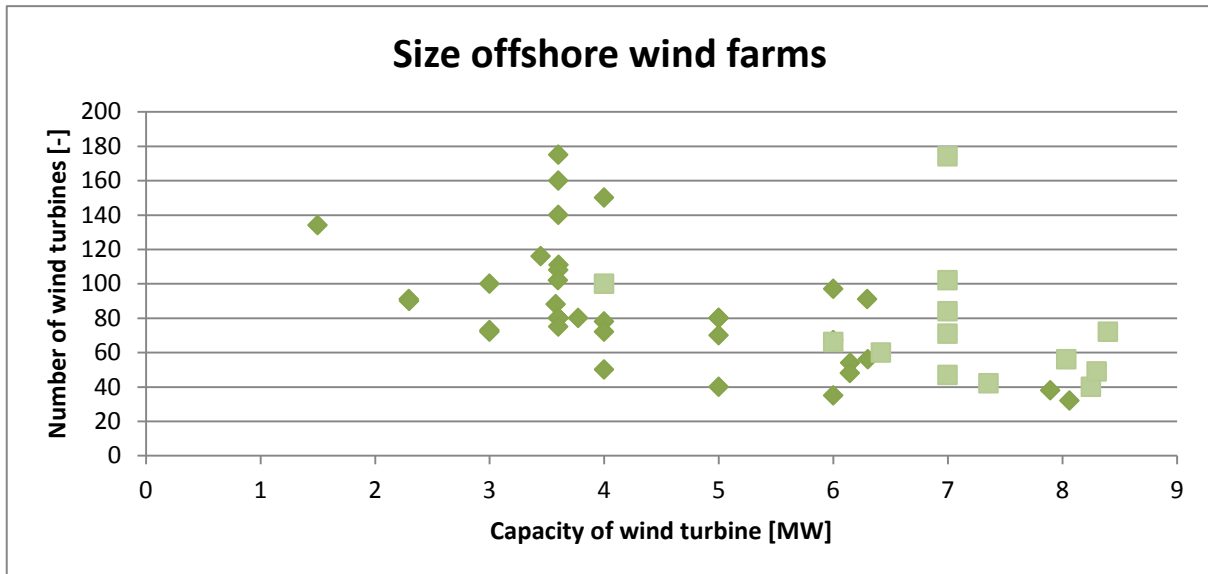


Figure 3-6 - Size of constructed and under construction offshore wind farm (rectangular= under construction)

### 3.3 OFFSHORE WIND TURBINE FOUNDATIONS

The main difference between onshore and offshore wind turbines is the foundation. Onshore wind turbines are founded on pile foundations or on a large concrete raft foundation, see Figure 3-7. The dimensions of the foundations depend on the soil characteristics at the project location and the installed capacity and characteristics of the wind turbine.



Figure 3-7 - Foundation onshore wind turbine (cte-wind.com)

The offshore wind turbine foundations are more complex and have more characteristics that have to be met:

- Depth of water
- Water flow velocity
- Wave conditions

The most important characteristic to choose the foundation type is the water depth. In Figure 3-8 different types of foundations are given that could be applied for offshore wind turbines. At very large water depths floating foundations are applied. For smaller water depths the use of monopiles, jacket and gravity based foundations are applied. The different types of foundations for shallow water are given in Figure 3-8 and Figure 3-9.



Figure 3-8 - Different types of offshore wind turbine foundations (energy.gov, 2017)

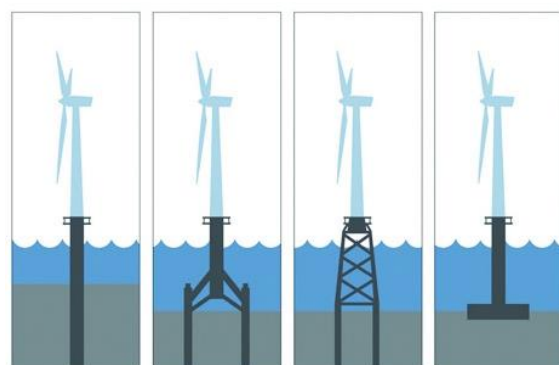


Figure 3-9 - Main types of offshore wind foundations (theengineer.co.uk, 2012)

GBFs can be applied for all water depths but there are four main types of construction and transportation. These four methods are given in Figure 3-10. In this figure also the applicability of the different foundation types are given with respect to the installed depth. The abbreviations in Figure 3-10 mean:

- L-FO: Lifted-Foundation
- L-IT: Lifted + Integrated Transport
- F-FO: Floated + Foundation only
- F-IT: Floated + Integrated Transport

Integrated transport means that the wind turbine is installed on the gravity based foundation before immersion. For shallower depth up to a meter of 30 the GBF can be lifted but when the depths are larger the foundations are too heavy to lift. Then other transportation methods are needed. As it can be seen in Figure 3-10 the GBF has the advantage that it can be applicable to larger water depths than other foundation types.

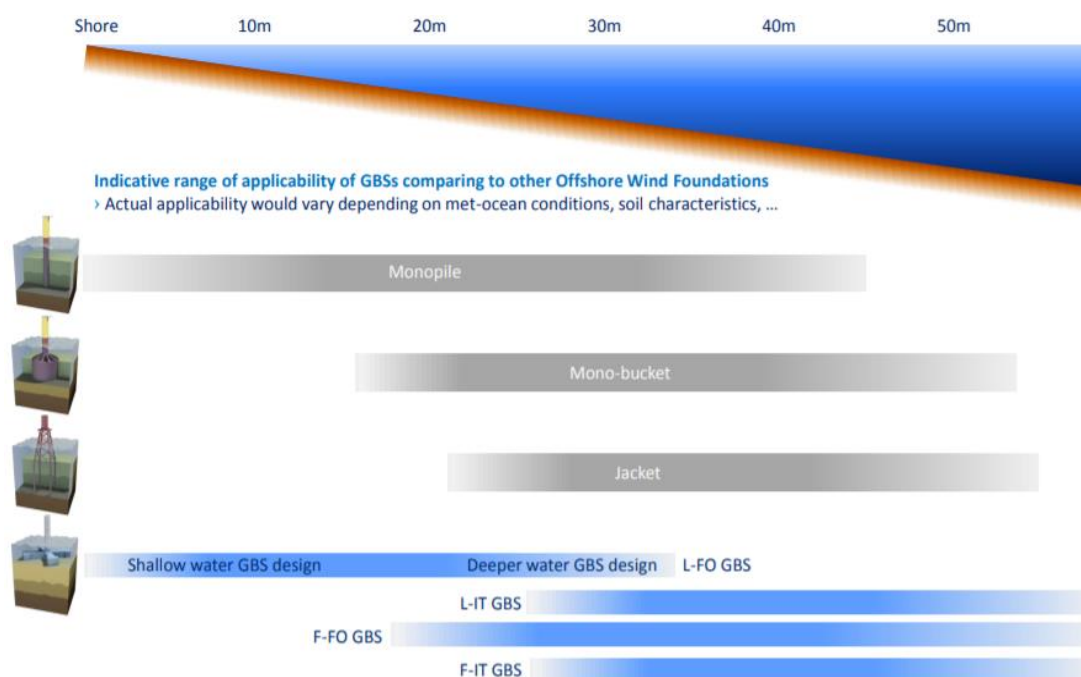


Figure 3-10 - Applicability per foundation type as function of water depth (carbontrust.com, 2015)

The main property of a GBF is the large weight. Therefore a GBF is mainly constructed of reinforced concrete and steel elements, both with a high volumetric weight. The main characteristic of a gravity based foundation is the large weight and the low centre of gravity. The stability of the wind turbine is created with the dead weight and the large diameter of the foundation. Some examples of gravity based foundations are given in Figure 3-11 till Figure 3-14.

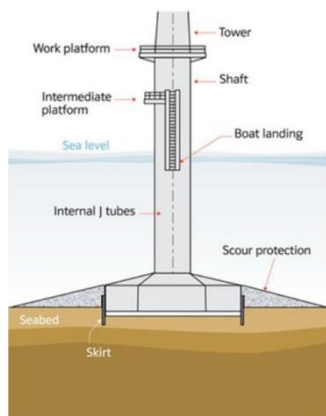


Figure 3-11 - Characteristics of a GBF (4coffshore.com, 2013)



Figure 3-12 - Fécamp GBF (4coffshore.com, 2013)



Figure 3-13 - Strabag GBF (slideshare.net, 2012)

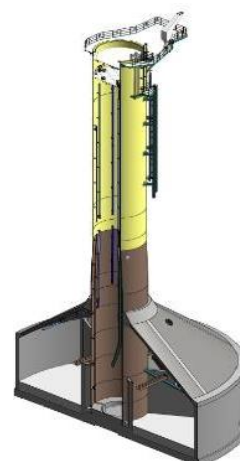


Figure 3-14 - Blyth GBF (strukton.nl, 2016)

The major part, 78.8% in 2015, of existing offshore wind turbines are founded with a monopile foundation, against 10.4% that is founded with gravity based foundations (carbontrust.com, 2015). The major disadvantage of monopiles is the restriction in size by buckling and therefore larger monopiles, in length and diameter requires a lot of steel which increases the weight and the cost. Also the transportation of monopiles is challenging because it is a single piece to transport and the dimensions of the largest monopiles now have a length of 84.4 metre with a diameter of 7.8 meter and a weight of around 1300 tons (Boskalis.com). Another disadvantage is the hammering process to hammer the foundation into the seabed. This causes a lot of noise and vibrations which is not good for the environmental life in the sea and at the seabed.

The trend for offshore wind is that offshore wind farms will be developed in deeper waters. The question is till what depth the monopiles could be profitable comparing to other foundation types like the GBF. In the case where hard ground conditions are present, like rock or overconsolidated clays the hammering process could be challenging or even impossible. Then the GBF could be a good alternative. At sand bottoms GBF have to compete with monopiles and other foundations and the most cost-efficient solution is chosen.

### 3.4 CONCLUSION HISTORY OF WIND INDUSTRY

The development in the wind energy industry is large. The scale of wind turbines increased rapidly and an important transition from onshore wind energy to offshore wind energy is made. The most important difference between onshore and offshore wind turbines is the type of foundation. For offshore wind turbines several foundation types are available depending on the water depth. A relatively new type of foundation is the gravity based foundation. This foundation ensures stability for the wind turbine due to the large weight. The advantages of these foundations are the applicability at larger water depths and that no piling activities are needed.

## Chapter 4: CASE DESCRIPTION

To develop a new construction and transportation method for a large number of GBFs for a windfarm on commercial scale a specific case is developed. First a reference case where GBFs are used is given: the C-Power project on the Thornton Bank. Then a new realistic hypothetical case study is described where a new construction and transportation method could be used for. For the case study the boundary conditions are given which are important to develop an optimal construction and transportation method. In this chapter the first design part is executed, indicated in blue in Figure 4-1.

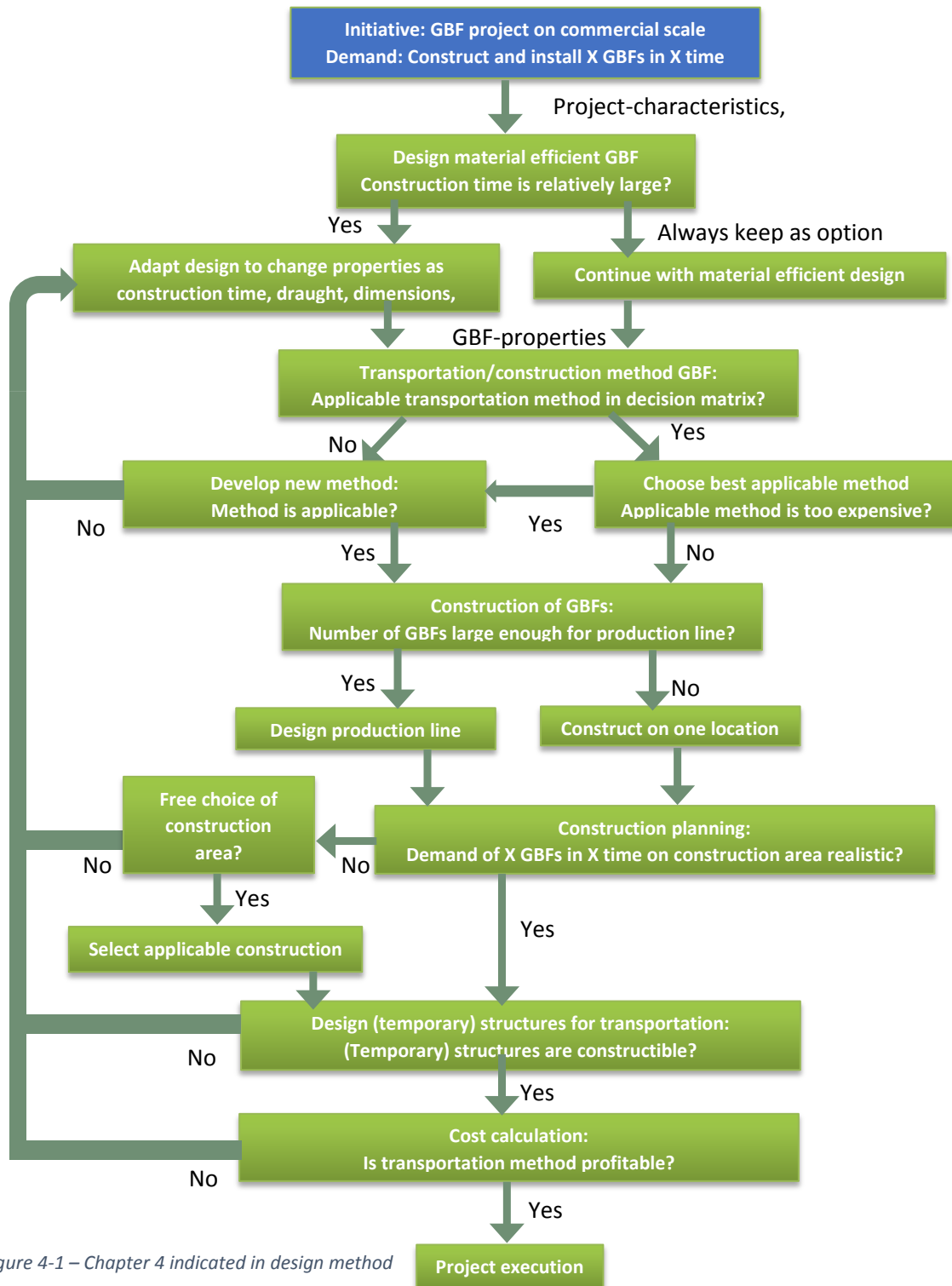


Figure 4-1 – Chapter 4 indicated in design method

## 4.1 REFERENCE CASE: C-POWER PROJECT ON THE THORNTON BANK

In this paragraph the reference case is described. First the project characteristics are described. The project location and the construction area are described and at last the environmental conditions like wave heights, water levels, soil conditions and weather conditions are given.

### 4.1.1 Project characteristics

C-Power is the first Belgium offshore wind farm. It consists of 54 wind turbines with a total capacity of 325.20 MW (c-power.be). The project is carried out in three phases. The characteristics of these three projects are given for each phase:

- Phase I: 6 wind turbines, founded with GBFs, with a capacity of 5 MW each.
- Phase II: 30 wind turbines, founded with jacket foundations, with a capacity of 6.15 MW each.
- Phase III: 18 wind turbines, founded with jacket foundations, with a capacity of 6.15 MW each.

The planning of these phases is given in Figure 4-2. The first phase started in 2008 and was finished halfway 2009. The construction of phases 2 and 3 has started after phase one was completely delivered and operational.

	2002	2003	2004	2005	2006	2007	2008	2009	2010	2011	2012	2013	2014	...
<b>Phase 1</b>	Permits & Engineering					Construction		Operation						
<b>Phase 2</b>							Permits & Engineering		Construction		Operation			
<b>Phase 3</b>							Permits & Engineering			Construction		Operation		

Figure 4-2 - Planning C-Power offshore wind farm (c-power.be)

#### 4.1.1.1 Project location

The C-Power wind farm is located in the North-Sea, northwest from the Belgium coast. The distance from the Belgian coast to the C-Power wind farm is 28.7 kilometer and the cable length is 35 kilometer (c-power.be). The location of the windfarm on the Thornton bank is displayed in Figure 4-3. The wind turbines, with the height dimensions are given in Figure 4-4.

In Figure 4-5 the layout of the C-Power wind farm is given. The construction phases are indicated with different colors. Phase I is indicated with yellow, phase II with blue and phase III with red. As can be seen, the foundation type is drawn in the figure: the yellow wind turbines of phase I have GBF foundations, the other have jacket foundations. Because of the GBFs the focus is on the first phase of the C-Power wind farm.



Figure 4-3 - Belgium offshore wind farm locations (otary.be)

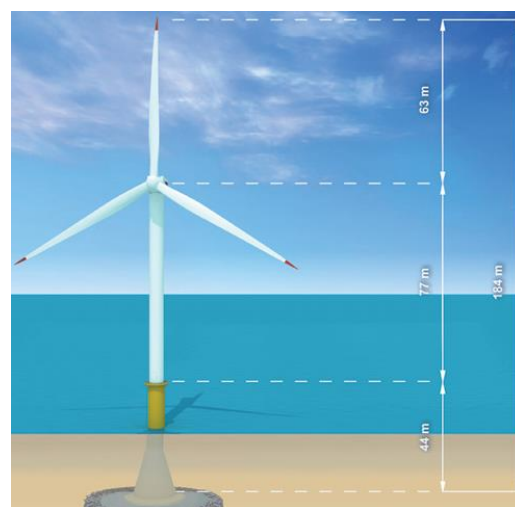


Figure 4-4 - Wind turbine Thornton bank phase I

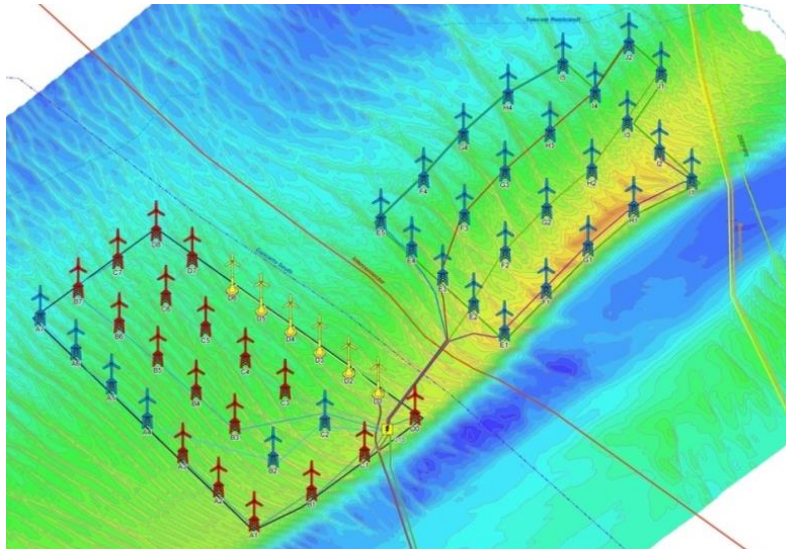


Figure 4-5 - Layout of C-Power wind farm (c-power.be)

#### 4.1.1.2 Construction area

The construction of the GBFs took place in the Port of Oostende, Belgium. Two construction areas are used to construct the GBFs and install the wind turbine parts. In this paragraph the construction areas are described. In the construction of the Thornton Bank wind farm phase I, two construction areas are used:

1. The so-called REBO Offshore site where the parts of the wind turbines are delivered and where vessels can berth.
2. A construction area, Halve Maan that is specially developed for the construction of the GBFs.

These two construction areas are described and in 0 a photo reportage of the construction of the GBFs included. The construction area of the GBFs is located in the black circle in Figure 4-6. In Figure 4-7 a closer look is given to that construction area, called “Halve Maan”.

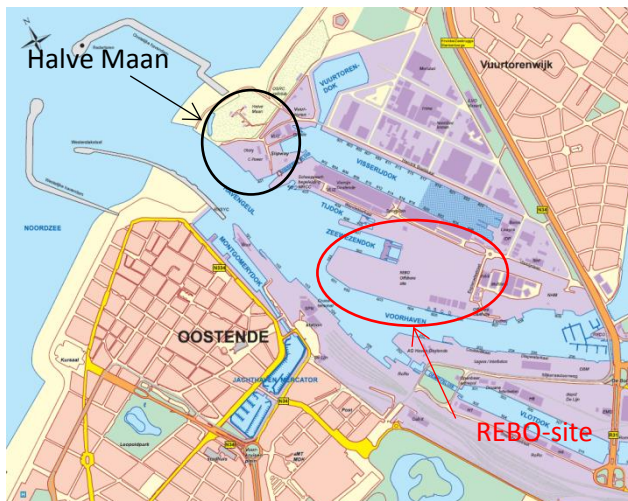


Figure 4-6 - Port of Oostende

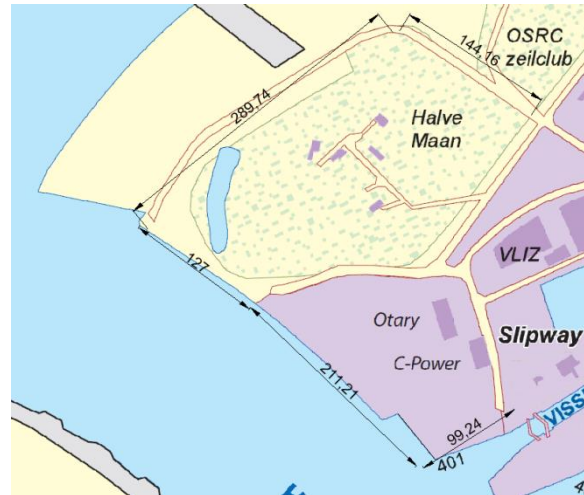


Figure 4-7 - Halve Maan and C-Power location with dimensions

At this area the construction works of the GBFs were performed. The GBFs are casted on platforms some meters above the surface. When the GBFs were ready several SPMTs drove under the GBFs and the GBFs are placed on the SPMTs. The GBFs are transported to the water and the vessel Rambiz lifted the 3000 ton heavy foundations from the quay wall partly into the water, to reduce the lifting weight. In Figure 4-9 it is shown how the GBFs are lifted from the quay wall into the water with the use of the heavy lift vessel Rambiz.

The delivery and lifting operations of the wind turbine parts took also place in the port of Oostende. The lifting operations are executed on a specific storage area of the Renewable Energy Base Oostende terminal (REBO). REBO is a company with some private and public shareholders. Deme owns 30% of the shares and the other shares are from Artes, Port Oostende and PMV. This construction area is described in paragraph 4.2.1 because this area is used to construct the GBFs from the case study.

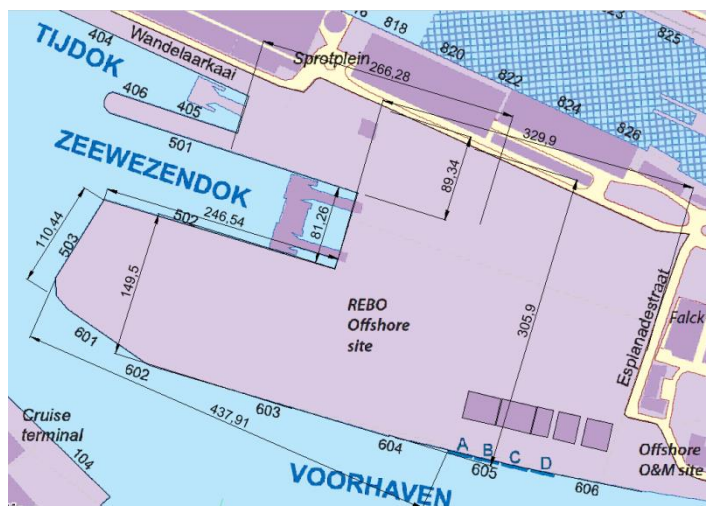


Figure 4-8 - REBO Offshore Site with dimensions



Figure 4-9 - Lifting operation of GBF from the quay wall into the water (c-power.be)

## 4.2 CASE STUDY: SEASTAR AND MERMAID OFFSHORE WIND FARMS

To develop a new construction and transportation method a case study is described. Two offshore wind farm locations are chosen where the wind turbines will be founded with GBFs. These locations are located in the Belgium part of the North Sea.

The Belgium government has set a target to produce more green energy. The target for the energy capacity of offshore wind is to increase the capacity from 877 MW in April 2018 (beginoffshoreplatform.be) to 2200 MW in 2020 and to 4000 MW in 2030 (belgianoffshoreplatform.be, 2017). The plans for the offshore wind farms to reach a total capacity of 4000 MW are displayed in Figure 4-3. The windfarms Seastar and Mermaid still have to be developed and constructed, see Figure 4-3 for the locations. The capacities of the wind farms are 246 MW and 266 MW. The water depth at the Mermaid wind farm location varies from 30 till 35 meter depth and at the Seastar location from 25-30 meter depth. A bathymetry map of the location of the Mermaid and Seastar wind farms are given in Figure A-22 and Figure A-23 in Annex D, at page 168.

The depth of the Mermaid wind farm is the largest and therefore the case study is performed on the foundation type for this location. These one have the larger dimensions and the larger weight. For the number of GBFs it is decided to choose to construct both wind farms with GBFs. The proposed wind farms have a total capacity of 512 MW and with a capacity of 8 MW per wind turbine 64 wind turbines are needed

### 4.2.1 Construction area

The construction of the GBF will take place on the same location as in the reference case: On the REBO Offshore Site and/or on the "Halve Maan". The construction areas with some dimensions are given in Figure 4-7 and Figure 4-8.

The REBO terminal is a terminal with quay walls and storage areas with a high bearing capacity. The most important characteristics are:

- 90 hectares on 5 sites.
- 800 meter of adapted heavy quays with a capacity from 4 till 20 ton/m<sup>2</sup>.
- Storage areas with a capacity of 10 ton/m<sup>2</sup>.

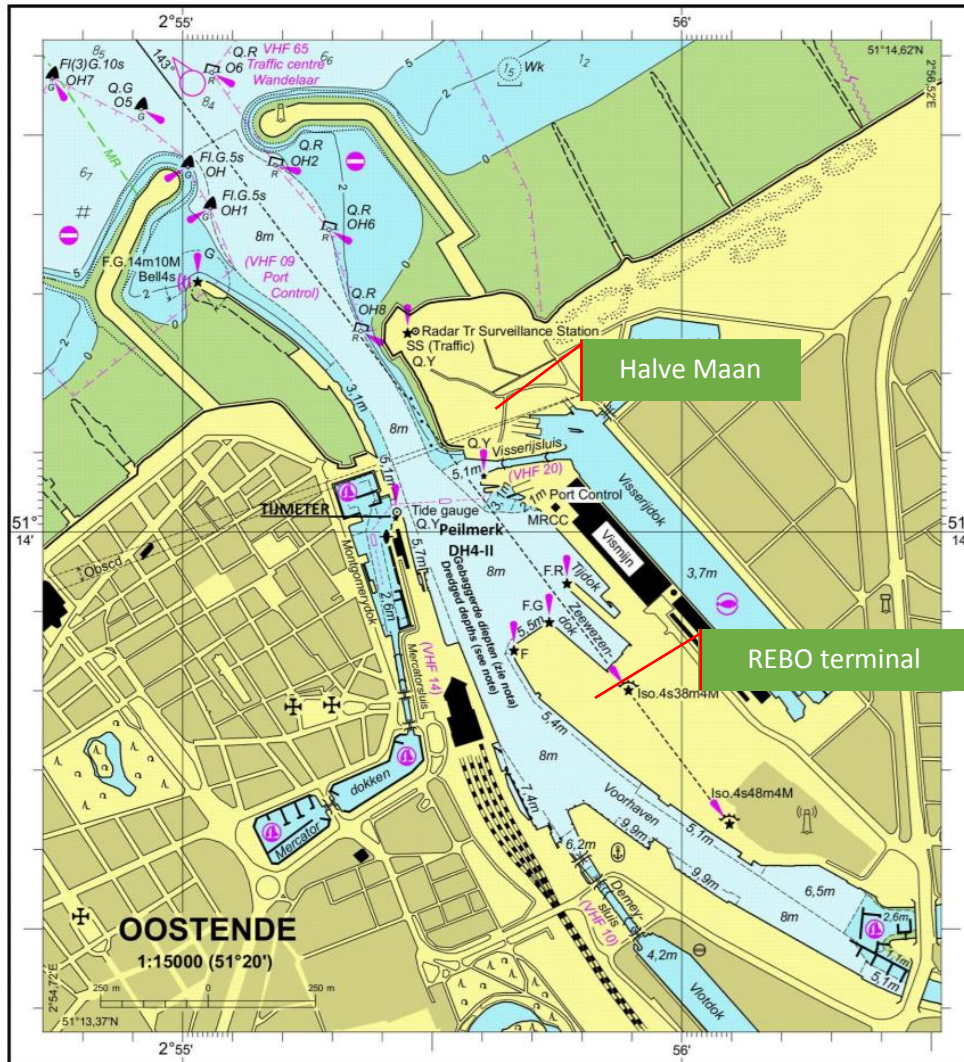


Figure 4-10 - Port of Oostende map with guaranteed depth

- Minimal guaranteed available depth of 8 meter in front of quay wall.

A part of the port of Oostende is displayed in Figure 4-6. With a red oval the REBO offshore site is indicated and in Figure 4-8 a closer look to the REBO offshore site is given.

The properties of the quay walls are given in Table 4-1.

Berth	501	502	503	603-604
Depth [m]	8	8	7	5
Berth length [m]	200	180	110	200
Strengthened seabed in front of quay	No	No	Yes	No

Table 4-1 - Properties REBO Offshore site quay walls

The available depth in front of the quay walls and in the port channels is an important parameter for the transportation of the caissons. The available depths must be larger than the draught of the caisson. The minimum guaranteed depth of the main channel in the Port of Oostende is 8 meter, see Figure 4-10. The guaranteed depth given by the Port of Oostende is relative to the Lowest Astronomical Tide (LAT). In Annex E two detailed bathymetry maps at the quay walls at the Halve Maan and the REBO Offshore Site are included.

#### 4.2.1.1 Soil conditions

The soil conditions at the two construction areas are consulted from the Belgian Government (dov.vlaanderen.be). In Annex F two CPTs are included and from these CPTs two sand layers are indicated. For foundation purposes for eventual (temporary) structures to fulfil the transportation operations these sand layers are important to create sufficient bearing capacity.

Location	Sand layer 1 [m TAW]	Sand layer 2 [m TAW]
Halve Maan	-7 till -11	From -15
REBO Offshore Site	-10 till -11	From -17

Table 4-2 - Sand layers at REBO Offshore Site and Halve Maan

#### 4.2.1.2 Environmental conditions

The environmental conditions are given with respect to water levels, waves and wind. First the water levels are described and thereafter the waves and wind data is described.

##### 4.2.1.2.1 Water level in port of Oostende

The water levels of the tides for high water and low water of the period 2001-2010 are given in Figure 4-11 and Figure 4-12. The water levels at the port of Oostende are given relative to TAW, the meaning of TAW is "Tweede Algemene Waterpassing". TAW is a reference height used in Belgium. The height of the REBO offshore terminal is 6.80 TAW and 7.3m LAT. The data of Figure 4-11 and Figure 4-12 is converted to a Cumulative Density Function (CDF) in the LAT reference system and this result in graphs displayed in Figure 4-13 and Figure 4-14.

TAW cm	HW										Totaal 10 jaren	%
	2001	2002	2003	2004	2005	2006	2007	2008	2009	2010		
<-300	0	1	1	1	0	0	0	0	2	1	6	0,09
300 - 309	0	0	1	3	1	0	0	1	0	1	7	0,10
310 - 319	0	0	0	5	0	0	1	0	2	1	9	0,13
320 - 329	1	3	4	5	4	5	2	6	3	2	35	0,50
330 - 339	4	6	4	5	9	5	7	10	8	2	60	0,85
340 - 349	4	8	8	9	13	11	8	7	7	4	79	1,12
350 - 359	7	14	13	15	14	15	15	15	12	12	132	1,87
360 - 369	19	18	19	17	19	18	20	15	15	24	184	2,61
370 - 379	24	25	30	29	39	43	31	24	26	35	306	4,34
380 - 389	46	33	40	25	35	36	24	36	37	33	345	4,89
390 - 399	44	39	54	43	48	36	40	35	46	35	420	5,95
400 - 409	40	39	47	64	51	62	43	55	47	50	498	7,06
410 - 419	46	56	56	44	53	45	47	50	70	49	516	7,31
420 - 429	65	62	43	49	64	68	47	53	56	39	546	7,74
430 - 439	61	67	55	71	70	66	69	57	67	56	639	9,05
440 - 449	58	90	63	65	59	73	70	69	59	54	660	9,35
450 - 459	72	76	76	56	59	46	66	69	62	70	652	9,24
460 - 469	79	59	51	65	61	53	65	49	60	71	613	8,69
470 - 479	50	37	55	60	37	46	34	58	53	46	476	6,75
480 - 489	37	24	40	36	23	27	52	51	33	36	359	5,09
490 - 499	15	22	24	24	20	13	22	21	23	32	216	3,06
500 - 509	15	19	11	6	9	22	15	8	10	31	146	2,07
510 - 519	12	3	6	3	5	10	13	10	6	14	82	1,16
520 - 529	5	3	1	3	6	3	4	5	0	4	34	0,48
530 - 539	0	1	2	3	4	2	3	2	0	3	20	0,28
540 - 549	1	1	1	0	2	1	2	0	0	0	8	0,11
550 - 559	0	0	0	0	0	0	2	1	0	1	4	0,06
560 - 569	0	0	0	0	0	0	0	0	1	0	1	0,01
>569	0	0	0	1	0	0	3	0	0	0	4	0,06
TOTAAL	705	706	705	707	705	706	705	707	705	706	7057	100

Figure 4-11 - Frequencies of High Water levels

TAW cm	LW										Totaal 10 jaren	%
	2001	2002	2003	2004	2005	2006	2007	2008	2009	2010		
<-70	1	0	0	0	0	0	0	1	0	0	2	0,03
-70 - -61	0	0	0	0	0	0	0	1	0	0	1	0,01
-60 - -51	1	3	0	0	2	1	0	1	1	1	10	0,14
-50 - -41	2	1	3	0	2	5	1	1	2	3	20	0,28
-40 - -31	3	10	10	9	7	11	7	5	6	3	67	0,95
-30 - -21	12	18	10	8	13	11	16	14	14	18	130	1,84
-20 - -11	24	20	23	20	21	16	21	20	24	13	202	2,86
-10 - -1	37	29	31	39	36	34	27	26	31	24	314	4,45
0 - 9	45	45	45	36	38	47	34	54	43	55	442	6,26
10 - 19	52	50	60	51	55	57	58	44	51	79	557	7,89
20 - 29	84	71	60	83	76	61	72	59	76	53	695	9,85
30 - 39	68	84	80	70	62	75	62	74	82	77	734	10,40
40 - 49	43	70	72	65	67	72	71	71	61	79	671	9,51
50 - 59	76	66	70	72	62	58	49	68	62	65	648	9,18
60 - 69	79	56	48	43	62	61	61	53	59	60	582	8,25
70 - 79	35	53	46	40	52	52	49	51	49	479	6,79	
80 - 89	42	34	35	50	42	40	51	44	40	46	424	6,01
90 - 99	34	33	32	40	36	28	32	42	34	31	342	4,85
100 - 109	18	19	25	35	24	23	34	19	21	19	237	3,36
110 - 119	13	18	21	24	14	19	27	20	18	12	186	2,64
120 - 129	15	10	10	9	14	15	9	18	14	6	120	1,70
130 - 139	9	4	9	8	7	4	9	8	7	4	69	0,98
140 - 149	5	6	5	4	3	7	1	6	1	4	42	0,60
150 - 159	1	0	4	1	4	3	2	3	3	2	23	0,33
160 - 169	2	2	5	3	0	0	4	1	2	3	22	0,31
170 - 179	1	2	1	0	0	3	2	1	2	0	12	0,17
180 - 189	2	1	0	2	3	0	0	1	0	0	9	0,13
190 - 199	0	0	0	0	2	1	0	0	0	0	3	0,04
>199	1	2	0	0	1	1	3	4	0	1	13	0,18
TOTAAL	705	705	705	708	705	705	705	708	705	705	7056	100

Figure 4-12 - Frequencies of Low Water tides (afdelingkust.be)

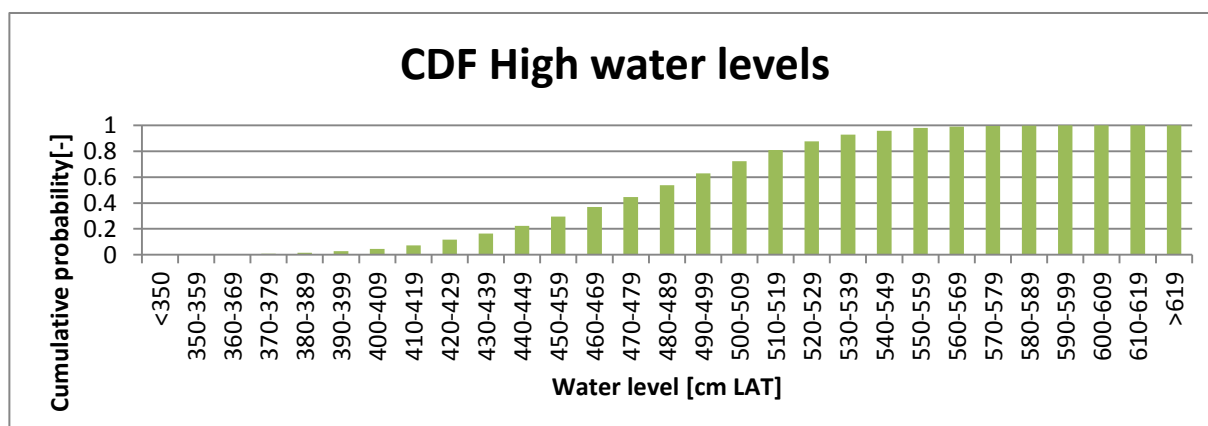


Figure 4-13 - Cumulative density function of high water levels at Port of Oostende

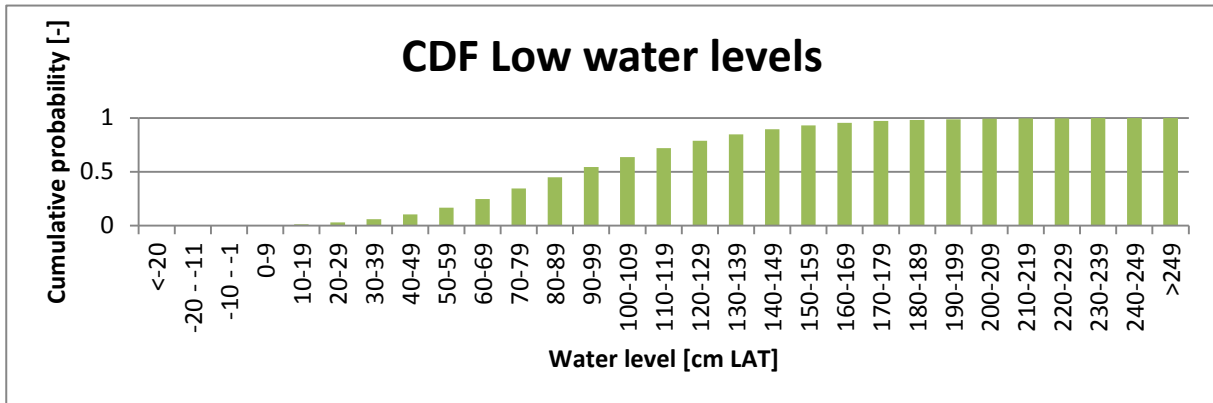


Figure 4-14 - Cumulative density function low waters at Port of Oostende

#### 4.2.1.2.2 Weather conditions

The weather conditions at the port of Oostende are presented in this paragraph. The main weather characteristics are displayed in Figure 4-15. In the legend the precipitation, temperatures and wind speeds are given. An important parameter is the temperature for casting concrete. When the maximum temperature is exceeding the 4 degrees Celsius and at night the temperature is below zero degrees measures are needed to

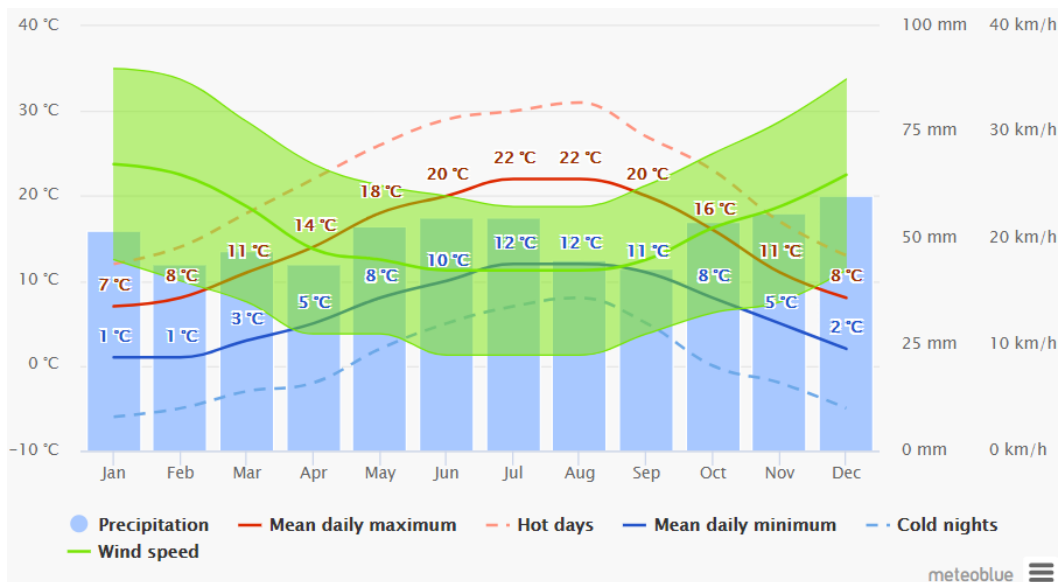


Figure 4-15 - Weather characteristics at Oostende (meteoblue.com)

cast concrete, as described in the NEN 6722 norm (betoncentrale.nl). In Figure 4-17 the maximum temperatures are given at Oostende. On average there are 21.4 days per year when concrete could not be casted. Excluding the weekends this result in 15 working days per year. Measures could be taken to isolate fresh concrete, and then the non-working days could be decreased, otherwise casting activities cannot go on and delay is inevitably.

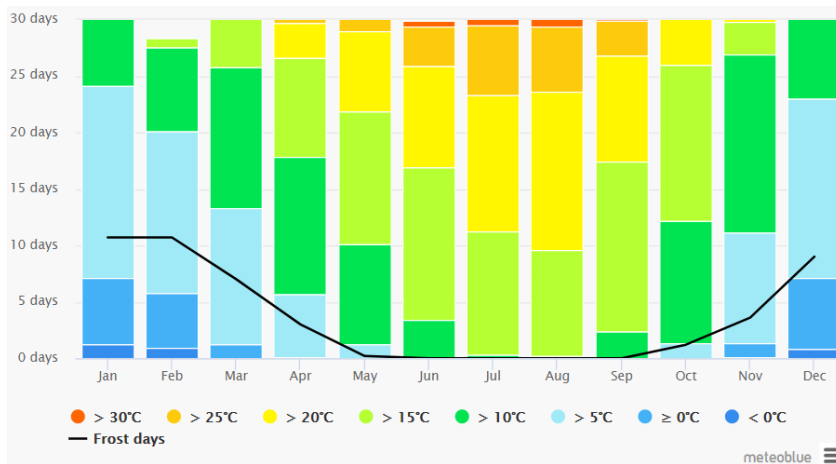


Figure 4-17 - Maximum temperatures at Oostende (meteoblue.com)

The wind directions and wind speeds are displayed in Figure 4-16. The main wind direction is from the Southwest. The main channel of the port of Oostende is in the northwest direction and this is positive for the wave climate.

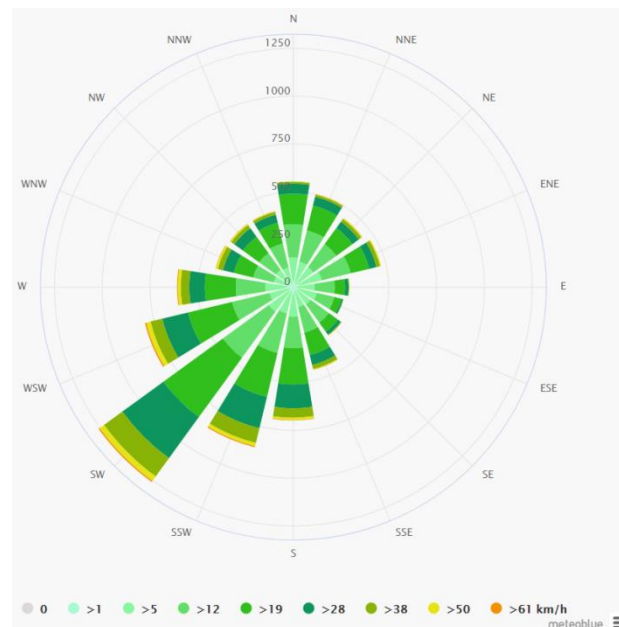


Figure 4-16 - Wind rose at Oostende (meteoblue.com)

#### 4.2.1.2.3 Wave conditions

The wave conditions at the Mermaid offshore wind farm location and at the port entrance are presented Table 4-3. The data from which the results are derived are described and displayed with three figures for each location in Annex H:

- Probability density function of wave heights with significant wave height
- Cumulative density function of wave heights
- Wave spectrum with the derived peak period

Location	Significant wave height [m]	Peak period [s]
<b>Mermaid</b>	2.10	7.5
<b>Port entrance</b>	1.05	6.5

Table 4-3 - Important wave parameters at Mermaid location and port entrance

The significant wave height at the REBO offshore site and Halve Maan are 1.05 because the measurements are in front of the port entrance with a similar depth, so there is no shoaling. The main wave direction at this location is North West so no diffraction takes place, see Figure 4-18.

The design wave height for constructions at the port is two times the significant wave height; therefore the design wave height is 2.10 meter (Schiereck, 2012).

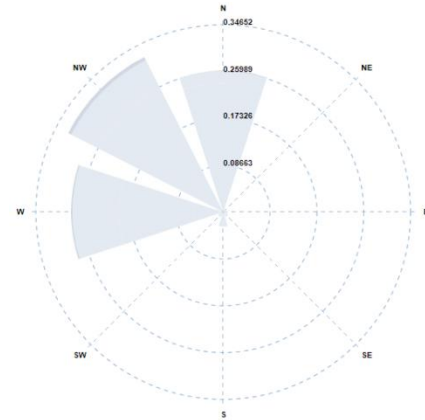


Figure 4-18 - Wave rose for port entrance location (metoceanview.com)

### 4.3 CONCLUSION CASE STUDY

The first design method step is executed in this chapter a reference case is used to develop a realistic case study for the application of a large number of gravity based foundation for offshore wind turbines.

At the Thornton Bank the Deme-Group has installed 5 gravity based foundations. In future the offshore wind farms Mermaid and Seastar Deme is also involved in the construction. In the case study it is assumed that the two wind farms both are founded with gravity based foundations. The construction takes place on the REBO offshore site and/or at the construction area “De Halve Maan”. The boundary conditions of the port are described and the most important case study characteristics are:

- Number of GBFs: 64
- Capacity wind turbine: 8 MW
- Timeframe: 2 year
- Water levels: see figures

With the information in this chapter the next step in the design method can be executed: “Design materiaefficient GBF”. The case study is placed in the constructed offshore wind farms in Figure 4-19, as it can be seen it is one of the larger offshore wind farms.

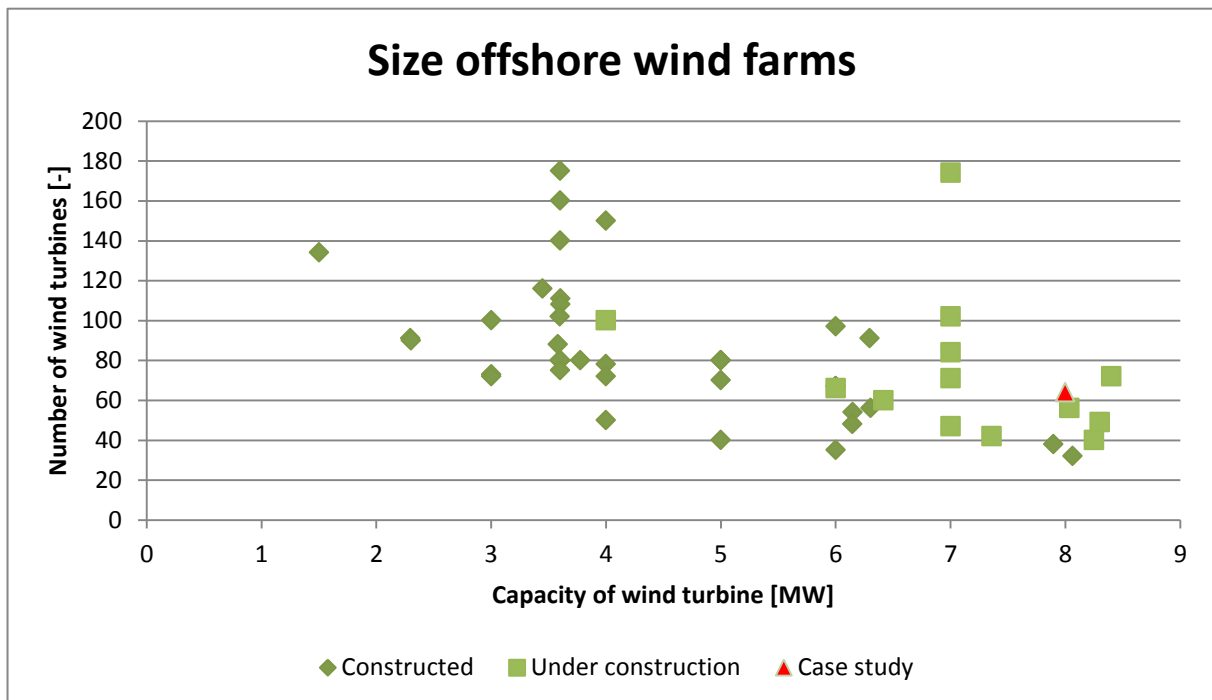


Figure 4-19 - Size of case study indicated in existing and under construction offshore windfarms

## Chapter 5: MATERIALEFFICIENT GBF DESIGN

In this chapter a materialefficient GBF is designed. The input from chapter 4 is used as boundary conditions. First the main functions of a GBF are described and the choice of the geometry is given. The design of the GBF is checked on the stability during transportation and stability during operation. At last the construction time of this GBF is given in a planning and the question is answered if the construction time is relatively large. In the design method this is the second step, see Figure 5-1. Due to one dominant requirement of the circular base slab which is the optimal geometry the secondary design method is executed with one design, therefore the evaluation procedure is very short.

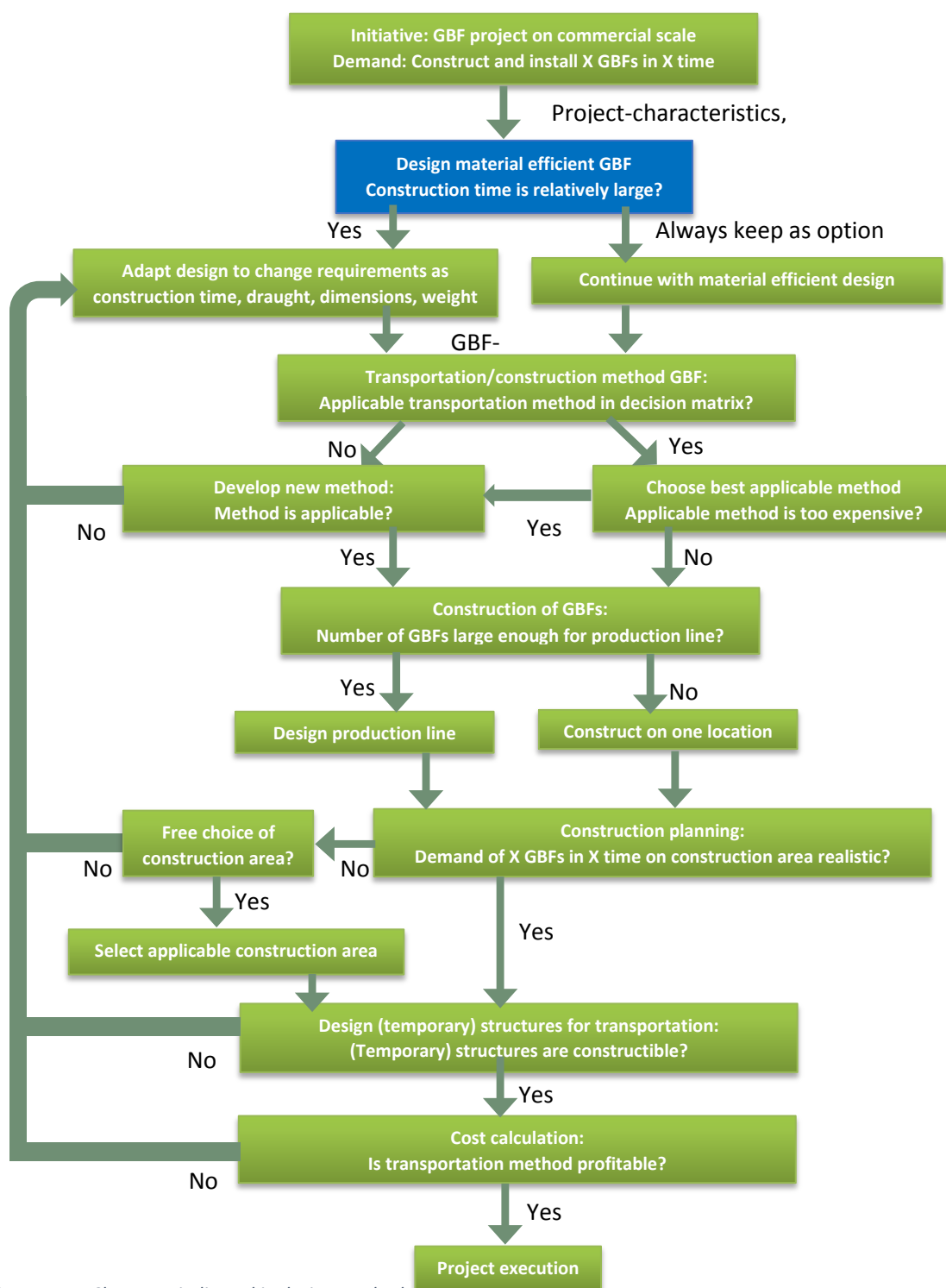


Figure 5-1 – Chapter 5 indicated in design method

## 5.1 GBF PROPERTIES

Gravity based foundations for offshore wind turbines can have different geometries and dimensions. In paragraph 3.3 at Figure 3-11 till Figure 3-14 some examples for gravity based foundations for offshore wind turbines are given. The main similarities of these GBFs are the large weight of the base and the low center of gravity. Concrete and steel are the main construction materials, both with a large weight.

The main function of a gravity based foundation is to ensure stability for the wind turbine. On the wind turbine several forces are present and they are indicated in Figure 5-2.

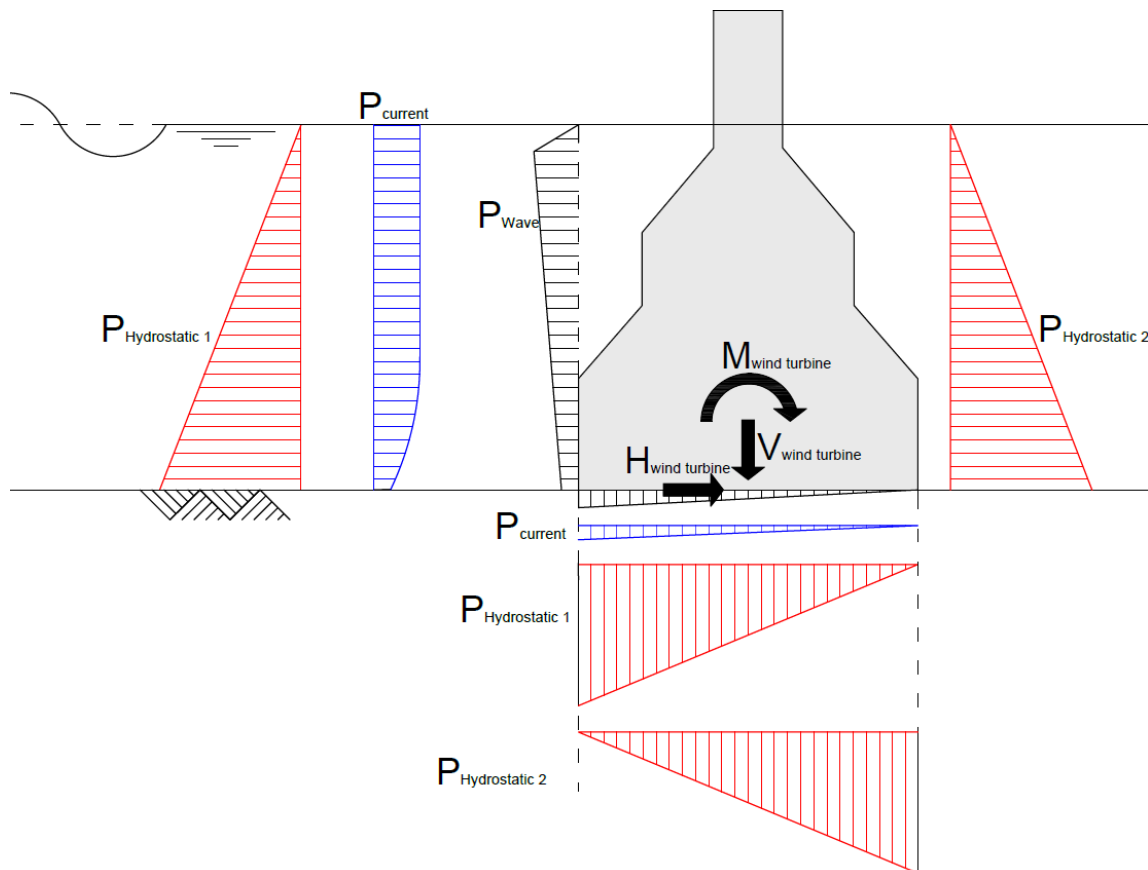


Figure 5-2 - Forces on installed GBF

The gravity based foundation is directly prone to the following environmental forces:

- Hydrostatic pressure
- Current
- Waves
- Wind

Besides the environmental forces directly on the GBF the wind turbine induce a moment, shear force and a vertical force on the GBF.

The wind forces on the wind turbine are transferred with the so-called transition piece to the foundation. The wind force induces a large moment around the center of gravity of the system. To ensure stability, the weight of the foundation must be sufficiently large. The subsoil has to bear the reaction forces for the weight, horizontal forces and rotational moments.

Usually, gravity based foundations are made in the dry and transported into the water to tow them to the place of immersion. An important criterion is that the gravity based foundation is able to float and is stable in the current, waves and wind.

The weight of some reference projects are given in Table 5-1 for an overview of what order of magnitude the deadweight could be expected. The dimensions of the base of the reference projects are given in Table 5-1. The order of magnitude of the weight of the elements is around 65-100 kN/m<sup>2</sup> and the order of magnitude for the dimensions are around 20-40 meter, depending on wind turbine capacity, water depth and environmental conditions.

	Weight [ton]	Diameter bottom slab [m]	Weight [kN/m <sup>2</sup> ]	Capacity wind turbine [MW]	Draught [m]
<b>Thornton Bank</b>	3000	23.5	68	5.1	6.75
<b>Confidential</b>	7250	32	88	8	8.8
<b>Confidential</b>	11,016	38	95	10	9.5

Table 5-1 - Properties GBF of reference projects (c-power.be)

As can be seen in Table 5-1 all GBFs of reference projects are circular. A circular foundation is the most efficient geometry:

- The forces from currents and waves are smallest for a circular foundation. The forces could be present from all directions and the advantage of a circular foundation is that the properties are identical in all directions.
- For the stability criteria a circular foundation is preferable because the contact area is the largest with the smallest dimensions of the GBF, a circle is the most efficient geometry to create the largest area with the smallest perimeter. Again the stability of the subsoil must be guaranteed for all directions and with a circular foundation this is identical in all directions.
- A circular foundation is the most efficient geometry with the amount of material needed to construct a GBF.

## 5.2 PROGRAM OF REQUIREMENTS GBF DESIGN

The preliminary design of a GBF is adopted from reference projects. In this report only the external stability is checked. The thicknesses of the concrete elements are assumed to be sufficient. For the external stability during transport and in the operation phase the following requirements hold:

- The GBF must be stable during transport, therefore a check is performed on:
  - Static stability
  - Dynamic stability
- The GBF must be stable in the operational phase, therefore a check is performed on:
  - Bearing capacity
  - Shear capacity
  - Rotational stability
- The stability calculations must be performed according to the Eurocodes.

### 5.3 GBF DESIGN

Based on the reference projects, a preliminary design is made for a GBF, see Figure 5-3. The calculation for the stability criteria determines the base slab diameter. A first estimation of a base slab diameter of 35 meter is used in this design. After the stability calculations the minimal diameter which ensures stability is calculated.

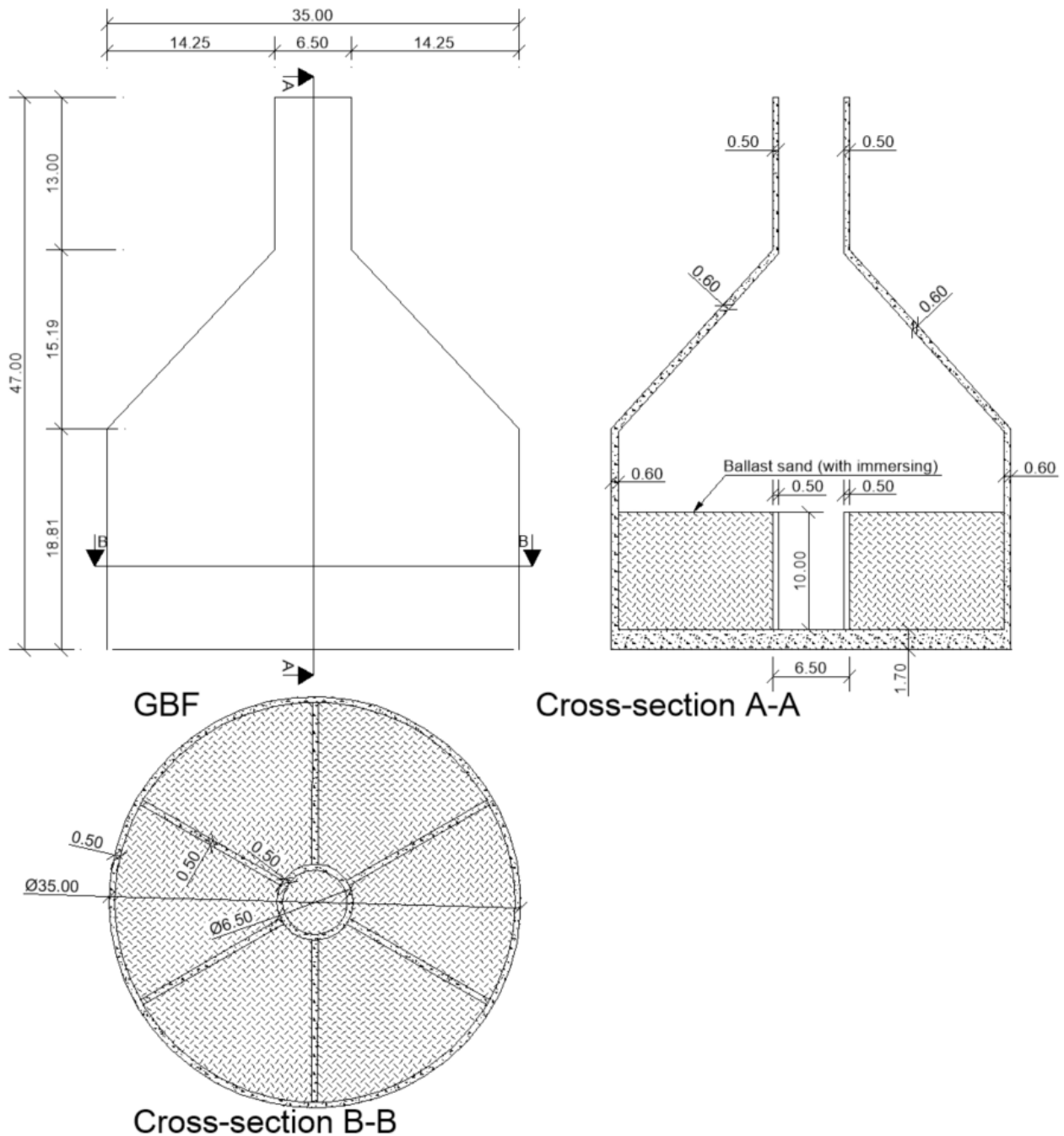


Figure 5-3 - Preliminary design of GBF

### 5.3.1 Starting points

For the calculation of the dimensions of the GBF the Eurocode guidelines are used. In the calculation Design Approach 2 (DA2) is performed. This means that the partial factors are given in the set of A1, R2 and M1, see Figure 5-4. The partial factors according to the Eurocode are displayed in Figure 5-4.

**Table 3.3.1 Partial factors on actions ( $\gamma_F$ ) or the effects of actions ( $\gamma_E$ )**

Action	Symbol	Set	
		A1	A2
Permanent	Unfavourable	$\gamma_G$	1,35
	Favourable		1,0
Variable	Unfavourable	$\gamma_Q$	1,5
	Favourable		0

**Table 3.3.2 Partial resistance factors for spread foundations ( $\gamma_R$ )**

Resistance	Symbol	Set		
		R1	R2	R3
Bearing	$\gamma_{Rv}$	1,0	1,4	1,0
Sliding	$\gamma_{Rh}$	1,0	1,1	1,0

**Table 3.3.3 Partial factors for soil parameters ( $\gamma_M$ )**

Soil parameter	Symbol	Value	
		M1	M2
Shearing resistance	$\gamma_\phi^1$	1,0	1,25
Effective cohesion	$\gamma_c$	1,0	1,25
Undrained strength	$\gamma_{cu}$	1,0	1,4
Unconfined strength	$\gamma_{qu}$	1,0	1,4
Effective cohesion	$\gamma_c$	1,0	1,4
Weight density	$\gamma_\gamma$	1,0	1,0

<sup>1</sup> This factor is applied to  $\tan \phi'$

Figure 5-4 - Load factors according the Eurocode (Molenaar & Voorendt, 2018)

The GBF must be stable during the operational phase. According to the Eurocode a safety factor of 1.4 is included for the bearing capacity of the subsoil and 1.1 for the sliding capacity. For the weight a weight factor of 1.0 is applied when the load is favorable and 1.35 when the load is unfavorable.

The loads on the GBF are taken from reference projects. For a project with a 10 MW wind turbine the horizontal load and bending moment, including an environmental partial load factor are:

- Horizontal load: 98,145 kN
- Moment: 1,000,350 kNm

To translate the design loads from the reference project to the case study the following procedure is executed:

- **Horizontal load:**  
The horizontal load on the wind turbine is assumed to be proportional to the capacity of the wind turbine. Therefore the load is multiplied by 0.8 and this result in a design load of 78,516kN.
- **Moment:**  
The moment applied on the foundation consist of a horizontal force and a lever arm. These two aspects are both taken into account. For the horizontal force the same procedure is followed as for the horizontal load: multiplying with a factor of 0.8.  
A 10 MW wind turbine is higher than an 8 MW turbine. With a reference case the hub height of an 8 MW wind turbine is set on 109 meter above sea level. The hub height of the 10 MW of the reference case has a height of 144 meter. Therefore the lever arm is multiplied by 109/144. To calculate the moment the following calculation is performed:

$$M_{8MW} = M_{10MW} \cdot 0.8 \cdot \frac{109}{144} = 605,768 \text{ kNm} \quad (4)$$

The environmental load factor of 1.35 is included in this value; therefore these loads are the design loads.

To calculate the stability of the GBF five stability criteria are applied:

- Stability during transportation phase:
  - Static stability
  - Dynamics stability
- Stability during operational phase:
  - Shear capacity of soil
  - Bearing capacity of soil
  - Rotational stability

The stability of the different criteria is calculated. With the unity check (UC) the stability of the different phenomena can be determined. The unity check is given by:

$$UC = \frac{F_{Ed}}{F_{Rd}} \leq 1 \quad (5)$$

Where:

$$F_{Ed} = \text{Design load}$$

$$F_{Rd} = \text{Resistance design capacity}$$

The unity of the load and resistance capacity could be several force related parameters for example, Newton, Newtonmeter, Newton per square meter etcetera. The only restriction is that the unity is similar to end up with a unitless unity check.

To calculate the stability criteria the weight of the GBF is important. The stability of the GBF is determined for various diameters. In the following paragraphs the calculation is performed for a GBF with a diameter of 35 meter and a height of 47 meter. In 0 the Matlab script is shown which is used for the calculation for the most optimal diameter. To determine the minimal diameter which guarantees stability the unity check is calculated in paragraph 5.2.9 and plotted for various diameters.

### 5.3.2 Weight

The weight of the GBF is determined by adding up the volume of concrete and multiplying it with the volumetric weight. The GBF is subdivided in 5 parts, of these parts the volumes of the applied material is determined and multiplying it with the volumetric density the weight is determined, see Table 5-2. The total weight of the GBF is 9969 ton.

The weight is determined with the formula:

$$W_{GBF} = V_c \cdot \gamma_c \quad (6)$$

Where:

$$W_{GBF} = \text{Weight of GBF [kg]}$$

$$V_c = \text{Volume of concrete [m}^3\text{]}$$

$$\gamma_c = \text{Volumetric density concrete} = 2400 \text{ [kg/m}^3\text{]}$$

$$\text{Where: } V_c = \begin{cases} \frac{1}{4} \cdot \pi \cdot D_{bs}^2 \cdot h_c & \text{For base slab} \\ \frac{1}{4} \pi \cdot (D_{out}^2 - D_{in}^2) \cdot h_c & \text{For hollow cyinders(7)} \\ \frac{1}{3} \pi \cdot h_c \left( (R_{out}^2 + R_{out}r_{out} + r_{out}^2) - (R_{in}^2 + R_{in}r_{in} + r_{in}^2) \right) & \text{For hollow cone} \end{cases}$$

Where:

$$D_{bs} = \text{Base slab diameter [m]}$$

$$h_c = \text{Height of concrete element [m]}$$

$D_{out}$  = Outer diameter of cylindrical part GBF [m]  
 $D_{in}$  = Inner diameter of cylindrical part GBF [m]  
 $R_{out}$  = Outer radius of cone bottom [m]  
 $R_{in}$  = Inner radius of cone bottom [m]  
 $r_{out}$  = Outer radius of cone top [m]  
 $r_{in}$  = Inner radius of cone top [m]

Part	Weight [ton]
Base slab	3925
Cylinder	2663
Inner walls +inner cylinder	1209
Cone	1878
Tower	294
<b>Total</b>	<b>9969</b>

Table 5-2 - Weight of GBF of 35m diameter

### 5.3.3 Draught

The buoyancy force on a floating element is given by the weight of the displaced water. The buoyancy force then is given by the formula:

$$F_{buoy} = V_{dw} \cdot \rho_w \quad (8)$$

Where:

$$\begin{aligned}
 F_{buoy} &= \text{Buoyancy force on GBF [kN]} \\
 V_{dw} &= \text{Volume of immersed part GBF [m}^3\text{]} \\
 \rho_w &= \text{Volumetric density of water} = 10,05 \text{ [kN/m}^3\text{]}
 \end{aligned}$$

Assuming that only the cylindrical part of the GBF is under water, the volume of the immersed part can be calculated with:

$$V_{dw} = \frac{1}{4} \pi \cdot D_{bs}^2 \cdot d \quad (9)$$

The total weight of the GBF is 9969 ton, to calculate the draught the following formula is used:

$$F_{buoy} = W_{GBF} \cdot g \quad (10)$$

$$V_{dw} \cdot \frac{\rho_w}{g} = W_{GBF} \quad (11)$$

The height is calculated and the assumption that only the cylindrical part is under water is good. Because the draught is not larger than the height of the cylindrical part of the GBF the submerged volume can be described as:

$$\frac{1}{4} \cdot \pi \cdot D_{bs}^2 \cdot d \cdot \frac{\rho_w}{g} = W_{GBF} \quad (12)$$

$$h_u = \frac{W_{GBF} \cdot g}{\frac{1}{4} \pi \cdot D_{bs}^2 \cdot \rho_w} = \frac{9969 \cdot 9.81}{\frac{1}{4} \pi \cdot 35^2 \cdot 10.05} = 10.11 \text{ m} \quad (13)$$

The draught is 10.11 meter.



$$\overline{KG} = \frac{\sum(V_i \cdot e_i \cdot \gamma_i)}{\sum(V_i \cdot \gamma_i)} \quad (20)$$

Where:

$V_i$  = Volume of element  $i$  [ $m^3$ ]

$e_i$  = Distance between centre of gravity of element  $i$  and reference level [ $m$ ]

$\gamma_i$  = Volumetric weight of element  $i$  [ $kN/m^3$ ]

The factors are determined of each element and are displayed in Table 5-3.

		$V_i [m^3]$	$e_i [m]$	$\gamma_i \left[ \frac{kN}{m^3} \right]$	$V_i \cdot e_i \cdot \gamma_i$	$V_i \cdot \gamma_i$
$i = 1$	Base slab	1636	0.85	23.54	32,732	38,508
$i = 2$	Cylinder	1110	10.26	23.54	267,870	26,121
$i = 3$	Inner walls	504	5.85	23.54	79,464	11,860
$i = 4$	Cone	782	23.37	23.54	439,730	18,419
$i = 5$	Tower	123	40.5	23.54	116,830	2,885
				$\Sigma$	936,626	97,793

Table 5-3 - Factors used to calculate the distance KG for a GBF diameter of 35 meter

The result is a distance of:

$$\overline{KG} = \frac{936,626}{97,793} = 9.58 \text{ m}$$

All distances are known and the metacentric height can be calculated:

$$h_m = 5.05 + 7.57 - 9.58 = 3.05 \text{ m}$$

Because the metacentric height is larger than 0.5 the GBF is statically stable.

### 5.3.5 Dynamic stability

Also the dynamic stability is very important to ensure that the GBF could be towed to its final location. First the wave climate is determined. This is done for two locations:

- At the port entrance of Oostende
- At the final immersion location at the Mermaid offshore wind farm

From the available wave data the probabilistic density function (PDF) and cumulative density function (CDF) are derived and displayed in Annex H in Figure A-32 and Figure A-33 for the port entrance location and in Figure A-36 and Figure A-37 for the Mermaid location. In the PDF figures the significant wave height is indicated. The wave spectrum at the port entrance and the Mermaid locations are displayed in Figure 5-6 and in Figure 5-7, from these figures the peak periods are the most important result. The most important results are summarized in Table 5-4, the peak periods are displayed in Figure 5-6 and Figure 5-7.

Location	Significant wave height [m]	Peak period [s]
<b>Mermaid</b>	2.10	7.5
<b>Port entrance</b>	1.05	6.5

Table 5-4 - Most important wave parameters

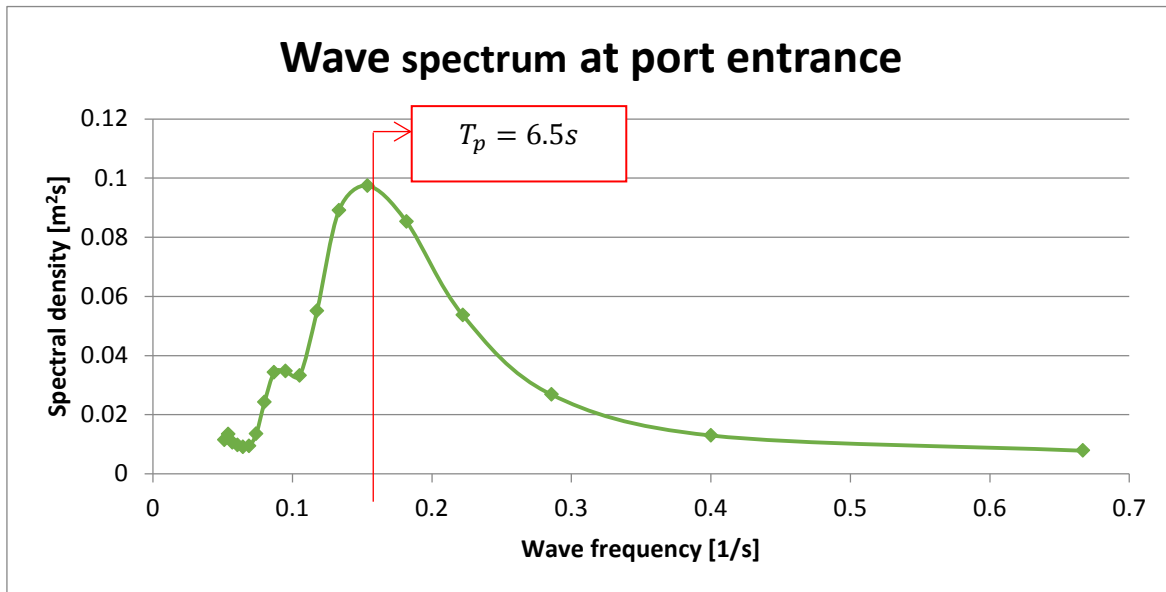


Figure 5-6 - Wave spectrum at port entrance (Data: metoceanview.com)

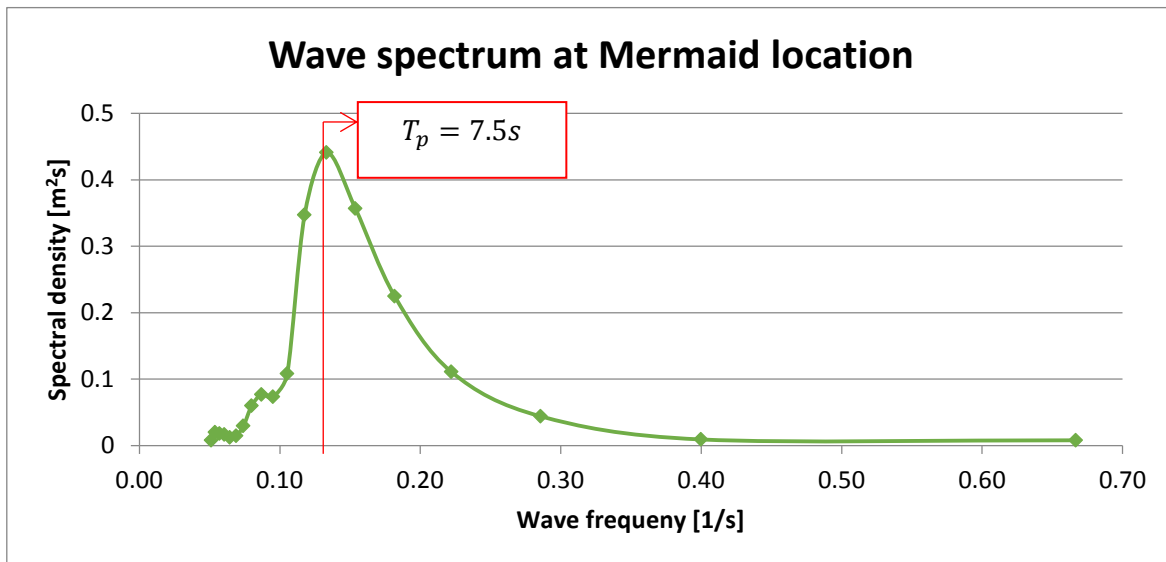


Figure 5-7 – Wave spectrum at Mermaid location (Data: metoceanview.com)

The natural oscillation period may not be in the range of the wave spectrum. The formula to calculate the natural oscillation period is (Voorendt, Molenaar, & Bezuyen, 2016):

$$T_0 = \frac{2 \cdot \pi \cdot j}{\sqrt{h_m \cdot g}} \quad (21)$$

Where:

$$j = \text{Polar inertia radius of the element [m]}$$

The polar inertia radius can be calculated with:

$$j = \sqrt{\left(\frac{I_{polar}}{A}\right)} \quad (22)$$

Where:

$$I_{polar} = \text{Polar moment of inertia [m}^4\text{]}$$

$A = \text{Area of concrete in a vertical cross – section [m}^2\text{]}$

The polar moment of inertia can be calculated with:

$$I_{polar} = \int_A r^2 dA = I_{xx} + I_{zz} \quad (23)$$

Where:

$$I_{xx} = \text{Polar moment of inertia around } z - \text{axis [m}^4\text{]}$$

$$I_{zz} = \text{Polar moment of inertia around } x - \text{axis [m}^4\text{]}$$

Because the geometry is rather complex the polar moment of inertia is estimated with the help of AutoCAD software. The Polar moment of inertia is equal to 262,400 m<sup>4</sup>. This value is implemented and the results are:

$$j = \sqrt{\frac{I_{polar}}{A}} = \sqrt{\frac{262,400}{1038}} = 15.91 \text{ m} \quad (24)$$

This result in a natural oscillation period of:

$$T_0 = \frac{2 \cdot \pi \cdot j}{\sqrt{h_m \cdot g}} = \frac{2 \cdot \pi \cdot 15.91}{\sqrt{3.04 \cdot 9.81}} = 18.30 \text{ s} \quad (25)$$

The natural oscillation period is at the spectrum where almost no wave energy is present, the natural oscillation period is higher than the peak wave period and therefore it is concluded that the GBF is dynamically stable.

### 5.3.6 Shear capacity

The environmental forces induce shear forces between the GBF and the subsoil. The subsoil has to resist these shear force. The resistance capacity of the subsoil is given as:

$$\tau_{max} = f_f \cdot \sigma'_n \quad (26)$$

Where:

$$\tau_{max} = \text{Maximum shear stress capacity [kN/m}^2\text{]}$$

$$f_f = \text{Coefficient of friction[-]} = \tan(\delta)$$

$$\delta = \text{Angle of friction between concrete and sand [}^\circ\text{]}$$

$$\sigma'_n = \text{Effective normal stress under the foundation [kN/m}^2\text{]}$$

The coefficient between sand and concrete is usually between 40 and 50 degree. In this calculation the lower bound of 40 degrees is applied. In the calculation of the effective normal stress is the partial factor for favourable weight applied: ( $\gamma_{G,fav} = 1.0$ ). The total weight of the GBF is used and the buoyancy force is subtracted from the weight to calculate the effective normal stress. The horizontal design shear stress is calculated with:

$$\tau_d = \frac{\Sigma H}{A} = \frac{78516}{962} = 81.6 \frac{\text{kN}}{\text{m}^2} \quad (27)$$

The Unity check is given as:

$$UC = \frac{\tau_d}{\tau_{max}/\gamma_{R,h}} \quad (28)$$

Where:

$$\tau_d = \text{Design value shear stress [N/m}^2\text{]}$$

$$\gamma_{R,h} = \text{Eurocode partial factor sliding (= 1.1)[-]}$$

In Table 5-5 the input values and the results are given. The GBF is stable regarding sliding.

Parameter	Value	Unit
$f_f$	0.84	[-]
$\sigma_n'$	215	[N/mm <sup>2</sup> ]
$\tau_{max}$	180	[N/mm <sup>2</sup> ]
$\tau_d$	82	[N/mm <sup>2</sup> ]
$UC$	0.50	[-]

Table 5-5 - Result of shear capacity calculation for GBF with 35m diameter

### 5.3.7 Bearing capacity

The bearing capacity of the subsoil can be determined with the Brinch-Hansen formula. The formula to determine the bearing capacity is as follows (Molenaar & Voorendt, 2018):

$$p'_{max} = c' N_c s_c i_c + \sigma'_q N_q s_q i_q + 0,5 \gamma' B_{eff} N_\gamma s_\gamma i_\gamma \quad (29)$$

The subscript  $q$  is for surcharge on the sea bottom and because next to the GBF no extra surcharge is present this factor is equal to zero. The subscript  $c$  refers to the cohesion in the soil, because gravel and sand is present and the cohesion of these soils is zero, these factors also can be neglected. Therefore the Brinch-Hansen formula is reduced to:

$$p'_{max} = 0,5 \gamma' B_{eff} N_\gamma s_\gamma i_\gamma \quad (30)$$

Where:

$$\begin{aligned} \gamma' &= \text{Effective volumetric weight of soil under foundation [N/m}^3\text{]} \\ B_{eff} &= \text{Effective width of foundation area [m]} \\ N_\gamma &= \text{Bearing capacity factor [-]} \\ s_\gamma &= \text{Shape factor [-]} \\ i_\gamma &= \text{Inclination factor [-]} \end{aligned}$$

The Bearing capacity factors are given as:

$$N_\gamma = (N_q - 1) \tan(1.32\varphi') \quad (31)$$

Where:

$$N_q = \frac{1 + \sin(\varphi')}{1 - \sin(\varphi')} \cdot e^{\pi \tan(\varphi')} \quad (32)$$

$$\varphi' = \text{Angle of internal friction [}^\circ\text{]}$$

The shape factor is given as:

$$s_\gamma = 1 - 0.3 \frac{B_{eff}}{L_{eff}} \quad (33)$$

Where:

$$L_{eff} = \text{Effective length of foundation [m]}$$

Because the foundation is circular, there are some formulas needed to estimate the effective area, length and width, see Figure 5-8.

Where  $A_{eff}$  is calculated with:

$$A_{eff} = 2 \left( R^2 \arccos\left(\frac{e}{R}\right) - e \sqrt{R^2 - e^2} \right) \quad (34)$$

The width and length are given with:

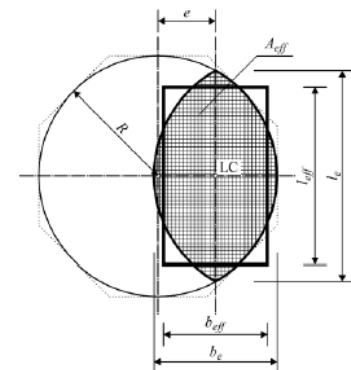


Figure 5-8 – Principle of effective dimensions of a circular foundation

$$b_e = 2(R - e) \quad (35)$$

$$l_e = 2R\sqrt{1 - \left(1 - \frac{b_e}{2R}\right)^2} \quad (36)$$

The effective foundation area can now be presented with a rectangle with an effective length and effective width:

$$l_{eff} = \sqrt{A_{eff} \cdot \frac{l_e}{b_e}} \quad (37)$$

$$b_{eff} = \frac{l_{eff}}{l_e} b_e \quad (38)$$

At last the inclination factor is given:

$$i_\gamma = \left(1 - \frac{\Sigma H_{unfav}}{\Sigma V_{fav} + A_{eff} c' \cot(\varphi')}\right)^3 \quad (39)$$

Applying sand and gravel the cohesion ( $c'$ ) is zero and the formula for the inclination factor is reduced to:

$$i_\gamma = \left(1 - \frac{\Sigma H_{unfav}}{\Sigma V_{fav}}\right)^3 \quad (40)$$

Where:

$$\begin{aligned} \Sigma H_{unfav} &= \text{Total horizontal force on foundation with unfavorable partial factor [N]} \\ \Sigma V_{fav} &= \text{Sum of vertical force on foundation with favorable partial factor [N]} \end{aligned}$$

Now all factors are known the maximum characteristic bearing capacity can be calculated:

$$p'_{max} = 0,5\gamma' B_{eff} N_\gamma s_\gamma i_\gamma \quad (41)$$

After calculating the characteristic value of the bearing capacity the maximum pressure of the GBF is calculated. The maximum vertical bearing capacity of the subsoil may not be exceeded. Therefore the maximum vertical stress is calculated at the edge of the GBF, where the maximum stress is present. This can be done with the following formula:

$$\sigma'_{GBF,max} = \frac{\Sigma V_{unfav}}{A} + \frac{\Sigma M}{W_{bs}} \quad (42)$$

Where:

$$\begin{aligned} A &= \text{Area of base slab [m}^2\text{]} \\ \Sigma M &= \text{Sum of all moments [kNm]} \\ W_{bs} &= \text{Moment of resistance of base slab [m}^3\text{]} \end{aligned}$$

Symbol	Value	Unit	Symbol	Value	Unit	Symbol	Value	Unit
<b>A</b>	962	[m <sup>2</sup> ]	$i_\gamma$	0.49	[-]	<b>R</b>	17.5	[m]
<b>A<sub>eff</sub></b>	822.7	[m <sup>2</sup> ]	$l_e$	34.77	[m]	$s_\gamma$	0.73	[-]
<b>b<sub>e</sub></b>	31.0	[m]	<b>L<sub>eff</sub></b>	30.37	[m]	$\Sigma V_{unfav}$	376735	[kN]
<b>B<sub>eff</sub></b>	27.1	[m]	$N_q$	37.75	[-]	$W_{bs}$	4209	[m <sup>3</sup> ]
<b>c'</b>	0	[kN/m <sup>2</sup> ]	$N_\gamma$	40.14	[-]	$\gamma'$	13.5	[kN/m <sup>3</sup> ]
<b>e</b>	2.00	[m]	$\sigma'_{GBF,max}$	535	[kN/m <sup>2</sup> ]	$\varphi'$	36	[°]
<b>H<sub>unfav</sub></b>	78516	[kN]	<b>p'<sub>max</sub></b>	2661	[kN/m <sup>2</sup> ]	$\Sigma M$	605768	[kNm]

Table 5-6 - Values for bearing capacity

The unity check is as follows:

$$UC = \frac{\sigma'_{GBF,max}}{p'_{max}/\gamma_{R;V}} \leq 1 \quad (43)$$

Where:

$$\begin{aligned} \sigma'_{GBF,max} &= \text{Maximal effective foundation pressure [kN/m}^2\text{]} \\ p'_{max} &= \text{Maximum bearing capacity subsoil [kN/m}^2\text{]} \\ \gamma_{R;V} &= \text{Eurocode partial factor on bearing capacity (= 1.4)[-]} \end{aligned}$$

Applying all values this results in a unity check of 0.28.

### 5.3.8 Rotational stability

The rotational stability can be calculated with the formula:

$$e_R = \frac{\sum H}{\sum V_{fav}} \cdot h_{COG} \leq \frac{D_{GBF}}{8} \quad (44)$$

Where:

$$\begin{aligned} e_R &= \text{Distance from the middle of the structure to the intersection point} \\ &\quad \text{of the resulting force and the bottom line of the structure [m]} \\ \sum M &= \text{Sum of the acting moments [kNm]} \\ h_{COG} &= \text{Height of Centre of Gravity [m]} \\ D_{GBF} &= \text{Diameter of base slab [m]} \end{aligned}$$

The unity check is given as:

$$UC = \frac{e_R}{\frac{D_{GBF}}{8}} \leq 1 \quad (45)$$

The result and input to calculate the unity check for the rotational stability are given in Table 5-7. The result is a unity check of 0.83.

Parameter	Value	Unit
$\sum H$	78,516	[kN]
$\sum V_{fav}$	206,450	[kN]
$h_{COG}$	9.58	[m]
$D_{GBF}$	35	[m]
$e_R$	3.64	[m]
$UC$	0.83	[-]

Table 5-7 - Input and results of rotational stability for GBF with 35m diameter

### 5.3.9 Optimal diameter for stability

All calculations have a unity check lower than one and therefore the GBF is stable. It might be that the base slab diameter can be reduced in diameter which is cheaper, lighter and takes less space to construct. To determine the optimal diameter the calculation is performed for various base slab diameters. The unity checks as function of the base slab diameter are given in Figure 5-9. As it can be seen in that figure the unity checks are all below 1 when the diameter of the base slab is 33 meter. Therefore the GBF is designed with a diameter of 33 meter. The stability calculation is performed with the use of Matlab software, the script with all calculated values is included in 0. The governing stability parameter is the rotational stability. When the diameter is tried to optimize this unity check could be decreased by increasing the weight of the GBF. This is negative for the construction, transportation and draught. Therefore this optimization is not executed.

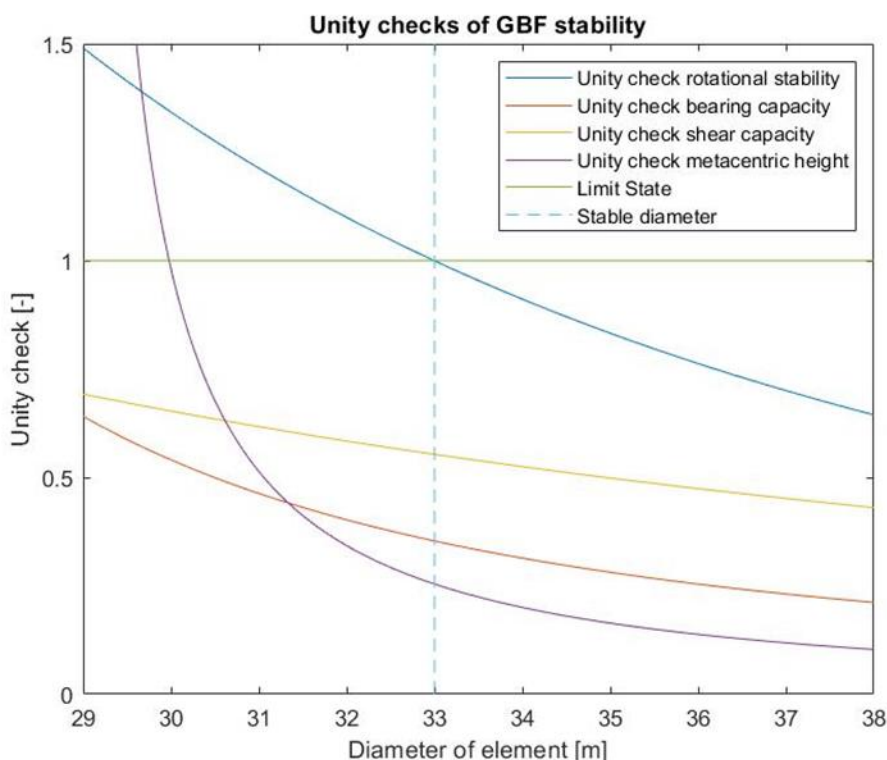


Figure 5-9 - Stability criteria as function of base slab diameter

With a GBF with a 33 meter diameter base slab the draught is 10.45 meter and the weight is 9157 ton.

The most important values for a GBF with a 33 meter diameter base slab are given in Table 5-8. All other values are included in a table in 0.

Property	Value	Unit
<b>Draught</b>	10.45	[m]
<b>Weight empty</b>	9157	[ton]
<b>Weight per square meter</b>	105.03	[kN/m <sup>2</sup> ]
<b>Weight installed</b>	44,294	[ton]
<b>Volume of concrete</b>	3815	[m <sup>3</sup> ]

Table 5-8 - Properties of 33 meter diameter base slab

## 5.4 CONSTRUCTION PLANNING

The construction time of the GBF is an important parameter because 64 GBFs must be constructed in a period of two years. Normally a planning is created by calculating the amount of volume of materials and divide then by the production rate. Because this GBF is not a standard structure and construction procedures are difficult due to the height, an estimation is given of the construction times based on production times. A choice is made for the type of formwork which is applied to cast concrete:

- Bottom slab: Traditional formwork
- Cylindrical part: gliding formwork
- Conical part: Traditional formwork
- Internal walls: System formwork
- Tower: Traditional formwork

Due to the large number of GBFs it is assumed that the purchase of a gliding formwork system is profitable comparing to applying system of traditional formwork to the cylinder. The construction time is explained for the several GBF elements:

The construction of the formwork to cast the base slab takes 3 weeks. The reinforcement can be started to braid one week after the start of the formwork construction, this construction action also takes three weeks. The base slab has a volume of 1454 m<sup>3</sup>. With a casting rate of 100 m<sup>3</sup>/hour, two days of concrete casting are reserved. After a period of hardening of one week the formwork is removed what takes one week.

Then the gliding formwork system can be installed which takes two weeks, the casting procedure takes 120 hours with a gliding velocity of 0.15 m/hour. The uninstallation of the gliding formwork takes one week. Equally to the gliding formwork the inner walls can be constructed, see the planning.

Then the cone can be constructed which is the most difficult part, due to the complex geometry. The construction of the formwork takes 4 weeks and the steel braiding two weeks. Due to the geometry and the large height these actions are not executed at the same time. The construction time to install the formwork at the tower is estimated at three weeks.

The planning for the GBF is given in Figure 5-10. In total the construction of a GBF takes 25 weeks. When 64 GBFs must be constructed in two years a shorter construction time of the GBF is preferable. If the construction planning can be reduced this has a large positive effect on the total construction time and costs.

Structural element	Concrete volume [m <sup>3</sup> ]	Volume per meter height (Gliding formwork) [m <sup>3</sup> /m]
<b>Base slab</b>	1454	-
<b>Outer wall</b>	1045	61.08
<b>Inner walls</b>	503	-
<b>Tower</b>	123	9.46
<b>Total</b>	<b>3125</b>	-

Table 5-9 - Concrete volumes of circular GBF

### 5.4.1 Learning curve

The planning described in paragraph 5.4 is a planning without applying a learning curve. A learning curve means that a certain construction action the first time takes longer because every construction action is 'new'. After executing a construction action several times the time needed decreases. In the planning of the construction of all GBFs a learning curve of 60%-80%-100% is included, the learning curve is used in chapter 8 where the planning of the entire project is made. This means that the construction time of the first GBF must be divided by 0.60, the second with 0.80 and the third and higher by 1.00. For the construction planning which takes 26 weeks the first GBF is constructed in 43.33 weeks, the second GBF in 32.5 and the third and higher in 26 weeks.

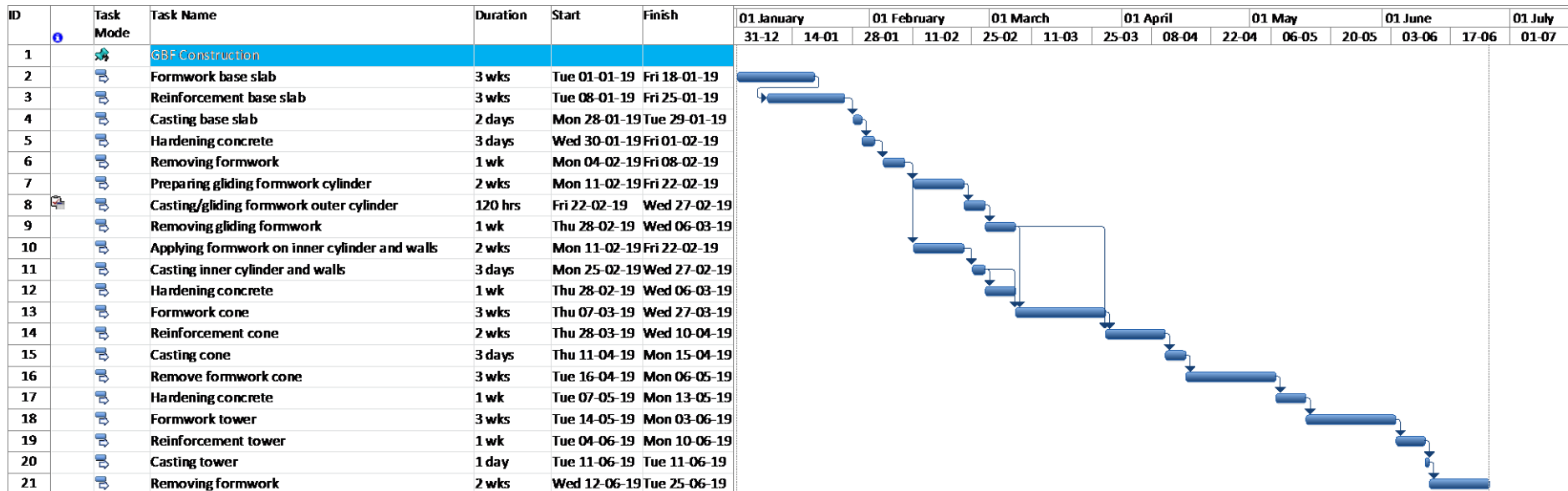


Figure 5-10 - Construction planning circular GBF

## 5.5 CONCLUSION MATERIALEFFICIENT GBF DESIGN

The design of the GBF from a reference project is used for the design of the structural elements. In this chapter the external stability is calculated for the following phenomena:

- Shear capacity
- Bearing capacity
- Rotational stability
- Static floating stability
- Dynamic floating stability

To design the most materialefficient GBF all stability criteria are calculated for various base slab diameters. This chapter includes an example calculation for a base slab of 35 meter. This diameter seems to be too large and can be decreased. By plotting the stability criteria as a unity check against the base slab diameter it is concluded that a minimal diameter of 33 meter fulfills all requirements.

The construction planning is created and a construction period of 26 weeks is needed to construct one GBF. With a construction period of 26 weeks the first GBF is constructed in 43.33 weeks, the second in 32.5 and the third in 26 weeks. At each construction area just three GBFs can be constructed in 2 years. This means that there are 22 construction locations needed which need a lot of area. Therefore it is decided that the construction time is too large period and it is chosen to follow the “Yes”-direction in the design method. In the next chapter the design is adapted to create a better constructability and decrease of the construction time.

## Chapter 6: ADAPTED GBF DESIGN

In this chapter the design of the GBFs is adapted. Due to the relatively long construction time of the GBFs an alternative design is made what is less materialefficient but has a better constructability and therefore a shorter construction time. In Figure 6-1 it is indicated in which phase of the design method this chapter is placed. The previous chapter describes a relatively large construction time for the GBFs and therefore the Yes-direction is followed to the design phase: Adapt design to change requirements. In this chapter the same holds as for the previous, due to the expertise of a design expert only one alternative is designed. Therefore the evaluation phase is very short due to one solution.

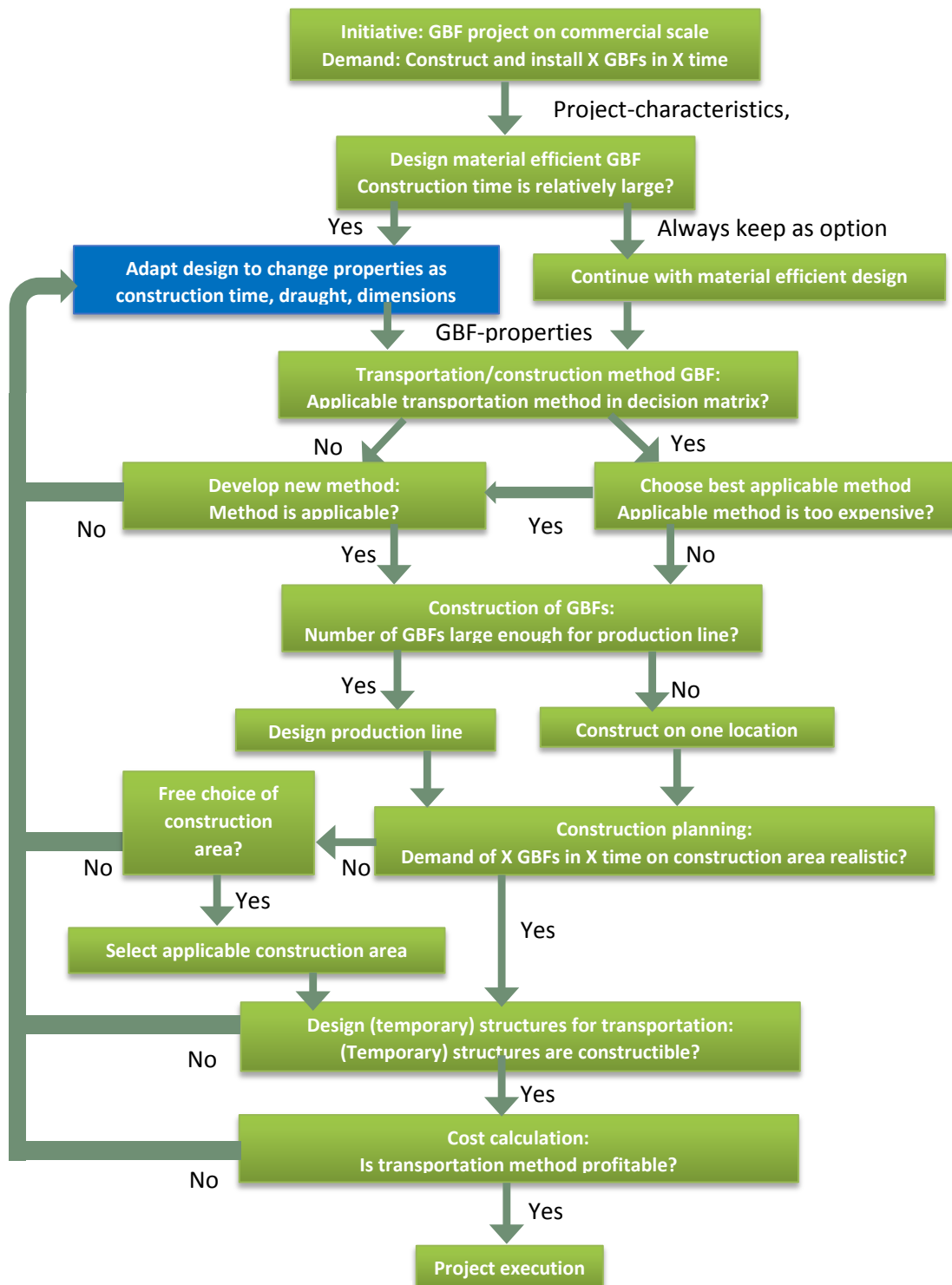


Figure 6-1 – Chapter 6 indicated in design method

## 6.1 PROBLEMATIC CONSTRUCTION ELEMENTS IN ORIGINAL DESIGN

For the composed case study 64 GBFs have to be constructed in two years. This means that a high production rate of GBFs is necessary. Because construction time is the most important parameter in the production process, the constructability of the GBFs is very important. The GBF design given in paragraph 5.3 has two difficult construction parts:

- Conical part:  
The conical part is a difficult part to construct because of the complex geometry. The geometry of the conical part is difficult to construct formwork, which is generally done with traditional formwork, and to cast. The conical part has a curved geometry and formwork is hard to apply on curved geometries. The formwork must be applied on a large height, this makes the formwork construction more difficult what increases the construction time and is more dangerous for workmen.
- Tower:  
The tower is also a difficult part to construct. A gliding formwork is difficult to place because this is at a height of 34 meter above the ground. Traditional formwork is a solution but either this placement is difficult at this heights.

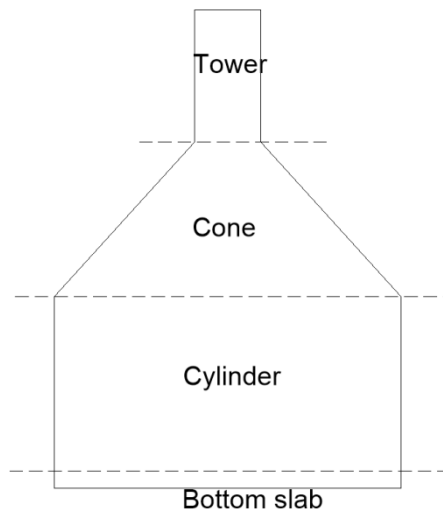


Figure 6-2 - Elements of GBF

Due to these difficulties the construction time of a GBF is large. To decrease the construction time, the design of the GBF could be adapted for a better constructability.

## 6.2 PROGRAM OF REQUIREMENTS CONSTRUCTION METHOD

To do some adaptations on the design of the GBF the following program of requirements is given:

- The conical part must be replaced or adapted to improve the constructability and decrease the risk on delay due to complex construction geometry.
- The tower part must be adapted to improve constructability and to reduce the risk on delay of the construction of the GBF.

As a sub-requirement the following requirement is given:

- The risks for human injury due to construction actions on large height must be mitigated.

## 6.3 STARTING POINTS

The GBF design is adapted in cooperation with some design experts of DIMCO. The conical element and the tower are very difficult to apply formwork on and to cast concrete. The large height where the construction activities must be executed causes longer execution times and large risks for workmen. The most important changes on the GBF design are:

- The base of the GBF is made hexagonal
- Twelve prefabricated plates are casted to construct the conical part
- The inner cylinder and the tower are constructed as one concrete element.

The geometrical adaptations of the design are given in Figure 6-3. The conical part is replaced by twelve plates to close the transition between the outer walls and the tower of the GBF. Plates to close the transitional part are prefabricated and placed by land based cranes. Two connections are designed to connect these plates to the

GBF. A concrete ring connection is designed to connect the plates with the inner cylinder, see Figure 6-4. On the other side the plate is connected to the outer walls by a post-tensioned connection, see Figure 6-5. This is only a design principle and no calculations for the strength of this connection are performed. Due to the adaptations the stability must be recalculated to determine the outside dimensions and the weight of the GBF.

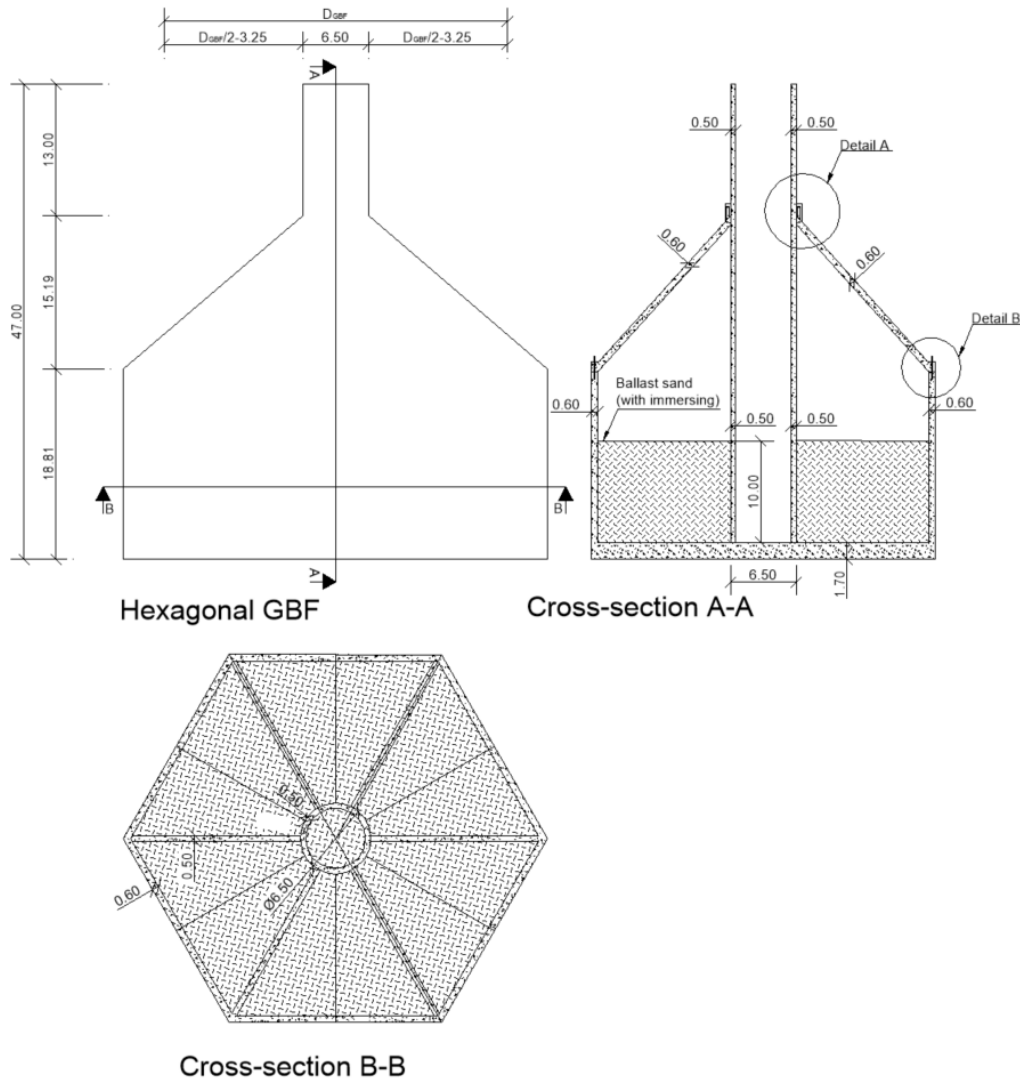


Figure 6-3 - Adapted design for better constructability

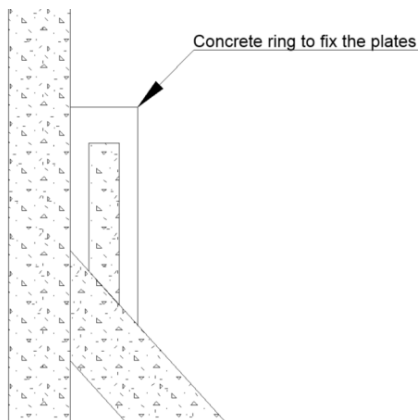


Figure 6-4 – Principle of ring connection Detail A

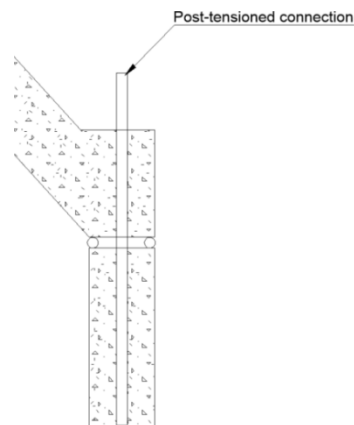


Figure 6-5 – Principle of post-tensioned connection

Because the hexagonal bottom slab not really has a diameter, Figure 6-6 is used for the definition of dimensions. The diameter is defined as the distance  $2R$ . To ensure stability in the transporting phase and installed phase similar calculations as in chapter 5 are performed. Some minor adaptations are present in the calculation of the stability. These adaptations are for example the formulas for base slab area, concrete volume and other geometrical changes. These adaptations are included in the Matlab script in 0.

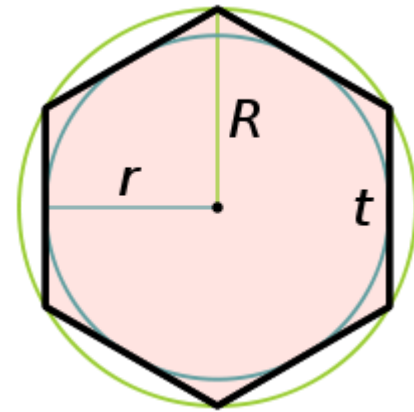


Figure 6-6 - Dimensions of hexagon

## 6.4 OPTIMAL DIAMETER

The unity checks to determine the stability of the element are plotted as function of the diameter ( $2R$ ). To ensure stability of the adapted design the stability criteria as described in 5.2 are used. The result in Figure 6-7 where the unity checks are plotted against the diameter is used to determine the minimal diameter of the GBF which is 37.5 meter. Because the geometry is hexagonal the horizontal forces induced by the flow and waves is larger, therefore some reserve capacity is included for this unknown increase in horizontal force. The stability calculation is performed with the use of Matlab software, the script is included in 0.

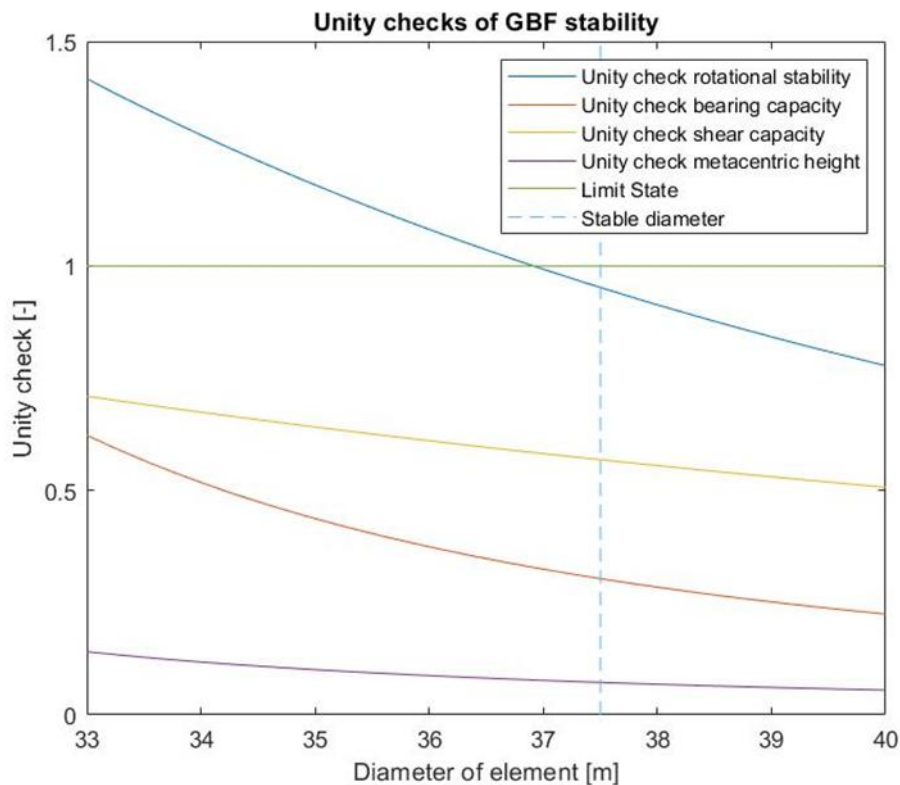


Figure 6-7 - Stability determination of hexagonal GBF by using unity checks for varying base slab diameter

A check on the dynamic stability is performed to ensure also dynamic stability. The metacentric height is 6.92 meter and the polar moment of inertia is  $242,233 \text{ m}^4$ . This results in a natural oscillation period of 11.93 seconds. In that region little wave energy is present and the GBF is dynamically stable.

The most important design values for a hexagonal GBF with a diameter of 37.5 meter are given in Table 6-1.

Property	hexagonal GBF	Circular GBF	Unit
<b>Draught</b>	11.21	10.45	[m]
<b>Weight</b>	10,495	9157	[ton]
<b>Weight per square meter</b>	112.7	105.03	[kN/m <sup>3</sup> ]
<b>Volume of concrete</b>	4373	3815	[m <sup>3</sup> ]
<b>Weight of plate</b>	163	-	[ton]

Table 6-1 - Parameters hexagonal GBF design with a diameter of 37.5 meter and circular GBF with diameter of 33 meter

A visual comparison between the hexagonal with a diameter of 37.5 meter and a circular GBF with a diameter of 33 meter is given in Figure 6-8. The hexagonal base slab needs a large foundation area, this is due to the less efficient geometry regarding stability. Another reason is the slightly higher center of gravity due to the tower which is constructed from base slab to the top.

Because the construction and transportation method interact with each other no decision is made on the circular or hexagonal design. At chapter 7 the most optimal combination is chosen.

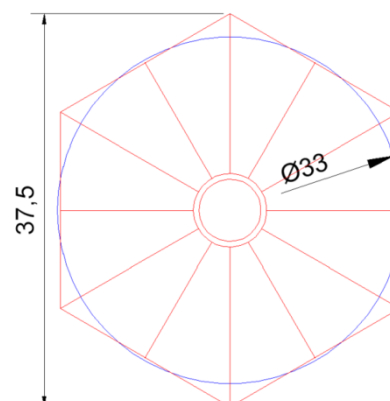


Figure 6-8 - Hexagonal and circular base slab

## 6.5 CONSTRUCTION PLANNING

A choice is made for the type of formwork which is applied to cast concrete:

- Bottom slab: Traditional formwork
- Cylindrical part: Gliding formwork
- Internal walls: System formwork
- Internal cylinder: Gliding formwork

Due to the large number of GBFs it is assumed that the purchase of a couple of gliding formworks is profitable comparing to applying system of traditional formwork. The amount of reinforcement steel is calculated using 175 kg/m<sup>3</sup>.

Structural element	Volume of concrete [m <sup>3</sup> ]	Volume per meter height (Gliding formwork) [m <sup>3</sup> /m]	Steel [kg]
<b>Base slab</b>	1553	-	271,775
<b>Outer wall</b>	1137	66.45	198,975
<b>Inner walls</b>	447	-	78,225
<b>Inner cylinder</b>	426.9	9.42	74,708
<b>Total</b>	<b>4373</b>	-	<b>623,683</b>

The following starting points are used to create a planning:

- Concrete casting: 100 m<sup>3</sup>/hour
- Gliding formwork: 15 cm/hour

The first step is to construct the base slab. The formwork is applied and this takes 3 weeks. After the first week the reinforcement is started to braid and takes 3 weeks. The base slab has a volume of 1553 m<sup>3</sup>, therefore the casting is performed in two days. After three days of hardening the concrete has a compressive strength of 36.5 N/mm<sup>2</sup> and then the preparation of the gliding formwork is applied. The compressive strength in time can be calculated according the formulas given in Annex G. The preparation of the formwork takes one week for the internal cylinder and two weeks for the outer cylinder. The casting has a vertical speed of 15 cm/hour

which is a concrete usage for the outer walls  $10.0 \text{ m}^3/\text{hour}$  and for the inner cylinder  $1.4 \text{ m}^3/\text{hour}$ . With the speed of  $15 \text{ cm}/\text{hour}$  the outer cylinder is casted in 5 days and the inner cylinder in 14 days. The removing of the formwork requires for both gliding formworks 7 days. Then again a hardening period of 7 days is implemented before the internal walls are placed. The placement of these internal walls is done by system formwork. The system formwork is lifted over the outer cylinder and placed. The six walls are casted and this will take 21 days. The planning is included in Figure 6-9.

Then the GBF is finished and can be transported into the water. The total planning for constructing a GBF takes 19 weeks and 1 week is reserved to transport the GBF and restore the area for the next one, so 20 weeks is used.

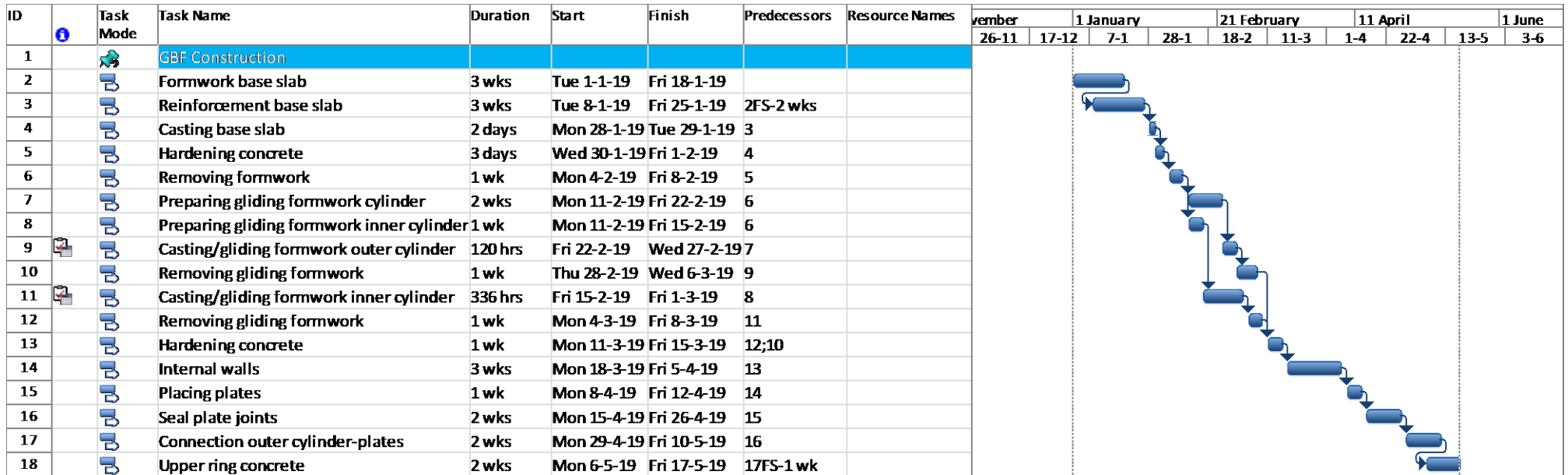


Figure 6-9 - Construction planning of GBF

## 6.6 CONCLUSION HEXAGONAL DESIGN

Regarding the two construction plannings given in Figure 5-10 and Figure 6-9 the following results are obtained:

- With the hexagonal GBF design no traditional formwork is needed to construct the cone. With the circular GBF design this formwork must be applied by workmen at large height.
- The tower part is constructed with a gliding formwork, this reduces the construction actions on large height.
- The construction time of a hexagonal GBF design reduce the construction time with 6 weeks (23%) per GBF.
- The amount of material needed is approximately  $558\text{m}^3$  (13%) more for the hexagonal design.

Because the construction and transportation are not independent on each other a choice can be made for the design for developing a new transportation method. The best combination of construction method and transportation method is developed in the next chapter where the next 3 design method steps are considered.

## Chapter 7: TRANSPORTATION AND CONSTRUCTION METHOD

With the design of two different GBF designs in chapter 5 and chapter 6 we end up with one design which is the most materialefficient and the other one which has a better constructability and therefore a smaller construction time. Now the question is how the GBFs can be constructed and can be transported from the quay wall into water. In the design method this is indicated in Figure 7-1 in blue. The GBF-properties which are described in chapter 5 and 6 are used as input to design the most optimal construction and transportation method. Because for this chapter more solutions are present the full secondary design method is applied.

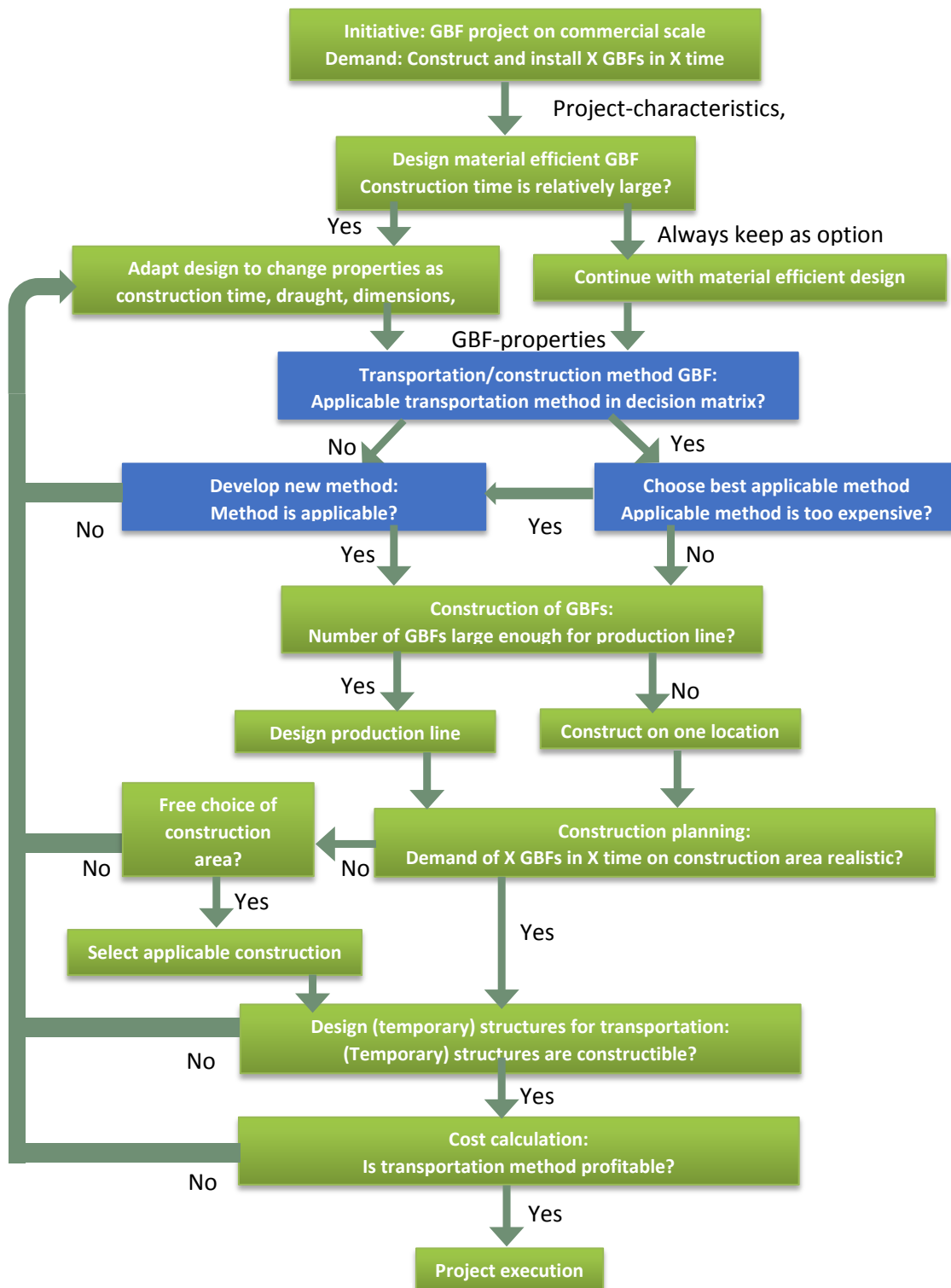


Figure 7-1 – Chapter 7 indicated in design method

After designing the GBF and develop the construction method of the GBFs the transportation method must be chosen to transport the GBFs from the quay wall into the water. In this chapter first the characteristics of the case study and GBF design are applied on the decision matrix and a cost estimation is performed. Then an alternative transportation method is designed for which a brainstorm session is executed. At the end of the chapter the most appropriate transportation method is chosen.

## 7.1 APPLYING THE DECISION MATRIX

In paragraph 2.4 at page 13 the main transportation methods are given for transportation on land and from land into water. In this chapter also the decision matrix is given which is developed in Annex A. With the construction of GBFs for offshore wind turbines at commercial scale the decision matrix can be used to check which construction and transportation methods could be applicable. The project characteristics of an offshore wind farm on commercial scale are as follows:

- Dimensions of GBF: <50x50m
- Draught of GBF: >10m
- Weight: 5000-15,000 ton
- Number of elements: >20
- Level of existing infrastructure: High

Applying these project characteristics the table can be reduced as displayed in Table 7-1. The project characteristics are indicated with red circles.

Construction method	Dimensions up to Length x Width [m x m]			Draught of element [m]			Weight [ton]			Number of elements			Level of existing infrastructure		Casting independent on weather conditions
	<50x50	50x50-150x75	>150x75	<5	5-10	>10	<5,000	5,000-15,000	>15,000	<10	10-20	>20	Little	High	
Factory	✓	✓	✓	✓	✓	✗	✓	✓	✓	✗	✗	✓	✗	✓	+
Casting basin	✓	✓	✓	✓	✓	✗	✓	✓	✓	✓	✗	✗	✗	✓	-
Syncrolift	✓	✓	✗	✓	✓	✗	✓	✓	✓	✗	✓	✓	✓	✓	-
Semi-submersible vessel	✓	✓	✓	✓	✓	✓	✓	✓	✓	✓	✓	✓	✓	✓	-
Dry dock	✓	✓	✓	✓	✓	✗	✓	✓	✓	✓	✓	✗	✗	✓	-
Floating dock	✓	✓	✗	✓	✓	✓	✓	✓	✓	✓	✓	✗	✓	✓	-
Building on pontoons	✓	✗	✗	✓ <sup>(1)</sup>	✓ <sup>(1)</sup>	✓ <sup>(1)</sup>	✓	✓	✓	✓	✗	✗	✓	✓	-
Land based crane	✓	✗	✗	✓	✓	✓	✓	✗	✗	✓	✓	✓	✓	✓	-
Heavy lift vessel	✓	✓	✗	✓	✓	✓	✓	✓	✗	✓	✓	✗	✓	✓	-

(1): Depends on available dimensions of sluices in the proximity

Table 7-1 - Decision matrix applied on project with GBF

Because the decision matrix could have some exceptions some remarks are made to each construction method.

- **Factory:**  
A factory with the use of one or two basins is not applicable due to the large draught of the element. The basins will have very long slopes and therefore need a large area which is not present at the port. Built a factory in the neighbourhood may cause problems with the available draught. Often the water level outside the factory basins is insufficient, a water depth of more than 10 meter occurs not often close to the border of a water body.
- **Casting basin:**  
The option of a casting basin is not applicable because of the large depth and therefore a large area is needed. Because of the high number of elements several batches are needed and this will increase the cost rapidly. Often the water level outside the basin is insufficient, a water depth of more than 10 meter occurs not often close at the water line.

- Syncrolift:  
The syncrolift is not applicable without adaptations because the draught of the element is large. The construction site is at the REBO Offshore Terminal where the guaranteed depth in front of the quay wall is 8 meter. Due to the tide the construction of a syncrolift could be possible but the channel must be deepened and a check must be performed to ensure stability for the existing quay walls. Also an analysis on the water levels must be performed to check if the water depth is sufficient in a certain time period. A main disadvantage is a fixed construction in front of the quay wall. Therefore this option is excluded and is not feasible.
- Semi-submersible vessel:  
As indicated in the decision matrix the use of a semi-submersible vessel is possible. Due to the large number of elements and the timeframe of the project the costs for the semi-submersible vessel are large.
- Dry dock:  
The draught of the elements is too large for the majority of the dry docks. Only 25% of the dry docks available worldwide have a draught of 12 meter or larger, see Figure A-20 in Annex A. A second note is the number of elements. With the use of a dry dock several batches are needed and this will increase the time and the cost needed to construct the GBFs.
- Floating dock:  
A floating dock is an option to execute the project. However, due to the large number of elements several batches are needed and the costs of a floating dock are high. This option seems not to be cost-efficient.
- Building on pontoons:  
Constructing the GBFs on pontoons seems to be impractical. 64 GBFs are needed and therefore a large number of pontoons and area at the port are needed.
- Land based crane:  
The use of a land based crane to lift the GBF from the quay wall into the water is impossible due to the large weight. Obviously land based cranes can be used to lift smaller elements of a caisson in the construction method.
- Heavy lift vessel:  
The use of a heavy lift vessel is possible but there are only two heavy lift vessels in the world which can lift the GBFs, see Figure A-14 in Annex A. Due to the large number of elements the timeframe when a heavy lift vessel is needed is very large and this will increase the cost to a very high level.

The use of a semi-submersible vessel seems to be the only transportation methods possible. At a reference project of the Tuas port expansion, described in Annex A this solution is also chosen where the caisson properties are quite similar. The GBFs are constructed on the quay wall and can be transported to the semi-submersible vessel, which is berthed at the quay wall. A relatively small semi-submersible vessel could be used to submerge the GBFs due to the relatively small dimensions to other caisson types. However due to the large draught a lot of small semi-submersible vessels are not applicable which increases the cost.

There are two possibilities for executing the transportation method with a semi-submersible vessel with a production of a large number of GBFs:

- Storage area at construction area
- Storage area in water

### Storage area at construction area

The costs for renting a semi-submersible for a GBF with a diameter of around 35 meter and a draught of 11.2 meter are 20,000 €/day, see Table 7-2. This is excluding operational costs and these must be added to calculate the total cost per day. A technical document of the applicable semi-submersible vessel is included in Annex I. With the requirement of installing the offshore wind farm in two years the following estimation is done:

- Rental period of two full timeframes from 1 April till 1 October (install window)
- Preparation works on vessel of 20 days per timeframe
- Removing works on vessel of 20 days per timeframe

In total the renting days of the semi-submersible vessel are:

$$d_{rent} = d_{rent,year1} + d_{rent,year2} = (20 + 183 + 20) + (20 + 183 + 20) = 446 \text{ days} \quad (46)$$

Where:

$$d_{rent,year1} = \text{Total rental days for installation window 1 [days]}$$

$$d_{rent,year2} = \text{Total rental days for installation window 2 [days]}$$

The costs of renting a semi-submersible vessel consist of several cost items. In Table 7-2 the rental costs for a semi-submersible vessel are estimated. Because the mobilization costs are unknown because the rental firma is not known these costs are not included.

Category	Sub-category	Amount	Cost	Period	Cost	
<b>Rental cost</b>		1 (Semi-sub)	€ 20,000	(per day)	446 (days) € 8,920,000	
<b>Crew cost</b>	Project manager	1 (men)	€ 80	(per hour)	3568 (hours) € 285,440	
	Engineer	1 (men)	€ 70	(per hour)	3568 (hours) € 249,760	
	Deckhand	2 (men)	€ 30	(per hour)	3568 (hours) € 214,080	
<b>General preparatory works</b>		2 (periods)	€ 100,000	(per period)	- - € 200,000	
<b>Maintenance and repair</b>			€1500	(per day)	446 (days) € 669,000	
					<b>Total</b>	<b>€ 10,538,280</b>
					<b>Total per day</b>	<b>€ 23,628</b>

Table 7-2 - Cost estimation semi-submersible vessel with storage area at construction site

The result is a total cost of 10.5 million euro to use a semi-submersible vessel.

### Construction area in the water

Because of the large number of GBFs and the large area needed, is it presumable that the storage area must be designed in the water. In this case the semi-submersible vessels must be rented a longer period. It is assumed that the semi-submersible is in operation from that the first hexagonal GBF is constructed, which is the upper limit for renting the semi-submersible vessel. The construction of the hexagonal GBF takes 20 weeks.

$$d_{rent} = d_{rent,year1} + d_{rent,year2} = (365 - 20 \cdot 7) + (365) = 590 \text{ days} \quad (47)$$

The costs of renting a semi-submersible vessel by using a storage area in the water are shown in Table 7-3. The total costs are in this case 13.8 million euro.

Category	Sub-category	Amount	Cost	Period	Cost	
<b>Rental cost</b>		1 (Semi-sub)	€ 20,000	(per day)	590 (days) € 11,800,000	
<b>Crew cost</b>	Project manager	1 (men)	€ 80	(per hour)	4720 (hours) € 377,600	
	Engineer	1 (men)	€ 70	(per hour)	4720 (hours) € 330,400	
	Deckhand	2 (men)	€ 30	(per hour)	4720 (hours) € 283,200	
<b>General preparatory works</b>		1 (per-iods)	€ 100,000	(per period)	- - € 100,000	
<b>Maintenance and repair</b>			€1500	(per day)	590 (days) € 885,000	
					<b>Total</b>	<b>€ 13,776,200</b>
					<b>Total per day</b>	<b>€ 23,349</b>

Table 7-3 - Cost estimation semi-submersible vessel with storage area in water

The total costs are 10.5 or 13.8 million euro depending on the storage area location. This is a large amount of money and therefore it is tried to found an alternative transportation method to transport the GBFs from land into water is developed.

## 7.2 PROGRAM OF REQUIREMENTS

Because the solution with a semi-submersible vessel is in first instance rejected a new method is developed. To develop a new method to construct and transport the GBFs from land into water the following requirements are formulated:

- The construction of eventual (temporary) structures which able the transportation must be constructible and may not have a large impact on the surroundings: harbor, shipping traffic, no exceptional noise level and small amount of air pollution, small area use.
- The amount of material use of the (temporary) construction must be as low as possible
- The reusability of the (temporary) construction or materials is a positive aspect.
- It is desirable to leave the area in the original state after the execution of the project.
- The required space on the construction area to construct and transport the GBFs must be kept as low as possible.
- The transportation method is applicable to more type of caissons, when this is the case the flexibility for other caisson projects can reduce costs on comparable projects. The transportation structure can be used multiple times and the cost of construction can be divided on several projects.
- The transportation phase from land into the water may not take longer than the production rate of the GBFs.
- The risk of toppling over or falling down of a GBF during the transportation is not acceptable. This could cause injury and delay of the construction and transportation method.
- The availability of the transportation method must be high. The availability could depend on environmental factors as wind and high waves. Also during winter the executing of the transportation may go on if a storage area is used. With a low availability risks on delay are present.

With these requirements the evaluation of the different methods is performed by using a multi-criteria analysis. Because the construction and transportation is not fully apart from each other the possibility to do some minor adaptations on the construction method are possible.

### **7.3 BRAINSTORM SESSION**

Because the majority of the construction and transportation methods of Table 7-1 are not applicable and a semi-submersible vessel is expensive to use, a brainstorm session was organized to develop a new construction and transportation method. The results are five ideas to construct GBFs and transport them from land into water. For each method a choice is made to use the circular or hexagonal design. In this paragraph the ideas from the brainstorm session are described. Five main methods come out from the brainstorm session and these methods are described with the use of some basic drawings and description.

Methods:

- 1) Slipway
- 2) Prefab fabrication method
- 3) Prefab fabrication on quay wall, completion on water
- 4) Construct GBF on quay wall and lift it with portal crane
- 5) Immersion structure

On the next pages a description of each method is given with some basic drawings, dimensions and quantities are a first estimation and will change in all probability.

### 7.3.1 Method 1: Slipway

The first method uses a slipway to transport the GBFs from land into water. On the quay wall a number of locations are chosen to construct the hexagonal GBFs. The hexagonal design is chosen because of the less construction time and the lower risks on delay. The GBFs are built on a plateau that is placed on several skidding beams. On the quay wall a network of skidding beams is installed to transport the GBFs to the slipway, see Figure 7-2. On this slipway a platform is constructed to keep the GBF vertically, see Figure 7-3. The platform is moved into the water and when sufficient depth is available the GBF will float and can be towed to the immersion location. The number of building locations depends on the planning and the required amount of constructed GBFs per week.

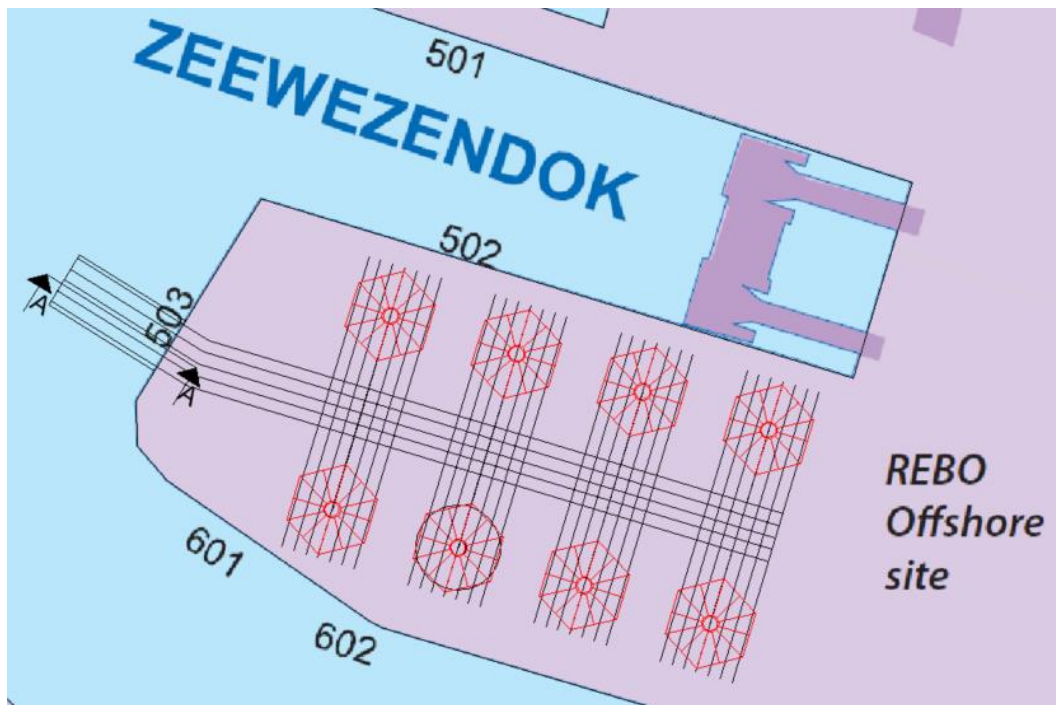


Figure 7-2 - Top view method 1

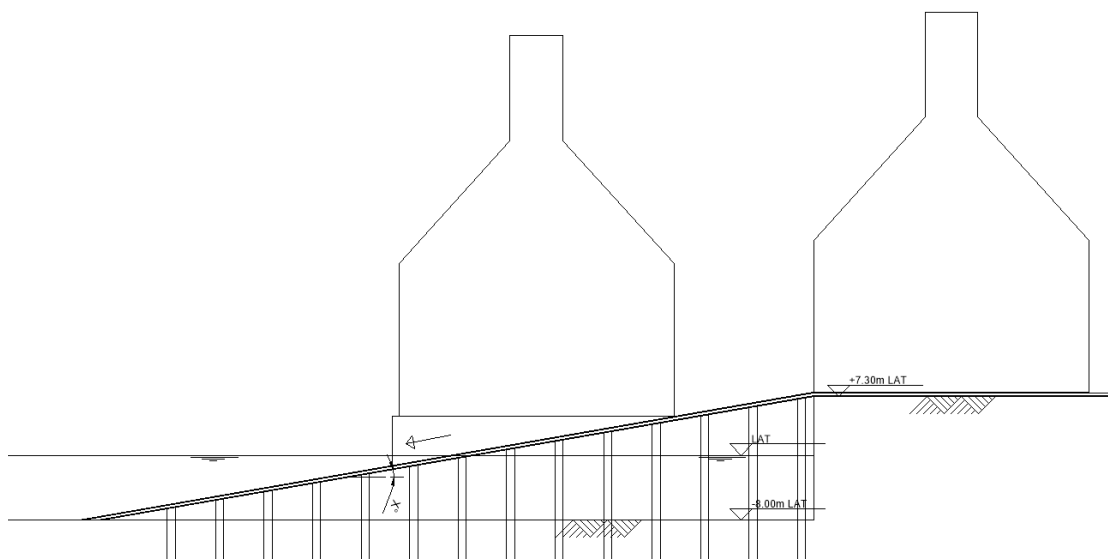


Figure 7-3 - Cross-section A-A Method 1

### 7.3.2 Method 2: Prefabrication method

In the prefabrication method the GBF is divided in four elements. The circular design is chosen because this design is more material efficient and the parts are prefabricated on multiple locations and now the conical part and tower do not have to be constructed on large heights. These parts are constructed on the quay wall and are connected to each other in a later stage, while floating in the Zeewezendok.

The GBFs are built in four pieces on the quay wall as can be seen in Figure 7-4:

- Bottom slab with short cylindrical part (grey)
- Cylindrical part and internal walls (blue)
- Conical part (green)
- Tower (red)

On the bottom slab a cylindrical part is constructed to create enough buoyancy to float when this part is lifted into the water. When this part is lifted in the water a second piece, the remainder cylindrical part and internal walls is installed on the bottom slab. Then the GBF is towed to the second location in the Zeewezendok where the conical part is lifted on the GBF. At last the GBF is towed to the third location where the tower is fixed on the GBF. The GBF now can be towed to the immersion location or to a storage location.

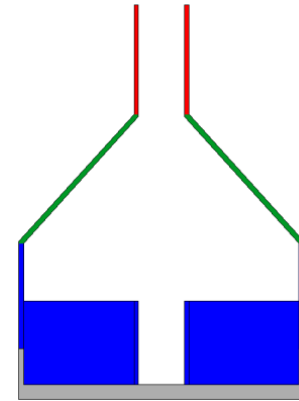


Figure 7-4 - Construction parts in production line

With this construction method the GBF can be lifted in different parts to reduce the lifting capacity of the equipment and the capacity of the storage area and quay walls of the REBO Offshore Site.

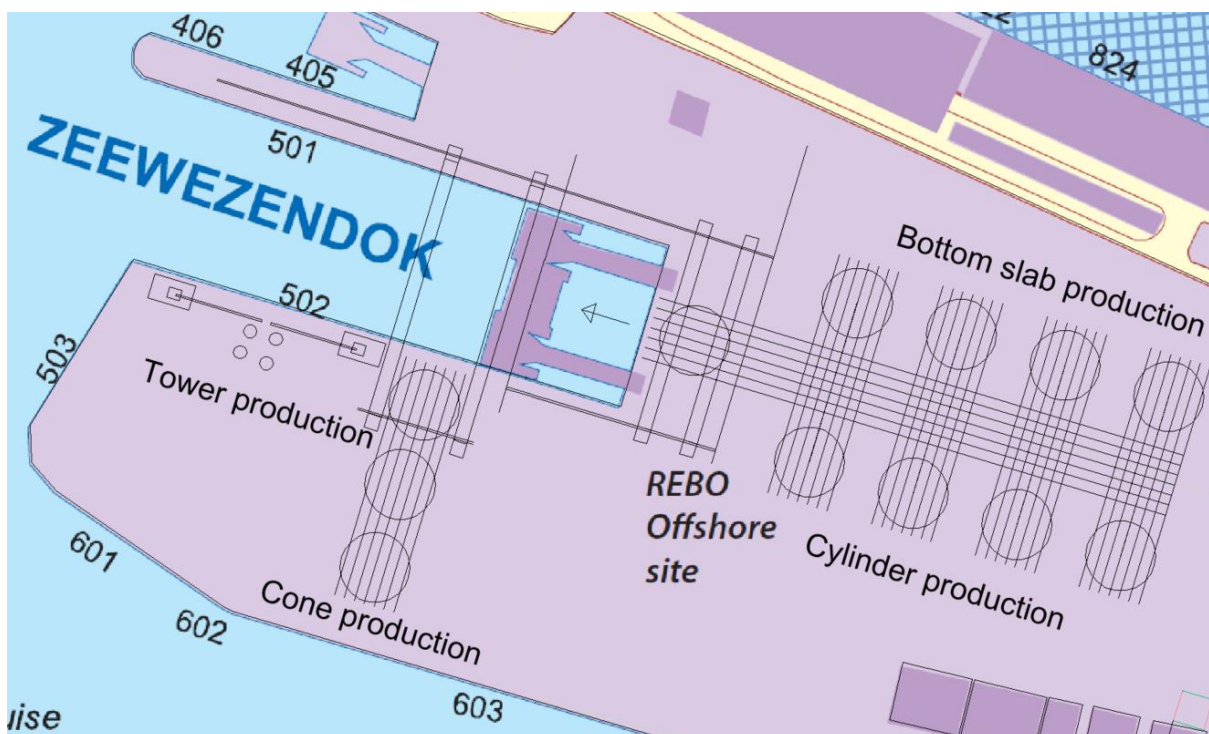


Figure 7-5 – Top view method 2

### 7.3.3 Method 3: Prefabrication on quay wall, completion on water

For this method the circular design is chosen because the weight of the plates to close the hexagonal GBF is too large to lift from the quay wall onto the GBFs in the water. The horizontal distance is too large to fulfil the lifting action with usual equipment.

The production of the bottom slab, with a part of the cylindrical part is indicated in Figure 7-6. After constructing the bottom slab it is transported by skidding beams to the portal crane where the elements are lifted and placed in the water where they float. The elements are completed on water where formwork is applied and concrete is casted. Within this method there are two options of execution:

- Method 3a:  
The minimal height of the cylindrical part is calculated to make it possible to immerse the GBF in the Zeewezendok. The top of the cylindrical part must be higher than the highest water level. The immersion is done to stabilize the element that it is fixed and will not sway and move. The working activities, like concrete casting are easier to execute when the element is not moving. When the GBF construction is finished the ballast is pumped out of the GBF and it is transported to the final immersion location.
- Method 3b:  
The cylindrical part is just set to make it possible to generate sufficient buoyancy. The element is floating and the further construction is executed. This saves costs for placing a gravel bed in the Zeewezendok.

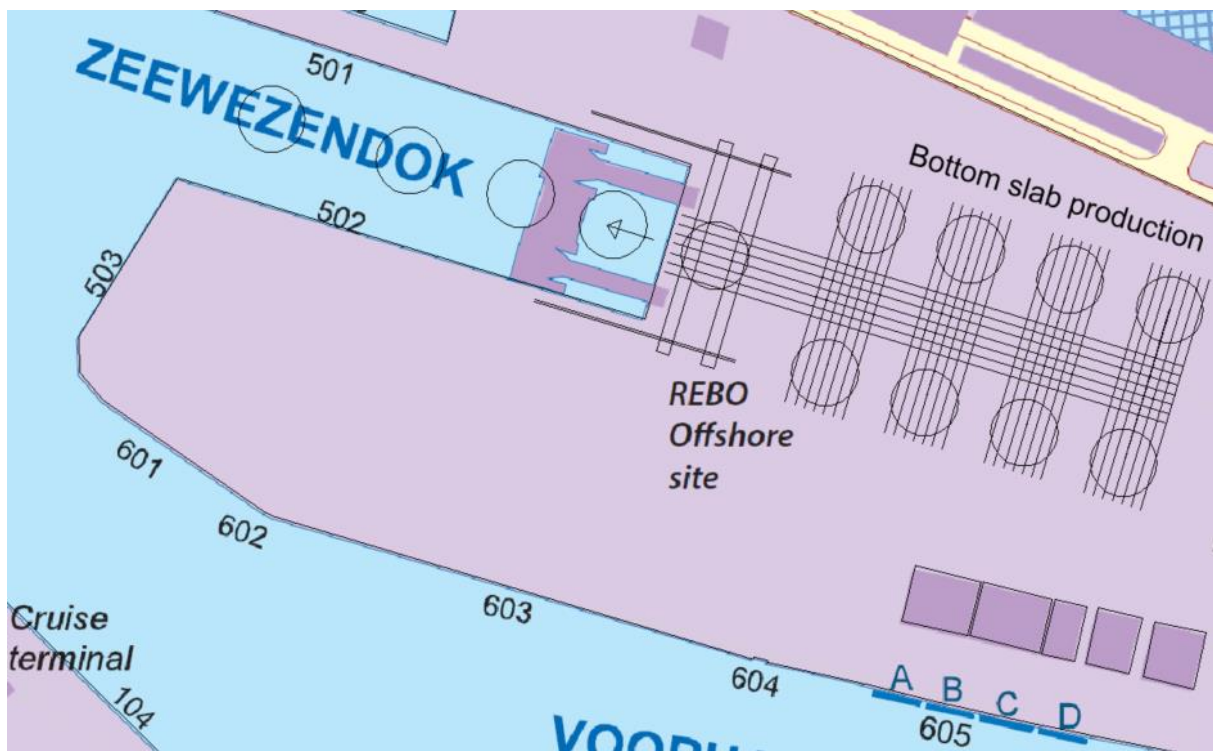


Figure 7-6 - Top view method 3

### 7.3.4 Method 4: Construct GBF on quay wall, lift action with portal crane

The GBFs are completely built on a platform on the skidding beams at the storage area. The GBFs are built according the hexagonal design to reduce the construction time. The GBFs are transported by the skidding beams to the portal crane. The portal crane lifts the GBF to the Zeewezendok, see Figure 7-7, Figure 7-8 and Figure 7-9. From there the GBF is towed to the final location.

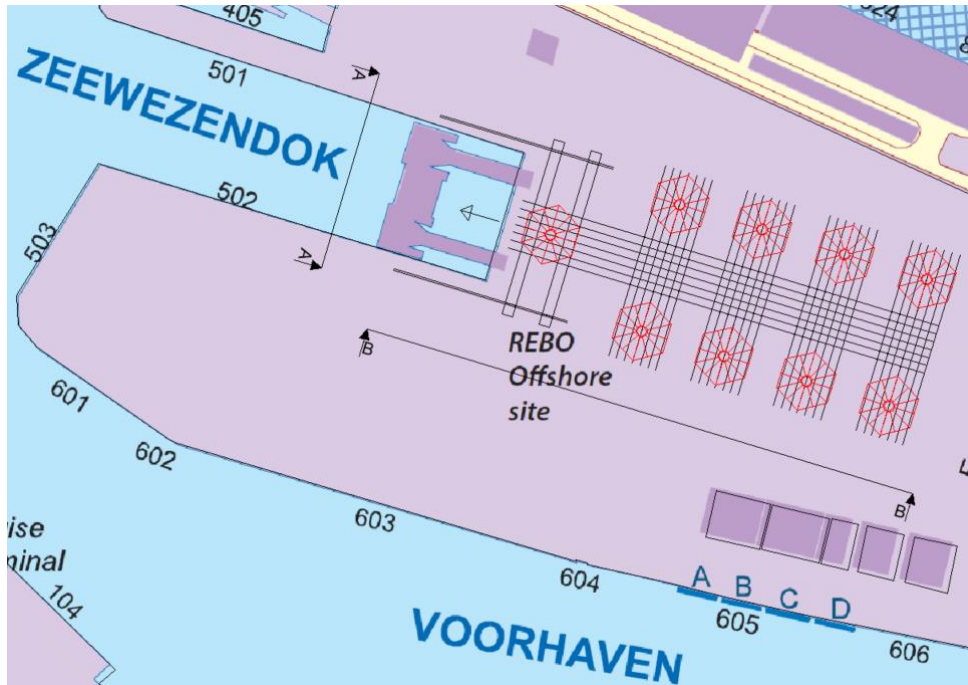


Figure 7-7 - Top view method 4

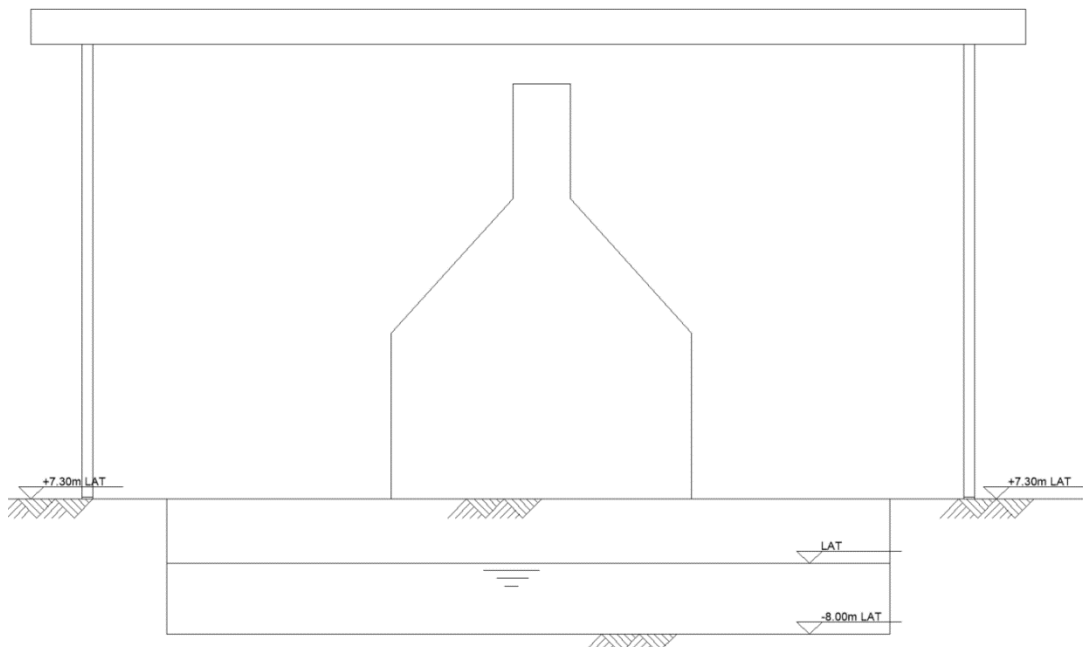


Figure 7-8 - View A-A method 4

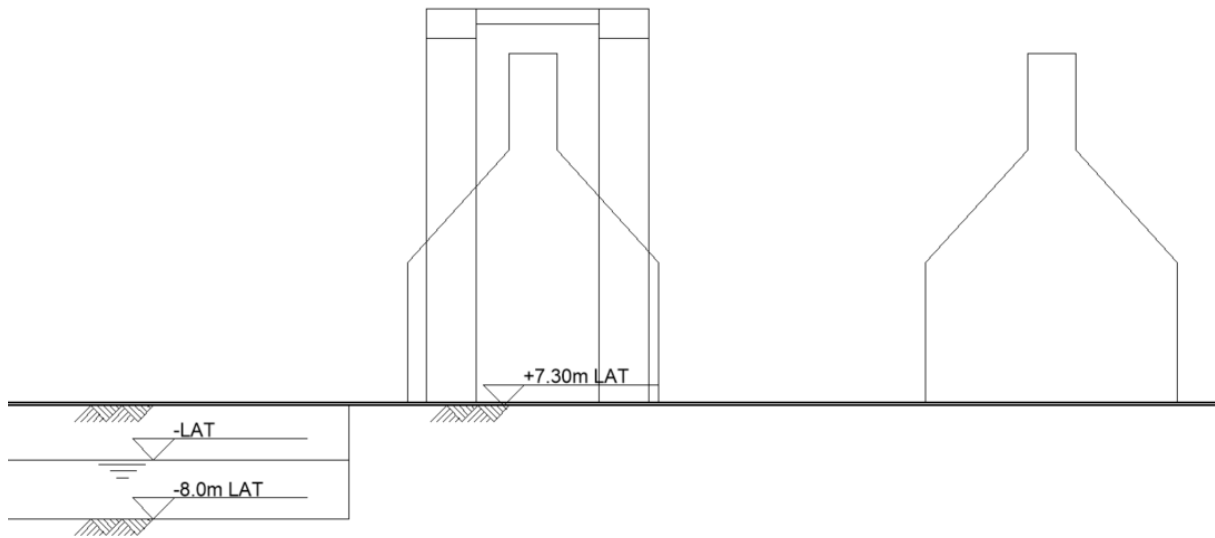


Figure 7-9 - Cross-section BB method 4

### 7.3.5 Method 5: Immersion platform

The GBFs are constructed on platforms on skidding beams. A choice is made to use the hexagonal design for a better constructability and lower construction time. When a GBF is fully constructed it is transported by skidding beams to the immersion platform. This platform is able to bear the deadweight of the GBF and can be immersed. The available depth at the quay walls is -8.0m LAT and therefore a deepening as displayed in Figure 7-11 might be needed. When the GBF floats above the immersion platform it can be towed to the immersion location at sea.

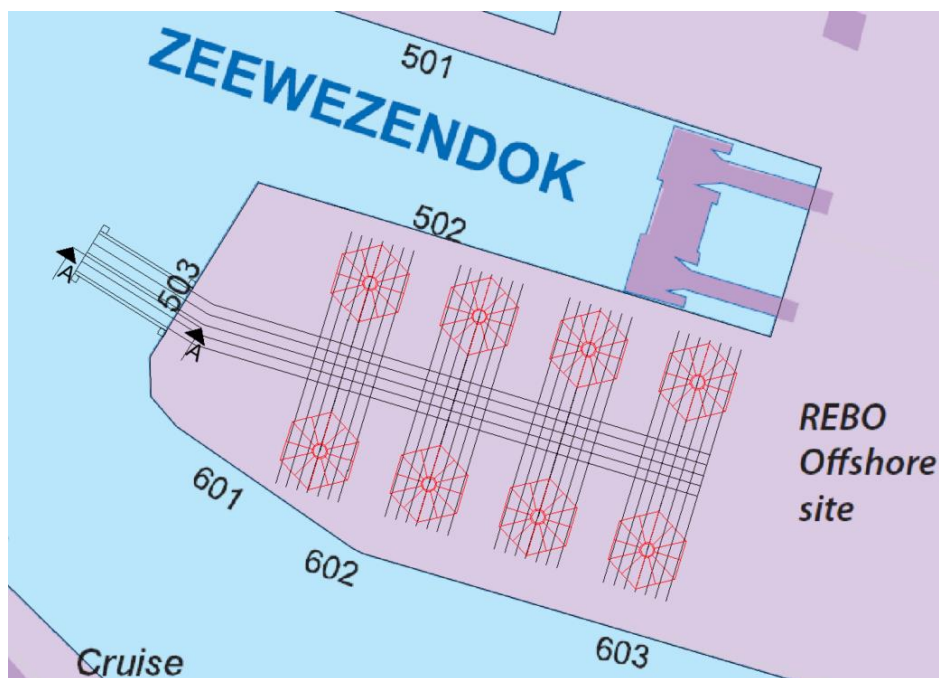


Figure 7-10 - Top view method 5

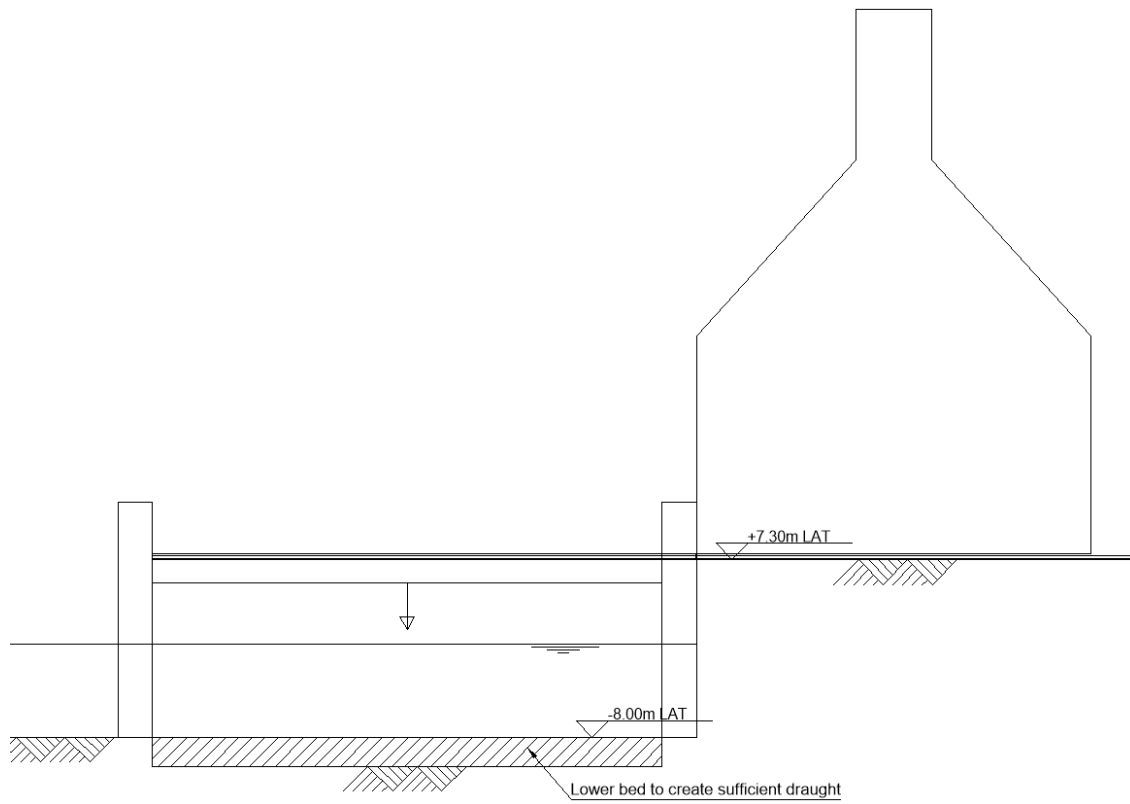


Figure 7-11 - Cross-section A-A method 5

## 7.4 APPLICABILITY OF THE NEW METHODS

The simulation phase is executed in this paragraph, the proposed methods from the brainstorm session are reviewed. The main question is if the proposed methods are feasible and could comply with the demands and boundary conditions.

For each method a short simulation is given. In each simulation the main functions of the transport process and some constructive elements are given to determine the constructability.

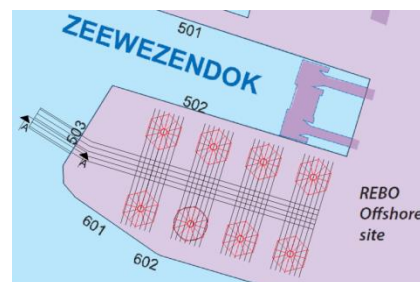


Figure 7-12 - Top view method 1

### 7.4.1 Method 1: Slipway

For this method two main transport actions are present, the transport on land by skidding beams and the transport from land to the water with a slipway construction, see Figure 7-12. The transport on land is executed with skidding beams, the main properties are described in paragraph 2.4.1.2 on page 14. The slipway construction with the main properties is described in this paragraph.

#### 7.4.1.1 Slipway construction

The slipway construction is displayed in Figure 7-13. The most important parameter of the slipway construction is the length of the construction. The shorter the length of the slipway the less cost the construction has and the less impact this construction has on the port activities.

The angle of the slipway must be as large as possible but then the platform to keep the GBF vertically will be higher, see Figure 7-13.

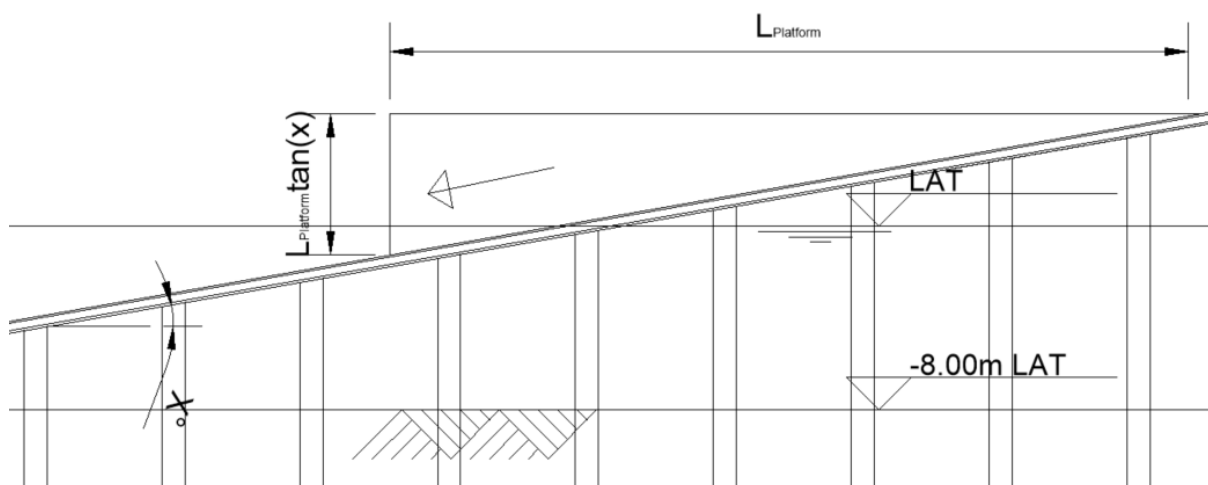


Figure 7-13 - Dimensions slipway platform

Due to the limited water depth the angle of the slipway construction could not be too large. A minimal draught of 11.21 meter is needed. To comply with 3 GBFs immersing a week the probability that the GBF will float from the platform with high water must be 20%. As can be seen from Figure 4-13 on page 31 this is a water height of +5.15m LAT. This gives a total available water depth of 13.15 meter. Subtracting the minimal draught plus 0.5 meter keel clearance the result is 1.44 meter. In Figure 7-14 the height of the slipway platform is plotted according the formula:

$$H_{platform} = L_{platform} \cdot \tan(x) \quad (48)$$

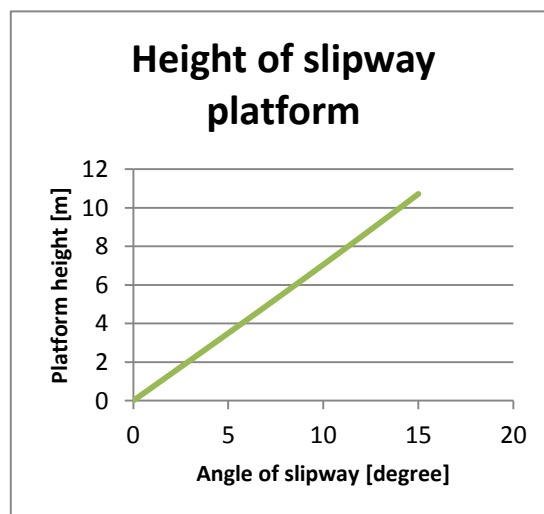


Figure 7-14 - Height of slipway platform with L=40m

Rewriting the formula the maximum angle can be determined and is 2.1 degrees. Now the length of the whole slipway construction can be determined and is 326 meter.

The forces on the slipway construction are indicated in Figure 7-15. With a GBF weight of around 10,000 tons the angle has a large influence on the parallel force on the slipway. With an angle of 2.1 degrees as calculated above this result in a parallel force of 3.6 MN.

Another option could be to construct the slipway further under water that the top of the platform is at the bottom level and a much smaller slipway construction is needed. In that case a large deepening in the port is needed and the constructability decreases. The forces on the rail of the slipway platform also increase, see Figure 7-15. Another problem is that with a larger angle the platform height also increases and the depth of the deepened part also, which cause rise in costs and sediment problems. The deepened part will be filled with sediment transport. This option seems not feasible and is therefore not seen as an option further in this report.

To construct this slipway construction there are some difficulties. The construction causes a lot of hinder in the port of Oostende. Due to the large dimensions there are a lot of sheet piles needed and the risk of a ship collision on the construction pit is very high because the construction pit is in the middle of the turning circle of the port. The slipway is at least 326 meter long and therefore the construction of the slipway is a difficult operation.

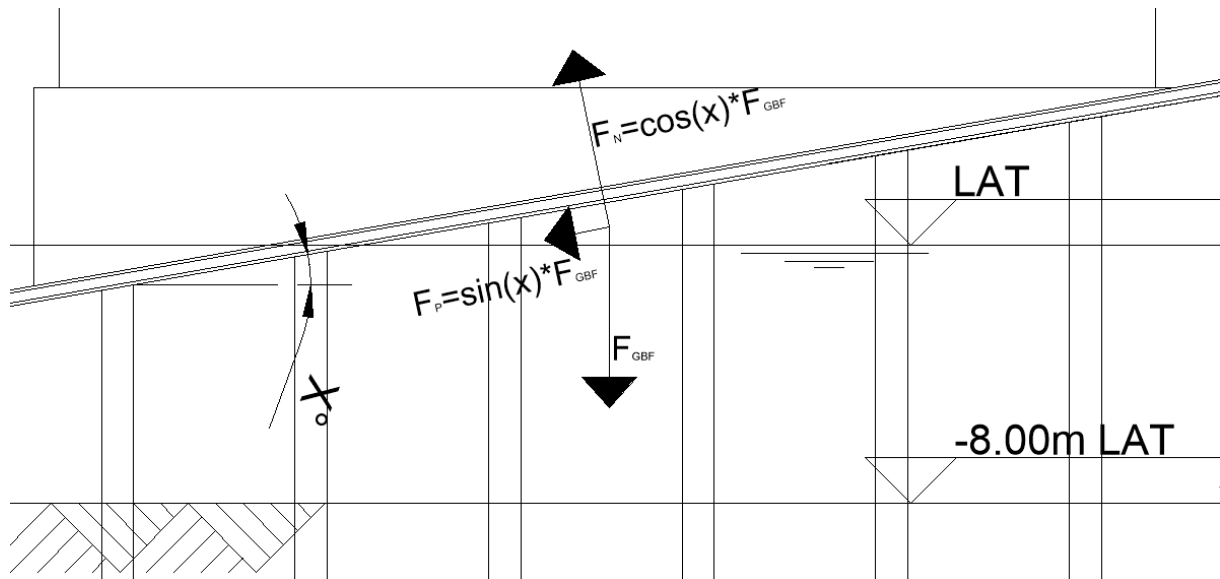


Figure 7-15 - Forces on the slipway construction

## 7.4.2 Method 2: Prefabrication method

In this method the GBFs are produced in four different elements. The original design is used because the cone production in this method causes no major problems.

### 7.4.2.1 Construction of GBF element

In the prefabrication method the GBF is divided in four elements:

- Bottom slab + part of cylinder
- Cylindrical part
- Conical part
- Tower

These four elements are built on the REBO area see Figure 7-16. The weights of these parts are given in Table 7-4. The first part is constructed till a height of 6 meter, one meter freeboard is available to avoid that

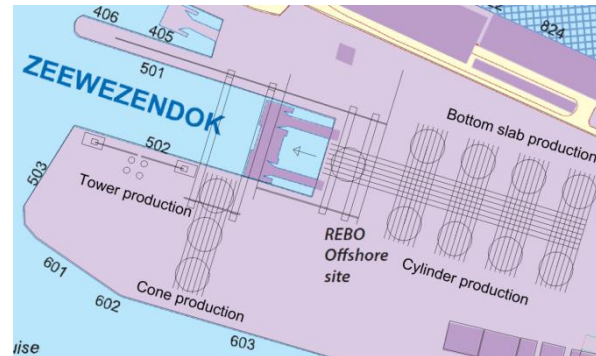


Figure 7-16 – Top view prefabrication method

water from waves flow in the GBF. The weight of the GBF till a height of 6 meter is, exclusive internal walls and internal cylinder, 4120 ton. With four hoisting points this is 10104 kN per hoisting point.

Part	Weight (D=33m) [ton]
<b>Bottom slab</b>	4120
<b>Cylindrical part with internal walls</b>	3645
<b>Conical part</b>	1728
<b>Tower</b>	294

Table 7-4 - Weights of GBF-parts

These concrete elements can be built with several techniques, for each part the most applicable techniques are chosen:

- Bottom slab: Traditional formwork
- Cylindrical part: Gliding formwork
- Conical part: Mall or traditional formwork
- Tower: Gliding formwork

Before estimating the construction times for the elements on the REBO site the area in the Zeewezendok is considered. The length of the dock is 250 meter long, therefore a maximum of 4 GBFs is assumed to be simultaneously in the dock. With a demand of 64 GBFs in two years a production rate of 0.6 GBFs per week is needed. This means that construction action in the Zeewezendok may not take longer than 1.67 weeks. Because climbing formworks on water has to be installed, used and removed this is hard to achieve.

### 7.4.2.2 Portal crane

With the weight, displayed in Table 7-4, the capacities of the two portal cranes and the land based cranes can be determined. The Portal cranes are modeled with the scheme, given in Figure 7-17 till Figure 7-20, the units are kilonewton and meters. Only the portal crane which lifts the base slab with the cylindrical part is displayed because this portal crane must lift the largest load. If this method appears to be the best method also the other cranes are worked-out.

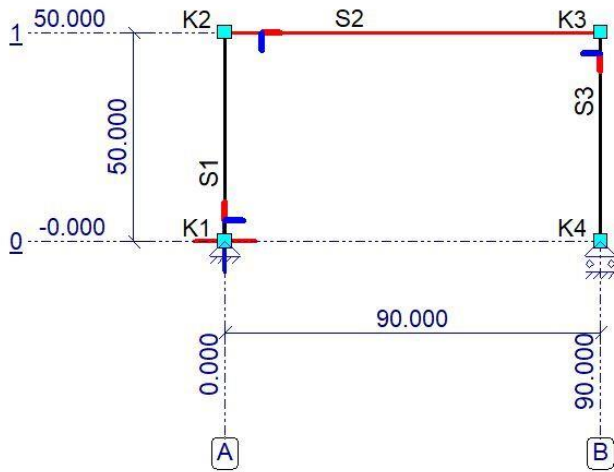


Figure 7-17 - Geometry of portal crane

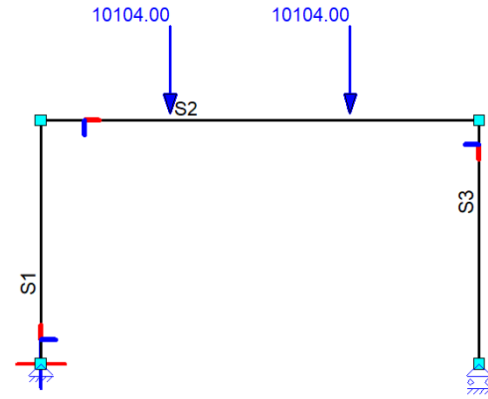


Figure 7-18 - Forces on portal crane



Figure 7-19 - Forces on foundation portal crane

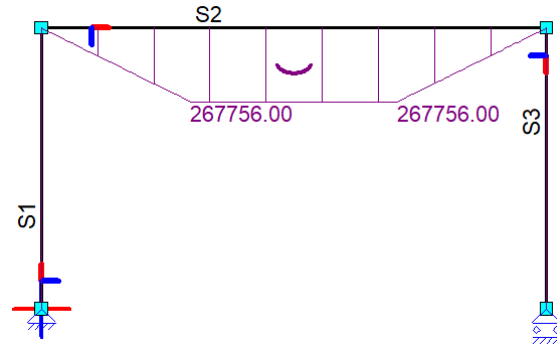


Figure 7-20 - Moment line portal crane

### 7.4.2.3 Land based cranes

The weight of the tower is very large for land-based cranes. The Demag AC 650 is one of the largest common All-Terrain cranes and has a capacity of 650 tons. However, this capacity is reached when the load is nearby the crane. The lifting capacities of this crane are displayed in Figure 7-21. To lift the tower on the GBF a minimal horizontal range of 20 meter is assumed at a height of 15 meters. The lifting capacity is around 100 ton and this is only one-third of the weight of the tower part. Lifting the tower on the GBF is therefore seen as impractical with land based cranes.

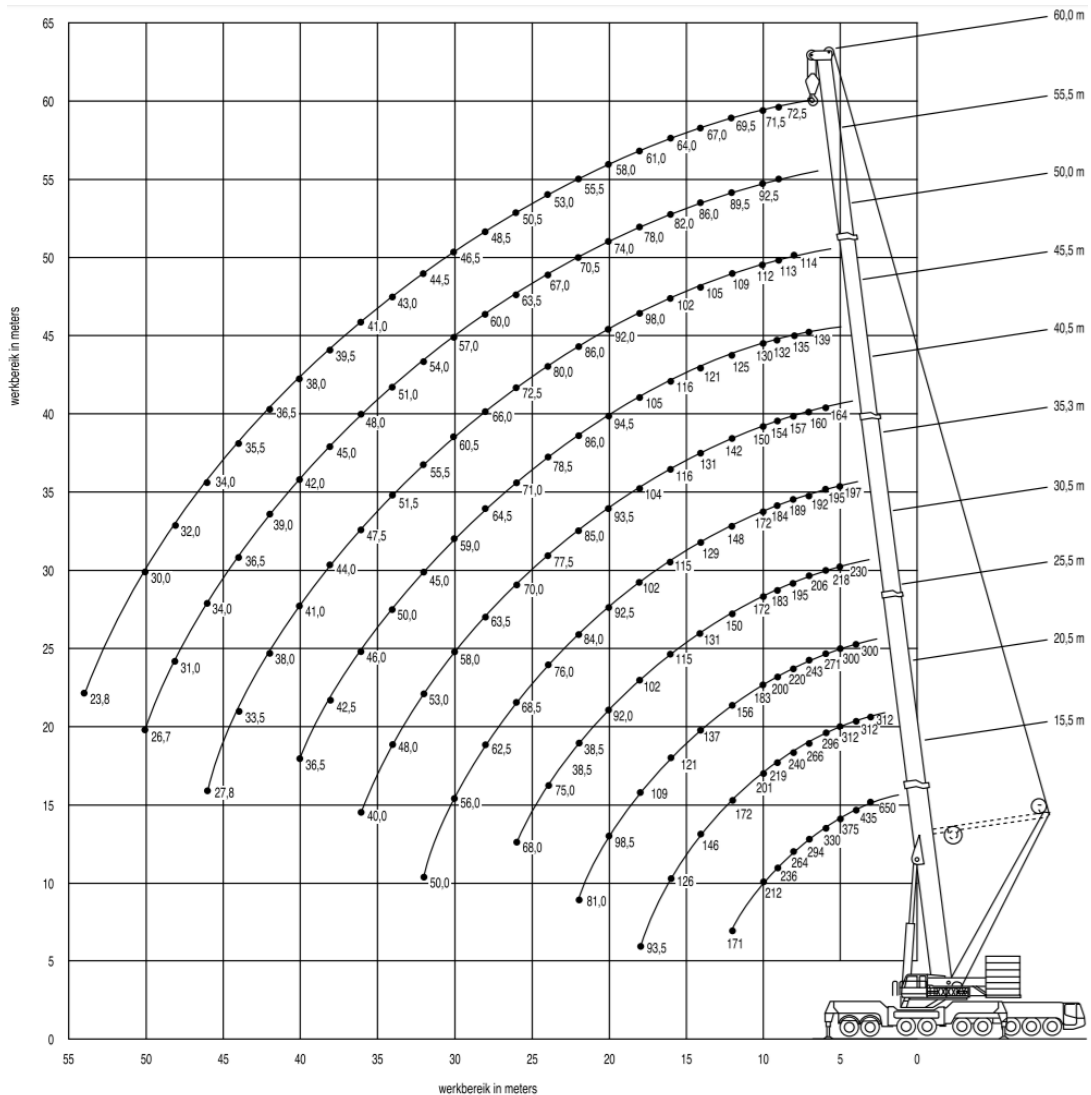


Figure 7-21 - Capacities and working range of Demag AC 650 (peinemann.nl)

### 7.4.3 Method 3: Prefabrication on quay wall, completion on water

In this method the construction of the bottom slab with a certain height of the cylindrical part are prefabricated on the quay wall. When the prefabricated part is constructed it is skidded to the portal crane where the GBF is lifted into the water.

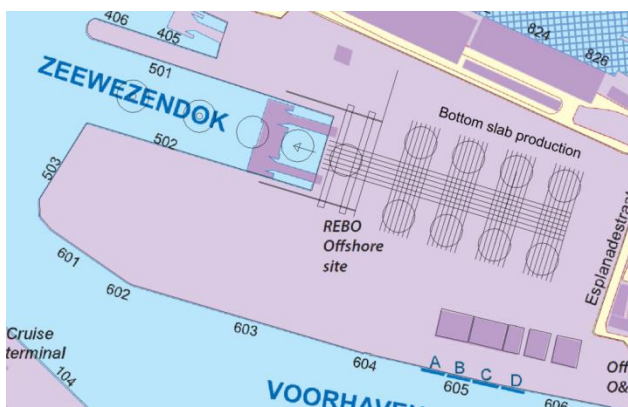


Figure 7-22 – Top view method 3

#### 7.4.3.1 Construction of GBF element

In this method two options are present to execute the construction of the GBFs. The GBF can be lifted into the water where the GBF is constructed while it is floating. The other option is to immerse the GBF and to finish it when it stands on the bottom. These methods are named method 3a and method 3b.

- **Method 3a:**  
The prefabricated part of the GBF must be constructed till a height that one meter freeboard is available in the floating phase to avoid that water is coming in the GBF from waves. This is a construction height of around 6 meter.
- **Method 3b:**  
The prefabricated part of the GBF must be constructed till a height that one meter freeboard is available when this element is immersed, in other words: The height of the element must be larger than the highest water level plus one meter. The highest water level is at +6m LAT see Figure 4-13 at paragraph 4.2.1.2.1. With a bottom level at -8m LAT the height of the element must be 15 meter. Because the cylindrical part ends at a level of 18.81 meter the choice is made to construct the GBF till 18.81 meter. To stop 3.81 meter before the end of the cylindrical part, lift it into the water and install the gliding formwork on water for the last 3.81 meter seems not practical.

The base slab is casted on the storage area and takes 6 weeks, see the planning in Figure 6-9. Then the cylindrical part must be casted and takes 3 weeks for method 3a and 2.5 week for method 3b. Then the elements must be lifted into the water. With a production rate of 0.6 GBFs per week six production lines at the REBO site are needed.

The number of production lines in the water with this method is limited. In the Zeewezendok 4 elements can be built simultaneously. With a required production rate of 0.6 GBFs per week a maximum allowable production time of 6.67 weeks is needed for 4 production lines. The conical part, the inner walls and inner cylinder must be constructed in these 6.67 weeks which is very hard, or even impossible, to achieve.

#### 7.4.3.2 Portal crane

The GBF must be lifted into the Zeewezendok by using a portal crane. The required lifting capacities are given in Table 7-5.

Lifting capacities	Weight (D=33m) [ton]
<b>Method 3a</b>	4120
<b>Method 3b</b>	5997

Table 7-5 - Lifting weights for method 3

These lifting capacities are high for portal cranes, especially with the span of 90 meter. The geometry of the portal crane, lifting forces, foundation reaction forces and moment line for method 3a are displayed in Figure 7-23 till Figure 7-26, the units are kilonewton and meters. For method 3b the same results are displayed in Figure 7-27 till Figure 7-30.

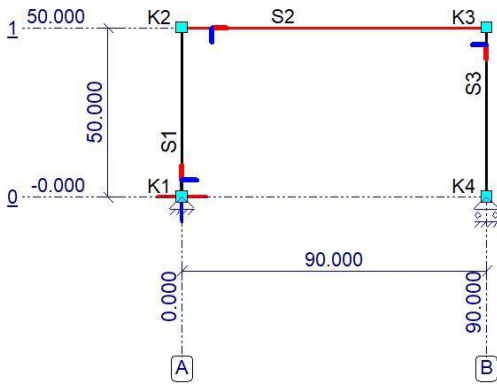


Figure 7-23 - Geometry of portal crane

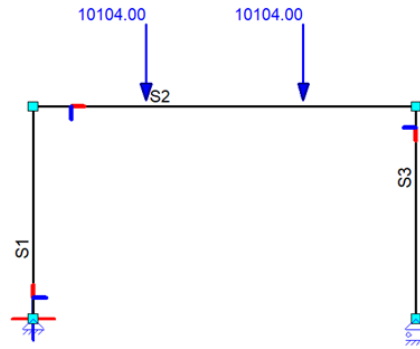


Figure 7-24 - Forces on portal crane method 3a



Figure 7-25 - Foundation forces method 3a

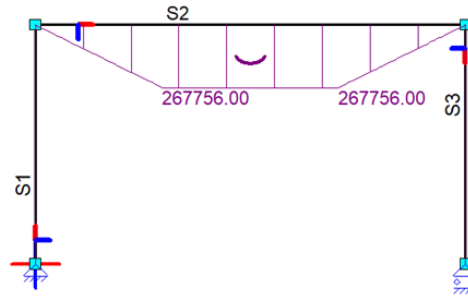


Figure 7-26 - Moment line method 3a

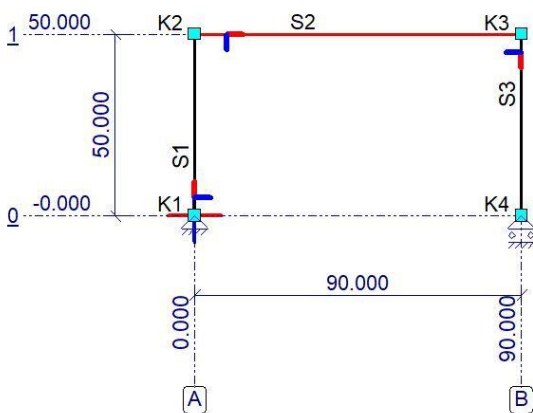


Figure 7-27 - Geometry portal crane

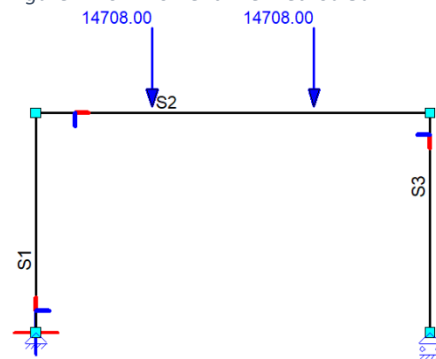


Figure 7-28 - Forces on portal crane method 3b

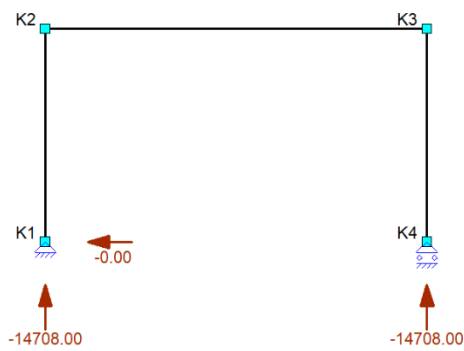


Figure 7-29 - Foundation forces method 3b

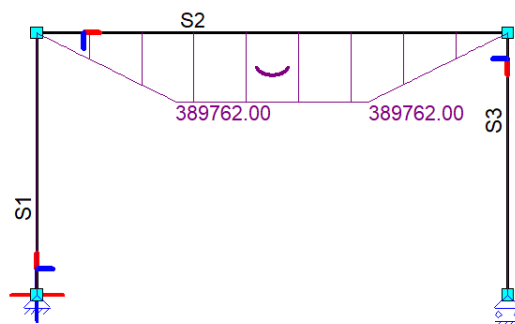


Figure 7-30 - Moment line method 3b

### 7.4.4 Method 4: Construct GBF on quay wall, lift with portal crane in water

In this method the GBF is fully constructed on the quay wall and the lifting operation is performed with a portal crane.

#### 7.4.4.1 Construction of GBF

See paragraph 5.5 for the construction time of 20 weeks per GBF. The conclusion is that 16 production lines are sufficient to construct and transport 64 GBFs from the quay wall into the water in the timeframe of two years, with applying the learning curve.

#### 7.4.4.2 Portal crane

The portal crane has to lift the complete elements from the quay wall into the water. The weight of the GBFs is 10,495 tons. This is a very large weight to lift, especially due to the large span of the portal crane which is 90 meters. The portal crane is modeled as a portal structure with two point loads which are in total the half of the total GBF weight, because there are two portal cranes to lift the total load. The weight induces the forces as displayed in Figure 7-32 till Figure 7-35, the units are kilonewton and meters. The foundation load is very high on the quay wall and a special foundation must be constructed along the rail construction of the portal crane. To construct this construction a huge investment cost must be done and a large part of the quay wall must be removed to construct the foundation of the portal crane.



Figure 7-31 - Top view method 4

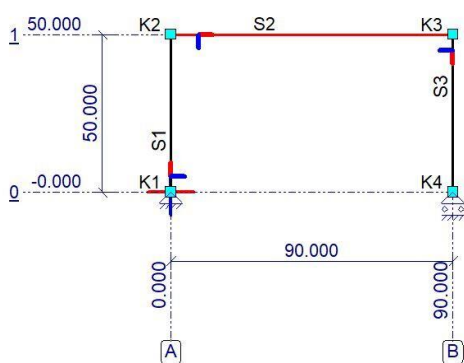


Figure 7-32 - Geometry of portal crane

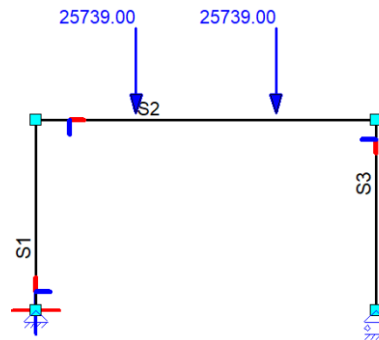


Figure 7-33 - Forces on portal crane

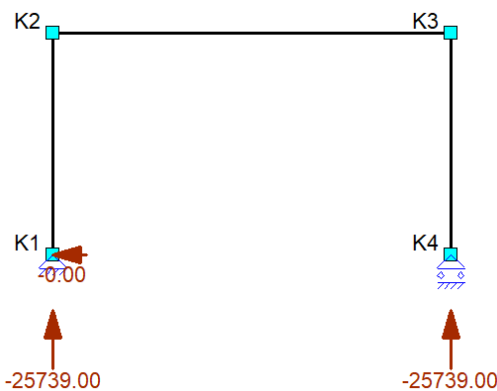


Figure 7-34 - Reaction forces on foundation

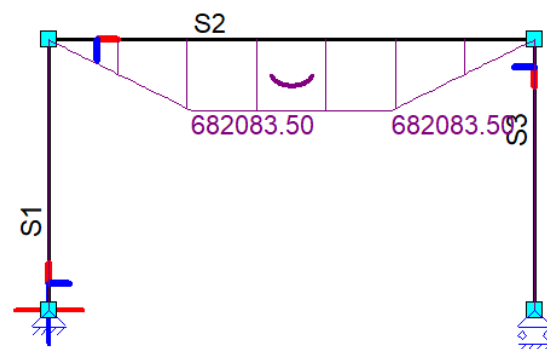


Figure 7-35 - Moment line for portal crane

## 7.4.5 Method 5: Immersion structure

In this method the GBFs are constructed on the quay wall whereafter the GBF is transported into the water by using an immersion structure.

### 7.4.5.1 Construction of GBF

See paragraph 5.5 for the construction time of 20 weeks per GBF. The conclusion is that 16 production lines are sufficient to construct and transport GBFs from the quay wall into the water with applying the learning curve.

### 7.4.5.2 Immersion structure

The immersion structure must be designed to achieve a minimal available draught of 11.2 meter for the GBF. An extra keel clearance of a half meter must be added. This result in a total available water depth of 11.7 meter. The water level that is exceeded in 20% of the high water is at +5.15m LAT. Therefore the platform may have a maximum construction height of 1.5 meter. When this is succeeded no deepening of the bed is needed and the constructability is higher. The forces in the immersion platform and the foundation depends on the type of foundation and for example the amount of piles. The elaboration of forces must be investigated when this method is worked-out. At the immersion structure a system must be installed which is able to lower the platform. This could be done by, for example, the use of a winch system or hydraulic jacks.

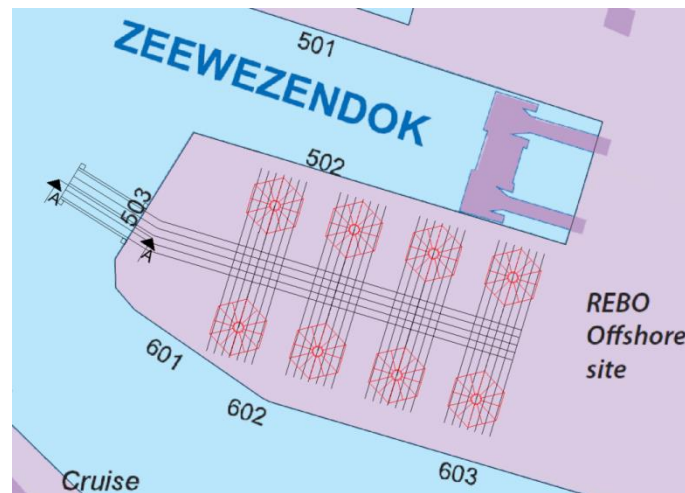


Figure 7-37 - Top view method 5

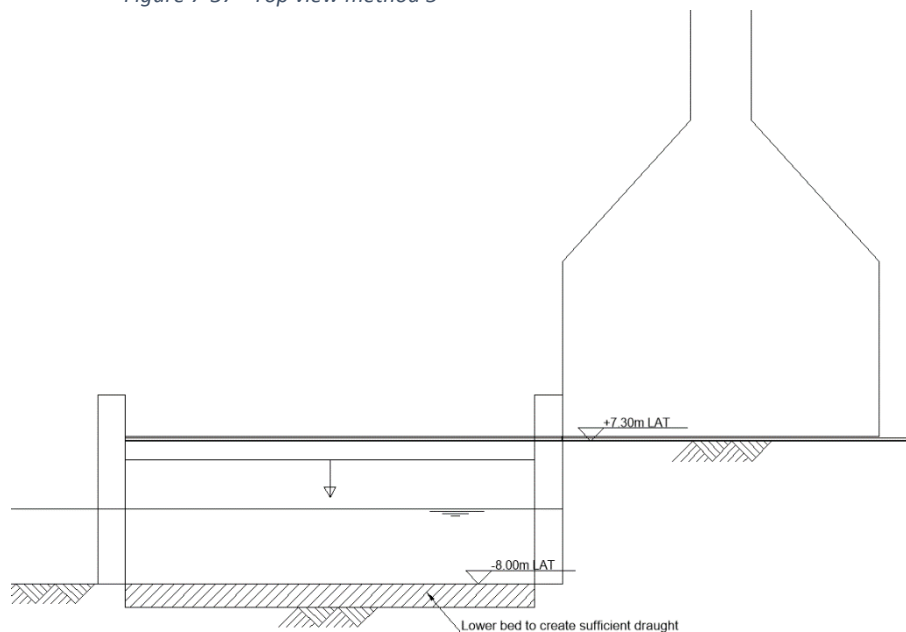


Figure 7-36 - Cross-section A-A method 5

## 7.5 MULTI-CRITERIA ANALYSIS

In this paragraph the methods are ranked to decide which method is the best solution for the construction and transportation of GBFs from land into water. First the criteria of the multi-criteria analysis (MCA) are described and thereafter the MCA is executed and an explanation of each criterion at the methods is presented.

### 7.5.1 Criteria

In the MCA several criteria are implemented, on each criterion a mark is given to all methods and at the end the method which scores the highest score is the most promising. The score is given with a scale from 1, which is bad till 10, which is excellent. For an example and more explanation an example is included in paragraph 1.5. The criteria from the program of requirements used in the MCA are:

- Constructability
- Amount of material use
- Reusability
- Required space
- Time
- Restoration of area
- Flexibility
- Risk during transportation
- Availability

### 7.5.2 Conclusion of the MCA

The result of the MCA is displayed in Table 7-6. The scores are given for each criterion for each method, from 1 which is bad till 10 which means excellent, and a final score is calculated. The final score is presented and method 5 found to be is the best method. The explanation of the scores is given in Table 7-7.

	Weight	Rating					Score				
		Method 1	Method 2	Method 3	Method 4	Method 5	Method 1	Method 2	Method 3	Method 4	Method 5
<b>Constructability</b>	0.20	4	2	6	4	8	0.80	0.40	1.20	0.80	1.60
<b>Amount of material</b>	0.10	4	6	8	7	5	0.40	0.60	0.80	0.70	0.50
<b>Reusability</b>	0.10	7	5	4	4	7	0.70	0.50	0.40	0.40	0.70
<b>Required space</b>	0.05	4	4	5	8	7	0.20	0.20	0.25	0.40	0.35
<b>Time</b>	0.15	8	2	2	8	8	1.2	0.3	0.3	1.2	1.2
<b>Restore</b>	0.10	4	5	8	8	6	0.40	0.50	0.80	0.80	0.60
<b>Flexibility</b>	0.10	6	3	5	6	7	0.60	0.30	0.50	0.60	0.70
<b>Risks</b>	0.15	8	3	4	7	8	1.20	0.45	0.60	1.05	1.20
<b>Availability</b>	0.05	6	4	5	6	8	0.30	0.20	0.25	0.30	0.40
<b>Total</b>	1						5.8	3.45	5.10	6.25	<b>7.25</b>

Table 7-6 – Multi-criteria analysis

According to the MCA the most promising method is method 5 and this method is chosen to investigate in the next phase of the report.

Criterion	Method 1: Slipway		Method 2: Prefabrication method		Method 3: Prefab on quay wall, completion on water		Method 4: Construct GBF on quay wall, lift with portal crane		Method 5: Immersion platform	
	Score	Description	Score	Description	Score	Description	Score	Description	Score	Description
Constructability	4	The constructability of the GBFs is good. There is no heavy lifting actions needed which is mostly the limiting factor. The slipway must be constructed to a large distance in the water area of the port. This is not good for the constructability.	2	The constructability of the GBFs is not good. The prefabricated elements must be connected to each other. These connections are hard to design and the execution to connect these parts when the GBF is floating is very difficult. Also the lifting capacity of land based cranes to lift the tower is insufficient.	6	The constructability of the prefab elements on the quay wall is good but the completion on water will cause problems. All equipment must be lifted to the water and a lot of cranes are needed. The lifting capacity of the portal crane must also be very high. A very large portal crane is needed.	4	The constructability of the GBFs is good. However the weight of the GBFs is that high that a portal crane that can lift these weight must be extremely high and strong. The quay walls are not designed for this high loads and extra foundation works are necessary. The constructability of the portal crane is not good.	8	The constructability of the GBFs is good. The constructability of the immersion platform is good, however if the thickness of the platform exceeds a certain height the harbor bottom must be deepened which could cause instability of the quay wall. The challenge is to construct the platform sufficiently slender.
	Amount of material use	4	The amount of material needed, is high due to the slipway platform which must be very long to create sufficient draught.	6	The amount of needed material is quite low, only two portal cranes are needed to construct.	8	The amount of needed material is low, only a portal crane must be installed.	7	The amount of needed material is low, only a large portal crane must be installed.	5

<b>Reusability</b>	7	The slipway construction can be used for new type of caisson projects on this construction location. When this structure is not founded with large piles the slipway construction might be transported to another project.	5	The portal cranes could be used for lifting operations. But due to the limited lifting area this is not very useful.	4	The portal crane can be used for lifting operations. Due to the limited lifting area this could only be used for a limited area.	4	The portal crane can be used for lifting operations. Due to the limited lifting area this could only be used for a limited area.	7	The slipway construction can be used for new type of caisson projects on this construction location. When this structure is not founded with large piles the immersion platform might be transported to another project.
<b>Required space</b>	4	The required space on the storage area is little. Only the production lines and the skidding line to the slipway take space on the construction area. However, the slipway has a large length into the port area which is not preferable.	4	The required space is large. For the construction of the base slab, cylindrical part, and tower several production lines are needed and this takes a lot of space on the storage area. On water the required space is large due to the construction on water.	5	The required space is little. Only the production lines and the skidding system to the slipway take space on the construction area. The portal crane is founded on the quay wall but do not need a lot of space. On water the required space is large due to the construction on water.	8	The required space is little. Only the production lines and the skidding line to the portal crane take space on the construction area. The portal crane is founded on the quay wall but do not need a lot of space.	8	The required space is little. Only the production lines and the skidding line to the immersion platform takes space on the construction area
<b>Time</b>	8	The elements can be fully constructed on land which means a high production rate and with this method the number of production lines can be adapted to construct sufficient GBFs in the restricted time period.	2	In this method the amount of production lines for each prefabricated part can be adapted to ensure that the GBFs are constructed in the restricted time period. However the construction on water is inadequate and the time restriction is not met by far.	2	The project execution time will not meet the target of 2 years. There are only four production lines possible on water and therefore each element must be finished in 6.67 weeks, which is not feasible.	8	The elements can be fully constructed on land which means a high production rate and with this method the number of production lines can be adapted to construct sufficient GBFs in the restricted time period.	8	The elements can be fully constructed on land which means a high production rate and with this method the number of production lines can be adapted to construct sufficient GBFs in the restricted time period.

<b>Restoration area</b>	4	The slipway is founded at the port location, therefore this slipway cannot be removed easily. The port loses a berth location. Another disadvantage is that the slipway is a long construction present in the port which may cause problems.	5	Due to the portal cranes a restriction is created at the storage area. The rails and portal cranes cause problems to the port function and also height restrictions are created. If the portal cranes are removed the rail and crane foundations must be restored into the original storage area.	6	Due to the portal crane a restriction at the storage area is created. The rails and portal cranes cause problems to the port function and also height restrictions are created. If the portal cranes are removed the rail and crane foundations must be restored into the original storage area.	6	Due to the portal crane a restriction at the storage area is created. The rails and portal cranes cause problems to the port function and also height restrictions are created. If the portal cranes are removed the rail and crane foundations must be restored into the original storage area.	6	The immersion platform causes a loss of a berth location. The immersion platform could be designed that it could be removed without harm to the quay walls. In that case the total port is in the same state as before the construction.
<b>Flexibility</b>	6	The slipway method could be used for other caisson construction projects. Only the platform must be replaced for a platform with the right dimensions. The weight may not exceed the design values.	3	This method is specifically applied to this caisson type. For other caisson constructions this method is not applicable.	5	This method could be applied for other caisson types, for less complex forms of caissons this method can more easily be applied to construct the caisson on water.	6	This method could be applied to all caisson types till the maximum capacity of the portal crane is reached. With very large weights of several thousands of tons this method is not profitable comparing to other transportation methods.	7	The immersion platform method can be used for any caisson type. The immersion platform could be designed for a certain design load and dimensions which are sufficient to the caisson. The draught is the limiting factor for the caisson. The construction height of the immersion platform could be in most cases not too large.
<b>Risk</b>	8	The GBF is not lifted from the ground and this minimizes the risk of toppling over of the GBFs. The risk on delay is severe. The construction is not a very complex operation which reduces the risks on delay. The construction of the GBFs is performed at several production locations. Delay on one or more GBFs will not harm the entire process.	3	The different elements are constructed on the quay wall and lifted above the Zeewezendok. The risk of failure of the construction method is severe because of the installation and lifting actions on water. Because of these complex construction actions the risk on delay of the construction of GBFs is severe.	4	The cylindrical part is constructed on the quay wall and lifted in the Zeewezendok where the construction of the GBF is finished. Because of instability of the GBF during construction the risk on instability and human injury is present. In the Zeewezendok the available space is limited and one production line is present. Due to the complex construction actions on water the risk of delay is high.	7	The GBFs are fully constructed on the quay wall with more production locations. Delay on one or more GBFs will not harm the entire process and therefore the risk on large delays in minimal. The GBFs are lifted from the quay wall into the water. Because this is one lifting action from land into water with a fully stable element the risks on damage and human harm is low.	8	The GBFs are fully constructed on the quay wall with more production locations. Delay on one or more GBFs will not harm the entire process and therefore the risk on large delays in minimal. The GBFs are not lifted which reduces the risk of toppling over of the GBFs. The risks therefore are minimal with an immersion platform.

<b>Availability</b>	6	The availability of the slipway platform is quite low. Due to the platform the GBF is not lifted and the wind is not an important factor to stop the transportation maneuver. Waves and shipping in the harbor decrease the availability, the slipway comes into the port and the shipping traffic could be hindered due to the large length.	4	Due to the large number of lifting actions this method is very dependent on the wind conditions. To complete a GBF multiple lifting actions are needed. The wave conditions are also important because one part is floating and other parts have to be installed on these.	5	The GBFs are largely built on the water. All materials must be transported to the GBFs and this is done by lifting actions. In the case of a floating GBF all construction actions must be performed on a swaying GBF which reduce the availability on some construction actions.	6	The GBFs are completely built on the quay wall. The GBF is lifted from the quay wall into the water and due to this only lifting action the availability not very high but due to the limiting lifting actions the risk on delay is mitigated.	8	The immersion platform has not a large length into the harbor, therefore the transportation process can be performed with a low dependence on the shipping traffic. Because no lifting actions are needed to transport the GBF the transportation method has low dependency on the wind conditions.
---------------------	---	---	---	--	---	---	---	--	---	---

Table 7-7 - Explanation of multi-criteria analysis

## **7.6 CONCLUSION CONSTRUCTION AND TRANSPORTATION METHODS**

In this chapter first the decision matrix is applied. The semi-submersible vessel is the only feasible option to transport the GBFs from land into water. The costs of the semi-submersible vessel are calculated and the costs are rather high with 10.5 or 13.8 million euro, depending on the storage area location. The objective is to develop a new construction and transportation method to transport the GBFs from land into water. A brainstormsession was organized and five methods are presented. In the synthesis and simulation phase the applicability and effects are determined and with the help of a multi-criteria analysis the best method is chosen, which is the immersion structure. This design step is executed and the Yes-direction is followed to the next design steps which are described in the next chapter.

## Chapter 8: CONSTRUCTION AND TRANSPORTATION PLANNING

The most optimal construction and transportation method is designed in chapter 7. The method is applicable to the GBFs and in this chapter the planning of the construction and transportation is considered. In Figure 8-1 the design method questions are indicated which are answered in this chapter. The 'design production line' and 'construct on one location' are both indicated because at the beginning of this chapter it is unknown which option is the best. Because for this chapter more solutions are present the full secondary design method is applied in this chapter.

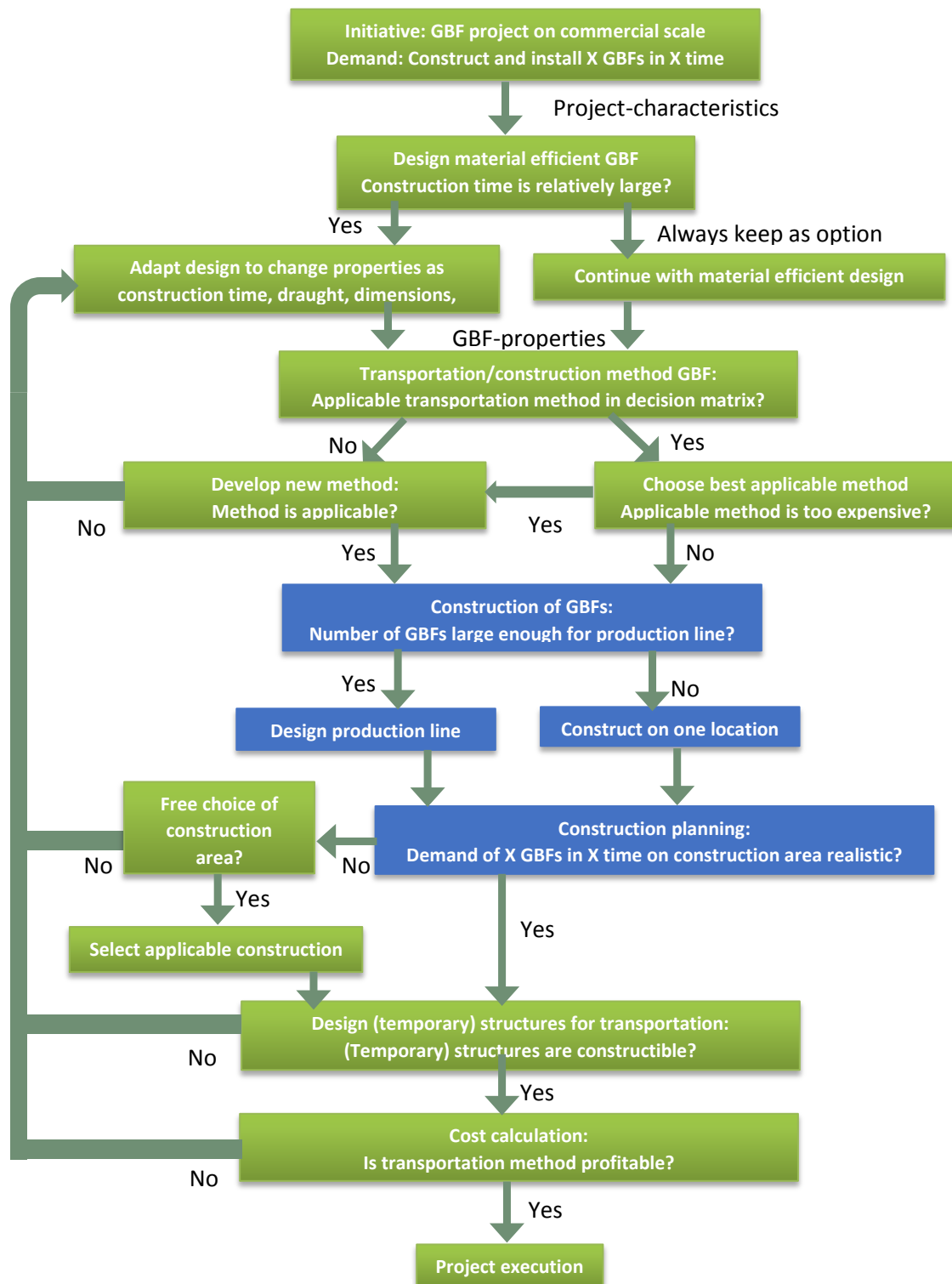


Figure 8-1 – Chapter 8 indicated in design method

After ranking the different methods the optimal construction planning to build and transport the GBFs from land into the water is considered. First the principle of a learning curve on a planning is explained, then the requirements on the most optimal planning and construction layout are given whereafter a multi-criteria analysis is performed to decide which of the three options the most optimal is.

## 8.1 MINIMIZING LEARNING CURVE

The planning described in paragraph 6.5 is a planning without applying a learning curve. A learning curve means that a certain construction action the first time takes longer because every construction action is 'new'. After executing a construction action several times the time needed decreases. In the planning a learning curve of 60%-80%-100% is included. This means that the construction time of the first GBF must be divided by 0.60, the second with 0.80 and the third and higher by 1.00. For the preliminary planning of 20 weeks, as described in 6.5 this means that the first GBF is constructed in 33 weeks, the second in 25 weeks and the third in 20 weeks. This implies per construction location 13 weeks extra for the first GBF and 5 weeks extra for the second GBF. The effect of a learning curve can be minimized by implementing a high repetition factor. When the construction can be divided in several stages and create a production line the amount of construction locations can be decreased and the learning curve effect is less. The more identical construction actions can be executed on a specific location the less effect the learning curve has on the construction time. To determine the effect of a learning curve three variants are described:

- Fixed location
- Production line
  - Production line with three construction locations
  - Production line with four construction locations

## 8.2 PROGRAM OF REQUIREMENTS

To develop construction planning methods some requirements are given where the construction planning must comply on. With the help of these requirements the most optimal method is chosen in the multi-criteria analysis.

- The 64 GBFs must be fully constructed and transported into the water within two years.
- The required area to execute the construction activities may not exceed the available areas. The less area the construction area layout takes the better it is.
- When the production is delayed and the 64 GBFs are not produced in the two available years the installation window has passed and this rapidly increase the costs. The risk on delay must be mitigated by mitigating measures.
- The needed equipment must be used as efficiently possible.
- The construction must be executed as efficient as possible. In other words: the learning effect must be minimized and waiting times due to an inefficient planning must be minimal.

### 8.3 CONSTRUCTION ON FIXED LOCATION

The first option is to construct the GBFs completely on a fixed location and transport the entire GBF to the immersion structure where it is transported into the water. With a production rate of 0.6 GBF per week, on average 2 GBFs per week must be completed. Because all GBFs could not be built simultaneously because of the large consumption of concrete by casting the bottom slab the start date of each GBF is set two days before the GBF is started to construct. In Figure 8-3 the planning is given of the construction on a fixed location. There are 16 construction locations needed to complete the construction in two years. The learning curve effect is due to this high number. On every 16 construction locations a 'loss' of 13 weeks on the first and 5 weeks on the second GBF construction must be taken into account. A high number of construction locations are needed and because lifting operations are executed simultaneously a large amount of equipment is needed.

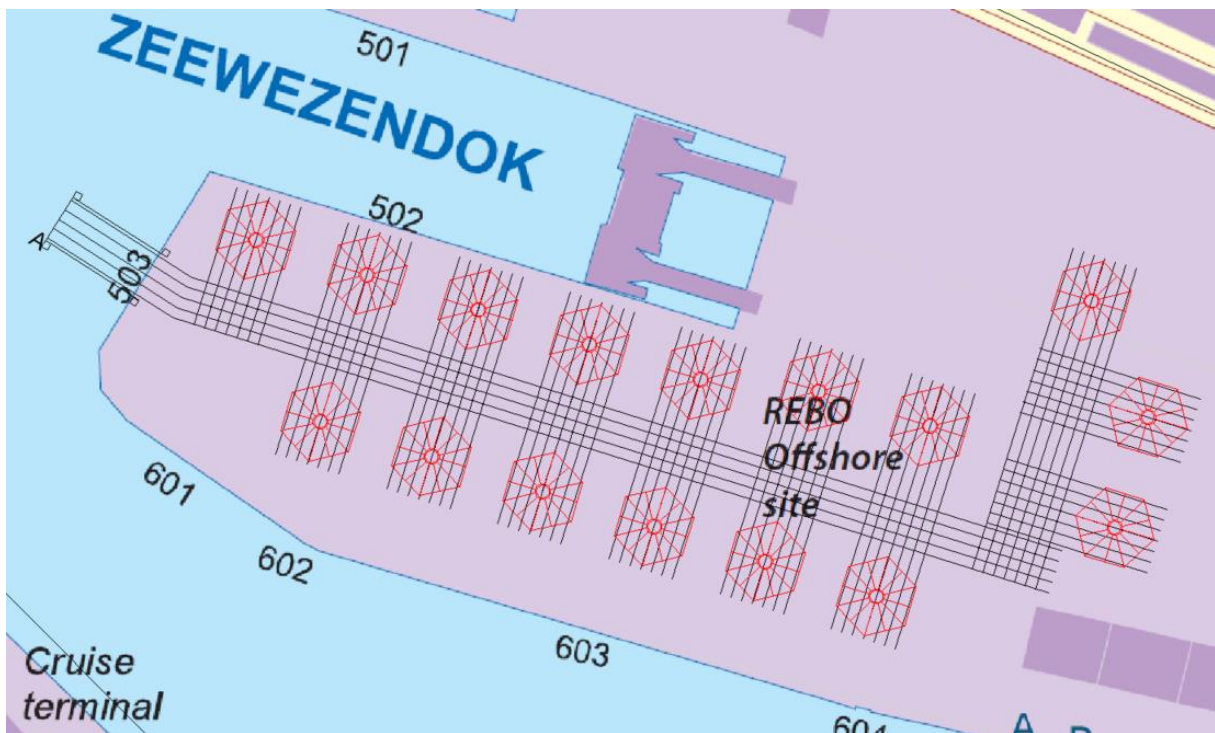


Figure 8-2 - Layout of REBO site with 16 fixed construction locations



## 8.4 CONSTRUCTION WITH A PRODUCTION LINE

The second variant is to construct the GBFs in a production line. The preliminary planning, to construct a hexagonal GBF which is given in paragraph 6.5 is used to group some construction actions. The result is displayed in Figure 8-4.

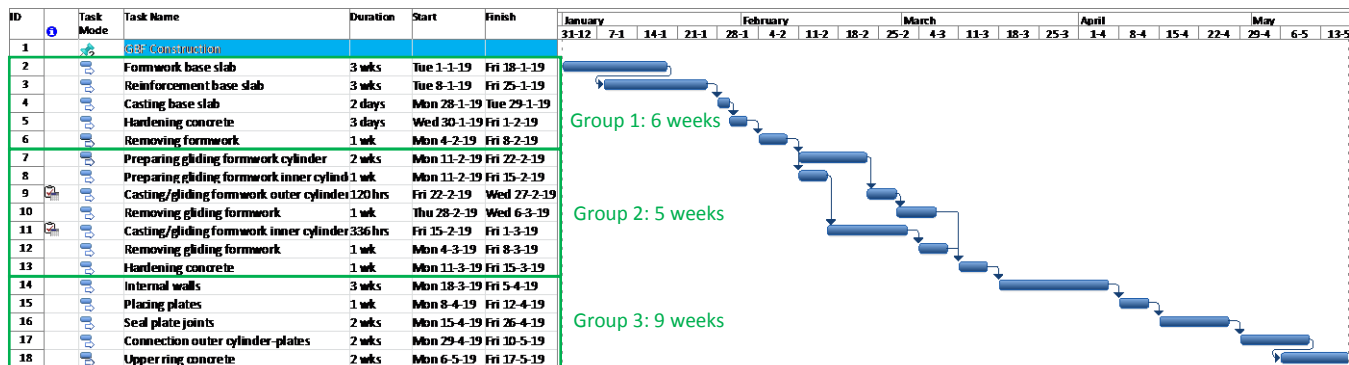


Figure 8-4 - Grouped construction actions

The first group consists of the construction of the base slab and takes in total 6 weeks. The second group consist the construction of the outer walls and inner cylindrical tower and takes in total 5 weeks. The third and last group of construction actions consist the construction of the inner walls and placing of the plates and the connection of the plates to the GBF, this group of actions takes 9 weeks. The third group of activities takes longer than the other two, therefore two options are investigated:

- Option 1: Each group of action has one construction location
- Option 2: Group 1 and group 2 have one construction location and group 3 has two construction locations.

### 8.4.1 Production line with three locations

All grouped construction activities have one construction location. The advantage of option 2 is that the learning curve has less influence on the working activities on group 3. The planning of the construction of the GBFs at one location is given in Figure 8-5. In a construction period of two years 8 GBFs are constructed per production line. With 8 production lines the construction of 64 GBFs can be executed in two years. This is a strict planning and no large delay is acceptable. Due to the larger execution time on the third location waiting times on location 1 and 2 are present.

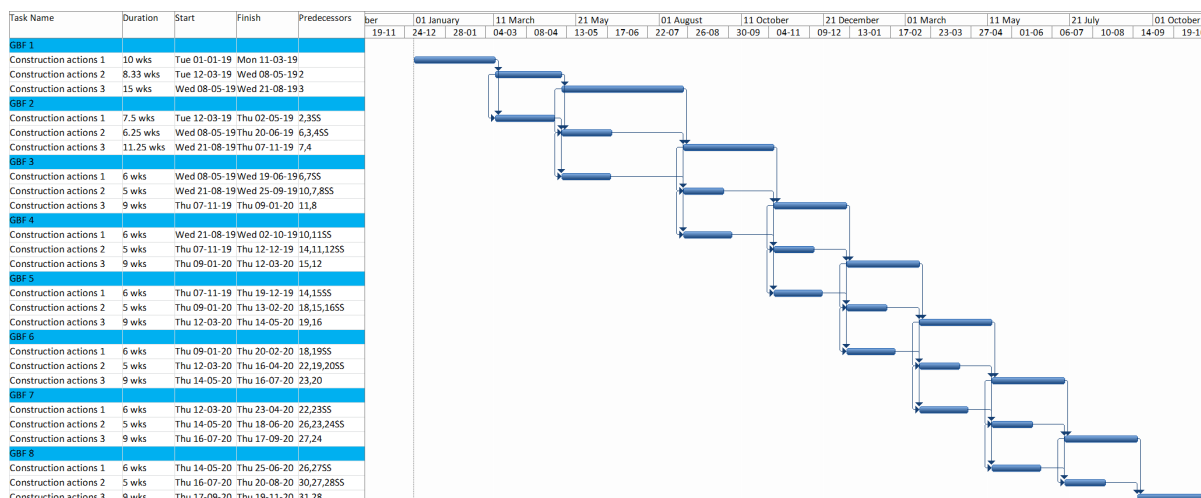


Figure 8-5 - Construction planning with the use of three locations (option 1)

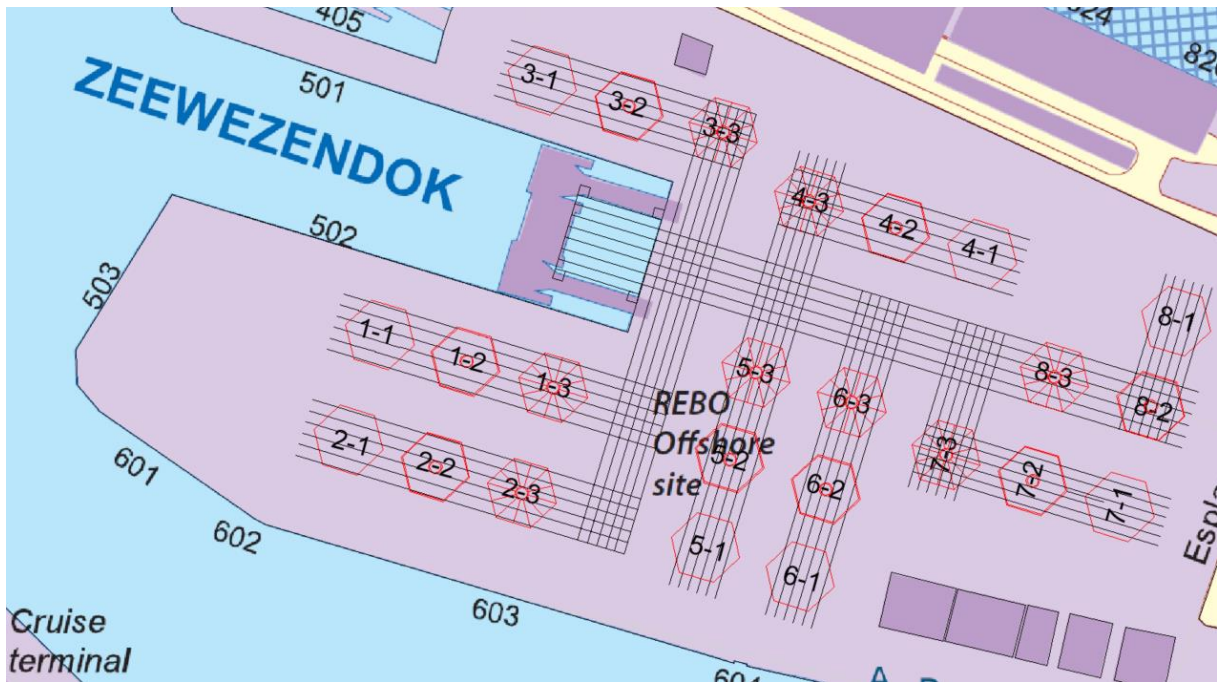


Figure 8-6 - Production lines on the REBO site with three locations (option 1)

In Figure 8-6 the production lines are drawn on the REBO site. The first number indicates the production line and the second number the group of construction actions.

### 8.4.2 Production line with four locations

Because the third group of construction activities takes longer, it is decided to use two locations to execute the construction actions of the third group. The groups are used to give a planning for one production line, see Figure 8-7. Because the third group is executed at two locations the learning curve is applied on both locations for the third group of construction actions.

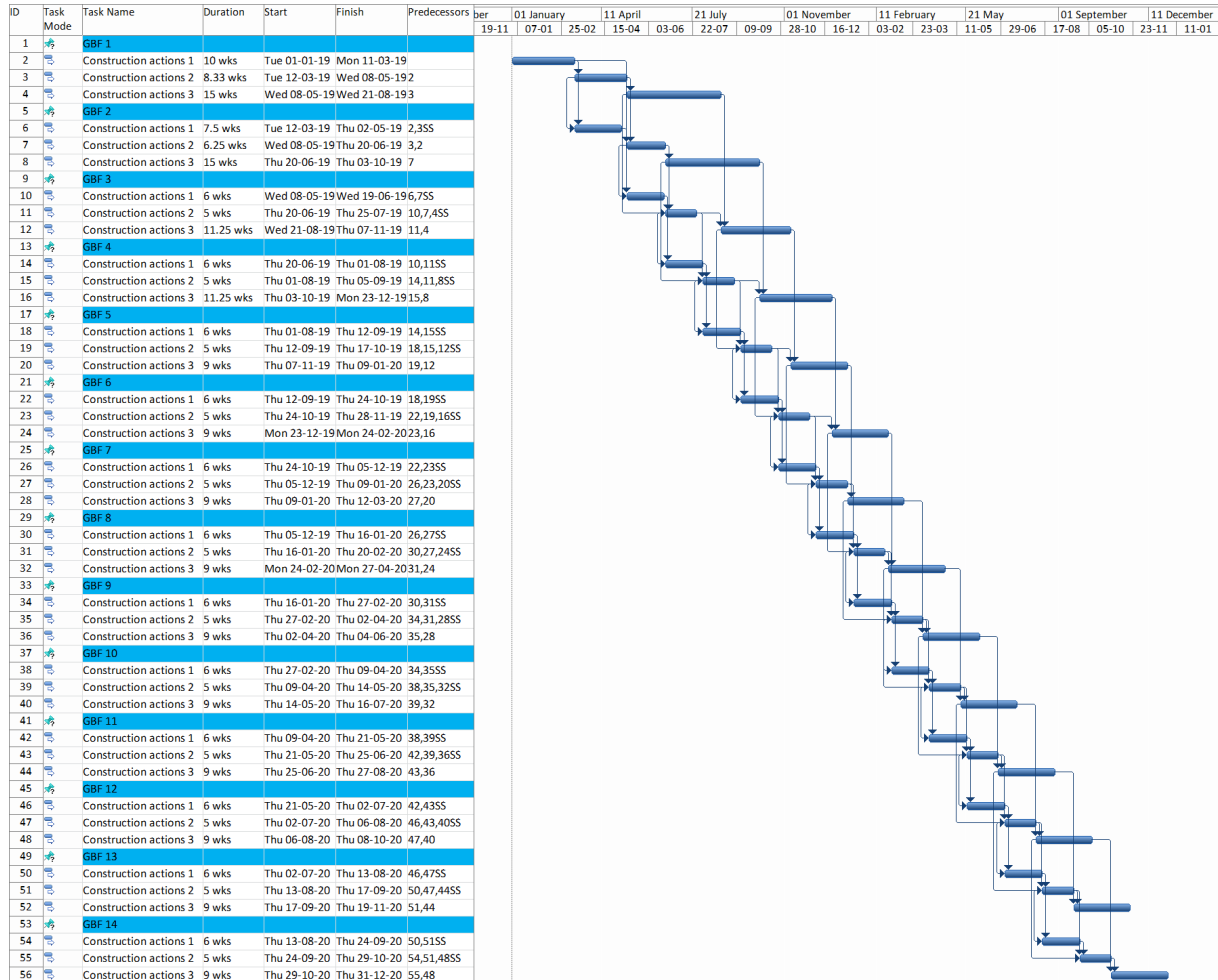


Figure 8-7 - Construction planning with the use of four locations (option 2)

According to the planning 14 GBFs can be constructed per production line in a period of two years. To fulfil the requirement of 64 GBFs in a period of two years, five production lines are sufficient. The use of five production lines implements a maximal production of 70 GBFs in two years, this reduces the risks of delay in the production process and some reserve capacity is available.

In Figure 8-8 the five production lines are drawn on the REBO offshore terminal. The numbers of the production locations is as follows:

Production line - Group of construction actions - Number of third construction location.

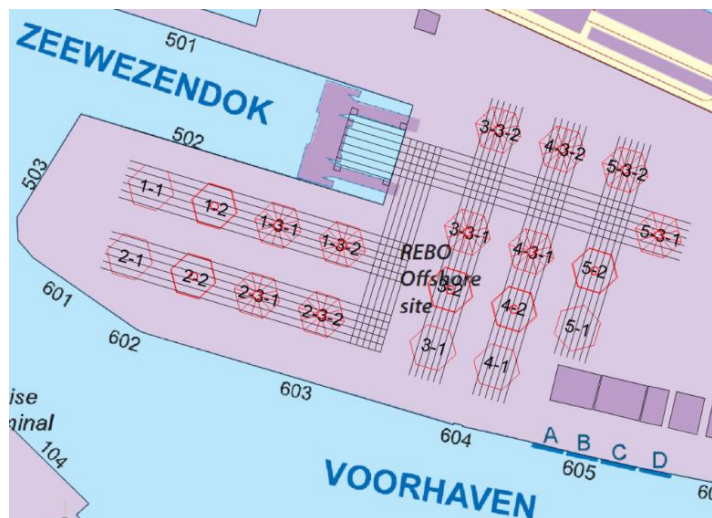


Figure 8-8 - Production line on REBO site with four locations (option 2)

## 8.5 DECISION ON CONSTRUCTION AND TRANSPORTATION PLANNING

To decide which option is the best, first some information about the options is given. The equipment and time that is needed differs for each planning and is presented in Table 8-1.

The working time is determined from the planning and with the total time needed to construct all GBFs the non-working time is calculated to give an indication about the efficiency of the three plannings.

Production	Area needed [locations]	Equipment					Working time [weeks]	Total time [weeks]	Non-Working time [weeks]
		Skidding beams [m]	Bottom slab formwork	Gliding formworks		Cranes for plates			
				Outer wall	Inner wall				
Fixed location	16 Locations	1523	16	16	16	32	1568	1568	0
Production line option 1	24 Locations	1940	8	8	8	16	1427	2359	932
Production line option 2	20 Locations	1532	5	5	5	20	1413	1971	558

Table 8-1 - Comparing the equipment of construction planning variants

Based on a multi-criteria analysis the most optimal construction method is determined. The execution is displayed in Table 8-2. From this MCA it can be concluded that the production line option 2 is the best method. The risk on delay is small and there are mitigation measures applicable. The amount of equipment needed is also quite low comparing to the other methods.

Multi-criteria analysis							
	Weight	Method 1	Method 2	Method 3	Method 1	Method 2	Method 3
Production rate	0.25	7	7	7	1.75	1.75	1.75
Exceeding area	0.10	8	6	7	0.80	0.60	0.70
Mitigation of risks	0.35	5	6	8	1.75	2.10	2.80
Efficient use of equipment	0.15	5	7	8	0.75	1.05	1.20
Efficient use of time	0.15	8	4	5	1.20	0.60	0.75
<b>Total</b>	<b>1</b>				<b>6.25</b>	<b>6.10</b>	<b>7.20</b>

Table 8-2 - Multi-criteria analysis construction and transport planning

The scores are given to each planning with help of the description in Table 8-3. The three construction area layouts and their planning are compared to each other by using the requirements as criteria. Per requirement the three construction planning are compared.

Criterion	Fixed location		Production line option 1		Production line option 2	
	Score	Description	Score	Description	Score	Description
<b>Construct 64 GBFs in 2 years</b>	7	The construction of 64 GBFs is feasible in the timeframe of 2 years.	7	The construction of 64 GBFs is feasible in the timeframe of 2 years.	7	The construction of 64 GBFs is feasible in the timeframe of 2 years.
<b>No exceeding of available area/ area needed</b>	8	There is no exceeding of available area. In total 16 construction locations are needed	6	There is no exceeding of available area. In total 24 construction locations are needed	7	There is no exceeding of available area. In total 20 construction locations are needed
<b>Mitigation of risks</b>	5	The risks are hard to mitigate, if the construction actions cannot be executed according to the planning a minimum of 16 GBFs are delivered too late. An extra construction location can be designed but because the complete construction of a GBF must be executed this increases the use of equipment and cost.	6	The risks can be mitigated by design a storage location on the quay wall. If a construction action has some difficulties and delays the already finished GBFs of the previous construction location can there be stored and an extra construction location of the delayed construction action can be designed. This is a relatively small adaptation to the construction process.	8	The risks already are mitigated because with full production 70 GBFs can be built in the timeframe of 2 years. Producing one GBF less per production line gives a total of 65 GBFs; a total delay of a whole GBF per production line still not give problems to the time schedule. Even if the delay is more than 6 GBFs an extra construction location can be implemented.
<b>Efficient use of equipment</b>	5	Because 16 production lines construct a few days after each other, a large amount of construction material and equipment at the same time is needed, see Table 8-1.	7	For each production line a complete set of equipment is needed. There are 8 production lines which imply that 8 sets of equipment are needed, see Table 8-1.	8	A production line is created with two, third locations. There are 5 sets of equipment needed for locations 1 and 2 and 10 of the third location, see Table 8-1.
<b>Efficient use of time</b>	8	The working time needed to construct the GBFs is the highest. No waiting time present so this is an efficient planning.	4	The time to construct the GBFs is low due to minimizing the learning effect. The more often a construction action can be repeated at a construction location the more efficient this is due to the learning curve. However, due to an inefficient planning there are 932 weeks of non-working time.	5	The time to construct the GBFs is the lowest of the methods. However, the non-working time is due to inefficiencies in the planning 558 weeks.

Table 8-3 - Comparison of construction and transportation planning

## 8.6 OPTIMIZING PLANNING

In the previous paragraphs the start date of the construction was set on the first of January 2019. The installation window of GBFs is from 1 April till 1 October. When the installation window has arrived no GBFs are constructed and this is not optimal. In Figure 8-9 the Production of GBFs is displayed. As it can be seen the first GBFs are produced at half august, the main part of the first installation window has passed and this is not optimal. To optimize the planning the start date must be chosen in a way that all GBFs are produced and installed in a timeframe of two years.

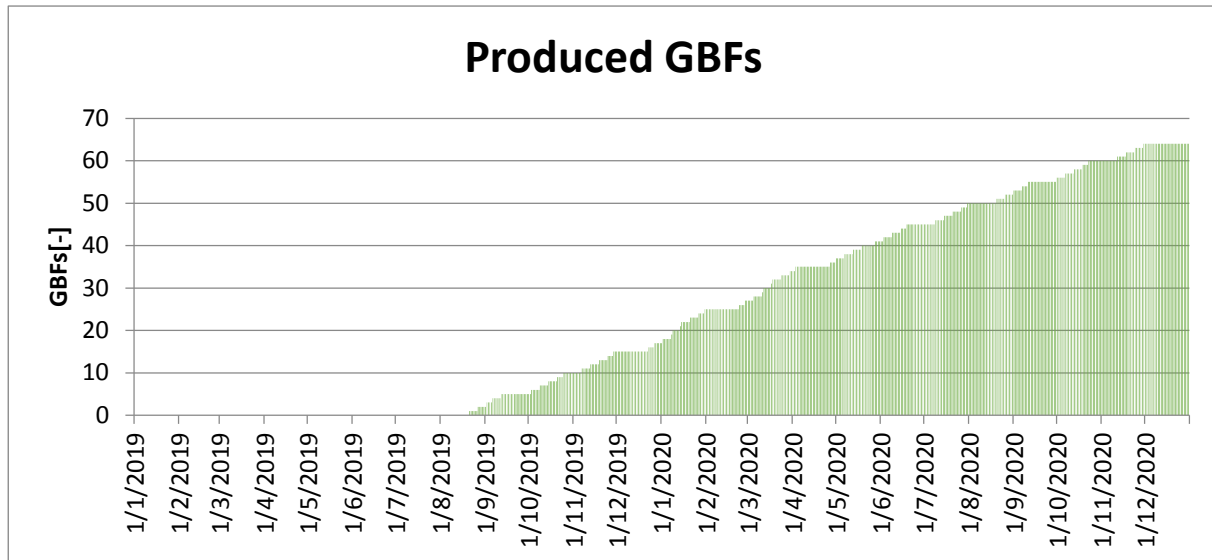


Figure 8-9 - Number of constructed GBFs

To optimize the planning some requirements are:

- The stock of GBFs must be kept as low as possible.
- The installation procedure may not be stopped because no GBFs are present in stock.
- The casting procedure of casting base slabs may not be coinciding because of the large concrete transport needed.

The planning is adapted and the construction activities now start at the ninth of august in 2019 and ends at the second of June 2020. According to Figure 8-11 a storage area must be designed where 26 GBFs temporary can be stored. Due to the optimization in the planning not two entire installation windows are used, the first installation window is from the fourth of July till the first of October, the second installation window is entirely used. The mean time to install a GBF, including bad weather windows, takes a half week.

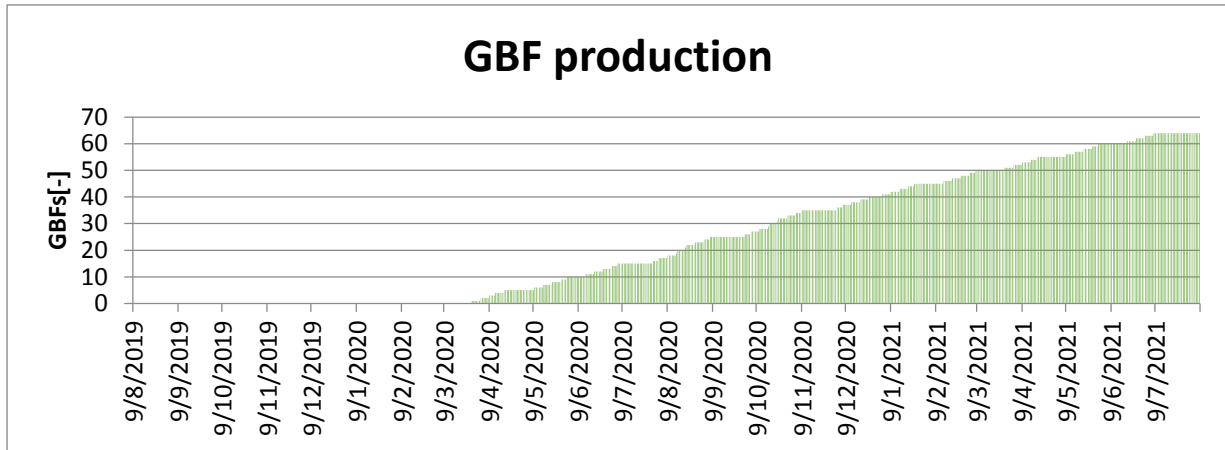


Figure 8-10 - GBF production adapted planning

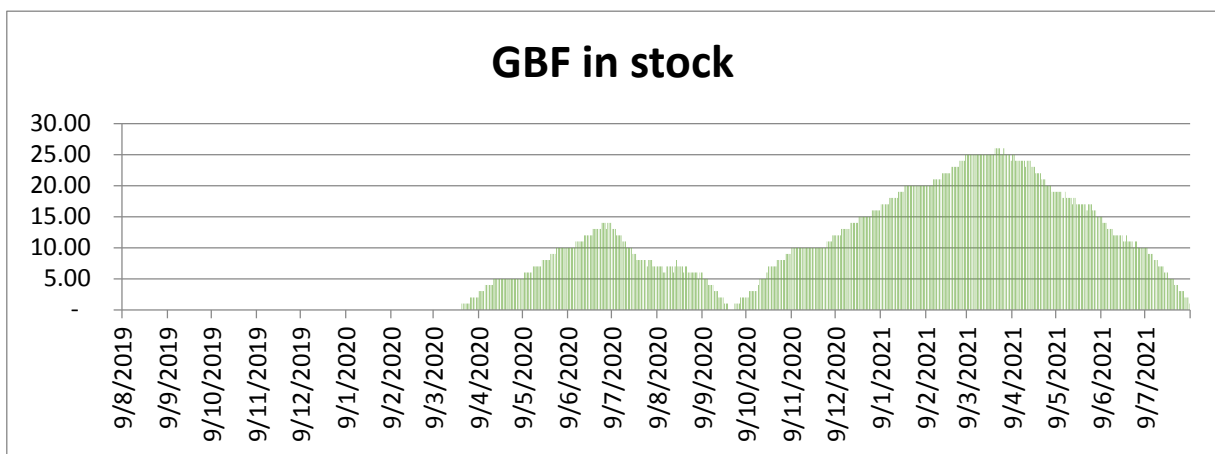


Figure 8-11 - Number of GBFs in stock

By planning the start of the first group of construction actions four days after each other the delay must be more than two days before the base slab casting coincide. This requirement is also satisfied.

Based on the construction area layouts the storage location must be designed in water. The construction area is quite full and there is no extra space for 26 GBFs. Because the planning is optimized a new number of renting days for a semi-submersible is estimated. For this number of days the total renting costs are calculated.

For the case study this means that the renting costs for a semi-submersible vessel are decreased. A period is needed from the start of the first installation window till August in the end of the second window. Because there is a chance of bad weather periods it is assumed that the semi-submersible vessel is rented for the whole second window. The extra available time on installation of the GBFs mitigates the risk of exceeding the installation window due to bad weather, one extra month is reserved for delay due to bad weather. There are twenty days reserved for the preparing and removing costs of equipment of the semi-submersible vessel. The rental days for a semi-submersible vessel are:

$$T_{c,ss} = d_{rent} \cdot C_{ss} = (20 + 548 + 20) \cdot 20,000 = 11,760,000 \text{ €} \quad (49)$$

Where:

$$\begin{aligned} T_{c,ss} &= \text{Total renting costs semi – submersible vessel [€]} \\ d_{rent} &= \text{Total renting period [days]} \\ C_{ss} &= \text{Rental cost of semi – submersible vessel [€/day]} \end{aligned}$$

The operational costs are also calculated and in Table 8-4 the total cost is presented, which is almost equal to the first cost estimation in Table 7-3.

Category	Sub-category	Amount	Cost	Period	Cost			
<b>Rental cost</b>		1	(Semi-sub)	€ 20,000	(per day)	588	(days)	€ 11,760,000
<b>Crew cost</b>	Project manager	1	(men)	€ 80	(per hour)	4704	(hours)	€ 376,320
	Engineer	1	(men)	€ 70	(per hour)	4704	(hours)	€ 329,280
	Deckhand	2	(men)	€ 30	(per hour)	4704	(hours)	€ 282,240
<b>General preparatory works</b>		1	(periods)	€ 100,000	(per period)	-	-	€ 100,000
<b>Maintenance and repair</b>				€1500	(per day)	588	(days)	€ 882,000
<b>Total</b>								<b>€ 13,729,840</b>
<b>Total/day</b>								<b>€ 23,350</b>

Table 8-4 - Renting costs of semi-submersible vessel

## 8.7 CONCLUSION CONSTRUCTION AND TRANSPORTATION PLANNING

In this chapter the question if the construction and transportation for the amount of 64 GBFs in a timeframe of 2 years is feasible is answered. To answer this question three methods are applied, one with the construction of a GBF fixed at one location, a method with three construction locations and a method with four locations. These methods are described in the synthesis and simulation phase and with a multi-criteria analysis the most optimal method is chosen: Construction of GBF on four locations. With this method the construction the large number of GBFs is feasible and the risks on delay are mitigated. The answer for this design step is answered and the Yes-direction is followed to the next design step: 'Design of the (temporary) structures', which is in this case the immersion structure.

## Chapter 9: DESIGN OF IMMERSION STRUCTURE

The design of the GBF, construction and transportation methods are determined, the construction process which is done as a production line is designed and in previous chapter the most optimal planning is given. With all these info the immersion structure can be designed. In the used design method this is one of the last steps before reaching the project execution phase, see Figure 9-1. For the platform of the immersion structure the secondary design method is applied to choose the best material. For the platform foundation one material can be chosen in advance because of the demand of a large contact area between the foundation and subsoil. Therefore the secondary design method again is performed without evaluation phase on the foundation.

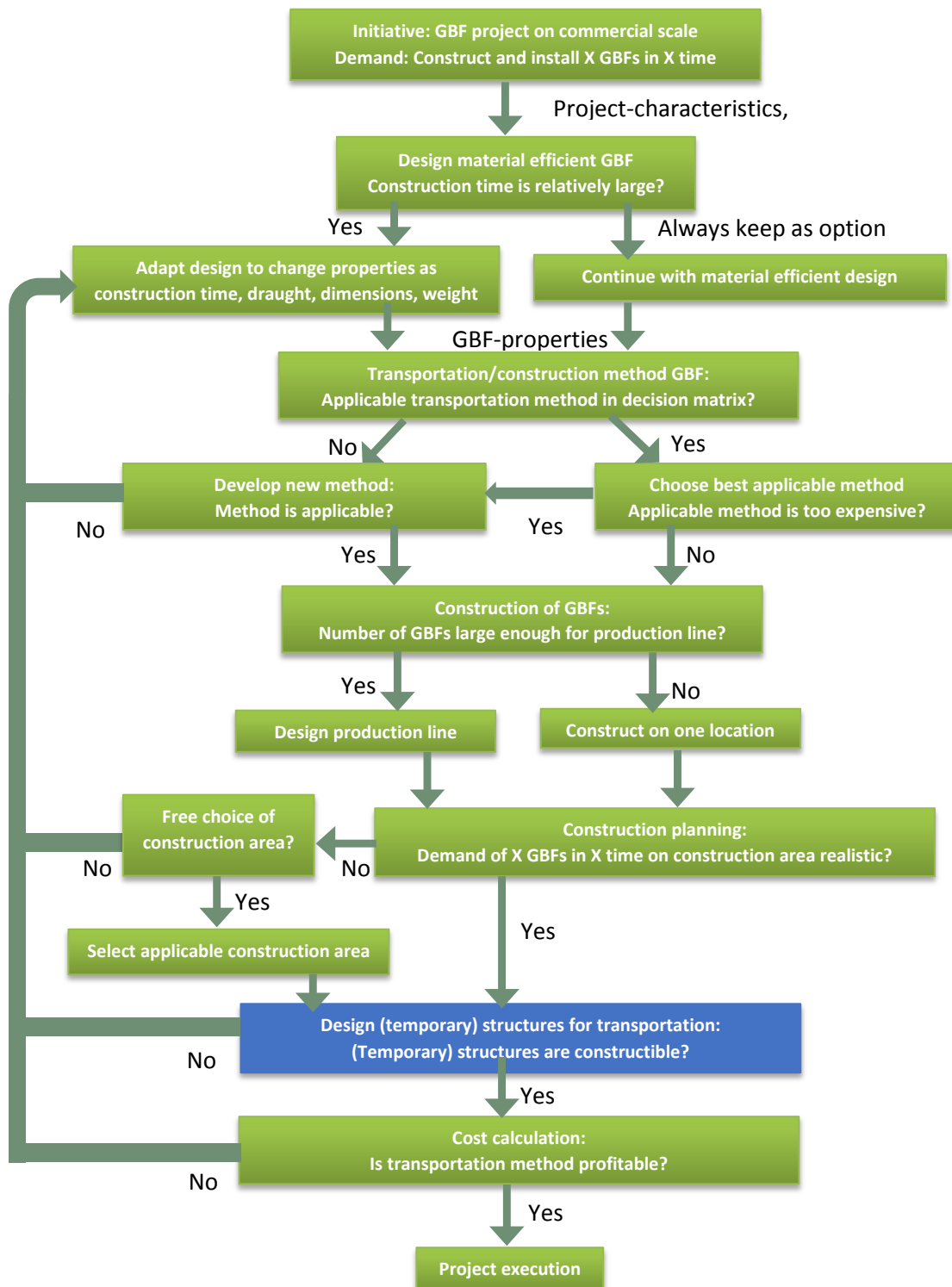


Figure 9-1 – Chapter 9 indicated in design method

To design the immersion structure first the function of the immersion structure is given. Then the calculation method is given according to the Eurocode and the program of requirements is given. The design of the immersion structure is done in two main parts, first the platform is designed and thereafter the foundation. Only a preliminary design is made to estimate the dimensions and to do a reliable cost estimation. If the structure is build a more extensive study must be performed on the structural design.

## 9.1 FUNCTION OF IMMERSION STRUCTURE

The immersion structure must fulfil the function of the transport from land into water of GBFs for offshore wind turbines. The procedure of the transport is given in step 1 till step 4 in Figure 9-2. In these drawings the basic principle is given. The design of the immersion platform follows in paragraph 9.4.1 and the design of the foundations are described in paragraph 9.4.3.

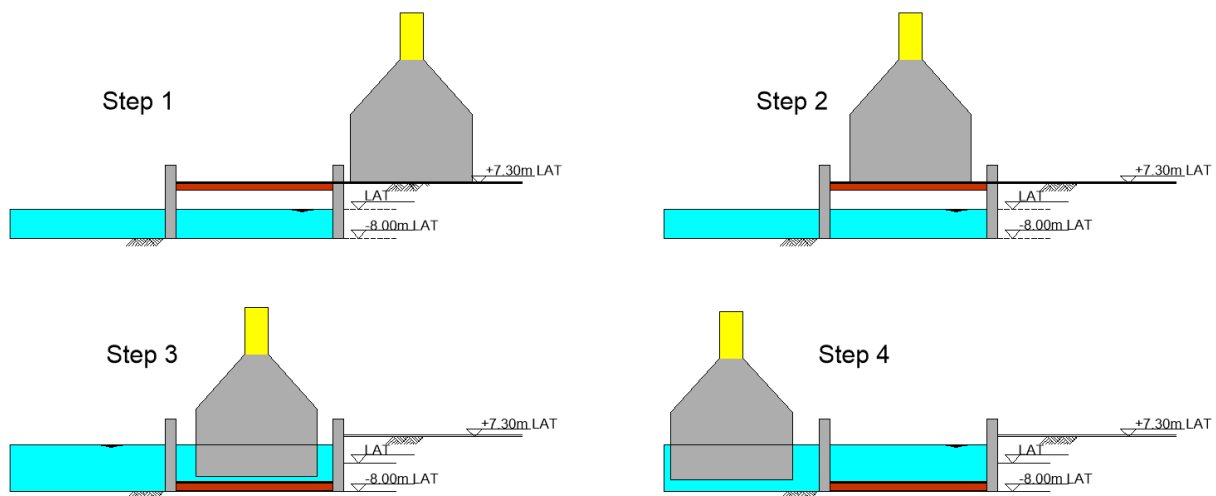


Figure 9-2 - Transportation of GBF from land into water

To fulfil the transportation of GBFs from land into water the immersion platform must bear the weight of the GBF. The structure must be able to lift and lower the platform. The total height of the platform may not be too large so that the minimal draught needed by the GBFs is not reached, otherwise the GBF will not float and the transportation action cannot be executed.

## 9.2 STARTING POINTS DESIGN IMMERSION STRUCTURE

For the static stability in water and the stability on the subsoil the same procedure as in chapter 5 and 6 is followed. For the calculation of the immersion platform structure the Eurocode guidelines are again followed. In the calculation Design Approach DA2 is performed. This means that the partial factors are given in the set of A1, R2 and M1, see Figure 9-3. For the structural calculations the capacity of materials are divided by factors as given in Figure 9-4 and Figure 9-5.

**Table 3.3.1 Partial factors on actions ( $\gamma_F$ ) or the effects of actions ( $\gamma_E$ )**

Action	Symbol	Set	
		A1	A2
Permanent	Unfavourable	1,35	1,0
	Favourable	1,0	1,0
Variable	Unfavourable	1,5	1,3
	Favourable	0	0

**Table 3.3.2 Partial resistance factors for spread foundations ( $\gamma_R$ )**

Resistance	Symbol	Set		
		R1	R2	R3
Bearing	$\gamma_{Rv}$	1,0	1,4	1,0
Sliding	$\gamma_{Rh}$	1,0	1,1	1,0

**Table 3.3.3 Partial factors for soil parameters ( $\gamma_M$ )**

Soil parameter	Symbol	Value	
		M1	M2
Shearing resistance	$\gamma_\phi^1$	1,0	1,25
Effective cohesion	$\gamma_c$	1,0	1,25
Undrained strength	$\gamma_{cu}$	1,0	1,4
Unconfined strength	$\gamma_{qu}$	1,0	1,4
Effective cohesion	$\gamma_c$	1,0	1,4
Weight density	$\gamma_\gamma$	1,0	1,0

<sup>1</sup> This factor is applied to  $\tan \phi'$

Figure 9-3 - Load factors according the Eurocode (Molenaar & Voorendt, 2018)

Design situations	$\gamma_c$ for concrete	$\gamma_s$ for reinforcing steel	$\gamma_s$ for prestressing steel
Persistent & Transient	1,5	1,15	1,15
Accidental	1,2	1,0	1,0

Figure 9-4 - Material factors for concrete structures (Molenaar & Voorendt, 2018)

type of material resistance	partial material factor $\gamma_m$
resistance of cross-sections of all steel classes	1,0

Figure 9-5 - Material factor for steel (Molenaar & Voorendt, 2018)

The weight of the GBF is  $112.7 \text{ kN/m}^2$ . This load is present where the GBF is placed on the immersion platform. Because the load is transferred from the quay wall to the middle of the platform the design criteria is that the whole platform is able to bear a distributed force of minimal  $112.7 \text{ kN/m}^2$ . The load factor for a permanent load is according to the Eurocodes 1.35 (Molenaar & Voorendt, 2018). The weight of the structure is a very important property of the GBF and during the construction this weight is intensively monitored. The GBFs are constructed and transported on a skidding system which uses jacks, the weight can be easily derived from the loads on the jacks. Therefore the load factor on the weight of the GBF is reduced and a partial factor of 1.1 is applied. This result in a design value of  $124 \text{ kN/m}^2$ . The partial factor on the selfweight of the platform structure is according to the Eurocode 1.35. The partial material factors for concrete and steel are 1.5 respectively 1.0, see Figure 9-4 and Figure 9-5. For the reinforcing steel and prestressing steel both a factor of 1.15 is used. For the hydrostatic forces it is assumed that the water level is at the top of the platform which causes higher forces, also a partial factor of 1.5 is applied on the hydrostatic forces.

### 9.3 PROGRAM OF REQUIREMENTS

A program of requirements is given to design the immersion platform:

- The dimensions of the platform must be designed in the way that a working width of 3 meter is available on all sides.
- The immersion platform must be able to bear a minimal weight of  $124 \text{ kN/m}^2$  present on the entire platform.
- The calculations are performed according to the Eurocode guidelines.
- The placement of the immersion platform must be done without foundation works. The immersion platform structure is directly placed on the bottom.
- The immersion platform includes ballast tanks to let the immersion platform float to transport it to another location where it can be used for other projects.
- Skidding beams are used for the transport of caissons on land and therefore the weight of a skid system is implemented in the immersion platform. The weight of skidding system and a steel plate on the platform is assumed to be  $5 \text{ kN/m}^2$ .
- The maximum allowable construction height of the immersion platform is 1.5 meter.
- The foundation of the structure must be stable with respect to:
  - Rotational capacity
  - Bearing capacity
  - Shear capacity
- The immersion platform structure may have a maximum draught of 10 meter.
- The immersion platform structure must have a metacentric height larger than 0.50 meter for stability.
- The weight of the immersion platform must be kept as low as possible.
- The material use must be kept as low as possible.
- The immersion platform can be adapted for larger and/or heavier caissons.

### 9.4 DESIGN PROCEDURE

The design calculation is done from top to bottom, for the design first simple hand calculations are performed whereafter the immersion structure is designed with the use of Scia Engineer. In this chapter the outcomes and a short explanation is given of the results obtained in Annex J.

- Platform:  
First the platform where the GBF stands on is designed. The weight of the GBF and additional material are implemented and the platform is designed in a way that it can bear the load.
- Concrete foundation:  
The foundation can be calculated when the load on the platform including self weight is known. The connection and lifting equipment of the immersion platform to the foundation is in the design of the concrete foundation applied with the help of a reference project. The lift equipment must be considered more extensively if this design is used for execution of this structure.
- Two connecting beams:  
To make the immersion platform stable a fixed connection between the two foundation legs must be designed.

### 9.4.1 Platform design

For the platform three materials are considered to construct a platform that could bear the weight of the GBF:

- Reinforced concrete
- Steel
- Prestressed concrete

Due to the requirement of a maximum platform height of 1.5 meter the materials reinforced concrete and prestressed concrete both are not applicable. The calculations of the platform in all three materials are included in Annex J. The result is a steel platform that consists of H-beams as given in Figure 9-6. The steel stress and deflection are given in Figure 9-7 and Figure 9-8.

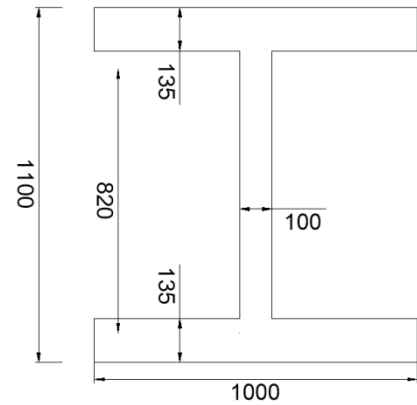


Figure 9-6 - Final design H-beam

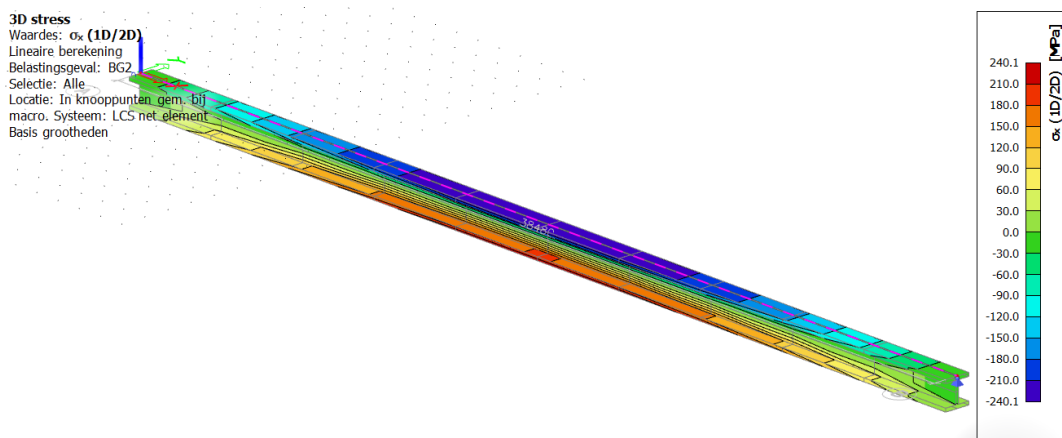


Figure 9-7 - Stresses in H-beam

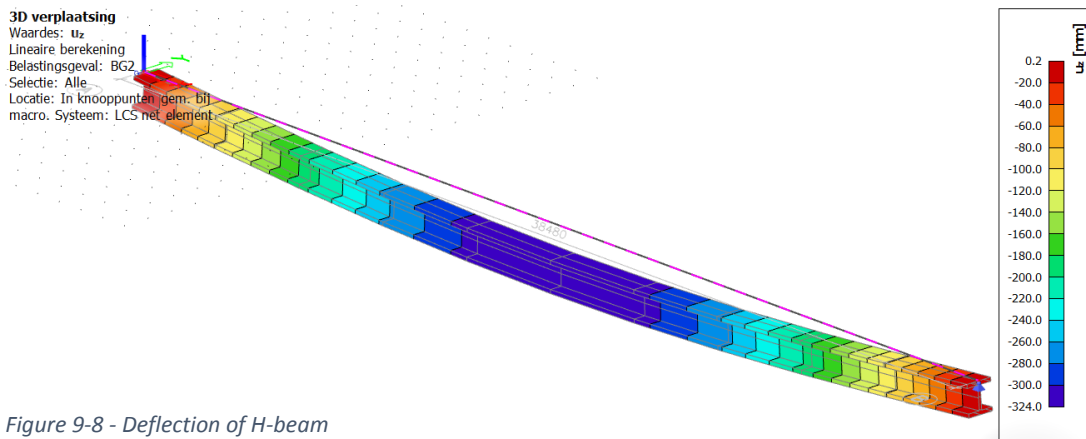


Figure 9-8 - Deflection of H-beam

The stresses according the Scia model are given in Figure 9-7 and the deflection is given in Figure 9-8. The maximum steel stress is around  $245 \text{ N/mm}^2$  and a reserve capacity is present for unforeseen forces for example wind or snow. The deflection of 32 cm over a span length of 38.48 meter is accepted and it is concluded that a steel beam construction could be designed to support the immersion platform. The height is 1.10 meter, 40 cm is left for the construction of the plate and skidding system above the beams.

A drawing of this platform is given in Figure 9-9 and Figure 9-10.

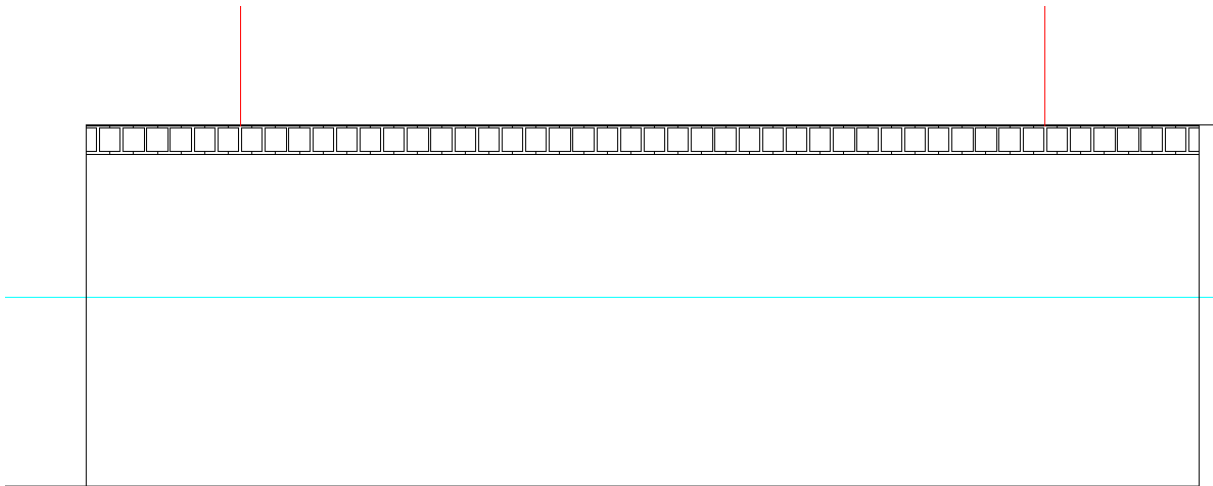


Figure 9-9 - Principle of steel beam supporting system

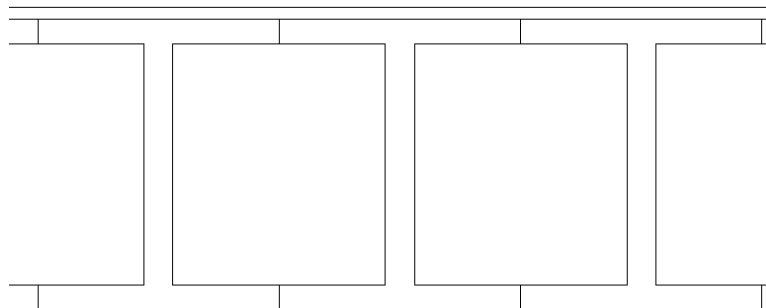


Figure 9-10 - Plate of immersion platform placed on H-beams

### 9.4.2 Lifting mechanism

A lifting mechanism must be designed to lower the platform with the GBF placed on it and to hoist the platform when the GBF is towed away. Only an indication of a feasible mechanism is shown to give an idea of what is possible. A winch system is chosen to use to lift and lower the platform, this is also done on the syncrolift that is used to transport the caissons for the flood defences at Venice from land into water, see Figure 9-11 and Figure 9-12.



Figure 9-11 - Winch system at Venice Mose project  
(newcivilengineer.com, 2011)



Figure 9-12 - Platform of Venice Mose project  
(newcivilengineer.com, 2011)

The caisson which is lowered with this winch system weights 25.000 tons and the dimensions and weight per square meter are somewhat higher but comparable with the GBF dimensions. With that knowledge it is assumed that the winch system is feasible on the immersion structure.

The weight of the winch system is subdivided in two main parts:

- Cables to lift the platform:
- Additional equipment for the rotation mechanism.

The cables to lift the platform are estimated with a basic formula and the weight of the additional equipment is estimated to be somewhat higher in weight than the cables.

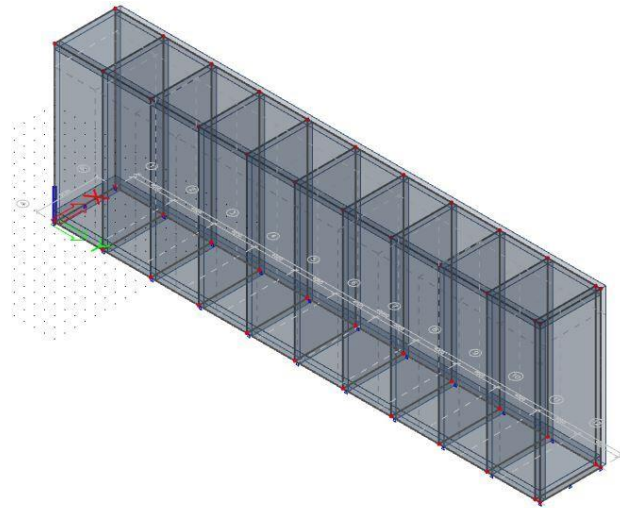


Figure 9-13 – Starting point of design foundation legs

- Cables to lift the platform:

The platform, including the GBF, weights 299,262kN, with a yield strength of the winch cables of 235 N/mm<sup>2</sup> the minimal surface area of steel cables is determined. A partial safety factor of 0.8 is included on the steel strength for the system, because not every cable is stretched equally in time.

$$A_{s,min} = \frac{W_{plat} + W_{GBF}}{0.8 \cdot f_{yd}} = \frac{(q_{steel} + q_{GBF} + q_{skid+plate}) \cdot A_{plat}}{0.8 \cdot 235} =$$

$$\frac{(36.47+124+5) \cdot 47 \cdot 38.48 \cdot 10^3}{188} = 1,591,821 mm^2 \quad (50)$$

Where:

$$f_{yd} = \text{Yield strength of steel cable [N/mm}^2\text{]}$$

The weight of the cables is estimated with the formula:

$$W_{cables} = A_{s,min} \cdot l_{cable} \cdot \rho_s = 1,591,821 \cdot 10^{-6} \cdot 15.3 \cdot 7800 = 189,968 \text{ kg} = 190 \text{ ton} \quad (51)$$

The weight of additional material to rotate the winches and to lift and lower the platform is assumed at 200 tons of steel.

### 9.4.3 Foundation

The foundation of the immersion platform has to resist the weight of the platform, must be stable on the bottom and must be stable to lower and raise the platform. Therefore it is decided to use reinforced concrete as material. With concrete a large contact area on the soil is created. Another advantage is that the internal forces mainly are compressive forces due to the platform weight, therefore concrete is applied. Because one of the requirements is that the platform is able to float internal space is required to pump water in and out. A calculation is performed to check the minimal thickness of the concrete elements. With the minimal thickness the width of the concrete foundation and the weight can be calculated. When the weight is calculated the minimal required internal space to let the platform float can be calculated and then the preliminary design is given. The starting point of the design is given in Figure 9-13. In principal the foundation consists of two large concrete hollow boxes with internal walls. The internal walls are implemented to reduce the bending moments and to prevent large concrete walls. The inner spaces could be applied as ballasting tanks. The width of the foundation is assumed to be 3 meters, the center to center distance between the walls is assumed to be 4 meter. The principle of how the forces interact on the foundation in a side view is shown in Figure 9-14.

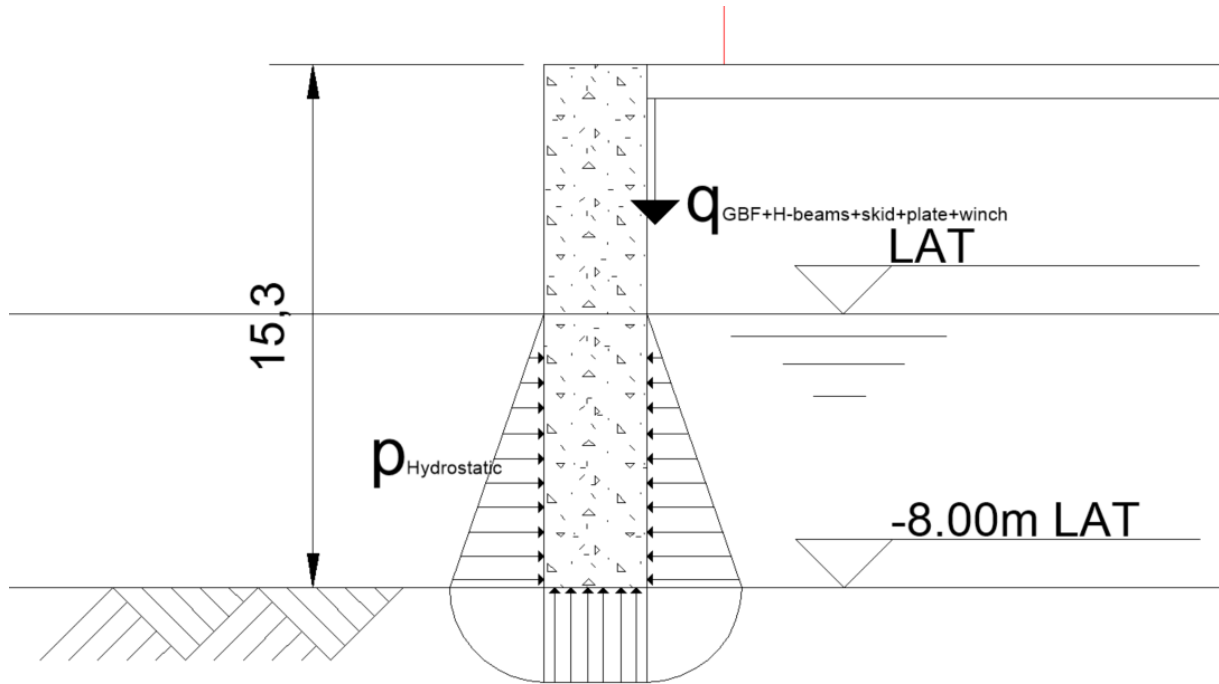


Figure 9-14 - Forces on concrete foundation (hydrostatic forces depends on water depth)

The forces are drawn on the concrete foundation which must resist the weight of the GBF, the H-beams, skidding beams, steel plate and the winch system. The calculation of the forces for the structure in operational phase is performed. When this solution is used at a project an extensive study on the dynamically loads in the floating, transporting and installing phase must be performed.

#### 9.4.3.1 Load conditions

The main loads which are present on the foundation of the immersion structure are described in this paragraph. The platform with the GBF weight, winch system, skidding beams, steel plate and H-beams and the hydrostatic pressure all interact on the concrete foundation. First the platform and GBF weight are given whereafter the hydrostatic forces on the platform are discussed.

##### Platform + GBF weight + Lift mechanism + skidding beams and steel plate:

- The force per square meter caused by the GBF on the platform is 112.7 kN/m<sup>2</sup>.
- The weight of the steel H-beams of the platform is self-weight and this is included in the Scia model. The weight of the platform is transferred to the immersion structure foundation.
- The lift mechanism weights in total 390 tons. Divide this equally over the edge of the immersion structure foundation this result in a total weight of 40.7 kN/m.
- The weight of the skidding beams and a steel plate over the H-beams is assumed at 5.0 kN/m<sup>2</sup>.

##### Hydrostatic pressure

The hydrostatic pressure is calculated with the formula:

$$p_h(d) = \rho_w g d \gamma_{Q,unfav} = 1025 \cdot 9.81 \cdot d \cdot 1.5 \quad (52)$$

Where:

$$\begin{aligned}
 p_h(d) &= \text{Hydrostatic pressure as function of depth [N/m}^2\text{]} \\
 g &= \text{Gravitational acceleration [m/s}^2\text{]} \\
 d &= \text{Depth [m]} \\
 \rho_s &= \text{Volumetric density water [kg/m}^3\text{]} \\
 \gamma_{Q,unfav} &= \text{Partial factor on unfavorable variable load (= 1.5)[-]}
 \end{aligned}$$

The hydrostatic pressure is proportional to the depth, the result of the hydrostatic force is zero at the top and  $153.8 \text{ kN/m}^2$  at the bottom, excluding partial factors. The forces under at the foundation are also  $153.8 \text{ kN/m}^2$ .

#### 9.4.3.2 Structural analysis

Because the foundation is an undetermined structure and it is impractical to calculate the internal forces by hand, a Scia Engineering model is applied. With this Scia model the forces in the cross-sections are calculated. The structure applied in the Scia model is given in Figure 9-15. The structure and the load case is symmetrical, therefore the results are given for one foundation leg only. The definitions of the walls are also given and are indicated in Figure 9-15 and Figure 9-16.

- 1: Upper slab
- 2: Bottom slab
- 3: Front and back wall
- 4: Side inner Wall
- 5: Side outer Wall
- 6: Connecting beam
- 7: Inner wall

The maximum forces in these cross-sections are given in Table 9-1. The results of the Scia model for all concrete elements are included in Annex J. For each structural element figures are given for the bending moments, shear forces and axial forces.

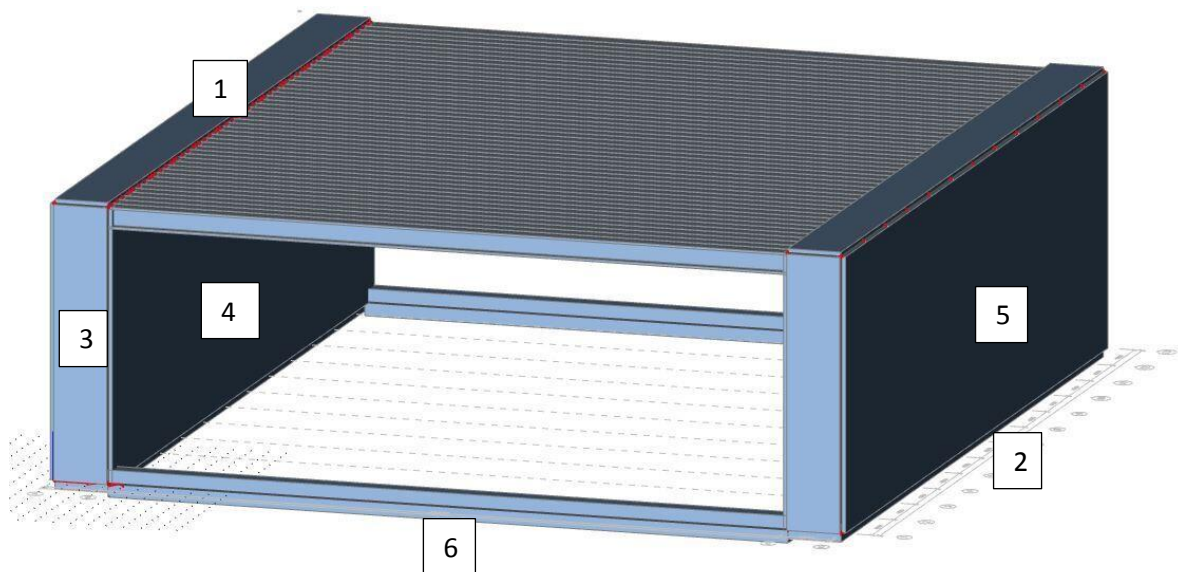


Figure 9-15 - Immersion platform as Scia Engineering model

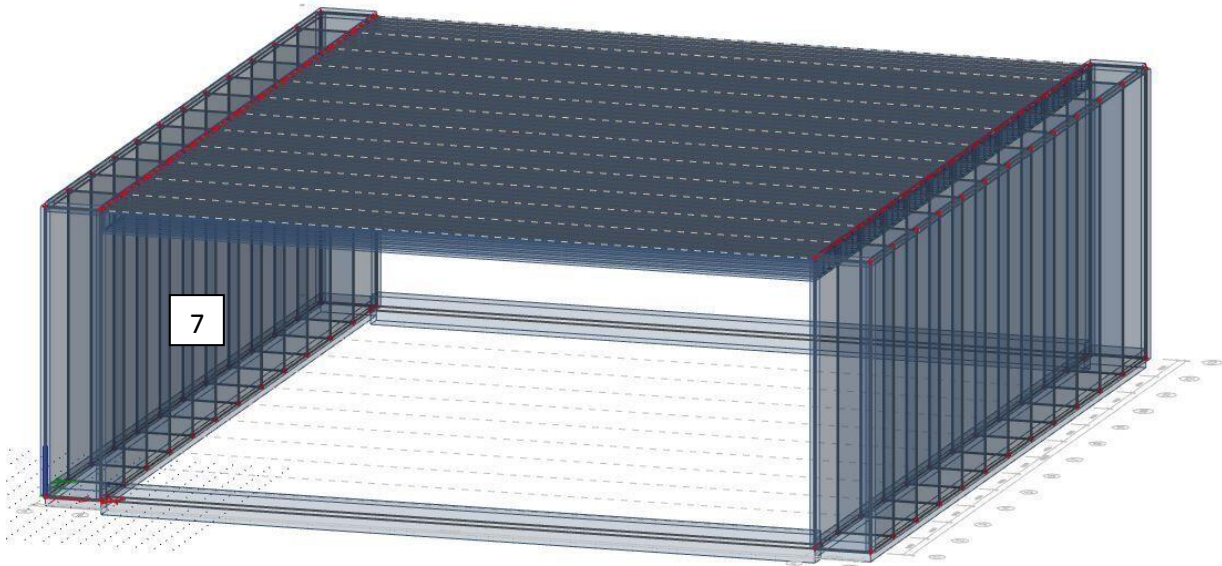


Figure 9-16 - Immersion platform transparent view

To determine the thicknesses of the foundation elements first the forces on the structure are calculated with a Scia Engineering model, in Annex J figures are included for the hydrostatic forces on the foundation legs, GBF load on the platform, the lifting mechanism on the foundation legs, the skidding beams and steel plate on the H-beams and for a visual interpretation of the linear increase of pressure by depth.

The forces in the Scia Engineer software are implemented with the characteristic values, no partial factors are present. To apply partial factors the load combination is created as is seen in Figure 9-17.

The following forces are adapted from the Scia results:

- $m_x$ : Bending moment in x-direction
- $m_y$ : Bending moment in y-direction
- $V_x$ : Shear force in x-direction
- $V_y$ : Shear force in y-direction
- $N_x$ : Axial force in x-direction
- $N_y$ : Axial force in y-direction

Naam	UGT-Set B (automatisch)
Omschrijving	
Type	EN-UGT (STR/GEO) Set B
Automatisch bijgewerkt	<input checked="" type="checkbox"/>
Constructie	Gebouw
Niet-lineaire combinatie	
Actieve coëfficiënten	<input checked="" type="checkbox"/>
<b>Inhoud van combinatie</b>	
BG1 - Self weight [-]	1,35
BG2 - Hydro [-]	1,50
BG3 - GBF [-]	1,10
BG4 - Lifting mechanism [-]	1,35
BG5 - Skid+plate [-]	1,00

Figure 9-17 - Load combinations used in Scia

Element	$d_0$ [mm]	$m_x$ [kNm]		$m_y$ [kNm]		$V_x$ [kN]		$V_y$ [kN]		$N_x$ [kN]		$N_y$ [kN]	
		Min	Max	Min	Max	Min	Max	Min	Max	Min	Max	Min	Max
<b>1: Upper slab</b>	500	-99	+51	-118	+85	-151	+563	-616	+616	-1792	+1020	-1144	+442
<b>2: Bottom slab</b>	1000	-787	+16815	-581	+1345	-2068	+15552	-4679	+4679	-2818	+20512	-2237	+5167
<b>3: Front wall</b>	500	-28	+424	-115	+142	-810	+822	-484	+310	-6824	+2781	-8044	+7939
<b>4: Side inner wall</b>	500	-904	+393	-3995	+461	-2363	+2363	-8241	+3127	-4958	+1564	-17742	-958
<b>5: Side outer wall</b>	500	-193	+326	-228	+312	-573	+573	-548	+635	-1237	+1647	-2078	+875
<b>6: Connecting slab</b>	1500	-6209	+26530	-298	+2434	-15601	+15601	-1155	+131	+6337	+9277	-295	+840
<b>7: Inner wall</b>	300	-36	+36	-89	+89	-181	+181	-336	+336	-1127	+159	-2633	+97

Table 9-1 - Result of internal forces of all structural elements

The structural minimal element thickness is chosen by calculating the minimal thickness for the case that all extremes are at one cross-section, see Table 9-2. In most cases this is unrealistic. Therefore this is the most conservative estimation of the concrete thicknesses. An example from the base slab of the immersion structure foundation is given in Figure A-86.

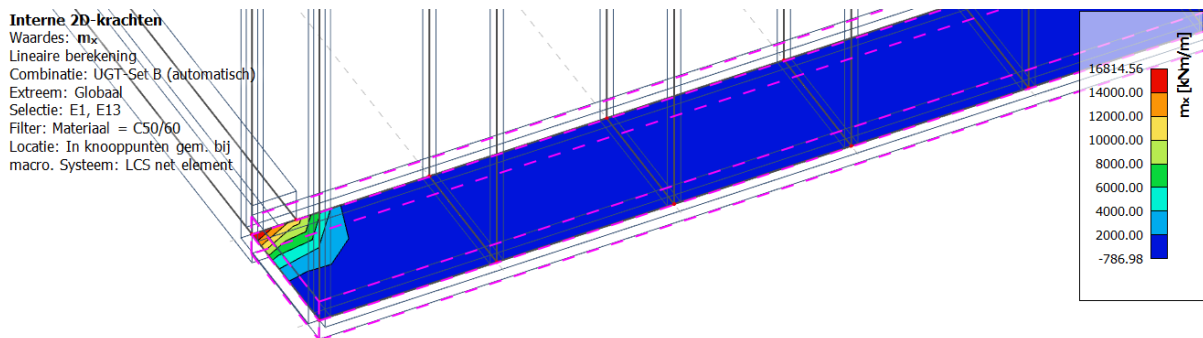


Figure 9-18 - Bending moment in x-direction for bottom slab

When the internal forces from a couple of meters from the connecting slab just a minimal thickness is needed of 455mm. Therefore a (conservative) estimation of the mean concrete thickness of 1.25 meter is done on the concrete bottom slab. Therefore in the design of the concrete thicknesses of the foundation legs a large optimization can be performed to reduce weight and material usage. This adaptation is applied on the most concrete elements, per element a short explanation is given:

- Upper slab: A minimum of 150 mm is used because of the constructability and minimal thickness.
- Front wall: Thickness is set on 650 mm because the extremes are not fixed in one location.
- Side inner wall: Thickness is changed to a mean thickness 500 mm. The minimal thickness at the main part of the side walls is 185mm but due to the placement of a lifting system local point loads could be implemented and therefore a mean thickness of 500 mm is chosen. When the lifting mechanism can be placed on the side inner wall this reduce the bending moments in other structural elements.
- Side outer wall: The thickness is changed to 500 mm due to the symmetry of the foundation leg, otherwise this thickness could be more decreased.
- Connecting slab: Comment made after showing Table 9-2.
- Inner wall: Thickness is set on 150 mm because of minimal thickness for constructability.

The assumed mean thicknesses are shown in Table 9-2.

Element	$d_0$ [mm]	$d_{min}$ [mm]	$d_{mean}$ [mm]
<b>1: Upper slab</b>	500	144	150
<b>2: Bottom slab</b>	500	2174	1250
<b>3: Front wall</b>	500	648	650
<b>4: Side inner wall</b>	500	637	500
<b>5: Side outer wall</b>	500	237	500
<b>6: Connecting slab</b>	1000	1870	H-beam
<b>7: Inner wall</b>	300	92	150

Table 9-2 – Calculated minimal thickness and estimated mean thickness of structural elements

With this calculation only a static analysis is done and a dynamic analysis must be performed for the transporting phase of the immersion structure. The outer dimensions of the GBF from the reference designs have a thickness of 500 mm. Therefore it can be assumed that the thicknesses, except for the upper slab, with a mean thickness of 500 mm are realistic.

A problem arises with the connection beam. This beam has a too large height. When the platform is lowered to the bottom a sill is present which the connecting beam is. Two possibilities to solve this problem are given:

- 1: Due to optimizations in the design the thickness could be reduced. The largest forces are present at the connection from the connecting slab and the side inner wall. An extensive analysis on this point is needed to reduce the concrete thickness.
- 2: The connecting beam could be replaced by a steel beam. When the identical beam as for the platform is used the beam can resist the forces. This beam has a height of 1.1 meter which is much lower. The steel stress according the Von Mises criteria is  $214 \text{ N/mm}^2$ , by applying the maximum shear force and bending moment at one location. See paragraph for the steel properties and explanation about the Von Mises criterion.

The second option is chosen to work out for the construction of the immersion platform.

#### 9.4.3.3 Stability

In Annex J, an example calculation is included for a foundation with a leg width of 3 meter to show the calculation principle. This foundation leg width fulfils the requirement on static stability in the floating phase but does not comply with the stability parameters of the subsoil during operation and the maximum allowable draught. Therefore the most optimal width of the foundation leg must be determined. The foundation leg must have a larger width. In Figure 9-19 the stability criteria and draught as function of the foundation leg width are shown. The unity checks must be below one to ensure stability, the draught has a maximum requirement of 10 meters and the metacentric height must be larger than 0.5 meter. The result is to design the immersion platform foundation legs with a width of 9.0 meter. A foundation leg width of 8.5 meter is just sufficient but because the design is a preliminary design and changes could be possible a leg width of 9.0 meter is chosen. It is recommended to execute the Scia model now with a foundation width of 9.0 meter. The results will differ from the first results and an iterative procedure must be executed. Because the design is only a preliminary design the thicknesses of the concrete elements are maintained and the foundation leg width of 9.0 meter is used. The most important parameters for the immersion structure with a foundation leg width of 9.0 meter are given in Table 9-3.

Parameter	Value	Unit
<b>Draught</b>	9.65	[m]
<b>Maximum weight</b>	229	[kN/m <sup>2</sup> ]

Table 9-3 - Values for immersion structure leg width=9m

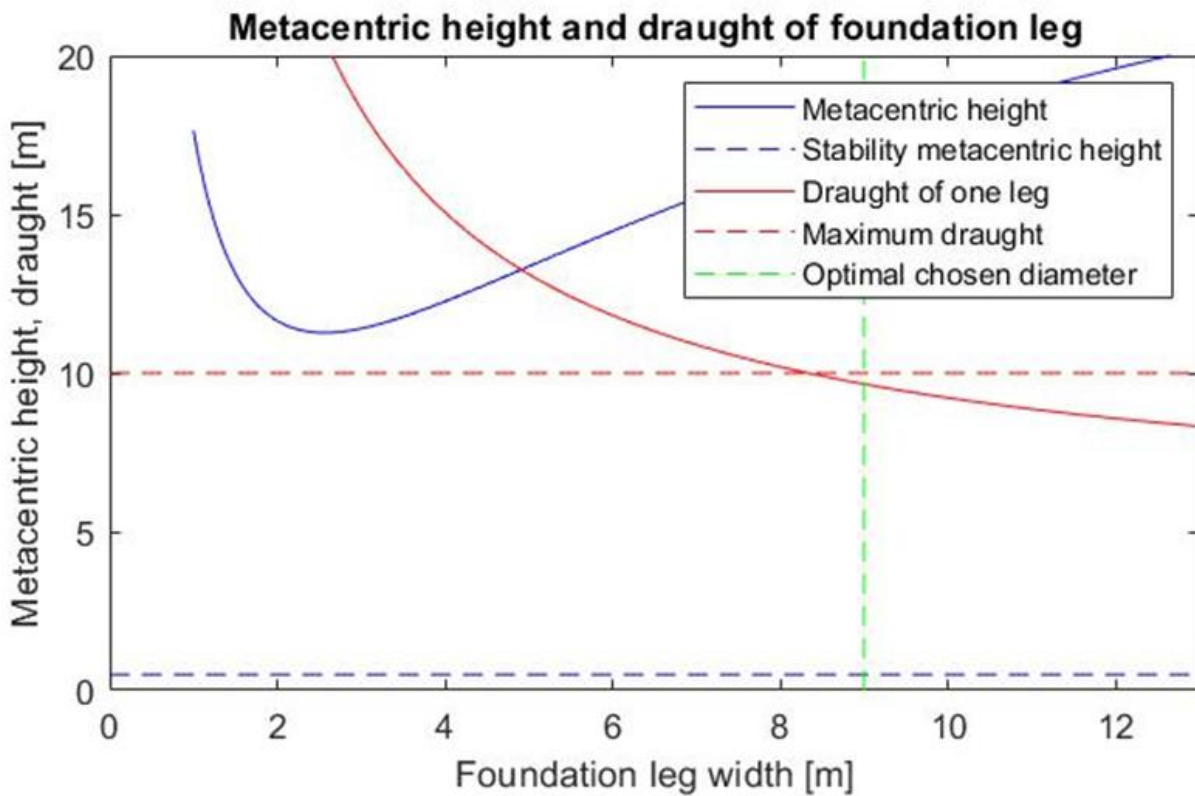
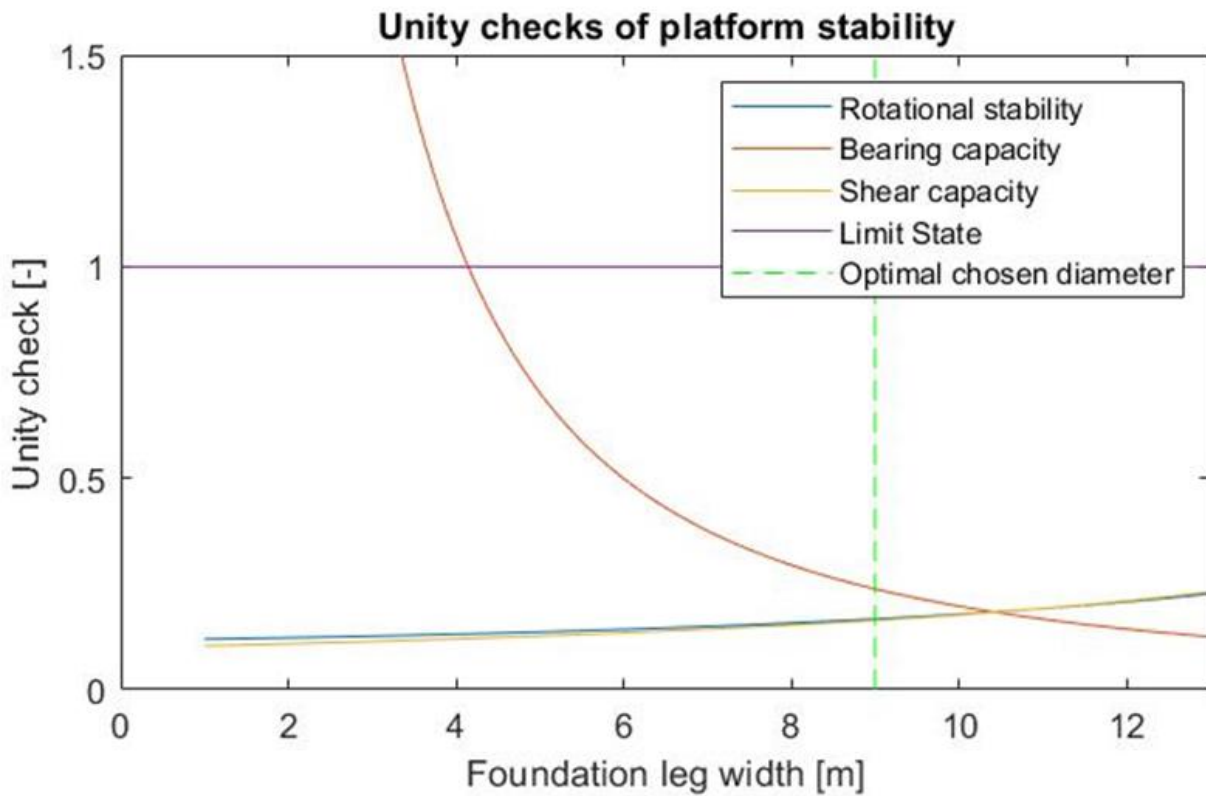


Figure 9-19 - Decision on foundation leg width

#### 9.4.4 Construction of immersion structure

Because the immersion structure itself is also a large structure which must be transported into the water the construction method of this immersion structure must be described. The length and width of the structure are 47 meter and 55 meter the immersion structure can be built on a dry or a floating dock, see Figure 9-20 and Figure 9-21. The immersion structure can be built in the majority of the dry docks and on a small part of the floating docks. A remark is made on the docks, the minimal available draught must be 10 meters. A dry dock is chosen due to the smaller renting costs.

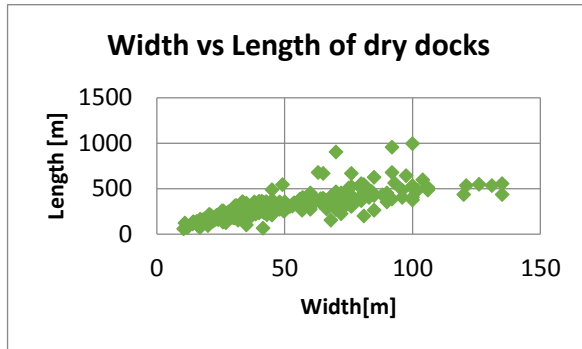


Figure 9-20 - Dimensions of available dry docks (Data: Wikipedia.org)

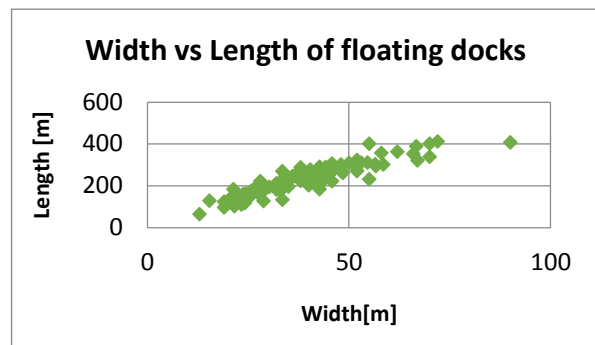


Figure 9-21 - Dimensions of floating docks

### 9.5 CONCLUSION AND RECOMMENDATIONS

The answer of the design step from this chapter was if the (temporary) structures are constructible. This question is answered with a yes. The immersion structure is designed in this chapter and consists of a platform, winch system and two concrete foundation legs.

The immersion structure is designed with a platform structure which consists of 47 H-beams as given in Figure 9-22. The connecting beam is also designed with this H-beam.

The concrete elements are designed according the dimensions in Table 9-4.

The draught of the platform is 9.65 meter.

Element	$d$ [mm]
1: Upper slab	150
2: Bottom slab	1250
3: Front wall	650
4: Side inner wall	500
5: Side outer wall	500
6: Connecting slab	H-beam
7: Inner wall	150

Table 9-4 - Thickness of concrete elements

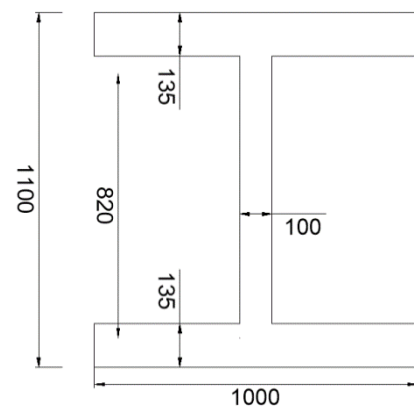


Figure 9-22 - Final design H-beam

Only a preliminary design is given of the immersion structure. The design is an iterative process and only the first iteration is executed. If the structure will be realized a more extensive design process must be executed. The concrete thicknesses could be adapted to design the most optimal concrete thicknesses at different locations where the internal forces are the highest. The connections between the foundation leg and the connecting beam and between the platform structure and foundation legs are not designed. When this design is executed the thickness of concrete elements might be changed and the stability criteria and draught change. In Figure 9-23 the immersion structure at the REBO Offshore Site and the principle of the submerging of the platform is shown. The upper platform lowers exactly between the two connecting beams and the optimal

draught is created. It is assumed that the 1 meter space between the quay wall and the immersion platform not have a large influence on the transporting system because the transporting system push the GBF from the quay wall and on the immersion platform the GBF can be towed to the middle of the platform. Therefore the one meter gap between the platform and the GBF is accepted.

This design step is answered with a yes and according the design method now only the cost calculation still has to be executed. This is done in the next chapter.

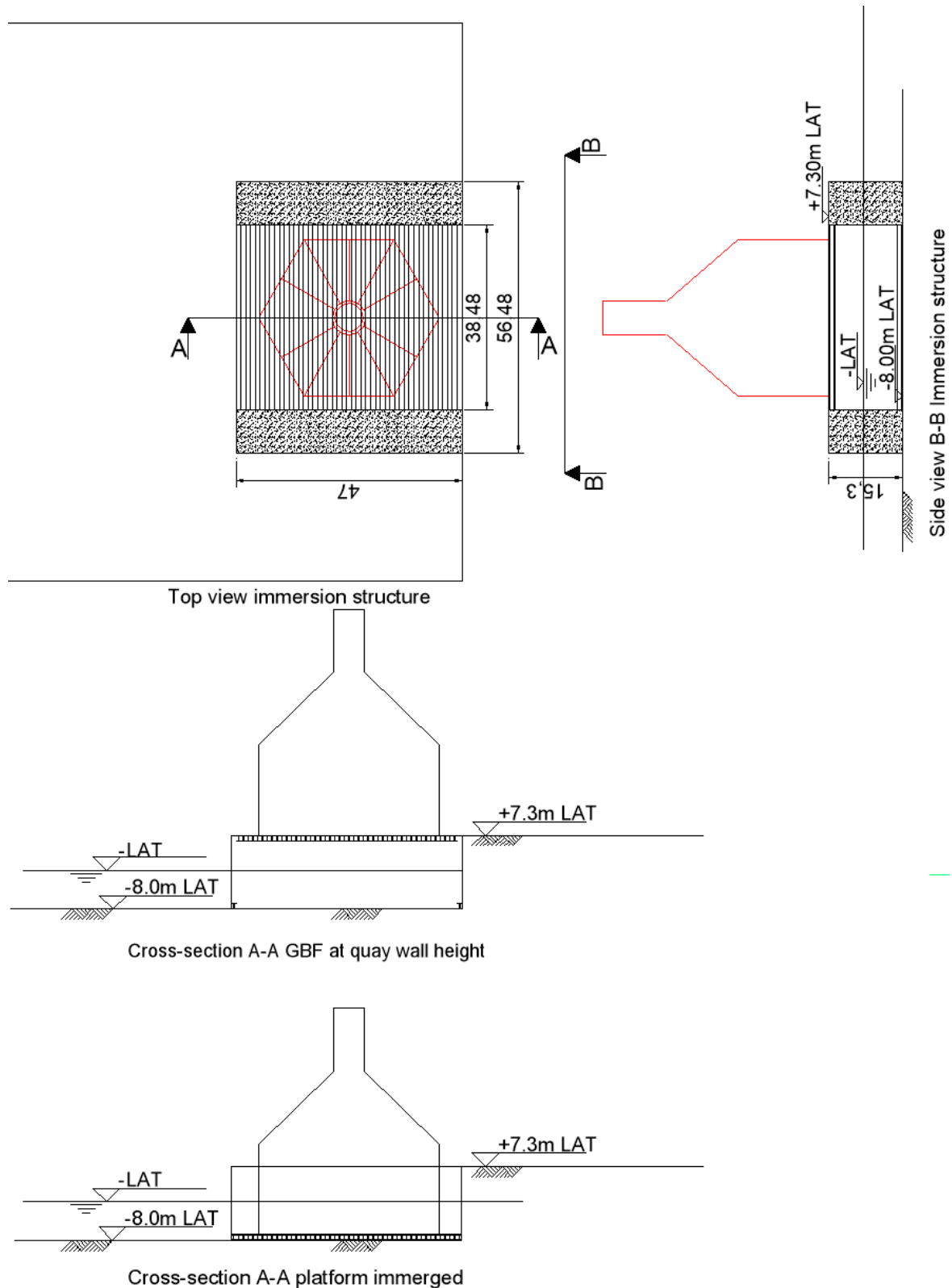


Figure 9-23 - Preliminary design immersion structure

## Chapter 10: COST CALCULATION

The last step in the design method is the cost calculation. If from the cost calculation turns out that the immersion structure is profitable above the semi-submersible vessel the project can be executed with the preliminary design of the immersion structure. When this is not the case and it turns out that the semi-submersible vessel is profitable some steps must be performed again with the new knowledge. The place of this chapter in the design process is indicated in blue in Figure 10-1.

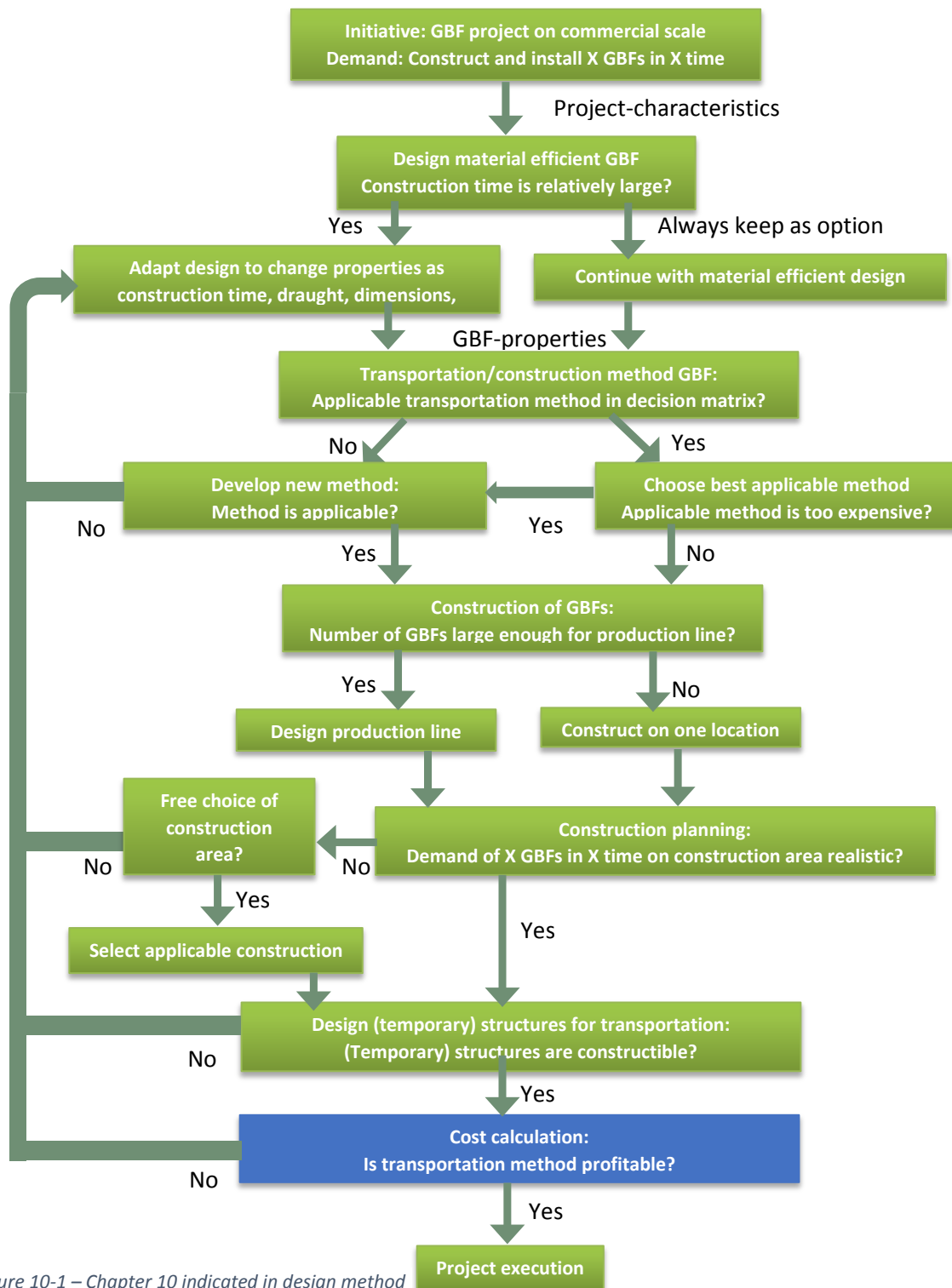


Figure 10-1 – Chapter 10 indicated in design method

In this chapter the applicability of the immersion structure is described. First the applicability of other caisson types and thereafter the applicability of the immersion structure at different port locations are described. After determining the applicability of the immersion structure on other projects the cost calculation is performed. A comparison is made between the use of the immersion structure and the semi-submersible vessel to distinguish which option is preferred.

## 10.1 APPLICABILITY OF IMMERSION STRUCTURE

The immersion structure has a large platform what can bear very large loads. There are, besides GBFs for offshore wind turbines a lot of other caisson types present. Other caisson reference projects are considered to determine the applicability of the immersion structure on other caisson types.

The immersion structure is specially designed for the REBO Offshore Site at the port of Oostende. The applicability of the immersion structure on other ports is also considered. First the applicability on other caissons is considered and thereafter the applicability on other quay walls.

### 10.1.1 Applicability on other caisson types

As mentioned in chapter 2 and in Annex A there is a large variety of types of caisson which are used for various purposes. The most common caisson types are:

- Breakwater
- GBF for wind turbines
- Quay wall
- Tunnel
- Bridge piers
- Flood defense

The applicability of the immersion platform structure depends on the weight per square meter. The characteristic strength of the immersion platform is 124 kN/m<sup>2</sup> for the weight of the GBF. Because this weight includes a partial safety factor of 1.1 the maximum design strength is 112 kN/m<sup>2</sup>. In Figure 10-2 the weight and the width of reference projects of several categories where caissons are applied are shown. The weight of the reference projects is between the 60 and 120 kN/m<sup>2</sup>. The applicability of the platform is displayed with a green

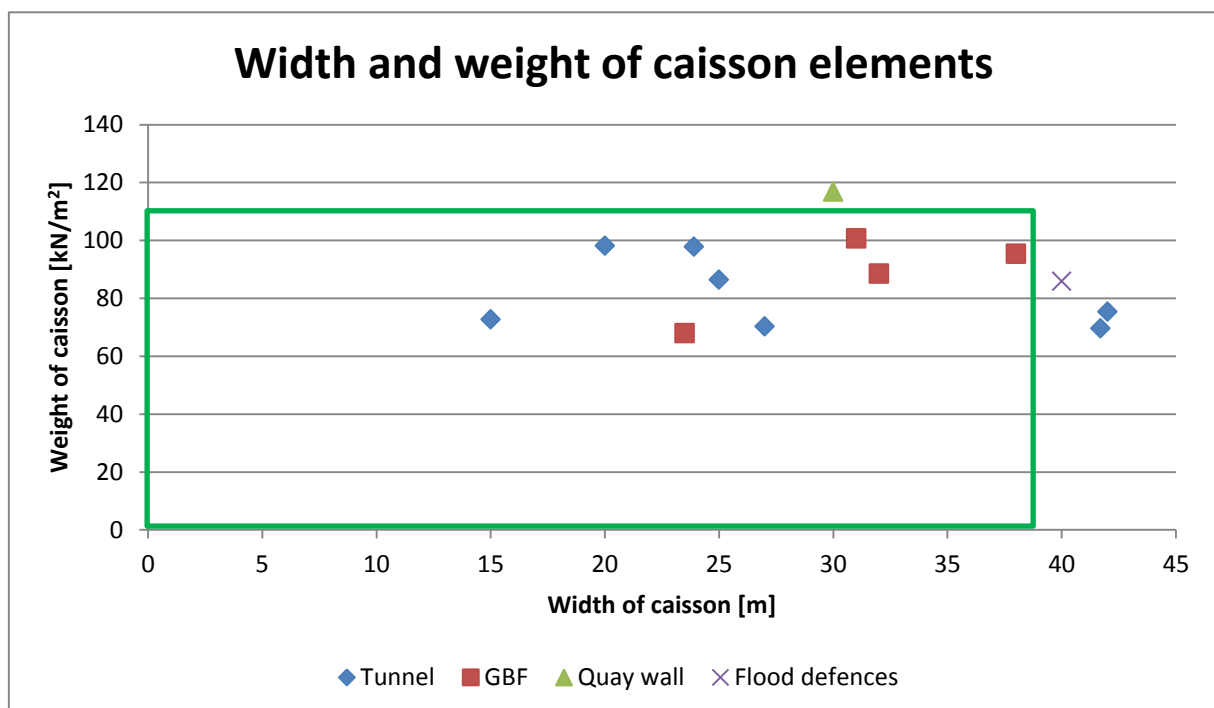


Figure 10-2 - Area of applicability of immersion platform

rectangular, in this area the designed immersion platform can be applied. The data on which Figure 10-2 is based, is displayed in Table 10-1.

Caisson	Dimensions						
	Weight [ton]	Length [m]	Width [m]	Height [m]	Diameter [m]	Weight [kN/m <sup>2</sup> ]	Draught [m]
<b>Tunnel</b>							
Femernbeltunnel	70000	217	42		-	75	7.36
Oresund tunnel	52000	176	41.7	8.5	-	70	6.78
Soderstromtunnel	20000	100	20	8.9	-	98	9.57
New Tyne Crossing	10000	90	15	8.5	-	73	7.09
Medway tunnel	30000	126	23.9	9.15	-	98	9.53
Roertunnel	29000	150	27	7.75		70	6.85
Shannon tunnel	22000	100	25	8.5		86	8.42
Busan	48000	180	26.46	9.97		99	9.65
<b>GBF</b>							
Thornton Bank	3000	-	-	-	23.5	68	6.62
Confidential	7250	-	-	-	32	88	8.63
Confidential	11016	-	-	-	38	95	9.30
Gravitas	7740	-	-	-	31	101	9.81
<b>Quay wall</b>							
Tuas port extension	15000	42	30	28	-	117	
<b>Flood defense</b>							
Venice flood defense	21000	60	40			86	8

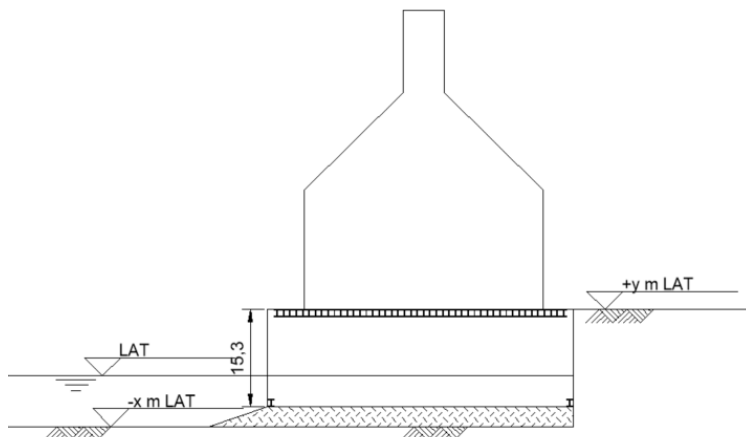
Table 10-1 - Properties of caisson construction projects

### 10.1.2 Applicability of immersion structure on port locations

The majority of the tunnel and GBF structures can be transported from land into the water by using the immersion platform. There are some other project or site characteristics that could be different with respect to the REBO Offshore Site in the port of Oostende:

- Quay wall is at larger height
- Quay wall is at lower height
- Caissons, especially tunnel elements, have a large length
- Weight is larger
  
- Quay wall is at a larger height:  
 If the quay wall is at a larger height than in the situation of the port of Oostende the platform could not reach the quay wall height, see Figure 10-3. In this case there are two options:
  - Design the immersion structure with an increased height. The drawback of this solution is that the draught of the immersion structure increases and the width of the foundation legs must be increased and the material usage is increasing.

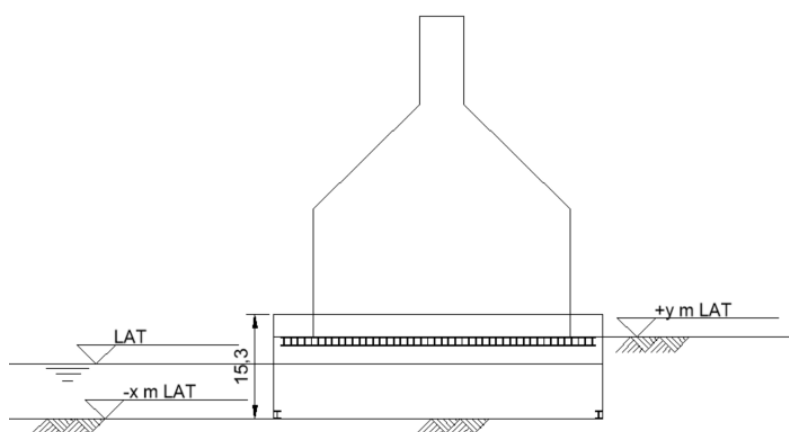
- The maximum draught of the most elements is smaller than 10 meter, see Table 10-1. Therefore the other solution is to place sand in front of the quay wall where the immersion structure can be placed on. Increasing the sand height in front of a quay wall has a positive influence on the quay wall capacity. After the project is finished the placed sand is removed and the harbour is in the original state. This solution is preferable to apply.



**Solution: Apply extra sand under structure**

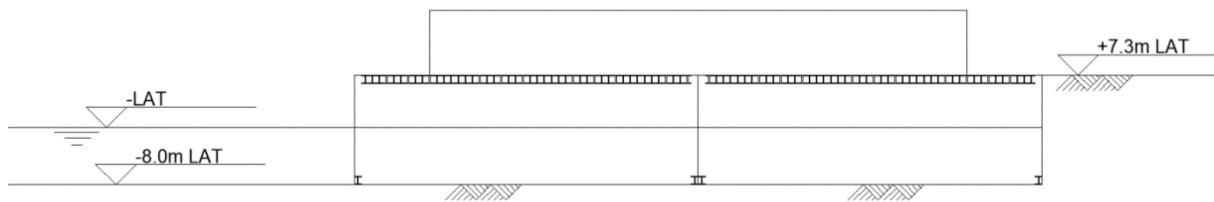
*Figure 10-3 - Solution for too high quay wall*

- Quay wall is at a smaller height:  
When the quay wall is at a smaller height the immersion structure can be placed in front of the quay wall and the foundation legs are higher than the quay wall. This is not a problem because the immersion platform can be lifted till quay wall height and the caisson can be transported on the platform and can be lowered in the water.
- Length of the element is larger than the platform:  
When the length of the caisson is too long an extra immersion structure could be build which could be placed next to the other immersion structure. The properties of structural elements will not change for a shorter or a longer structure because the structure is similar every distance between any inner wall. Only the connecting beam could be adjusted because for a longer immersion structure the forces are larger and vice versa for a shorter immersion structure. In Figure 10-5 the principle is displayed for a tunnel element, which is commonly an element with a relatively large length. The gap between two immersion structures is two meter, due to the connecting beams at the bottom. By the same argumentation as for the first problem this could not be a large problem.



**Solution: Immersion platform set on quay wall height**

*Figure 10-4 - Solution for a lower quay wall*



Longer tunnel element on two immersion structures

Figure 10-5 - Solution for a longer element

- The weight of the caisson is larger:  
If the weight of the caisson is larger than of the GBF used in the case study the steel platform can be adapted. The steel profiles could be replaced by heavier one for a project specific caisson. If the heavy caisson has a width that is smaller, the steel platform can be recalculated with a reduced weight and the immersion structure still might be used. In this case the steel stress must be checked to prevent failure of the platform.

The problems as described above all could be solved. There is only one caisson property which causes questions on the height of the platform. A minimal water depth to let the elements float is needed at the location. The immersion structure is designed for a draught of 11.2 meter of the GBFs from the case study. The available draught depends on the location where the immersion structure is placed. The draught of the immersion structure is the local water depth minus the height of the platform, which is around 1.5 meter. The maximum height of the immersion platform is at 15.3 meter. Therefore the water depth must be for most caisson projects around 12 meter. Because not all characteristics are known of various ports and quay walls it is recommended to do an extensive research on port parameters to design the optimal immersion structure height. The larger the height the more port areas could be used but the draught is also increasing and the immersion foundation legs also. However, this is negative for the material usage and the costs of the immersion structure.

### 10.1.3 Conclusion of applicability of immersion structure

Due to the applicability on other caisson projects the design could be adapted. With the dimensions as designed for the GBF transportation from the reference case the majority of the caissons projects can be executed. This is an important remark on the cost calculation. The total construction cost of the immersion platform not has to be paid for one project but could be depreciated over several projects.

## 10.2 CONSTRUCTION COST ESTIMATION OF IMMERSION PLATFORM

To calculate the construction costs of the immersion platform first the quantities are calculated, with the production rates first a planning is created from which the rental period of the dry dock can be estimated. When the planning is known the full construction costs of the immersion platform are calculated.

To calculate the cost of the construction of the immersion structure there are some important cost items:

- Rental costs dry dock
- Cost of several materials and equipment
  - Reinforced concrete
  - Steel for H-beams
  - Steel for lifting mechanism

- Formwork
- Labor costs

The unit prices and production rates which are used to give a cost estimation and a planning are given in Table 10-2 (Horst & Braam, 2016), the quantities indicated with a star are estimated and an explanation is given after this table.

Category	Sub-category	Quantity	Unit
<b>Dry dock</b>	Rental costs	40,000	[€/week]
	Crew, cranes, energy supply	20,000	[€/week]
<b>Concrete</b>	Slab	120	[€/m <sup>3</sup> ]
	Production rate concreting a slab	0.10	[man-hour/m <sup>3</sup> ]
	Wall	120	[€/m <sup>3</sup> ]
	Production rate concreting a slab	0.20	[man-hour/m <sup>3</sup> ]
	Casting concrete	100	[m <sup>3</sup> /hour]
<b>Reinforcing steel</b>	Material cost reinforcing steel	1000	[€/ton]
	Production rate braiding steel	10	[man-hour/ton]
<b>Formwork</b>	Cost plywood	20	[€/m <sup>2</sup> ]
	Cost install formwork	50	[€/m <sup>2</sup> ]
	Production rate formwork	0.5	[man-hour/m <sup>2</sup> ]
<b>Steel H-beam</b>	Steel (S355)	2000*	[€/ton]
	Production rate	32*	[man-hour/beam]
<b>Lifting mechanism</b>	Steel winch system	3500*	[€/ton]
	Production rate	5.80*	[man-hour/ton]
<b>Labour</b>	Cost man-hour	40	[€/man-hour]

Table 10-2 - Starting points cost estimation immersion structure

- Steel H-beam:  
The steel price for steel quality S235 is around 1500 euro per ton. According (Greven, 2014) the steel price for S355 is 2% higher. Due to the large cross-sectional dimensions and large length a conservative estimation of 2000 euro per ton is assumed.
- Production rate H-beam:  
The installation of the H-beams is assumed to be done by 8 men in 4 hours. The H-beam must be lifted by one or two cranes. With at both ends two workmen and with two supervisors this is in total eight workmen.
- Steel winch system:  
The steel winch system is constructed from steel, because the system is not known in detail a conservative cost rate of 3500 euro per ton is assumed. Due to the relatively small amount of steel needed for the winch system the total cost is not largely influenced when this cost rate appears to be too low.
- Production rate winch system:  
The winch system is installed on each H-beam. It is assumed that one system can be installed by three workmen in 1 day. Dividing the total weight of 390 ton over 94 installing, 4.14 ton per installation point is present. With 24 workmen hours this result in a production rate of 5.80 workmen hour per ton.

A planning is created and shown in Figure 10-6. Comments are made on the planning in chronological form:

- Prepare dry dock:  
A timeframe of two weeks is assumed to prepare the dry dock for construction activities.
- Formwork bottom slab leg 1:  
A total formwork of 563 square meters must be installed. With a production rate of 0.5 mh/m<sup>2</sup> this takes 1126 man-hours. With 14 workmen this can be done in two weeks.
- Casting concrete bottom slab:  
The bottom slab has a concrete volume of 528 m<sup>3</sup>. With a concrete casting production rate of 100 m<sup>3</sup>/s one day is reserved.
- Formwork front/back/side/inner walls leg 1:  
A total formwork of 2662 m<sup>2</sup> must be installed to cast all walls. With a production rate of 0.5 mh/m<sup>2</sup> this takes 5324 man-hours. Again by using 14 workmen this takes 10 weeks.
- Casting concrete front/back/side/inner walls leg 1:  
A total amount of concrete of 981 m<sup>3</sup> is needed. With a production rate of 100 m<sup>3</sup>/hour somewhat more than one day is needed, but because the concrete must be casted till a height of 15.3 two days are reserved.
- Formwork upper slab:  
A total formwork of 416 m<sup>2</sup> must be installed to cast the upper slab. With a production rate of 0.5 mh/m<sup>2</sup> this takes 832 man-hours. Again by using 14 workmen this takes 1.5 weeks. Because of the height and the more difficult placement 2 weeks is reserved to install formwork on the upper slab.
- Casting concrete upper slab:  
The upper slab consists of 63.5 m<sup>3</sup> concrete. With a concrete casting production rate of 100 m<sup>3</sup>/hour this operation takes approximately somewhat more than half an hour. Because the upper slab is at large height and because the concrete must harden the next days no extra activities can be executed and one day is reserved for this operation.
- Install lift mechanism:
  - Winch system:  
Per winch system on an H-beam it is assumed that three workmen can install one winch system a day.
  - H-beam:  
The installation of the H-beams is assumed to be done by 8 men in 4 hours. The H-beam must be lifted by one or two cranes. At both ends two workmen and two supervisors this is in total eight workmen. Two teams of three workmen install the winch systems to work with an equal production rate. Now the H-beams can be installed directly after the winch system is installed. Four days are left in between to work without influence of the winch system installation each activity.
- Restore dry dock in original state:  
All material and equipment present in the dry dock must be removed and the dry dock must be cleaned and restored in the old state. For these activities two weeks are estimated.

The construction activities are separated for foundation leg 1 and foundation leg 2. These activities are executed simultaneously. Due to the large concrete consumption of some activities these activities are not executed on the same day. In total the construction of the immersion platform takes 27 weeks.

With this outcome of 27 weeks the cost estimation can be executed as can be seen in Table 10-3. An extra percentage of 25% is reserved for additional and unforeseen costs. In total the construction of the immersion structure costs 19.1 million euro.

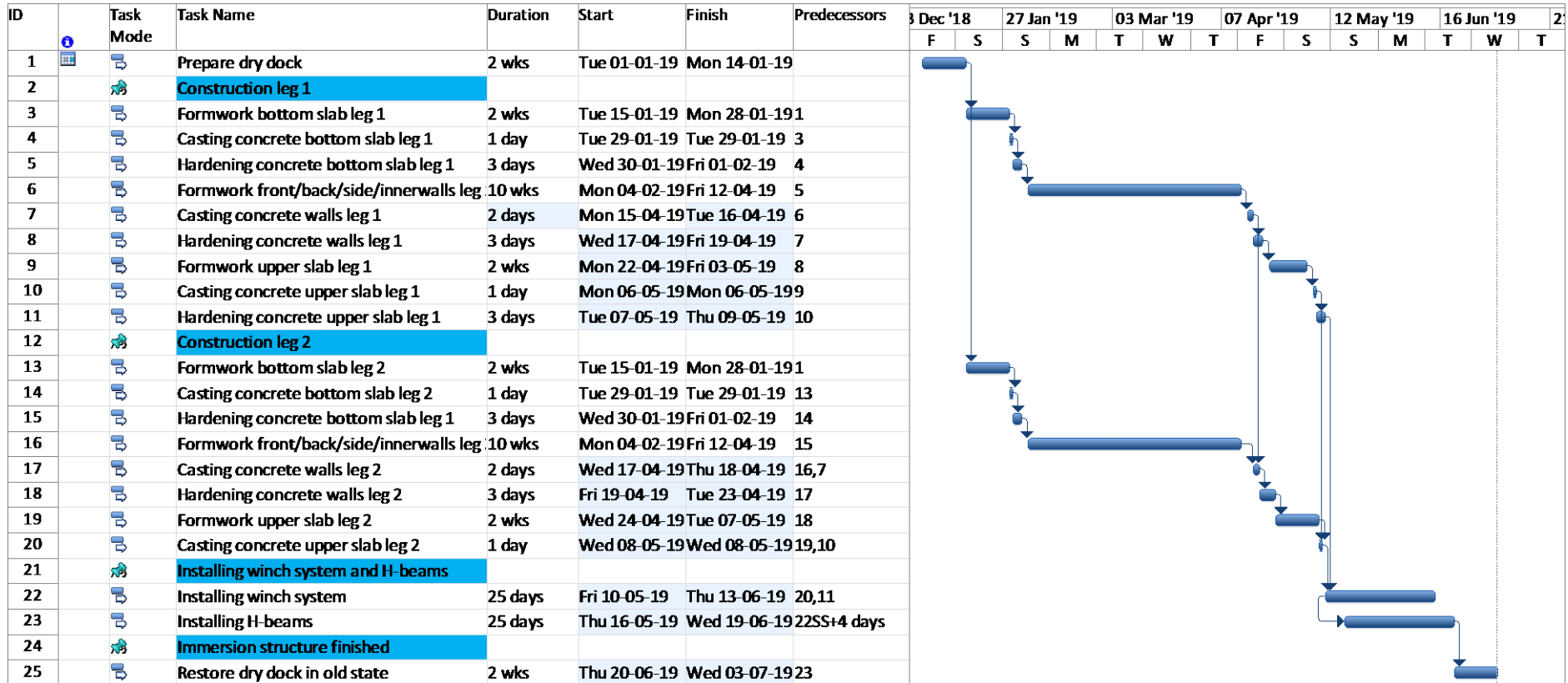


Figure 10-6 - Construction planning immersion structure

### Dry dock

-	Rent (incl. cranes and additional supplies)	26	(weeks)	€ 40,000	(Per week)	€ 1,040,000
-	Crew, energy supply etc.	26	(weeks)	€ 20,000	(Per week)	€ 520,000
					<b>Total</b>	<b>€ 1,560,000</b>
<b>Concrete</b>						
-	Slab	1,184	m3	€ 120	(Per m3)	€ 142,128
-	Wall	1,963	m3	€ 120	(Per m3)	€ 235,512
-	Concreting a slab	0.10	mh/m3			
-	Concreting a wall	0.20	mh/m3			
-	Labor	511	(mh)	€ 40	(Per mh)	€ 20,438
					<b>Total</b>	<b>€ 398,078</b>
<b>Reinforcing steel</b>						
-	Amount of steel	551	ton	€ 1,000	(Per ton)	€ 550,725
-	Labor	5,507	(mh)	€ 40	(Per mh)	€ 220,920
-	Production rate	10	(mh/ton)			
					<b>Total</b>	<b>€ 771,015</b>
<b>Formwork</b>						
-	Plywood	7,415	(m2)	€ 20	(Per m2)	€ 148,302
-	Preparation of formwork	7,415	(m2)	€ 50	(Per m2)	€ 370,755
-	Labor	3,708	(mh)	€ 40	(Per mh)	€ 148,302
-	Production rate	0.5	(mh/m2)			
					<b>Total</b>	<b>€ 667,359</b>
<b>Steel H-beam</b>						
-	H-beams	5191.6	(ton)	€ 2,000	(Per ton)	€ 10,383,200
-	Labor	1568	(mh)	€ 40	(Per mh)	€ 62,720
-	Nr of H-beams	49	(beam)			
-	Production rate	32	(mh/beam)			
					<b>Total</b>	<b>€ 10,445,920</b>
<b>Lifting mechanism</b>						
-	Steel winch system	390	(ton)	€3,500	(per ton)	€ 1,365,000
-	Labor	2260.9	(mh)	€40	(Per mh)	€ 90,435
-	Production rate	5.7971	(mh/ton)			
					<b>Total</b>	<b>€ 1,455,435</b>
					Subtotal costs	<b>€ 15,297,807</b>
					Additional costs (25%)	<b>€ 3,824,452</b>
					<b>Total cost</b>	<b>€ 19,122,259</b>

Table 10-3 - Cost estimation immersion structure

### 10.3 OPERATIONAL COST OF IMMERSION STRUCTURE

To calculate the operational cost of the immersion structure to execute the case study, it is assumed that 5 workmen are needed to operate the transportation operation. Another assumption is that in one workday the GBFs can be transported from land into water.

Also a cost factor for the maintenance and repair of the immersion platform is assumed at €15,000 per week. With an equal period of renting the semi-submersible vessel of 352 day this is equal to 50 weeks.

Workmen				Cost	
-	Workmenhours	5x8x64	[hours]	€40	(Per hour) € 102,400
-	Maintenance and repair	50	[weeks]	€10,000	(maintenance) € 500,000
					<b>Total</b> € 602,400

Table 10-4 - Total operational costs of immersion platform

Adding these costs with the construction costs the costs are 19.7 million euro to construct and use the immersion structure for the case study.

### 10.4 IMMERSION STRUCTURE APPLIED ON MORE PROJECTS

When the immersion structure is applied on one project the use of a semi-submersible vessels is profitable, the costs are approximately the half of the immersion structure. In this paragraph it is checked what the minimum amount of days for which the immersion structure is profitable.

The following starting points are used to calculate the cost of using the immersion structure per week:

	Value	unit
<b>Construction cost</b>	19.1	[million euro]
<b>Residual value</b>	15%	[initial value]
<b>Discount factor</b>	1.07	[-]
<b>Service life</b>	20	[years]
<b>Annuity</b>	0.110	[-]

Table 10-5 - Input for depreciation and interest cost estimation

The depreciation and interest is calculated with the following formula:

$$C_{D+I} = \frac{A}{U} \cdot \left(1 - \frac{V_R}{D_f^t}\right) \quad (53)$$

Where:

$$\begin{aligned}
 C_{D+I} &= \text{Depreciation and interest cost factor per week [\%]} \\
 A &= \text{Annuity [-]} \\
 U &= \text{Utilization factor [\%]} \\
 V_R &= \text{Redidual value [\%]} \\
 D_f &= \text{Discount factor [-]} \\
 t &= \text{Service time [years]}
 \end{aligned}$$

To calculate the depreciation and interest costs per week the following formula is applied:

$$C_{D+I,IS} = C_{D+I} \cdot T_c \quad (54)$$

Where:

$$\begin{aligned}
 C_{D+I,IS} &= \text{Depreciation and interest cost of immersion structure [€]} \\
 T_c &= \text{Total construction cost of immersion structure [€]}
 \end{aligned}$$

The minimal utilization of the immersion structure must be calculated to decide when the solution of applying the immersion structure is profitable. The rental and operational costs of the semi-submersible vessel is 163,450 euro per week. The immersion structure is profitable when the depreciation, interest and operational costs are lower than this value. The operational costs for the immersion structure are 12,048 euro per week. Therefore the depreciation and interest costs of the immersion structure must be lower than 151,402 euro per week. The minimal utilization factor is calculated to conclude if the immersion structure can be profitable. With a utilization factor of 22% both solutions have the equal costs.

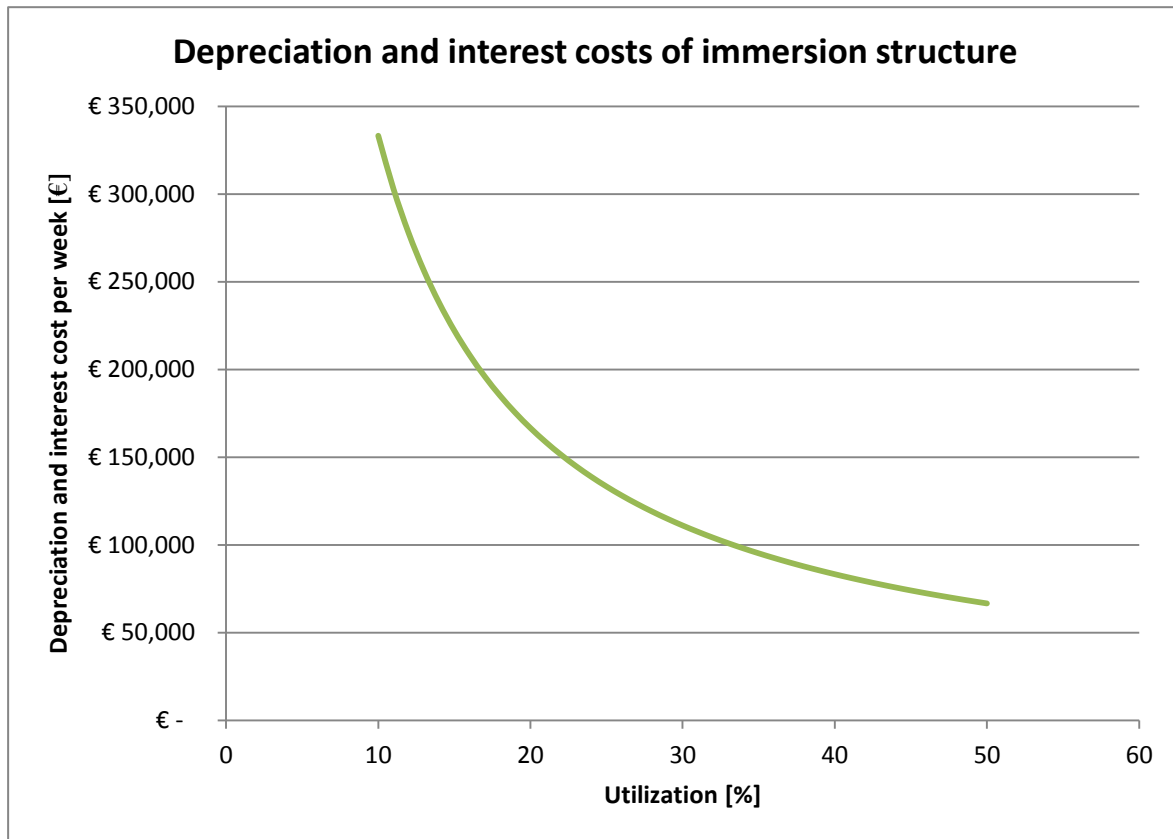


Figure 10-7 - Depreciation and interest costs as function of utilization

## 10.5 CONCLUSION

The costs to construct the immersion structure are 19.1 million euro. These costs are higher than the 13.8 million euro to rent a semi-submersible vessel for two windows to execute the transportation operation of the GBF from land into water for this project. The GBF design could be adapted to investigate a cost reduction of the immersion structure, a decrease in cross-sectional area of the H-beams could lead into a large cost reduction for the immersion platform. Otherwise it seems to be that renting a semi-submersible vessel is the best solution to execute the case study.

However, the immersion platform could be used for several projects. Therefore the utilization of the immersion structure is calculated to determine when this solution is profitable. The depreciation and interest costs are calculated from the immersion structure and compared with the rental costs of the semi-submersible vessel. The minimal utilization period to give a profitable solution is 22% in a lifetime of 20 years. Because 20 years is a very long time span and the developments are uncertain an extensive research must be executed to decide if the risks of constructing the immersion structure are too large or acceptable.

## Chapter 11: CONCLUSIONS AND RECOMMENDATIONS

---

The goal of this research is to try to find a new design method to find the optimal construction and transportation method for applying gravity based foundations for offshore foundation on commercial scale. The conclusions are given in paragraph 11.1 and the recommendations are described in paragraph 11.2.

### 11.1 CONCLUSIONS

The design objective is to investigate what is the most optimal construction and transportation method to construct a large number of gravity based foundations and transport them from land into water. In this report the answer is given on the research question:

*“What is the most optimal construction and transportation method for a large number of gravity based foundations for offshore wind turbines?”*

The new developed design method is applied and combining all design elements the most optimal construction is the use of a hexagonal GBF design which is fully constructed in a production line at the REBO site and transported on land on skidding beams to the, depending on future projects, immersion structure or semi-submersible vessel. The applicability of the immersion structure is shown in Figure 11-1.

To come to this final answer first a materialefficient design is designed which is stable during the transportation and operation phase. This results in a circular GBF with a minimal diameter of 33 meter. Because the constructability of the GBF is low and this causes a large construction time the design is adapted into a hexagonal shape. This GBF is stable during transportation and operational phase with a minimal diameter of 37.5 meter. This is less materialefficient but due to the better constructability this design could be an option.

The construction and transportation method interact with each other and therefore both designs must be considered to determine the optimal transportation method. In the decision matrix the project characteristics are used to determine which common transportation methods are applicable: only the semi-submersible vessel is applicable but has high costs: 10.5 or 13.8 million euro, depending on the storage area location. Therefore an alternative transportation method is tried to find with the help of a brainstorm session. The so-called immersion structure is found to be the best solution and this structure is designed.

After knowing the best applicable construction and transportation method a construction planning is developed. Three options are considered and the best solution according to the executed multi-criteria analysis is the use of 4 production lines with each 4 four construction locations. The construction of 64 GBFs in a period of two years is feasible and risks on delay are mitigated. Because there is no space to design the storage area at the construction the storage is done in the water. The semi-submersible vessel is rented in this case for a longer period which causes a rental cost of 13.8 million euro.

The construction and operation costs of the immersion structure are calculated and are 19.7 million euro. This is approximately double the renting and operation costs of a semi-submersible vessel for the case study. However, the immersion structure also is applicable to other caisson types which could make the immersion structure profitable. If there are in future projects where caissons must be constructed on land and are transported into the water the immersion structure can be profitable. A minimal utilization of 22% in a service time of 20 years is needed to be profitable. If this is not the case the semi-submersible vessel is a logical choice.

The developed design method is successfully applied on the case study. On projects where large caissons are involved it is not expected that the design method will not work. In this case study GBFs are implemented in the design method but in principle for each type of caisson this design method is applicable. One project characteristic is very important in the design method: the large amount of caissons which must be constructed and transported from the dry in the water. To give answer on the design method objectives a secondary design method is applied. This is functioning on some design objectives but when there is one parameter which is dominant above all other properties the secondary design method does not add much value to the outcome of the design. The solution of the immersion structure is added to the decision matrix in Figure 11-1.

Construction method	Dimensions up to Length x Width [m x m]			Draught of element [m]			Weight [ton]			Number of elements			Level of existing infrastructure		Casting independent on weather conditions
	<50x50	50x50 - 150x75	>150x75	<5	5-10	>10	<5,000	5,000-15,000	>15,000	<10	10-20	>20	Little	High	
Factory	✓	✓	✓	✓	☐	✗	✓	✓	✓	✗	✗	✓	✗	✓	+
Casting basin	✓	✓	✓	✓	☐	✗	✓	✓	✓	✓	✗	✗	✗	✓	-
Syncrolift	✓	✓	☐	✓	☐	✗	✓	✓	✓	✗	✓	✓	✓	✓	-
Semi-submersible vessel	✓	✓	✓	✓	✓	☐	✓	✓	✓	✓	✓	✓	✓	✓	-
Dry dock	✓	✓	✓	✓	☐	✗	✓	✓	✓	✓	✓	✗	✗	✓	-
Floating dock	✓	☐	✗	✓	✓	☐	✓	✓	✓	✓	✓	✗	✓	✓	-
Building on pontoons	✓	☐	✗	☐ <sup>(1)</sup>	☐ <sup>(1)</sup>	☐ <sup>(1)</sup>	✓	✓	✓	✓	✗	✗	✓	✓	-
Land based crane	✓	✗	✗	✓	✓	✓	✓	✗	✗	✓	✓	✓	✓	✓	-
Heavy lift vessel	✓	☐	✗	✓	✓	✓	✓	☐	✗	✓	✓	✗	✓	✓	-
Immersion structure	✓	☐	✗	✓	✓	☐	✓	✓	✓	✓	✓	✓	✓	✓	-

(1): Depends on available dimensions of sluices in the proximity

Figure 11-1 - Decision matrix with immersion structure

## 11.2 RECOMMENDATIONS

Because there are in the research question a lot of aspects which influence other aspects some recommendation are done to some aspects which must be investigated before this solution can be executed:

- Only the base slab diameter is changed to ensure external stability. The thicknesses of the elements are used from a reference project. The concrete thicknesses and reinforced steel quantities must be recalculated when the diameter changes.
- The environmental forces on the circular GBF geometry are not adapted for the use of a hexagonal shape. The change in forces must be investigated and implemented to calculate the stable diameter of the GBF.
- The prefabricated plates and the connections for the hexagonal GBF must be designed.
- A storage area must be designed for the amount of 26 GBFs which are finished during the season when installation is not possible.
- The immersion structure design might be adapted due a dynamic calculation in the transportation phase.
- The winch system of the immersion structure is adapted from a reference project and quantities are assumed, this system must be designed when it is decided to build the immersion structure.
- An extensive research on the market development of GBFs and/or other caisson structures must be executed to conclude if the immersion structure is profitable to realize and use.
- Because the new developed design method it is recommended to apply more case studies to investigate where problems will arise and to improve the method. The method assumes that with the use of suboptimizations an optimal result is obtained. Because the design is all about interactions it could be that another solution could be more optimal. This could be investigated and the design method can be optimized.

## BIBLIOGRAPHY

---

- 4coffshore.com*. (2013, June 5). Retrieved March 9, 2018, from <http://www.4coffshore.com/windfarms/gravity-based-support-structures-aid8.html>
- acciona-construccion.com*. (2018, February 15). Retrieved May 29, 2018, from <http://www.acciona-construccion.com/pressroom/in-depth/2017/febrero/the-kugira-the-vessel-that-builds-ports/>
- afdelingkust.be*. (n.d.). Retrieved May 11, 2018, from [http://www.afdelingkust.be/sites/default/files/atoms/files/10-jarig%20overzicht%20\\_getij.pdf](http://www.afdelingkust.be/sites/default/files/atoms/files/10-jarig%20overzicht%20_getij.pdf)
- bam.com*. (n.d.). Retrieved February 2, 2018, from [https://www.bam.com/sites/default/files/domain-606/documents/edf\\_er\\_blyth\\_brochure-606-14997770021779687906.pdf](https://www.bam.com/sites/default/files/domain-606/documents/edf_er_blyth_brochure-606-14997770021779687906.pdf)
- bamnuttall.co.uk*. (2016, September 6). Retrieved March 9, 2018, from <http://www.bamnuttall.co.uk/news/good-progress-at-blyth,38616580>
- beeldbank.rws.nl*. (n.d.). Retrieved May 29, 2018, from [https://beeldbank.rws.nl/MediaObject/Details/De\\_Tweede\\_Coentunnel\\_en\\_Bouwdok\\_Barendrecht\\_436898](https://beeldbank.rws.nl/MediaObject/Details/De_Tweede_Coentunnel_en_Bouwdok_Barendrecht_436898)
- belgianoffshoreplatform.be*. (n.d.). Retrieved April 23, 2018, from <http://www.belgianoffshoreplatform.be/nl/>
- belgianoffshoreplatform.be*. (2017, november 15). Retrieved april 23, 2018, from <http://www.belgianoffshoreplatform.be/app/uploads/cp-belga-etude-elia.pdf>
- betoncentrale.nl*. (n.d.). Retrieved May 14, 2018, from <http://www.betoncentrale.nl/media/bestanden/beton-brochure-beton-in-de-winter.pdf>
- Bijlaard, F., Abspoel, R., & Vries, P. d. (2013). *Staalconstructies*.
- Boskalis.com*. (n.d.). Retrieved January 29 2018, from <https://boskalis.com/about-us/fleet-and-equipment/offshore-vessels/heavy-transport-vessels.html>
- Boskalis.com*. (n.d.). Retrieved April 11, 2018, from <https://boskalis.com/about-us/projects/detail/offshore-wind-farm-monopile-installation-veja-mate.html>
- Bouygues-construction. (2018, February 14). *www.bouygues-construction.com*. Retrieved from <http://www.bouygues-construction.com/en/press/news/bouygues-construction-will-precaster-caissons-maritime-infrastructure-monaco-offshore-extension-project-marseille>
- Breugel, K. v., Braam, C., Veen, C. v., & Walraven, J. (2016). *Concrete Structures under Imposed Thermal and Shrinkage Demormations*. Delft.
- Carbon Trust. (2015). *Offshore wind industry review of GBSs*. Carbon Trust. Retrieved March 12, 2018, from <https://www.carbontrust.com/media/672062/ctc844-offshore-wind-industry-review-gbs-gravity-base-foundations.pdf>

- carbontrust.com*. (2015, November). Retrieved March 9, 2018, from <https://www.carbontrust.com/media/672062/ctc844-offshore-wind-industry-review-gbs-gravity-base-foundations.pdf>
- Cement&Betoncentrum. (2016). *Tabellen en grafieken*. Aeneas Media.
- cimc-raffles.com*. (n.d.). Retrieved May 28, 2018, from [http://www.cimc-raffles.com/en/enterprise/raffles/ability/production/taisun/201009/t20100917\\_7972.shtml](http://www.cimc-raffles.com/en/enterprise/raffles/ability/production/taisun/201009/t20100917_7972.shtml)
- cleantechnica.com*. (2014, June 22). Retrieved March 7, 2018, from <https://cleantechnica.com/2014/06/22/americas-first-wind-turbine-generated-electricity-1888/>
- concreteconstruction.net*. (n.d.). Retrieved June 14, 2018, from [http://www.concreteconstruction.net/\\_view-object?id=00000153-8bb6-dbf3-a177-9fbf56520000](http://www.concreteconstruction.net/_view-object?id=00000153-8bb6-dbf3-a177-9fbf56520000)
- c-power.be*. (n.d.). Retrieved April 13, 2018, from <http://www.c-power.be/index.php/project-phase-1/construction>
- c-power.be*. (n.d.). Retrieved April 20, 2018, from <http://www.c-power.be/index.php/project-phase-1/effective-works>
- c-power.be*. (n.d.). Retrieved April 20, 2018, from <http://www.c-power.be/index.php/general-info/windfarm-layout>
- cte-wind.com*. (n.d.). Retrieved March 7, 2018, from <http://www.cte-wind.com/vi/d-an-di-n-gio-qu-c-t/cac-cong-ty-con-c-a-chung-toi-qu-c-t/ctp-polska>
- Data: *deme-group.com*. (n.d.). Retrieved February 2, 2018, from <https://www.deme-group.com/geosea/meet-fleet>
- Data: *metoceanview.com*. (n.d.). Retrieved May 22, 2018, from <https://app.metoceanview.com/hindcast/>
- Data: *Wikipedia.org*. (n.d.). Retrieved January 29, 2018, from [https://en.wikipedia.org/wiki/Crane\\_vessel](https://en.wikipedia.org/wiki/Crane_vessel)
- deme-group.com*. (n.d.). Retrieved January 30, 2018, from <https://www.deme-group.com/nl/dec/news/eerste-fase-ontwikkeling-tuas-containerterminal-singapore-op-kruissnelheid>
- directindustry.com*. (n.d.). Retrieved May 28, 2018, from <http://www.directindustry.com/prod/terex-cranes-france-material-handling/product-7651-1561207.html>
- directindustry.es*. (n.d.). Retrieved May 29, 2018, from <http://www.directindustry.es/prod/pilosio-spa/product-56379-524934.html>
- dov.vlaanderen.be*. (n.d.). Retrieved May 15, 2018, from <https://www.dov.vlaanderen.be/portaal/?module=verkenner#ModulePage>
- drømstørre.dk*. (2003, Mai 12). Retrieved March 7, 2018, from <http://xn--drmstørre-64ad.dk/wp-content/wind/miller/windpower%20web/res/lacour1a.jpg>

- drømsjørre.dk*. (2003, July 23). Retrieved March 7, 2018, from <http://xn--drmstrre-64ad.dk/wp-content/wind/miller/windpower%20web/res/fls3.jpg> and <http://xn--drmstrre-64ad.dk/wp-content/wind/miller/windpower%20web/res/fls2.jpg>
- dutchwatersector.com*. (2013, May 9). Retrieved March 15, 2018, from <https://www.dutchwatersector.com/news-events/news/6022-strukton-awarded-contract-to-immersed-caissons-for-venice-storm-surge-barrier.html>
- energy.gov*. (2017, December 19). Retrieved March 7, 2018, from [https://www.energy.gov/sites/prod/files/styles/borealis\\_article\\_hero\\_respondxl/public/offshore%20wind%20crop.jpg?itok=IP-RCFcv](https://www.energy.gov/sites/prod/files/styles/borealis_article_hero_respondxl/public/offshore%20wind%20crop.jpg?itok=IP-RCFcv)
- energyclassroom.com*. (2004). Retrieved March 7, 2018, from <http://energyclassroom.com/wp-content/uploads/2014/08/1200-4.jpg>
- engineersireland.ie*. (n.d.). Retrieved May 29, 2018, from <https://www.engineersireland.ie/EngineersIreland/media/SiteMedia/groups/Divisions/civil/The-Formwork-to-the-Millau-Viaduct.pdf?ext=.pdf>
- femern.com*. (n.d.). Retrieved February 2, 2018, from <https://femern.com/en/Tunnel/Facts-on-the-tunnel/An-immersed-tunnel>
- Floatgen.eu*. (n.d.). Retrieved January 30, 2018, from <http://floatgen.eu/en>
- gantrex.com*. (n.d.). Retrieved May 28, 2018, from <https://www.gantrex.com/en-gu/stories-news-15-slipways-in-shipyard-industry>
- genewsroom.com*. (2018, March 1). Retrieved March 7, 2018, from <https://www.genewsroom.com/press-releases/ge-announces-haliade-x-worlds-most-powerful-offshore-wind-turbine-284260>
- Greven, S. (2014, January 16). *bouwenmetstaal.nl*. Retrieved from [https://www.bouwenmetstaal.nl/uploads/evenementen/07\\_greven\\_s.pdf](https://www.bouwenmetstaal.nl/uploads/evenementen/07_greven_s.pdf)
- Hertogh, M., Bosch-Rekvelde, M., & Houwing, E. (2017). *Integraal Ontwerp en Beheer*. Delft.
- Holthuijsen, L. H. (2007). *Waves in Oceanic and Coastal Waters*. New York: Cambridge University Press.
- Hordijk, D., & Lagendijk, P. (2017). *Lecture notes: Concrete structures*.
- Horst, A. v., & Braam, C. (2016). *Lecture Notes Construction Technology for civil engineering structures*.
- Krabbendam, R. (2016, May 5). *heavyliftnews.com*. Retrieved March 12, 2018, from <http://www.heavyliftnews.com/news/construction---installation-of-1st-caisson-at-tuas-terminal-port-phase-1>
- liebherr.com*. (n.d.). Retrieved May 28, 2018, from <https://www.liebherr.com/en/irl/products/mobile-and-crawler-cranes/mobile-cranes/lm-mobile-cranes/details/lm1120091.html>
- mammoet.com*. (n.d.). Retrieved May 23, 2018, from <https://www.mammoet.com/equipment/special-equipment/skidding-system/skidding-system/>

- Mammoet.com*. (n.d.). Retrieved February 2, 2018, from <http://www.mammoet.com/equipment/cranes/ring-cranes/ptc-200-ds/>
- Maritime and Port Authority Singapore. (n.d.). *Youtube.com*. Retrieved January 28, 2018, from <https://www.youtube.com/watch?v=cy13DhPIBZM>
- maritime-executive.com*. (n.d.). Retrieved March 6, 2018, from <https://www.maritime-executive.com/article/phase-1-of-tuas-terminal-development-begins#gs.Fs7NyQQ>
- meteoblue.com*. (n.d.). Retrieved May 14, 2018, from [https://www.meteoblue.com/en/weather/forecast/modelclimate/ostend\\_belgium\\_2789786](https://www.meteoblue.com/en/weather/forecast/modelclimate/ostend_belgium_2789786)
- metoceanview.com*. (n.d.). Retrieved June 14, 2018, from [app.metoceanview.com/hindcast](http://app.metoceanview.com/hindcast)
- Molenaar, W., & Voorendt, M. (2018). *Manual Hydraulic Structures*. Delft: TU Delft.
- mwps.world*. (2015, September). Retrieved March 7, 2018, from [https://www.mwps.world/wp-content/uploads/2015/09/Lagerwey-LW52\\_750kW-Wind-Turbine-d-2-300x3005.jpg](https://www.mwps.world/wp-content/uploads/2015/09/Lagerwey-LW52_750kW-Wind-Turbine-d-2-300x3005.jpg)
- navionics.com*. (n.d.). Retrieved April 23, 2018, from [webapp.navionics.com](http://webapp.navionics.com)
- newcivilengineer.com*. (2011, June 28). Retrieved March 15, 2018, from <https://www.newcivilengineer.com/latest/turning-the-tide/8616691.article>
- newcivilengineer.com*. (2011, February 10). Retrieved August 3, 2018, from <https://www.newcivilengineer.com/world-view/the-rolls-royce-of-caissons-in-venice/8611198.article>
- orsted.nl*. (2017, November 28). Retrieved March 9, 2018, from <https://orsted.nl/News-archive/2017/11/Borssele-1-2-eerste-windpark-met-rotor-van-167-meter>
- otary.be*. (n.d.). Retrieved april 23, 2018, from <http://www.otary.be/en/projects>
- peinemann.nl*. (n.d.). Retrieved June 5, 2018, from <http://www.peinemann.nl/nl/kranen/mobiele-hijskranen/at-kranen/650-tons-kraan/>
- Peire, K., Nonneman, H., & Bosschem, E. (2009, June). *iadc-dredging.com*. Retrieved from <https://www2.iadc-dredging.com/wp-content/uploads/2017/02/article-gravity-base-foundations-for-the-thornton-bank-offshore-wind-farm-115-3.pdf>
- peri-usa.com*. (n.d.). Retrieved May 29, 2018, from <https://www.peri-usa.com/projects/highrise-buildings-and-towers/21st-century-tower.html>
- Pictures: C-Power.be*. (n.d.). Retrieved April 23 2018, from <http://www.c-power.be/index.php/project-phase-1/effective-works>
- polyfluor.nl*. (n.d.). Retrieved May 28, 2018, from <http://www.polyfluor.nl/en/products/finished-products/ptfe-slide-bearing-sheets-skidway-systems/>
- research.engineering.ucdavis.edu*. (n.d.). Retrieved June 14, 2018, from <https://research.engineering.ucdavis.edu/gpa/wp-content/uploads/sites/43/2015/02/Quay-Wall-P2-Labeled.jpg>
- scheuerle.com*. (n.d.). Retrieved May 28, 2018, from [https://www.scheuerle.com/fileadmin/data\\_all/files/Self-Propelled\\_Transporters\\_EN.pdf](https://www.scheuerle.com/fileadmin/data_all/files/Self-Propelled_Transporters_EN.pdf)

- scheuerle.com*. (n.d.). Retrieved May 30, 2018, from [https://www.scheuerle.com/fileadmin/data\\_all/files/Scheuerle\\_SPMT\\_EN.pdf](https://www.scheuerle.com/fileadmin/data_all/files/Scheuerle_SPMT_EN.pdf)
- Schiereck, G. (2012). *Intoduction to Bed, bank and shore protection*. Delft: VSSD.
- sciencedirect.com*. (n.d.). Retrieved March 7, 2018, from <https://www.sciencedirect.com/science/article/pii/S1364032115011752>
- severnbridges.org*. (n.d.). Retrieved June 14, 2018, from <http://www.severnbridges.org/2012/05/01/building-the-second-bridge/>
- siemens.co.uk*. (2013). Retrieved March 9, 2018, from [http://www.siemens.co.uk/en/news\\_press/index/news\\_archive/2013/london-array-worlds-largest-offshore-wind-farm-inaugurated.htm](http://www.siemens.co.uk/en/news_press/index/news_archive/2013/london-array-worlds-largest-offshore-wind-farm-inaugurated.htm)
- slideshare.net*. (2012, September 3). Retrieved March 9, 2018, from <https://www.slideshare.net/niamhmcgrath1210/delivering-large-scale-offshore-wind>
- staaltabellen.nl*. (n.d.). Retrieved august 28, 2018, from <http://www.staaltabellen.nl/images/stories/pdf/044.pdf>
- strukton.com*. (2014, June 6). Retrieved July 30, 2018, from <https://www.strukton.com/projects/immersion-storm-surge-barrier-venice/>
- strukton.nl*. (2016, June 15). Retrieved March 9, 2018, from <https://www.strukton.nl/serveimage.ashx/?path=%2FGlobal%2FGroep%2FAfbeeldingen%2FNieuws%2F2016%2FGBF.png&action=resize&rw=600&rh=0&cat=local&mw=0&mh=0>
- tehnoros-ship.ru*. (n.d.). Retrieved March 15, 2018, from [http://tehnoros-ship.ru/eng/products/ship\\_launchng\\_lifting\\_equipment/syncrolifts/](http://tehnoros-ship.ru/eng/products/ship_launchng_lifting_equipment/syncrolifts/)
- theconstructor.org*. (n.d.). Retrieved May 29, 2018, from <https://theconstructor.org/concrete/precast-concrete-construction/273/>
- theconstructor.org*. (n.d.). Retrieved May 29, 2018, from <https://theconstructor.org/building/wooden-formwork-design-calculation-concrete/16697/>
- theengineer.co.uk*. (2012, April 30). Retrieved March 9, 2018, from <https://www.theengineer.co.uk/issues/30-april-2012/wind-energy-gets-serial/>
- theguardian.com*. (2008, October 17). Retrieved March 7, 2018, from <https://www.theguardian.com/environment/2008/oct/17/wind-power-renewable-energy>
- thinkdefence.co.uk*. (2015, February). Retrieved June 14, 2018, from <https://www.thinkdefence.co.uk/2015/02/north-sea-floods-1953-swords-ploughshares/>
- vallourec.com*. (2016, October 26). Retrieved March 15, 2018, from <http://www.vallourec.com/constructionsolutions/EN/E-Library/news/Pages/beatrice-blyth.aspx>
- Voorendt, M., Molenaar, W., & Bezuyen, K. (2016). *Hydraulic Structures - Caissons*. Delft.
- Walraven, J., & Braam, C. (2018). *Prestressed concrete*.
- windenergyfoundation.org*. (n.d.). Retrieved March 7, 2018, from <http://windenergyfoundation.org/about-wind-energy/history/>

## Annexes

---

Annex A	Construction and transportation methods of reference projects.....	135
Annex B	Matlab scripts.....	148
Annex C	Construction of Thornton bank Phase I.....	164
Annex D	Bathymetry offshore wind farm locations .....	168
Annex E	Detailed bathymetry Port of Oostende .....	169
Annex F	Cone Penetration tests .....	171
Annex G	Concrete hardening.....	173
Annex H	Wave characteristics .....	174
Annex I	Leaflet of applicable semi-submersible .....	177
Annex J	Design calculation immersion structure .....	182

## Annex A CONSTRUCTION AND TRANSPORTATION METHODS OF REFERENCE PROJECTS

Constructing offshore wind foundations have a lot of similarities with other construction projects where large concrete caissons are used. In principle the gravity based foundation is a large caisson, but with respect to tunnel elements, quay walls and flood defences the shape is different. The dimensions, weight and the required number of elements are often similar to other projects. In this annex several projects where large caissons are constructed are described. The considered projects are given in Table A-1. These projects are selected to give a selection of projects with each a different construction method.

Project and caisson type	Construction method
<b>Fehmarnbelttunnel (tunnel)</b>	Factory with two docks with different height
<b>Singapore TTP 1 (quay wall)</b>	Skidding beams with semi-submersible vessel
<b>Blyth Offshore Demonstrator Project (GBF)</b>	Use of dry dock
<b>FLOATGEN (floatable wind turbine foundation)</b>	Building on the water with help of pontoons
<b>Monaco floating breakwater (breakwater)</b>	Building on floating dock
<b>Thornton Offshore Wind Farm (GBF)</b>	Use of heavy lifting vessels
<b>Venice flood defence</b>	Use of syncrolift

Table A-1 - Projects from literature study where the construction method is described

In the considered projects the caissons are large in dimensions and weight. To construct and transport the caisson from the casting place into deeper water several transportation methods are possible. Of these seven projects the construction method is described and the range of possibilities and advantages and disadvantages are given.

### A.1. FEHMARNBELTTUNNEL: FACTORY WITH TWO DOCKS

The Fehmarnbelttunnel is an, still to build, immersed tunnel between Denmark and Germany, see Figure A-1.

When the project is finished, this tunnel will be the longest immersed tunnel in the world. The tunnel consists of 89 elements, each with a length of 217 meter and a weight of 73,000 ton. These elements will be casted at location in a specially built factory. Eight production lines are designed to deliver the large amount of elements.

#### A.1.1. Construction method

The Fehmarnbelttunnel will be built with the use of 89 elements. Each element consists of several segments. To clarify the construction method, the procedure of constructing one tunnel element is described. In Figure A-2 a top view of the factory is given where the different construction phases of the factory are indicated.

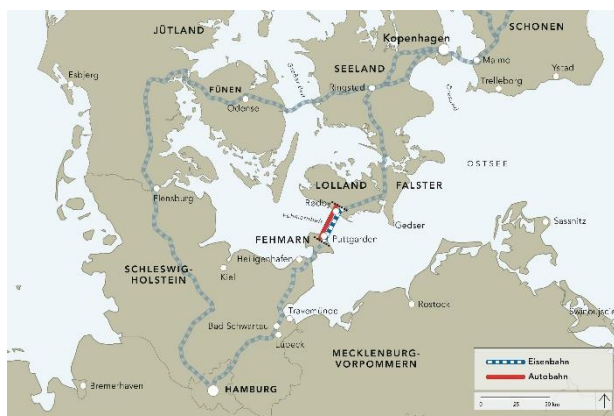


Figure A-1 - Map Fehmarnbelttunnel (femern.com)

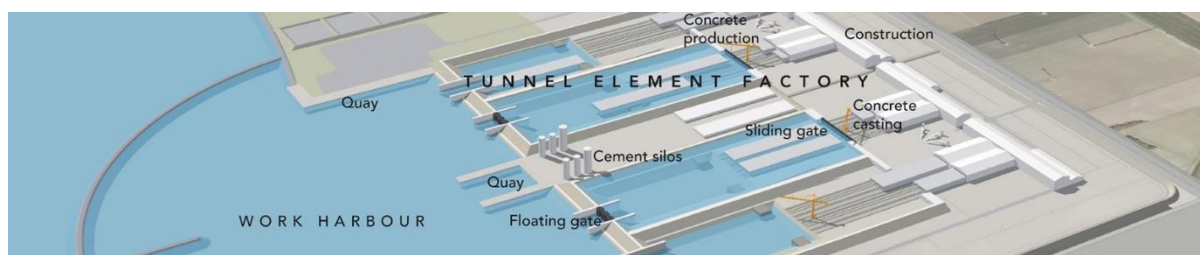


Figure A-2 - Tunnel Element Factory for Fehmarnbelttunnel (femern.com)

To construct a tunnel segment, the reinforcement net is constructed in the fabric hall. After the reinforcement net is constructed, the complete reinforcement net is transported to the casting place where the complete segment is casted. When this segment is cast it is transported over skidding beams to the curing room. During the curing process, the next segment will be already cast and will be fixed to the segment. In this way several segments can be constructed in a relatively short time. The casting process is given in Figure A-3. Several activities can go on continuously with this construction method.

The flow chart is given for 3 segments, but can go on until the number of elements is reached to construct one tunnel element.

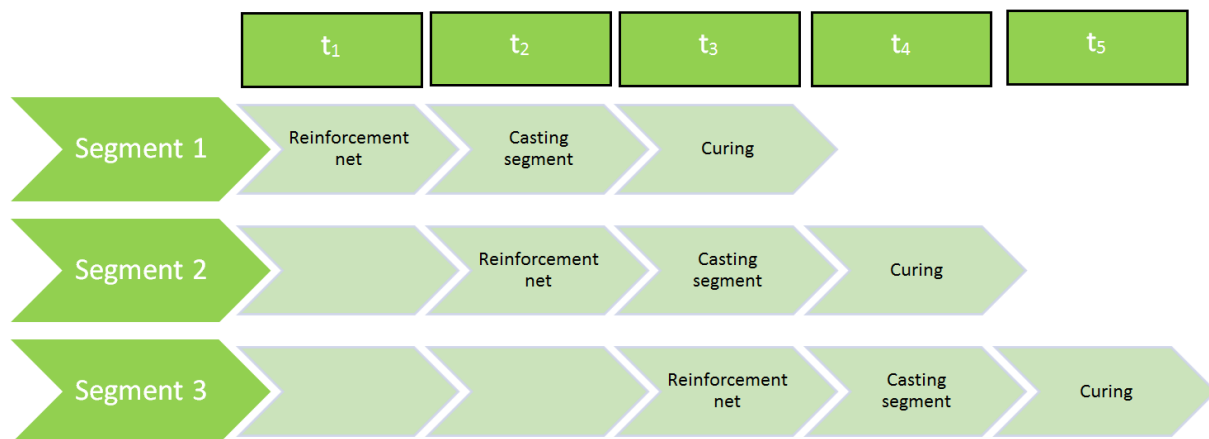


Figure A-3 - Production process tunnel element

When an element is finished the roll gate is closed behind the tunnel element and the basin is filled with water. The tunnel element floats and will be towed to the deeper part of the basin. Then the water will be lowered equal to the water level outside, see Figure A-2. The floatable gate opens and the elements will be towed to the tunnel alignment and will be immersed and connected to the previous tunnel element.

#### **A.1.1. Range of possibilities**

The advantage of a factory at the project location is that it is specially designed for a certain type of element, dimensions and weight. For every type of project a specially built factory can be a solution for the production of elements. However this type of constructing the caissons is only profitable when a project concerns a large number of caissons. A second demand for the transport of heavy elements to the final location is the proximity of water and the water has a sufficient depth.

#### **A.1.2. Advantages and disadvantages of the construction method**

The advantages and disadvantages must be considered to decide whether this construction method could be used and if it could be profitable. First the advantages of this construction method are discussed and afterwards the disadvantages:

- Project execution time:  
With the construction of a specially built factory the layout is optimally designed for the construction of elements. With an optimal layout and optimal conditions for casting and curing the time needed to construct the elements can be shortened in comparison a situation without a factory.
- Controlled conditions/quality:  
With the use of a factory the conditions in the factory halls can be optimized for the casting and curing procedure, the casting procedure is independent on local weather conditions. With optimal conditions the quality control of the concrete elements could be easier.

- Working conditions:  
The working conditions for personnel are good. In a factory hall the temperature can be controlled and workers do not have to work in rainy conditions or in low of high temperatures. This could increase the working rate of the personnel and shortens the construction time.

Nevertheless a factory is not built for every immersed tunnel project. There are several disadvantages that decide if this construction method is useful for a certain project or not:

- Costs:  
The costs to build a factory at the location are large. For the project a certain large number of concrete elements are needed to ensure a profitable use of a specially built fabric.
- Necessary area:  
The necessary area to build such a factory is relative large. Not at every project location such an area is available. When the factory cannot be built at the project location a location can be found more remote but the question is till which distance a factory is a profitable solution comparing with other construction methods.
- Environment:  
A factory has a negative impact on the local environment. A factory covers a large area and the noise and pollution of the activities harm the local environment. An important question is if the factory also could be used for other projects or that the factory must be decommissioned.
- Infrastructure:  
The presence of local infrastructure is an important aspect in the decision to build a project specific factory. Large amount of materials must be transported to the factory. This could be done over water or by road. The costs for a factory rapidly increase if these facilities are not present.

## A.2. SINGAPORE TUAS TERMINAL PORT PHASE 1: SEMISUBMERSIBLE VESSEL

Deme is involved in the project of a large harbour expansion in Singapore. The harbour will be expanded with 21 new berths with a total length of 8.6 kilometres. The harbour expansion will be constructed with the use of 222 concrete caissons with a height of 28 meters high (deme-group.com). The construction method is analysed and the advantages and disadvantages are given. The harbour expansion is displayed in Figure A-4. The project is in the execution phase and is planned to be finished in 2020.



Figure A-4 - Location of the Tuas port expansion (maritime-executive.com)

### A.2.1. Construction method

The caissons are built on the quay wall on several skidding beams. The full caisson, except the deck, is casted and the caisson is moved to the edge of the quay wall where a semi-submersible vessel is berthed. This situation is given in Figure A-5. The caisson is skidded on the vessel and the vessel navigates to deeper water where it can submerge. There, the semi-submersible vessel immerses partly and the caisson can be towed to its final location and it can be immersed, see Figure A-6.



Figure A-5 - Transportation of caisson on semi-submersible vessel (Krabbendam, 2016)



Figure A-6 - Construction method Singapore harbour extension (Maritime and Port Authority Singapore)

### A.2.2. Range of possibilities

With the use of a semi-submersible vessel the range of possibilities is large. Semi-submersible ships have dimensions large enough for the largest elements, the dimensions goes up to a length of 275 and a width of 70 meters. The capacity of semi-submersible vessels goes up to 117,000 tons (Boskalis.com). The possibility to build a project specific semi-submersible vessel could be, and is in this case, feasible. The larger the project scale the more likely it is that a project specific vessel is profitable. The only restriction is that the water depth in front of the quay wall is sufficient to berth the semi-submersible vessel. On the other hand: the draught of a large caisson is in most cases larger than of a semi-submersible vessel, so when the use of a semisubmersible vessel is not possible the caisson could not at all be transported by water.

### A.2.3. Pros and cons

For this construction method the following advantages and disadvantages must be considered before a construction method is chosen.

Advantages:

- Dimensions and weight:  
A main advantage of this construction method is that the dimensions of caissons are never too large for a semi-submersible vessel. In some special cases with large projects a special semi-submersible vessel could be built.
- Flexibility:  
The use of a semi-submersible vessel gives flexibility in the transport of caissons. Caissons could be transported in more rough conditions than the caisson on itself could resist.

Disadvantages:

- Cost:  
The costs of using a large semi-submersible vessel are large. The solution for this large project is to build a project specific semi-submersible vessel but this is only a solution if the contract sum is large comparing with the costs of building a vessel and the project duration is very long causing buying a vessel could be cheaper than renting. Another option is to rent a semi-submersible vessel to use in the timeframe of the project. The question is what the most profitable solution is.
- Depth:  
The main restriction is the depth in front of the quay wall.

### A.3. BLYTH OFFSHORE DEMONSTRATOR PROJECT: EXISTING DRY DOCK

The Blyth Offshore Demonstration Project is performed to investigate the use of gravity based foundation for offshore wind turbines. The gravity based foundations are displayed in Figure A-7. In total five wind turbines are produced in a dry dock and immersed in the North Sea. An available dry dock in Newcastle upon Tyne is used and the offshore wind turbines are immersed in front of the coast of the United Kingdom, see Figure A-8.



Figure A-7 - Gravity based foundation for wind turbine in dry dock (bam.com)



Figure A-8 - Location of the Blyth project (vallourec.com, 2016)

#### A.3.1. Construction method

In an available dry dock in Newcastle upon Tyne the construction of the gravity based foundations is performed. The dry dock has sufficient dimensions to produce all foundations in one batch. After the elements are constructed the dock is inundated and the foundations float. The foundations are towed out of the dry dock and are immersed in the North Sea.

#### A.3.2. Range of possibilities

The use of a dry dock is quite restricted. A dry dock must be in the proximity and then also the dimensions have to be sufficient. Dry docks are used to maintain vessels; therefore the bottom of some dry docks narrows to the bottom. The main issue why dry docks are not always used are the dimensions. In Figure A-9 the dimensions of available dry docks worldwide are given. The main part of the dry docks has a length till 400 meter and a width till 90 meter. Therefore the presence of a suitable dry dock in the proximity is uncertain. For larger, or more, elements it is harder to find a suitable dry dock. Especially for large projects where a lot of elements have to be produced there are not many suitable dry docks because the tunnel elements must be produced in several batches and this take a lot of time and have large costs.

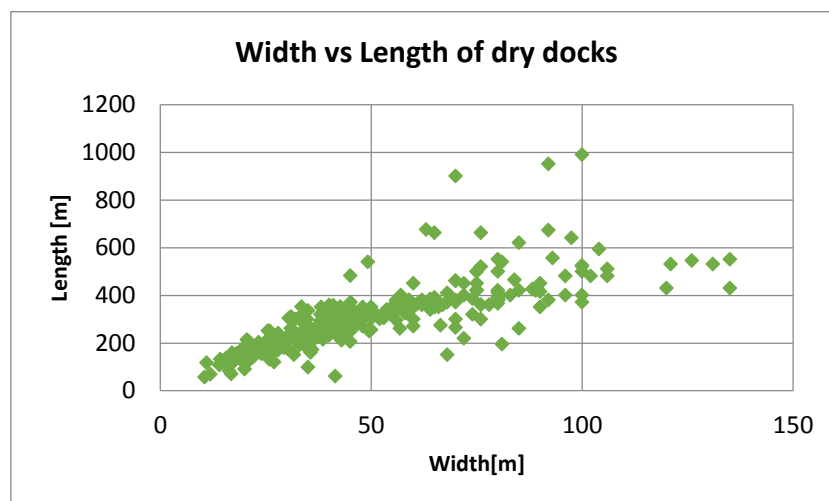


Figure A-9 - Dimensions of available dry docks (Data: Wikipedia.org)

### A.3.3. Advantages and disadvantages

The advantages and disadvantages of using a dry dock for a construction project are described. First the advantages are described and thereafter the disadvantages.

Advantages:

- Low cost:  
With the use of an available dry dock only minor construction works has to be performed to make the dry dock suitable. No construction site has to be constructed.
- Shorter project execution time:  
With the absence of the construction phase of a factory, construction pit or another type of construction place there is less time needed to complete the project and the project can be executed in a smaller timeframe.

Disadvantages:

- Fixed size:  
For a construction project a construction place can be designed with optimal dimensions. A certain length, width and depth can be designed and the construction place can be built. If a dry dock is chosen, the dimensions are fixed and could be not optimal to execute the project. If the dimensions are just too small to put an additional segment or element in a batch the construction phase will take more batches and time, this will cause an increase in cost.
- No controlled conditions:  
With using a dry dock the weather conditions could not be controlled. A roof could be built but this increase costs and could not be optimal with the use of cranes to lift materials in the dry dock.
- Available draught:  
The draught available at the dry dock is fixed. Therefore a lot of dry docks could be inappropriate to execute the caisson construction.

### A.3.4. Alternative of using a dry dock: Floating dock

In some projects like the construction of the Monaco floating breakwater a floating dock is used to construct the caisson in the dock (Bouygues-construction, 2018). In that case the construction method is quite similar but the construction takes place on water. This construction method has the same advantages and disadvantages except that the costs are higher comparing to the use of a dry dock. The use of a floating dock has one extra advantage and that is the flexibility of the construction location. With the use of a dry dock the dry docks are fixed on a place and with a floating dock the construction place can be moved to anywhere in the water with a sufficient water depth.

The supply of materials could be done by water or by land when the floating dock is berthed at the quay wall. Via water the supply of materials could be done more efficiently with larger quantities per arrival of a vessel instead of a truck.

The dimensions of existing floating docks are given in Figure A-10. It can be seen that the dimensions are quite smaller than dry docks.

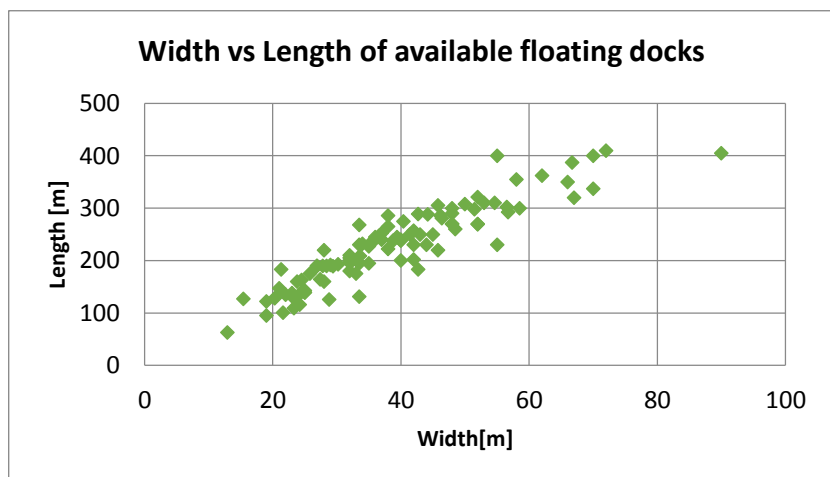


Figure A-10 - Width and lengths of available floating docks (Data: Wikipedia.org)

## A.4. FLOATGEN PROJECT: BUILDING ON WATER WITH HELP OF PONTOONS

To investigate the use of a floatable offshore wind turbine the FLOATGEN project is executed. The offshore wind turbines have a floatable foundation. This foundation is made of a large rectangular caisson. The floatable offshore wind turbine is displayed in Figure A-11. During the construction the rectangular caisson is built on three pontoons, see Figure A-12.



Figure A-11 – Animation of installed FLOATGEN foundation (Floatgen.eu)



Figure A-12 - Construction phase FLOATGEN foundation (Floatgen.eu)

### A.4.1. Construction method

The floatable foundations are constructed on three pontoons in front of a quay wall. First a working floor is created on the three pontoons, and then the caisson is constructed. When the construction of the caisson is finished the pontoons with the caisson on top are towed into a sluice. The water level in the sluice is lowered and the pontoon sinks to the bottom and is filled with water to 'fix' the pontoon at the bottom. Then the water level is raised and the caisson floats without connecting to the pontoons and can be transported and fulfil its function as a floatable foundation for an offshore wind turbine.

### A.4.2. Range of possibilities

This construction method is suitable for building projects where a small number of caissons are needed. When a large number of these wind turbines must be produced a very high number of pontoons are needed and the available area in a harbour could be insufficient. The carrying capacity of the pontoons is in most cases not the limiting factor. Pontoons have in general a carrying capacity till 15 ton per square meter and this is sufficient for most caisson types.

### A.4.3. Advantages and disadvantages

The use of pontoons have some advantages and disadvantages, these are described for this construction method.

Advantages:

- Additional working area:  
When there is insufficient area available at the quay walls the construction can be moved to pontoons in front of quay wall.
- High carrying capacity:  
Most pontoons have capacities of around 15 ton per square meter and this complies for most caisson types. The total deadweight per pontoon goes to around 20,000 tons. When the elements are too big or too heavy an extra pontoon could be used.

- Cost:  
The costs of using pontoons are lower than the use of expensive vessels like semi-submersible vessels or floating docks.

Disadvantages:

- Available area:  
Concerning projects with more elements the water area could be insufficient to position all pontoons.
- Sluice:  
The presence of a sluice with sufficient dimensions and depth is indispensable.

## A.5. THORNTON OFFSHORE WIND FARM

For the Thornton Offshore Wind Farm the transportation of the gravity based foundations is executed with SPMTs to the edge of the quay wall and the lifting operation from the quay wall into the water is executed with lifting equipment. The element can be built on the quay wall and the element can be lifted and placed in the water where it floats. Another option could be to build on a pontoon and with a heavy lift vessel lift it in the water where it floats. Then the lifting range can be shortened and this is positive for the lifting capacity of the heavy lifting vessel.



*Figure A-13 - Heavy lift vessel lifting a gravity based foundation  
(Peire, Nonneman, & Bosschem, 2009)*

### A.5.1. Range of possibilities

The possibilities are determined by the weight and the dimensions of the element. For lift vessels the capacities are given in Figure A-14.

With the focus on the fleet of Deme the next graph in Figure A-15 presents the lifting capacities of the vessels. The largest vessel of Deme is able to lift 5000 tons and the main part of the fleet has lifting capacities in the range of 400-1500 tons.

For land-based cranes the capacities differ from water-based equipment. The largest types of cranes are able to lift a weight of 5000 tons (Mammoet.com). This ring crane is displayed in Figure A-16. The majority of terrain cranes has a lifting capacity of several hundred tons. The disadvantage of a ring crane is the very large area needed for installation and that the cranes are not manoeuvrable. The cost of these cranes is also very high. At last, the availability of the cranes is low because the number of such cranes worldwide is little.

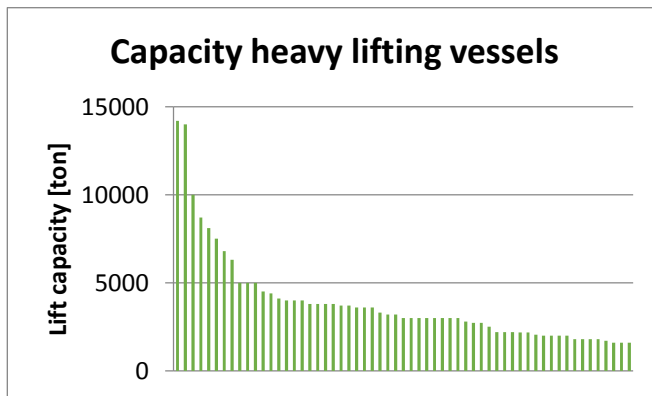


Figure A-14 - Lift capacity of heavy lift vessels (Data: Wikipedia.org)

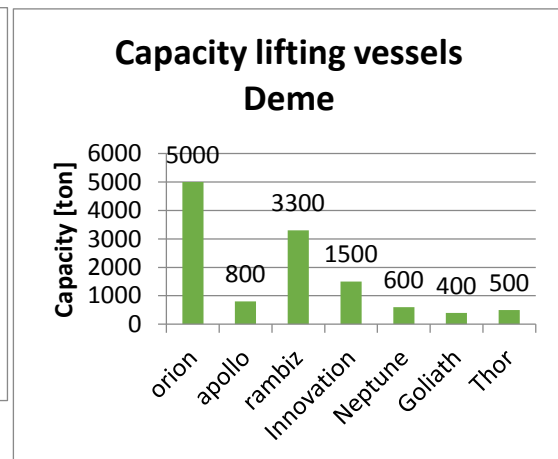


Figure A-15 - Lifting capacity Deme fleet (Data: deme-group.com)

### A.5.2. Advantages and disadvantages

Also with the use of cranes there are some advantages and disadvantages. These are given for the heavy lift vessels because this includes the main lifting operation of the heavy caissons in the Thornton Offshore Wind Farm project.

Advantages:

- Manoeuvrability:  
Heavy lift vessels are able to manoeuvre to the optimal position to lift the caisson. When the caisson is lifted the vessel could sail to the position where the caisson can be lowered into the water. With insufficient water depths this could be needed.
- Small lifting range:  
With the manoeuvrability of a vessel the crane on the vessel does not have to reach very far. This is positive for the lifting capacity of the crane.

Disadvantages

- Lifting capacity:  
The lifting capacity of the most heavy lift vessels is restricted to around 5000 tons, see Figure A-15. For higher lifting capacities there are only few heavy lift vessels available. With only few available the costs for renting a heavy lift vessel will be very high.



Figure A-16 - Ring crane (Mammoet.com)

## A.6. VENICE FLOOD DEFENCE: USE OF SYNCROLIFT

Venice is threatened by flooding due to the rising sea level but more due to the subsidence of the land. In the lagoon inlets, see Figure A-17, caissons, acting as flood defences, are immersed to protect the city of Venice.

A flood defence is constructed with the use of large caissons. The caissons are constructed on the quay wall and are transported by a rail construction to a syncrolift. This syncrolift can lower the caisson until the caisson floats due to the buoyancy of the water. A drawing of a syncrolift is included in Figure A-18 to explain the principle.



Figure A-17 - Type of flood defence, plan view of flood defence, location of immersing caissons (dutchwatersector.com, 2013)

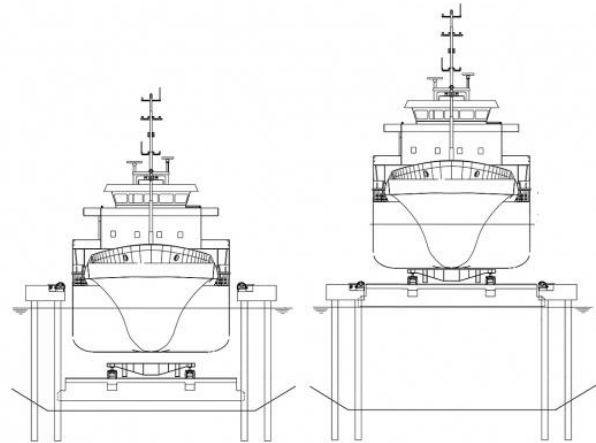


Figure A-18 - Drawing of Syncrolift (tehnoros-ship.ru)

The idea of a syncrolift originates from the shipbuilding industry. When a ship is built or must be repaired the ship is transported on a rail to the syncrolift platform and is lowered into the water, when the ship floats it can easily sail out from the platform. In the flood defence project in Venice a syncrolift is used for the large caissons. The construction area with the syncrolift is displayed in Figure A-19.



Figure A-19 - Construction area of flood defence in Venice lagoon (newcivilengineer.com, 2011)

#### A.6.1. Range of possibilities

Syncrolifts are mainly used for the launching of vessels but are sometimes used for the launching of a caisson. The ranges of possibilities are mainly determined by the dimensions and the weight capacity of the syncrolift.

- Capacity: Up to 30,000 tons (tehnoros-ship.ru)
- Dimensions: Up to 200 meter length and 40 meter width. (tehnoros-ship.ru)

The main limit of this method is the draught of the caisson. The available water depth indirectly causes the maximum available draught to apply this method.

#### A.6.2. Advantages and disadvantages

With using the syncrolift some advantages and disadvantages could be present. First the advantages whereafter the disadvantages are given.

Advantages:

- Time:  
With the use of a syncrolift a lot of elements can be launched in a short time. With a rail network on the quay wall the construction of several elements at the same time can be performed. There is no need of several batches as for the floating or dry dock and the construction could be a continuing process.

Disadvantages:

- Depending on water depth:  
The water depth in front of the syncrolift determines the maximum draught that could be created for the caissons. When this depth is insufficient the use of the syncrolift is not an option.
- Manoeuvrability:  
The syncrolift could be constructed in front of an existing quay wall. When this syncrolift is constructed it is a fixed structure and cannot be used at other locations as for the floating dock and heavy lift vessels is possible.

## **A.7. CONCLUSION CONSTRUCTION METHODS**

The advantages and disadvantages of the several construction methods are given and the most important characteristics of a project and caisson dimensions are implemented in a decision matrix. With the use of the decision matrix an overview is presented to several construction methods with their common applicability. First some comments and explanation is given per construction method whereafter the decision matrix is given.

In this chapter the main result of the literature study is given with the use of a decision matrix. In this matrix different construction methods are given with different project characteristics which could be present within a project. The characteristics in the matrix are:

- Dimension of caisson
- Draught
- Weight
- Number of elements
- Level of existing infrastructure
- Influence of weather conditions

These parameters are all described and applied on the different construction methods. For the quantities of several parameters a rough distinction is made. The boundaries of these parameters are not hard limits but give only an indication.

A green check mark is given when the construction method is applicable, a yellow equal to sign is given when this construction method is not always applicable and a closer look on the possibilities is needed. A red cross means that the construction method is in most cases not applicable. Nevertheless, with exceptional circumstances or equipment this option could always be feasible.

The result is given in Table A-2 at page 147, in paragraph A.7.1 till A.7.6 a short explanation per parameter is given of the choices for the decision matrix.

### **A.7.1. Dimensions**

The dimensions of caissons could be prescribed or optimal dimensions are designed for the most optimal caissons and construction method. In the decision matrix the dimensions are classified with three classes <50mx50m which could be gravity based foundations or quay walls, 50mx50m-150mx75m which could be for example elements for a breakwater or tunnel elements and larger elements of <150mx75m. For construction methods with the use of a factory, semi-submersible vessel, or a dry dock all available dimensions are

sufficient. For a floating dock, pontoons, land based crane and a heavy sea lift vessel the dimensions are restricted. For elements smaller than 50mx50m it is possible but for larger elements it causes more difficulties.

### A.7.2. Draught

To transport the caissons into deeper water the draught of an element is an important parameter. The draught of the caisson determines the required water depth. For a construction methods which use floating equipment the required water depth must be sufficient. With the use of a dry dock the depth of the dry dock must also be sufficient. In Figure A-20 and Figure A-21 the available depths of dry docks and floating docks are displayed. For the sufficiency of depth an extra keel clearance of 1 meter is applied. The depth is limited to the outside water level for the construction methods factory and casting basin. With large depths the casting basin also need very large dimensions, due to the slopes, and this is not desirable.

For dry docks the maximum draught of 12 meter is the maximum for which gives that 25% of the docks could be used. The dry dock has to be in the proximity, so the real probability that a dry dock could be used for caissons with a large draught than 13 meter is low. When a larger draught is needed the possibility is real low because the location of the dry dock is also important.

For floating docks the maximum is around 17 meter for which there are 15% of the floating docks left which could be possible for caisson construction. Floating docks can be towed to anywhere what is positive that every floating dock could be used anywhere where the available depth is sufficient.

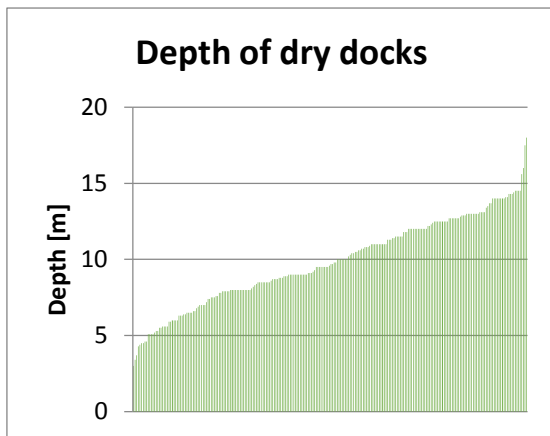


Figure A-20 - Depth of dry docks (Data: Wikipedia.org)

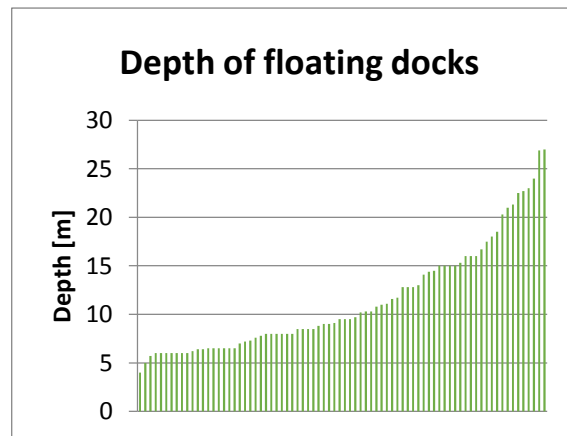


Figure A-21 - Depth of floating docks (Data: Wikipedia.org)

### A.7.3. Weight

The weight of an element depends on the volume of the applied materials. The weight of the caissons is restricted with some construction and transportation methods. The use of land based cranes is restricted till around 5000 tons; even in that case exceptional equipment is needed. For heavy sea lift vessels the lift capacity is given in Figure A-14. From that figure it can be seen that the number of vessels which could lift more than 5000 tons are low. Excepting few vessels, a larger lifting capacity than 10,000 tons is not possible. The master thesis is written for DIMCO, part of the Deme Group and in their fleet no lifting capacities above 5000 tons are present as displayed in Figure A-15 on page 143.

The carrying capacity of vessels or barges is in most cases sufficient. For construction methods which use the buoyancy of water to let the elements float, in theory there is no limit on the weight of a caisson.

### A.7.4. Number

The number of elements is an important parameter to select a construction method. Building a special factory to construct one or a few elements is absolutely not profitable and on the other hand, it is not profitable to cast many elements in a small dry dock because a lot of batches are needed. In the decision matrix a distinction is made for a number of characteristics and the suitable construction methods. For the heavy lifting vessel a comment must be made: The number of elements is not a limiting factor but when several batches must be

executed, the ratio of working time/non-working time is low and this is not profitable because the heavy lift vessels are very expensive.

#### A.7.5. Level of existing infrastructure

The level of existing infrastructure is always important to a project. When the level of infrastructure is high the supply of materials, workmen and equipment can be performed without problems. When the level of infrastructure is low, problems could occur with the supply and the project could take longer. A solution is to build temporary infrastructure to the project location but it has high costs. With some construction methods like a specially built factory and the use of a dry dock there a few locations possible and the existing infrastructure is important. With the other construction methods, like a floatable dock semisubmersible vessel, building on pontoons and the use of heavy lift vessels, the construction location could easily be changed to a location with good existing infrastructure. With these construction methods the construction is executed on floatable platforms or could be performed in an existing harbour.

#### A.7.6. Influence of weather conditions

Weather conditions influence the construction process. In some conditions the concrete curing will take longer and concrete could not be poured in temperatures below 0 degree Celsius. Welding is also dependent on weather conditions. When the weather conditions are bad the project could delay and run out of budget.

For quality it is also better to have a controlled environment. This is possible with the building of a special factory. The temperature and humidity could be influenced and rainy conditions are less important when the main part of the activities takes place inside the factory. Therefore the factory has a plus-sign to indicate the advantage and the other activities a minus-sign to indicate the disadvantage.

#### A.7.7. Decision matrix

The decision matrix, given in Table A-2, is designed by using the information above. With the use of this decision matrix the applicability of construction methods for a project could be considered.

Construction method	Dimensions up to Length x Width [m x m]			Draught of element [m]			Weight [ton]			Number of elements			Level of existing infrastructure		Casting independent on weather conditions
	<50x50	50x50-150x75	>150x75	<5	5-10	>10	<5,000	5,000-15,000	>15,000	<10	10-20	>20	Little	High	
Factory	✓	✓	✓	✓	⊘	✗	✓	✓	✓	✗	✗	✓	✗	✓	+
Casting basin	✓	✓	✓	✓	⊘	✗	✓	✓	✓	✓	✗	✗	✗	✓	-
Syncrolift	✓	✓	⊘	✓	⊘	✗	✓	✓	✓	✗	✓	✓	✓	✓	-
Semi-submersible vessel	✓	✓	✓	✓	✓	⊘	✓	✓	✓	✓	✓	✓	✓	✓	-
Dry dock	✓	✓	✓	✓	⊘	✗	✓	✓	✓	✓	✓	✗	✗	✓	-
Floating dock	✓	⊘	✗	✓	✓	⊘	✓	✓	✓	✓	✓	✗	✓	✓	-
Building on pontoons	✓	⊘	✗	⊘ <sup>(1)</sup>	⊘ <sup>(1)</sup>	⊘ <sup>(1)</sup>	✓	✓	✓	✓	✗	✗	✓	✓	-
Land based crane	✓	✗	✗	✓	✓	✓	✓	✗	✗	✓	✓	✓	✓	✓	-
Heavy lift vessel	✓	⊘	✗	✓	✓	✓	✓	⊘	✗	✓	✓	✗	✓	✓	-

(1): Depends on available dimensions of sluices in the proximity

Table A-2 - Decision matrix

## Annex B MATLAB SCRIPTS

In this annex three Matlab scripts are included:

- Stability for circular GBF
- Stability for hexagonal GBF
- Stability for immersion structure

### B.1 MATLAB SCRIPT CIRCULAR GBF

```
clear all
close all

%-----INPUT-----
% Eurocode factors
Partial_EC_Fac_Bear = 1.4; % Partial factor on bearing capacity according to the Eurocode [-]
Partial_EC_Fac_slid = 1.1; % Partial factor on sliding capacity according to the Eurocode [-]
Partial_EC_Fac_fav_V = 1.0; % Partial factor on weight favorable [-]
Partial_EC_Fac_unfav_V = 1.35; % Partial factor on weight unfavorable [-]

% General
Y_c = 2400*9.81/1000; % Volumetric weight concrete [kN/m3]
Y_w = 1025*9.81/1000; % Volumetric weight water [kN/m3]
Y_s = 15.70; % Volumetric weight sand infill [kN/m3]
g = 9.81; % Gravitational acceleration [m/s2]

% Input Base slab
D_Base_slab = linspace(25,40,750); %Diameter of base slab [m]
h_Base_slab = 1.7; % Height of base slab [m]

% Input Cylinder
t_Cyl = 0.6; % Thickness cylindrical wall [m]
Height_end_cyl = 18.81; % Height of cylindrical part [m]

% Input Inner walls
N_Walls = 6; % Number of internal walls [-]
h_Walls = 10; % Height of internal walls [m]
D_inner_cyl = 6.5; % Diameter of inner cylinder [m]
t_Walls = 0.5; % Thickness of inner walls [m]
t_inner_cyl = 0.5; % Thickness of inner cylinder [m]

% Input Cone
D_Cone_up_out = 6.5; % Diameter at top of cone [m]
t_Cone = 0.6; % Thickness of cone [m]
h_Cone = 15.19; % Height of cone [m]

% Input Tower
t_Tower = 0.5; % Thickness of tower [m]
D_Tower_out = 6.5; % Outer diameter of tower [m]
h_Tower = 13.0; % Height of tower [m]

h_GBF = 47.0; % Height of total GBF [m]

%-----Input Brinch Hansen-----
Moment_Tot = 1000350*.8*(109/(94+50)); %Total moment [kNm]
Hor_Tot = 98145*.8; %Total horizontal force [kN]

% Soil parameters
Int_fric_angle = 36*2*pi/360; %Angle of internal friction [Radians]
Angle_bet_c_s = 40*2*pi/360; %Angle of friction between sand and concrete [Radians]
Coef_friction = tan(Angle_bet_c_s); %Coefficient of friction [-]

% Water level
WL_HT = 40; % Water depth at high tide [m]
WL_LT = 32; % Water depth at low tide [m]
WL_MSL = 35; % Depth of water at Mean Sea Level [m]
Wave_Height = 5.5; % Extreme wave height [m]

%Wind turbine
Weight_wind_turbine = 11000; % Weight of wind turbine [kN]

for i=1:(length(D_Base_slab));
```

```

% Geometric calculations
A_Base_slab(i) = 1/4*pi*D_Base_slab(i)^2; % Base slab area [m2]
R_Base_slab(i) = D_Base_slab(i)/2; % Radius of GBF [m]
Mom_of_Res_Base_slab(i) = pi*D_Base_slab(i)^3/32; % Moment of resistance base slab [m3]

D_Cyl_out(i) = D_Base_slab(i); % Outer cylindrical diameter [m]
D_Cyl_in(i) = D_Cyl_out(i) - 2 * t_Cyl; % Inner cylindrical diameter [m]
h_Cyl = Height_end_cyl - h_Base_slab; % Height of cylinder [m]

angle(i) = atan(h_Cone / (0.5 * D_Base_slab(i) - 0.5 * D_Tower_out)); %Angle of cone [radian]
D_Cone_bot_out(i) = D_Base_slab(i); % Outer diameter bottom cone [m]
D_Cone_bot_in(i) = D_Base_slab(i) - (2 * t_Cone)/sin(angle(i)); % Inner diameter bottom cone [m]
D_Cone_up_in(i) = D_Cone_up_out - (2* t_Cone)/sin(angle(i)); % Inner diameter cone [m]

D_Tower_in = D_Tower_out - 2 * t_Tower; % Inner diameter tower [m]
l_Walls(i) = D_Base_slab(i)/2 - t_Cyl - D_inner_cyl/2; % length of inner walls [m]

%Volume/Weight calculation

V_Base_slab(i) = 1/4*pi*D_Base_slab(i)^2*h_Base_slab; % Volume base slab [m3]
W_Base_slab(i) = V_Base_slab(i) * Y_c; % Mass of base slab [kN]

V_Cyl(i) = 1/4*pi*(D_Cyl_out(i)^2-D_Cyl_in(i)^2)*h_Cyl; % Volume cylinder [m3]
W_Cyl(i) = V_Cyl(i)*Y_c; % Mass of base slab [kN]

V_Inner_walls(i) = N_Walls * l_Walls(i) * t_Walls * h_Walls + 1/4 * pi * (D_inner_cyl^2 - (D_inner_cyl - 2 * t_inner_cyl)^2) * h_Walls; %Volume of internal walls [m3]
W_Inner_walls(i) = V_Inner_walls(i) * Y_c; % Mass of internal walls [kN]

V_Cone(i) = 1/3*pi*h_Cone*((0.5*D_Cone_bot_out(i))^2+0.5*D_Cone_bot_out(i)*0.5*D_Cone_up_out+(0.5*D_Cone_up_out)^2)-1/3*pi*h_Cone*((0.5*D_Cone_bot_in(i))^2+0.5*D_Cone_bot_in(i)*0.5*D_Cone_up_in(i)+(0.5*D_Cone_up_in(i))^2); %Volume of cone [m3]
W_Cone(i) = V_Cone(i)*Y_c; % Mass of cone [kN]

V_Tower = 1/4*pi*(D_Tower_out^2-D_Tower_in^2)*h_Tower; % Volume of tower [m3]
W_Tower = V_Tower * Y_c; % Mass of tower [kN]

V_tot(i) = V_Base_slab(i) + V_Cyl(i) + V_Inner_walls(i) + V_Cone(i) + V_Tower; % Volume of total GBF [m3]
W_Tot_ch(i) = W_Base_slab(i) + W_Cyl(i) + W_Inner_walls(i) + W_Cone(i) + W_Tower; % Mass of total GBF [kN]

Weight_ch(i) = W_Tot_ch(i)/A_Base_slab(i); % Total weight per square meter [kN/m2]
Draught(i) = W_Tot_ch(i)/(A_Base_slab(i)*Y_w); % Draught of GBF [m]
Weight_d_unfav = Weight_ch(i) * Partial_EC_Fac_unfav_V;
Weight_d_fav = Weight_ch(i);

V_GBF_outer(i) = 1/4*pi*D_Base_slab(i)^2 * (h_Base_slab + h_Cyl)+ 1/3*pi*h_Cone*(0.5*D_Cone_bot_out(i)^2+(0.5*D_Cone_bot_out(i)*0.5*D_Cone_up_out+(0.5*D_Cone_up_out)^2)+(WL_MSL - h_GBF + h_Tower)*1/4*pi*D_Tower_out^2; %Volume of total GBF [m3]
COG(i) = (V_Base_slab(i)*h_Base_slab/2 + V_Inner_walls(i)*(h_Base_slab+h_Walls/2)+V_Cyl(i)*(h_Base_slab+h_Cyl/2) + V_Cone(i)*(h_Base_slab+h_Cyl+h_Cone/3)+V_Tower*(h_Base_slab+h_Cyl+h_Cone+h_Tower/2))/V_tot(i); %Height of Centre of Gravity [m]

%-----Metacentric height: h_m=KB+BM+-KG>0.50m

KB(i) = 1/2 * Draught(i); % KB-distance [m]
BM(i) = (1/4 * pi * (0.5*D_Base_slab(i))^4) / (A_Base_slab(i) * Draught(i)); % BM-distance [m]

%Factors to determine KG: [1]:Bottom slab [2]:Cylinder [3]: Inner Walls [4]: Cone [5]:Tower
Sum_Base_slab(i) = V_Base_slab(i) * h_Base_slab/2 * Y_c;
Sum_Cyl(i) = V_Cyl(i) * (h_Base_slab + h_Cyl/2) * Y_c;
Sum_Inner_walls(i) = V_Inner_walls(i) * (h_Base_slab + h_Walls/2) * Y_c;
Sum_Cone(i) = V_Cone(i) * (h_Base_slab + h_Cyl + 1/3 * h_Cone) * Y_c;
Sum_Tower = V_Tower * (h_Base_slab + h_Cyl + h_Cone + h_Tower/2) * Y_c;

Den_Base_slab(i) = V_Base_slab(i) * Y_c;
Den_Cyl(i) = V_Cyl(i) * Y_c;

```

```

Den_Inner_walls(i)= V_Inner_walls(i) * Y_c;
Den_Cone(i)      = V_Cone(i) * Y_c;
Den_Tower       = V_Tower *Y_c;
KG(i)           = (Sum_Base_slab(i) + Sum_Cyl(i) +Sum_Inner_walls(i) + Sum_Cone(i) +
Sum_Tower) / (Den_Base_slab(i) + Den_Cyl(i) + Den_Inner_walls(i) + Den_Cone(i) + Den_Tower);
%KG-distance [m]

h_m(i)         = KB(i) + BM(i) - KG(i); % Metacentric height [m]
UC_meta(i)     = 0.5/h_m(i);           % UC Metacentric height [m]

%-----Calculation Brinch Hansen-----
Weight_GBF_Full_unfav(i)= Partial_EC_Fac_unfav_V*(W_Tot_ch(i) + (V_GBF_outer(i) - V_tot(i) -
1*1/4*pi*D_Tower_out^2)*Y_s); % Weight of filled GBF including unfav partial factor[kN]
Weight_GBF_Full_fav(i)  = Partial_EC_Fac_fav_V*(W_Tot_ch(i) + (V_GBF_outer(i) - V_tot(i) -
1*1/4*pi*D_Tower_out^2)*Y_s); %Weight of filled GBF including fav partial factor [kN]
Weight_GBF_Full_ch(i)   = (W_Tot_ch(i) + (V_GBF_outer(i) - V_tot(i) -
1*1/4*pi*D_Tower_out^2)*Y_s); % Characteristic weight of filled GBF [kN]

Eff_Weight_GBF_Full_unfav(i) = (Weight_GBF_Full_unfav(i) + Weight_wind_turbine -
V_GBF_outer(i) * Y_w) / A_Base_slab(i); % Eff weight of filled GBF per square meter incl.
unfav partial factor[kN/m2]
Eff_Weight_GBF_Full_fav(i)= (Weight_GBF_Full_fav(i) + Weight_wind_turbine - V_GBF_outer(i) *
Y_w) / A_Base_slab(i); % Eff Weight of filled GBF per square meter incl. fav partial
factor [kN/m2]
Eff_Weight_GBF_Full_ch(i) = (Weight_GBF_Full_ch(i) + Weight_wind_turbine - V_GBF_outer(i) *
Y_w) / A_Base_slab(i); %Characteristic Eff weight of filled GBF per square meter [kN/m2]

Vert_tot_unfav(i)= Eff_Weight_GBF_Full_unfav(i)*A_Base_slab(i); % Total
effective weight GBF incl. part. fact. unfav [kN]
Vert_tot_fav(i) = Eff_Weight_GBF_Full_fav(i)*A_Base_slab(i); % Total
effective weight GBF incl. part. fact. fav [kN]
Vert_tot_ch(i) = Eff_Weight_GBF_Full_ch(i)*A_Base_slab(i); % Total
characteristic effective weight GBF [kN]

%----Shear capacity----
Tau_max(i) = tan(Angle_bet_c_s) * Eff_Weight_GBF_Full_fav(i); % Maximal
allowable shear force per square meter [kN/m2]
Resist_hor_force(i) = Tau_max(i) * A_Base_slab(i); % Maximal allowable shear force [kN]
UC_Shear_capacity(i) = (Hor_Tot) / (Resist_hor_force(i)/Partial_EC_Fac_slid);
% Unity check shear force [-]

%----Bearing capacity-----
ecc_unfav(i) = Hor_Tot/(Eff_Weight_GBF_Full_unfav(i)*A_Base_slab(i))*COG(i); %
Eccentricity [m]
b_e(i) = 2 * (R_Base_slab(i)-ecc_unfav(i)); % Width of circle segment [m]
l_e(i) = 2 * R_Base_slab(i)*sqrt(1-(1-b_e(i)/(2*R_Base_slab(i)))^2);
% Length of circle segment [m]
A_eff(i) = 2 * (R_Base_slab(i)^2*acos(ecc_unfav(i)/R_Base_slab(i))-
ecc_unfav(i)*sqrt(R_Base_slab(i)^2-ecc_unfav(i)^2)); % Effective area foundation [m2]
l_eff(i) = sqrt(A_eff(i)*l_e(i)/b_e(i)); % Effective length of foundation [m]
b_eff(i) = l_eff(i)/l_e(i)*b_e(i); % Effective width of foundation [m]
s_gamma(i) = 1 - 0.3 * b_eff(i)/l_eff(i); % Shape factor [-]
N_q = (1 + sin(Int_fric_angle)) / (1 - sin(Int_fric_angle)) * exp( pi *
tan(Int_fric_angle)); % Bearing capacity factor [-]
N_gamma = (N_q - 1) *tan(1.32*Int_fric_angle);% Bearing capacity factor [-]
gamma = 13.5; % Effective weight subsoil [kN/m3]
i_gamma(i) = (1-Hor_Tot/Vert_tot_unfav(i))^3; % Inclination factor [-]
Max_vert_force(i) = Vert_tot_unfav(i)/A_Base_slab(i)+Moment_Tot/Mom_of_Res_Base_slab(i);
% Maximal vert force [kN/m2]
Max_bearing_cap(i) = (1/2*gamma*b_eff(i)*N_gamma*s_gamma(i)*i_gamma(i)); % Maximal
bearing cap [kN/m2]
UC_Bearing_cap(i) = Max_vert_force(i)/(Max_bearing_cap(i)/Partial_EC_Fac_Bear);
% Unity Check bearing capacity [-]

%-----Rot stability-----
ecc_fav(i) = Hor_Tot/(Eff_Weight_GBF_Full_fav(i)*A_Base_slab(i))*COG(i);
Max_rot_eR(i) = D_Base_slab(i)/8; % Maximal acceptable eccentricity [m]
UC_Rot_Stab(i) = ecc_fav(i)/Max_rot_eR(i); % Unity Check rotational stability [-]

end

figure() %UC-figure
plot(D_Base_slab, UC_Rot_Stab,'DisplayName','Unity check rotational stability')
hold on
plot(D_Base_slab, UC_Bearing_cap,'DisplayName','Unity check bearing capacity')
hold on
plot(D_Base_slab, UC_Shear_capacity,'DisplayName','Unity check shear capacity')

```

```

hold on
plot(D_Base_slab, UC_meta, 'DisplayName', 'Unity check metacentric height')
hold on
plot([25,45], [1,1], 'DisplayName', 'Limit State')
hold on
plot([33,33], [0,2], '--', 'DisplayName', 'Stable diameter')
xlabel('Diameter of element [m]')
title('Unity checks of GBF stability')
ylabel('Unity check [-]')
ylim([0,1.5])
xlim([29,38])
legend()

figure() %zoom in figure
plot(D_Base_slab, UC_Rot_Stab, 'DisplayName', 'Unity check rotational stability')
hold on
plot(D_Base_slab, UC_Bearing_cap, 'DisplayName', 'Unity check bearing capacity')
hold on
plot(D_Base_slab, UC_Shear_capacity, 'DisplayName', 'Unity check shear capacity')
hold on
plot([25,45], [1,1], 'DisplayName', 'Limit State')
xlabel('Diameter of element [m]')
title('Unity checks of GBF stability')
ylabel('Unity check [-]')
ylim([0,1.5])
xlim([32,35])
legend()

figure() % Parameters GBF
subplot(3,1,1)
plot(D_Base_slab, Draught)
title('Draught of element')
ylabel('Draught [m]')
xlim([29,38])

subplot(3,1,2)
plot(D_Base_slab, Weight_ch)
title('Weight of GBF')
ylabel('Weight [kN/m^2]')
xlim([29,38])
hold on

subplot(3,1,3)
plot(D_Base_slab, V_tot)
title('Volume of concrete')
xlabel('Diameter of element [m]')
ylabel('Concrete [m^3]')
xlim([29,38])

clear all
close all

```

Parameter	Value	Parameter	Value
A_Base_slab	962.11	N_q	37.75
A_eff	822.69	N_Walls	6.00
angle	0.82	Partial_EC_Fac_Bear	1.40
Angle_bet_c_s	0.70	Partial_EC_Fac_fav_V	1.00
b_e	31.01	Partial_EC_Fac_slid	1.10
b_eff	27.09	Partial_EC_Fac_unfav_V	1.35
BM	7.57	R_Base_slab	17.50
Coef_friction	0.84	Resist_hor_force	173235.97
COG	9.58	s_gamma	0.73
D_Base_slab	35.00	Sum_Base_slab	32732.11
D_Cone_bot_in	33.35	Sum_Cone	439731.05
D_Cone_bot_out	35.00	Sum_Cyl	267870.87
D_Cone_up_in	4.85	Sum_Inner_walls	79463.59
D_Cone_up_out	6.50	Sum_Tower	116828.76
D_Cyl_in	33.80	t_Cone	0.60
D_Cyl_out	35.00	t_Cyl	0.60
D_inner_cyl	6.50	t_inner_cyl	0.50
D_Tower_in	5.50	t_Tower	0.50
D_Tower_out	6.50	t_Walls	0.50
Den_Base_slab	38508.37	Tau_max	180.06
Den_Cone	18419.34	UC_Bearing_cap	0.28
Den_Cyl	26121.00	UC_meta	0.16
Den_Inner_walls	11860.24	UC_Rot_Stab	0.83
Den_Tower	2884.66	UC_Shear_capacity	0.50
Draught	10.11	V_Base_slab	1635.59
ecc_fav	3.64	V_Cone	782.34
ecc_unfav	2.00	V_Cyl	1109.45
Eff_Weight_GBF_Full_ch	214.58	V_GBF_outer	28946.24
Eff_Weight_GBF_Full_fav	214.58	V_Inner_walls	503.75
Eff_Weight_GBF_Full_unfav	391.57	V_tot	4153.65
g	9.81	V_Tower	122.52
gamma	13.50	Vert_tot_ch	206454.58
h_Base_slab	1.70	Vert_tot_fav	206454.58
h_Cone	15.19	Vert_tot_unfav	376735.29
h_Cyl	17.11	W_Base_slab	38508.37
h_GBF	47.00	W_Cone	18419.34
h_m	3.05	W_Cyl	26121.00
h_Tower	13.00	W_Inner_walls	11860.24
h_Walls	10.00	W_Tot_ch	97793.61
Height_end_cyl	18.81	W_Tower	2884.66
Hor_Tot	78516.00	Wave_Height	5.50
i	1.00	Weight_ch	101.64
i_gamma	0.50	Weight_d_fav	101.64
Int_fric_angle	0.63	Weight_d_unfav	137.22
KB	5.05	Weight_GBF_Full_ch	486516.29
KG	9.58	Weight_GBF_Full_fav	486516.29
l_e	34.77	Weight_GBF_Full_unfav	656796.99
l_eff	30.37	Weight_wind_turbine	11000.00
l_Walls	13.65	WL_HT	40.00
Max_bearing_cap	2666.09	WL_LT	32.00
Max_rot_eR	4.38	WL_MSL	35.00
Max_vert_force	535.48	Y_c	23.54
Mom_of_Res_Base_slab	4209.24	Y_s	15.70
Moment_Tot	605767.50	Y_w	10.06
N_gamma	40.14		

Table A-3 Values for circular GBF-design with a diameter of 35 meter

Parameter	Value	Parameter	Value
A_Base_slab	855.30	N_q	37.75
A_eff	706.03	N_Walls	6.00
angle	0.85	Partial_EC_Fac_Bear	1.40
Angle_bet_c_s	0.70	Partial_EC_Fac_fav_V	1.00
b_e	28.46	Partial_EC_Fac_slid	1.10
b_eff	24.79	Partial_EC_Fac_unfav_V	1.35
BM	6.52	R_Base_slab	16.50
Coef_friction	0.84	Resist_hor_force	156124.77
COG	9.77	s_gamma	0.74
D_Base_slab	33.00	Sum_Base_slab	29098.18
D_Cone_bot_in	31.41	Sum_Cone	404774.97
D_Cone_bot_out	33.00	Sum_Cyl	252296.98
D_Cone_up_in	4.91	Sum_Inner_walls	74731.25
D_Cone_up_out	6.50	Sum_Tower	116828.76
D_Cyl_in	31.80	t_Cone	0.60
D_Cyl_out	33.00	t_Cyl	0.60
D_inner_cyl	6.50	t_inner_cyl	0.50
D_Tower_in	5.50	t_Tower	0.50
D_Tower_out	6.50	t_Walls	0.50
Den_Base_slab	34233.16	Tau_max	182.54
Den_Cone	16955.11	UC_Bearing_cap	0.35
Den_Cyl	24602.34	UC_meta	0.25
Den_Inner_walls	11153.92	UC_Rot_Stab	1.00
Den_Tower	2884.66	UC_Shear_capacity	0.55
Draught	10.44	V_Base_slab	1454.01
ecc_fav	4.12	V_Cone	720.15
ecc_unfav	2.27	V_Cyl	1044.95
Eff_Weight_GBF_Full_ch	217.54	V_GBF_outer	25803.70
Eff_Weight_GBF_Full_fav	217.54	V_Inner_walls	473.75
Eff_Weight_GBF_Full_unfav	395.35	V_tot	3815.37
g	9.81	V_Tower	122.52
gamma	13.50	Vert_tot_ch	186062.26
h_Base_slab	1.70	Vert_tot_fav	186062.26
h_Cone	15.19	Vert_tot_unfav	338145.98
h_Cyl	17.11	W_Base_slab	34233.16
h_GBF	47.00	W_Cone	16955.11
h_m	1.97	W_Cyl	24602.34
h_Tower	13.00	W_Inner_walls	11153.92
h_Walls	10.00	W_Tot_ch	89829.18
Height_end_cyl	18.81	W_Tower	2884.66
Hor_Tot	78516.00	Wave_Height	5.50
i	1.00	Weight_ch	105.03
i_gamma	0.45	Weight_d_fav	105.03
Int_fric_angle	0.63	Weight_d_unfav	141.79
KB	5.22	Weight_GBF_Full_ch	434524.91
KG	9.77	Weight_GBF_Full_fav	434524.91
I_e	32.69	Weight_GBF_Full_unfav	586608.63
I_eff	28.47	Weight_wind_turbine	11000.00
I_Walls	12.65	WL_HT	40.00
Max_bearing_cap	2246.29	WL_LT	32.00
Max_rot_eR	4.13	WL_MSL	35.00
Max_vert_force	567.05	Y_c	23.54
Mom_of_Res_Base_slab	3528.11	Y_s	15.70
Moment_Tot	605767.50	Y_w	10.06
N_gamma	40.14		

Table A-4 - Values for circular GBF-design with a diameter of 33 meter

## B.2 MATLAB SCRIPT HEXAGONAL GBF

```

clear all
close all

%-----INPUT-----
% Eurocode factors
Partial_EC_Fac_Bear = 1.4; % Partial factor on bearing capacity according to the Eurocode [-]
Partial_EC_Fac_slid = 1.1; % Partial factor on sliding capacity according to the Eurocode [-]
Partial_EC_Fac_fav_V = 1.0; % Partial factor on weight favorable [-]
Partial_EC_Fac_unfav_V = 1.35; % Partial factor on weight unfavorable [-]

% General
Y_c = 2400*9.81/1000; % Volumetric weight concrete [kN/m3]
Y_w = 1025*9.81/1000; % Volumetric weight water [kN/m3]
Y_s = 15.70; % Volumetric weight sand infill [kN/m3]
g = 9.81; % Gravitational acceleration [m/s2]

% Input Base slab
D_Base_slab = linspace(20,50,500); %Diameter of base slab [m]
h_Base_slab = 1.7; % Height of base slab [m]

% Input Cylinder
thick_Cyl = 0.6; % Thickness cylindrical wall [m]
Height_end_cyl = 18.81; % Height of cylindrical part [m]

% Input Inner walls
N_Walls = 6; % Number of internal walls [-]
h_Walls = 10; % Height of internal walls [m]
D_inner_cyl = 6.5; % Diameter of inner cylinder [m]
t_Walls = 0.5; % Thickness of inner walls [m]
t_inner_cyl = 0.5; % Thickness of inner cylinder [m]

%Input "cone"
N_Elements = 6; % Number of prefabricated elements [-]
t_Elements = 0.6; % Thickness of prefabricated elements [-]
h_Plates = 15.19; % Height of Plates [m]

% Input Tower
t_Tower = 0.5; % Thickness of tower [m]
D_Tower_out = 6.5; % Outer diameter of tower [m]
h_Tower = 13.0; % Height of tower [m]

h_GBF = 47.0; % Height of total GBF [m]

%-----Input Brinch Hansen-----
Moment_Tot = 1000350*.8*(109/(94+50)); %Total moment [kNm]
Hor_Tot = 98145*.8; %Total horizontal force [kN]

% Soil parameters
Int_fric_angle = 36*2*pi/360; %Angle of internal friction [Radians]
Coeff_fricition = tan(Int_fric_angle); %Coefficient of friction [-]
Angle_bet_c_s = 40*2*pi/360; %Angle of friction between sand and concrete [Radians]

% Water level
WL_HT = 40; % Water depth at high tide [m]
WL_LT = 32; % Water depth at low tide [m]
WL_MSL = 35; % Depth of water at Mean Sea Level [m]
Wave_Height = 5.5; % Extreme wave height [m]

%Wind turbine
Weight_wind_turbine = 11000; % Weight of wind turbine [kN]

for i=1:(length(D_Base_slab));
% Geometric calculations
R_Base_slab(i) = D_Base_slab(i)/2; % Radius of GBF [m]
r_Base_slab(i) = sqrt(3)/2*R_Base_slab(i)
A_Base_slab(i) = 3*sqrt(3)/2*(R_Base_slab(i))^2; % Base slab area [m2]
Mom_of_Res_Base_slab(i) = pi*D_Base_slab(i)^3/32; % Moment of resistance base slab [m3]

t_Cyl_out(i) = R_Base_slab(i); %Outer cylindrical dia [m]
h_Cyl = Height_end_cyl - h_Base_slab; %Height of cylinder [m]
t_Cyl_in(i) = t_Cyl_out(i)-2*thick_Cyl*tan(30*2*pi/360);

angle(i) = atan(h_Plates / (r_Base_slab(i) - 0.5 * D_Tower_out));
t_Elements_vert(i)=t_Elements/cos(angle(i));

```

```

D_Tower_in      = D_Tower_out - 2 * t_Tower;                % Inner diameter tower      [m]

l_Walls(i)      = D_Base_slab(i)/2 - thick_Cyl - D_inner_cyl/2;% length of inner walls  [m]

%Volume/Weight calculation

V_Base_slab(i) = 2*r_Base_slab(i)^2*sqrt(3)*h_Base_slab;    %Volume base slab      [m3]
W_Base_slab(i) = V_Base_slab(i) * Y_c;                      % Mass of base slab    [kN]

V_Cyl(i)        =6*((t_Cyl_in(i) + t_Cyl_out(i))/2) * thick_Cyl * h_Cyl; %Volume cylinder[m3]
W_Cyl(i)        = V_Cyl(i)*Y_c;                             % Mass of base slab    [kN]

V_Inner_walls(i) = N_Walls * l_Walls(i) * t_Walls * h_Walls; %Volume of internal walls
W_Inner_walls(i) = V_Inner_walls(i) * Y_c;                  % Mass of internal walls [kN]

V_Inner_Cyl(i)  = 1/4 * pi * (D_inner_cyl^2 - (D_inner_cyl - 2 * t_inner_cyl)^2) * (h_GBF - h_Base_slab);
W_Inner_Cyl(i)  = V_Inner_Cyl(i)*Y_c;

V_Plates(i)     = (A_Base_slab(i)-1/4*pi*D_Tower_out^2)*t_Elements/cos(angle(i)); %Volume of cone [m3]
W_Plates(i)     = V_Plates(i)*Y_c;                          %Mass of cone         [kN]

V_tot(i)        = V_Base_slab(i) + V_Cyl(i) + V_Inner_walls(i) + V_Inner_Cyl(i) + V_Plates(i); %Volume of total GBF [m3]
W_Tot(i)        = W_Base_slab(i) + W_Cyl(i) + W_Inner_walls(i) + W_Inner_Cyl(i) + W_Plates(i); %Mass of total GBF [kN]

Weight_ch(i)    = W_Tot(i)/A_Base_slab(i);                  % Total weight per square meter[kN/m2]
Draught(i)      = W_Tot(i) / (A_Base_slab(i)*Y_w);         % Draught of GBF      [m]
Weight_d_unfav(i)=Partial_EC_Fac_unfav_V*Weight_ch(i);
Weight_d_fav(i) =Partial_EC_Fac_fav_V*Weight_ch(i);

V_GBF_outer(i) = A_Base_slab(i) * (h_Base_slab + h_Cyl) + 1/2*h_Plates*A_Base_slab(i)+(WL_MSL - h_GBF + h_Tower)*(1/4*pi*D_Tower_out^2); %Volume of total GBF [m3]
COG(i)          = (V_Base_slab(i)*h_Base_slab/2 + V_Inner_walls(i)*(h_Base_slab+h_Walls/2) + V_Inner_Cyl(i)*((h_GBF-h_Base_slab)/2)+ V_Cyl(i)*(h_Base_slab+h_Cyl/2) + V_Plates(i)*(h_Base_slab+h_Cyl+h_Plates/3))/V_tot(i); %Height of Centre of Gravity [m]

%-----Metacentric height: h_m=KB+BM+-KG>0.50m

KB(i)           = 1/2 * Draught(i);                          % KB-distance [m]
BM(i)           = (0.0601*D_Base_slab(i)^4) / (A_Base_slab(i) * Draught(i)); % BM-distance [m]

%Factors to determine KG: [1]:Bottom slab [2]:Cylinder [3]: Inner Walls [4]: Cone [5]:Tower
Sum_Base_slab(i) = V_Base_slab(i) * h_Base_slab/2 * Y_c;
Sum_Cyl(i)       = V_Cyl(i) * (h_Base_slab + h_Cyl/2) * Y_c;
Sum_Inner_walls(i)= V_Inner_walls(i) * (h_Base_slab + h_Walls/2) * Y_c;
Sum_Inner_Cyl(i) = V_Inner_Cyl(i) * ((h_GBF-h_Base_slab)/2)*Y_c;
Sum_Plates(i)   = V_Plates(i) * (h_Base_slab + h_Cyl + 1/3 * h_Plates) * Y_c;

Den_Base_slab(i) = V_Base_slab(i) * Y_c;
Den_Cyl(i)       = V_Cyl(i) * Y_c;
Den_Inner_walls(i)= V_Inner_walls(i) * Y_c;
Den_Inner_Cyl(i) = V_Inner_Cyl(i) * Y_c;
Den_Plates(i)   = V_Plates(i) * Y_c;

KG(i)           = (Sum_Base_slab(i) + Sum_Cyl(i) +Sum_Inner_walls(i) +Sum_Inner_Cyl(i) + Sum_Plates(i)) / (Den_Base_slab(i) + Den_Cyl(i) + Den_Inner_walls(i)+ Den_Inner_Cyl(i) + Den_Plates(i)); %KG-distance [m]

h_m(i)          = KB(i) + BM(i) - KG(i); % Metacentric height [m]
UC_meta(i)      = 0.5/h_m(i); % UC Metacentric height [m]

%-----Calculation Brinch Hansen-----
Weight_GBF_Full(i) = W_Tot(i) + ((V_GBF_outer(i) - V_tot(i) - 1*1/4*pi*D_Tower_out^2))*Y_s; % Characteristic weight of filled GBF [kN]
Weight_GBF_Full_fav(i) = Partial_EC_Fac_fav_V*Weight_GBF_Full(i);
% Weight of filled GBF incl. fav. part. fac [kN]
Weight_GBF_Full_unfav(i) = Partial_EC_Fac_unfav_V*Weight_GBF_Full(i);
% Weight of filled GBF incl. unfav. part. fac [kN]

```

```

Eff_Weight_GBF_Full(i) = (Weight_GBF_Full(i) + Weight_wind_turbine - V_GBF_outer(i) * Y_w) /
A_Base_slab(i); % Characteristic weight of filled GBF per square meter [kN/m2]
%[kN/m2]
Eff_Weight_GBF_Full_fav(i) = (Weight_GBF_Full_fav(i) + Partial_EC_Fac_fav_V *
Weight_wind_turbine - V_GBF_outer(i) * Y_w) / A_Base_slab(i); % Weight of filled GBF per
square meter incl. part. fav. fact [kN/m2]
Eff_Weight_GBF_Full_unfav(i)=(Weight_GBF_Full_unfav(i) +
Partial_EC_Fac_unfav_V*Weight_wind_turbine - V_GBF_outer(i) * Y_w) / A_Base_slab(i); % Weight
of filled GBF per square meter incl. part. unfav. fact [kN/m2]

Vert_tot(i) = Eff_Weight_GBF_Full(i)*A_Base_slab(i);% Total effective weight GBF [kN]
Vert_tot_fav(i) = Vert_tot(i)*Partial_EC_Fac_fav_V;% Total effective weight GBF incl.
part. fav. fac. [kN]
Vert_tot_unfav(i) = Vert_tot(i)*Partial_EC_Fac_unfav_V; % Total effective weight GBF
incl. part unfav fact. [kN]

%---Shear capacity---
Tau_max(i) = tan(Angle_bet_c_s) * Eff_Weight_GBF_Full_fav(i); % Maximal
allowable shear force per square meter [kN/m2]
Resist_hor_force(i) = Tau_max(i) * A_Base_slab(i); % Maximal allowable shear force [kN]
UC_Shear_capacity(i) = Hor_Tot / (Resist_hor_force(i)/Partial_EC_Fac_slid);
% Unity check shear force [-]

%---Bearing capacity-----
ecc(i) = Hor_Tot/(Eff_Weight_GBF_Full_unfav(i)*A_Base_slab(i))*COG(i);
%Moment_Tot/Vert_tot(i) ; % Eccentricity [m]
b_e(i) = 2 * (R_Base_slab(i)-ecc(i)); % Width of circle segment [m]
l_e(i) = 2 * R_Base_slab(i)*sqrt(1-(1-b_e(i)/(2*R_Base_slab(i)))^2);
% Length of circle segment [m]
A_eff(i) = 2 * (R_Base_slab(i)^2*acos(ecc(i)/R_Base_slab(i))-
ecc(i)*sqrt(R_Base_slab(i)^2-ecc(i)^2)); % Effective area foundation [m2]
l_eff(i) = sqrt(A_eff(i)*l_e(i)/b_e(i)); % Effective length of foundation [m]
b_eff(i) = l_eff(i)/l_e(i)*b_e(i); % Effective width of foundation [m]

s_gamma(i) = 1 - 0.3 * b_eff(i)/l_eff(i); % Shape factor [-]
N_q = (1 + sin(Int_fric_angle)) / (1 - sin(Int_fric_angle)) * exp( pi *
tan(Int_fric_angle)); % Bearing capacity factor [-]
N_gamma = (N_q - 1) * tan(1.32*Int_fric_angle); % Bearing capacity factor [-]
gamma = 13.5; % Effective weight subsoil [kN/m3]
i_gamma(i) = (1-Hor_Tot/Vert_tot_unfav(i))^3; % Inclination factor [-]
Max_vert_force(i) = Vert_tot_unfav(i)/A_Base_slab(i)+Moment_Tot/Mom_of_Res_Base_slab(i);
% Maximal vert force [kN/m2]
Max_bearing_cap(i) = (1/2*gamma*b_eff(i)*N_gamma*s_gamma(i)*i_gamma(i));
% Maximal bearing cap [kN/m2]
UC_Bearing_cap(i) = Max_vert_force(i) / (Max_bearing_cap(i)/Partial_EC_Fac_Bear);
% Unity Check bearing capacity [-]

%-----Rot stability-----
ecc_fav(i) = Hor_Tot/(Eff_Weight_GBF_Full_fav(i)*A_Base_slab(i))*COG(i);
Max_rot_eR(i) = D_Base_slab(i)/8; % Maximal acceptable eccentricity [m]
UC_Rot_Stab(i) = ecc_fav(i)/Max_rot_eR(i);% Unity Check rotational stability [-]

end

figure() %UC-figure
plot(D_Base_slab, UC_Rot_Stab,'DisplayName','Unity check rotational stability')
hold on
plot(D_Base_slab, UC_Bearing_cap,'DisplayName','Unity check bearing capacity')
hold on
plot(D_Base_slab, UC_Shear_capacity,'DisplayName','Unity check shear capacity')
hold on
plot(D_Base_slab, UC_meta, 'DisplayName', 'Unity check metacentric height')
hold on
plot([25,45],[1,1],'DisplayName','Limit State')
xlabel('Diameter of element [m]')
title('Unity checks of GBF stability')
ylabel('Unity check [-]')
ylim([0,1.5])
xlim([30,40])
legend()

figure() %zoom in figure
plot(D_Base_slab, UC_Rot_Stab,'DisplayName','Unity check rotational stability')
hold on
plot(D_Base_slab, UC_Bearing_cap,'DisplayName','Unity check bearing capacity')
hold on

```

```
plot(D_Base_slab, UC_Shear_capacity, 'DisplayName', 'Unity check shear capacity')
hold on
plot(D_Base_slab, UC_meta, 'DisplayName', 'Unity check metacentric height')
hold on
plot([25,45], [1,1], 'DisplayName', 'Limit State')
hold on
plot([37.5,37.5], [0,2], '--', 'DisplayName', 'Stable diameter')
xlabel('Diameter of element [m]')
title('Unity checks of GBF stability')
ylabel('Unity check [-]')
ylim([0,1.5])
xlim([33,40])
legend()
```

Parameter	Value	Parameter	Value
A_Base_slab	913.39	Partial_EC_Fac_slid	1.10
A_eff	669.65	Partial_EC_Fac_unfav_V	1.35
angle	0.86	r_Base_slab	16.24
Angle_bet_c_s	0.70	R_Base_slab	18.75
b_e	27.57	Resist_hor_force	151967.32
b_eff	23.98	s_gamma	0.74
BM	11.61	Sum_Base_slab	31074.38
Coef_friction	0.73	Sum_Cyl	273697.59
COG	10.29	Sum_Inner_Cyl	227676.28
D_Base_slab	37.50	Sum_Inner_walls	70511.93
D_inner_cyl	6.50	Sum_Plates	456775.54
D_Tower_in	5.50	t_Cyl_in	18.06
D_Tower_out	6.50	t_Cyl_out	18.75
Den_Base_slab	36558.10	t_Elements	0.60
Den_Cyl	26689.18	t_Elements_vert	0.92
Den_Inner_Cyl	10051.93	t_inner_cyl	0.50
Den_Inner_walls	10524.17	t_Tower	0.50
Den_Plates	19133.30	t_Walls	0.50
Draught	11.21	Tau_max	166.38
ecc	2.45	thick_Cyl	0.60
ecc_fav	4.46	UC_Bearing_cap	0.36
Eff_Weight_GBF_Full	198.28	UC_meta	0.07
Eff_Weight_GBF_Full_fav	198.28	UC_Rot_Stab	0.95
Eff_Weight_GBF_Full_unfav	360.74	UC_Shear_capacity	0.57
g	9.81	V_Base_slab	1552.76
gamma	13.50	V_Cyl	1133.59
h_Base_slab	1.70	V_GBF_outer	24151.14
h_Cyl	17.11	V_Inner_Cyl	426.94
h_GBF	47.00	V_Inner_walls	447.00
h_m	6.92	V_Plates	812.66
h_Plates	15.19	V_tot	4372.95
h_Tower	13.00	Vert_tot	181107.60
h_Walls	10.00	Vert_tot_fav	181107.60
Height_end_cyl	18.81	Vert_tot_unfav	244495.26
Hor_Tot	78516.00	W_Base_slab	36558.10
i	1.00	W_Cyl	26689.18
i_gamma	0.31	W_Inner_Cyl	10051.93
Int_fric_angle	0.63	W_Inner_walls	10524.17
KB	5.61	W_Plates	19133.30
KG	10.29	W_Tot	102956.68
l_e	32.10	Wave_Height	5.50
l_eff	27.92	Weight_ch	112.72
l_Walls	14.90	Weight_d_fav	112.72
Max_bearing_cap	1508.95	Weight_d_unfav	152.17
Max_rot_eR	4.69	Weight_GBF_Full	412953.40
Max_vert_force	384.69	Weight_GBF_Full_fav	412953.40
Mom_of_Res_Base_slab	5177.19	Weight_GBF_Full_unfav	557487.09
Moment_Tot	605767.50	Weight_wind_turbine	11000.00
N_Elements	6.00	WL_HT	40.00
N_gamma	40.14	WL_LT	32.00
N_q	37.75	WL_MSL	35.00
N_Walls	6.00	Y_c	23.54
Partial_EC_Fac_Bear	1.40	Y_s	15.70
Partial_EC_Fac_fav_V	1.00	Y_w	10.06

Table A-5 - Values for hexagonal GBF-design with a 'diameter' of 37 meter

### B.3 MATLAB SCRIPT IMMERSION STRUCTURE

```

clear all
close all

%-----Input-----
Y_c = 23.54; %Volumetric weight concrete [kN/m3]
Y_w = 10.05; %Volumetric weight water [kN/m3]

Leg_Height = 15.3; %Height of leg [m]
Leg_Length = 47; %Length of base [m]
Leg_Width = linspace(1,15,1000); %Width of concrete foundation [m]
h_Ballast = 11; %Height of ballast [m]
Part_Platt_Installed = 4/47; %Part of H-beams dur. transp. [-]

h_plat_top = 15.3; %Height of platform [m]
W_GBF = 1.0296e+05; %Weight of GBF [kN]
W_Platt = 48857.9; %Weight of platform [kN]
W_lift_mech = 390*9.81; %Weight of lifting mechanism [kN]

h_beam = 1.1; %Height of beam [m]
Wat_depth_max = +6; %Maximum water depth [mLAT]
Wat_depth_min = 0; %Minimum water depth [mLAT]
Bottom_level = -8; %Bottom depth [mLAT]
h_quay_wall = +7.30; %Quay wall height [m]

% Eurocode factors
Partial_EC_Fac_Bear = 1.4; %Partial factor on bearing capacity according to the Eurocode [-]
Partial_EC_Fac_slid = 1.1; %Partial factor on sliding capacity according to the Eurocode [-]
Partial_EC_Fac_fav_V = 1.0; %Partial factor on weight favorable [-]
Partial_EC_Fac_unfav_V = 1.35; %Partial factor on weight unfavorable [-]

% Soil parameters
Int_fric_angle = 36*2*pi/360; %Angle of internal friction [Radians]
Angle_bet_c_s = 40*2*pi/360; %Angle of friction between sand and concrete [Radians]
Coef_friction = tan(Angle_bet_c_s); %Coefficient of friction [-]

for i=1:length(Leg_Width)

nr_inner_walls = 11; %Number of inner walls [-]

Bottom_Slab_Thickness= 1.25; %Thickness bottom slab [m]
Upper_Slab_Thickness = 0.15; %Thickness upper slab [m]
Side_Wall_Thickness = 0.5; %Thickness side walls [m]
Front_Back_Wall = 0.65; %Thickness of front/back walls [m]
Inner_Walls_Thickness= 0.15; %Thickness of inner walls [m]

V_Bottom(i) = Bottom_Slab_Thickness * Leg_Width(i)*Leg_Length;
V_Upper(i) = Upper_Slab_Thickness * Leg_Width(i)*Leg_Length;
V_Side = 2*Leg_Length*(Leg_Height-Upper_Slab_Thickness-
Bottom_Slab_Thickness)*Side_Wall_Thickness;
V_Front_Back(i) = 2*(Leg_Height-Upper_Slab_Thickness-Bottom_Slab_Thickness)*(Leg_Width(i)-
2*Side_Wall_Thickness)*Front_Back_Wall;
V_Inner(i) = nr_inner_walls*(Leg_Height-Upper_Slab_Thickness-
Bottom_Slab_Thickness)*(Leg_Width(i)-2*Side_Wall_Thickness)*Inner_Walls_Thickness;

V_Ballast(i) = (h_Ballast-Bottom_Slab_Thickness)*(Leg_Width(i)*Leg_Length-
(2*Side_Wall_Thickness-nr_inner_walls*Inner_Walls_Thickness-2*Front_Back_Wall));
W_Ballast(i) = V_Ballast(i)*Y_w;

V_Leg(i) = V_Bottom(i) + V_Upper(i) + V_Side + V_Front_Back(i) + V_Inner(i);
W_Leg(i) = V_Leg(i) * Y_c;
A_Leg(i) = Leg_Length*Leg_Width(i);
W_Tot_with_GBF(i) = W_GBF + W_Platt + 2*W_Leg(i)+W_lift_mech;
W_Tot_without_GBF(i) = W_Platt+ 2*W_Leg(i)+W_lift_mech;
W_Tot_with_GBF_Ballast(i) = W_Tot_with_GBF(i)+W_Ballast(i);
W_Tot_with_GBF_Ballast_unfav(i)= Partial_EC_Fac_unfav_V*W_Tot_with_GBF_Ballast(i);
W_Tot_without_GBF_Ballast(i) = W_Tot_without_GBF(i)+W_Ballast(i);

A_Tot(i) = 2 * Leg_Length * Leg_Width(i);
V_und_wat_low(i) = A_Tot(i) * (Wat_depth_min-Bottom_level);
V_und_wat_high(i) = A_Tot(i) * (Wat_depth_max-Bottom_level);

COG(i) = (1/2 * Leg_Height * 2 * W_Leg(i)+ W_Platt * (h_plat_top-
1/2*h_beam)) / (2*W_Leg(i)+W_Platt);

% %-----Calculation Brinch Hansen-----

```

```

Vert_tot_min(i) = Partial_EC_Fac_fav_V*W_Tot_without_GBF_Ballast(i); % Total min weight [kN]
Vert_tot_max(i) = Partial_EC_Fac_unfav_V*W_Tot_with_GBF_Ballast(i); % Total max weight [kN]

Vert_tot_eff_min(i) = (Vert_tot_min(i) - V_und_wat_high(i)*Y_w) / A_Tot(i); % Total eff.
weight/m2 incl. fav factor [kN/m2]
Vert_tot_eff_max(i) = (Vert_tot_max(i) - V_und_wat_low(i)*Y_w) / A_Tot(i); % Total eff.
weight/m2 incl. unfav factor [kN/m2]
Vert_tot_eff_Shear(i)=(Vert_tot_min(i)- V_und_wat_high(i)*Y_w) / A_Tot(i); % Total eff. for
shear [kN/m2]

Vert_tot_eff_min_A(i)=Vert_tot_eff_min(i)*A_Tot(i); %Total effective weight incl. fav.
factor [kN/m2]
Vert_tot_eff_max_A(i)=Vert_tot_eff_max(i)*A_Tot(i); %Total effective weight incl unfav
factor [kN/m2]

Hor_Tot = 1.5*0.04 * W_GBF;
Mom_Tot = Hor_Tot*h_plat_top;

%----Shear capacity----
Tau_max(i) = Coef_friction * Vert_tot_eff_Shear(i); % Maximal
allowable shear force per square meter [kN/m2]]
UC_Shear_capacity(i) = (Hor_Tot/A_Tot(i))/(Tau_max(i)/Partial_EC_Fac_slid); % Unity check
shear force [-]

%----Bearing capacity-----
ecc(i) = Hor_Tot/(Vert_tot_eff_max_A(i))*COG(i); % Eccentricity [m]
l_eff(i) = Leg_Length-2*ecc(i); % Effective length of foundation [m]
b_eff = Leg_Width; % Effective width of foundation [m]
A_eff(i) = 2*l_eff(i)*b_eff(i); % Effective area foundation [m2]
s_gamma(i) = 1 - 0.3 * b_eff(i)/l_eff(i); % Shape factor [-]
N_q = (1 + sin(Int_fric_angle)) / (1 - sin(Int_fric_angle)) * exp( pi *
tan(Int_fric_angle));% Bearing capacity factor [-]
N_gamma = (N_q - 1) *tan(1.32*Int_fric_angle); % Bearing capacity factor [-]
gamma = 13.5; % Effective weight subsoil
i_gamma(i) = (1-Hor_Tot/(Vert_tot_eff_max_A(i)))^3;% Inclination factor [-]
Max_vert_force(i) = Vert_tot_eff_max_A(i)/A_Tot(i) +
Mom_Tot/(1/6*2*Leg_Width(i)*Leg_Length^2); % Maximal vert force [kN/m2]
Max_bearing_cap(i) = (1/2*gamma*b_eff(i)*N_gamma*s_gamma(i)*i_gamma(i));
% Maximal bearing cap [kN/m2]
UC_Bearing_cap(i) = (Max_vert_force(i)) / (Max_bearing_cap(i)/Partial_EC_Fac_Bear);
%Unity Check bearing capacity [-]

%-----Rot stability-----
ecc_fav(i) = Hor_Tot/(Vert_tot_eff_min(i)*A_Tot(i))*COG(i);
Max_rot_eR = Leg_Length/6; % Maximal acceptable eccentricity [m]
UC_Rot_Stab(i) = ecc_fav(i)/Max_rot_eR;

%-----Metacentric Height complete platform-----
Draught(i) = (Part_Platt_Installed * W_Platt + 2*W_Leg(i)+W_lift_mech)/(A_Tot(i)*Y_w);
KB(i) = 1/2*Draught(i);
BM(i) = (2*1/12*Leg_Width(i)*Leg_Length^3) / (A_Tot(i) * Draught(i)); % BM-distance
[m]

%Factors to determine KG: [1]:Platform [2]:Upper slabFront/back wall [3] Front/back
wallInner
#walls [4] Inner Walls Side wall inner [5] Side wall [6] Bottom slab

Sum_Platt(i) = Part_Platt_Installed*W_Platt * (h_plat_top-0.5*h_beam);
Sum_Upper_Slab(i) =2*(V_Upper(i) * Y_c* (15.3-0.5*Upper_Slab_Thickness));
Sum_Front_Back(i) =2*(V_Front_Back(i)*h_plat_top/2*Y_c);
Sum_Inner_Walls(i) =2*(V_Inner(i)*h_plat_top/2*Y_c);
Sum_Side_Wall =2*(V_Side*Y_c*h_plat_top/2);
Sum_Bottom_Slab(i) =2*(V_Bottom(i)*Y_c*Bottom_Slab_Thickness/2);
Sum_Lift_Mech =W_lift_mech*Leg_Height;

Sum_Sum=Sum_Platt(i)+Sum_Upper_Slab(i)+Sum_Front_Back(i)+Sum_Inner_Walls(i)+Sum_Side_Wall+Sum_B
ottom_Slab(i)+Sum_Lift_Mech;
Den_Platt(i) =Part_Platt_Installed*W_Platt;
Den_Upper_Slab(i) =2*V_Upper(i)*Y_c;
Den_Front_Back(i) =2*V_Front_Back(i)*Y_c;
Den_Inner_Walls(i) =2*V_Inner(i)*Y_c;
Den_Side_Wall =2*V_Side * Y_c;
Den_Bottom_Slab(i) =2*V_Bottom(i)*Y_c;
Den_Lift_Mech =W_lift_mech;

KG(i)
=(Sum_Lift_Mech+Sum_Platt(i)+Sum_Upper_Slab(i)+Sum_Front_Back(i)+Sum_Inner_Walls(i)+Sum_Side_Wa

```

```

ll+Sum_Bottom_Slab(i)) /
(Den_Lift_Mech+Den_Platt(i)+Den_Upper_Slab(i)+Den_Front_Back(i)+Den_Inner_Walls(i)+Den_Side_Wal
l+Den_Bottom_Slab(i));
h_m(i)          = KB(i) + BM(i) - KG(i); % Metacentric height [m]
UC_meta(i)      = 0.5/h_m(i);           % UC Metacentric height [m]

end

subplot(2,1,1) %UC-figure
plot(Leg_Width, UC_Rot_Stab, 'DisplayName', 'Rotational stability')
hold on
plot(Leg_Width, UC_Bearing_cap, 'DisplayName', 'Bearing capacity')
hold on
plot(Leg_Width, UC_Shear_capacity, 'DisplayName', 'Shear capacity')
hold on
plot([0,45],[1,1], 'DisplayName', 'Limit State')
xlabel('Foundation leg width [m]')
title('Unity checks of platform stability')
ylabel('Unity check [-]')
ylim([0,1.5])
xlim([0,13])
plot([9.0,9.0],[0,50], '--g', 'DisplayName', 'Optimal chosen diameter')
legend()
hold on

subplot(2,1,2)
plot(Leg_Width, h_m, 'b', 'DisplayName', 'Metacentric height')
hold on
plot([0,45],[0.5,0.5], '--b', 'DisplayName', 'Stability metacentric height')
plot(Leg_Width, Draught, 'r', 'DisplayName', 'Draught of one leg')
plot([0,45],[10,10], '--r', 'DisplayName', 'Maximum draught')
hold on
title('Metacentric height and draught of foundation leg')
xlabel('Foundation leg width [m]')
ylabel('Metacentric height, draught [m]')
ylim([0,20])
xlim([0,13])
plot([9.0,9.0],[0,50], '--g', 'DisplayName', 'Optimal chosen diameter')
legend()
figure()

plot(Leg_Width, h_m, 'DisplayName', 'Metacentric Height')
hold on
plot(Leg_Width, Draught, 'DisplayName', 'Draught')
legend()

figure()
plot(Leg_Width, h_m, 'DisplayName', 'Metacentric height')
hold on
plot(Leg_Width, Draught, 'DisplayName', 'Draught')
legend()
xlabel('Foundation leg width [m]')
ylabel('Metacentric height and Draught [m]')
ylim([0,20])
xlim([0,10])
plot([0,45],[0.5,0.5], '--b', 'DisplayName', 'Stability metacentric height')
plot([0,45],[10,10], '--r', 'DisplayName', 'Maximum draught')
title('Draught and metacentric height of immersion structure')

figure()
plot(Leg_Width, UC_Rot_Stab, 'DisplayName', 'Rotational stability')
hold on
plot(Leg_Width, UC_Bearing_cap, 'DisplayName', 'Bearing capacity')
hold on
plot(Leg_Width, UC_Shear_capacity, 'DisplayName', 'Shear capacity')
hold on
plot([0,45],[1,1], 'DisplayName', 'Limit State')
xlabel('Foundation leg width [m]')
title('Unity checks of platform stability')
ylabel('Unity check [-]')
ylim([0,1.5])
xlim([0,10])
%plot([10,10],[0,50], '--g', 'DisplayName', 'Optimal chosen diameter')
legend()
hold on

```

Parameter	Value	Parameter	Value
A_eff	278.82	Partial_EC_Fac_fav_V	1.00
A_Leg	141.00	Partial_EC_Fac_slid	1.10
A_Tot	282.00	Partial_EC_Fac_unfav_V	1.35
Angle_bet_c_s	0.70	s_gamma	0.98
b_eff	3.00	Side_Wall_Thickness	0.50
BM	10.05	Sum_Bottom_Slab	5186.16
BM_Leg	0.05	Sum_Bottom_Slab_Leg	2593.08
Bottom_level	-8.00	Sum_Den_Leg	21955.99
Bottom_Slab_Thickness	1.25	Sum_Front_Back	13016.25
Coef_friction	0.84	Sum_Front_Back_Leg	6508.13
COG	11.39	Sum_Inner_Walls	16520.63
Den_Bottom_Slab	8297.85	Sum_Inner_Walls_Leg	8260.32
Den_Bottom_Slab_Leg	4148.93	Sum_Lift_Mech	58536.27
Den_Front_Back	1701.47	Sum_Platt	61332.26
Den_Front_Back_Leg	850.74	Sum_Side_Wall	235293.83
Den_Inner_Walls	2159.56	Sum_Side_Wall_Leg	117646.92
Den_Inner_Walls_Leg	1079.78	Sum_Sum	405045.58
Den_Lift_Mech	3825.90	Sum_Sum_Leg	142588.52
Den_Platt	4158.12	Sum_Upper_Slab	15160.17
Den_Side_Wall	30757.36	Sum_Upper_Slab_Leg	7580.09
Den_Side_Wall_Leg	15378.68	Tau_max	211.04
Den_Upper_Slab	995.74	UC_Bearing_cap	1.86
Den_Upper_Slab_Leg	497.87	UC_meta	0.04
Draught	18.31	UC_Rot_Stab	0.13
Draught_Leg	15.49	UC_Shear_capacity	0.11
ecc	0.26	Upper_Slab_Thickness	0.15
ecc_fav	0.99	V_Ballast	1393.76
Front_Back_Wall	0.65	V_Bottom	176.25
gamma	13.50	V_Front_Back	36.14
h_Ballast	11.00	V_Inner	45.87
h_beam	1.10	V_Leg	932.71
h_m	11.40	V_Side	653.30
h_m_Leg	1.30	V_und_wat_high	3948.00
h_plat_top	15.30	V_und_wat_low	2256.00
h_quay_wall	7.30	V_Upper	21.15
Hor_Tot	6177.60	Vert_tot_eff_max	941.98
i	1.00	Vert_tot_eff_max_A	265637.38
i_gamma	0.93	Vert_tot_eff_min	251.51
Inner_Walls_Thickness	0.15	Vert_tot_eff_min_A	70925.70
Int_fric_angle	0.63	Vert_tot_eff_Shear	251.51
KB	9.16	Vert_tot_max	288310.18
KB_Leg	7.75	Vert_tot_min	110603.10
KG	7.80	W_Ballast	14007.31
KG_Leg	6.49	W_GBF	102960.00
I_eff	46.47	W_Leg	21955.99
Leg_Height	15.30	W_lift_mech	3825.90
Leg_Length	47.00	W_Platt	48857.90
Leg_Width	3.00	W_Tot_with_GBF	199555.79
Max_bearing_cap	742.70	W_Tot_with_GBF_Ballast	213563.10
Max_rot_eR	7.83	W_Tot_with_GBF_Ballast_unfav	288310.18
Max_vert_force	984.76	W_Tot_without_GBF	96595.79
Mom_Tot	94517.28	W_Tot_without_GBF_Ballast	110603.10
N_gamma	40.14	Wat_depth_max	6.00
N_q	37.75	Wat_depth_min	0.00
nr_inner_walls	11.00	Y_c	23.54
Part_Platt_Installed	0.09	Y_w	10.05
Partial_EC_Fac_Bear	1.40		

Table A-6 - Values for immersion structure with a foundation leg width of 3 meter

Parameter	Value	Parameter	Value
A_eff	838.19	Partial_EC_Fac_fav_V	1.00
A_Leg	423.00	Partial_EC_Fac_slid	1.10
A_Tot	846.00	Partial_EC_Fac_unfav_V	1.35
Angle_bet_c_s	0.70	s_gamma	0.94
b_eff	9.00	Side_Wall_Thickness	0.50
BM	19.07	Sum_Bottom_Slab	15558.47
BM_Leg	0.77	Sum_Bottom_Slab_Leg	7779.23
Bottom_level	-8.00	Sum_Den_Leg	37041.13
Bottom_Slab_Thickness	1.25	Sum_Front_Back	52065.02
Coef_friction	0.84	Sum_Front_Back_Leg	26032.51
COG	10.47	Sum_Inner_Walls	66082.52
Den_Bottom_Slab	24893.55	Sum_Inner_Walls_Leg	33041.26
Den_Bottom_Slab_Leg	12446.78	Sum_Lift_Mech	58536.27
Den_Front_Back	6805.88	Sum_Platt	61332.26
Den_Front_Back_Leg	3402.94	Sum_Side_Wall	235293.83
Den_Inner_Walls	8638.24	Sum_Side_Wall_Leg	117646.92
Den_Inner_Walls_Leg	4319.12	Sum_Sum	534348.89
Den_Lift_Mech	3825.90	Sum_Sum_Leg	207240.18
Den_Platt	4158.12	Sum_Upper_Slab	45480.52
Den_Side_Wall	30757.36	Sum_Upper_Slab_Leg	22740.26
Den_Side_Wall_Leg	15378.68	Tau_max	48.97
Den_Upper_Slab	2987.23	UC_Bearing_cap	0.24
Den_Upper_Slab_Leg	1493.61	UC_meta	0.03
Draught	9.65	UC_Rot_Stab	0.17
Draught_Leg	8.71	UC_Shear_capacity	0.16
ecc	0.22	Upper_Slab_Thickness	0.15
ecc_fav	1.31	V_Ballast	4143.26
Front_Back_Wall	0.65	V_Bottom	528.75
gamma	13.50	V_Front_Back	144.56
h_Ballast	11.00	V_Inner	183.48
h_beam	1.10	V_Leg	1573.54
h_m	17.39	V_Side	653.30
h_m_Leg	-0.46	V_und_wat_high	11844.00
h_plat_top	15.30	V_und_wat_low	6768.00
h_quay_wall	7.30	V_Upper	63.45
Hor_Tot	6177.60	Vert_tot_eff_max	352.63
i	1.00	Vert_tot_eff_max_A	298325.50
i_gamma	0.94	Vert_tot_eff_min	58.36
Inner_Walls_Thickness	0.15	Vert_tot_eff_min_A	49373.65
Int_fric_angle	0.63	Vert_tot_eff_Shear	58.36
KB	4.83	Vert_tot_max	366343.90
KB_Leg	4.36	Vert_tot_min	168405.85
KG	6.51	W_Ballast	41639.79
KG_Leg	5.59	W_GBF	102960.00
I_eff	46.57	W_Leg	37041.13
Leg_Height	15.30	W_lift_mech	3825.90
Leg_Length	47.00	W_Platt	48857.90
Leg_Width	9.00	W_Tot_with_GBF	229726.06
Max_bearing_cap	2157.16	W_Tot_with_GBF_Ballast	271365.85
Max_rot_eR	7.83	W_Tot_with_GBF_Ballast_unfav	366343.90
Max_vert_force	366.89	W_Tot_without_GBF	126766.06
Mom_Tot	94517.28	W_Tot_without_GBF_Ballast	168405.85
N_gamma	40.14	Wat_depth_max	6.00
N_q	37.75	Wat_depth_min	0.00
nr_inner_walls	11.00	Y_c	23.54
Part_Platt_Installed	0.09	Y_w	10.05
Partial_EC_Fac_Bear	1.40		

Table A-7 - Values for immersion structure with a foundation leg width of 9 meter

## Annex C CONSTRUCTION OF THORNTON BANK PHASE I

In this annex several pictures are given where the construction method for the offshore foundations is given. At each picture a short explanation is included about the construction actions. The construction of the GBFs foundation took 57 weeks. A short overview is given to explain the construction method.

### CONSTRUCTION METHOD

Year-Week	Picture	Explanation
2007-30		Preparation of the construction site "De Halve Maan" at the port of Oostende, Belgium.
2007-34		The bottom slab of an offshore wind turbine foundation is under construction. In this picture the reinforcement of the bottom slab is created. The bottom slab is casted on beams on a certain height that a self-propelled modular transporter (SPMT) can drive under the slab to load it.
2007-37		The bottom slab is casted and the formwork of the conical part is applied.

<p><b>2007-42</b></p>		<p>The formwork is applied higher and a large part of the conical shape is casted.</p>
<p><b>2007-48</b></p>		<p>The conical part of one of the GBFs is completed and two others are in the phase of casting the conical part. The formwork is installed on the lower conical part of the other two. In total 6 GBFs are constructed.</p>
<p><b>2008-05</b></p>		<p>Installing the sea cable location on the conical part of the GBF.</p>
<p><b>2008-07</b></p>		<p>A lifting lug installed on the bottom slab of the GBF.</p>

<p><b>2008-12</b></p>		<p>Construction of the top platform where the auxiliaries piece has to be installed.</p>
<p><b>2008-16</b></p>		<p>Installation of the auxiliaries at the top platform of the GBF. This is the upper part where the wind turbine is installed at sea.</p>
<p><b>2008-17</b></p>		<p>Transport of the GBF by a self-propelled modular transporter (SPMT) from the construction place to the edge of the quay wall.</p>

<p><b>2008-17</b></p>		<p>Lifting operation of a GBF from the quay wall by the lifting vessel “Rambiz”.</p>
<p><b>2008-19</b></p>		<p>The installed GBF on the sea bottom. Only the top part is visible above the water line.</p>
<p><b>2008-28</b></p>		<p>The foundations are filled with material to increase the weight for stability.</p>

Table A-8 - Short explanation of construction method of GBF for the Thornton bank Phase I (Pictures: C-Power.be)

## Annex D BATHYMETRY OFFSHORE WIND FARM LOCATIONS

In this annex two bathymetry maps are given of the water depth of the offshore wind locations Mermaid and Seastar. First a map of the Mermaid location is given whereafter the bathymetry map of the wind farm Seastar is given. As it can be seen the depth of the Seastar location is till 30 meter and the depth at the Mermaid location till a depth of 35 meter.

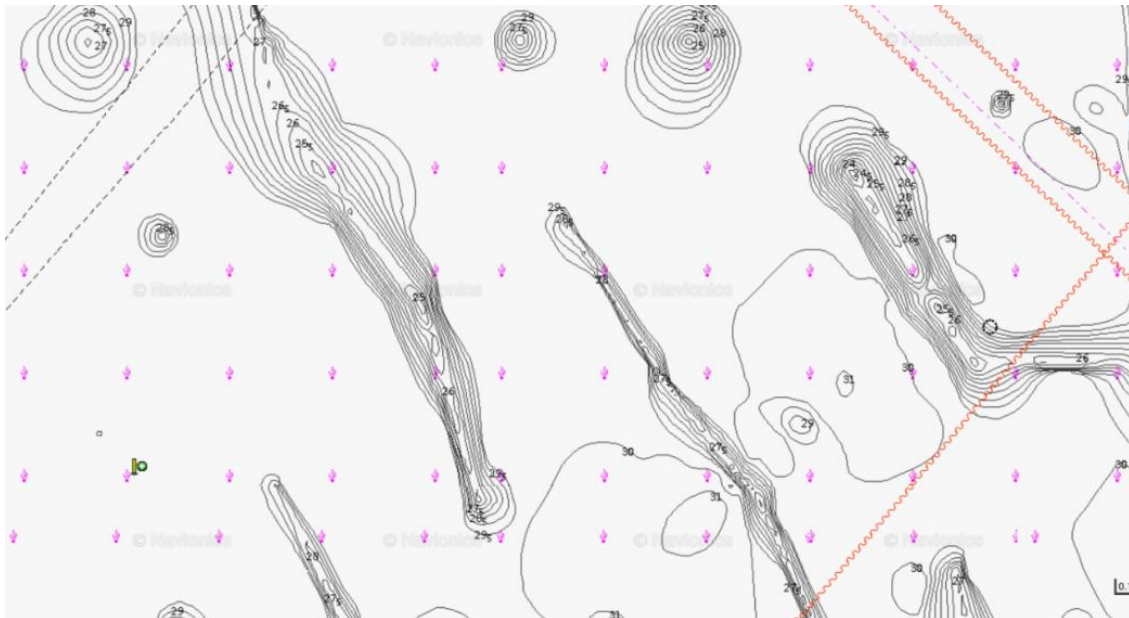


Figure A-22 - Bathymetry map Seastar offshore wind farm (navionics.com)

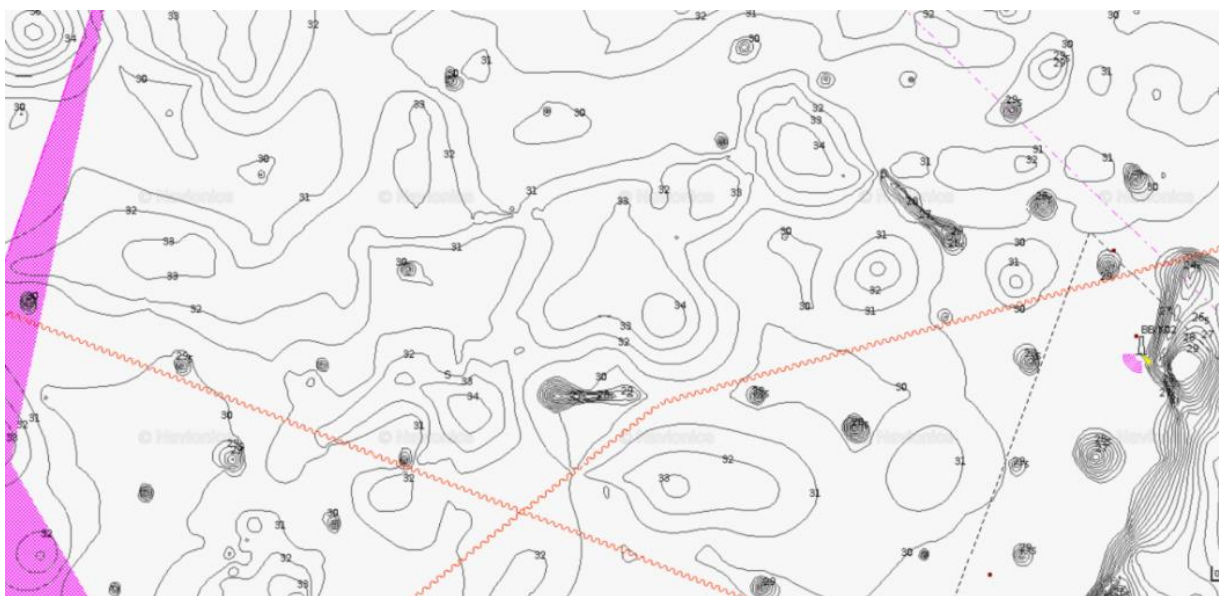


Figure A-23 - Bathymetry map Mermaid offshore wind farm (navionics.com)



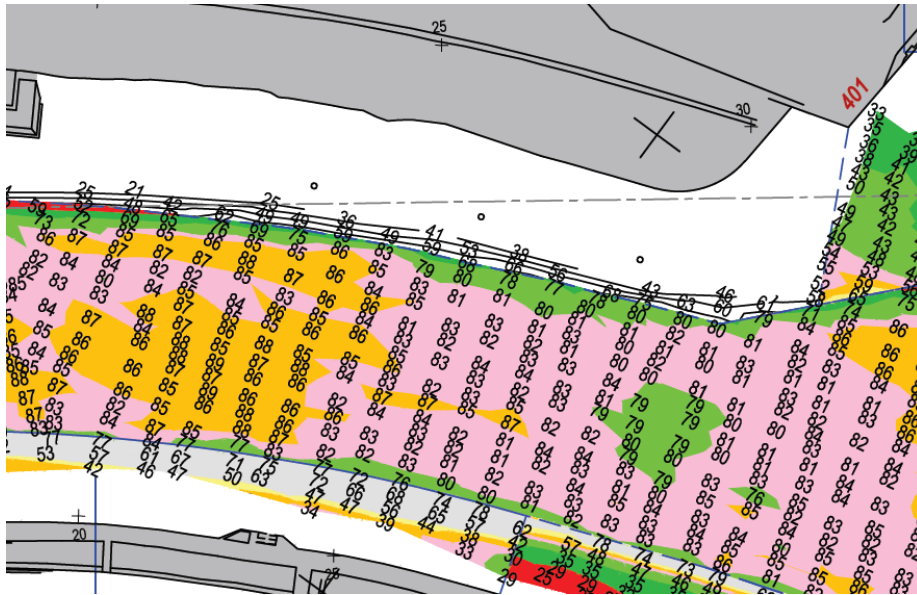


Figure A-25 - Bathymetry map at Otary/Halve Maan [dm LAT]

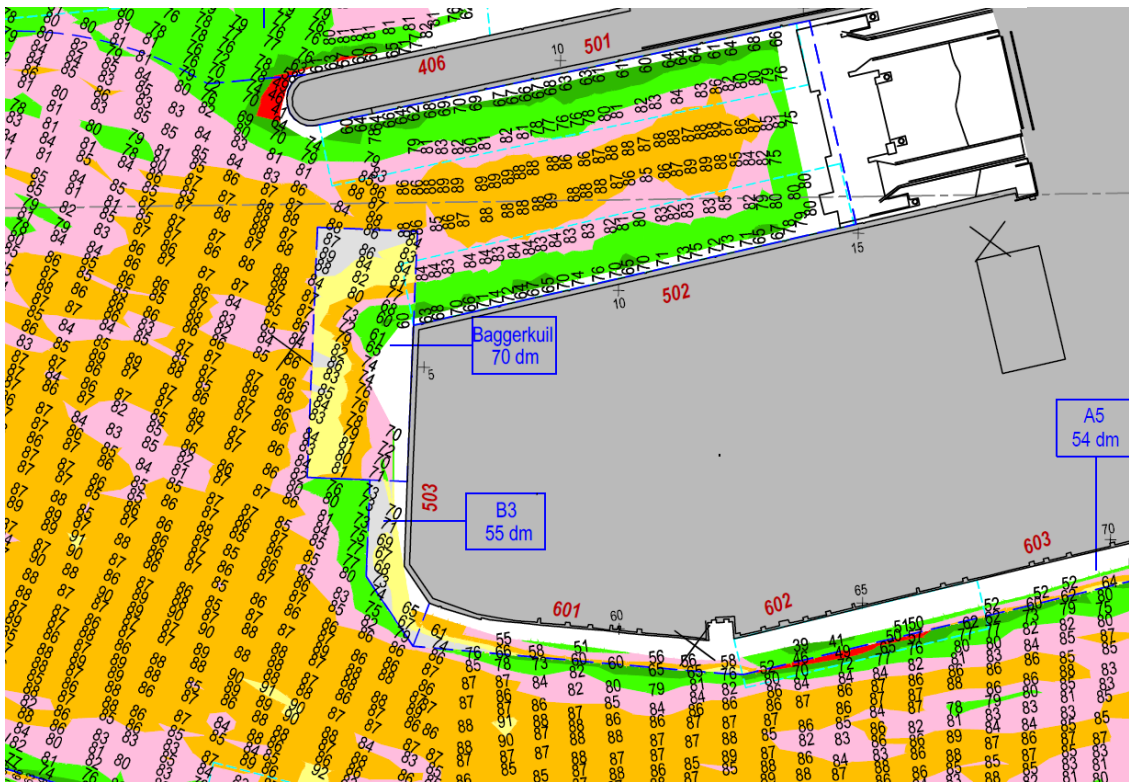


Figure A-26 - Bathymetry map at REBO Offshore Site [dm LAT]

## Annex F CONE PENETRATION TESTS

At the port of Oostende several CPTs are provided from the website of Databank Ondergrond Vlaanderen (dov.vlaanderen.be). In Figure A-27 and Figure A-28 orange circles indicate available CPTs.



Figure A-27 - Available CPTs at REBO Offshore Site



Figure A-28 - Available CPTs at Halve Maan

Two CPTs are included at the next page. Important are the two sand layers, in Table A-9 an overview is given of the present sand layers.

Location	Sand layer 1 [m TAW]	Sand layer 2 [m TAW]
<b>Halve Maan</b>	-7 till -11	From -15
<b>REBO Offshore Site</b>	-10 till -11 m	From -17

Table A-9 - Sand layers at REBO Offshore Site and Halve Maan

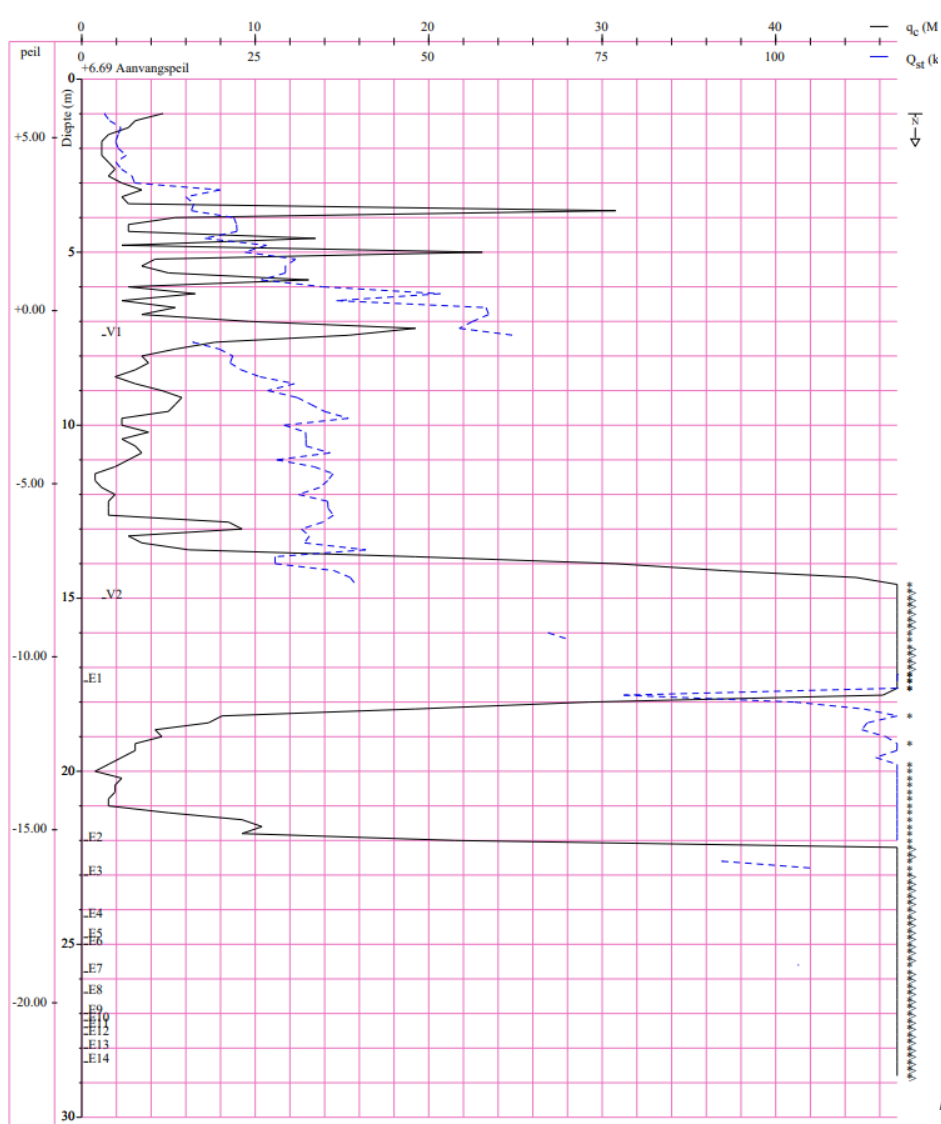


Figure A-30 - CPT at REBO Offshore Site

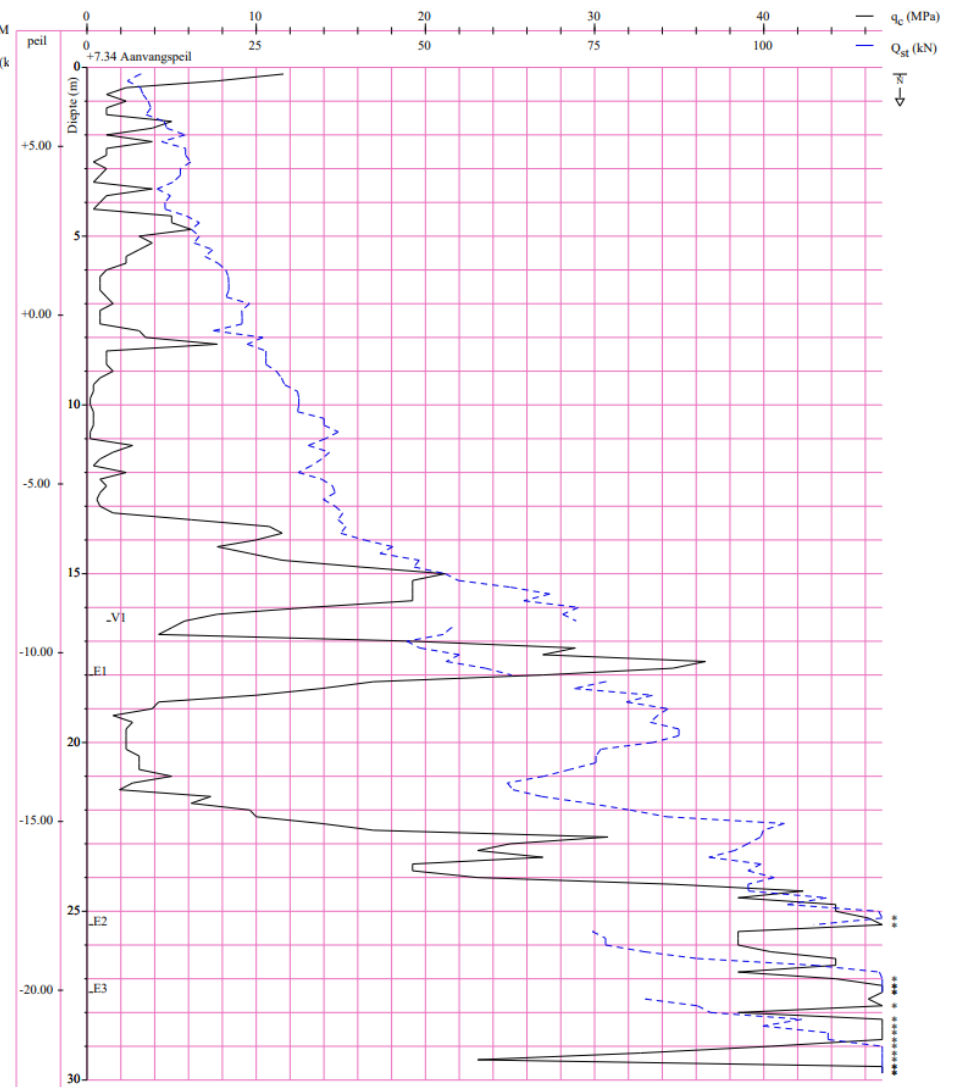


Figure A-29 - CPT at Halve Maan

## Annex G CONCRETE HARDENING

The hardening of concrete is given by the next formula (Breugel, Braam, Veen, & Walraven, 2016):

$$\beta_{cc}(t) = e^{s \left[ 1 - \left( \frac{28}{t/t_1} \right) \right]}$$

Where:

$B_{cc}(t)$  = Coefficient, depending on the age  $t$  [-]  
 $s$  = Cement depending factor (0.38 for rapid hardening concrete) [-]  
 $t$  = Age of concrete (days)  
 $t_1 = 1$  [days]

The strength of the casted concrete can be computed with the formula:

$$f_{cm}(t) = \beta_{cc} \cdot f_{cm}$$

Where:

$f_{cm}(t)$  = Mean compressive strength concrete at time  $t$  [ $N/mm^2$ ]  
 $f_{cm}$  = Mean compressive cylinder strenght after 28 days [ $N/mm^2$ ]

As mentioned the concrete class C55/67 is used. Applying the concrete compression strength the result is given as a graph given in Figure A-31.

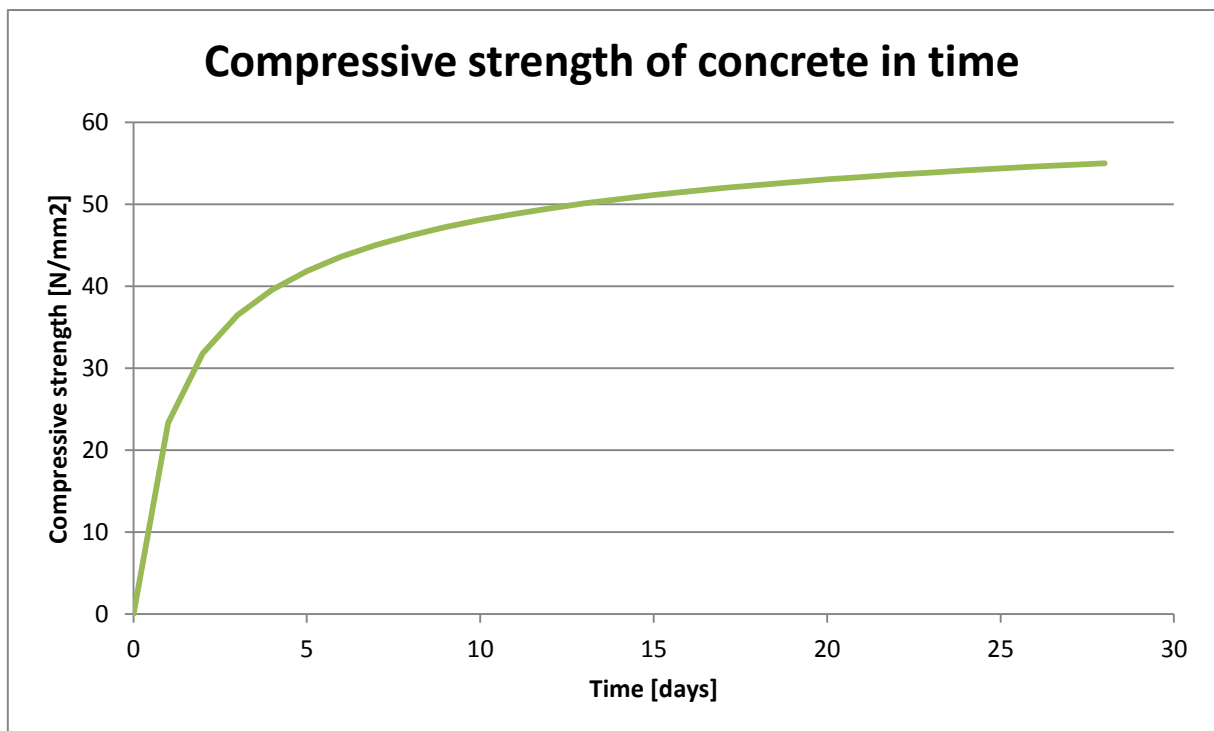


Figure A-31 -Compressive strength of concrete in time

## Annex H WAVE CHARACTERISTICS

In this annex the wave characteristic for the offshore wind farm location and at the port location are calculated. The data comes from metoceanview.com where the wave data is available. From these wave data the two most important parameters, the significant wave height and the peak period calculated.

The significant wave height is given as the mean height of the one-third highest waves:

$$H_{\frac{1}{3}} = \frac{1}{N/3} \sum_{j=1}^{N/3} H_j$$

Where:

$N$  = Number of waves in data [-]

$j$  = Rank number of wave [-]

$H_j$  = Height of the  $j$ 'th wave [m]

$H_{\frac{1}{3}}$  = Significant wave height [m]

The peak period is given as the period with the maximum energy in the wave spectrum.

The data from which the results are derived are described and displayed with three figures for each location in:

- Probability density function of wave heights with significant wave height
- Cumulative density function of wave heights
- Wave spectrum with the derived peak period

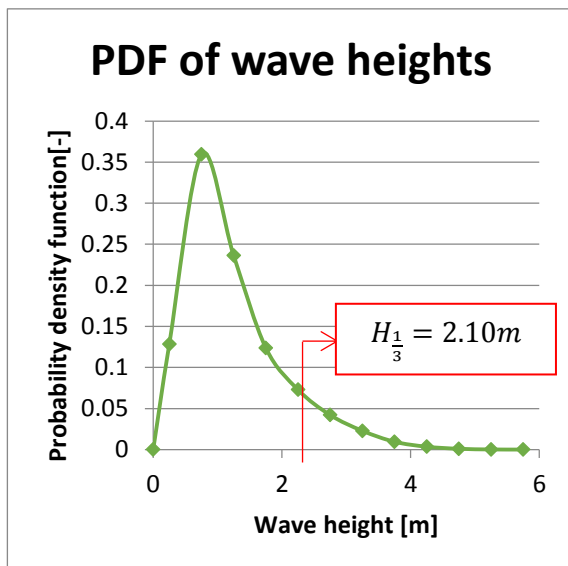


Figure A-32 - PDF of the wave height at the Mermaid offshore wind farm (Data: metoceanview.com)

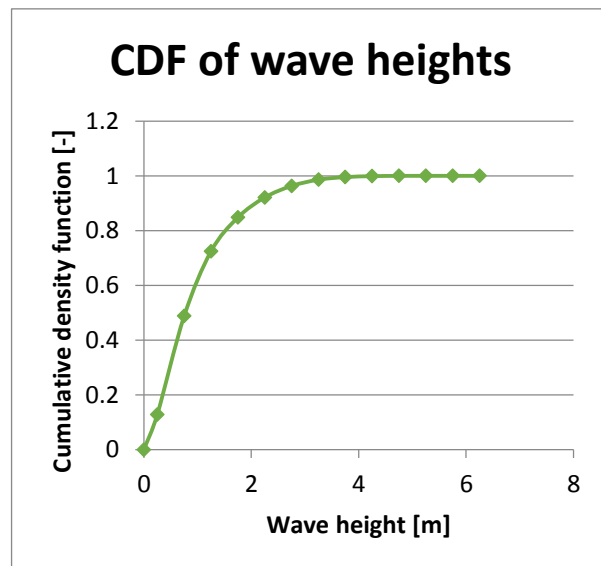


Figure A-33 - CDF of the wave height at the Mermaid offshore wind farm (Data: metoceanview.com)

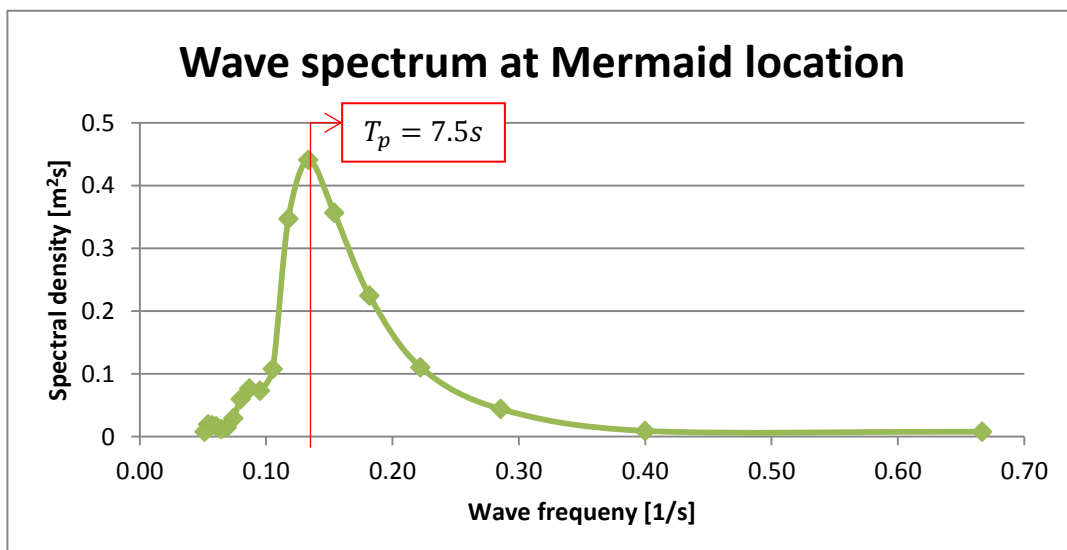


Figure A-34 - Spectral density at Mermaid location (Data: metoceanview.com)

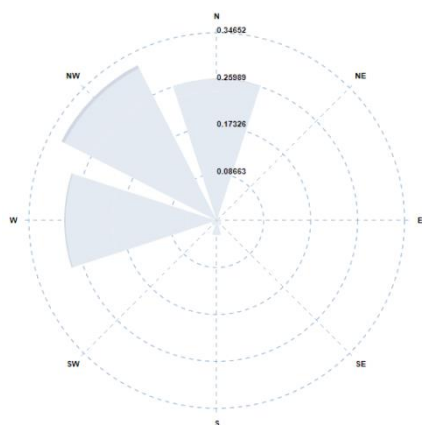


Figure A-35 - Wave rose for port entrance location

The significant wave height at the REBO offshore site and Halve Maan are 1.05 because the measurements are in front of the port entrance with a similar depth, so there is no shoaling. The main wave direction at this location is North West so no diffraction takes place, see Figure 4-18.

The design wave height for constructions at the port is two times the significant wave height; therefore the design wave height is 2.10 meter (Schierreck, 2012).

Location	Significant wave height [m]	Peak period [s]
<b>Mermaid</b>	2.10	7.5
<b>Port entrance</b>	1.05	6.5

Table A-10 - Important wave parameters at Mermaid location and port entrance

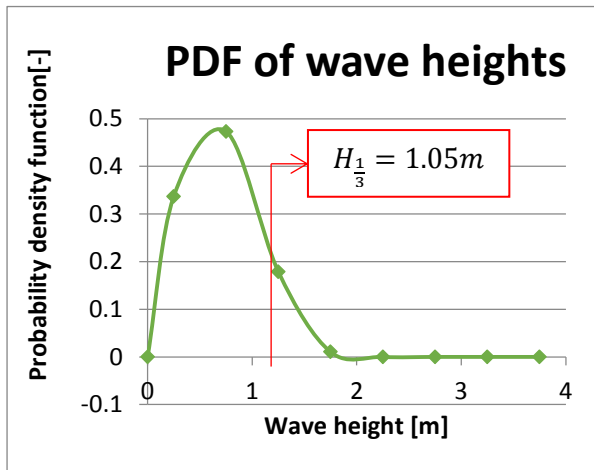


Figure A-36 - Probability density function of wave heights at Oostende port entrance (Data: metoceanview.com)

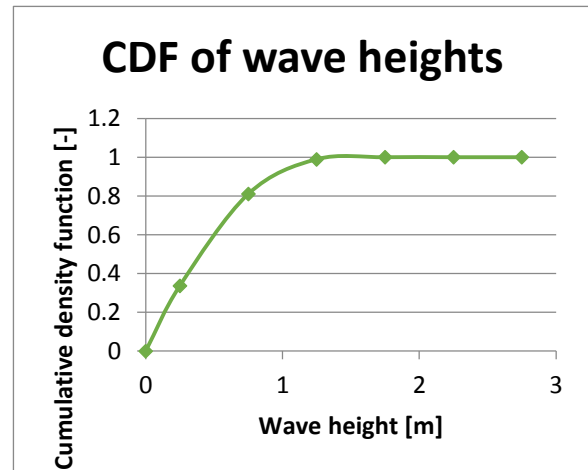


Figure A-37 - Cumulative density function of wave heights at Oostende port entrance (Data: metoceanview.com)

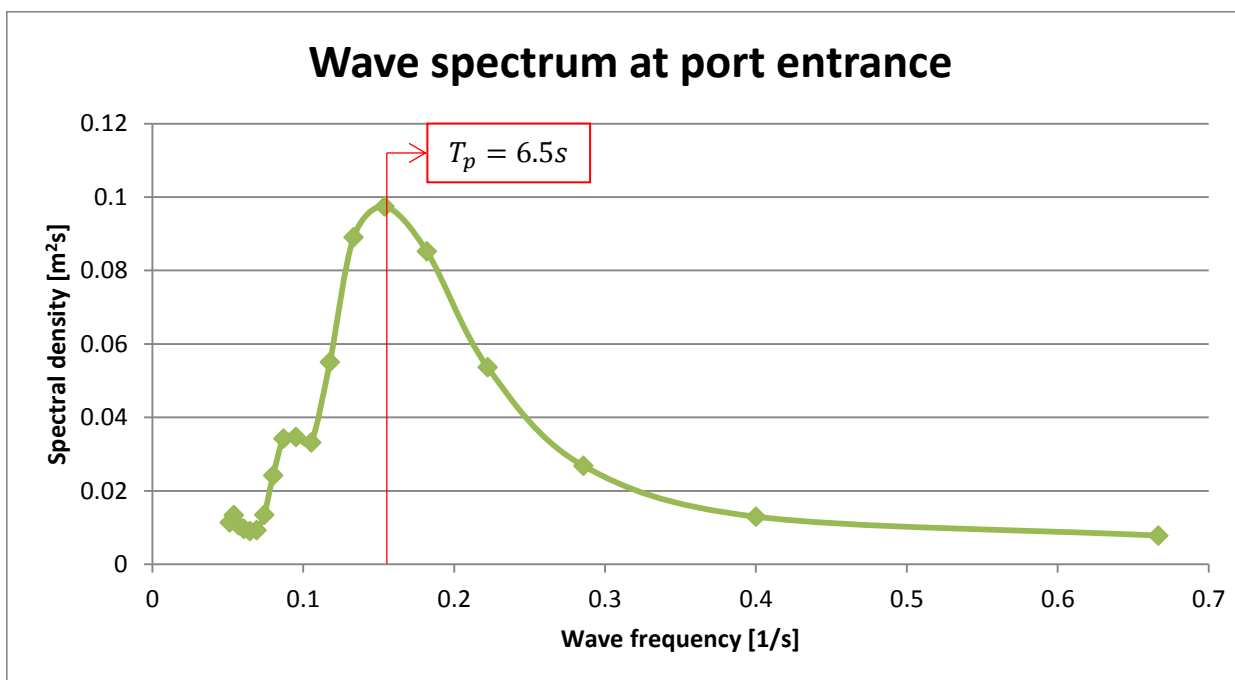


Figure A-38 - Wave spectrum at port entrance (Data: metoceanview.com)

## Annex I LEAFLET OF APPLICABLE SEMI-SUBMERSIBLE



- Submersible to 12.5 m forward / 16.7 m aft above deck
- Launching of jackets up to 10,000 t
- Heavy cargo up to 30,000 t
- Voluminous cargo up to 5,150 m<sup>3</sup>
- Extreme deck strength of 35 t/m<sup>2</sup>
- Ballast water treatment system
- Ice Class ICE-C

### **BOABARGE 37/38**

Semi Submersible Heavy Lift and  
Launching Cargo Barge

## **B** BOABARGE 37

### General Information

Vessel's Name	BOABARGE 37
Flag	Norwegian, NOR
Port of Registry	Trondheim
Call Sign	LG8610
Class Society	DNV
Class Notations	+A1 ICE-CDK(+) DAT(-10)C -Barge for Deck Cargo
Year built	2015
Builder	Nanjing Wujiazui Shipbuilding Co. Ltd.
Place built	Nanjing, China
Owner	Boa Barges AS
Manager	Boa Management AS

### Dimensions

Length, Overall	152 m (498.7 ft)
Breadth, Moulded	38 m (124.7 ft)
Depth, Moulded	9.15 m (30 ft)
Draught - Max	6.92 m (22.7 ft)
Draught - Min	1.50 m (4.9 ft)
Air Draught (from keel to top of mast)	29.95 m (98.3 ft)
Web Frame Spacing	2 m (6.6 ft)
Long. Stiffener Spacing	0.61 m (2.0 ft)
Gross Tonnage	15,185 t
Net Tonnage	4,555 t

### Cargo Capacities

Deadweight (T = 6.920 m)	29,500
Deck space	5,150 m <sup>2</sup>
Deck strength	35 t/m <sup>2</sup>
Launching Capacity	up to 10,000 t jacket

### Submerging Depth

Submerging (Without floatation tanks) when grounding at stern	12.5 m (41 ft) above deck fwd 16.7 m (54.8 ft) above deck aft
Submerging (free floating) with 15 m (49.2 ft) high floatation tanks positioned aft on main deck	12.5 m (41 ft) above deck fwd 13.0 m (42.6 ft) above deck aft
2 additional floating tanks for free floating submerging operations	LxBxH: 20 m x 4.575 m x 15 m

### Tank Capacities

Ballast tanks	46,000 m <sup>3</sup>
Bilge tanks	35 m <sup>3</sup>
Sewage	14.8 m <sup>3</sup>
Fresh water	25 m <sup>3</sup>
Fuel (MDO)	45 m <sup>3</sup>
Lub. Oil Store	0.64 m <sup>3</sup>
Hydr. Oil Store	128 m <sup>3</sup>
Misc. Oil Store	0.64 m <sup>3</sup>

### Ballast System

Ballast Pumps (Diesel Driven)	2 x 5,200 m <sup>3</sup> /hr
Ballast Pumps (Electric Driven)	2 x 750 m <sup>3</sup> /hr
Service Pump (Electric Driven)	1 x 900 m <sup>3</sup> /hr
Ballast Tanks	27 in pontoon, 2 in deckhouse
Remote operated pumps, valves and sounding system from control room	
Ejector stripping system for all ballast tanks	

### Power Supply

Main Generators	2 x 310 kVA (2 x 248 Kw), 440 V, 60 Hz 1 x 210 kVA (1 x 168 Kw), 440 V, 60 Hz
Work Generator	1 x 37 kVA (1 x 30 Kw), 440 V, 60 Hz
Equipment on deck	230 V and 440 V
Shore Power Connections	230 V and 440 V

### Anchor & Mooring Equipment

Anchor Winches	2 x hydraulic winches
Anchors	2 x SPEK 6900 kg, 2 x 330 m x 64 mm K3
Capstans	3 x 12 t pull
Work Winches	2 x double drum on winch deck
Rope Capacities	220 m x 40 mm (721.8 ft x 1.57 in) 150 m x 60 mm (492.1 ft x 2.36 in)
Bollards	Size 500, Capacity SWL 100 t

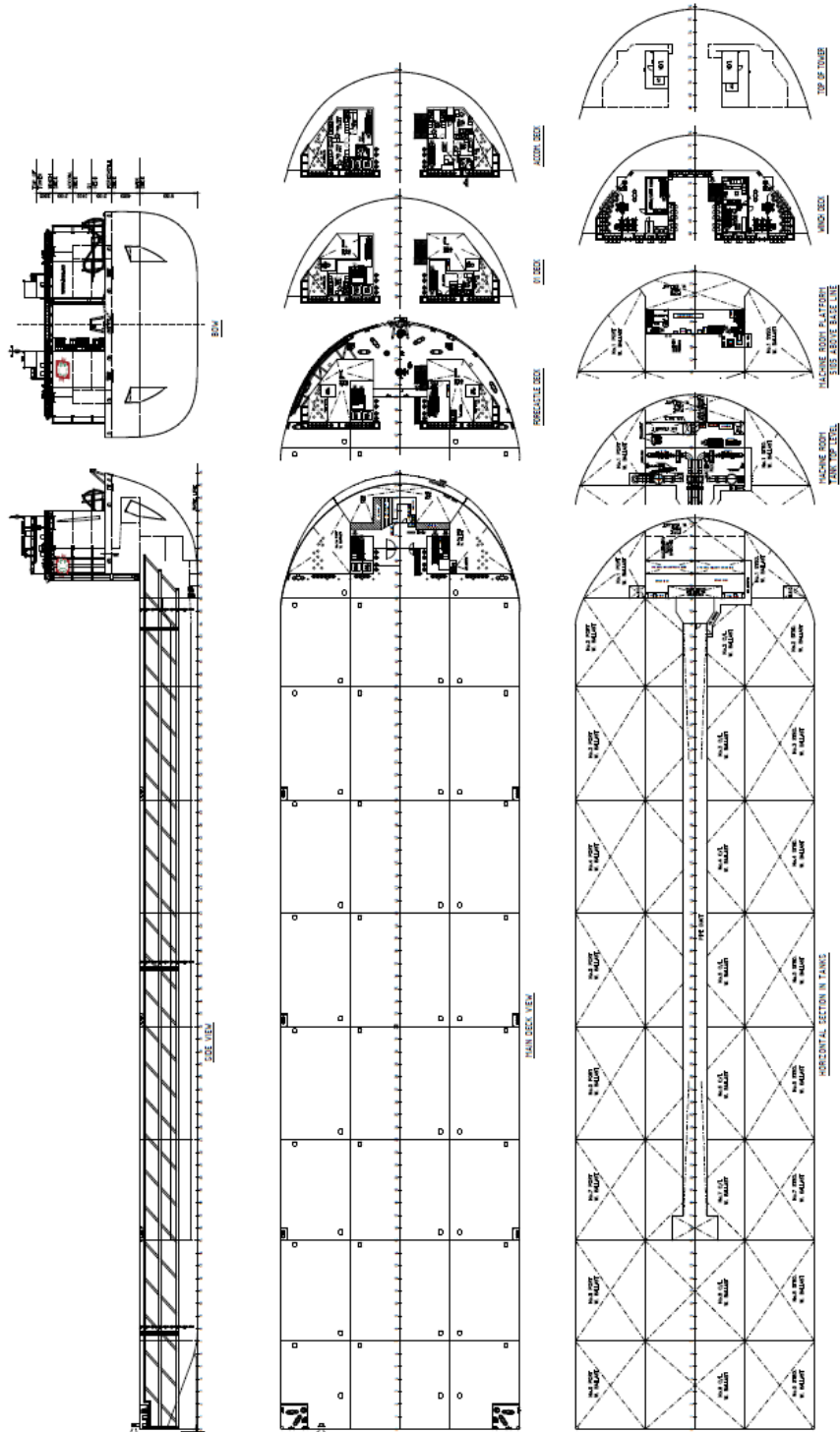
### Towing Equipment

Towing Bridle	Each legs 26.5 m (87 ft), tow plate and 9 m (29.5 ft) long fore runner
Bridle chain	78mm K3, MBL 4500 KN, Max. Bollard Pull 208.5 t
Recovery System	Recovery winch and A-frame with chain on fore-castle deck
Emergency Towing	152 m x 80 mm wire installed in a rack on fore-castle deck, port side
Towing Brackets	3 forward 750 t MBL, 2 aft 300 t MBL

### Accommodation

Accommodations	20 beds
Day Room	1
Meeting Room	1







**CORPORATE HEADQUARTERS**

**BOA Management AS**  
Strandveien 43  
7067 Trondheim  
Norway  
+47 73 99 11 99  
chartering@boa.no

[www.boa.no](http://www.boa.no)

Every effort has been made to ensure that all information contained in this brochure is accurate and up-to-date, however all specifications are subject to change without notice and should be verified. Boa accepts no liability or responsibility for any action taken based on the information presented in this brochure. Boa encourages interested parties to verify the contents of this brochure when in doubt.

© BOA - January 2018

## Annex J DESIGN CALCULATION IMMERSION STRUCTURE

To design the immersion structure first the function of the immersion structure is given. Then the calculation method is given according to the Eurocode and the program of requirements is given. The design of the immersion structure is done in two main parts, first the platform is designed and thereafter the foundation. Only a preliminary design is made to estimate the dimensions and to do a reliable cost estimation. If the structure is build a more extensive study must be performed on the structural design.

### J.1 FUNCTION OF IMMERSION STRUCTURE

The immersion structure must fulfil the function of the transport from land into water of GBFs for offshore wind turbines. The procedure of the transport is given in step 1 till step 4 in Figure A-39. In these drawings the basic principle is given. The design of the immersion platform follows in paragraph J.4.1 and the design of the foundations is described in paragraph J.4.3.

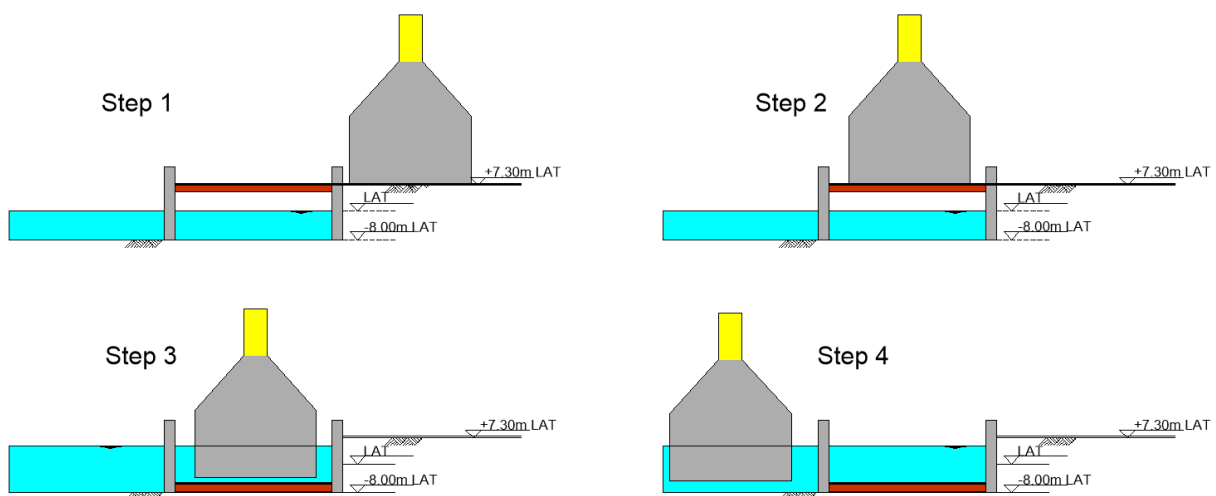


Figure A-39 - Transportation of GBF from land into water

To fulfil the transportation of GBFs from land into water the immersion platform must bear the weight of the GBF. The structure must be able to lift and lower the platform. The total height of the platform may not be too large so that the minimal draught needed by the GBFs is not reached, otherwise the GBF will not float and the transportation action cannot be executed.

### J.2 STARTING POINTS DESIGN IMMERSION PLATFORM

For the static stability in water and the stability on the subsoil the same procedure as in chapter 5 and 6 is followed. For the calculation of the immersion platform structure the Eurocode guidelines are again followed. In the calculation Design Approach 2 (DA2) is performed. This means that the partial factors are given in the set of A1, R2 and M1, see Figure A-40. For the structural calculations the capacity of materials are divided by factors as given in Figure A-41 and Figure A-42.

**Table 3.3.1 Partial factors on actions ( $\gamma_F$ ) or the effects of actions ( $\gamma_E$ )**

Action	Symbol	Set	
		A1	A2
Permanent	Unfavourable	1,35	1,0
	Favourable	1,0	1,0
Variable	Unfavourable	1,5	1,3
	Favourable	0	0

**Table 3.3.2 Partial resistance factors for spread foundations ( $\gamma_R$ )**

Resistance	Symbol	Set		
		R1	R2	R3
Bearing	$\gamma_{Rv}$	1,0	1,4	1,0
Sliding	$\gamma_{Rh}$	1,0	1,1	1,0

**Table 3.3.3 Partial factors for soil parameters ( $\gamma_M$ )**

Soil parameter	Symbol	Value	
		M1	M2
Shearing resistance	$\gamma_\varphi^1$	1,0	1,25
Effective cohesion	$\gamma_c$	1,0	1,25
Undrained strength	$\gamma_{cu}$	1,0	1,4
Unconfined strength	$\gamma_{qu}$	1,0	1,4
Effective cohesion	$\gamma_c$	1,0	1,4
Weight density	$\gamma_\gamma$	1,0	1,0

<sup>1</sup> This factor is applied to  $\tan \varphi'$

Figure A-40 - Load factors according the Eurocode (Molenaar & Voorendt, 2018)

Design situations	$\gamma_c$ for concrete	$\gamma_s$ for reinforcing steel	$\gamma_s$ for prestressing steel
Persistent & Transient	1,5	1,15	1,15
Accidental	1,2	1,0	1,0

Figure A-41 - Material factors for concrete structures (Molenaar & Voorendt, 2018)

type of material resistance	partial material factor $\gamma_m$
resistance of cross-sections of all steel classes	1,0

Figure A-42 - Material factor for steel (Molenaar & Voorendt, 2018)

The weight of the GBF is  $112.7 \text{ kN/m}^2$ . This load is present where the GBF is placed on the immersion platform. Because the load is transferred from the quay wall to the middle of the platform the design criteria is that the whole platform is able to bear a distributed force of minimal  $112.7 \text{ kN/m}^2$ . The load factor for a permanent load is according to the Eurocodes 1.35 (Molenaar & Voorendt, 2018). The weight of the structure is a very important property of the GBF and during the construction this weight is intensively monitored. The GBFs are constructed and transported on a skidding system which uses jacks, the weight can be easily derived from the loads on the jacks. Therefore the load factor on the weight of the GBF is reduced and a partial factor of 1.1 is applied. This result in a design value of  $124 \text{ kN/m}^2$ . The partial factor on the selfweight of the platform structure is according to the Eurocode 1.35. The partial material factors for concrete and steel are 1.5 respectively 1.0, see Figure A-41 and Figure A-42. For the reinforcing steel and prestressing steel both a factor of 1.15 is used. For the hydrostatic forces it is assumed that the water level is at the top of the platform which causes higher forces, also a partial factor of 1.5 is applied on the hydrostatic forces.

### J.3 PROGRAM OF REQUIREMENTS

A program of requirements is given to design the immersion platform:

- The dimensions of the platform must be designed in the way that a working width of 3 meter is available on all sides.
- The immersion platform must be able to bear a minimal weight of  $124 \text{ kN/m}^2$  present on the entire platform.
- The calculations are performed according to the Eurocode guidelines.
- The placement of the immersion platform must be done without foundation works. The immersion platform structure is directly placed on the bottom.
- The immersion platform includes ballast tanks to let the immersion platform float to transport it to another location where it can be used for other projects.
- Skidding beams are used for the transport of caissons on land and therefore the weight of a skid system is implemented in the immersion platform. The weight of skidding system and a steel plate on the platform is assumed to be  $5 \text{ kN/m}^2$ .
- The maximum allowable construction height of the immersion platform is 1.5 meter.
- The foundation of the structure must be stable with respect to:
  - Rotational capacity
  - Bearing capacity
  - Shear capacity
- The immersion platform structure may have a maximum draught of 10 meter.
- The immersion platform structure must have a metacentric height larger than 0.50 meter for stability.
- The weight of the immersion platform must be kept as low as possible.
- The material use must be kept as low as possible.
- The immersion platform can be adapted for larger and/or heavier caissons.

### J.4 DESIGN PROCEDURE

The design calculation is done from top to bottom, for the design first simple hand calculations are performed whereafter the immersion structure is designed with the use of Scia Engineer:

- Platform:  
First the platform where the GBF stands on is designed. The weight of the GBF is implemented and the platform is designed in a way that it can bear the load of the GBF.
- Concrete foundation:  
The foundation can be calculated when the load of the platform including self weight is known. The connection and lift equipment of the immersion platform to the foundation is in the design of the concrete foundation applied with the help of a reference project. The lift equipment must be considered more extensively if this design is used for execution of such a project.

The immersion structure consists of several different elements. In the design the elements are:

- Platform structure
- Two foundation legs
- Two connecting beams between the foundation legs on the bed.

#### J.4.1 Platform design

To design the platform a first assumption must be made to the connection of the platform to the foundation. The platform is hinged on the foundation legs. This reduces the bending moments in the foundation legs and is positive for the design of the foundation legs. A fixed connection is hard to design, especially when the platform also must be lowered and raised. A first idea is to design the platform as is given in.

First a hand calculation is performed to estimate the forces on the immersion platform by a distributed load. The platform is hinged on two sides, the design load is on the entire platform equally distributed, therefore the

slab can be modeled as a simply supported structure as displayed in Figure A-43. In this figure a one meter strip of the platform is taken.

The formula to calculate the bending moment at midspan for a simply supported structure with an equally distributed load is:

$$M_{mid} = \frac{1}{8} \cdot (q_{GBF} + q_{skid+plate}) \cdot l^2 \quad (55)$$

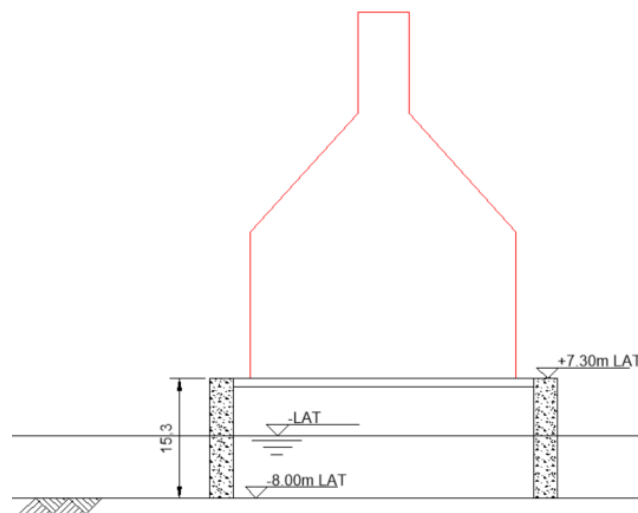
Where:

$M_{mid}$  = Bending moment at midspan [kNm]  
 $q$  = Distributed load [kN/m]  
 $l$  = Length of span [m]

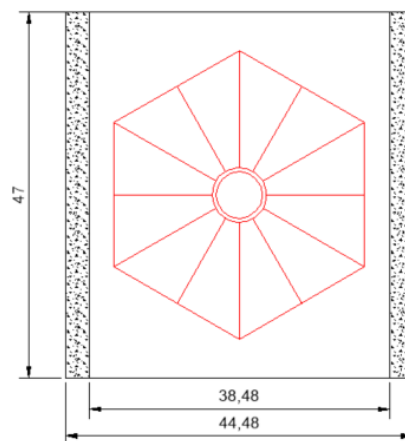
$$M_{Mid} = \frac{1}{8} \cdot (124 + 5) \cdot 38.48^2 = 23,876 \text{ kNm}$$

This results in a bending moment of 23,876 kNm.

In Figure A-44 till Figure A-47 the platform is displayed with a bending moment line, shear force diagram and support reactions, the units are kN and meter.



Side view Immersion platform



Top view Immersion platform

Figure A-43 - Preliminary design immersion platform

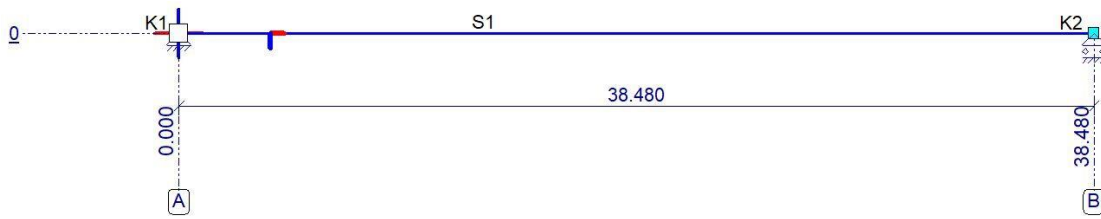


Figure A-44 - Geometry and supports of immersion platform

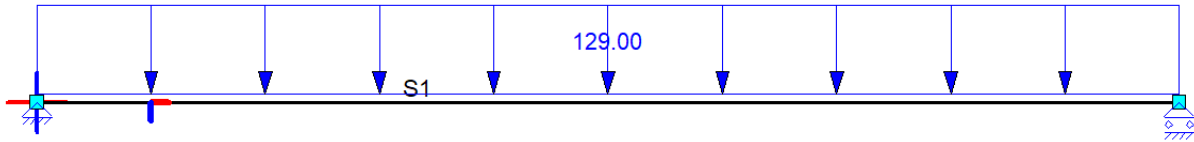


Figure A-45 - Distributed load of GBF, skid system and steel platform

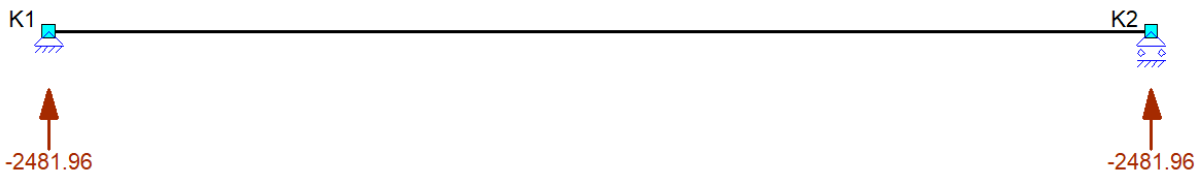


Figure A-46 - Foundation reaction forces

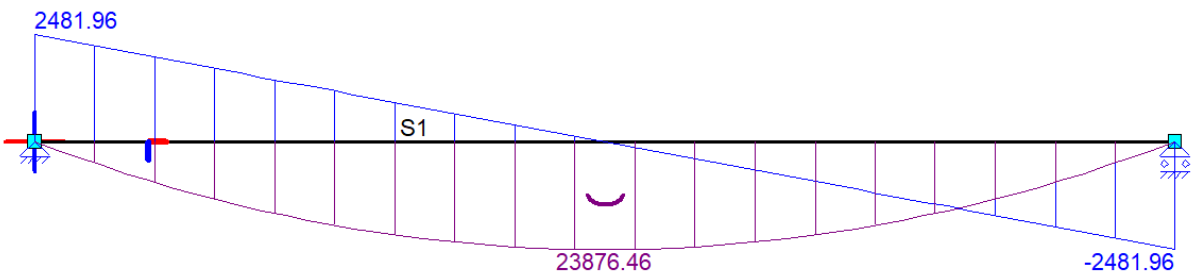


Figure A-47 - Bending moment (purple) and shear force (blue)

In Figure A-48 a 2D model is applied to check if a 1D calculation is an appropriate model for the 2D platform. The values are quite similar and therefore the strip method is applicable, also when a steel plate is installed on the platform structure.

**Interne 2D-krachten**  
 Waardes:  $m_y$   
 Lineaire berekening  
 Belastingsgeval: BG2  
 Extreem: Globaal  
 Selectie: Alle  
 Locatie: In knooppunten gem. bij macro. Systeem: LCS net element

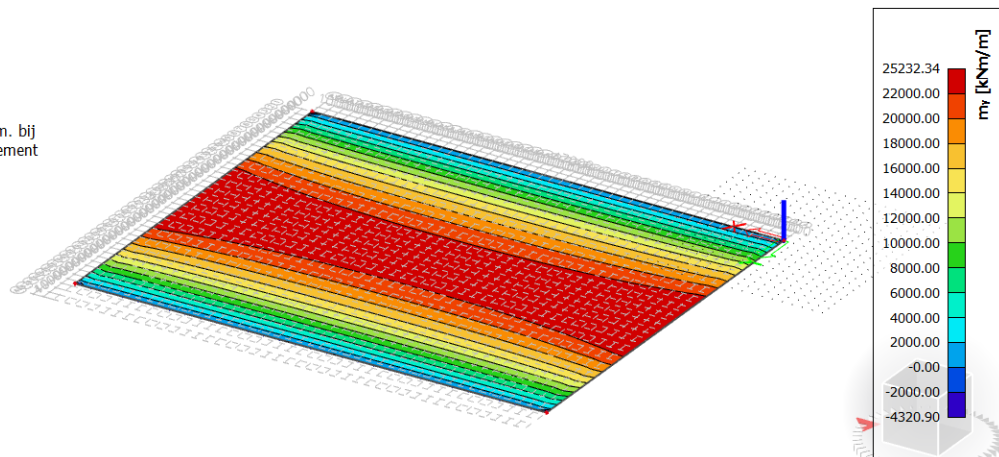


Figure A-48 - Bending moment in 2D platform

Because the platform must resist very high bending moments the construction of the platform can be done in three different types of materials:

- Steel
- Reinforced concrete
- Prestressed concrete.

For these three main options a calculation is performed if the materials are applicable and what the dimensions of these materials are.

#### J.4.1.1 Steel construction

The main advantage of a steel construction is the relatively low weight and high strength. The steel stress may not exceed the maximum allowable steel strength. The maximum allowable stress in the steel is given in the steel class, for example, S235 can have a maximum stress of 235 N/mm<sup>2</sup>.

The maximum stress is given by the Von Mises criteria (Bijlaard, Abspoel, & Vries, 2013):

$$\sqrt{\sigma_x^2 + 3\tau^2} \leq \frac{f_y}{\gamma_m} \quad (56)$$

Where:

$$\begin{aligned} \sigma_x &= \text{Stress due to bending moment [N/mm}^2\text{]} \\ \tau &= \text{Stress due to shear forces [N/mm}^2\text{]} \\ f_y &= \text{Maximum allowable yield stress [N/mm}^2\text{]} \\ \gamma_m &= \text{Partial factor steel (= 1.0)[-]} \end{aligned}$$

The stress due to bending is given by (Bijlaard, Abspoel, & Vries, 2013):

$$\sigma_x = \frac{M_{Ed}}{W_{y,min}} \quad (57)$$

Where:

$$\begin{aligned} M_{Ed} &= \text{Design value bending moment [Nm]} \\ W_{y,min} &= \text{Moment of resistance around } y - \text{axis [m}^3\text{]} \end{aligned}$$

The shear stress in a flange of a steel profile is given by:

$$\tau_{Ed,flange} = \frac{V_{z,Ed} \cdot S_{y,f}^a}{I_y \cdot t_f} \quad (58)$$

The shear stress in the web is given as:

$$\tau_{Ed,web} = \frac{V_{z,Ed} \cdot S_{y,w}^a}{I_y \cdot t_w} \quad (59)$$

The maximum shear stress capacity of a beam is given by:

$$V_{z,Rd} = \min\left(\frac{t_f}{S_{y,f}^a}, \frac{t_w}{S_{y,w}^a}\right) \cdot I_y \frac{f_y}{\sqrt{3}} \quad (60)$$

Where:

$$\begin{aligned} t_f &= \text{Flange thickness [mm]} \\ t_w &= \text{Web thickness [mm]} \end{aligned}$$

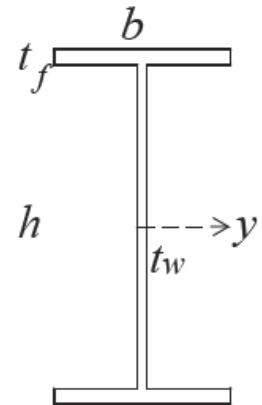


Figure A-49 - Definitions for a H-profile (Bijlaard, Abspoel, & Vries, 2013)

$$S_{y,(f \text{ or } w)}^a = \text{Shear moment flange or web} [mm^3]$$

$$I_y = \text{Moment of inertia around } y - \text{axis} [mm^4]$$

$$V_{z,Ed} = \text{Design value shear force} [N]$$

$$f_y = \text{Yield stress capacity} (= 355) [N/mm^2]$$

First the point at midspan is used to estimate the dimensions of the steel beam.

$$M_{Ed} = 23,876 \cdot 10^6 \text{ Nmm}$$

We apply the largest HEB profile in the common steel tables: HEB 1000. The minimal moment of resistance of this H-beam is  $12895 \times 10^3 \text{ mm}^3$  (staaltabellen.nl).

The steel stress for a HEB 1000 is calculated:

$$\sigma_x = \frac{M_{Ed}}{W_{y,min}} \leq \frac{f_y}{\gamma_m} \quad (61)$$

$$\sigma_x = \frac{23876 \cdot 10^6}{12895 \cdot 10^3} \leq \frac{f_y}{1.0} \quad (62)$$

$$f_y \geq 1852 \frac{N}{mm^2} \quad (63)$$

Applying a steel quality S355 the stress is more than 5 times too high at midspan. This means that a specific steel H-beam must be designed to bear the large internal forces.

The minimal moment of resistance is calculated which is needed to fulfil the requirement at midspan for only the GBF weight, skid system and steel plate is:

$$W_{min} = \frac{M_{Ed}}{\sigma_x} \cdot \gamma_m = \frac{23876 \cdot 10^6}{355} \cdot 1.0 = 6.73 \cdot 10^7 \text{ mm}^3 \quad (64)$$

Because this moment of resistance is without the weight of the steel profile the weight of the steel H-beams are added.

Weight of steel:

$$q_{H-beam} = A_s \cdot \rho_s \cdot g \cdot \gamma_{G,unfav} = A_s \cdot 7800 \cdot 9.81 \cdot 1.35 \text{ kN/m} \quad (65)$$

Where:

$$\rho_s = \text{Volumetric weight steel} (= 7800) [kg/m^3]$$

The steel beam is designed to resist the bending moments. Then the beam is checked on the shear forces and the Von Mises criteria. The dimensions of the new designed beam are given in Figure A-50. The following factors are calculated as follows:

Cross-sectional area:

$$A_s = h \cdot b - (h - 2 \cdot t_f) \cdot (b - t_w) \quad (66)$$

Moment of inertia with applying the Steiner rule:

$$I_{yy} = \frac{1}{12} t_w \cdot (h - 2t_f)^3 + 2 \cdot \left( \left( \frac{1}{12} \cdot t_w \cdot t_f^3 + \left( \frac{1}{2} h - \frac{1}{2} t_f \right)^2 \cdot t_f \cdot b \right) \right) \quad (67)$$

$$W_{y,min} = \frac{I_y}{\frac{h}{2}} \quad (68)$$

Because the calculation is an iterative process only the final dimensions of the steel H-beam are given in Table A-11 and a design is shown in Figure A-50. The total weight of the platform with the H-beams, GBF weight and the skid system and the steel plate, including partial factors, is:

$$q_{tot} = q_{GBF} + q_{H-beam} + q_{skid+plate} = 124 + 26.22 + 5 = 150.2 \text{ kN/m}$$

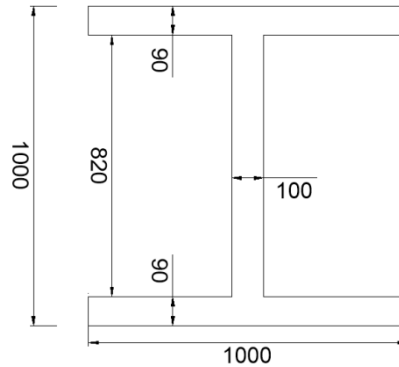


Figure A-50 - H-beam design

Property	Value	Unit	Property	Value	Unit
$h$	1000	[mm]	$q_{plat}$	5	[kN/m]
$b$	1000	[mm]	$q_{steel}$	26.22	[kN/m]
$t_f$	90	[mm]	$q_{tot}$	150.2	[kN/m]
$t_w$	90	[mm]	$I_y$	$4.15 \cdot 10^{10}$	[mm <sup>4</sup> ]
$A$	253,800	[mm <sup>2</sup> ]	$W_{y,min}$	$8.30 \cdot 10^7$	[mm <sup>3</sup> ]

Table A-11 - Properties designed steel beam (S355)

The H-beam fulfills the requirement on bending moments:

$$f_y = \frac{M_{Ed}}{W_{y,min}} = \frac{27803.6 \cdot 10^6}{8.30 \cdot 10^7} = 334 \leq 355 \text{ N/mm}^2$$

A check must be performed on the shear stress capacity. The shear capacity is calculated with (Bijlaard, Abspoel, & Vries, 2013):

$$V_{z,Rd} = \min\left(\frac{t_f}{S_{y,f}^a}, \frac{t_w}{S_{y,w}^a}\right) \cdot I_y \frac{f_y}{\sqrt{3}} \quad (69)$$

Where:

$$S_{y,f}^a = \frac{1000}{2} \cdot 90 \cdot \frac{1000-90}{2} = 2.05 \cdot 10^7 \text{ mm}^3 \quad (70)$$

$$S_{y,w}^a = 1000 \cdot 90 \cdot \left(\frac{1000-90}{2}\right) + \frac{1}{2} \cdot \left(\frac{1000}{2} - 90\right)^2 = 4.10 \cdot 10^7 \text{ mm}^3 \quad (71)$$

The result is a capacity of:

$$V_{z,Rd} = \min\left(\frac{90}{2.05 \cdot 10^7}, \frac{90}{4.10 \cdot 10^7}\right) \cdot 4.05 \cdot 10^{10} \cdot \frac{355}{\sqrt{3}} = 1.82 \cdot 10^7 \text{ N} \quad (72)$$

The maximum shear stress in the beam is  $2.481 \cdot 10^6 \text{ N}$  and therefore the profile is applicable at the supports, where the shear force is maximal.

To estimate the stresses from the whole span the Von Mises criteria is plotted as function of the x-coordinate of the span, see Figure A-51. From the figure can be concluded that the criteria on bending moment has larger influence than the shear stress criteria and no exceedance of maximum steel stress is present.

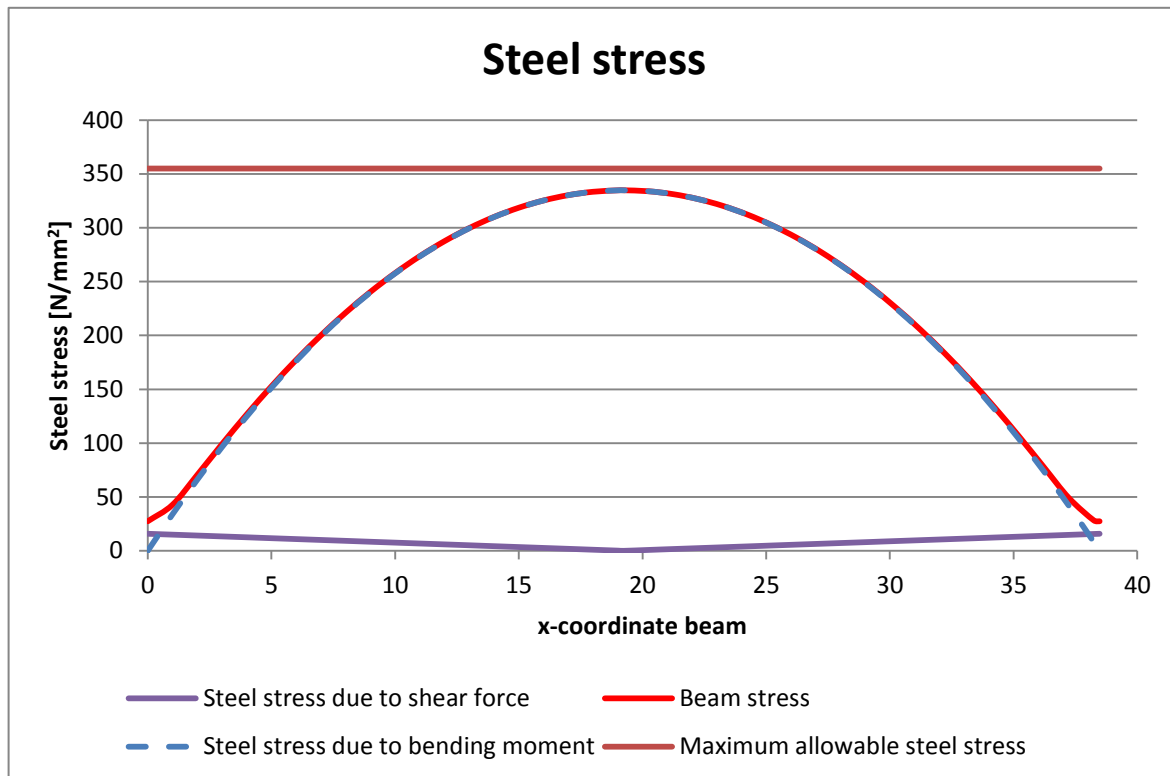


Figure A-51 – Von Mises criteria plotted as function of x-coordinate

Also the deformation of the H-beam is of importance. A large deflection must be prevented. To calculate the beam deflection the following formula is applied:

$$w_{mid} = \frac{5}{384} \cdot \frac{q_{tot} \cdot l^4}{E \cdot I_y} \quad (73)$$

Where:

$$\begin{aligned}
 w_{mid} &= \text{Deflection at midspan [m]} \\
 q_{tot} &= \text{Distributed load [N/m]} \\
 l &= \text{Span length [m]} \\
 E &= E - \text{modulus steel } (= 210 \cdot 10^9) [\text{Nm}] \\
 I_y &= \text{Moment of inertia [m}^4]
 \end{aligned}$$

By implementing the values this results in:

$$w_{mid} = \frac{5}{384} \cdot \frac{150.2 \cdot 10^3 \cdot 38.48^4}{210 \cdot 10^9 \cdot 4.15 \cdot 10^{-2}} = 0.49m \quad (74)$$

To check the outcomes of the calculations the beam is modelled in the software package Scia Engineer. The internal stresses and displacements are shown in Figure A-52 and Figure A-53. The stress profile of the Von Mises criteria and from Scia Engineer is similar. The maximum stress is not exceeded and the profile is applicable. The deflection of the beam is also similar to the calculations. For design purposes the dimensions of the beam could be larger to decrease the deflections.

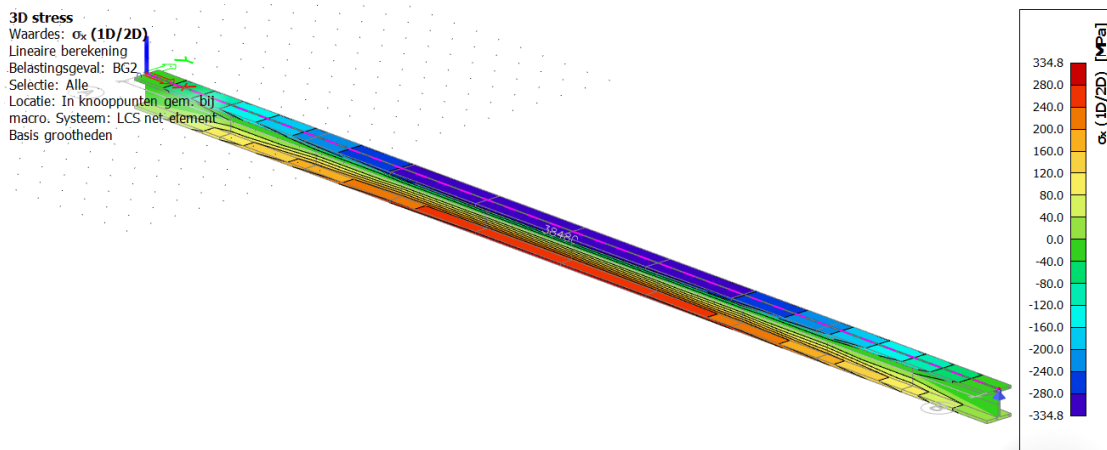


Figure A-52 - Stress in H-beam due to  $q_{tot}$

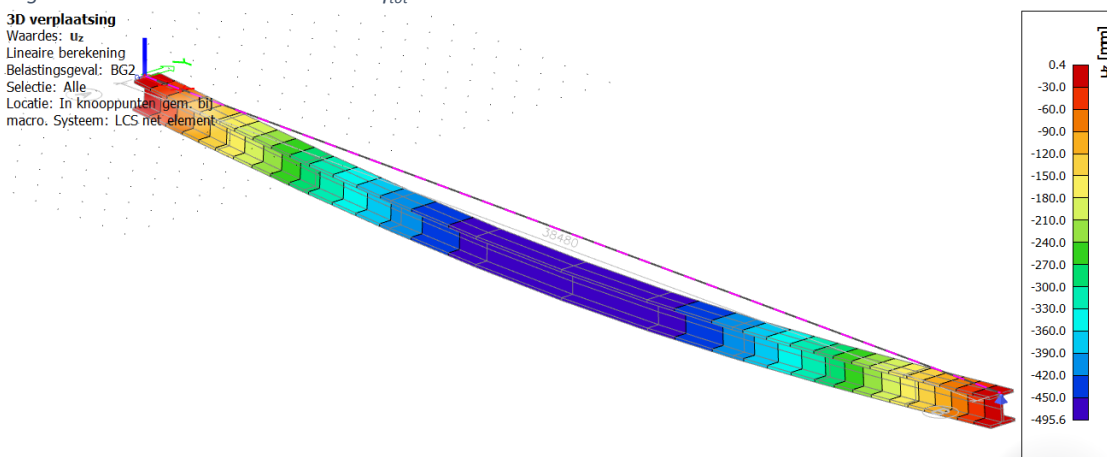


Figure A-53 - Displacement of H-beam

The H-beam deflection of 50 cm is quite high. An important requirement is the small construction height of the platform structure. This extra deflection is not accounted in the total construction height. The GBF stands on the structure and cause the major part of the deflection, when the structure is lowered under water the effective weight of the GBF decreases until the GBF floats. At the moment the GBF floats the weight on the platform is zero and the deflection is negligible. But for the transportation of the GBF from land onto the platform this could cause problems. Therefore the H-beam is designed heavier to reduce the deflection. The new dimensions are given in Table A-12 and are shown in Figure A-54. In Figure A-55 the Von Mises criteria, in Figure A-56 the internal stresses and in Figure A-57 the deflection are shown.

Property	Value	Unit	Property	Value	Unit
$h$	1100	[mm]	$A$	353000	[mm <sup>2</sup> ]
$b$	1000	[mm]	$q_{steel}$	36.47	[kN/m]
$t_f$	135	[mm]	$q_{tot}$	160	[kN/m]
$t_w$	100	[mm]	$I_y$	$6.8 \cdot 10^{10}$	[mm <sup>4</sup> ]
			$W_{y,min}$	$1.78 \cdot 10^8$	[mm <sup>3</sup> ]

Table A-12 - Dimensions of heavier designed H-beam

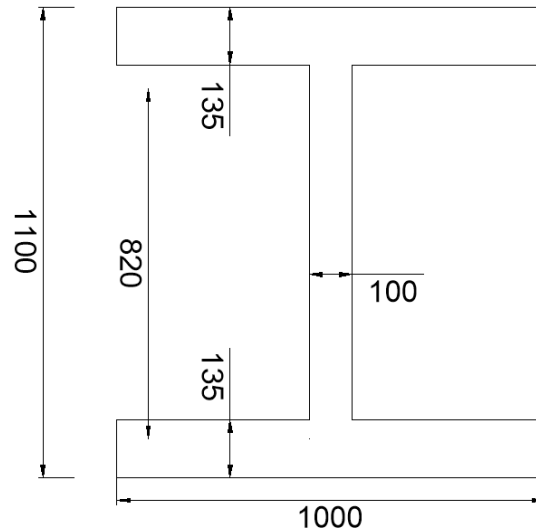


Figure A-54 - Final design H-beam

Applying these dimensions of the H-beam the Von Mises stresses are shown in Figure A-55, the stresses according the Scia model are given in Figure A-56 and the deflection is given in Figure A-57. The maximum steel stress is around  $245 \text{ N/mm}^2$  and a reserve capacity is present for unforeseen forces for example wind or snow. The deflection of 32 cm over a span length of 38.48 meter is accepted and it is concluded that a steel beam construction could be designed to support the immersion platform. The height is 1.10 meter, 40 cm is left for the construction of the plate and skidding system above the beams.

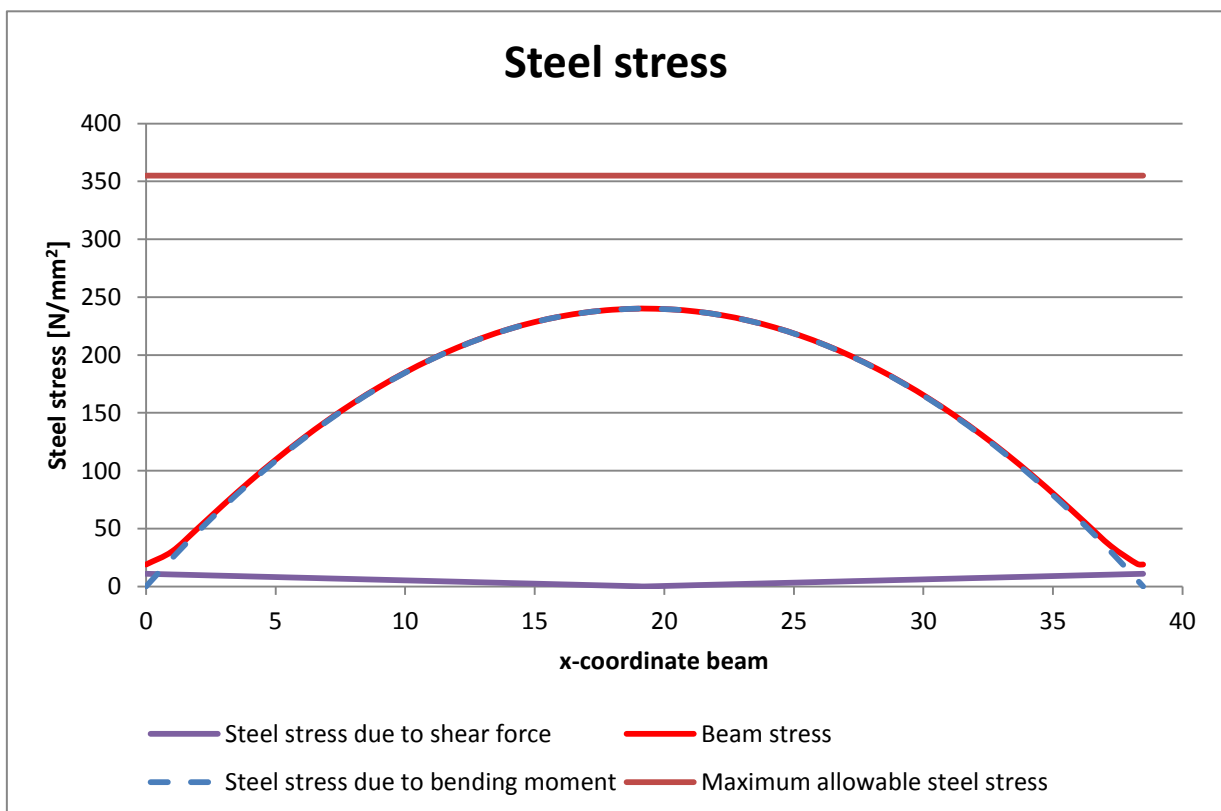


Figure A-55 - Von Mises criteria plotted as function of x-coordinate

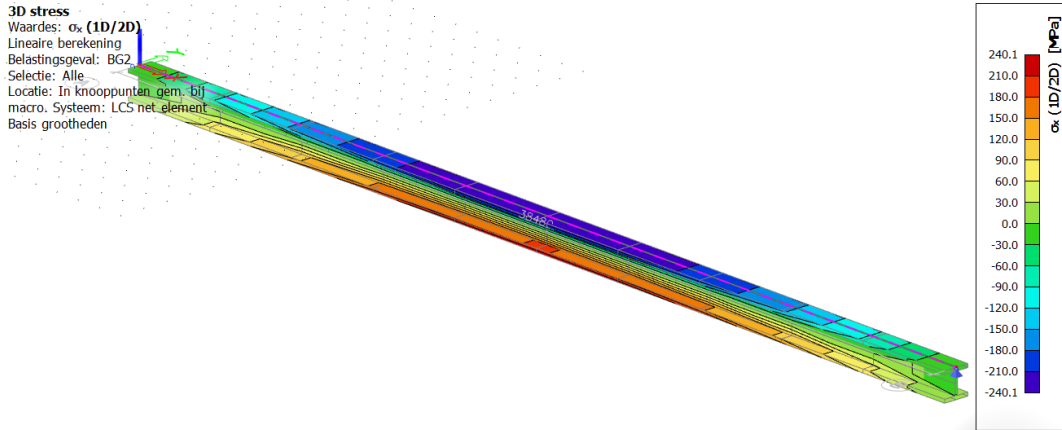


Figure A-56 - Stresses in final design H-beam

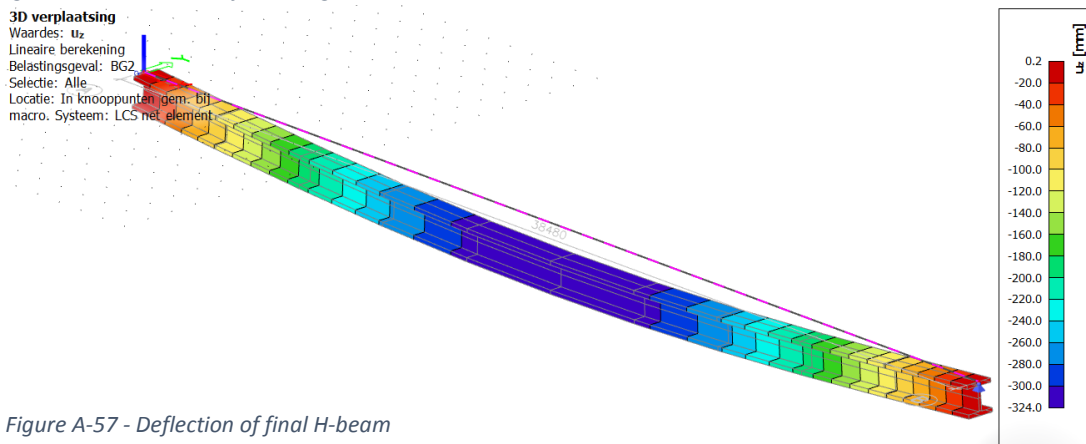


Figure A-57 - Deflection of final H-beam

#### J.4.1.2 Reinforced concrete

Another option could be to build the platform construction with reinforced concrete. The capacity of a concrete beam can be calculated with a cross-section where the forces are indicated in Figure A-58:

$$M_{Ed} = N_s \cdot z \quad (75)$$

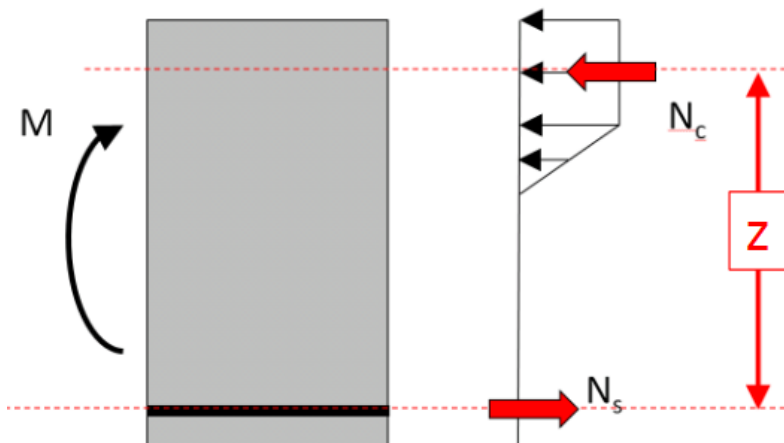


Figure A-58 - Forces on reinforcement concrete cross-section (Hordijk & Lagendijk, 2017)

Where:

- $N_c$  = Compressive force in concrete [N]
- $N_s$  = Tension force in steel [N]
- $z$  = Internal lever arm ( $\approx 0.9d$ ) [m]
- $M_{Ed}$  = Design value bending moment in crosssection [Nm]

For the calculation a maximum height of 1200 mm is used. The width of a concrete element is according to rule of thumb the half of the height: 600 mm

The characteristic weight of the concrete element is 18 kN/m. The extra moment at midspan caused by selfweight is calculated with:

$$q_{cd} = q_c \cdot \gamma_{G,unfav} = 18 \cdot 1.35 = 24.3 \text{ kN/m}$$

$$M_{c,mid} = \frac{1}{8} \cdot (q_{cd} + q_{GBF} + q_{skid+plate}) \cdot l^2 = \frac{1}{8} \cdot (24.3 + 124 + 5) \cdot 38.48^2 = 28,374 \text{ kNm} \quad (76)$$

$$N_c = N_s = \frac{M_{Ed}}{z} = \frac{28374}{0.9 \cdot 1.2} = 26,272 \text{ kN} \quad (77)$$

Where:

$$M_{c,mid} = \text{Bending moment at midspan in concrete [kNm]}$$

$$q_c = \text{Weight of concrete element per meter [kN/m]}$$

To calculate the minimal amount of reinforcing steel the following formula is applied:

$$A_{s,needed} = \frac{N_s}{f_{yd}} = \frac{26,272,327}{435} = 60,396 \text{ mm}^2 \quad (78)$$

Where:

$$f_{yd} = \frac{f_y}{\gamma_s} = \frac{500}{1.15} = 435 \frac{\text{N}}{\text{mm}^2} \quad (79)$$

This gives a reinforcement ratio of:

$$\frac{A_{s,needed}}{A_c} = \frac{60,396}{600 \cdot 1200} \cdot 100\% = 8.39\% \quad (80)$$

Where:

$$f_y = \text{Yield strength reinforcement [N/mm}^2]$$

$$f_{yd} = \text{Design yield strength reinforcement [N/mm}^2]$$

$$A_{s,needed} = \text{Minimal surface of needed reinforcement [mm}^2]$$

$$A_c = \text{Cross – sectional area concrete [mm}^2]$$

The reinforcement ratio in this concrete element is too high, see Figure A-59 for the maximum reinforcement ratios. The calculation is performed for one meter width, when the full cross-section of one meter width is used the maximum reinforcement ratio is also exceeded; therefore use of a reinforced concrete structure to support the platform is not applicable.

C20/25	C25/30	C30/37	C35/45	C40/50	C45/55
1,23	1,54	1,85	2,15	2,46	2,77
C50/60	C55/67	C60/75	C70/85	C80/95	C90/105
3,08	3,03	3,01	3,10	3,31	3,55

Figure A-59 - Maximum reinforcement ratio per concrete class (Cement&Betoncentrum, 2016)

#### J.4.1.3 Prestressed concrete

To determine the applicability of a prestressed concrete structure a preliminary design of a concrete element is made. A rule of thumb is that the thickness of the element is around 1/33 of the length. The thickness is in first instance assumed to be 1.20 meter. In Figure A-60 a first estimation of the concrete profile is given.

The cross-sectional parameters which are needed to determine the applicability of a prestressed concrete element are calculated as follows:

The cross-sectional area is calculated with:

$$A_c = 1000 \cdot 1200 - 500 \cdot 700 = 0.85 \cdot 10^6 \text{ mm}^2 \quad (81)$$

The extra weight of the prestressed concrete beam can be calculated by multiplying the area by the density which is 2400 kg/m<sup>3</sup>:

$$q_c = A_c \cdot \rho_c \cdot g = 0.85 \cdot 10^6 \cdot 2400 \cdot 9.81 = 21.25 \text{ kN/m} \quad (82)$$

Where:

$$q_c = \text{Characteristic weight of prestressed concrete element per meter [kN/m]}$$

To calculate the design load the weight is multiplied by the partial weight factor of 1.35:

$$q_{cd} = q_c \cdot \gamma_{G,unfav} = 21.25 \cdot 1.35 = 28.69 \text{ kN/m} \quad (83)$$

Where:

$$q_{cd} = \text{Design weight of concrete element per meter [kN/m]}$$

Calculating the bending moment at midspan, caused by the design weight of the concrete element:

$$M_{E,G} = \frac{1}{8} \cdot (q_{cd} + q_{skid+plate}) \cdot l^2 = 6237 \cdot 10^6 \text{ Nmm} \quad (84)$$

The bending moment at midspan, caused by selfweight and variable GBF weight are:

$$M_{E,G+Q} = \frac{1}{8} \cdot (q_{cd} + q_{GBF} + q_{skid+plate}) \cdot l^2 = 29187 \text{ kNm}$$

The moment of inertia is:

$$I_y = \frac{1}{12} \cdot b_{out} \cdot h_{out}^3 - \frac{1}{12} \cdot b_{in} \cdot h_{in}^3 = 1.3 \cdot 10^{11} \text{ mm}^4 \quad (85)$$

Because the cross-section is symmetrical the moment of resistance is equal for the top fiber and bottom fiber:

$$W_{ct} = W_{cb} = \frac{I_y}{\frac{1}{2}h} = \frac{1.3 \cdot 10^{11}}{\frac{1}{2} \cdot 1200} = 2.17 \cdot 10^8 \text{ [mm}^3\text{]} \quad (86)$$

The upward pressure from the tendons can be calculated with the formula:

$$q_p = \frac{8 \cdot P_{m,\infty} \cdot f}{l^2} \quad (87)$$

Where:

$$P_{m,\infty} = \text{Working prestressing force in concrete element [kN]}$$

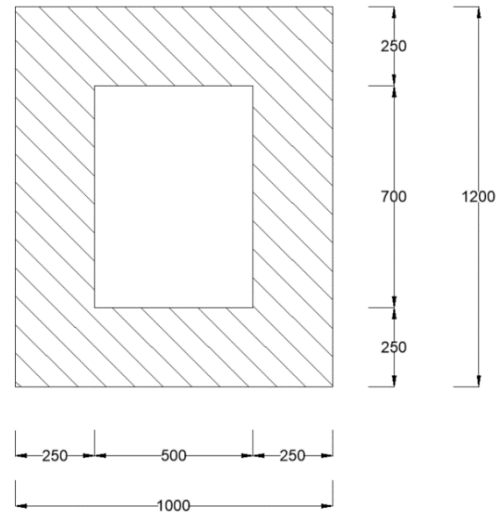


Figure A-60 - Preliminary design prestressed concrete girder

$$f = \text{Drape of tendon [m]}$$

The values as given in Table A-13 are used for the calculation of the prestressed element.

Parameter	Value	Unit	Parameter	Value	Unit
$A_c$	$0.85 \cdot 10^6$	$[mm^2]$	$l$	38.48	$[m]$
$f$	400	$[mm]$	$W_{cb}$	$2.17 \cdot 10^8$	$[mm^3]$
$W_{ct}$	$2.17 \cdot 10^8$	$[mm^3]$	$M_{E,G}$	$6237 \cdot 10^6$	$[Nmm]$
$M_{E,G+Q}$	$29187 \cdot 10^6$	$[Nmm]$	$\sigma_{cd}$	30	$[N/mm^2]$

Table A-13 - Properties prestressed concrete element

Where:

$$\sigma_{cd} = \text{Compressive design strength of concrete [N/mm}^2\text{]}$$

The principle of prestressed concrete is to preload the concrete element by tendons. In Figure A-61, a tendon is drawn in a concrete cross-section. By tensioning the tendon an upward pressure is created. With this upward pressure the resultant downward force is decreased.

To check if a prestressed concrete element is applicable there are three checks needed:

- No tensile stresses at bottom fiber at  $t=\infty$
- No exceedance of maximum allowable compressive capacity at  $t=0$  at bottom fiber
- No tensile stresses at top fiber at  $t=0$ .

For the calculating of the checks the parameters are used from Table A-13.

**Check 1: No tensile stresses at bottom fiber at  $t=\infty$ . With this check the minimal tensioning force is calculated** (Walraven & Braam, 2018).

$$\sigma_c \leq 0 \quad (88)$$

$$-\frac{P_{m,\infty}}{A_c} - \frac{\frac{1}{8} \frac{f}{l^2} P_{m,\infty} \cdot l^2}{W_{cb}} + \frac{M_{E,G+Q}}{W_{cb}} \leq 0 \quad (89)$$

$$P_{m,\infty} \geq \frac{\frac{M_{E,G+Q}}{W_{cb}}}{\frac{1}{A_c} + \frac{f}{W_{cb}}} = \frac{\frac{29187 \cdot 10^6}{2.17 \cdot 10^8}}{\frac{1}{0.85 \cdot 10^6} + \frac{400}{2.17 \cdot 10^8}} = 4.45 \cdot 10^7 [N] \quad (90)$$

$$P_{m,0} \geq \frac{P_{m,\infty}}{0.8} = \frac{4.96 \cdot 10^7}{0.8} = 5.57 \cdot 10^7 [N] \quad (91)$$

**Check 2: No exceedance of maximum allowable compressive capacity at  $t=0$  at bottom fiber. With this check the maximum tensioning force is calculated** (Walraven & Braam, 2018).

$$\sigma_{cb} \geq -\sigma_{cd} \quad (92)$$

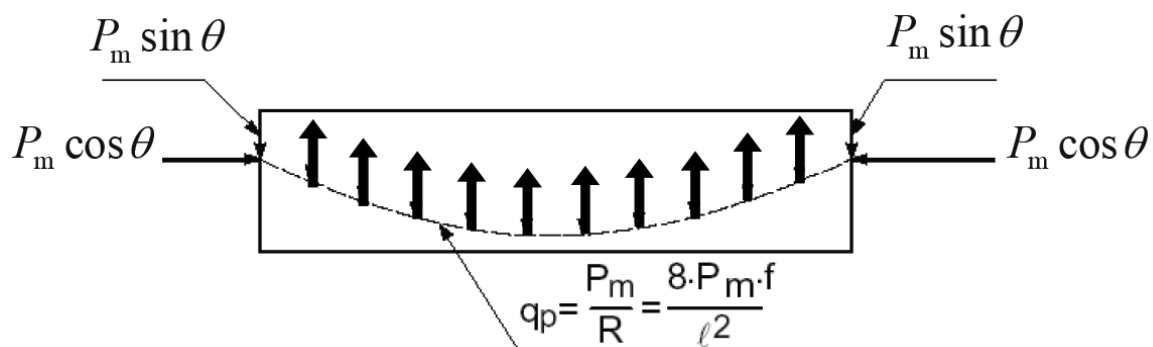


Figure A-61 - Principle of prestressing (Walraven & Braam, 2018)

$$-\frac{P_{m,0}}{A_c} - \frac{\frac{1}{8} \frac{8f}{l^2} P_{m,0} \cdot l^2}{W_{cb}} + \frac{M_{E,G}}{W_{cb}} \geq -\sigma_{cd} \quad (93)$$

$$P_{m,0} \leq \frac{\sigma_{cd} + \frac{M_{E,G}}{W_{cb}}}{\frac{1}{A_c} + \frac{f}{W_{cb}}} \quad (94)$$

Where the maximum allowable compressive strength is given by:

$$\sigma_{cd} = 0.6 \cdot f_{ck} = 0.6 \cdot 50 = 30 \text{ N/mm}^2 \quad (95)$$

The initial stress is calculated:

$$P_{m,0} \leq \frac{30 + \frac{6237 \cdot 10^6}{2.17 \cdot 10^8}}{\frac{1}{0.85 \cdot 10^6} + \frac{f}{2.17 \cdot 10^8}} = 1.95 \cdot 10^7 \text{ N} \quad (96)$$

**Check 3: No tensile stresses at top fiber at t=0. With this check the maximum tensioning force is calculated** (Walraven & Braam, 2018).

$$\sigma_{ct} \leq 0 \quad (97)$$

$$-\frac{P_{m,0}}{A_c} + \frac{\frac{1}{8} \frac{8f}{l^2} P_{m,0} \cdot l^2}{W_{ct}} - \frac{M_{E,G}}{W_{ct}} \leq 0 \quad (98)$$

$$P_{m,0} \leq \frac{\frac{M_{E,G}}{W_{ct}}}{\frac{1}{A_c} + \frac{f}{W_{ct}}} \leq \frac{\frac{6237 \cdot 10^6}{2.17 \cdot 10^8}}{\frac{1}{0.85 \cdot 10^6} + \frac{f}{2.17 \cdot 10^8}} = 4.30 \cdot 10^7 \text{ N} \quad (99)$$

After performing the three checks the following results are achieved:

$$P_{m,0} \geq 5.57 \cdot 10^7 \text{ N}; P_{m,0} \leq 1.95 \cdot 10^7 \text{ N}; P_{m,0} \leq 4.30 \cdot 10^7 \text{ N} \quad (100)$$

The prestressing force must be higher than  $5.57 \cdot 10^7$  and lower than  $1.95 \cdot 10^7$  Newton. These two requirements cannot be fulfilled simultaneously and therefore this prestressed element is not feasible. This is due to the relatively small self-weight of the platform and the very large weight of the GBF which is placed on the platform. To carry the GBF a large prestressing is needed to prevent tension at the bottom fiber, when the GBF is not present this large prestressing causes tension at the top fiber.

#### J.4.1.4 Decision on platform structure

The materials reinforcement concrete and prestressed concrete are not applicable when a maximum construction height of 1.5 meter is available. Therefore no multi-criteria analysis is executed and the solution is found in steel H-beams to support the immersion platform. A drawing of this platform is given in Figure A-62 and Figure A-63.

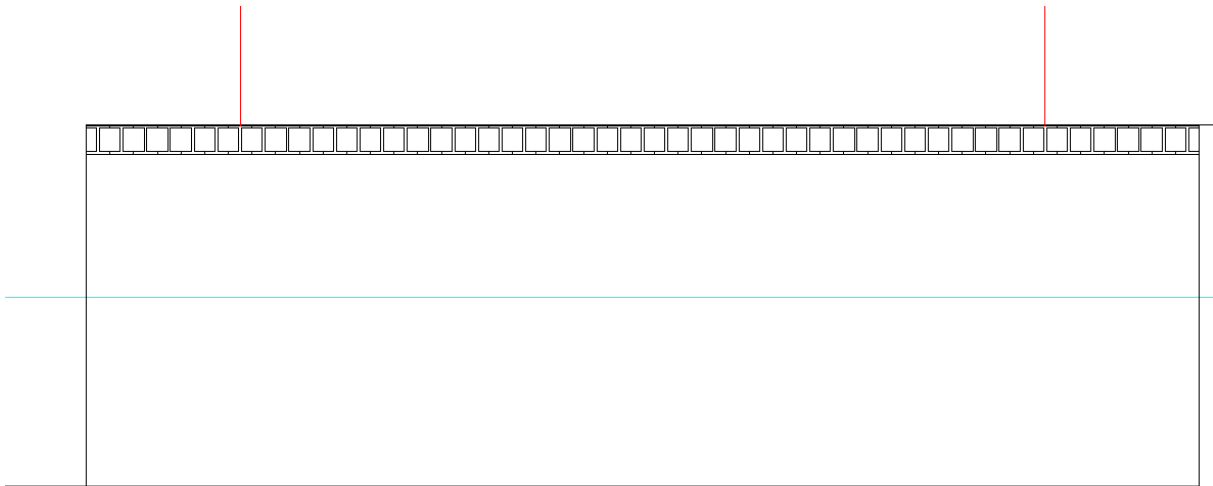


Figure A-62 - Principle of steel beam supporting system

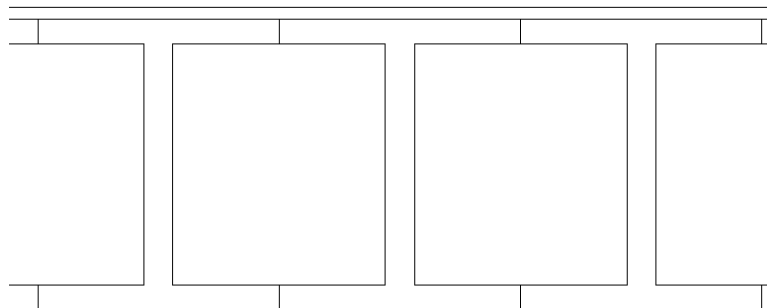


Figure A-63 - Plate of immersion platform placed on H-beams

#### J.4.2 Lifting mechanism

A lifting mechanism must be designed to lower the platform with the GBF placed on it and to hoist the platform when the GBF is towed away. Only an indication of a feasible mechanism is shown to give an idea of what is possible. A winch system is chosen to use to lift and lower the platform, this is also done on the syncrolift that is used to transport the caissons for the flood defences at Venice from land into water, see Figure A-64 and Figure A-65.



Figure A-64 - Winch system at Venice Mose project  
(newcivilengineer.com, 2011)



Figure A-65 - Platform of Venice Mose project  
(newcivilengineer.com, 2011)

The caisson which is lowered with this winch system weights 25,000 tons and the dimensions and weight per square meter are somewhat higher but comparable with the GBF dimensions. With that knowledge it is assumed that the winch system is feasible on the immersion structure.

The weight of the winch system is subdivided in two main parts:

- Cables to lift the platform:
- Additional equipment for the rotation mechanism.

The cables to lift the platform are estimated with a basic formula and the weight of the additional equipment is estimated to be somewhat higher in weight than the cables.

- Cables to lift the platform:

The platform, including the GBF, weights 299,262kN, with a yield strength of the winch cables of 235 N/mm<sup>2</sup> the minimal surface area of steel cables is determined. A partial safety factor of 0.8 is included on the steel strength for the system, because not every cable is stretched equally in time.

$$A_{s,min} = \frac{W_{plat} + W_{GBF}}{0.8 \cdot f_{yd}} = \frac{(q_{steel} + q_{GBF} + q_{skid+plate}) \cdot A_{plat}}{0.8 \cdot 235} =$$

$$\frac{(36.47+124+5) \cdot 47 \cdot 38.48 \cdot 10^3}{188} = 1,591,821 mm^2 \quad (101)$$

Where:

$$f_{yd} = \text{Yield strength of steel cable [N/mm}^2\text{]}$$

The weight of the cables is estimated with the formula:

$$W_{cables} = A_{s,min} \cdot l_{cable} \cdot \rho_s = 1,591,821 \cdot 10^{-6} \cdot 15.3 \cdot 7800 = 189,968[kg] = 190 ton \quad (102)$$

The weight of additional material to rotate the winches and to lift and lower the platform is assumed at 200 tons of steel.

#### J.4.3 Foundation

The foundation of the immersion platform has to resist the weight of the platform, must be stable on the bottom and must be stable to lower and raise the platform. Therefore it is decided to use reinforced concrete as material. With concrete a large contact area on the soil is created. Another advantage is that the internal forces mainly are compressive forces due to the platform weight, therefore concrete is applied. Because one of the requirements is that the platform can float internal space is required to pump water in and out. A calculation is performed to check the minimal thickness of the concrete elements. With the minimal thickness the width of the concrete foundation and the weight can be calculated. When the weight is calculated the minimal required internal space to let the platform float can be calculated and then the preliminary design is given. The starting point of the design is given in Figure A-66. In principal the foundation consists of two large concrete hollow boxes with internal walls. The internal walls are implemented to reduce the bending moments and to prevent large concrete walls. The inner spaces could be applied as ballasting tanks. The width of the foundation is assumed to be 3 meters, the center to center distance between the walls is assumed to be 4 meter. The principle of how the forces interact on the foundation in a side view is shown in Figure A-67.

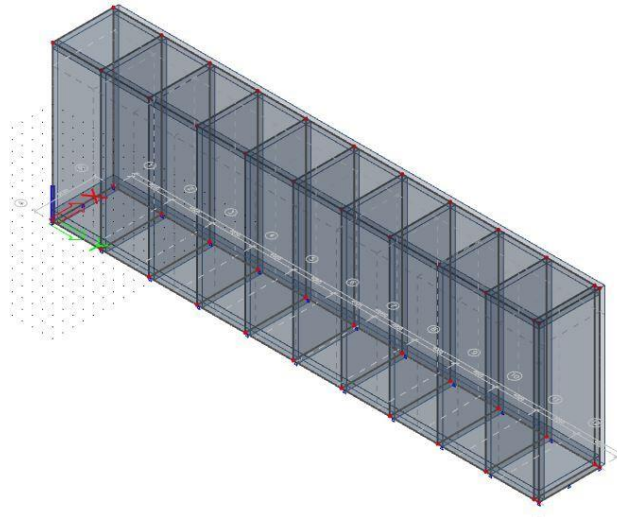


Figure A-66 – Starting point of design foundation legs

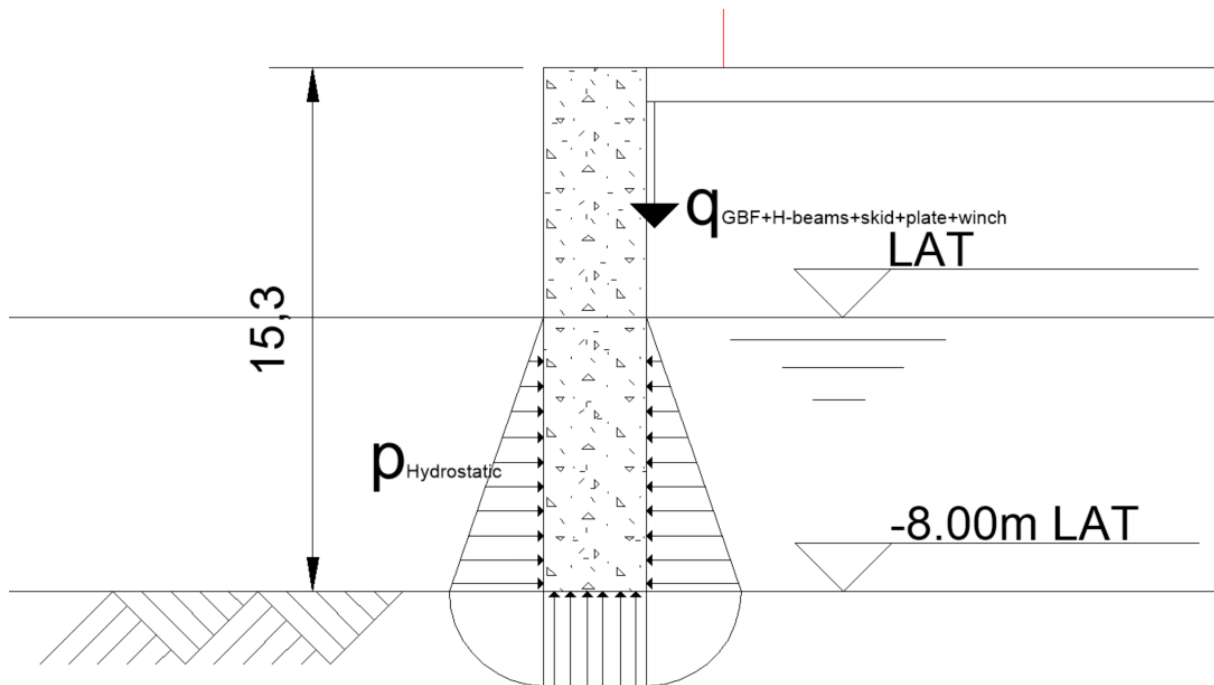


Figure A-67 - Forces on concrete foundation (hydrostatic forces depends on water depth)

The forces are drawn on the concrete foundation which must resist the weight of the GBF, the H-beams, skidding beams, steel plate and the winch system. The calculation of the forces for the structure in operational phase is performed. When this solution is used at a project an extensive study on the dynamically loads in the floating, transporting and installing phase must be performed.

#### J.4.1.5 Load conditions

The main loads which are present on the foundation of the immersion structure are described. The platform with the GBF weight, winch system, skidding beams, steel plate and H-beams and the hydrostatic pressure all interact on the concrete foundation. First the platform and GBF weight are given whereafter the hydrostatic forces on the platform are discussed.

#### Platform + GBF weight + Lift mechanism + skidding beams and steel plate:

- The force per square meter caused by the GBF on the platform is 112.7 kN/m<sup>2</sup>.
- The weight of the steel H-beams of the platform is self-weight and this is included in the Scia model. The weight of the platform is transferred to the immersion structure foundation.
- The lift mechanism weights in total 390 tons. Divide this equally over the edge of the immersion structure foundation this result in a total weight of 40.7 kN/m.
- The weight of the skidding beams and a steel plate over the H-beams is assumed at 5.0 kN/m<sup>2</sup>.

#### Hydrostatic pressure

The hydrostatic pressure is calculated with the formula:

$$p_h(d) = \rho_w g d \gamma_{Q,unfav} = 1025 \cdot 9.81 \cdot d \cdot 1.5 \quad (103)$$

Where:

$$\begin{aligned}
 p_h(d) &= \text{Hydrostatic pressure as function of depth [N/m}^2\text{]} \\
 g &= \text{Gravitational acceleration [m/s}^2\text{]} \\
 d &= \text{Depth [m]} \\
 \rho_s &= \text{Volumetric density water [kg/m}^3\text{]} \\
 \gamma_{Q,unfav} &= \text{Partial factor on unfavorable variable load (= 1.5)[-]}
 \end{aligned}$$

The hydrostatic pressure is proportional to the depth, the result of the hydrostatic force is zero at the top and 153.8 kN/m<sup>2</sup> at the bottom, excluding partial factors. The forces under at the foundation are also 153.8 kN/m<sup>2</sup>.

#### J.4.1.6 Structural analysis

Because the foundation is an undetermined structure and it is impossible to calculate the internal forces by hand, a Scia Engineering model is applied. With this Scia model the forces in the cross-sections are calculated. The structure applied in the Scia model is given in Figure A-68. The structure and the load case is symmetrical, therefore the results are given for one foundation leg only. The definitions of the walls are also given and are indicated in Figure A-68 and Figure A-69.

1. Upper slab
2. Bottom slab
3. Front wall
4. Side inner Wall
5. Side outer Wall
6. Connecting beam
7. Inner wall

The maximum forces in these cross-sections are given in Table A-14. For each structural element figures are given for the bending moments, shear forces and axial forces.

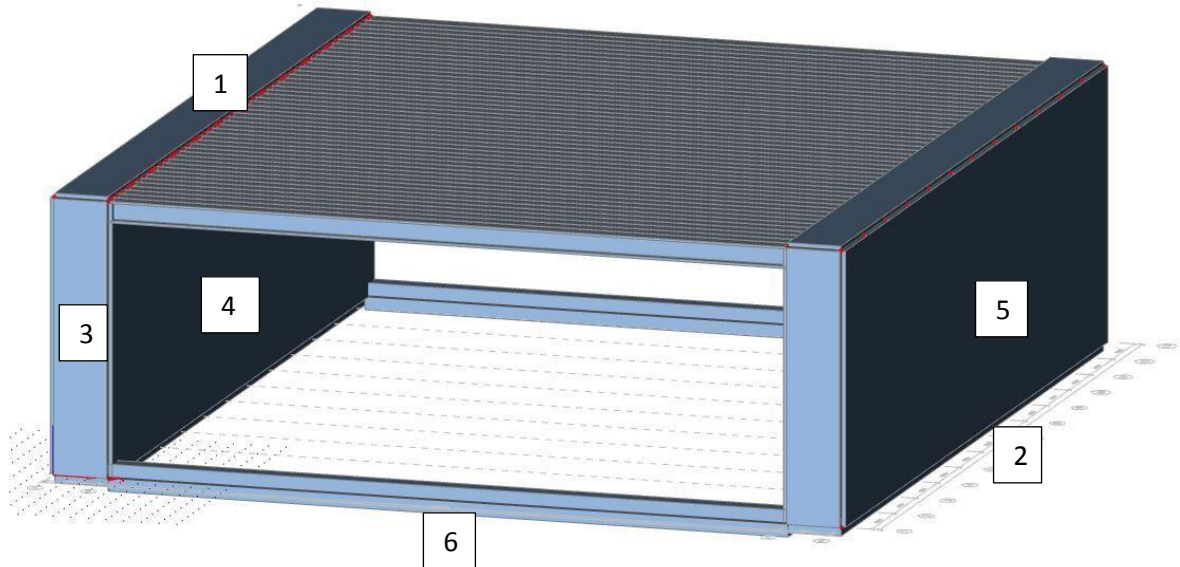


Figure A-68 - Immersion platform as Scia Engineering model

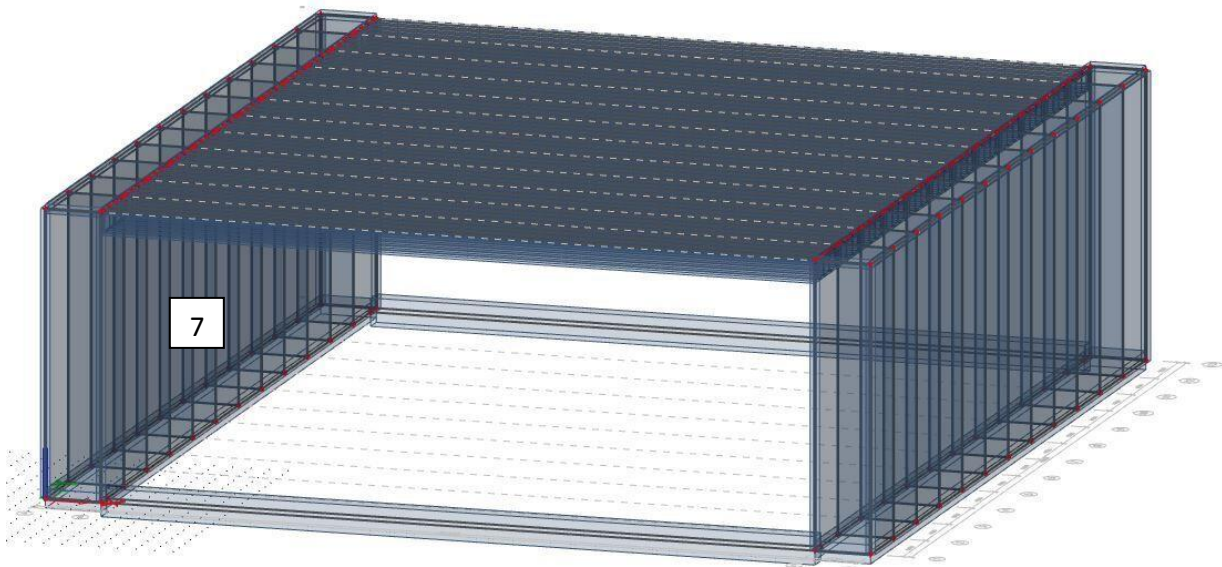


Figure A-69 - Immersion platform transparent view

To determine the thicknesses of the foundation elements first the forces on the structure are applied in a Scia Engineering model, see Figure A-70 for the hydrostatic forces on the foundation legs, Figure A-71 for the GBF load on the platform, Figure A-72 for the lifting mechanism on the foundation legs, Figure A-73 for the skidding beams and steel plate on the H-beams and Figure A-74 for a visual interpretation of the linear increase of pressure by depth.

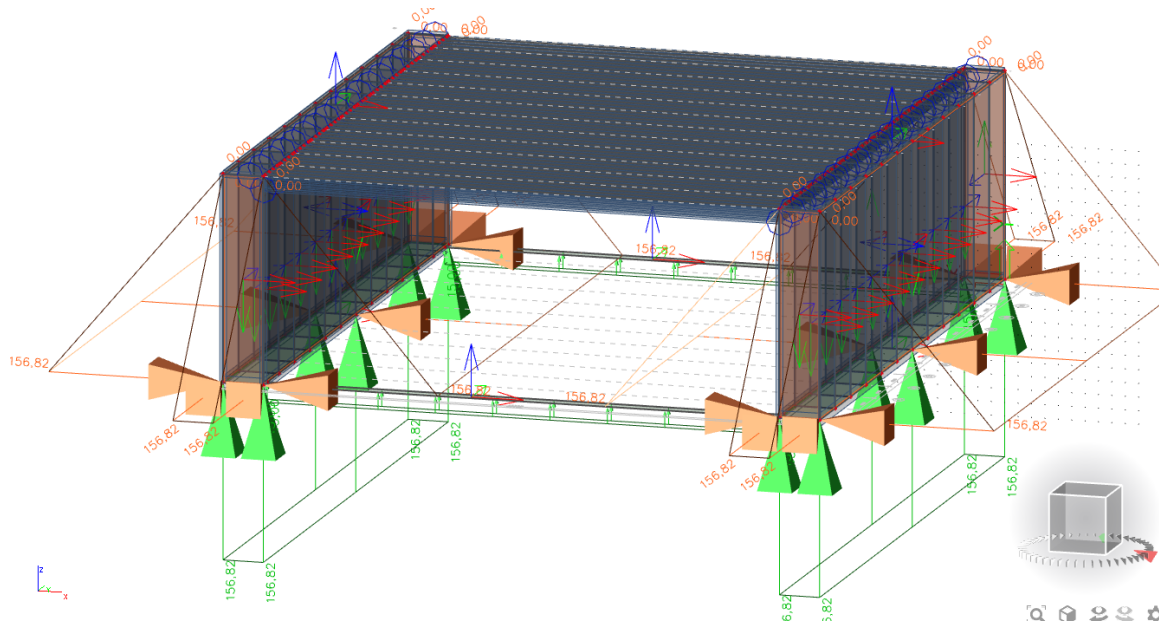


Figure A-70 – BG 2: Hydrostatic pressure on immersion structure

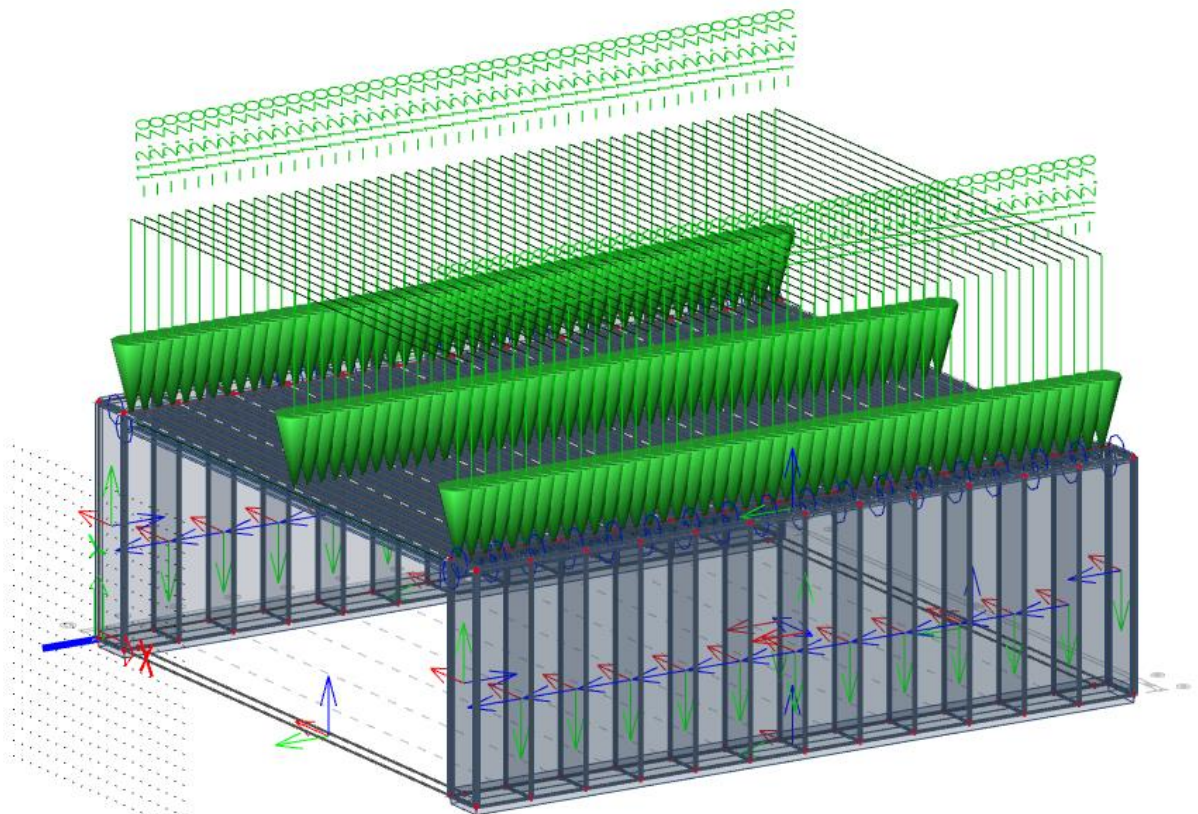


Figure A-71 – BG 3: GBF load on platform

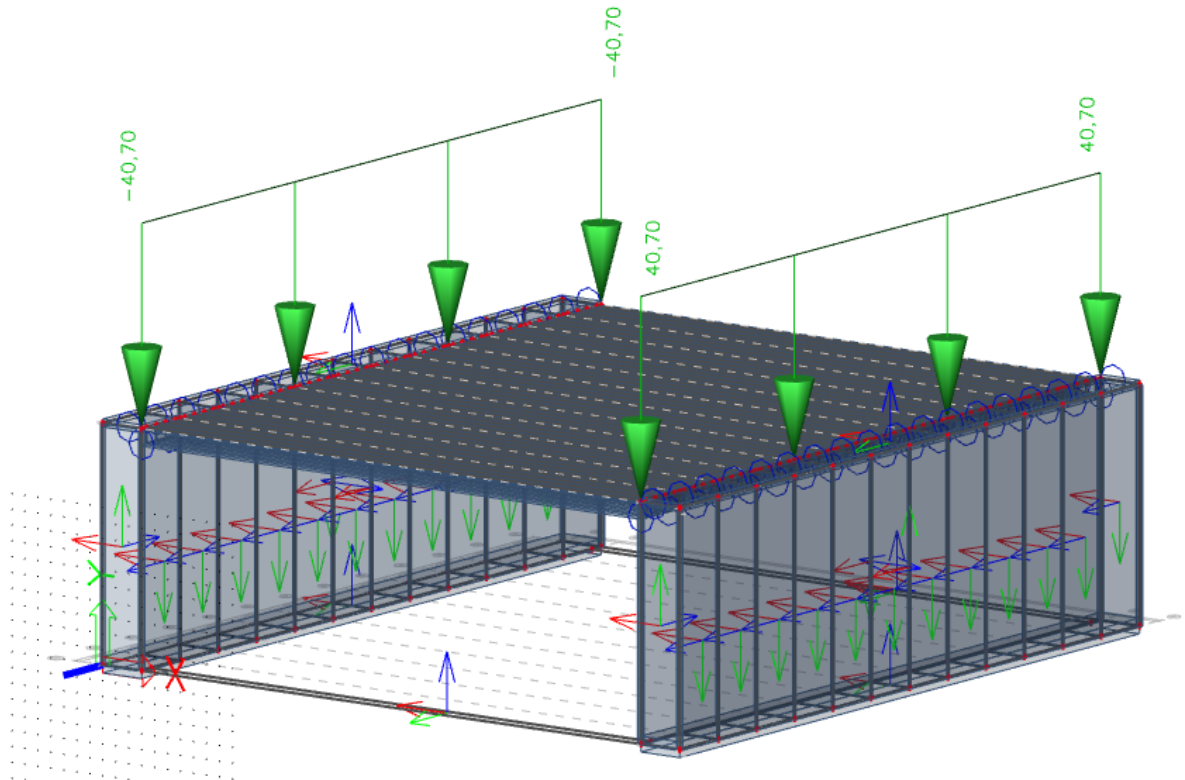


Figure A-72 – BG 4: Lifting mechanism on side inner walls

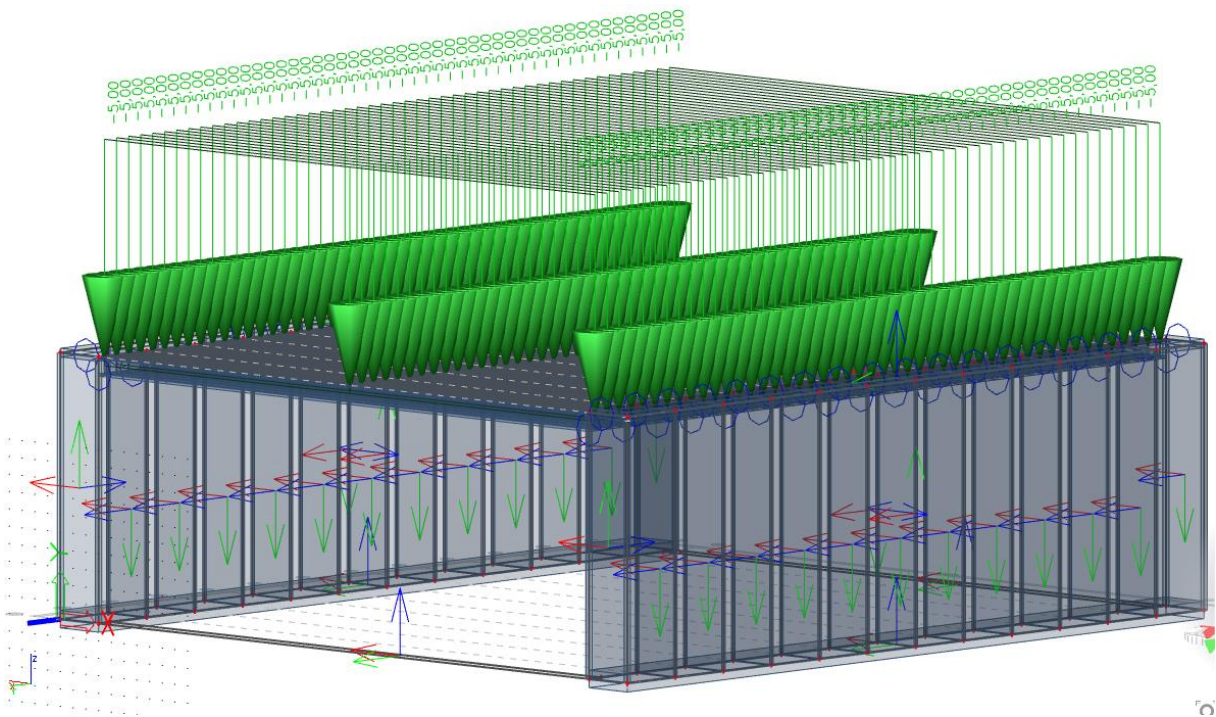


Figure A-73 - BG 5: Skidding beams and plate

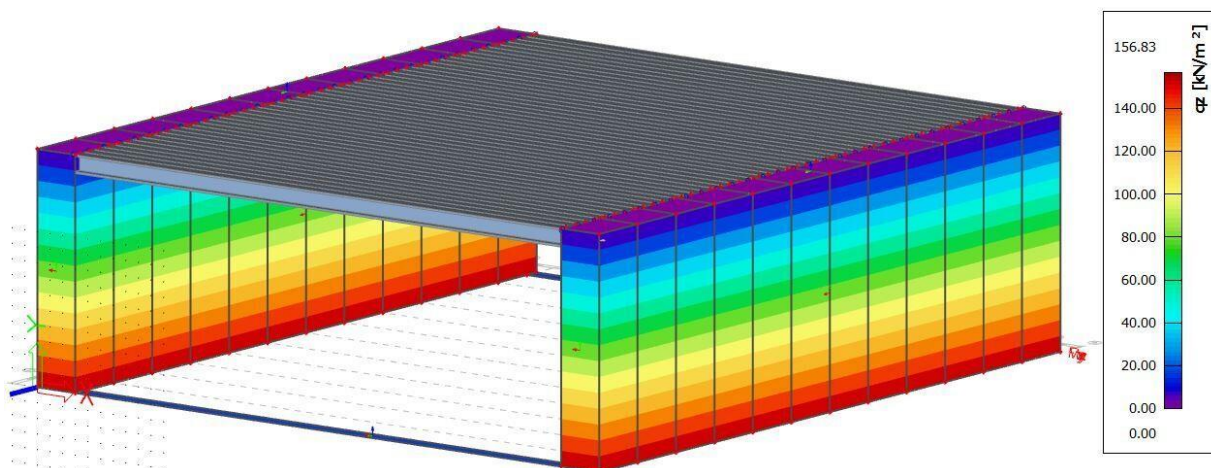


Figure A-74 - Values of hydrostatic pressure on immersion platform

The forces in the Scia Engineer software are implemented with the characteristic values, no partial factors are present. To apply partial factors the load combination is created as is seen in Figure A-75.

The following forces are adapted from the Scia results:

- $m_x$ : Bending moment in x-direction
- $m_y$ : Bending moment in y-direction
- $V_x$ : Shear force in x-direction
- $V_y$ : Shear force in y-direction
- $N_x$ : Axial force in x-direction
- $N_y$ : Axial force in y-direction

In the Scia software the orientations are implemented as shown in the figures. Each element has an orientation with a local x, y and z-axis and the global orientation of the model is given in the left lower corner.

#### J.4.1.6.1 Result of structural analysis side outer wall

The results for the side outer wall are shown in Figure A-78 till Figure A-83. The minimal and maximal values from these figures are used to determine the minimal thickness of the concrete elements. In Table A-14 the values of all elements are summarized.

To check the order of magnitude of the forces in the side outer wall a simple hand calculation is performed.

The hydrostatic forces act on the side outer wall and this wall is supported by the four rigid supports (walls) and the forces are transferred to the closest wall. This is shown in Figure A-76 where a section between two inner walls is taken.

The highest bending moments are expected at the cross section of the lines at 2 meter from the bottom slab. To estimate the bending moments the scheme in Figure A-77 is used.

At a water depth of 13.3 the forces of are:

$$q_{hydro} = \rho_w \cdot g \cdot \gamma_{Q,unfav} \cdot h = 200.5 \text{ kN/m}$$

This leads into the bending moment and shear forces:

$$M_1 = M_2 = \frac{1}{12} \cdot q_{hydro} \cdot l^2 = \frac{1}{12} \cdot 200.5 \cdot 4^2 = 267.3 \text{ kNm}$$

Naam	UGT-Set B (automatisch)
Omschrijving	
Type	EN-UGT (STR/GEO) Set B
Automatisch bijgewerkt	<input checked="" type="checkbox"/>
Constructie	Gebouw
Niet-lineaire combinatie	
Actieve coëfficiënten	<input checked="" type="checkbox"/>
<b>Inhoud van combinatie</b>	
BG1 - Self weight [-]	1,35
BG2 - Hydro [-]	1,50
BG3 - GBF [-]	1,10
BG4 - Lifting mechanism [-]	1,35
BG5 - Skid+plate [-]	1,00

Figure A-75 - Load combinations used in Scia

$$V_1 = V_2 = \frac{1}{2} \cdot q_{hydro} \cdot 4 = \frac{1}{2} \cdot 200.5 \cdot 4 = 401 \text{ kN}$$

Compare these values with Figure A-78 and Figure A-80 these values have the same order of magnitude.

The Scia model results for all other structural elements are included in paragraph J.6

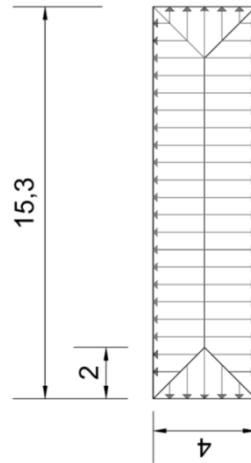


Figure A-76 - Load distribution side outer wall

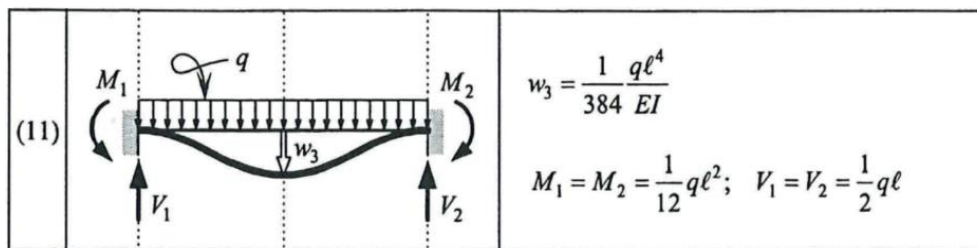


Figure A-77 - Bending moments at the supports for a fixed-fixed beam (Molenaar & Voorendt, 2018)

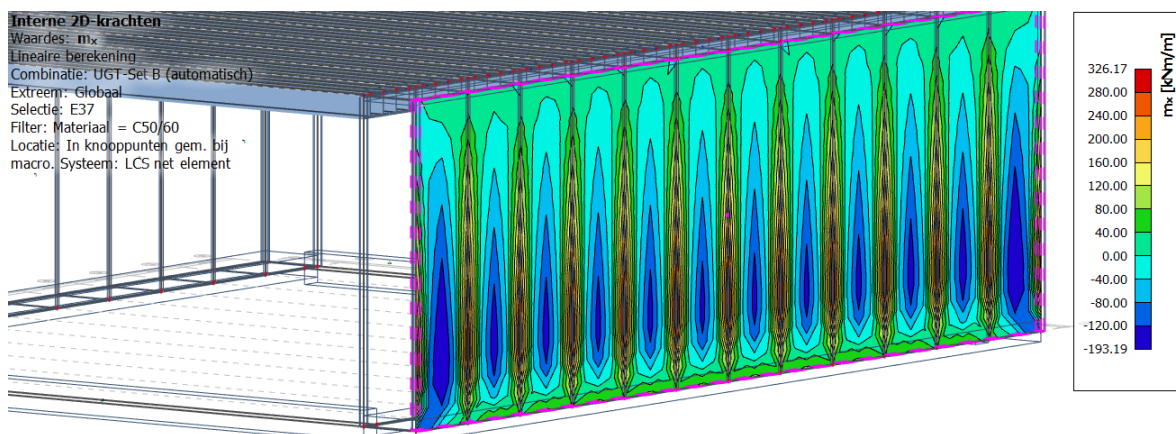


Figure A-78 - Result of bending moment in x-direction for side outer wall

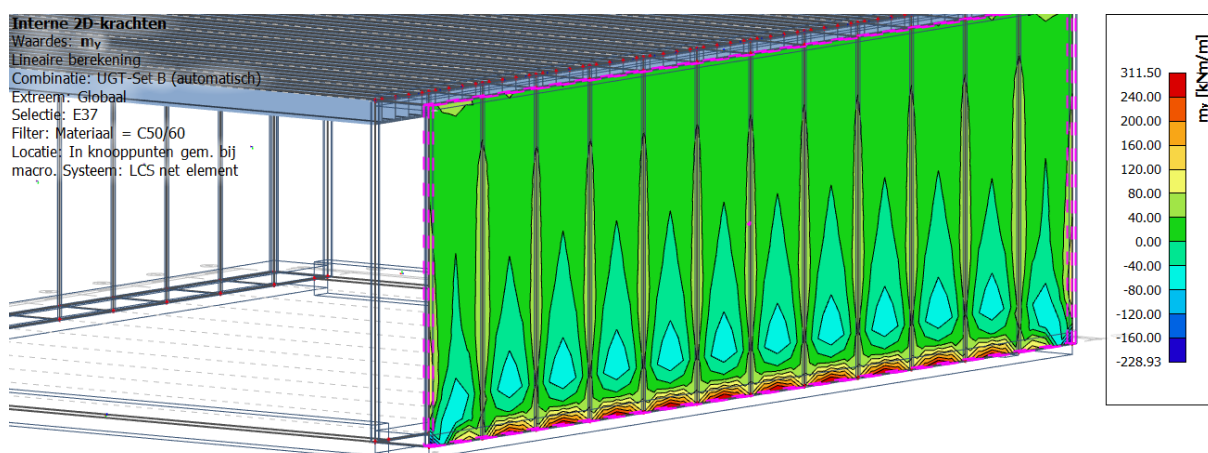


Figure A-79 - Result of bending moment in y-direction for side outer wall

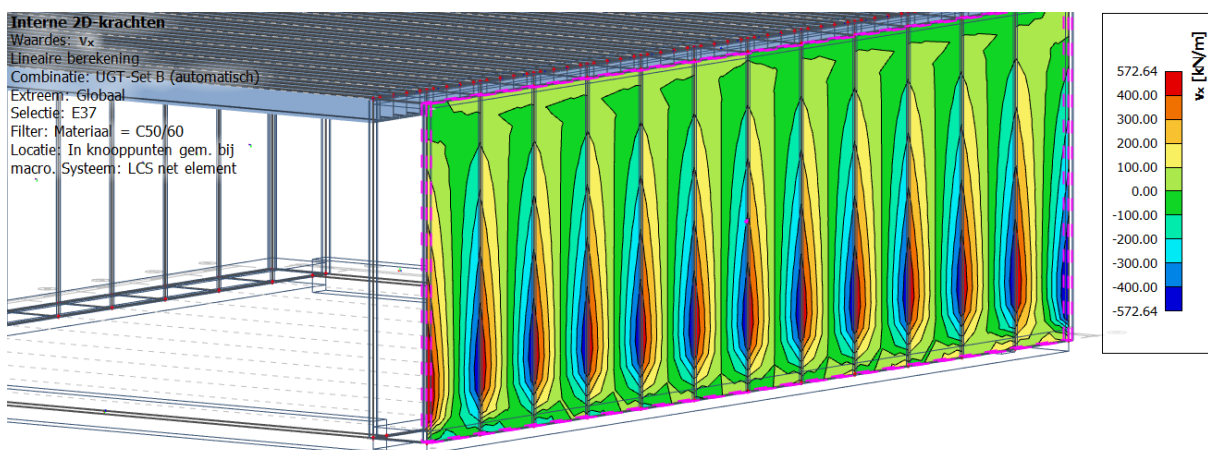


Figure A-80 - Result of shear force in x-direction for side outer wall

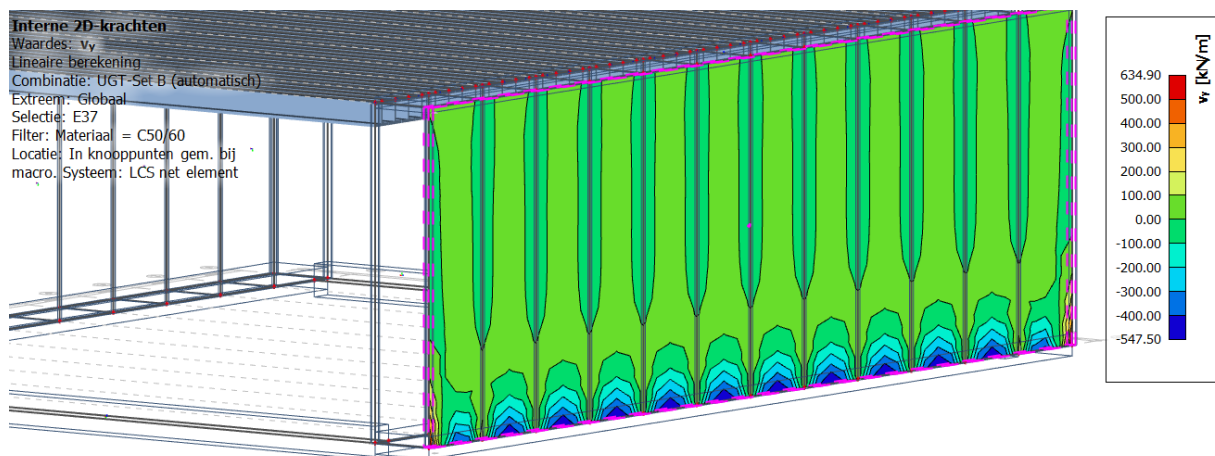


Figure A-81 - Result of shear force in  $y$ -direction for side outer wall

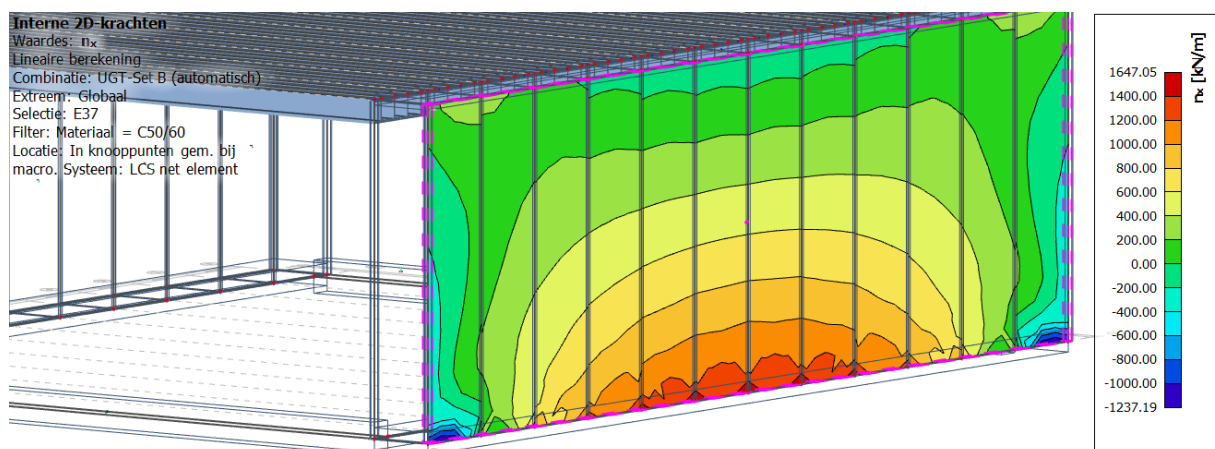


Figure A-82 - Result of axial force in  $x$ -direction for side outer wall

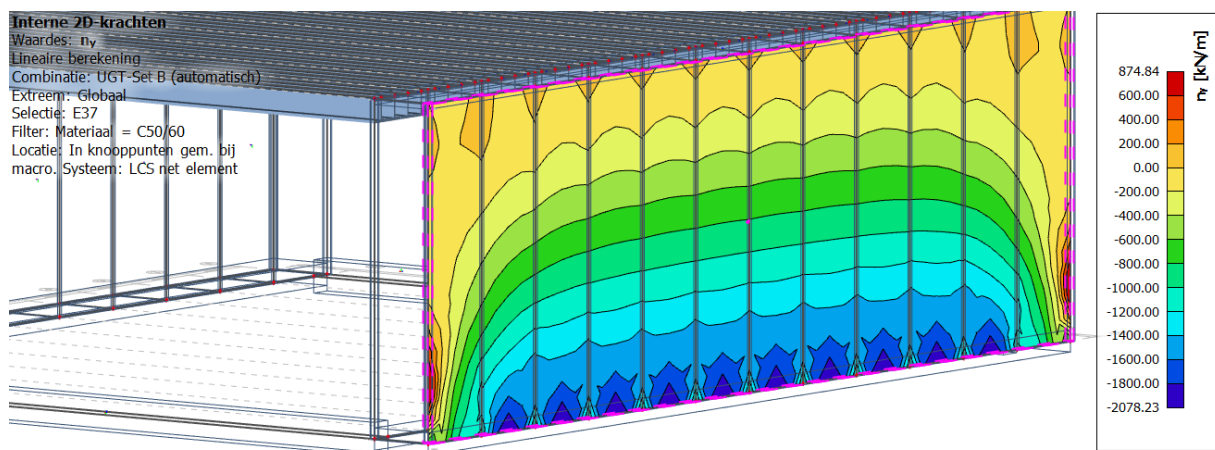


Figure A-83 - Result of axial force in  $y$ -direction for side outer wall

Element	$d_0$ [mm]	$m_x$ [kNm]		$m_y$ [kNm]		$V_x$ [kN]		$V_y$ [kN]		$N_x$ [kN]		$N_y$ [kN]	
		Min	Max	Min	Max	Min	Max	Min	Max	Min	Max	Min	Max
<b>1: Upper slab</b>	500	-99	+51	-118	+85	-151	+563	-616	+616	-1792	+1020	-1144	+442
<b>2: Bottom slab</b>	1000	-787	+16815	-581	+1345	-2068	+15552	-4679	+4679	-2818	+20512	-2237	+5167
<b>3: Front wall</b>	500	-28	+424	-115	+142	-810	+822	-484	+310	-6824	+2781	-8044	+7939
<b>4: Side inner wall</b>	500	-904	+393	-3995	+461	-2363	+2363	-8241	+3127	-4958	+1564	-17742	-958
<b>5: Side outer wall</b>	500	-193	+326	-228	+312	-573	+573	-548	+635	-1237	+1647	-2078	+875
<b>6: Connecting slab</b>	1500	-6209	+26530	-298	+2434	-15601	+15601	-1155	+131	+6337	+9277	-295	+840
<b>7: Inner wall</b>	300	-36	+36	-89	+89	-181	+181	-336	+336	-1127	+159	-2633	+97

Table A-14 - Result of internal forces of all structural elements

#### J.4.1.6.2 Calculation of minimal thickness of elements

In this paragraph the results on the side outer wall are used to determine the minimal thickness of this element. This calculation is performed for all elements of the immersion structure and the final results are displayed in Table A-16.

The element must fulfill requirements on three different internal forces: the bending moments, shear forces and axial forces. For all criteria must hold:

$$M_{Rd} \geq M_{Ed} \quad ; \quad V_{Rd} \geq V_{Ed} \quad ; \quad N_{Rd} \geq N_{Ed} \quad (104)$$

Where the subscripts holds:

$$\begin{aligned} R_d &= \text{Resistance capacity} \\ E_d &= \text{Design value} \end{aligned}$$

The calculation procedure is explained for these three cases.

#### Bending moment calculation

To determine the bending moment capacity a rule of thumb is used, see Figure A-84.

$$M_{Rd} = N_s \cdot z \quad (105)$$

Where:

$$z \approx 0.9 \cdot d_m \quad (106)$$

And:

$$N_s = f_{yd} \cdot A_{s,max} = f_{yd} \cdot d_m \cdot b \cdot \rho_{l,max} \quad (107)$$

With:

$$d_m = \text{Minimal height of element needed for resistance of bending moment [mm]}$$

To calculate the minimal height of an element these formulas can be rewritten in:

$$d_m = \sqrt{\frac{M_{Ed}}{\rho_{l,max} \cdot b \cdot f_{yd} \cdot 0.9}} \quad (108)$$

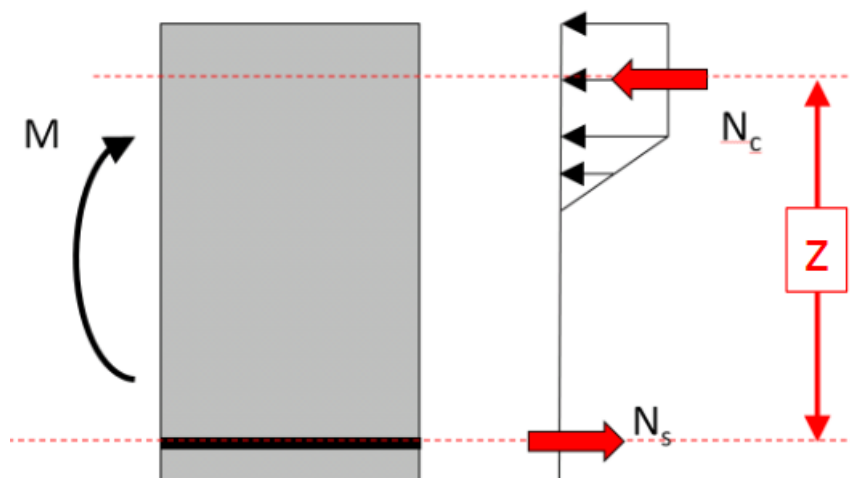


Figure A-84 - Forces on reinforcement concrete cross-section (Hordijk & Lagendijk, 2017)

### Shear force calculation

To calculate the shear force resistance the following formula is applied (Hordijk & Lagendijk, 2017):

$$V_{Rd,c} = \frac{0.18}{\gamma_c} \cdot k \cdot (100\rho_l f_{ck})^{\frac{1}{3}} b_w d \quad (109)$$

With a minimum value of:

$$V_{Rd,c} = v_{min} b_w d \quad (110)$$

In which:

$$v_{min} = 0.035 k^{\frac{3}{2}} \cdot f_{ck}^{\frac{1}{2}} \quad (111)$$

Where:

$$k = 1 + \sqrt{\frac{200}{d}} \quad (112)$$

When the minimal required shear force resistance cannot be reached, shear reinforcement can be applied, see Figure A-65. With a formula to calculate equilibrium in forces the minimal amount of reinforcement can be calculated:

$$V_{Rd,s} = \frac{A_{sw}}{s} \cdot z \cdot \cot(\theta) \cdot f_{ywd} \quad (113)$$

Rewriting this formula and assume  $V_{Rd,s} = V_{Ed}$  the minimal surface of reinforcing steel per length can be calculated with:

$$\frac{A_{sw}}{s} = \frac{V_{Ed}}{z \cdot \cot(\theta) \cdot f_{ywd}} \quad (114)$$

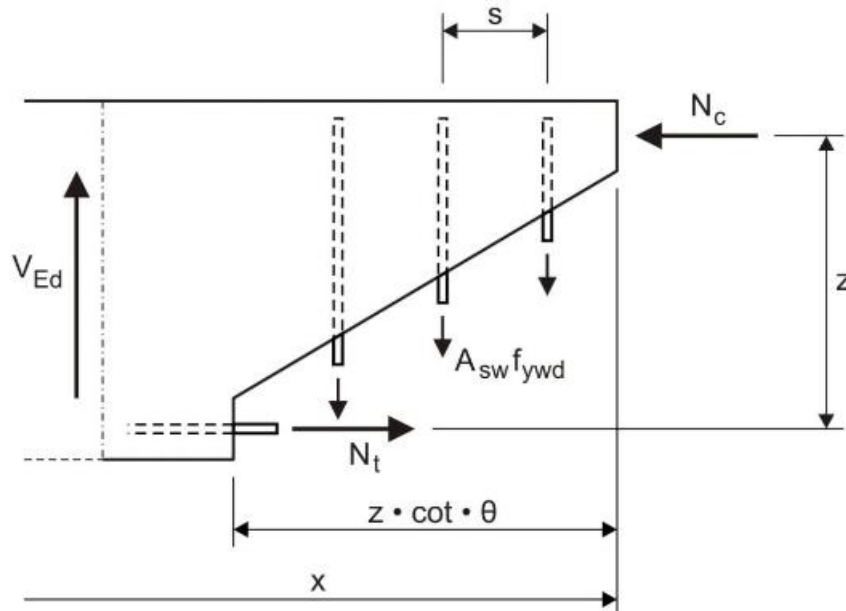


Figure A-85 - Principle of shear reinforcement (Hordijk & Lagendijk, 2017)

### Axial force calculation

For the axial force on the elements two situations are present:

- Axial tensioning force
- Axial compressive force

Concrete has a low tension capacity and a high compression capacity. Therefore steel is used to resist the tension forces. The low concrete capacity is therefore not implemented in the formula. To calculate the resistance to an axial tensioning force the following formula is applied:

$$N_{Rd} = A_{s,req,t} \cdot f_{yd} \quad (115)$$

By implementing  $N_{Rd} = N_{Ed}$  this can be rewritten in:

$$A_{s,req,t} = \frac{N_{Ed}}{f_{yd}} \quad (116)$$

Where:

$$A_{s,req,t} = \text{Minimal amount of reinforcement for tension force [mm}^2\text{]}$$

$$f_{yd} = \text{Design value reinforcing steel [N/mm}^2\text{]}$$

When a compressive force is present at a cross-section the capacity can be calculated with:

$$N_{Rd} = A_c \cdot f_{cd} + A_{s,req,t} \cdot f_{yd} + A_{s,req,c} \cdot f_{yd} \quad (117)$$

Where:

$$A_c = \text{Cross – sectional area concrete [mm}^2\text{]}$$

$$f_{cd} = \text{Compressive design strength concrete [N/mm}^2\text{]}$$

$$A_{s,req,c} = \text{Cross – sectional area of compressive steel reinforcement, if needed [mm}^2\text{]}$$

Because reinforcement is costly to apply the compressive strength of the concrete is used to fulfil the requirement to compressive force. This formula without the reinforcement is rewritten in:

$$A_c = \frac{N_{Rd}}{f_{cd}} \quad (118)$$

$$d_{nc} = \frac{N_{Rd}}{f_{cd} \cdot b} \quad (119)$$

The use of compressive reinforcement steel is rarely applied because the concrete has a large compressive capacity.

The calculation for the outer side wall of a foundation element is executed to show the calculation principle. The calculation is performed on all structural elements but only the procedure is explained on the side outer wall of the immersion platform.

#### J.4.1.6.3 Calculation of minimal thickness of the side outer wall element

In this paragraph the results on the side outer wall are used to determine the minimal thickness of this element. The results per meter width are shown in Table A-15.

Internal force upper slab	Lower bound value	Upper bound value
$m_x$ [kNm]	-193.19	+326.17
$m_y$ [kNm]	-228.93	+311.50
$V_x$ [kN]	-572.64	+572.64
$V_y$ [kN]	-547.50	+634.90
$N_x$ [kN]	-1237.19	+1647.05
$N_y$ [kN]	-2078.23	+874.84

Table A-15 - Maximum internal forces for side outer wall

The calculation procedure is given as follows:

1. Estimate initial thickness by bending moment capacity, use maximal reinforcement ratio.
2. Check the minimal thickness for the axial compressive capacity.
3. Calculate the amount of reinforcement for the axial tension capacity
4. The maximum reinforcement ratio is now exceeded, increase iteratively the thickness of the element till the reinforcement ratio equals the maximum.
5. Calculate the shear force capacity. Apply shear reinforcement if needed.
6. Check if all situations fulfill the requirements.

### 1: Bending moment calculation

$$d_m = \max\left(\sqrt{\frac{M_{Ed,X}}{\rho_{l,max} \cdot b \cdot f_{yd} \cdot 0.9}}, \sqrt{\frac{M_{Ed,Y}}{\rho_{l,max} \cdot b \cdot f_{yd} \cdot 0.9}}\right) = \max\left(\sqrt{\frac{326.17 \cdot 10^6}{0.0308 \cdot 1000 \cdot 435 \cdot 0.9}}, \sqrt{\frac{311.50 \cdot 10^6}{0.0308 \cdot 1000 \cdot 435 \cdot 0.9}}\right) = \max(136, 146) = 161 \text{ mm} \quad (120)$$

### 2: Axial compressive force calculation

$$d_{nc} = \frac{N_{Rd}}{b \cdot f_{cd}} = \frac{2078.23 \cdot 10^3}{1000 \cdot \frac{50}{1.5}} = 62 \text{ mm} \quad (121)$$

### 3: Axial tension force calculation

$$A_{s,req,t} = \frac{N_{Ed}}{f_{yd}} = \frac{1647.05 \cdot 10^3}{435} = 3786 \text{ mm}^2 \quad (122)$$

$$\rho_l = \rho_{lm} + \frac{A_{s,req,t}}{b \cdot d} = 0.0308 + \frac{3786}{1000 \cdot 161} = 0.0543 [-] \quad (123)$$

### 4: Iterative procedure to satisfy maximum reinforcement ratio.

The iterative procedure is executed with Excel where the input is the thickness of the concrete element and where the output is the maximum resistance and the reinforcement ratio. The procedure is executed till both criteria are satisfied. The result is a minimum thickness of 237 mm.

### 5: Calculate the shear force capacity. Apply shear reinforcement if necessary.

Now the calculation for shear resistance capacity of the slab is calculated.

$$V_{Rd,c} = \frac{0.18}{\gamma_c} \cdot k \cdot (100 \rho_l f_{ck})^{\frac{1}{3}} b_w t_v \quad (124)$$

First the k value is calculated:

$$k = \min\left(1 + \sqrt{\frac{200}{d}}, 2.0\right) = \min\left(1 + \sqrt{\frac{200}{237}}, 2.0\right) = 1.92 \quad (125)$$

The minimum value now can be calculated:

$$v_{min} = 0.035 k^{\frac{3}{2}} \cdot f_{ck}^{\frac{1}{2}} = 0.035 \cdot 1.92^{\frac{3}{2}} \cdot 50^{\frac{1}{2}} = 0.66 \frac{N}{\text{mm}^2} \quad (126)$$

With a minimum value for the capacity of the cross-section of:

$$V_{Rd,c,min} = v_{min} b_w d = 0.66 \cdot 1000 \cdot 237 = 156 \text{ kN} \quad (127)$$

Now all factors are known the maximum capacity is calculated:

$$V_{Rd,c} = \frac{0.18}{\gamma_c} \cdot k \cdot (100 \rho_l f_{ck})^{\frac{1}{3}} b_w d = \frac{0.18}{1.5} \cdot 1.92 \cdot (100 \cdot 0.0308 \cdot 50)^{\frac{1}{3}} \cdot 1000 \cdot 237 = 293 \text{ kN} \quad (128)$$

The shear force on the cross-section is too high to resist without shear reinforcement. Therefore the minimal amount of shear reinforcement is calculated:

$$\frac{A_{sw}}{s} = \frac{V_{Ed}}{z \cdot \cot(\theta) \cdot f_{ywd}} = \frac{634.90 \cdot 10^3}{0.9 \cdot 237 \cdot \cot(30) \cdot \frac{500}{1.15}} = 3.95 \frac{mm^2}{mm} \quad (129)$$

## 6: Check all situations

Check the three main requirements:

$$M_{Rd} \geq M_{Ed} \quad ; \quad V_{Rd} \geq V_{Ed} \quad ; \quad N_{Rd,t} \geq N_{Ed,t} \quad ; \quad N_{Rd,c} \geq N_{Ed,c} \quad (130)$$

$$326 \geq 326 \quad ; \quad 635 \geq 635 \quad ; \quad 1647 \geq 1647 \quad ; \quad 7900 \geq 2078 \quad (131)$$

### Conclusion:

The minimal thickness of the side outer wall is 237 mm. This is in the static situation. Due to the requirements of transporting and floating the forces are dynamically and the minimal thickness could be larger.

#### J.4.1.6.4 Design thickness of structural elements

The calculation as performed in the previous paragraph is repeated for all elements. In Table A-16 the thicknesses of the structural elements are shown. A note is made to the choice of the thickness of the side outer wall, this thickness is adapted to the side inner wall. Due to the requirement of floating it is preferable to design the foundation symmetrical.

Element	$d_0$ [mm]	$d_{min}$ [mm]
1: Upper slab	500	144
2: Bottom slab	500	2174
3: Front wall	500	648
4: Side inner wall	500	637
5: Side outer wall	500	237
6: Connecting slab	1000	1870
7: Inner wall	300	92

Table A-16 - Minimal thicknesses due to the internal forces at one location

The structural element thickness is chosen by calculating the minimal thickness for the case that all extremes are at one cross-section. In most cases this is unrealistic. Therefore this is the most conservative estimation of the concrete thicknesses. An example from the base slab of the immersion structure foundation is given in Figure A-86.

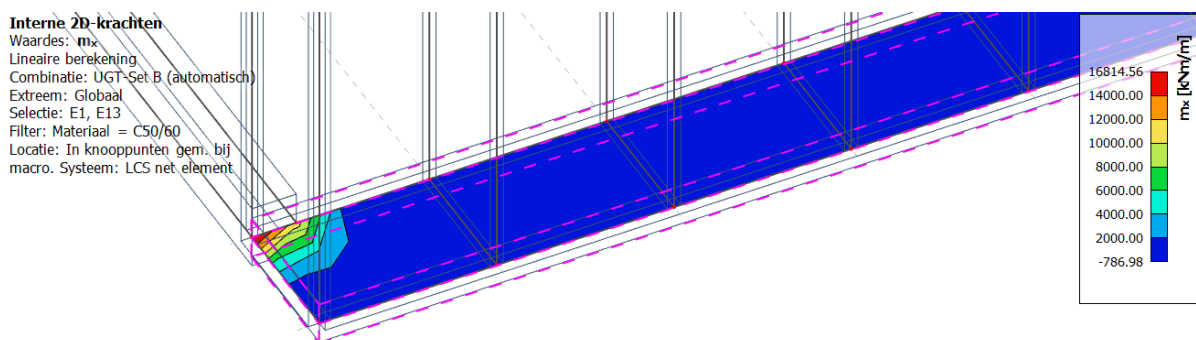


Figure A-86 - Bending moment in x-direction for bottom slab

When the internal forces from a couple of meters from the connecting slab just a minimal thickness is needed of 455mm. Therefore a (conservative) estimation of the mean concrete thickness of 1.25 meter is done on the concrete bottom slab. Therefore in the design of the concrete thicknesses of the foundation legs a large optimization can be performed to reduce weight and material usage. This adaptation is applied on the most concrete elements, per element a short explanation is given:

- Upper slab: A minimum of 150 mm is used because of the constructability and minimal thickness.
- Front wall: Thickness is set on 650 mm because the extremes are not fixed in one location.

- Side inner wall: Thickness is changed to a mean thickness 500 mm. The minimal thickness at the main part of the side walls is 185mm but due to the placement of a lifting system local point loads could be implemented and therefore a mean thickness of 500 mm is chosen. When the lifting mechanism can be placed on the side inner wall this reduce the bending moments in other structural elements.
- Side outer wall: The thickness is changed to 500 mm due to the symmetry of the foundation leg, otherwise this thickness could be more decreased.
- Connecting slab: Comment made after showing Table A-17.
- Inner wall: Thickness is set on 150 mm because of minimal thickness for constructability.

The assumed mean thicknesses are shown in Table A-17.

Element	$d_0$ [mm]	$d_{min}$ [mm]	$d_{mean}$ [mm]
<b>1: Upper slab</b>	500	144	150
<b>2: Bottom slab</b>	500	2174	1250
<b>3: Front wall</b>	500	648	650
<b>4: Side inner wall</b>	500	637	500
<b>5: Side outer wall</b>	500	237	500
<b>6: Connecting slab</b>	1000	1870	H-beam
<b>7: Inner wall</b>	300	92	150

Table A-17 - Estimated mean thickness of structural elements

With this calculation only a static analysis is done and a dynamic analysis must be performed for the transporting phase of the immersion structure. The outer dimensions of the GBF from the reference designs have a thickness of 500mm. Therefore it can be assumed that the thicknesses, except for the upper slab, with a mean thickness of 500 are realistic.

A problem arises with the connection beam. This beam has a too large height. When the platform is lowered to the bottom a sill is present which the connecting beam is. Two possibilities to solve this problem are given:

- 3: Due to optimizations in the design the thickness could be reduced. The largest forces are present at the connection from the connecting slab and the side inner wall. An extensive analysis on this point is needed to reduce the concrete thickness.
- 4: The connecting beam could be replaced by a steel beam. When the identical beam as for the platform is used the beam can resist the forces. This beam has a height of 1.1 meter which is much lower. The steel stress according the Von Mises criteria is  $214 \text{ N/mm}^2$ , by applying the maximum shear force and bending moment at one location. See paragraph J.4.1.1 for the steel properties and explanation about the Von Mises criterion.

The second option is chosen to work out for the construction of the immersion platform.

#### J.4.1.7 Stability

To check the stability of the immersion structure during the transportation and operational phase there are two checks performed:

1. Static stability during transport
2. Stability on subsoil during operational phase

The immersion structure must be stable on the subsoil. An important requirement is that the foundation is placed on the subsoil without the using of piling. Therefore it is chosen to design the foundation with a large contact area on the subsoil. The principle of the calculation is similar to the calculation of the stability of the GBFs. The calculation is performed in this paragraph for the immersion structure. Besides the requirement on

stability also the stability in the floating phase is important. Therefore the most important parameters of the foundation of the immersion structure are:

- Shear capacity
- Bearing capacity
- Rotational stability
- Metacentric height

These stability criteria depend on several design parameters. The width of the foundation leg is chosen as parameter to design the most optimal foundation for the immersion platform. In the calculation which is performed in the next paragraphs a foundation leg width of 3 meters is assumed, the same width as in the applied Scia model.

For the load conditions at the calculation of the stability parameters the favorable weight of the immersion structure is the lowest possible, only the selfweight of the structure with the partial load factor and the unfavorable weight is the highest weight possible, with the placed GBF on it and the unfavorable load factor.

#### J.4.1.7.1 Weight

The weight of the foundation is calculated by adding the volume of concrete for all structural elements. Multiplying the volume with the volumetric weight of concrete the mass of the foundation legs is calculated. At last the platform weight is added to the foundation weight and the total mass is known:

$$V_{leg} = V_{Upper\ slab} + 2 \cdot V_{Side\ wall} + V_{front,back\ wall} + V_{Bottom\ slab} + V_{Inner\ walls} \quad (132)$$

$$V_{leg} = 21.2 + 2 \cdot 653.3 + 36.1 + 176.3 + 45.9 = 932.7 \text{ m}^3 \quad (133)$$

$$W_{leg} = V_{leg} \cdot \gamma_c = 932.7 \cdot 23.54 = 21,956 \text{ kN} \quad (134)$$

$$W_{tot} = 2 \cdot W_{leg} + W_{plat} + W_{lift} = 2 \cdot 21,956 + 48,858 + 3,826 = 96,596 \text{ kN} \quad (135)$$

The weight of the GBF is added to calculate the maximum weight. The Eurocode factors for weight are included in the next paragraphs.

$$W_{max} = W_{tot} + W_{GBF} = 96,596 + 102,960 = 199,556 \text{ kN} \quad (136)$$

#### J.4.1.7.2 Static floating stability

The immersion structure has two foundation legs, a platform and two connecting beams. To reduce weight and decrease the draught it is assumed that four of the 47 H-beams of the immersion platform are installed during the transportation phase. The check for stability is done with a calculation procedure similar with the GBF floating stability in Chapter 5 and 6. First the draught is calculated where after the static stability by calculating the metacentric height is performed.

$$W_{tot,float} = 2 \cdot W_{leg} + \frac{4}{47} \cdot W_{plat} + W_{lift} = 51,896 \text{ kN} \quad (137)$$

The draught of a foundation leg is given according next formula:

$$2 \cdot (b_{leg} \cdot l_{leg} \cdot d) \cdot \rho_w = W_{tot,float} \quad (138)$$

$$d = \frac{W_{Leg}}{\rho_w \cdot A_{Leg}} = \frac{51896}{2 \cdot 10.05 \cdot 47 \cdot 3} = 18.31 \text{ m} \quad (139)$$

Where:

$$b_{leg} = \text{Width of foundation leg [m]}$$

$$l_{leg} = \text{Length of foundation leg [m]}$$

$$d = \text{Draught [m]}$$

The draught is 18.31 meter.

The GBF have to be stable in the floating phase. To ensure stability the metacentric height has to be minimal 0.5 meter (Voorendt, Molenaar, & Bezuyen, 2016). To determine the metacentric height Figure A-87 and following formula are used: (Voorendt, Molenaar, & Bezuyen, 2016)

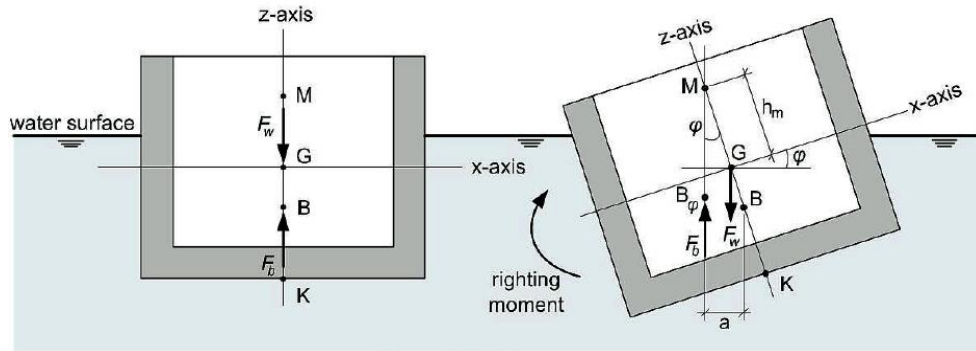


Figure A-87 – Stability of a floating element

$$h_m = \overline{KB} + \overline{BM} - \overline{KG} \quad (140)$$

Where:

$\overline{KB}$  = Distance of centre of buoyancy and bottom element [m]

$\overline{BM}$  = Distance centre of buoyancy and metacentre [m]

$\overline{KG}$  = Distance between bottom element and centre of gravity [m]

To calculate the distances the following formulas are used:

$$\overline{KB} = \frac{1}{2}d \quad (141)$$

With a draught of 18.31 meter the distance KB equals 9.16 meter.

$$\overline{BM} = \frac{I_{yy}}{V_{dw}} \quad (142)$$

Where:

$I_{yy}$  = Area moment of inertia[m<sup>4</sup>]

$V_{dw}$  = Volume of immersed part of element [m<sup>3</sup>]

The area moment of inertia of a rectangular geometry with help of the rule of Steiner is computed. The minimal moment of inertia is calculated, the floating platform is determined in x and y direction with the formula:

$$I = \min(I_{yy}, I_{xx}) = \min\left(2 \cdot \left(\frac{1}{12} \cdot l_{leg}^3 \cdot b_{leg}\right), 2 \cdot \left(\frac{1}{12} \cdot b_{leg}^3 \cdot l_{leb} + b_{leg} \cdot l_{leg} \cdot (l_{span} + b_{leg})^2\right)\right) \quad (143)$$

$$I_{yy} = \min\left(2 \cdot \left(\frac{1}{12} \cdot 47^3 \cdot 3\right), 2 \cdot \left(\frac{1}{12} \cdot 3^3 \cdot 47 + 3 \cdot 47 \cdot (38.5 + 3)^2\right)\right) = \min(51912, 485886)$$

The volume of the immersed part is:

$$V_{dw} = 2 \cdot b_{leg} \cdot l_{leg} \cdot d \quad (144)$$

This results in:

$$\overline{BM} = \frac{51912}{5163.76} = 10.05 \text{ m} \quad (145)$$

To calculate the distance between the bottom of the element and the centre of gravity the following formula is applied:

$$\overline{KG} = \frac{\sum(V_i \cdot e_i \cdot \gamma_i)}{\sum(V_i \cdot \gamma_i)} \quad (146)$$

Where:

$V_i$  = Volume of element  $i$  [ $m^3$ ]

$e_i$  = Distance between centre of gravity of element  $i$  and reference level [ $m$ ]

$\gamma_i$  = Volumetric weight of element  $i$  [ $kN/m^3$ ]

The factors are determined of each element and are displayed in Table A-18.

		$V_i [m^3]$	$e_i [m]$	$\gamma_i \left[ \frac{kN}{m^3} \right]$	$V_i \cdot e_i \cdot \gamma_i$	$V_i \cdot \gamma_i$
<b><math>i = 1</math></b>	Upper slab	42.3	15.225	23.54	15160.17	995.74
<b><math>i = 2</math></b>	Side walls	1306.6	7.65	23.54	235196.60	30744.65
<b><math>i = 3</math></b>	Front + Back wall	72.28	7.65	23.54	13016.25	1701.47
<b><math>i = 4</math></b>	Inner walls	91.74	7.65	23.54	16520.63	2159.56
<b><math>i = 5</math></b>	Bottom slab	352.5	0.625	23.54	5186.16	8297.85
<b><math>i = 6</math></b>	Platform	54.33	14.75	76.52	61322.80	4157.33
<b><math>i = 7</math></b>	Lifting mechanism	50.00	15.3	76.52	58537.80	3826.00
				$\Sigma$	404940.41	51882.61

Table A-18 - Factors used to calculate the distance  $KG$

The result is a distance of:

$$\overline{KG} = \frac{404,940.41}{51882.61} = 7.80 \text{ m} \quad (147)$$

All distances are known and the metacentric height can be calculated:

$$h_m = 9.16 + 10.05 - 7.80 = 11.41 \text{ m} \quad (148)$$

Because the metacentric height is larger than 0.5 the immersion structure is statically stable. The draught and the metacentric height as function of the foundation leg width are displayed in Figure A-88. The metacentric height is not a problem for the static stability. Due to the large BM-factor caused by the long distance between the legs the structure is very stable. To design the structure with a maximum draught of 10 meters the foundation legs must be around 8 meters width. Now the stability on the soil is determined and with these two requirements the final foundation leg width must be determined.

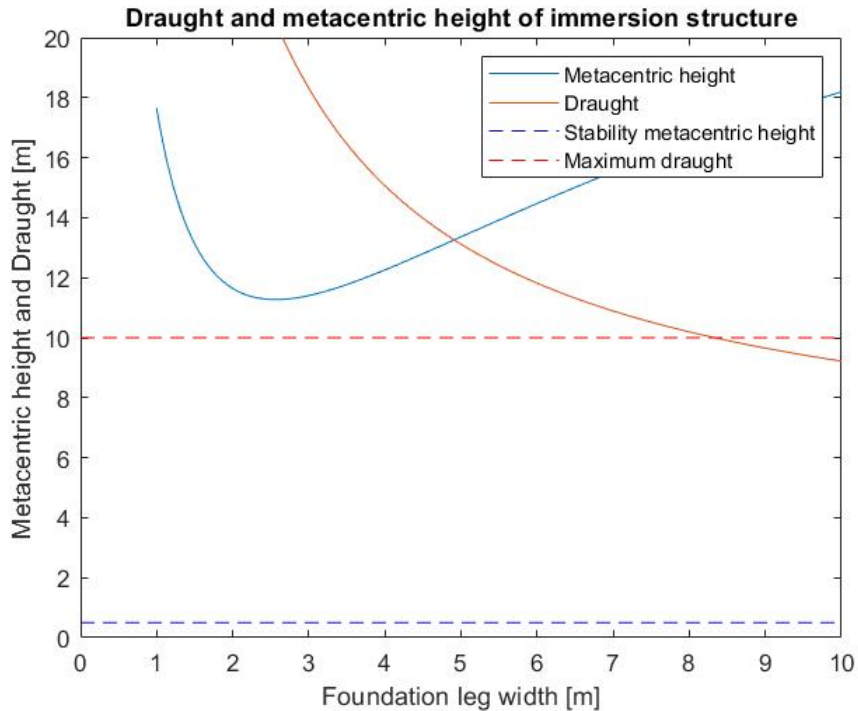


Figure A-88 - Draught and metacentric height as function of foundation leg width

The stability on the subsoil is calculated, in this check it is assumed that the immersion structure immerse with the help of ballasting water till a height at mean sea level.

#### J.4.1.7.3 Shear capacity

The sliding of the GBF on the immersion platform generates shear forces between the immersion platform and the subsoil. The subsoil has to resist these shear force. The resistance capacity of the subsoil is given as:

$$\tau_{max} = f_f \cdot \sigma'_n \quad (149)$$

Where:

$f_f =$  Coefficient of friction[-] =  $\tan(\delta)$

$\delta =$  Angle of friction between concrete and sand [°]

$\sigma'_n =$  Effective normal stress under the foundation [ $kN/m^2$ ]

The coefficient between sand and concrete is usually between 40 and 50 degree. In this calculation the lower bound of 40 degrees is applied. The maximum design value of the horizontal shear stress, caused by transporting the GBF on the platform is calculated with:

$$\tau_d = \frac{\sum H_{unfav}}{A} = \frac{1.5 \cdot 4044}{282} = 21.5 \frac{N}{mm^2}$$

In the calculation of the effective normal stress is the partial factor for favourable weight applied: ( $\gamma_{G,fav} = 1.0$ ). The total weight of the immersion platform is used and the buoyancy force is subtracted from the weight to calculate the effective normal stress. The Unity check is given as:

$$UC = \frac{\tau_d}{\tau_{max}/\gamma_{R,h}} \quad (150)$$

Where:

$$\begin{aligned}\tau_d &= \text{Design value shear stress [N/m}^2\text{]} \\ \tau_{max} &= \text{Maximum shear capacity subsoil [N/m}^2\text{]} \\ \gamma_{R,h} &= \text{Eurocode partial factor sliding (= 1.1)[-]}\end{aligned}$$

Because a large weight is present and a relatively low horizontal force

a small unity check as calculated was expected.

Parameter	Value	Unit
$f_f$	0.84	[-]
$\sigma_n'$	251.5	[kN/m <sup>2</sup> ]
$\tau_{max}$	211.3	[kN/m <sup>2</sup> ]
$\tau_d$	21.5	[kN/m <sup>2</sup> ]
<b>UC</b>	0.11	[-]

Table A-19 - Result of shear capacity calculation

#### J.4.1.7.4 Bearing capacity

The bearing capacity of the subsoil can be determined with the Brinch-Hansen formula. The formula to determine the bearing capacity is as follows:

$$p'_{max} = c'N_c S_c i_c + \sigma'_q N_q s_q i_q + 0,5\gamma' B_{eff} N_\gamma s_\gamma i_\gamma \quad (151)$$

The subscript  $q$  is for surcharge on the sea bottom and because next to the GBF no extra surcharge is present these factor is equal to zero. The subscript  $c$  refers to the cohesion in the soil, because gravel and sand is present, both with a cohesion of zero, these factors also can be neglected. Therefore the Brinch-Hansen formula is reduced to:

$$p'_{max} = 0,5\gamma' B_{eff} N_\gamma s_\gamma i_\gamma \quad (152)$$

Where:

$$\begin{aligned}\gamma' &= \text{Effective volumetric weight of soil under foundation [kN/m}^3\text{]} \\ B_{eff} &= \text{Effective width of foundation area [m]} \\ N_\gamma &= \text{Bearing capacity factor [-]} \\ s_\gamma &= \text{Shape factor [-]} \\ i_\gamma &= \text{Inclination factor [-]}\end{aligned}$$

The bearing capacity factors are given as:

$$N_\gamma = (N_q - 1) \tan(1.32\varphi') \quad (153)$$

Where:

$$N_q = \frac{1+\sin(\varphi')}{1-\sin(\varphi')} \cdot e^{\pi \tan(\varphi')} \quad (154)$$

$$\varphi' = \text{Angle of internal friction [}^\circ\text{]}$$

The shape factor is given as:

$$s_\gamma = 1 - 0.3 \frac{B_{eff}}{L_{eff}} \quad (155)$$

Where:

$$L_{eff} = \text{Effective length of foundation area [m]}$$

Because the foundation is rectangular the effective width can be calculated with:

$$b_{eff} = b - 2e \quad (156)$$

Where:

$$\begin{aligned}B_{eff} &= \text{Effective width of foundation area [m]} \\ b &= \text{Width of foundation [m]} \\ e &= \text{Eccentricity [m]}\end{aligned}$$

At last the inclination factor is given:

$$i_{\gamma} = \left(1 - \frac{\Sigma H_{unfav}}{V_{unfav} + A_{eff} c' \cdot \cot(\varphi')}\right)^3 \quad (157)$$

Applying sand and gravel the cohesion is zero and the formula for the inclination factor is reduced to:

$$i_{\gamma} = \left(1 - \frac{\Sigma H_{unfav}}{\Sigma V_{fav}}\right)^3 \quad (158)$$

Where:

$$H_t = \text{Total characteristic horizontal force on foundation [N]}$$

$$\Sigma V_{fav} = \text{Total vertical force on foundation with favorable partial factor [N]}$$

Now all factors are known the maximum characteristic bearing capacity can be calculated:

$$p'_{max} = 0,5\gamma' B_{eff} N_{\gamma} s_{\gamma} i_{\gamma} \quad (159)$$

After calculating the characteristic value of the bearing capacity the maximum pressure of the GBF is calculated. The maximum vertical bearing capacity may not be exceeded. Therefore the maximum vertical stress is calculated at the edge of the immersion structure, where the maximum stress is present. This can be done with the following formula:

$$\sigma'_{is,max} = \frac{\Sigma V_{unfav}}{A} + \frac{\Sigma M}{W_{bs}} \quad (160)$$

Where:

$$\sigma_{is,max} = \text{Maximum pressure of immersion structure on subsoil [kN/m}^2\text{]}$$

$$A = \text{Area of base slab [m}^2\text{]}$$

$$\Sigma V = \text{Sum of all effective vertical forces design value [kN]}$$

$$\Sigma M = \text{Sum of all moments [kNm]}$$

$$W_{bs} = \text{Moment of resistance of base slab [m}^3\text{]}$$

Symbol	Value	Unit	Symbol	Value	Unit	Symbol	Value	Unit
<b>A</b>	282	[m <sup>2</sup> ]	<b>i<sub>γ</sub></b>	0.93	[-]	<b>s<sub>γ</sub></b>	0.98	[-]
<b>A<sub>eff</sub></b>	278.82	[m <sup>2</sup> ]	<b>L<sub>eff</sub></b>	46.47	[m]	<b>ΣV<sub>unfav</sub></b>	288310	[kN]
<b>B<sub>eff</sub></b>	3	[m]	<b>N<sub>q</sub></b>	37.75	[-]	<b>W<sub>bs</sub></b>	2209	[m <sup>3</sup> ]
<b>c'</b>	0	[kPa]	<b>N<sub>γ</sub></b>	40.14	[-]	<b>γ'</b>	13.5	[kN/m <sup>3</sup> ]
<b>e</b>	0.26	[m]	<b>σ'<sub>is,max</sub></b>	1065	[kN/m <sup>2</sup> ]	<b>φ'</b>	36	[°]
<b>ΣH<sub>unfav</sub></b>	6066	[kN]	<b>p'<sub>max</sub></b>	743	[kN/m <sup>2</sup> ]	<b>ΣM</b>	94517	[kNm]

Table A-20 - Values used to calculate bearing capacity of subsoil

The unity check is as follows:

$$UC = \frac{\sigma'_{plat,max}}{p'_{max}/\gamma_{R;\gamma}} \leq 1 \quad (161)$$

Where:

$$p'_{max} = \text{Maximum bearing capacity subsoil [N/m}^2\text{]}$$

$$\gamma_{R;\gamma} = \text{Eurocode partial factor on bearing capacity (= 1.4)[-]}$$

Applying all values the result is a unity check of 1.77. This unity check is larger than 1 and therefore the foundation legs must be designed with an increase in width. The vertical maximum pressure of 1065 is also very high.

#### J.4.1.7.5 Rotational stability:

The rotational stability can be calculated with the formula:

$$e_R = \frac{\sum H_{unfav}}{\sum V_{fav}} \cdot h_{COG} \leq \frac{L_{foundation}}{6} \quad (162)$$

Where:

$e_R$  = Distance from the middle of the structure to the intersection point of the resulting force and the bottom line of the structure [m]

$\sum M$  = Sum of the acting moments design value [Nm]

$h_{COG}$  = Height of Centre of Gravity [m]

$D_{GBF}$  = Diameter of base slab [m]

The unity check is given as:

$$UC = \frac{e_R}{L_{Foundation}/6} \leq 1 \quad (163)$$

The result and input to calculate the unity check for the rotational stability are given in Table A-21.

All checks are now performed and the immersion structure fulfils the requirements on the shear capacity and the rotational stability. Because the pressure on the subsoil is too large with a foundation leg width of 3 meter. the foundation leg width must be increased. The stability parameters are plotted as function of the leg width and are displayed in Figure A-89.

Parameter	Value	Unit
$\sum H_{unfav}$	6066	[kN]
$\sum V_{fav}$	70923	[kN]
$h_{COG}$	11.39	[m]
$L_{foundation}$	47	[m]
$e_R$	0.99	[m]
$UC$	0.13	[-]

Table A-21 - Input and results of rotational stability

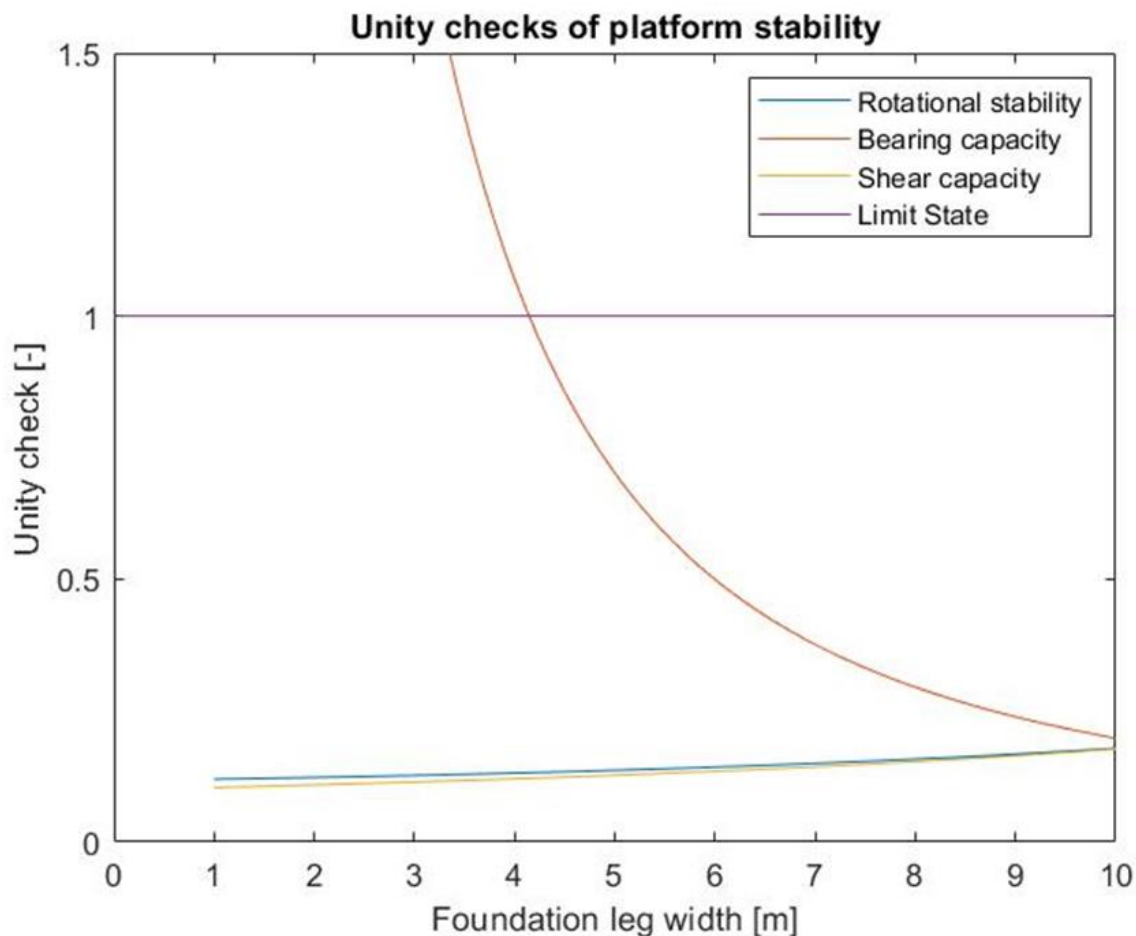


Figure A-89 – Stability criteria as function of foundation leg width

#### J.4.1.7.6 Optimal dimension of foundation leg

The example calculation for a foundation with a leg width of 3 meter fulfil the requirement on static stability in the floating phase but does not comply with the stability parameters of the subsoil during operation and the maximum allowable draught. Therefore the most optimal width of the foundation leg must be determined. The foundation leg must have a larger width. In Figure A-90 the stability criteria and draught as function of the foundation leg width are shown. The unity checks must be below one, the draught has a maximum of 10 meters and the metacentric height must be larger than 0.5 meter. The result is to design the immersion platform foundation legs with a width of 9.0 meter. A foundation leg width of 8.5 meter is just sufficient but because the design is a preliminary design and changes could be possible a leg width of 9.0 meter is chosen. It is recommended to execute the Scia model now with a foundation width of 9.0 meter. The results will differ from the first results and an iterative procedure must be executed. Because the design is only a preliminary design the thicknesses of the concrete elements are maintained and the foundation leg width of 9.0 meter is used. The most important parameters for the immersion structure with a foundation leg width of 9.0 meter are given in Table A-22.

Parameter	Value	Unit
Draught	9.65	[m]
Maximum weight	229	[kN/m <sup>2</sup> ]

Table A-22 - Values for immersion structure leg width=9m

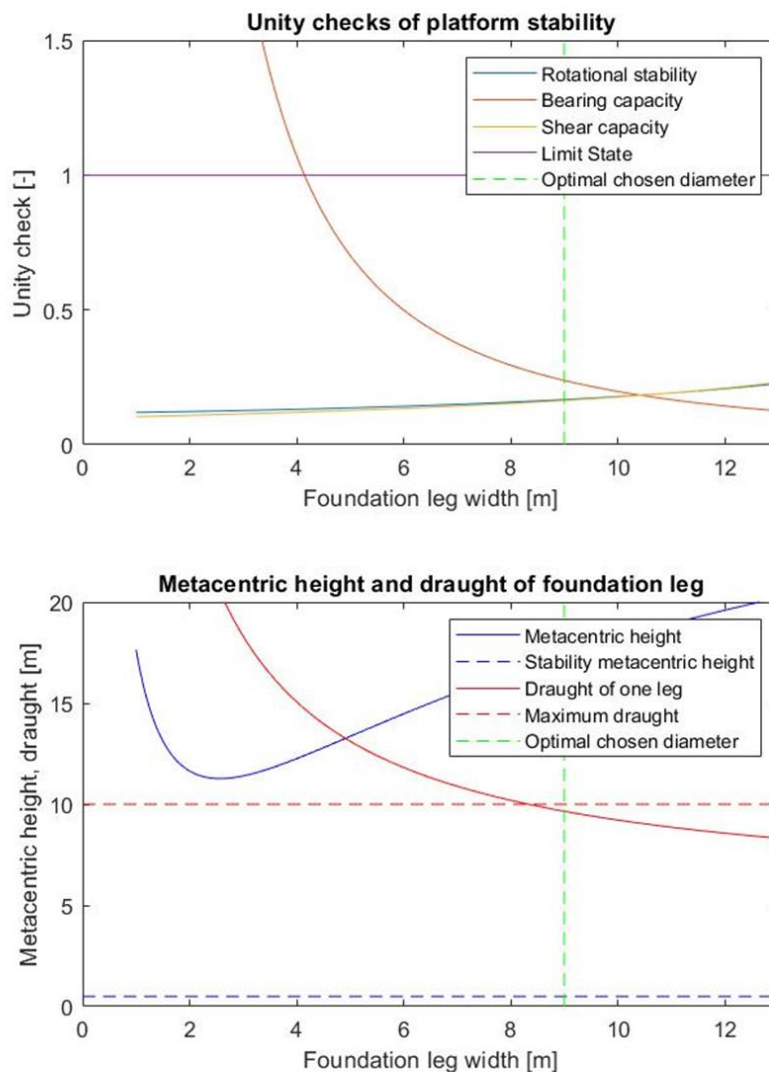


Figure A-90 - Decision on foundation leg width

#### J.4.4 Construction of immersion structure

Because the immersion structure itself is also a large structure which must be transported into the water the construction method of this immersion structure must be described. The length and width of the structure are 47 meter and 55 meter the immersion structure can be built on a dry or a floating dock, see Figure A-91 and Figure A-92. The immersion structure can be built in the majority of the dry docks and on a small part of the floating docks. A remark is made on the docks, the minimal available draught must be 10 meters. A dry dock is chosen due to the smaller renting costs.

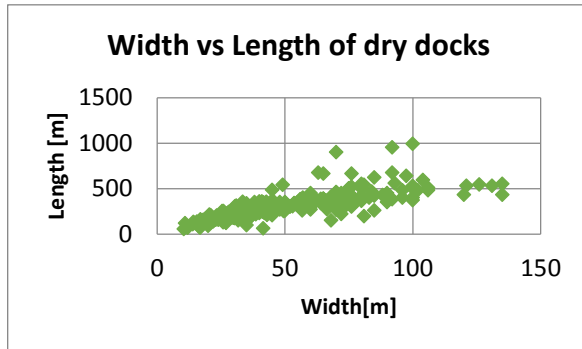


Figure A-91 - Dimensions of available dry docks (Data: Wikipedia.org)

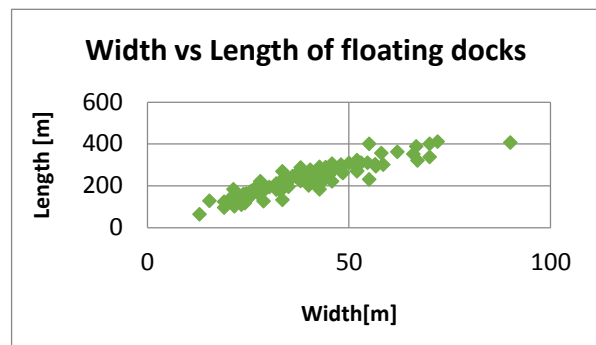


Figure A-92 - Dimensions of floating docks

### J.5 CONCLUSION AND RECOMMENDATIONS

The answer of the design step from this chapter was if the (temporary) structures are constructible. This question is answered with a yes. The immersion structure is designed in this chapter and consists of a platform, winch system and two concrete foundation legs.

The immersion structure is designed with a platform structure which consists of 47 H-beams as given in Figure A-93. The connecting beam is also designed with this H-beam.

The concrete elements are designed according the dimensions in Table A-23.

The draught of the platform is 9.65 meter.

Element	$d[mm]$
1: Upper slab	150
2: Bottom slab	1250
3: Front wall	650
4: Side inner wall	500
5: Side outer wall	500
6: Connecting slab	H-beam
7: Inner wall	150

Table A-23 - Thickness of concrete elements

Only a preliminary design is given of the immersion structure. The design is an iterative process and only the first iteration is executed. If the structure will be realized a more extensive design process must be executed. The concrete thicknesses could be adapted to design the most optimal concrete thicknesses at different locations where the internal forces are the highest. The connections between the foundation leg and the connecting beam and between the platform structure and foundation legs are not designed. When this design is executed the thickness of concrete elements might be changed and

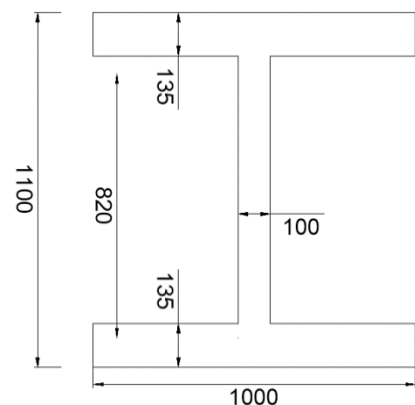


Figure A-93 - Final design H-beam

the stability criteria and draught change. In Figure A-94, the immersion structure is shown at the REBO Offshore Site. The upper platform lowers exactly between the two connecting beams and the optimal draught is created. It is assumed that the 1 meter space between the quay wall and the immersion platform not have a large influence on the transporting system because the transporting system push the GBF from the quay wall and on the immersion platform the GBF can be towed to the middle of the platform. Therefore the one meter gap between the platform and the GBF is accepted.

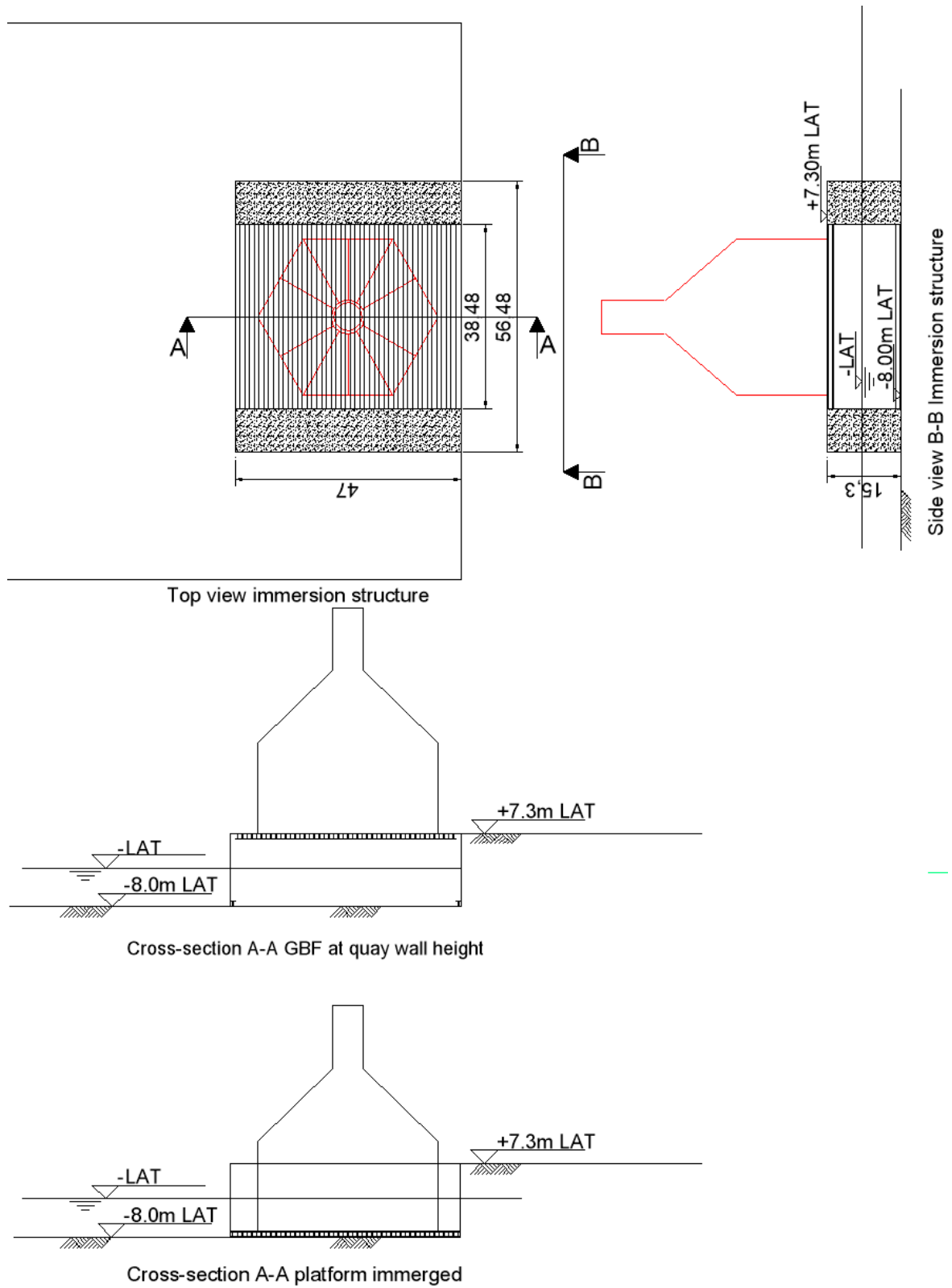


Figure A-94 - Preliminary design immersion structure

## J.6 RESULTS PER STRUCTURAL ELEMENT

The results are given for the seven different structural elements. The order from 1 till 7 is followed. For each structural element the figures are given and thereafter the values are summarized in a table. After the results of the seven structural elements all values are summarized in one table and the minimal thickness can be calculated.

### Upper slab

The results of the calculation with Scia for the upper slab are given in Figure A-95 till Figure A-100.

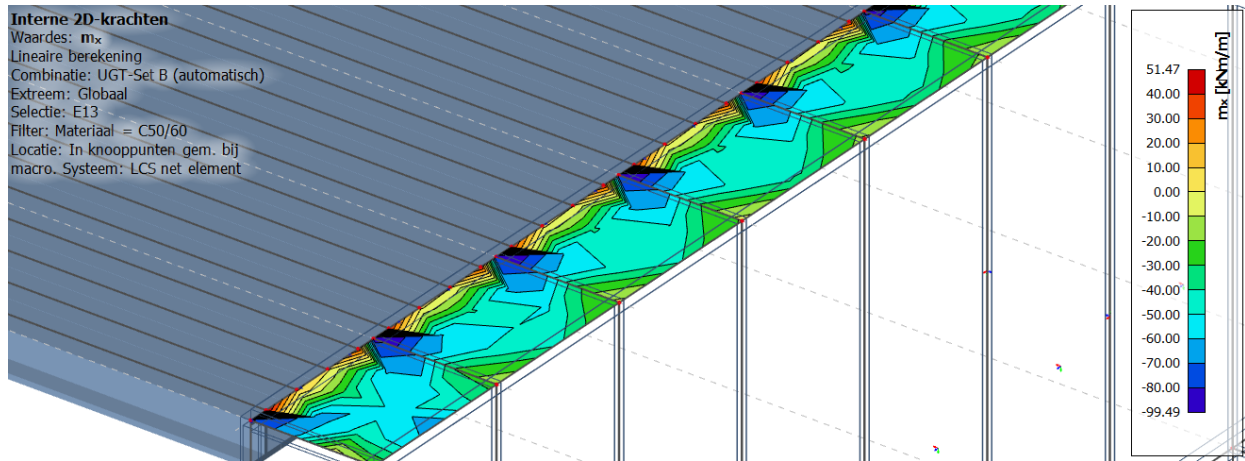


Figure A-95 - Result of bending moment in x-direction for upper slab

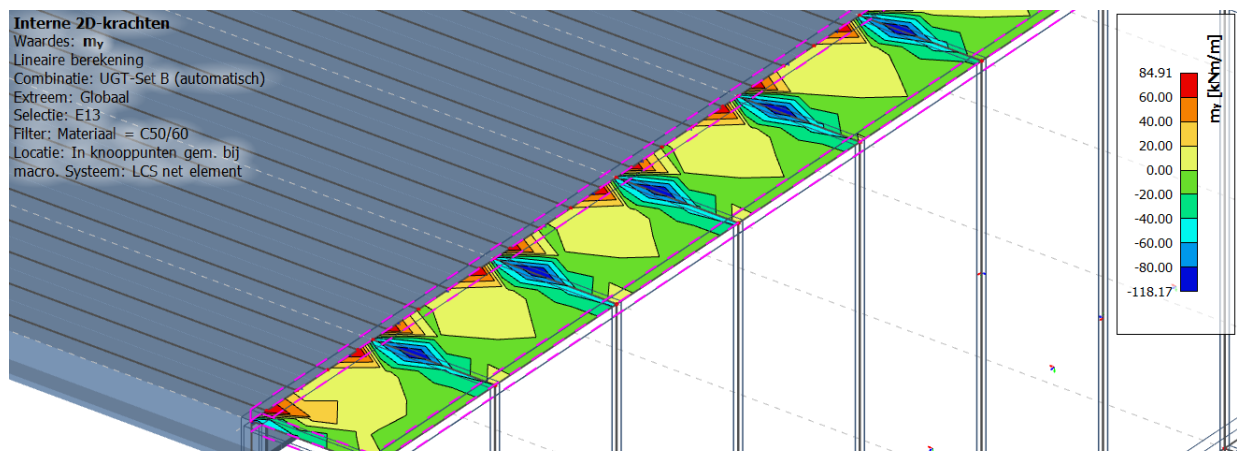


Figure A-96 - Result of bending moment in y-direction for upper slab

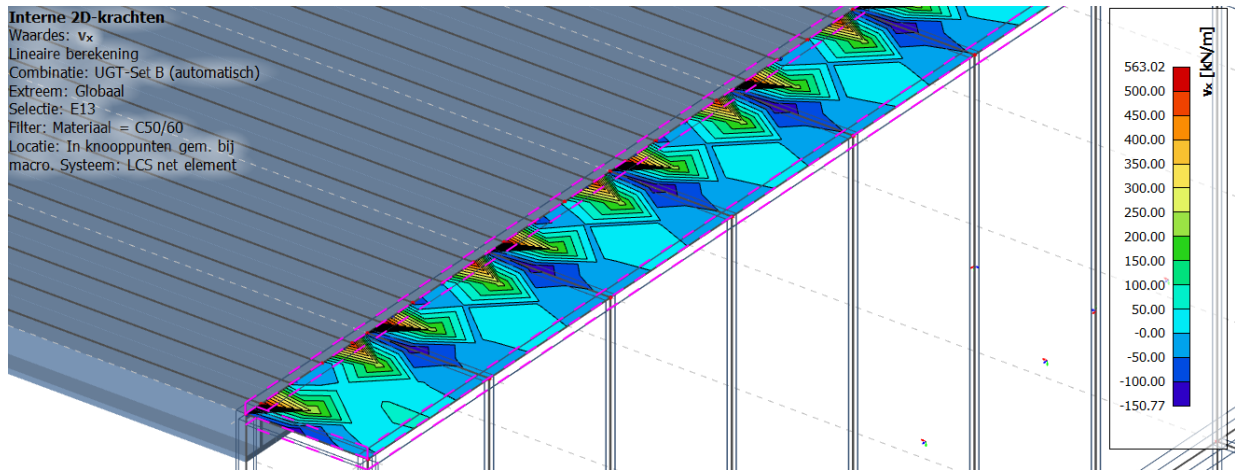


Figure A-97 - Result of shear force in x-direction for upper slab

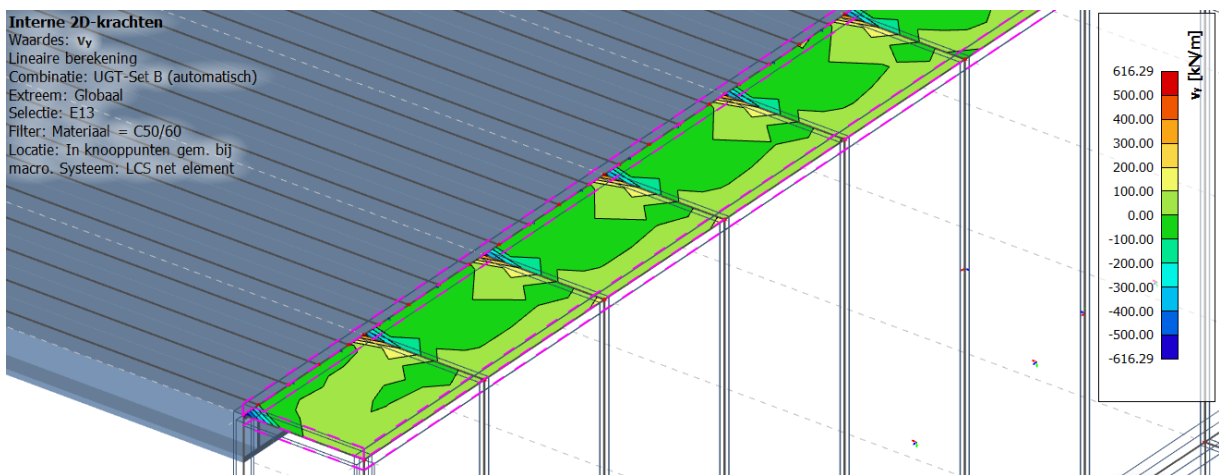


Figure A-98 - Result of shear force in y-direction for upper slab

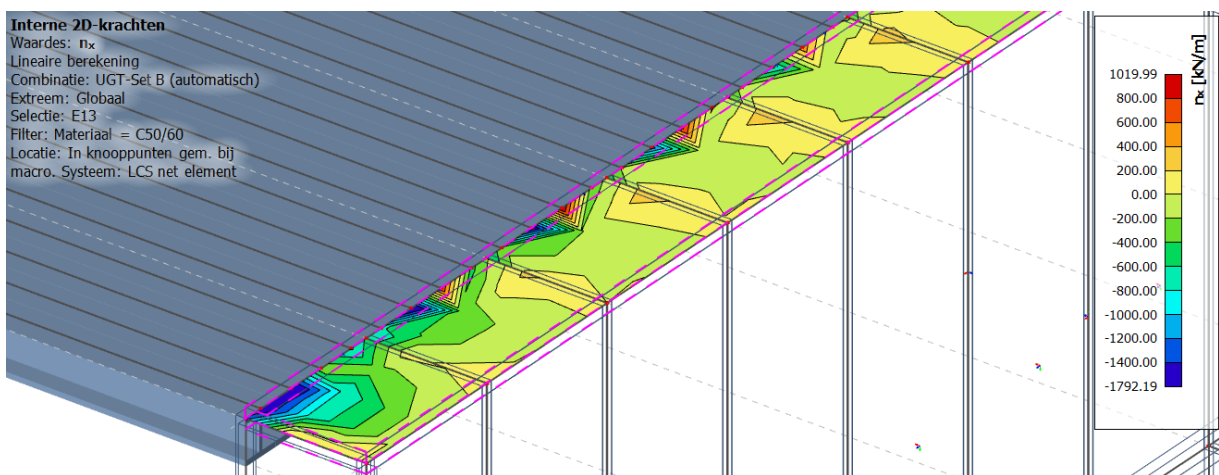


Figure A-99 - Result of axial force in x-direction for upper slab

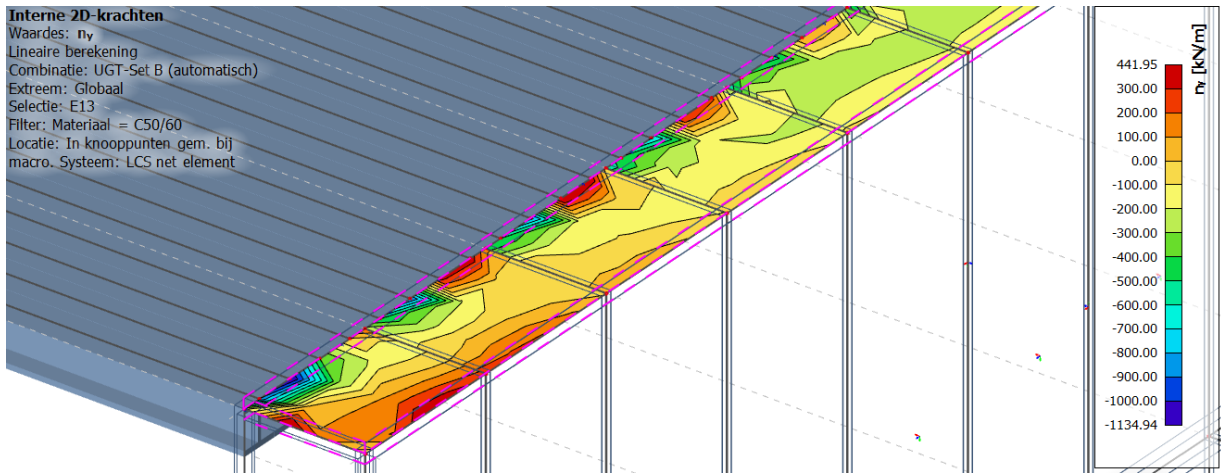


Figure A-100 - Result of axial force in y-direction for upper slab

The maximum values of the internal forces are given in Table A-24.

Internal force upper slab	Lower bound value	Upper bound value
$m_x$ [kNm]	-99.49	+51.47
$m_y$ [kNm]	-118.17	+84.91
$V_x$ [kN]	-150.77	+563.02
$V_y$ [kN]	-616.29	+616.29
$N_x$ [kN]	-1792.19	+1019.99
$N_y$ [kN]	-1143.94	+441.95

Table A-24 - Maximum values of internal forces upper slab

### Bottom slab

The results of the calculation with Scia for the bottom slab are given in Figure A-101 till Figure A-106.

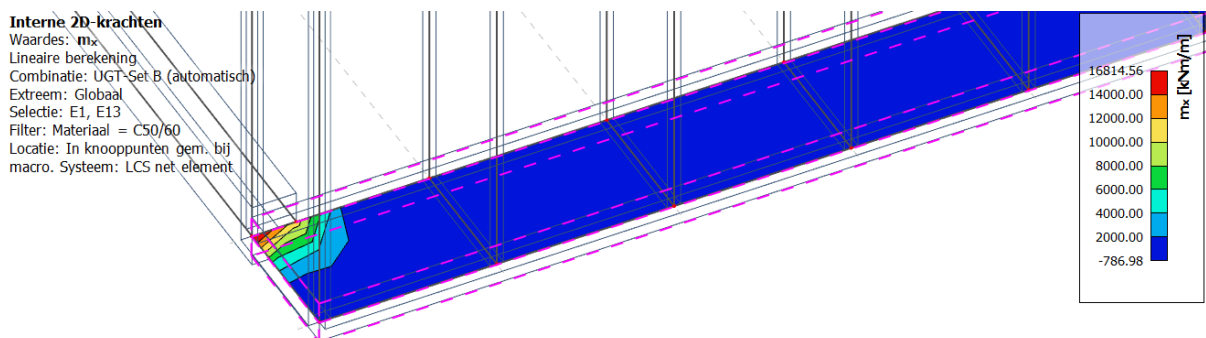


Figure A-101 - Result of bending moment in x-direction for bottom slab

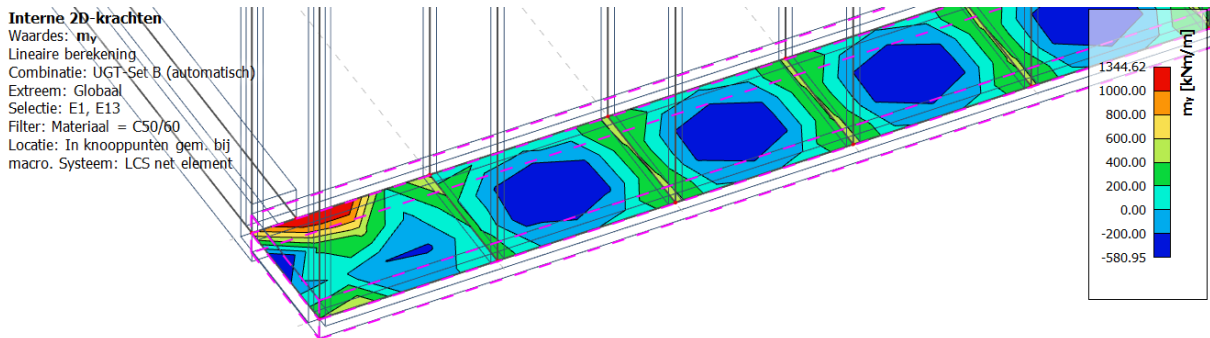


Figure A-102 - Result of bending moment in y-direction for bottom slab

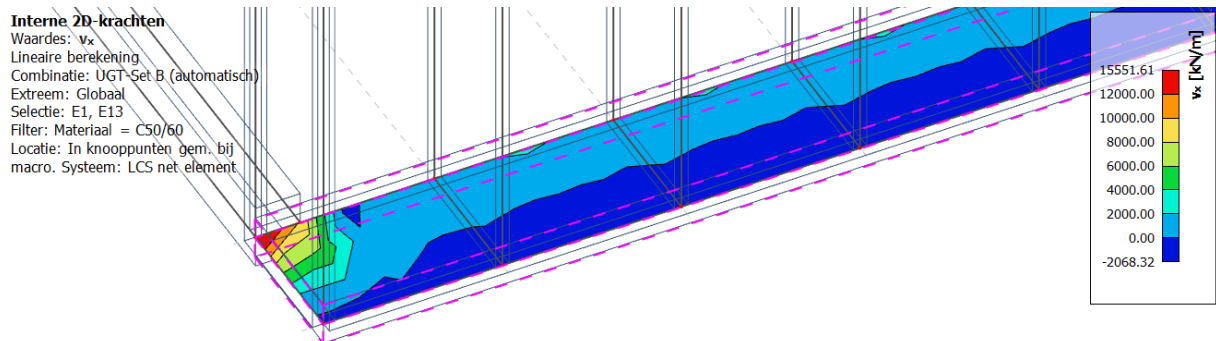


Figure A-103 - Result of shear force in x-direction for bottom slab

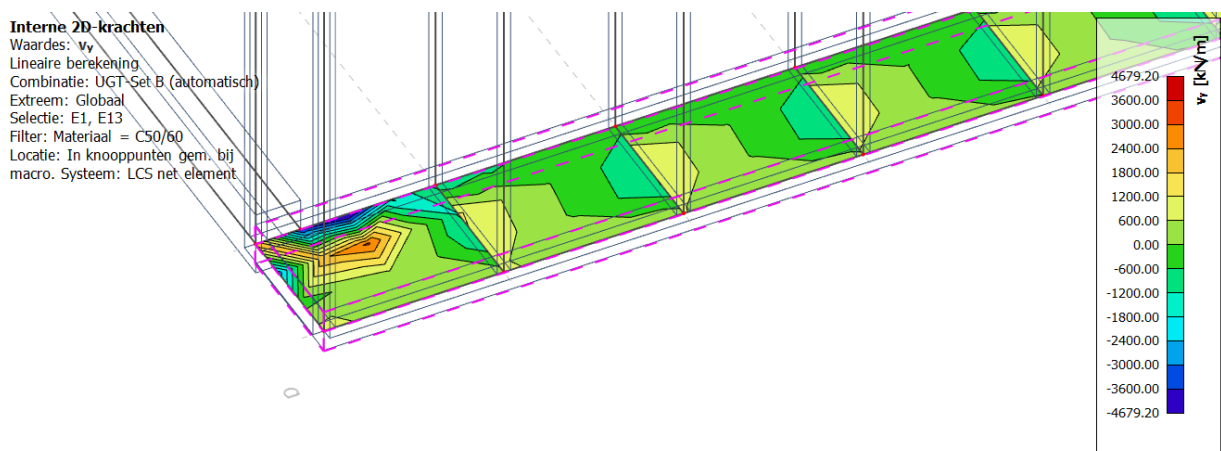


Figure A-104 - Result of shear force in y-direction for bottom slab

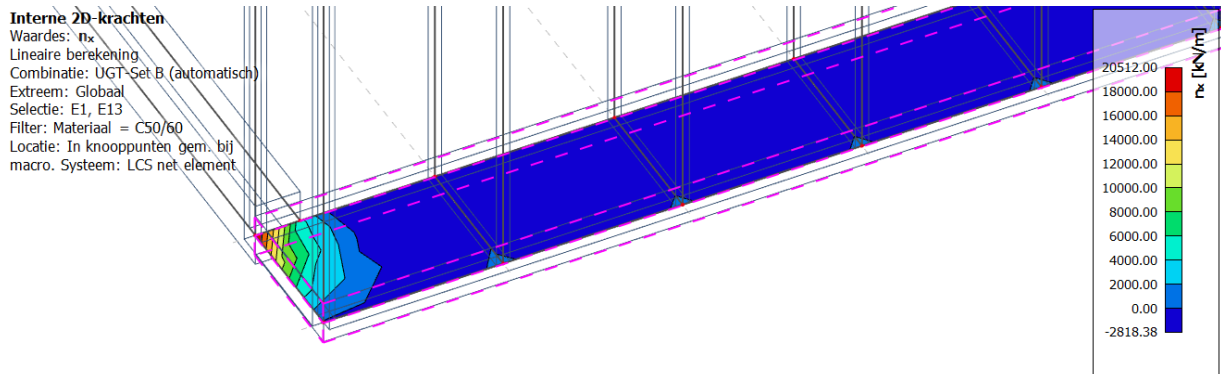


Figure A-105 - Axial forces in x-direction for bottom slab

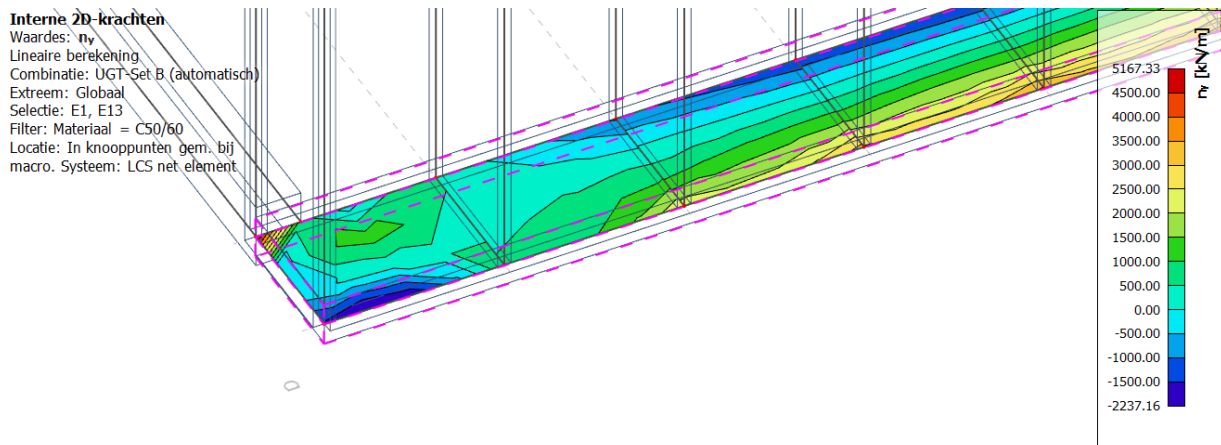


Figure A-106 - Axial forces in y-direction for bottom slab

The maximum values of the internal forces are given in Table A-25.

Internal force upper slab	Lower bound value	Upper bound value
$m_x$ [kNm]	-786.98	+16814.56
$m_y$ [kNm]	-580.95	+1344.62
$V_x$ [kN]	-2068.32	+15551.61
$V_y$ [kN]	-4679.20	+4679.20
$N_x$ [kN]	-2818.38	+20512.00
$N_y$ [kN]	-2237.16	+5167.33

Table A-25 - Maximum values of internal forces upper slab

## Front wall

The results of the calculation with Scia for the front wall are given in Figure A-107 till Figure A-112.

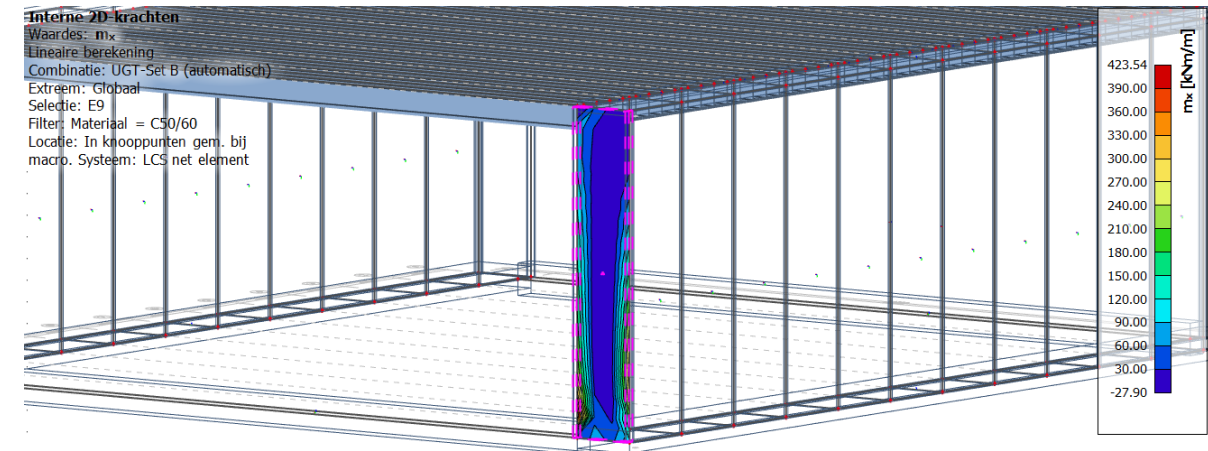


Figure A-107 - Result of bending moment in x-direction for front wall

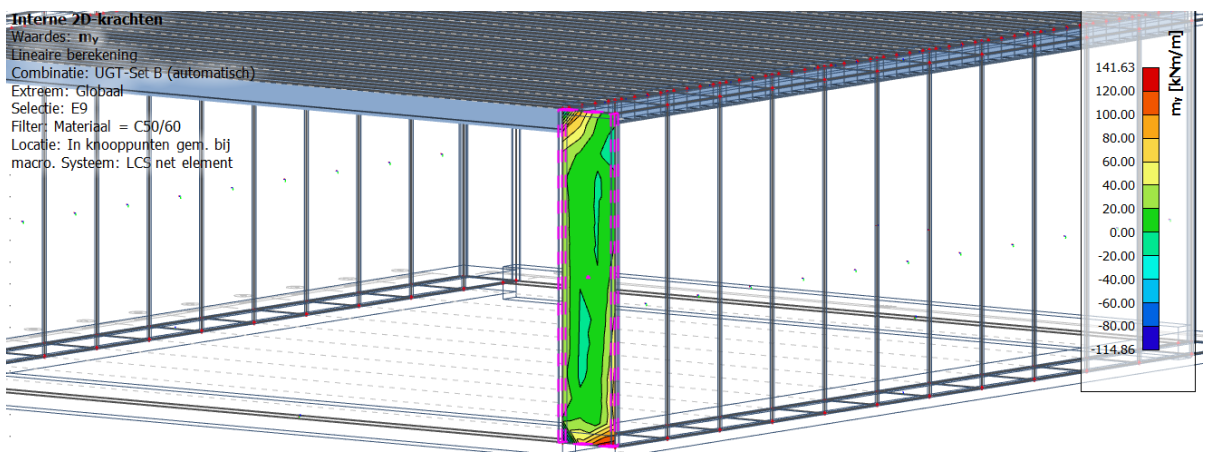


Figure A-108 - Result of bending moment in y-direction for front wall

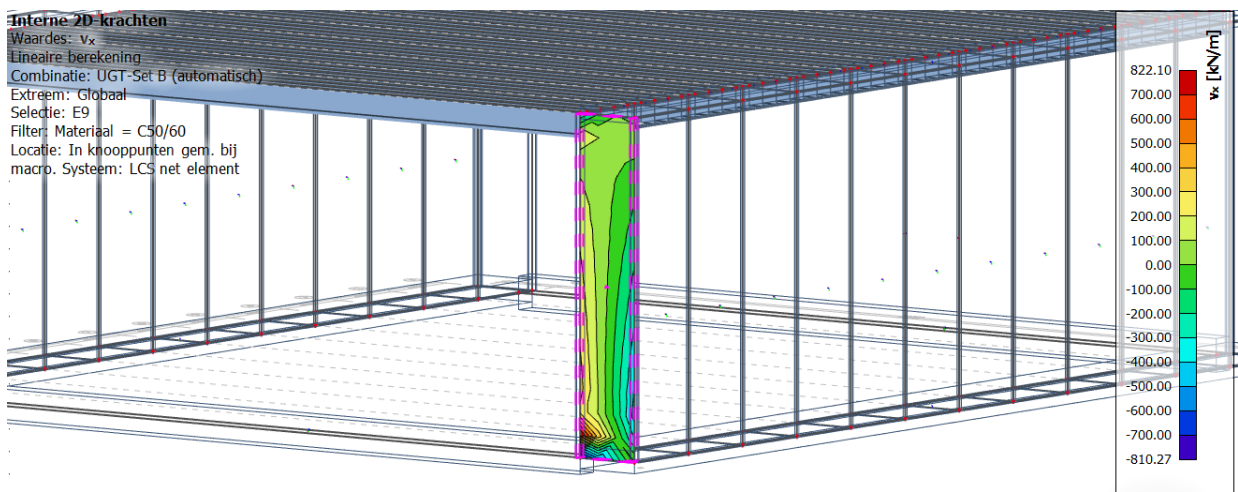


Figure A-109 - Result of shear force in x-direction for front wall

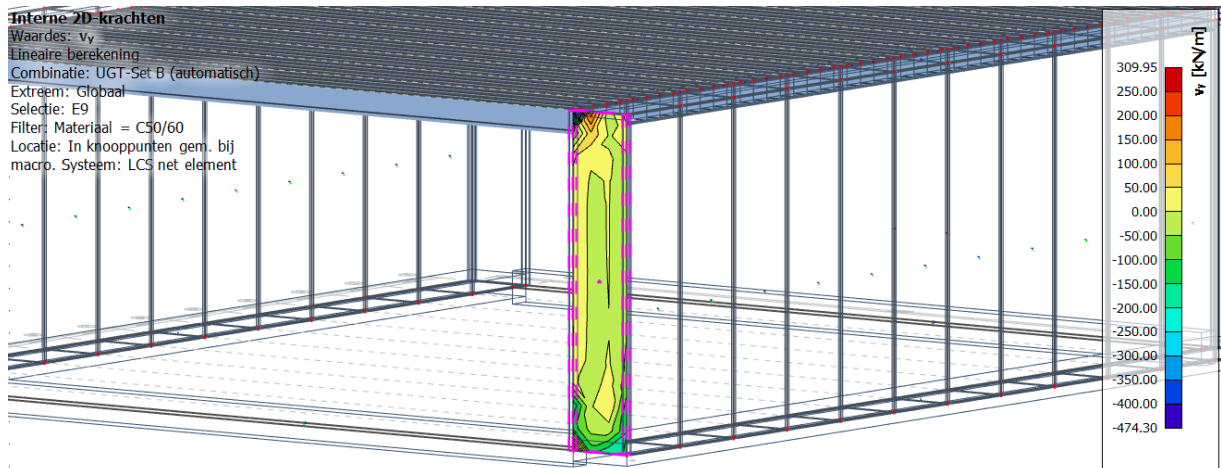


Figure A-110 - Result of shear force in y-direction for front wall

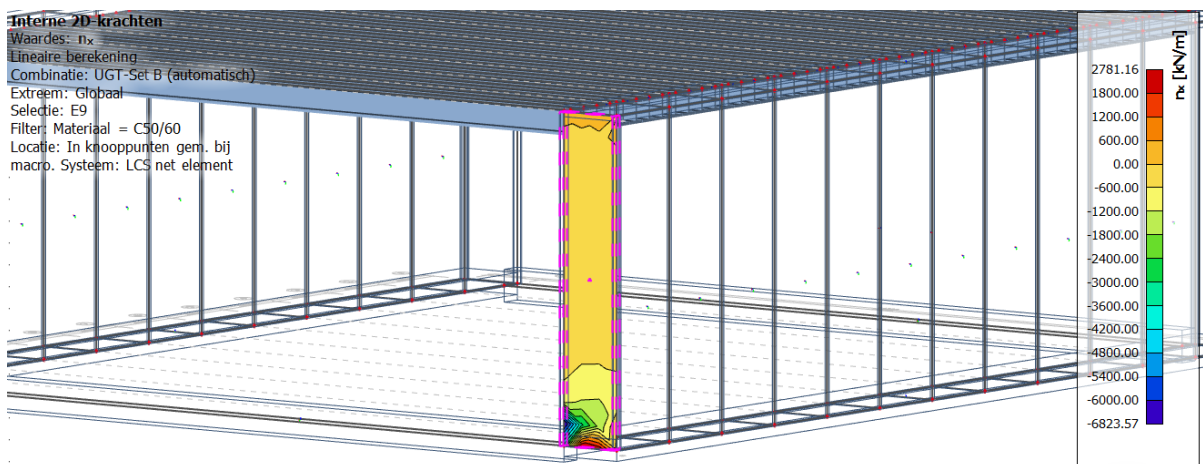


Figure A-111 - Result of axial force in x-direction for front wall

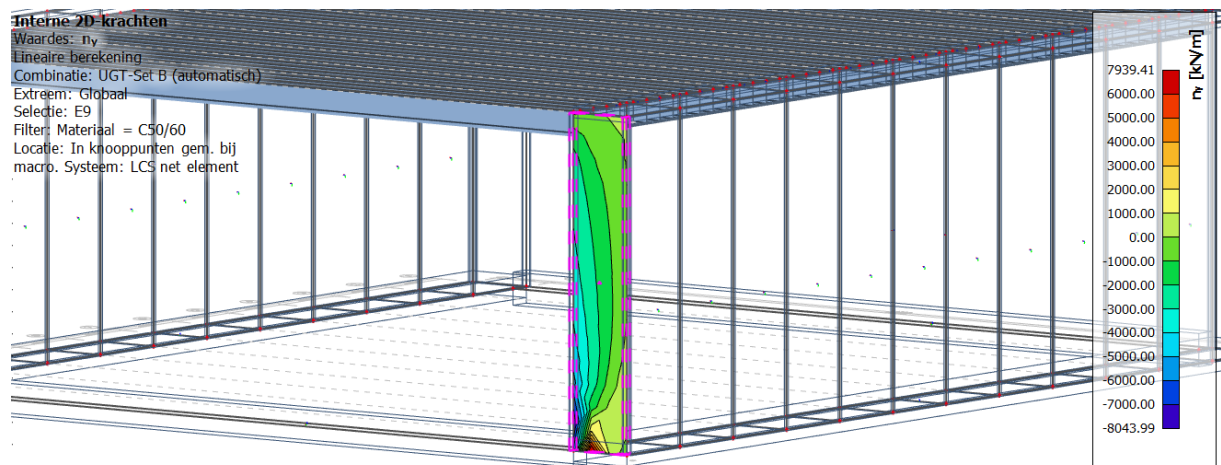


Figure A-112 - Result of axial force in y-direction for front wall

The maximum values of the internal forces are given in Table A-26.

Internal force upper slab	Lower bound value	Upper bound value
$m_x$ [kNm]	-27.90	+423.54
$m_y$ [kNm]	-114.86	+141.63
$V_x$ [kN]	-810.27	+822.10
$V_y$ [kN]	-474.30	+309.95
$N_x$ [kN]	-6823.57	+2781.16
$N_y$ [kN]	-8043.99	+7939.41

Table A-26 - Maximum values of internal forces upper slab

### Side inner wall

The results of the calculation with Scia for the side inner wall are given in Figure A-113 till Figure A-118.

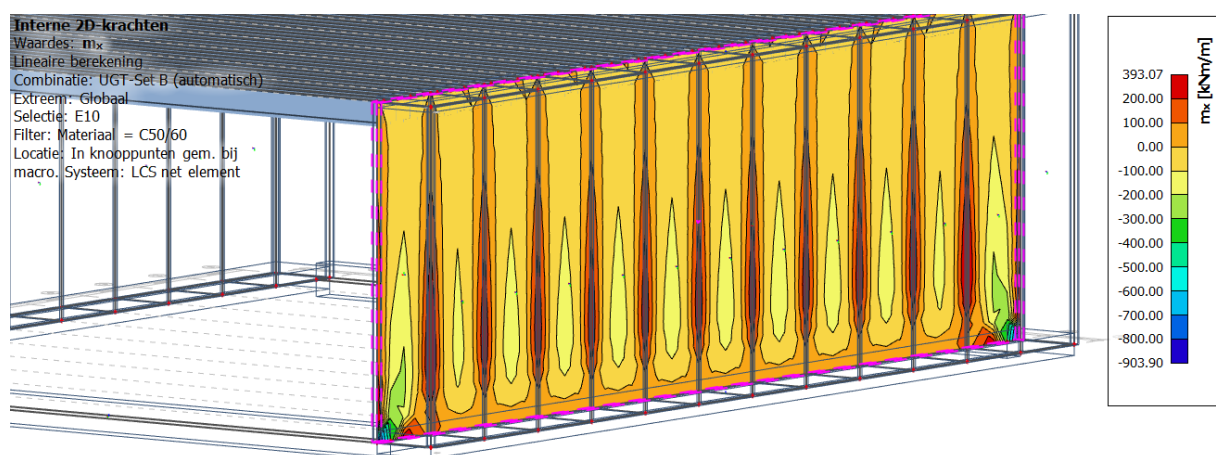


Figure A-113 - Result of bending moment in x-direction for side inner wall

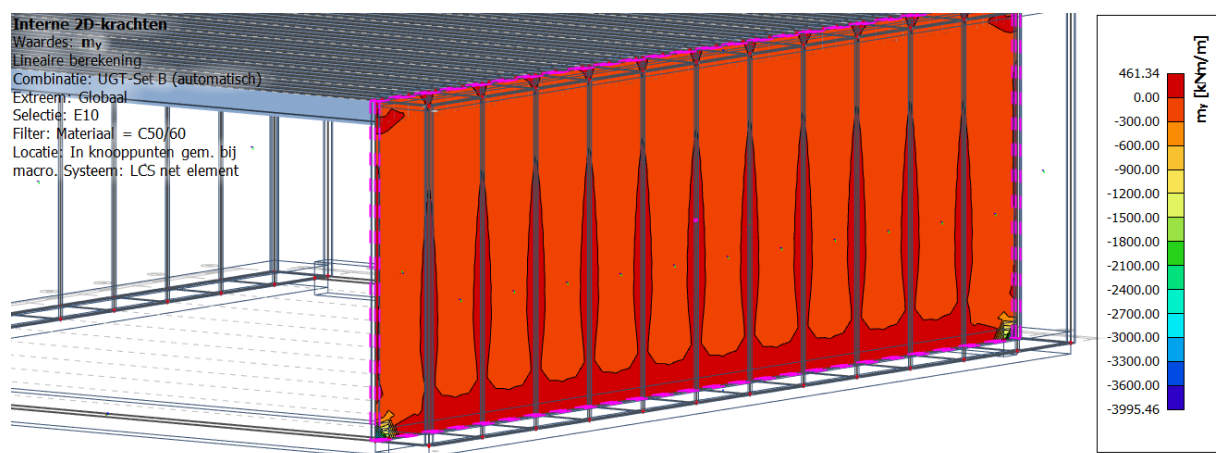


Figure A-114 – Result of bending moment in y-direction for side inner wall

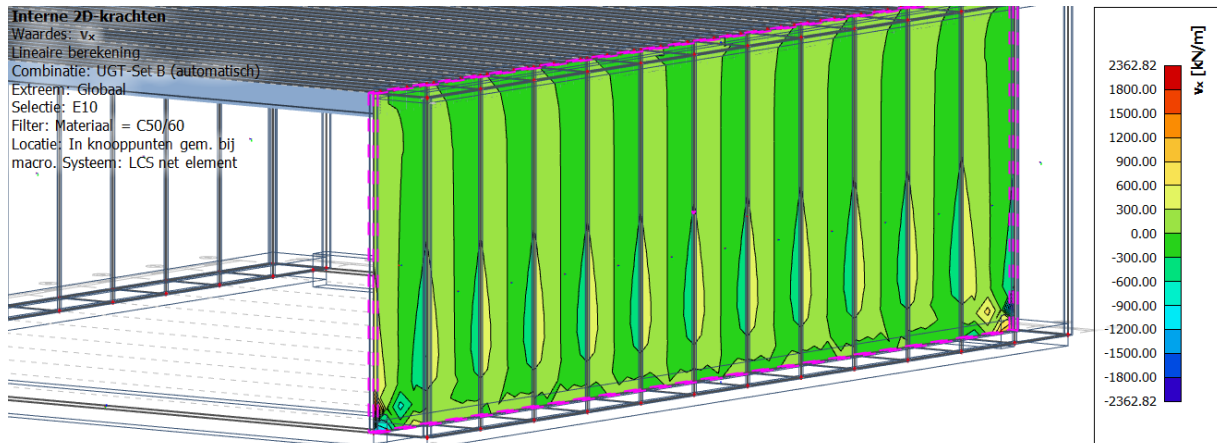


Figure A-115 - Result of shear force in x-direction for side inner wall

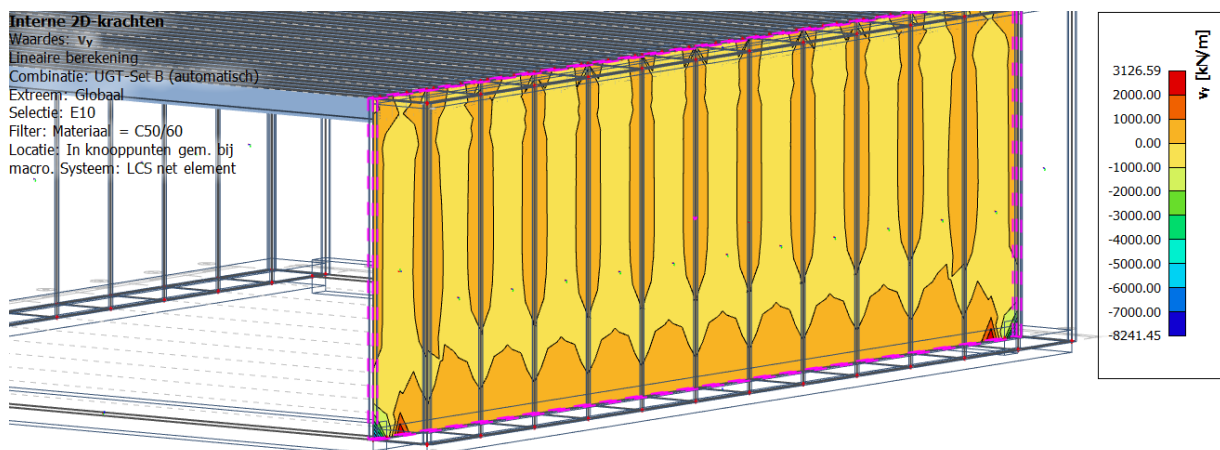


Figure A-116 - Result of shear force in y-direction for side inner wall

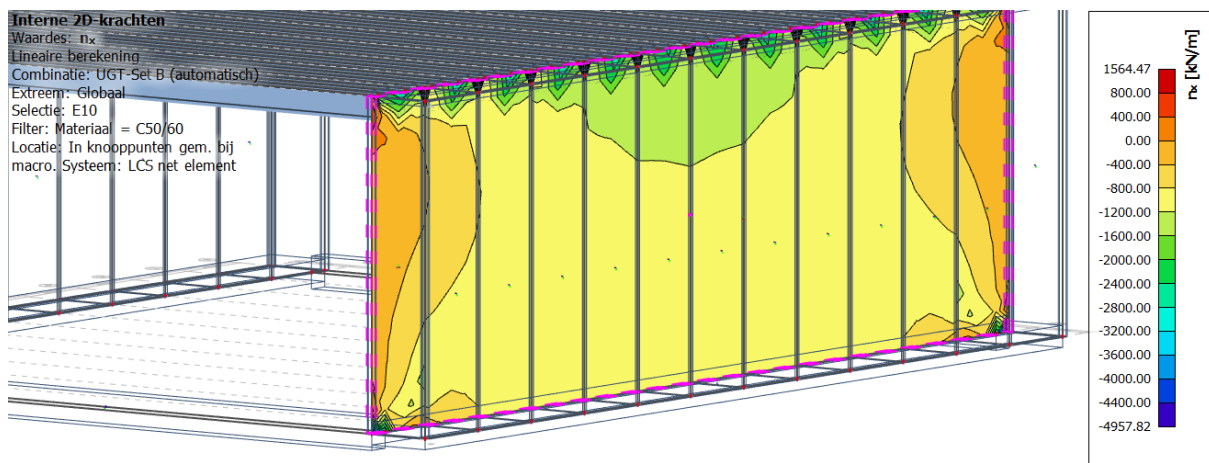


Figure A-117 - Result of axial force in x-direction for side inner wall

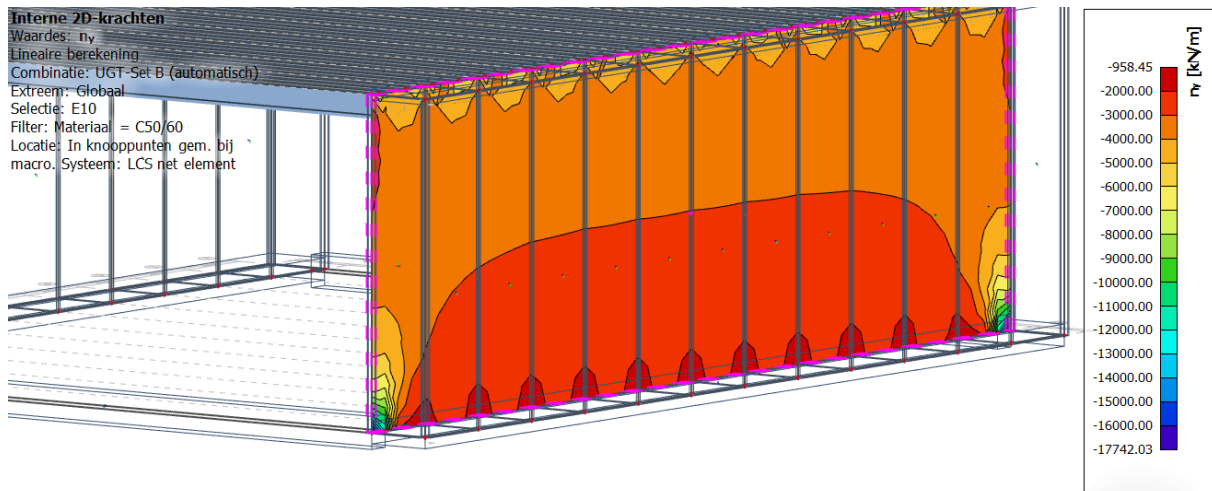


Figure A-118 - Result of axial force in y-direction for side inner wall

The maximum values of internal forces are given in Table A-27.

Internal force upper slab	Lower bound value	Upper bound value
$m_x$ [kNm]	-903.90	+393.07
$m_y$ [kNm]	-3995.46	+461.34
$V_x$ [kN]	-2362.82	+2362.82
$V_y$ [kN]	-8241.45	+3126.59
$N_x$ [kN]	-4957.82	+1564.47
$N_y$ [kN]	-17742.03	-958.45

Table A-27 - Maximum values of internal forces side inner wall

### Side outer wall

The results of the calculation with Scia for the side outer wall are given in Figure A-119 till Figure A-124.

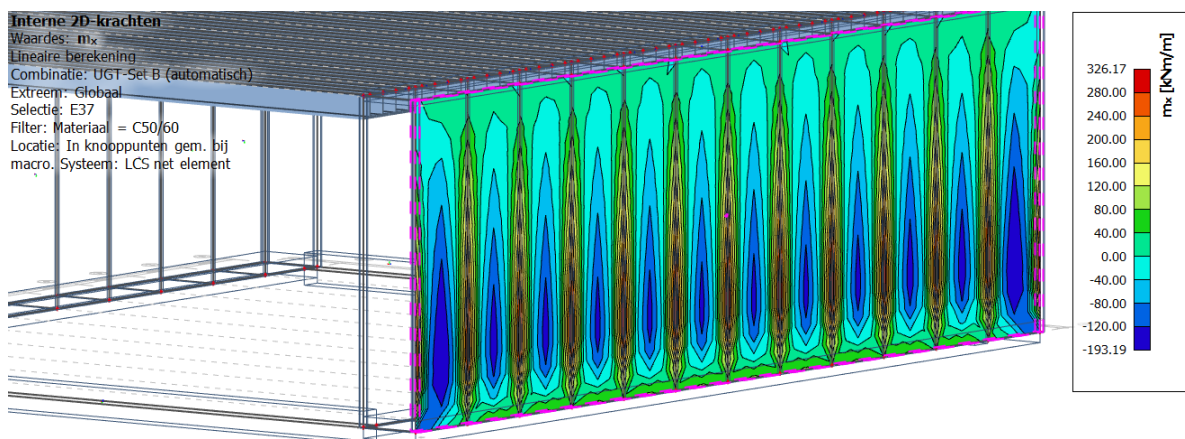


Figure A-119 - Result of bending moment in x-direction for side outer wall

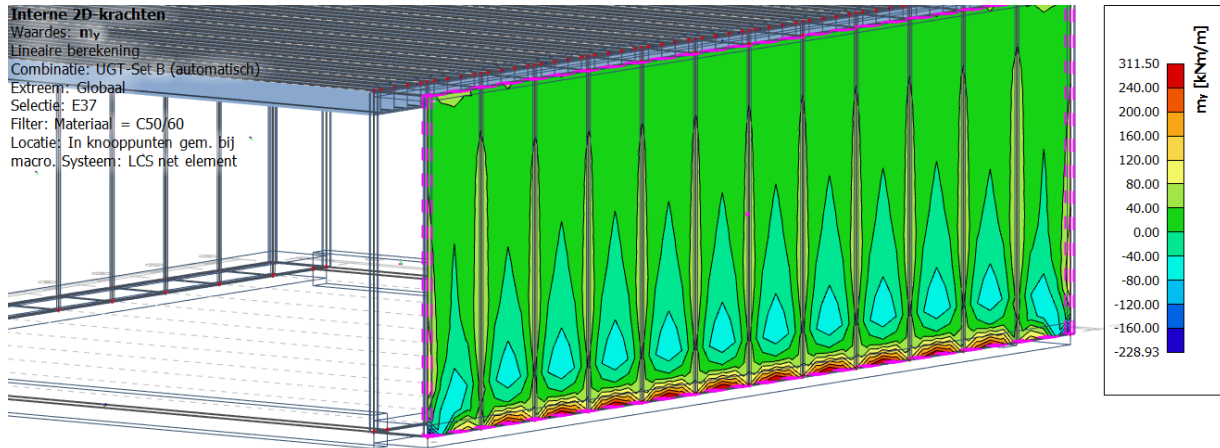


Figure A-120 - Result of bending moment in  $y$ -direction for side outer wall

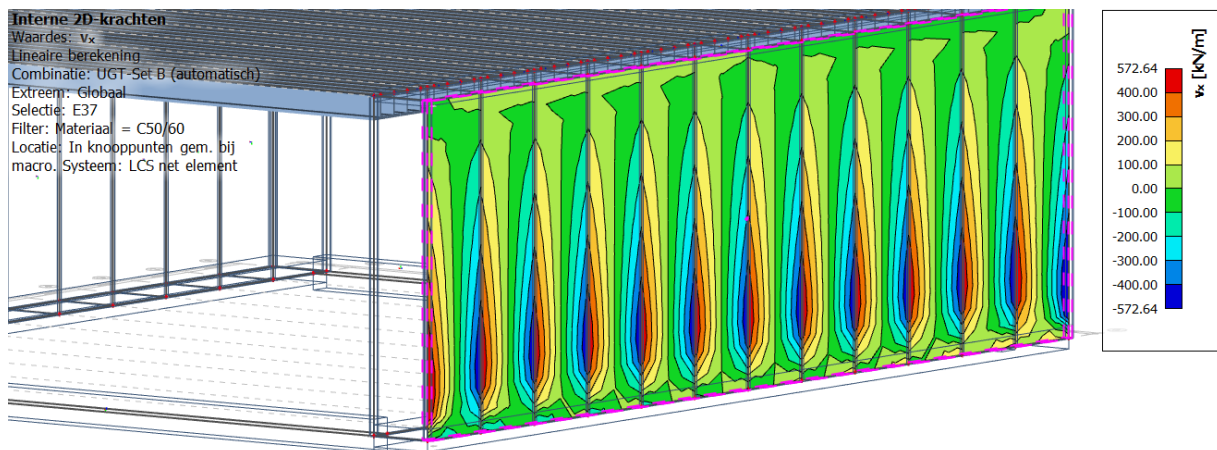


Figure A-121 - Result of shear force in  $x$ -direction for side outer wall

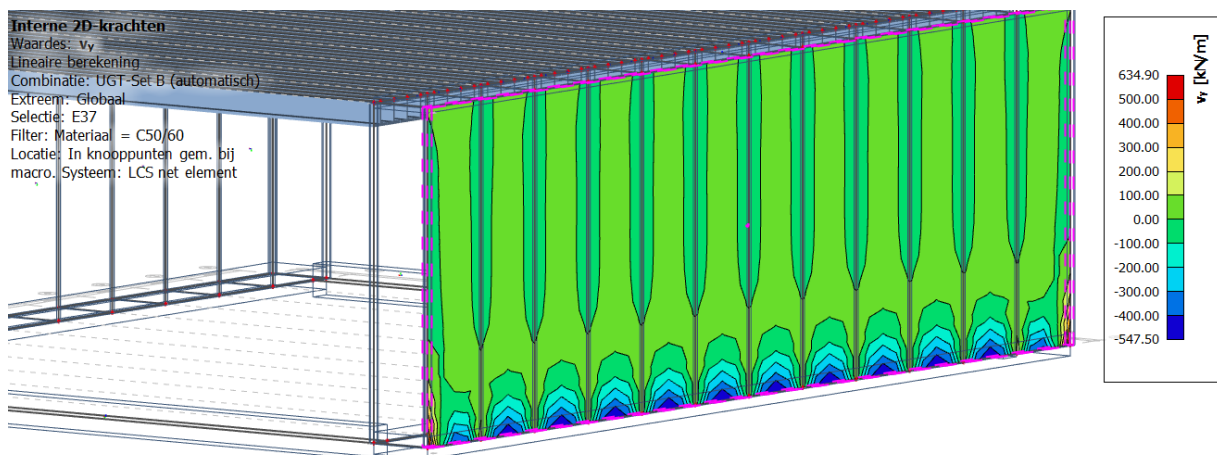


Figure A-122 - Result of shear force in  $y$ -direction for side outer wall

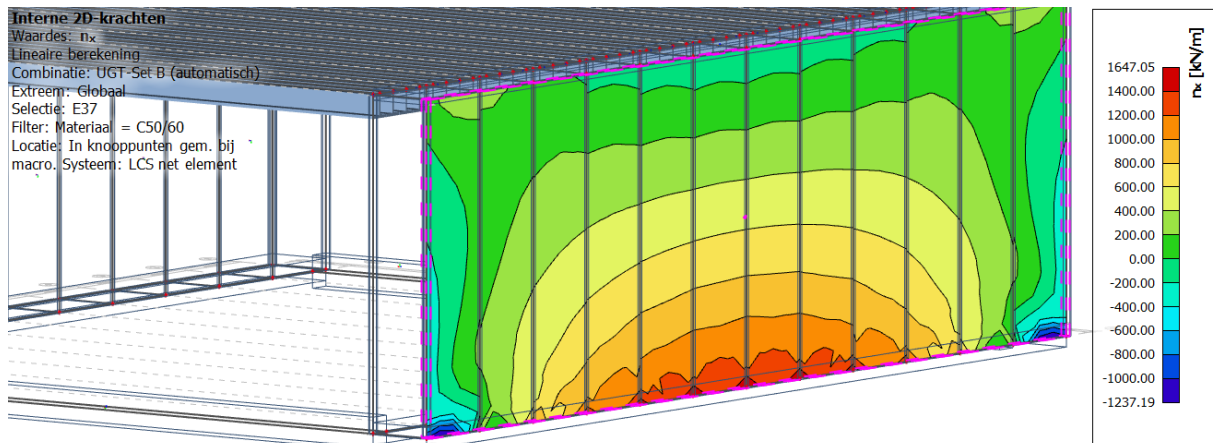


Figure A-123 - Result of axial force in x-direction for side outer wall

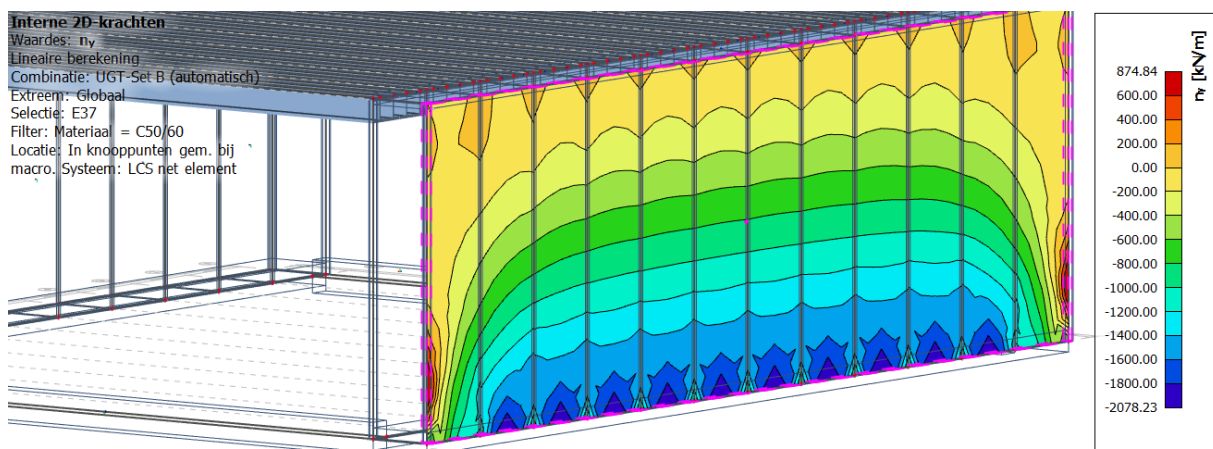


Figure A-124 - Result of axial force in y-direction for side outer wall

The maximum values of internal forces are given in Table A-28.

Internal force upper slab	Lower bound value	Upper bound value
$m_x$ [kNm]	-193.19	+326.17
$m_y$ [kNm]	-228.93	+311.50
$V_x$ [kN]	-572.64	+572.64
$V_y$ [kN]	-547.50	+634.90
$N_x$ [kN]	-1237.19	+1647.05
$N_y$ [kN]	-2078.23	+874.84

Table A-28 - Maximum values of internal forces side outer wall

### Connecting beam

The results of the calculation with Scia for the connecting beam are given in Figure A-125 till Figure A-130.

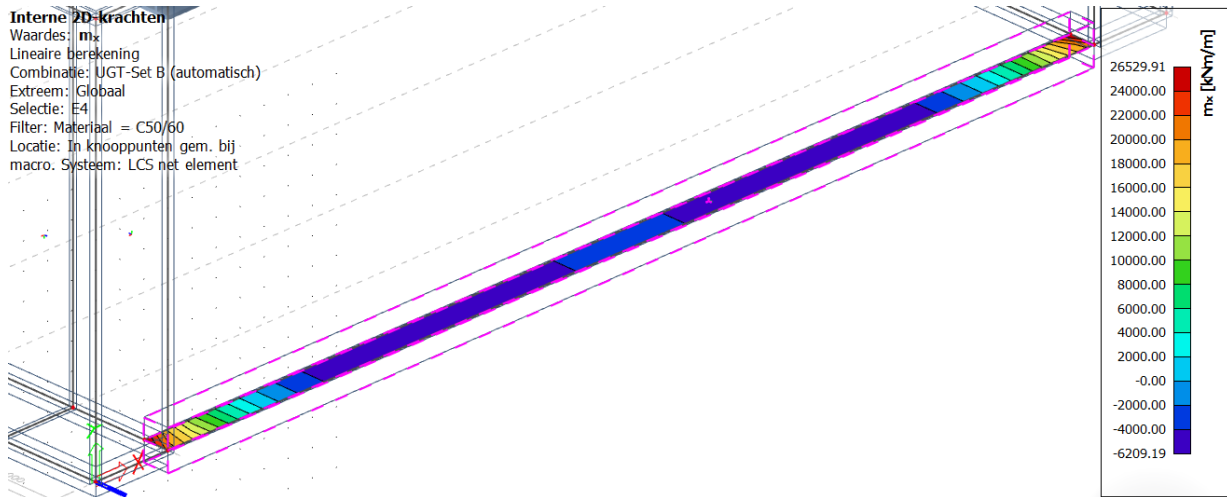


Figure A-125 - Result of bending moment in x-direction for connecting beam

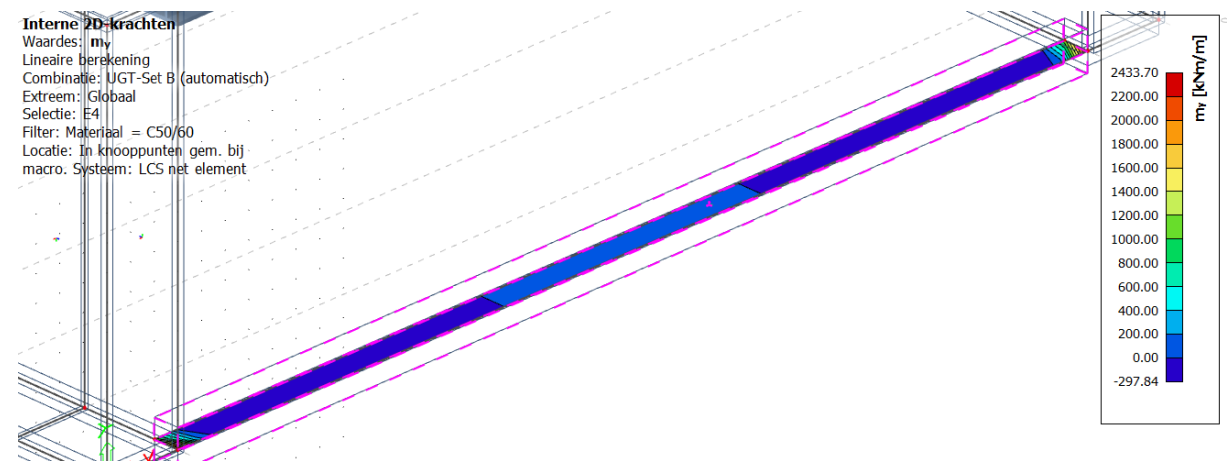


Figure A-126 - Result of bending moment in y-direction for connecting beam

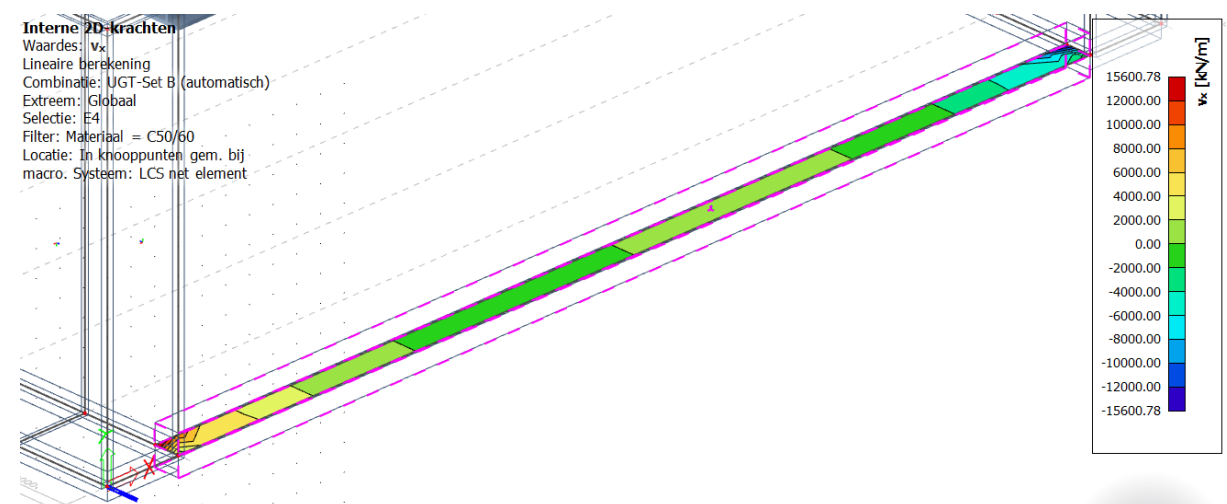


Figure A-127 - Result of shear force in x-direction for connecting beam

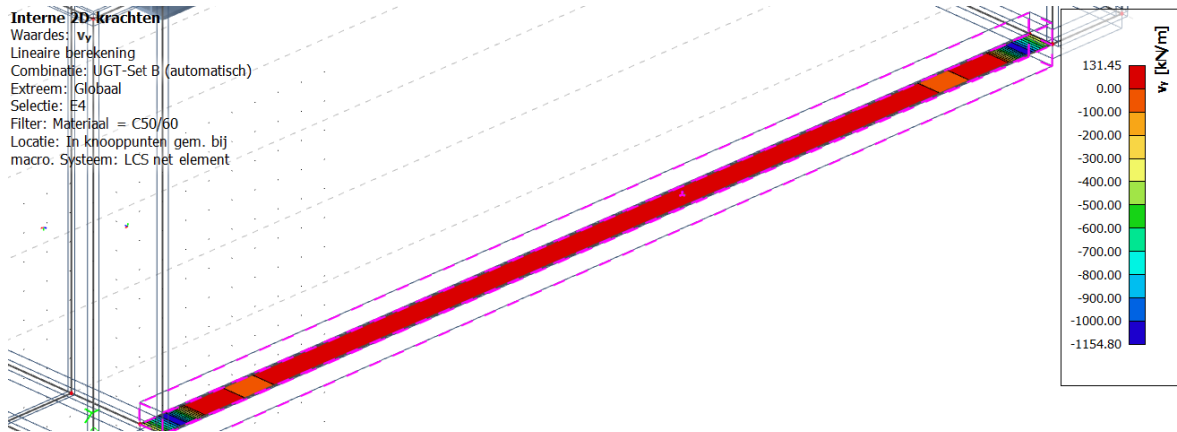


Figure A-128 - Result of shear force in y-direction for connecting beam

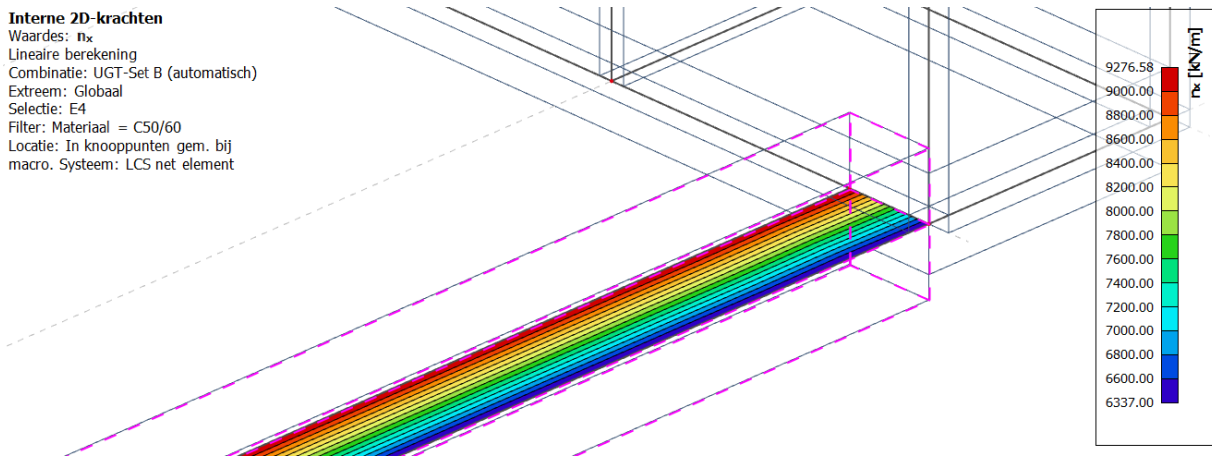


Figure A-129 - Result of axial force in x-direction for connecting beam

**Interne 2D-krachten**  
 Waardes:  $m_y$   
 Lineaire berekening  
 Combinatie: UGT-Set B (automatisch)  
 Extreem: Globaal  
 Selectie: E4  
 Filter: Materiaal = C50/60  
 Locatie: In knooppunten gem. bij  
 macro. Systeem: LCS net element

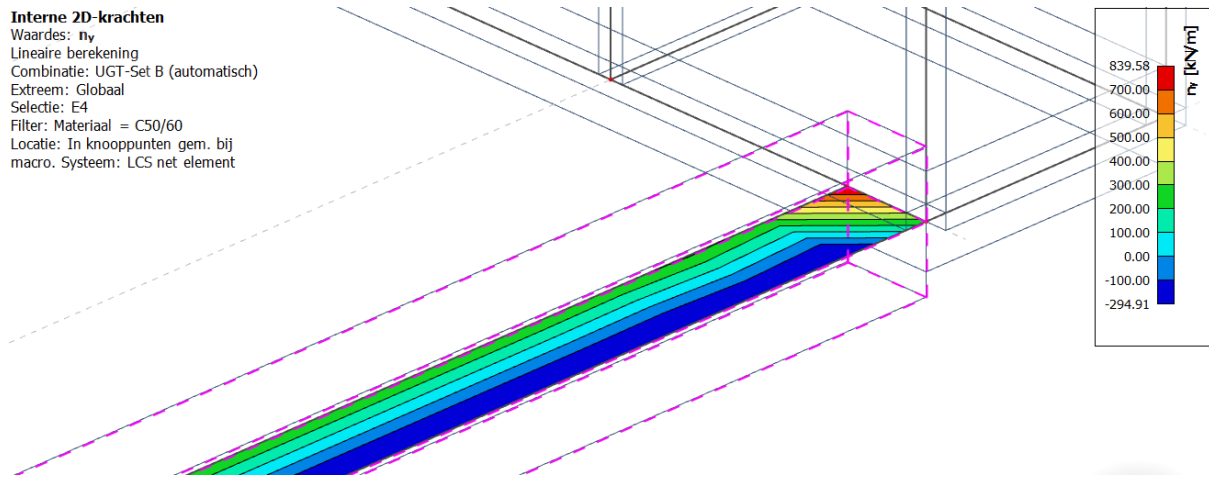


Figure A-130 - Result of axial force in y-direction for connecting beam

The maximum values of internal forces are given in Table A-29.

Internal force upper slab	Lower bound value	Upper bound value
$m_x$ [kNm]	-6209.19	+26529.91
$m_y$ [kNm]	-297.84	+2433.70
$V_x$ [kN]	-15600.78	+15600.78
$V_y$ [kN]	-1154.80	+131.45
$N_x$ [kN]	+6337.00	+9276.58
$N_y$ [kN]	-294.91	+839.58

Table A-29 - Maximum values of internal forces connecting slab

### Inner wall

The results of the calculation with Scia for the inner walls are given in Figure A-131 till Figure A-136.

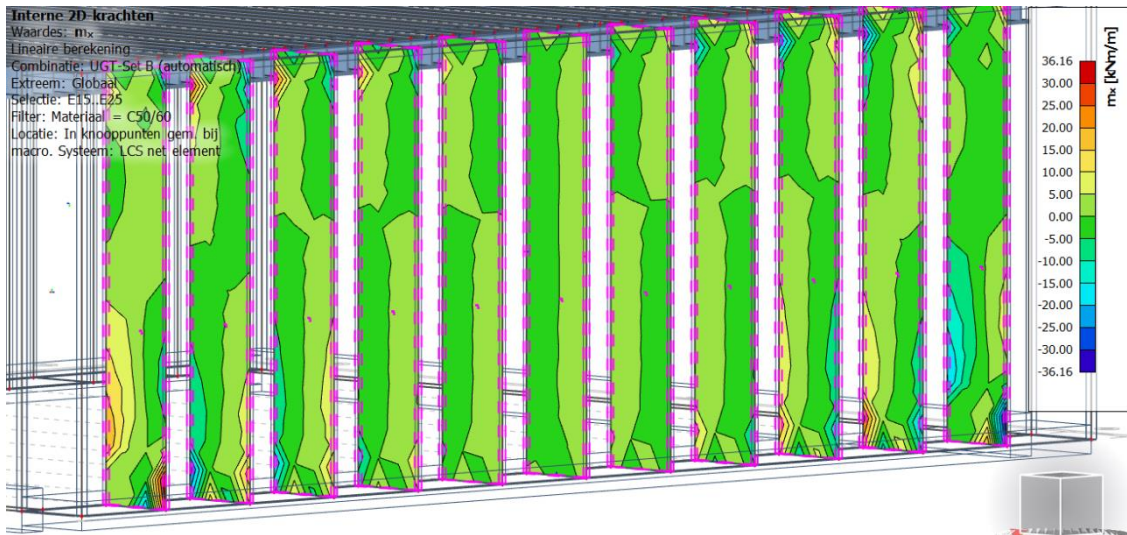


Figure A-131 - Result of bending moment in x-direction for inner walls

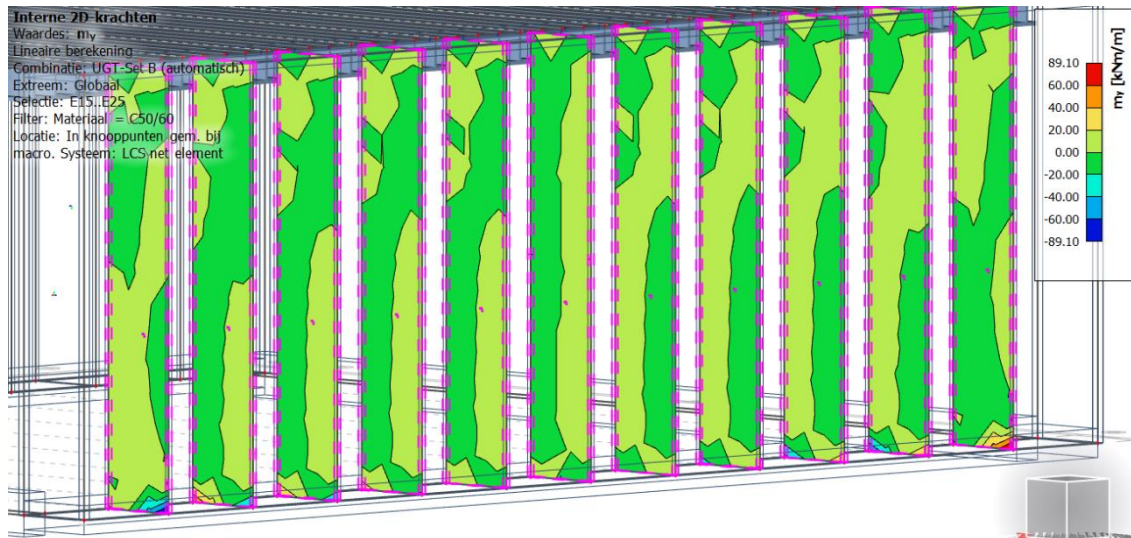


Figure A-132 - Result of bending moment in y-direction for inner walls

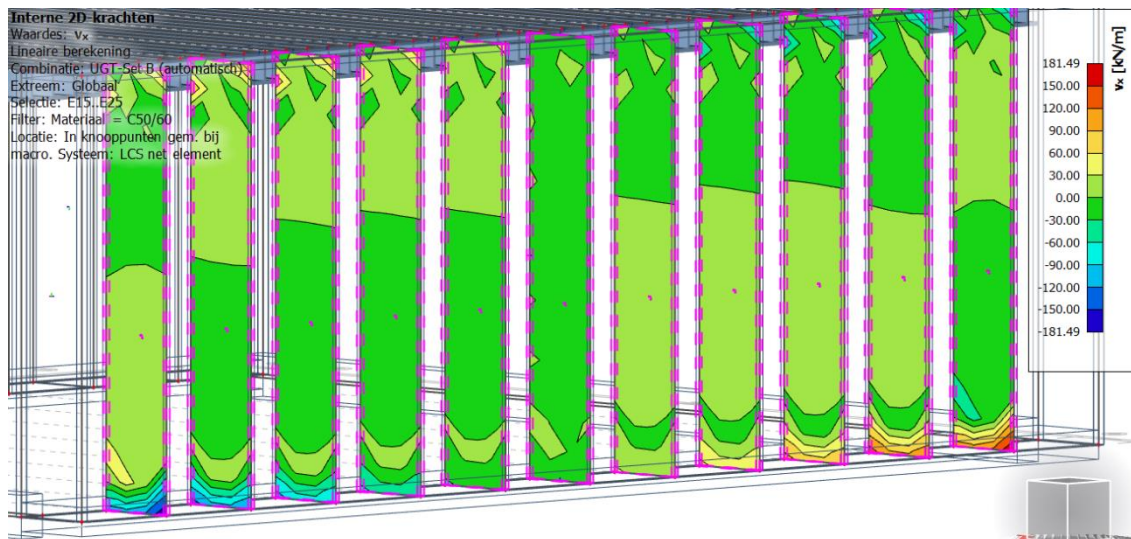


Figure A-133 - Result of shear force in x-direction for inner walls

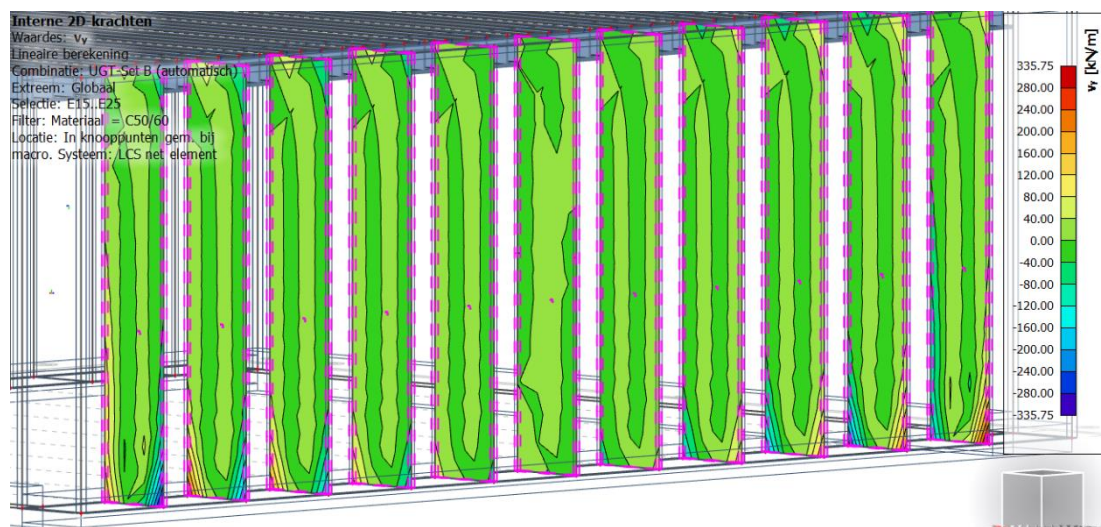


Figure A-134 - Result of shear force in y-direction for inner walls

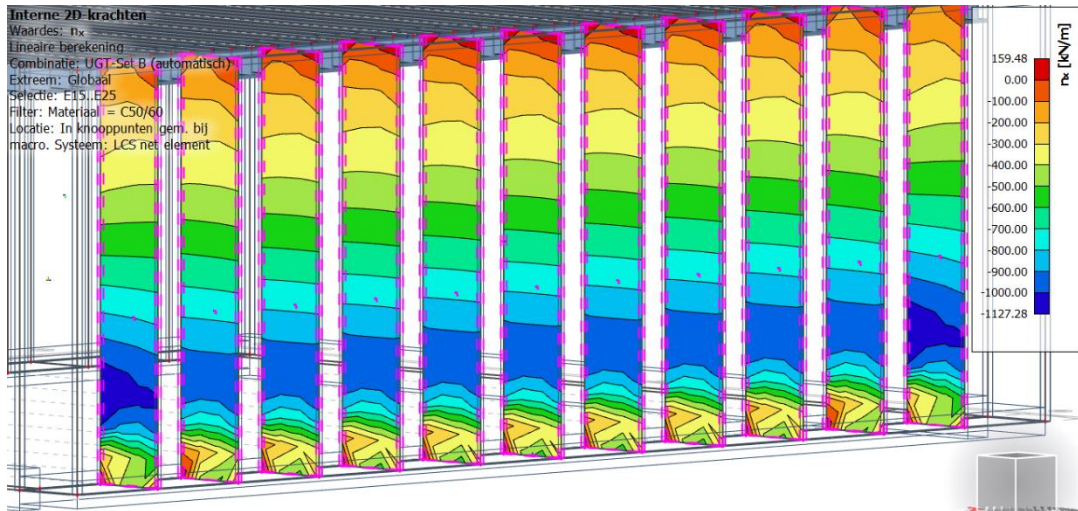


Figure A-135 - Result of axial force in x-direction for inner walls

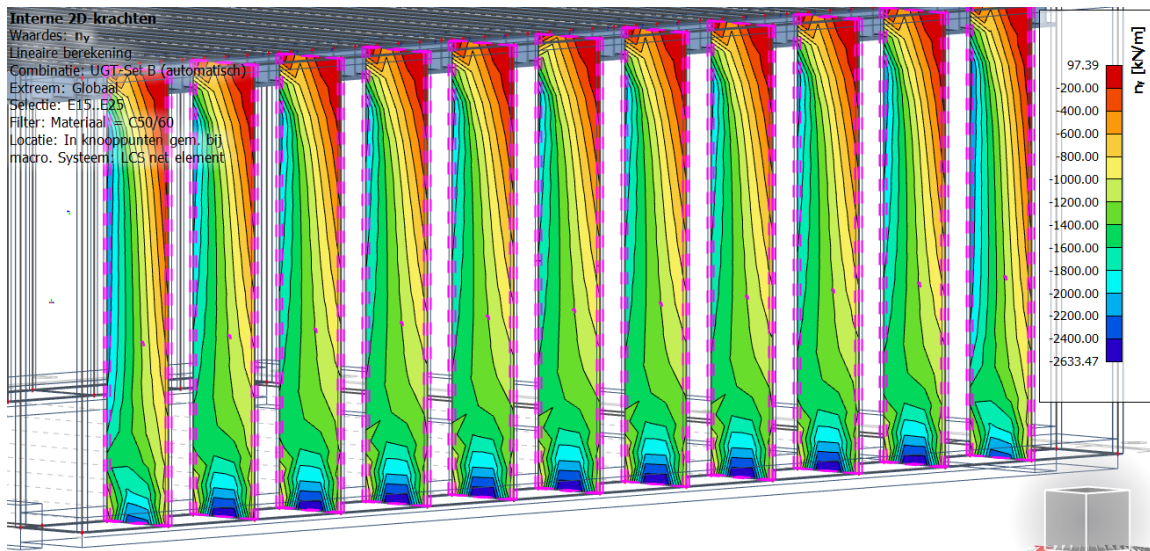


Figure A-136 - Result of axial force in y-direction for inner walls

The maximum values of internal forces are given in Table A-30.

Internal force upper slab	Lower bound value	Upper bound value
$m_x$ [kNm]	-36.16	+36.16
$m_y$ [kNm]	-89.10	+89.10
$V_x$ [kN]	-181.49	+181.49
$V_y$ [kN]	-335.75	+335.75
$N_x$ [kN]	-1127.28	+159.48
$N_y$ [kN]	-2633.47	+97.39

Table A-30 - Maximum values of internal forces inner walls